THE PREPARATION AND CHARACTERIZATION OF STRUCTURALLY STABLE 5-COORDINATE POLYSTANNANES

by

Aman Ullah Khan

Master of Science in Molecular Science,

Ryerson University, Toronto, Canada, 2010

A dissertation presented to Ryerson University

in partial fulfillment of the requirements for the degree of Doctor of Philosophy

in the Program of Molecular Science

Toronto, Ontario, Canada, 2014

AUTHOR'S DECLARATION

I hereby declare that I am the sole author of this dissertation. This is a true copy of the dissertation, including any required final revisions, as accepted by my examiners.

I authorize Ryerson University to lend this dissertation to other institutions or individuals for the purpose of scholarly research

I further authorize Ryerson University to reproduce this dissertation by photocopying or by other means, in total or in part, at the request of other institutions or individuals for the purpose of scholarly research.

I understand that my dissertation may be made electronically available to the public.

THE PREPARATION AND CHARACTERIZATION OF STRUCTURALLY STABLE 5-COORDINATE POLYSTANNANES

Aman Ullah Khan, Molecular Science, Ryerson University, 2014

ABSTRACT

Tetraorganotin compounds $[2\text{-}(MeOCH_2)C_6H_4]SnR_3$ (R = Me, n-Bu, Ph) containing a C,O-chelating ligand were prepared in good yield from the reaction of the R_3SnCl and $[2\text{-}(MeOCH_2)C_6H_4]Li$. Tethered organotin compounds $Ph_3Sn(CH_2)_3OC_6H_4R$ (R = Ph, H, CF_3, OCH_3) were prepared in good yield from the hydrostannylation reactions of the corresponding vinyl ethers with Ph_3SnH. Conversion of two organotin compounds to triorganotin chlorides and diorganotin chlorides, $(Ph_{3\text{-}n}Cl_nSn(CH_2)_3OC_6H_4R$; R = H, Ph: n = 1, 2), was successfully carried out and characterisation afforded by NMR spectroscopy. X-ray crystallographic studies revealed a tetrahedral geometry for the tetraorganotin $Ph_3Sn(CH_2)_3OC_6H_4CF_3$, while five-coordinate trigonal bipyramidal structures with relatively short Sn-O (2.7-2.8 Å) interactions were observed for both mono- $(Ph_2ClSn(CH_2)_3OC_6H_4R$; R = H, Ph) and dichloride $(PhCl_2Sn(CH_2)_3OC_6H_4R$; R = H, Ph) species. Penta-coordinate diorganotin dichlorides containing a C,N- chelating ligand $[2\text{-}(Me_2NCH_2)C_6H_4]RSnCl_2$ (R = Me, n-Bu, Ph) or C,O- chelating ligand $[2\text{-}(MeOCH_2)C_6H_4]RSnCl_2$ (R = Me, n-Bu, Ph) were prepared by treating $RSnCl_3$ with the lithiated salts $[2\text{-}(Me_2NCH_2)C_6H_4]Li$ and $[2\text{-}(MeOCH_2)C_6H_4]Li$ respectively. Organotin chlorides were successfully reduced with $LiAlH_4$ or $NaBH_4$ to produce novel hydrides. Catalytic dehydrocoupling of diorganotin dihydrides to yield polystannanes was explored using a variety of dehydrocoupling catalysts such as Wilkinson's catalyst, Cp_2ZrMe_2 or TMEDA. In almost every instance this resulted in the formation of yellow coloured gummy polymeric materials of moderate molecular weights (Mw = 1×10^4 - 1×10^5 Da) and PDI's (1.3-2.0). The stability of polystannanes containing

tethered O or *C,N-* or *C,O-*chelating ligands was investigated in both solid and in solution using NMR and UV-Vis spectroscopies. These studies revealed an enhanced stability to ambient light in the solid state and in solution in the dark when compared to known poly(dialkyl)stannanes.

ACKNOWLEDGEMENTS

Dedication

I dedicated this to my parents, my wife Gulshan Ara and sons Rizwan, Shahryar and Shehroze

for their endless love, support and encouragement.

Table of Contents

List of Tables:

List of Figures:

List of Schemes:

List of Abbreviations:

Å	Angstrom
AIBN	Azobisisobutyronitrile
AOs	Atomic orbitals
BC	Before Christ
CP-MAS	Cross polarization-Magic angle spinning
d	Days
Da	Daltons
DCM	Dichloromethane
DME	Dimethylethane
DSC	Differential Scanning Calorimetry
Et-	Ethyl
Et_2O	Diethyl ether
GPC	Gel Permeation Chromatography
h	Hours
Hex-	Hexyl
HMPA	Hexamethylphosphoramide
HOMO	Highest occupied molecular orbital
Hz	Hertz
LUMO	Lowest unoccupied molecular orbital
Me-	Methyl
M_n	Number average molecular weight
MO	Molecular orbital
M_w	Weight average molecular weight
Myr	Myrtanyl
NMR	Nuclear Magnetic Resonance
O_h	Octahedral
PDI	Polydispersity index
Ph-	Phenyl

ppm	Parts per million
RI	Refractive index
RT	Room temperature
SP	Square pyramidal
t-Bu	Tertiary butyl
TBP	Trigonal bipyramidal
TEPO	2,2,6,6-Tetramethylpiperidinyloxy
THF	Tetrahydrofuran
TMEDA	Tetramethylethylenediamine
UV	Ultra Violet
VT	Variable temperature

1.0 Tin (Sn):

Tin is the oldest known metal in the periodic table. It has been used to increase the hardness of copper since 3500 BC and helped to start the Bronze Age. It was first isolated as a pure metal in 800 BC.[1] Its abundance in the earth's surface is about 2 ppm, with Cassiterite, SnO_2, the most important ore of tin. China and South East Asia produce 75% of the world's production of tin and $\approx$ 18% from South America.[2] Tin is the first metallic element of Group 14 in the periodic table with atomic number 50, atomic mass 118.90 g/mol and a ground state valence shell electronic configuration $5s^2 5p^2$. It has 10 stable isotopes which is the highest number for any element of the periodic table. Tin has three NMR active isotopes (^{115}Sn, ^{117}Sn and ^{119}Sn) each with spin ½. More commonly ^{117}Sn (7.61%) and ^{119}Sn (8.58%) nuclei are used for NMR experiments due to their relatively high natural abundance. For tin chemistry, ^{119}Sn NMR spectroscopy has become a routine tool with NMR chemical shifts ranging from +4000 to -2500 ppm with the ^{119}Sn resonance for SnMe$_4$ assigned to $\delta = 0$ ppm.[2] Tin most commonly exists in either a Sn(II) or Sn(IV) oxidation state with tetravalent structures preferred for most organotin compounds. The majority of organic and inorganic Sn(IV) compounds possess sp^3 hybridization and adopt a tetrahedral structure, e.g. SnX$_4$ (Figure 1). The coordination number at tin can be increased through hybridization to form 5- and 6-coordinated complexes. These hybridized orbitals can accept electrons from ligands to form coordination geometries which are trigonal bipyramidal, TBP (SnX$_5$) or octahedral, O$_h$ (SnX$_6$) respectively.

Tetrahedral   Trigonal bipyramidal   Octahedral
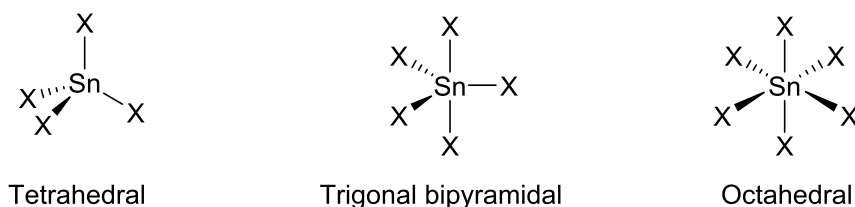
Figure 1: Geometry of different Sn(IV) compounds.

1.1 Organotin compounds:

In 1849, the first organotin compound, diethyltin diiodide, was synthesized by Frankland[3] and shortly thereafter the first oligo- or polystannane was reported by Löwig in 1852.[4] Löwig studied the reaction of iodoethane with Sn/K or Sn/Na alloys and obtained Et_3SnH and Et_3Sn-$SnEt_3$. The development of organotin chemistry slowed for the next fifty years with only 37 papers published by 1900. Organotin chemistry was revolutionized shortly thereafter with the availability of organomagnesium halides as alkylating and arylating agents. These reagents were widely used to produce R_4Sn type compounds. In 1903, Pope and Peachey described the synthesis of a number of tetraalkyl- and tetraarylstannanes by reacting a suitable Grignard reagent with $SnCl_4$ or alkyltin halide.[5] Kocheshkov discovered the redistribution reaction between R_4Sn and $SnCl_4$ in 1929 which afforded tri-, di- and mono-organostannyl chloride species.[6] In 1936, Yngve discovered the heat stabilizing ability of organotins on polyvinyl chloride. In 1937, a summary of the early work of organotins was published in *Organometallische Chemie* by Krause and von Grosse.[7]

1.2 Hypervalent/ Hypercoordinate compounds:

In recent years, research interest in compounds with non-classical chemical bonds has increased extensively.[8] These include the derivatives of silicon, germanium[9-12] and tin.[13,14] The expansion in the coordination sphere of these elements is caused by additional intra- or intermolecular coordination interactions. In the early 1960's it was demonstrated that organotin compounds have the ability to expand their coordination spheres.[15,16] In 1969, the term "hypervalent" was introduced by Musher to explain the structure of compounds that required octet expansion for the central atom (e.g. PCl_5, SiF_6, etc.).[17] The ions or molecules of the elements of Group 15-18 that possess more electrons than the octet within a valence shell are deemed

hypervalent.[17] Compounds of elements from Groups 1, 2 or 14 as the central atom are also included in the family of hypervalent compounds. Hypervalent bonds in 5- or 6-coordinate compounds of Ge, Sn and Pb differ from the hypervalent bonds of S, P and Cl derivatives. In this case, the donor lone pair of Group 14 elements is supplied by the ligand as the central atom has no ns^2 lone pair. The first structurally characterized pentacoordinated organotin compound was a $PyMe_3SnCl$ in 1963.[18] In the last three decades, five (TBP, SP) and six (O_h) coordinated tin compounds have been extensively studied. Compounds of main group elements containing (N) electrons more than the octet in a valence shell associated with the central atom (E) directly bound to ligands (L) are known as hypervalent compounds. Therefore, the simple designation *N-E-L* is used to describe hypervalent molecules (Figure 2).[18]

10-E-5	10-E-5	12-E-6
TBP	SP	O_h
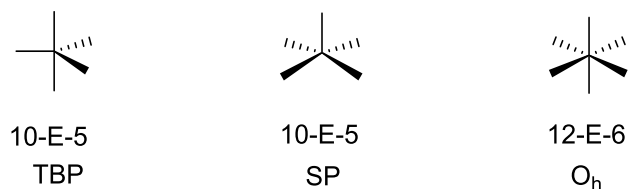
Figure 2: The principle coordination geometries of 5- and 6-coordinate Sn compounds. The formation of hypervalent bonds containing a 5- and 6-coordinated central atom can be interpreted by two concepts; the d-orbital concept or the 3c-4e bond concept.

1. *The d-orbital concept*:

According to this classical concept, filled *s* and *p* atomic orbitals along with vacant $5d$-orbitals are involved in bond formation and cause an increase in the coordination number from 4 to 5 or 6 for Group 14 containing species. Two electronic configurations are envisioned to hold additional electrons that exceed the octet within the valence shell; dsp^3 or d^2sp^3.[8] Sn has five vacant $5d$ AOs which could participate in the formation of penta- and hexacoordinate structures. However, computational studies have shown that the nd AOs of Group 14 atoms (Ge, Sn and Pb)

are too diffuse and too high in energy to participate in bonding[8] (more detail provided in the 3c-4e bond concept: below).

2. *3c-4e bond concept:*

This concept excludes the contribution of $5d$ orbitals in hypervalent bonding for penta- and hexacoordinate structures. In 1951, Pimentel and Rundle proposed the idea of a 3c-4e bond using molecular orbital theory.[20] A simple description of the 3c-4e bond model is the delocalization of one pair of bonding electrons to the two other substituents. The 3c-4e model suggests that ns^2 orbitals of metal atom (E) could be used for bonding to equatorial ligands resulting in two-center bonds, while the np_z orbital could interact with an appropriate orbital of the axial substituent (*L*) and a lone pair of the donor atom (*N*) to form a hypervalent, 3c-4e bond. Initially, the concept of 3c-4e bond was not readily adopted by researchers, but progress in computational studies and the efforts of Kutzelnigg *et al.*[21] have made this idea generally acceptable today. The hypervalent bonding of molecules has also been investigated by von Schleyer *et al.*[22] who concluded that the *d*-orbital concept is incorrect and these orbitals are not important in the acceptance of electrons beyond the octet. It has been determined that it is not possible for the *d* orbitals to hold extra electron density because of the high energy gap between n(sp) and nd, which makes the number of available metal orbitals deficient. From theoretical calculations, it has been established that in main group elements, participation of *d* orbitals for hybridization with *s* and *p* orbitals of third period and heavier is negligible. Therefore, a 3c-4e bond is an electron-rich bond and the non-bonding molecular orbital becomes the highest occupied orbital. In the 3c-4e bond, the central atom has less than four pairs of electrons in the valence shell and does not exceed the Lewis octet due to the distribution of extra electron density on to ligands or substituents. Figure 3 represents the simplest MO diagram of the 3c-4e bond.
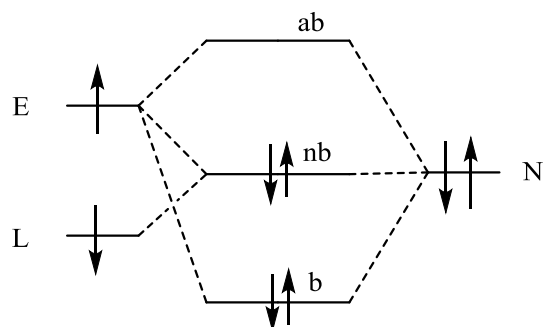
b = bonding, nb = non-bonding, ab = antibonding

Figure 3: The MO diagram of a (3c-4e) bond in hypervalent compounds.

In Group 14, the hypervalency of both Sn and Si has been intensively studied in comparison to Ge, with even fewer studies for compounds of Pb. In a pentacoordinated TBP molecule, the hypervalent bond is typically seen in the axial position. Four methods were proposed by Akiba[8] to construct a 3c-4e bond of a pentacoordinated molecule experimentally (Figure 4); a) add two free radicals to coordinate with a pair of unshared electrons in a *p* orbital, b) add two pairs of unshared electrons to coordinate a vacant *p* orbital, c) add a pair of unshared electrons to coordinate with σ* orbital of E-X bond (e.g., sulphonium, phosphonium etc.), d) add a pair of unshared electrons to coordinate with the σ* orbital of E-X bond of a neutral molecule (e.g., Si and Sn).
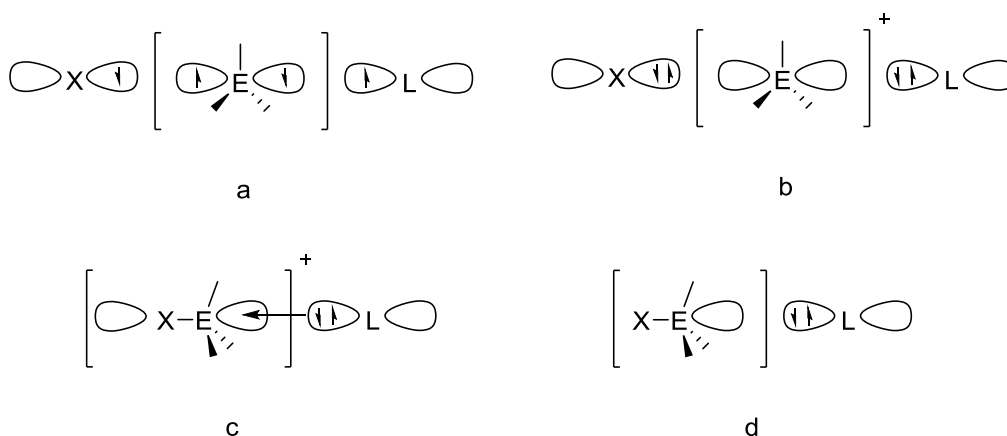
Figure 4: Proposed methods to make (3c-4e) bonds.[8]

Hypervalent bonds are favourably formed when these conditions are present:

1. The electronegativity of the ligands is typically higher than the central E atom.

2. For trigonal bipyramidal molecules, ligands having higher electronegativity form the hypervalent bond with central atom E and tend to occupy axial positions.

3. The E-L bonds are longer in penta- and hexacoordinate compounds than in tetrahedral molecules.

1.3 Hypervalent/ Hypercoordinate compounds of Group 14:

1.3.1 Hypercoordinate organotin compounds containing *C,N*-chelating ligands:

Hypervalent compounds of organotin derivatives with ligands containing an intramolecular Sn-N interaction have been known since 1960.[23] These tin species have been extensively studied by single-crystal X-ray diffraction and NMR (^{1}H, ^{13}C, ^{119}Sn) spectroscopy. The strength of the Sn-N interaction can be inferred from the bond distance; the smaller the distance, the stronger the donor-acceptor interaction. It is also observed that as the Sn-N distance decreases, the Sn-X (X = F, Cl, Br, I) bond becomes longer. This is consistent with the model shown in Figure 4(d). The ^{119}Sn NMR spectra of hypervalent triorganotin(IV) compounds exhibit a single resonance for the central tin atom, shifted up-field with respect to a structurally similar non-hypervalent analog.

Organotin(IV) compounds possessing the 2-(Me_2NCH_2)C_6H_4- organic ligand with nitrogen as donor atom or other related potentially chelating organic ligands have been extensively investigated both in solution and in the solid state. Interest in these types of organotin compounds has been largely due to their unusual structural properties[14,24] and potential biological uses.[25] The different types of organotin compounds utilizing the 2-(Me_2NCH_2)C_6H_4- ligand can be classified as mono-, di-, tri- and tetraorganotin(IV) compounds.

1.3.1.1 Tetraorganotin compounds containing *C,N*-chelating ligands:

The more commonly used *C,N*-chelating ligands are shown in Figure 5. Ligands i-iv and vii can form five membered hypervalent compounds while v and vi form six membered chelate rings.[26]

M = Si, Ge, Sn
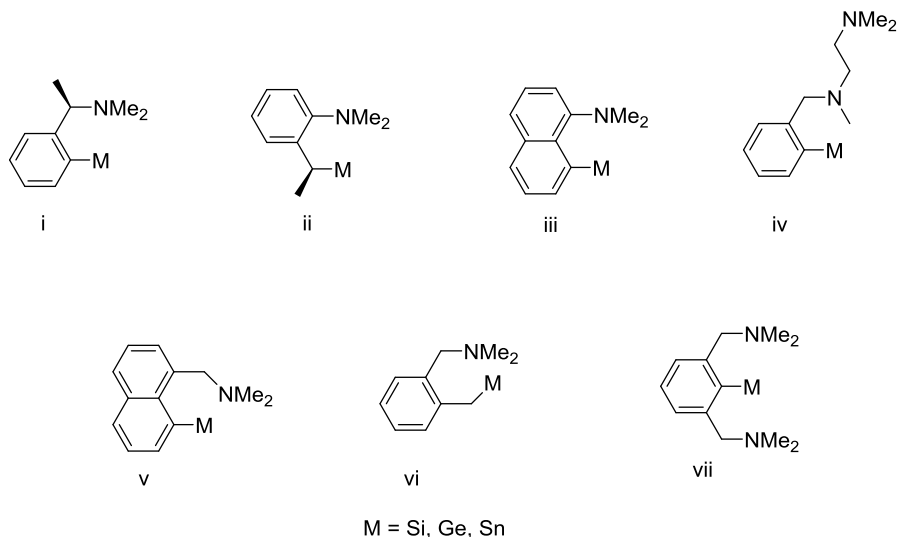
Figure 5: Most commonly used *C,N*-chelating ligands.

The important structural feature of these ligands is that the Sn-N intramolecular coordination results in an increase of the coordination number at tin from 4 to 5 or 6 for i to iv and v to vi respectively.

Organotin compounds containing these ligands can be synthesized by heteroatom facilitated ortho-lithiation followed by reaction with organotin halides. Jastrzebski *et al.*[27] reported the synthesis of 8-(dimethylamino)-1-naphthyl lithium etherate by reacting the equimolar amount of 1-(dimethylamino)naphthalene with *n*-BuLi in Et$_2$O. The 8-(dimethylamino)-1-naphthyl lithium etherate was treated with Me$_3$MCl (M = Si, Sn) to obtain the corresponding Group 14 derivatives. Reaction of 8-(dimethylamino)-l-naphthyl lithium with Me$_3$SnCl or Ph$_3$SnCl afforded high yields of 8-(dimethylamino)-l-naphthyltrimethyltin and 8-(dimethylamino)-l-naphthyltriphenyltin, respectively (Scheme 1).[28] Tetraorganotin compounds were initially

considered as unlikely to extend their coordination number due to the poor acceptor properties of these tin centers.[14]
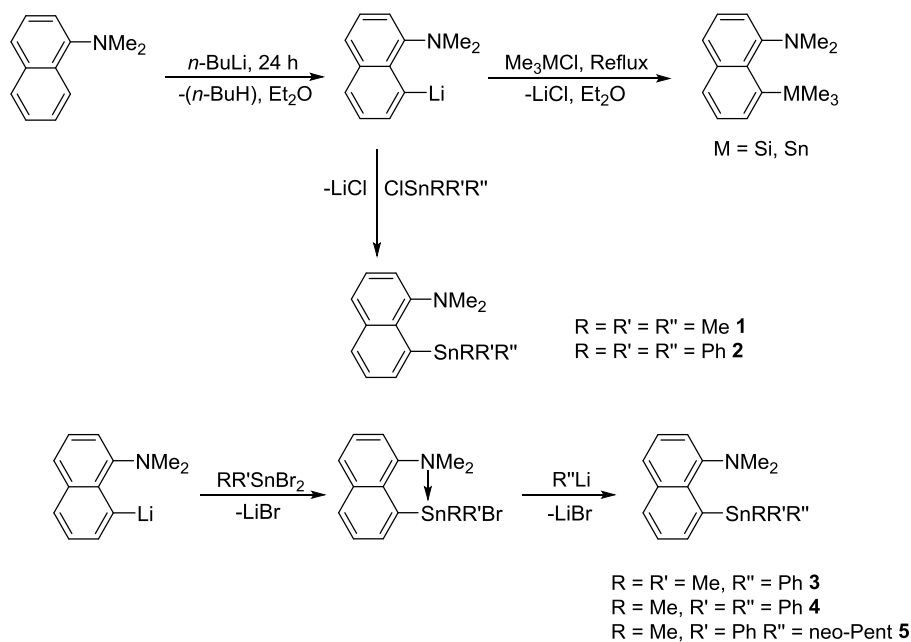
Scheme 1: Synthesis of tetraorganotin compounds.[25,26]
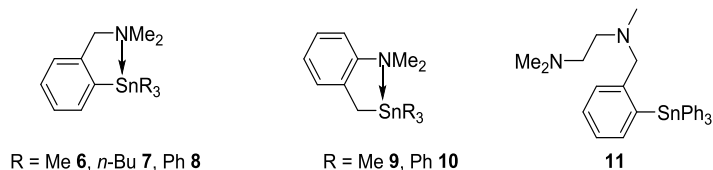
Figure 6: Tetraorganotin compounds.

NMR (^{1}H, ^{13}C, [119]Sn) spectroscopic studies have provided information concerning the structure of tin compounds with *C,N*-chelating ligands in solution. These studies indicate that the ^{119}Sn NMR chemical shift of such compounds is strongly dependent on the type of substituent and coordination number of tin.[14]

In compounds **1-5**, the stable geometry of the 8-(dimethylamino)-1-naphthyl group ensures a Sn-N coordination bond. An X-ray structure of **2** reveals tin in TBP geometry with the N atom and one of the phenyl rings at axial positions.[28] The [119]Sn chemical shifts of compounds **1-4** show that the replacement of methyl by phenyl groups enhances the up-field shift of Sn resonances due

8

to an increasing Sn-N interaction. A significant upfield shift of the [119]Sn resonance for **6** compared to the unsubstituted analogue Me$_3$SnPh is likely due to the presence of a Sn-N intramolecular interaction.

Table 1: Comparison of the [119]Sn chemical resonances of tin compounds containing a *C,N*-ligand and structurally similar unsubstituted analogue.

Compound	[119]Sn δ (ppm)	Unsubstituted analogue	[119]Sn δ (ppm)
1	-46.0[28]	C$_{10}$H$_7$SnMe$_3$	-31.8[37]
2	-155.3[28]	C$_{10}$H$_7$SnPh$_3$	-
3	-81.7[28]	C$_{10}$H$_7$SnPhMe$_2$	-
4	-110.4[28]	C$_{10}$H$_7$SnPh Me$_2$	-
5	-97.3[28]	C$_{10}$H$_7$SnMe$_3$	-31.8[37]
6	-50.0	Me$_3$SnPh	-28.6[338]
7	-50.0[29b]	Bu$_3$SnPh	-41.7[39]
8	-168.5[34]	Ph$_4$Sn	-137.0
9	-0.8[32]	C$_6$H$_4$CH$_2$SnMe$_3$	3.5[36]
10	-122.2[32]	C$_6$H$_4$CH$_2$SnPh$_3$	-118.0[37]
11	-148.0[35]	-	-

A comparison of ^{119}Sn NMR chemical shifts of tin compounds containing a *C,N*-ligand and their unsubstituted analogues given in Table 1 indicate that compounds **9**-**10** (Figure 6) have no apparent intramolecular interaction between Sn and N as there is only a slight upfield shift in their resonances compared to their unsubstituted analogues. A possible reason for the absence of an intramolecular interaction, particularly in compound **10**, is due to the energetically favourable structure having a bulky SnR$_3$ substituent perpendicular to the plane of aryl ring, keeping the tin atom away from the potential donor atoms.

1.3.1.1a Solution Structure of tetraorganotin compounds 1, 3-5:

The relatively small 52 Hz $^2J_{117/119Sn-1H}$ coupling values for the methyl protons present in compounds **1**, **3**-**5** are indicative of a tetrahedral geometry at tin.[30-33] The presence of two resonances for the -NMe$_2$ group in **5** containing a stable chiral center suggest a blockage of

pyramidal inversion at nitrogen, and may be a result of strong Sn-N coordination or steric considerations. The ^{1}H and ^{13}C chemical shift values of the -NMe$_2$ in compounds **1**-**5** are relatively insensitive to Sn-N coordination. The methyl groups of -NMe$_2$ in these compounds have ^{13}C chemical resonances at $\approx$ 48 ppm, very close to that of the free 1-(dimethylamino)naphthalene (46.2 ppm). A small upfield shift of 2.2 ppm results with the substitution of phenyl for methyl at the tin center.[32]

1.3.1.2 Synthesis of organotin halides containing *C,N*-chelating ligands:

Organotin halides have been synthesized by a variety of methods. The most commonly used method is the conversion of alkyl or aryl halides into Grignard reagents in THF or Et$_2$O and their subsequent reaction with SnCl$_4$ to produce tetraorganotin compounds. Tri- and diorganotin compounds can be synthesized by the comproportionation (or Kocheskov redistribution) reactions of tetraorganotin compounds with SnCl$_4$ (Scheme 2).[42]

$$RBr \xrightarrow[\text{Et}_2\text{O or THF}]{\text{Mg turnings}} RMgBr \xrightarrow[\text{Et}_2\text{O}]{0.2 \text{ eq. SnCl}_4} R_4Sn$$

$$2R_2SnCl_2 \xleftarrow[\text{neat}]{2 \text{ eq. SnCl}_4} R_4Sn \xrightarrow[\text{neat}]{3 \text{ eq. SnCl}_4} 4RSnCl_3$$

$$R_2SnCl_2 \xrightarrow[\text{neat}]{R_4Sn} 2RSnCl_3$$

R = Alkyl or Aryl groups
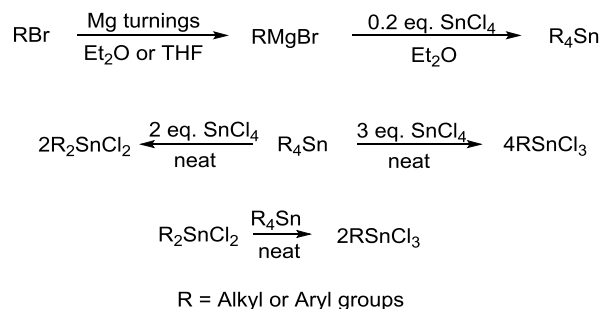
Scheme 2: Synthesis of organotin halides.

The R$_2$SnCl$_2$ species are more conveniently accessed using the Kocheskov equilibrium (Scheme 2). During this reaction RSnCl$_3$ is produced as an intermediate which immediately reacts with a tetraorganotin species to produce a diorganotin dihalide. Different techniques were reported to obtain pure tetraorganotin compounds. Caseri *et al.* used a 5% HCl solution for tetraalkyltin compounds[40] and saturated solution of NH$_4$Cl for tetraaryltin compounds.[41] Uhlig *et al.* purified tetraaryltin compounds by filtration of reaction mixtures through celite and extraction of the

residues with DCM.[42] Deacon *et al*. prepared diorganotin dihalides by reacting tetraorganotin compounds with a stoichiometric solution of Br_2 or I_2 in $CHCl_3$. The halobenzene by-product was removed by prolonged drying under reduced pressure.[43]

Hypercoordinated diorganotin halides containing *C,N*-chelated ligands can be synthesized by reacting $[2\text{-}(Me_2NCH_2)C_6H_4]Li$ with R_nSnCl_{4-n} (R = L, Me, *n*-Bu, Ph) under inert atmosphere. Another method for the synthesis of diorganotin halides is the solvent-free ligand redistribution reaction between $[2\text{-}(Me_2NCH_2)C_6H_4]Sn$ and $SnCl_4$. These may also be synthesized from the direct reaction of $[2\text{-}(Me_2NCH_2)C_6H_4]Li$ and $SnCl_4$ (Scheme 3).[49]
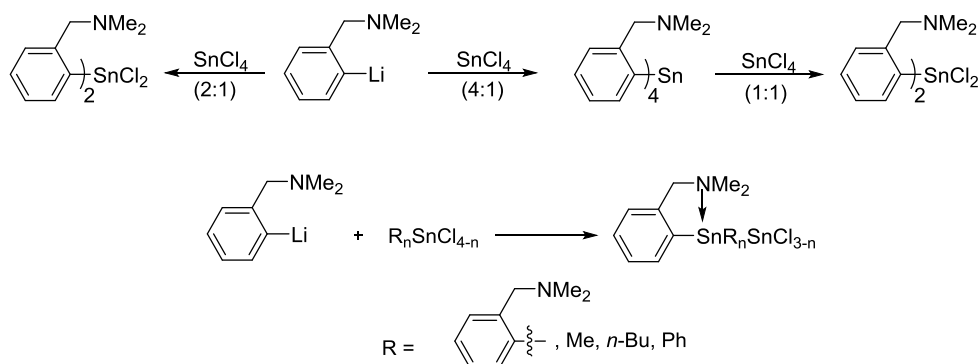
Scheme 3: Routes for the synthesis of hypercoordinated organotin halides.

1.3.1.3 Triorganotin halides containing *C,N*-chelating ligands:

There are a number of triorganotin halides (Figure 7) containing *C,N*-chelating ligands such as $2\text{-}(Me_2NCH_2)C_6H_4\text{-}$. The presence of a Sn-N intramolecular interaction in these species has been established by crystallography[44] and ^{119}Sn CP-MAS NMR[45] (Cross Polarization-Magic Angle spinning) techniques in the solid state as well as by solution multinuclear NMR spectroscopy.[29b,46]

R = H **12a-c**   R' = R" = Me **a**
R = Me **13a-c**   R' = Me, R" = Ph **b**
R = Et **14a-c**   R' = R" = Ph **c**
R = i-Pr **15a-c**
R = t-Bu **16a-c**

R = Me, R' = Ph, X = Cl **17**
R = R' = Ph, X = Cl **18**
R = R' = Me, X = Cl **19**
R = R' = n-Bu, X = Br **20**
R = R' = n-Bu, X = Cl **21**
R = R' = t-Bu, X = Cl **22**

23

R = H **24**   R' = R" = Me **a**
                R' = Me, R" = Ph **b**
                R' = R" = Ph **c**

R = R' = Me **25**
R = Me, R' = Ph **26**

R = R'= Me **27**
R = Me, R' = Ph **28**
R = R' = Ph **29**
R = Me, R' =(-) menthyl **30**
R = Ph, R' =(-) menthyl **31**

32
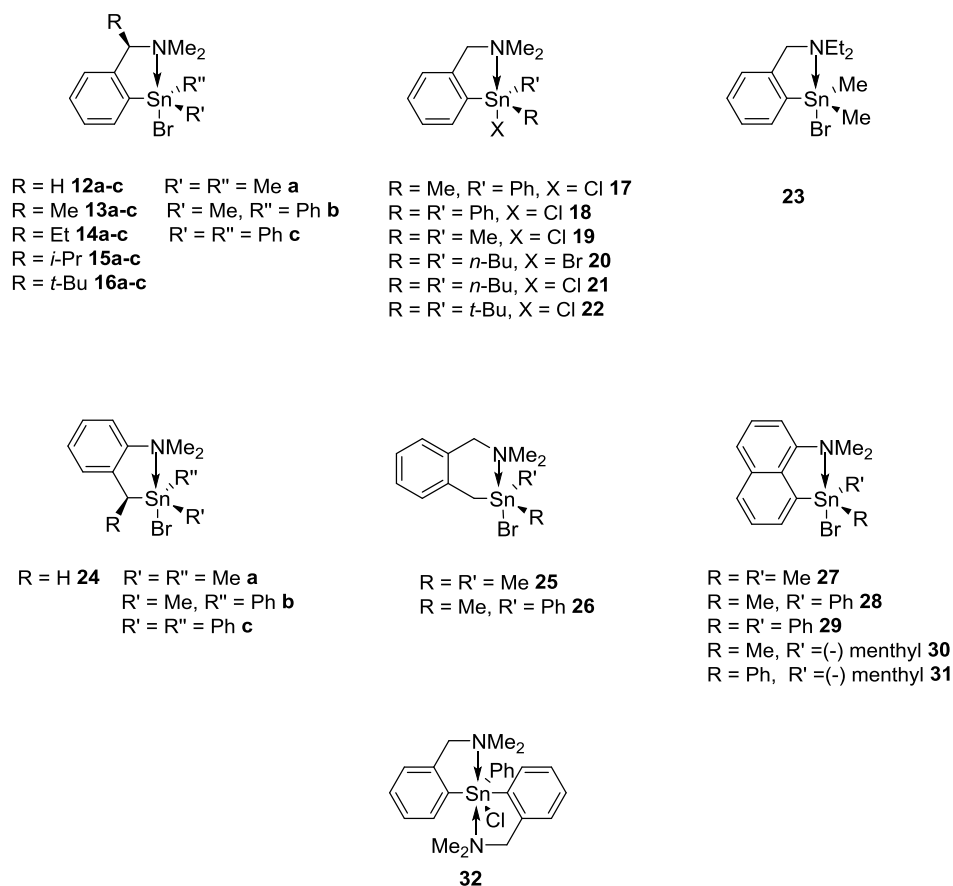
Figure 7: 5-coordinate triorganotin halides.

1.3.1.3a Synthesis:

R = Me **12a**, Ph **12c**
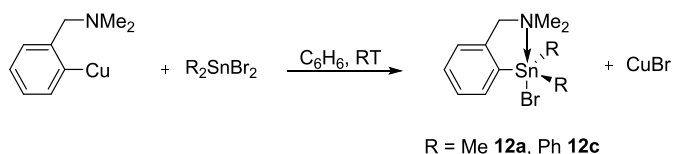
Scheme 4: Synthesis of compounds **12a** and **12c**.[47]

van Koten *et al*. prepared compounds **12a** and **12c** by treating the [2-(Me$_2$NCH$_2$)C$_6$H$_4$]Cu tetramer with diorganotin dihalides (Scheme 4).[47] Compounds **13** and **14** were prepared by lithiation of 2-Me$_2$NCH(R)C$_6$H$_5$ with t-BuLi. Compounds **15** and **16** were synthesized by lithium/halogen exchange reactions of 2-Me$_2$NCH(R)C$_6$H$_5$ (R = isopropyl, t-butyl) with n-BuLi because the presence of bulky substituents greatly reduces accessibility to the ortho site. The

reaction of $SnBr_2Me_2$, $SnBr_2MePh$, $SnBr_2Ph_2$ with the lithiated species afforded hypervalent compounds **13**(**a-c**) and **16**(**a-c**) as white coloured crystalline solids (Scheme 5).[56a]
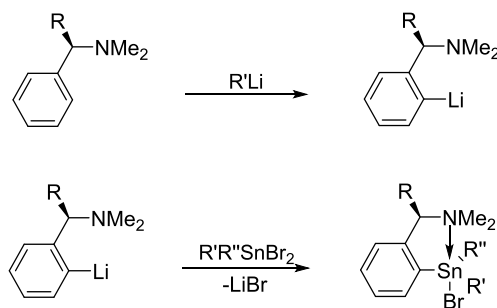
Scheme 5: Synthesis of **13**(**a-c**) and **16**(**a-c**).[28]

Compounds **17**, **18** and **19** were previously reported by both Rippstein *et al.*[48] and Varga *et al.*[49] and were synthesized by reacting $[2-(Me_2NCH_2)C_6H_4]Li$ with their respective diorganotin dihalides. Alternatively, **17** was obtained by reacting $[2-(Me_2NCH_2)C_6H_4]Li$ with a solution of $SnMePhBr_2$ in Et_2O.[50] Compounds **21**[51], **22**[52], and **32**[48,29a] were synthesized from the reactions of a 1:1 of $n\text{-}Bu_2SnCl_2$, $t\text{-}Bu_2SnCl_2$ and 1:2 ratio of $PhSnCl_3$ with $[2-(Me_2NCH_2)C_6H_4]Li$ in C_6H_6 at room temperature. Compound **23** was prepared by reacting Me_2SnBr_2 with $[2-(Et_2NCH_2)C_6H_4]Li$.[53]

1.3.1.3b Structural studies:

The x-ray crystal structure determination of $[2-(Me_2NCH_2)C_6H_4]SnPh_2Br$ **12c** reveals a five-coordinate distorted TBP geometry at the tin center, with three carbon ligands, including the built-in ligand and the bromine atom in equatorial and axial positions, respectively. A N-Sn-Br bond angle of 171° and Sn-N bond length of 2.51 Å was observed for **12c**. The Sn-N bond distance may be the result of a balance between the inherent Sn-N bond strength and the skeletal strain in the five-membered chelate ring.[54] These observations provide evidence of an intramolecular interaction between Sn and N.

The configurational stability of the triorganotin bromides having either the tin center (Figure 7) (R'$\neq$R'', **12b** and **24b**), or the benzyl carbon atom (R $\neq$ H) or both (**12b**-**16b**) as chiral centers were investigated extensively by variable temperature NMR spectroscopy.[47,50,56a] Tin compounds **25** and **26** have a six-membered chelate ring where the tin centers have configurational stability only at low temperature (below 0 °C),[50] while triorganotin bromides having a flexible five-membered chelate ring (**13b**-**16b**, **17** and **24b**) are considerably more stable on the NMR time scale (up to 130 °C). These fluxional processes were studied by the ^{1}H NMR of **12b** at variable temperatures. The diastereotopicity of the methyl protons of the -NMe$_2$ group was observed by ^{1}H NMR spectroscopy at low temperature, indicating the inertness of Sn-N coordination on the NMR time scale. At higher temperature, the -NMe$_2$ resonances coalesce due to the process of Sn-N dissociation/association. The process (Figure 8) by which -NMe$_2$ methyl groups become homotopic consists of four steps including Sn-N dissociation, rotation around the C$_{benzyl}$-N bond, pyramidal inversion at nitrogen and finally Sn-N association. On the NMR time scale this process is quite fast above 0 °C. [32,33,54,55,56a] Finally, it was found that the tin center has configurational stability up to 130 °C on the NMR time scale in triorganotin bromides having a rigid five-membered chelate ring (**28, 30, 31**).[27] The ^{1}H NMR analysis of **25** and **26** containing a six-membered chelate ring reveal the existence of both the process of dissociation/association and inversion of configuration at tin centers.[50] The ^{1}H NMR spectrum of compound **26** at -40 °C showed an AB pattern for both benzylic -CH$_2$ groups and two resonances for -NMe$_2$ group. This indicates the stability of the Sn-N interaction and configuration of tin on the NMR time scale. At -30 °C, it was observed that -NMe$_2$ resonances coalesce, with no change of the AB pattern up to 0 °C. This suggests that on NMR time scale, only the Sn-N dissociation/association process becomes

rapid. Above 0 ºC, the coalescence of the two AB patterns to two singlets show that inversion of configuration at tin centers is rapid.[50]
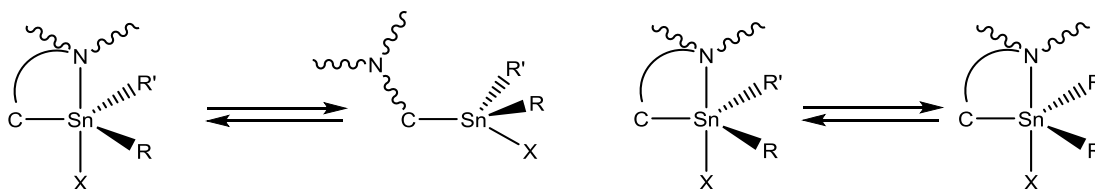
Figure 8: Two basic fluxional processes of a *C,N*-chelating ligand containing R_3SnCl.

R = Me **13 b'**
R = Et **14 b'**
R = *i*-Pr **15 b'**
R = *t*-Bu **16 b'**

R = Me **13 b"**
R = Et **14 b"**
R = *i*-Pr **15 b"**
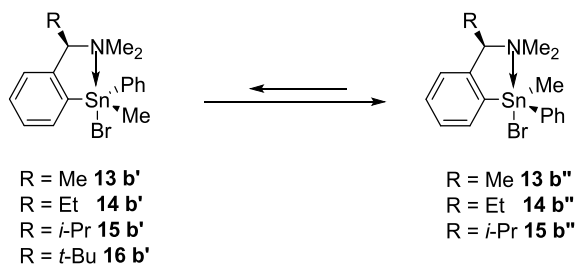
Scheme 6: Diastereoisomers of **13b**-**16b**.

Compounds **13b**-**16b** possess two chiral centres; one at the benzylic carbon and one at the tin atom. NMR (^{1}H and ^{119}Sn) spectroscopy indicate the presence of two different diastereoisomers for **13b**-**15b** and a single isomer for **16b** as shown in Scheme 6. The coordination geometry at the tin atoms of compounds **21** and **22** is trigonal bipyramidal having the carbon atoms and more electronegative atoms (N, Cl) at equatorial and axial positions respectively. The Sn-N bond distance in **22** is 2.904(14) Å which is significantly longer than in **21** (2.510(5) Å) and other known triorganotin compounds. The downfield ^{119}Sn NMR resonance of 18.5 ppm for **22** is in contrast with the resonances of similar types of 5-coordinate compounds with strong Sn-N interactions such as $LSn(n\text{-Bu})_2Cl$ ($\delta = -51.7$ ppm), $LSn(n\text{-Bu})_2F$ ($\delta = -77.1$ ppm), $LSn(t\text{-Bu})_2F$ ($\delta = -92.1$ ppm), $LSnMe_2F$ ($\delta = -53.8$ ppm) where $L = 2\text{-}(Me_2NCH_2)C_6H_4\text{-}$. Variable temperature (VT) ^{1}H and ^{119}Sn NMR studies of **22** in different solvents and in the solid state concluded that its geometry is distorted trigonal pyramidal, but with a significantly weaker Sn-N interaction.[52]

15

The geometry of **32** can be explained in two different ways. It may be a prototypical distorted trigonal bipyramidal geometry for organotin having a *C,N*-chelating ligand located in equatorial positions where both the chlorine and nitrogen atoms are in axial positions. Here the non-coordinated nitrogen atom lies out of the tin coordination sphere and does not coordinate to tin (Sn–N1 and Sn-N2 distances at 2.4752(17) and 3.5174(19) Å respectively). Alternatively, it may be regarded as a distorted octahedron, with C1 and C10, N1 and Cl1, and N2 and C19 in mutual pseudo *trans* positions. The Sn–N1 and Sn-N2 distances are 2.5345(18) and 3.2736(19) Å for the second molecule and the bond angle between C1-Sn-C10 in these molecules is 130.66º and 134.15º instead of 180º. The asymmetric crystal unit cell of **32** show two independent molecules having small differences in some bond distances and angles.[29a]

Triorganotin compounds tend to favour pentacoordination in the presence of donor molecules due to the increased Lewis acidity of tin. Compounds in Figure 7 contain a potentially intramolecularly coordinating *C,N*-chelating ligand capable of forming a five membered chelate ring. The tin center in these compounds has TBP geometry having the carbon ligands at equatorial sites and the more electronegative nitrogen and halogen atoms at axial positions. NMR (^{1}H, ^{13}C and ^{119}Sn) studies of these compounds suggest that they have same structure in both the solid state and in solution. However, fluxional processes become more frequent at higher temperature on the NMR time scale.

Table 2: [119]Sn chemical shifts and Sn-N distance of triorganotin halides.

Compounds	R	R'	R"	[119]Sn shift(δ) ppm	Sn-N distance (Å)
12a	H	Me	Me	-50.0[26,47]	-
12b	H	Me	Ph	-111.0[26,57]	-
12c	H	Ph	Ph	-182.0[26,47]	2.511(12)[54]
13a	Me	Me	Me	-55.7[56a]	-
13b	Me	Me	Ph	-117.0 and -117.7[56a]	2.476(7)[56a]
13c	Me	Ph	Ph	-206.9[56a]	-
14a	Et	Me	Me	-53.8[56a]	-
14b	Et	Me	Ph	-112.6 and -115.1[56a]	-
14c	Et	Ph	Ph	-187.5[56a]	-
15a	i-Pr	Me	Me	-46.1[56]	-
15b	i-Pr	Me	Ph	-111.1 and -113.9[26]	-
15c	i-Pr	Ph	Ph	-181.6[56a]	-
16a	t-Bu	Me	Me	-35.4[56a]	-
16b	t-Bu	Me	Ph	-102.7[56a]	2.552(5),2.482(5)[56a]
16c	t-Bu	Ph	Ph	-165.3[56a]	-
20	H	n-Bu	n-Bu	-44.9[29b]	2.510(5)[58]
22	H	t-Bu	t-Bu	18.5	2.904(14)[52]
24a	H	Me	Me	22.8[32]	-
24b	H	Me	Ph	-46.5[32]	-
24c	H	Ph	Ph	-122.1[32]	-
25	-	Me	Me	-25.0[50]	-
26	-	Me	Ph	-94.8[50]	-
27	-	Me	Me	-38.7[27]	-
28	-	Me	Ph	-97.5[27]	2.496(6)[28]
29	-	Ph	Ph	-165.1[27]	-

^{1}H NMR spectra of compounds **13b**-**13d**, **14b**-**14d**, **15b**-**15d** and **16b**-**16d** reveal a TBP structure for tin, where the C-ligands occupy equatorial positions and the N an axial position. For compounds **13b**-**15b**, two distinct patterns were observed in their ^{1}H NMR spectra indicative of two diastereoisomers. These observations are supported by the presence of a chiral center in these molecules. The $^2J_{117\text{-}119\text{Sn-1H}}$ coupling of 65 Hz for triorganotin bromides **13b**-**16b** and **13a**-**16a** having one and two methyl groups bonded to tin also confirm the TBP geometry.[56a]

The ^{119}Sn NMR data for trioganotin halides (Table 2) suggest that the formation of pentacoordinated species results in a relatively large upfield shift of ^{119}Sn NMR resonance

compared to similar four coordinate tin species. For example, the ^{119}Sn NMR resonance for **12c**-**16c** range from δ = -105 to -145 ppm compared to δ = -60 ppm for Ph$_3$SnBr.[56b] The upfield shift of ^{119}Sn resonances is also consistent with the substitution of methyl for phenyl groups. The ^{119}Sn chemical shifts of triorganotin halides in these studies are independent of temperature (between -80 to 100 ºC) suggesting that even in the presence of fluxional process involving Sn-N dissociation-association observable by ^{1}H and ^{13}C NMR spectroscopy, the Sn center retains its pentacoordinated geometry. Two well resolved ^{119}Sn resonances were also observed for compounds **13c**-**16c** indicative of the existence of two diastereoisomers.

The VT ^{119}Sn NMR of **25** and **26** indicate a strong temperature dependence, with an increasing downfield shift observed with increasing temperature. A significant ^{119}Sn NMR chemical shift variation was observed for **25** and **26** from -49.4 ppm and -131.1 ppm at -85 ºC to -6.2 ppm and -72.0 ppm at 100 ºC, respectively. This downfield shift may be due to the predominance of tetrahedral coordination geometry for the tin centres at the higher temperature. The five membered ring in compounds **12**-**24** and **27**-**31** are more flexible than in **25** and **26** and this increased flexibility may promote Sn-N dissociation, resulting in tetracoordinate tin species and a downfield shift of the ^{119}Sn NMR resonance.

1.3.1.4 Diorganotin dihalides containing *C,N*-chelating ligands:

R' = H, R = Me, X = Cl **33**, Br **34**
R' = H, R = Ph, X = Cl **35**, Br **36**
R' = H, R = *n*-Bu, X = Cl **37**, F **38**
R' = H, R = *t*-Bu, X = Cl **39**
R" = Me, R = Me, X = Br **40**

X = F **41**, Cl **42**, Br **43**, I **44**
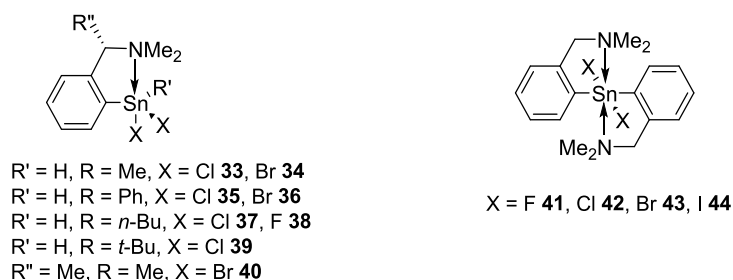
Figure 9: Diorganotin dihalides.

1.3.1.4a Synthesis:

Diorganotin(IV) dihalides **33**, **35** and **37** are compounds of interest in this thesis as they can be used directly or after modification to dihydrides as potential monomers. van Koten *et al.*[59] synthesized compounds **33** and **35** by reacting [2-(Me$_2$NCH$_2$)C$_6$H$_4$]$_4$Cu$_4$ with MeSnCl$_3$ and PhSnCl$_3$ respectively in C$_6$H$_6$ at room temperature. Rippstein *et al.*[48] prepared **35** from the reaction of [2-(Me$_2$NCH$_2$)C$_6$H$_4$]Li with PhSnCl$_3$ in Et$_2$O and purified by toluene extraction. Novák *et al.*[29a] reacted the [2-(Me$_2$NCH$_2$)C$_6$H$_4$]Li salt with PhSnCl$_3$ in C$_6$H$_6$ to prepare **35**. Varga *et al.*[51] synthesized compound **37** by reacting [2-(Me$_2$NCH$_2$)C$_6$H$_4$]Li with *n*-BuSnCl$_3$ in C$_6$H$_6$ and purified the product by extraction with hot petroleum ether. Compound **38** was obtained by reacting compound **37** with KF in MeOH at room temperature. Compounds **42** and **44** were also synthesized by reacting [2-(Me$_2$NCH$_2$)C$_6$H$_4$]Li with SnX$_4$ (X = Cl, I) in a 2:1 ratio.

1.3.1.4b Structural studies:

In compounds **35** and **37** the distance between Sn-N is 2.444(5) Å and 2.458(5) Å respectively. These hypercoordinated molecules have a 3c-4e *trans* configuration ((N(1)-Sn(1)-Cl(1) = 168.15º(12), 171.61º(15) respectively) that contribute to a strong intramolecular Sn-N interaction. The molecules possess a distorted TBP (*C,N*-)CSnCl$_2$ core (hypervalent 10-Sn-5).[29a,51] Compounds **35** and **37** share two common features in their molecular structures;[41] a strong coordination between the Sn and N atoms of the pendant Me$_2$NCH$_2$ arm that result in an increase in the coordination number at tin, and the SnC$_3$N ring folded along Sn(1)--CH$_2$ atoms.

The tin atoms in compounds **42** and **44** are bound to two L groups (L = 2-(Me$_2$NCH$_2$)C$_6$H$_4$)) and two *cis*-bonded halides (Cl, I) with the molecules possessing pseudo octahedral geometry. The C-Sn-C bond angle for **42** and **44** are 152.47º(7) and 157.97º(11) respectively, whereas the ideal bond angle for octahedral geometry is 180º. Similarly, the N-Sn-N

angles are 108.47º(4) for **42** and 103.65º(7) for **44** compared to the ideal 90º. Comparatively large

Sn-N distances of 2.6179(13) Å for **42**, and 2.537(2) Å and 2.648(2) Å for **44** were observed.

Table 3: ^{119}Sn chemical shifts and Sn-N distances of diorganotin halides.

Compounds	R"	R'	X	^{119}Sn Shift(δ) ppm	Sn-N distance (Å)
33	H	Me	Cl	-94.0[26, 59]	-
34	H	Me	Br	-141.4[26,59]	-
35	H	Ph	Cl	-167.6	2.444(5)[57]
36	H	Ph	F	-	-
37	H	*n*-Bu	Cl	-104.3,[29b] 103.0[51]	2.428(3)[64], 2.458[57]
38	H	*n*-Bu	F	-	2.494[51]
39	H	*t*-Bu	Cl	-	-
40	Me	Me	Br	-145.0[26,59]	-
41	L	L	F	-216.1	2.496(2), 2.597(1)[60]
42	L	L	Cl	-252.8	2.6179(13)[29a]
43	L	L	Br	-269.6[29b,59]	-
44	L	L	I	-347.4	2.537(2), 2.648(2)[29a]

The ^{119}Sn NMR chemical shift data of pentacoordinated diorganotin dihalides **33** (δ = -94.0

ppm), **34** (δ = -141.4 ppm), and the triorganotin halide **12a** (δ = -50.0 ppm) show an upfield shift

relative to their 4-coordinate analogues. Substitution of the Cl in **33** with Br in **34** produced a

downfield shift of about 50 ppm. A similar trend was observed for the diorganotin dihalide **37**

(^{119}Sn δ = -104.3 ppm) and triorganotin halide **20** (δ = -44.9 ppm).

1.3.1.5 Monoorganotin trihalides containing *C,N*-chelating ligands:
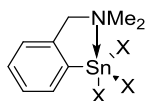
X = Cl **45**, Br **46**, I **47**

Figure 10: Monoorganotin halides.[61]

Compounds **45**-**47** were obtained in low yields from the reaction of a 1:1 ratio of LLi and

SnX$_4$ (L = [2-(Me$_2$NCH$_2$)C$_6$H$_4$]Li, X = Cl, Br, I). A strong intramolecular Sn-N interaction in the

hypervalent compounds **45**-**47** was observed from an up-field shift of the ^{119}Sn resonances (δ = -

227.4, -408 (broad), and -944.4 ppm)[61] compared to the trihalophenyl compounds, $PhSnX_3$ (δ = -61.3, -227.2 and -699.9 ppm).[62] The Lewis acidity of the tin atom decreases with the lower electronegativity of X which is evident from the $^3J_{119Sn-1H}$ coupling constant for **45-47** (132.0, 128.6 and 126.2 Hz). A distorted TBP geometry is observed in all compounds and the bond distance of the Sn-N dative interaction in **45-47** is 2.380(2), 2.402(3) and 2.436(4) Å, respectively. A slight increase in the Sn-N bond distance going from **45** to **47** is related to the relative electronegativities and sizes of X.[61]

Data obtained for organotin compounds containing *C,N*-chelating ligands in non-coordinating apolar solvents indicate the existence of intramolecular Sn-N donor-acceptor interactions of variable strength. It increases with the decreasing number of organic substituents at the tin center.[27b] The ^{119}Sn NMR data of **45-47** show the influence of additional coordination on chemical shift, which is relatively minor in the case of tetraorganotin compounds, but results in large upfield shifts for triorganotin halides and diorganotin dihalides.[26]

1.3.2 Organotin hydrides containing *C,N*-chelating ligands:

The preparation of organotin hydrides was first reported by Kraus and Geer in 1922 by reacting Me_3SnNa with HCl in liquid ammonia.[63] A revolution in the synthesis of tin hydrides occured in 1947 when Finholt *et al*. reported a convenient method to reduce organotin chlorides with lithium aluminum hydride ($LiAlH_4$).[64] Afterwards, this method was successfully used for the synthesis of R_nSnH_{4-n}. The most frequently used methods for the preparation of organotin hydrides involve reducing agents such as silicon, lithium and boron hydrides. Some other methods such as thermal decomposition of organotin formates, hydrolysis of stannyl metallic compounds and ligand exchange between organotin compounds are less commonly used.[65]

$$R_3SnX \; + \; MH \longrightarrow R_3SnH \; + \; MX$$

$$R_3SnOCHO \longrightarrow R_3SnH \; + \; CO_2$$

$$R_2SnHLi \; + \; R'X \longrightarrow R'R_2SnH \; + \; LiX$$

$$R_3SnH \; + \; R'_3SnX \longrightarrow R_3SnX \; + \; R'_3SnH$$
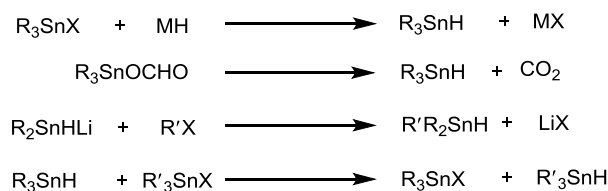
Scheme 7: The preparation of organotin hydrides.[65]

Organotin hydrides with chelating ligands containing donor atoms such as N, P or O atom have received increasing attention in recent years due to their unusual structural properties as well as their industrial and pharmacological applications.[74,75] The donor-acceptor interaction between Sn and the donor atom of the ligand is the most interesting aspect of these molecules. Surprisingly, there are few examples of hydrides having Sn-N intramolecular interactions reported in literature.[66-72] These donor-acceptor interactions have been confirmed by various techniques such as X-ray crystallogaphy[76] and NMR spectroscopy.[66-72, 76]

1.3.2.1 Triorganotin hydrides containing *C,N*-chelating ligands:

R' = R" = Ph **48**, *n*-Bu **49**, *t*-Bu **50**, Me **51**

R = Ph **52**, Men **53**

Men = Menthyl

54

R = Ph **55**, Men **56**
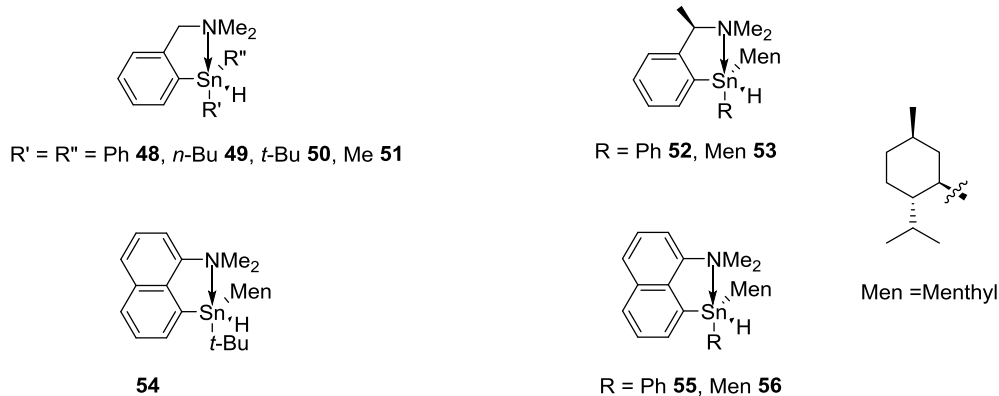
Figure 11: Triorganotin hydrides.

1.3.2.1a Synthesis:

Turek *et al.*[66] prepared triorganotin hydrides **48-50** by reacting [2-(Me$_2$NCH$_2$)C$_6$H$_4$]R$_2$SnX (R = Ph, *n*-Bu, *t*-Bu and X = Cl) with K(BEt$_3$)H in a 1:1 ratio in THF at -20º C and stirring at room temperature for 5 days. These hydrides show typical ^{1}H NMR (C$_6$D$_6$) hydride resonances at 6.98, 5.83 and 6.01 ppm for **48**, **49** and **50** respectively. Compound **51** was prepared from the reaction

of [2-[(Me$_2$NCH$_2$)C$_6$H$_4$]SnMe$_2$Br or the analogous chloride with LiAlH$_4$ in THF.[67] Compound **52** was prepared by treating the 2-[(Me$_2$NCHMe)C$_6$H$_4$-] ligand containing triorganotin monohalides with NaBH$_4$ in EtOH, as LiAlH$_4$ was found to decompose the halide. Hydrides **53**-**56** were also obtained by treating the corresponding chlorides with LiAlH$_4$.[68]

1.3.2.1b Structural studies:

For triorganotin hydrides the ^{1}H NMR resonance for the proton directly bonded to the tin atom varies between 4.5-7.5 ppm.[65] The presence of a $^{117/119}$Sn couplings is a characteristic feature in ^{1}H NMR spectra of these compounds. The magnitude of this coupling is dependent on substituents bonded to tin. Tin hydrides which contain bulky alkyl groups have relatively smaller values of $^1J_{117/119Sn\text{-}1H}$ whereas tin hydrides containing aromatic rings cause an increase in $^1J_{117/119Sn\text{-}1H}$ coupling. The characteristic changes of the NMR chemical shifts for Sn and N and the values of coupling constants of $J_{117/119Sn\text{-}13C}$ and $J_{117/119Sn\text{-}15N}$ support the existence of substantive donor-acceptor interactions. Examples of tin hydrides having a donor-acceptor interaction between Sn and N include the triorganotin hydrides with 2-(*N,N*-dimethylaminomethyl)phenyl and 2-(4-isopropyl-2-oxazolinyl)-5-phenyl substituents[77,78] and diorganotin dihydrides containing 2-(4-isopropyl-2-oxazolinyl)-5-phenyl as chelating ligands and phenyl, methyl, *n*-butyl and *t*-butyl substituents (Figure 13).[66,69]

For hypercoordinated tin hydrides **60**-**62** as shown in Figure 13, the Sn-N interaction is evident from the increase in the value of coupling constants. A comparison of $^1J_{117/119Sn\text{-}1H}$ coupling between tetravalent compound **57**, **58**, and **59** and pentavalent **60**, **61** and **62** show the difference in the nature of substituents bound to tin (Table 4).[65,70]

δ = 7.02 ppm
$J(^1\text{H}-^{119}\text{Sn})$ = 1936 Hz

4.66 ppm
1744 Hz

4.84 ppm
1609 Hz

57

58

59
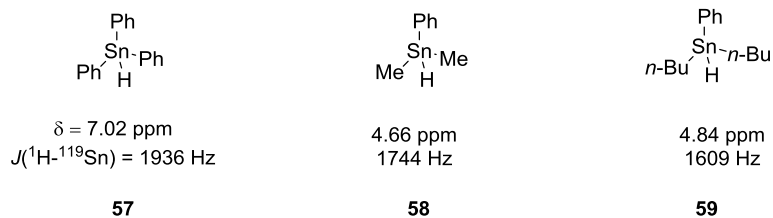
Figure 12: Structure of triorganotin hydrides without chelating ligand.

$R^1 = R^2 = $ Ph **60**
$R^1 = R^2 = $ Me **61**
$R^1 = R^2 = $ n-Bu **62**
$R^1 = $ Ph, $R^2 = $ t-Bu **63**
$R^1 = $ Me, $R^2 = $ t-Bu **64**
$R^1 = $ Ph, $R^2 = $ Me **65**
$R^1 = $ Me, $R^2 = $ n-Bu **66**

R = Me **67**
R = Ph **68**
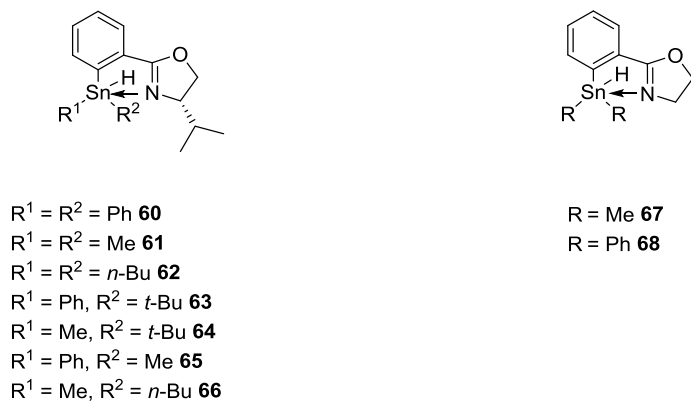
Figure 13: Structures of hydrides containing chelating ligands.

Hydrides **65-72** were synthesized by Cmoch *et al.*[69, 71,72] by reacting the monohalides (Br, I) with NaBH$_4$ in EtOH at 0-25 ℃. Unfortunately, X-ray structures of these low melting hydrides have not yet been reported. There is only one example of a triorganotin hydride, **54**, which has been structurally determined by X-ray crystallography. The structure of **54** revealed the presence of both epimers in 1:1 ratio. The coordination geometry of **54** is a monocapped tetrahedron having only a weak Sn-N interaction; evident from the very long Sn-N distances of 2.931(3) and 2.885(3) Å in this molecule.

Table 4: ^1H and ^{119}Sn NMR data of hypercoordinate triorganotin hydrides.

Compound	δ ^1H(ppm)Sn-H	δ ^{119}Sn or δ ^{117}Sn (ppm)	$J_{117/119Sn-1H}$(Hz)
48	6.98	-180.9	2128[66]
49	5.83	-113.2	1627[66]
50	6.01	-90.0	1638[66]
51	5.64	-30.2	1696/1777[67]
52	6.46	-136.7, -166.8	1904/1920[67]
53	5.99	-141.3	1671[68]
54	6.37, 6.20	-91.3, -94.8	1723/1803, 1717/1797[76]
55	6.71, 6.91	-140.0, -115	1980, 1955[68]
56	6.31	-104.6	1729[68]
60	7.62	-158.5	2167/2070[70]
61	6.20	-129.0	1753[69]
62	6.42	-92.0	1503[69]
63	7.15, 7.35	-102.0, 118.9	1480/1549, 1832/1908[71]
64	6.35, 6.46	-60.0, -91.0	1380/1444, 1692/1770[71]
65	6.66, 6.67	-160.0, -159.2	1933/2022, 1897/1985[72]
66	6.14, 6.14	-112.1, -117.7	1615/1688, 1548/1615[72]
67	6.09	-128.8	1597/1971[72]
68	7.41	-180.6	1850/1937[72]

1.3.2.2 Diorganotin dihydrides containing *C,N*-chelating ligands:
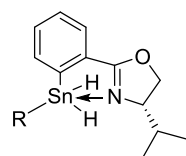
R = Me **69**, Ph **70**

Figure 14: Hypercoordinated diorganotin dihydrides.

Dihydrides **69** and **70** (Figure 14) were prepared by Matkowska *et al.*[72] from the reaction

of dihalides (I, Br) with NaBH$_4$ in EtOH at 0-25 ºC. These compounds have two distinct hydrogen

atoms directly bonded to tin. The comparison of $^1J_{117/119Sn-1H}$ coupling constants of coordinated hydrides for **69** and **70** and noncoordinated analogues $PhMeSnH_2$ and Ph_2SnH_2 provides evidence that Sn-N interaction/coordination can cause both a strong decrease and increase of $^1J_{117/119Sn-1H}$ coupling constant for **69** and negligible/strong coupling increase for **70** (Table 5). The effect of temperature $^1J_{117/119Sn-1H}$ on coupling constants for these species were also investigated. It was concluded that the variation in the values of coupling constants at different temperatures may be due to the axial/equatorial positions of hydrogen atoms; one is axial and one is equatorial in **69** and both are equatorial in **70**. $^{117/119}$Sn satellites in the ^{1}H NMR spectra are doubled due to the presence of intramolecular Sn–N coordination.

Table 5: $^1J_{117/119Sn-1H}$ coupling constants of coordinated and non-coordinated hydrides.

Compound	^{1}H (ppm) Sn-H	$J_{117/119Sn-H}$ (Hz)	Unsubstituted analogue	$J_{117/119Sn-H}$ (Hz)
69	6.17-6.04	1615/1703, 1888/1987	$PhMeSnH_2$	1771/1835[73]
70	6.78-6.64	1853/1940, 2059/2155	Ph_2SnH_2	1842/1928[73]

1.3.3 Si, Ge and Pb compounds containing a *C,N*-chelating ligand:

Hypervalent silicon compounds (Figure 15) have been known since the beginning of 19th century.[77] Boyer *et al*.[78] prepared and characterized a number of these compounds, including **72**, **81**, **94** and **96** which were structurally studied by both X-ray crystallography and solution NMR spectroscopy. The geometry of these hypercoordinated silicon compounds was exclusively distorted TBP having the nitrogen atom at an axial position. Five- and six-membered chelate rings were formed in case of **81**, **94** and **97** respectively. Here the five-membered rings remain planar whereas the six-membered ring, such as **97**, folds about the Si-CH$_2$ group axis. The naphthyl group in **81** and the phenyl group in **94** and **97** occupy the second axial position of the TBP complexes.

Equatorial sites of TBP geometry were occupied by two hydrogen atoms in **81** and **94**, whereas one hydrogen atom and one methyl group are found in **97**. A comparison of the geometries of **98b**-**e** (Figure 16) by X-ray diffraction revealed intramolecular coordination between the donor nitrogen atom and silicon center, resulting in five coordinate geometries.

R' = H, R = Me **71**
R' = H, R = F **72**
R' = Me, R = Me **73**
R' = Me, R = F **74**

R' = H, R = Ph **75**
R' = Me, R = Ph **76**
R' = H, R = Np **77**
R' = Me, R = Np **78**

R' = H, R = Ph **79**
R' = Me, R = Ph **80**
R' = H, R = Np **81**
R' = Me, R = Np **82**

R = Me, X = F **83**
R = Me, X = Cl **84**
R = Et, X = Cl **85**

R' = Me, R = H, X = F **86**
R' = Me, R = H, X = Cl **87**
R' = Me, R = H, X = Br **88**
R' = Me, R = Np, X = H **89**
R' = Me, R = Np, X = F **90**
R' = Me, R = Np, X = Cl **91**

92

93

94

95

96

97
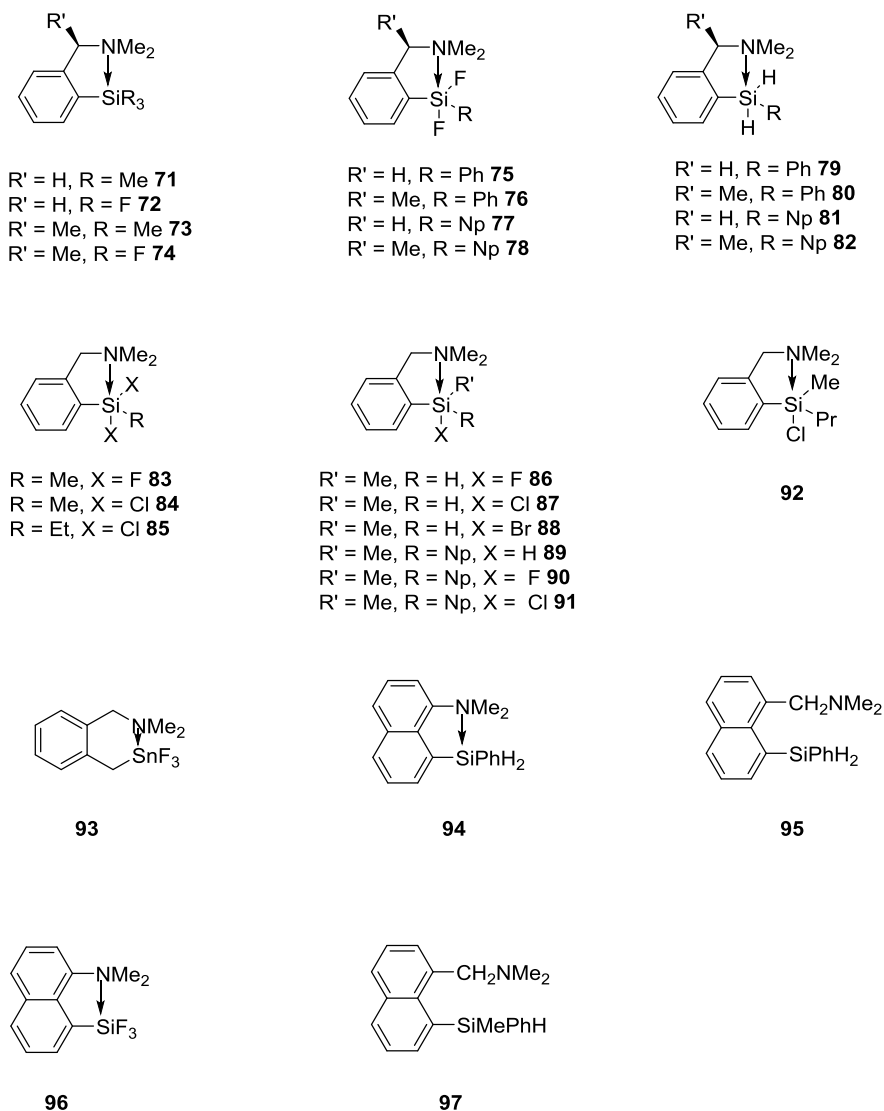
Figure 15: Si compounds containing a *C,N*-chelating ligand.

In most of these hypervalent compounds the axial positions are occupied by the donor atom with the halogen or hydride located in a *trans* configuration. The distance between donor and acceptor is significantly longer than a normal single bond distance between these two atoms. In

the case of **98e**, the distance between the datively bonded Si and N atoms is 2.03 Å, whereas length

of covalent bond between these atoms is 1.77 Å.

X =
Me$_3$ **98a**
Me$_2$Cl **98b**
MeCl$_2$ **98c**
Cl$_3$ **98d**
F$_3$ **98e**
ClF$_2$ **98f**
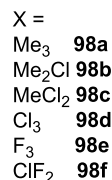
Figure 16: Organosilicon compounds containing a *C,N*-chelating ligand.[79]

Table 6: ^{29}Si chemical shift data for five- vs four-coordinate silanes

Compound	δ(^{29}Si) ppm	Compound	δ(^{29}Si) ppm	Δδ(^{29}Si) ppm
71	-4.8	SiMe$_3$Ph[78]	-4.1	-0.7
72	-102.2	SiF$_3$Ph[78]	-72.8	-29.4
81	-47.2	SiH$_2$Ph(C$_{10}$H$_7$)[78]	-35.6	-11.6
82	-52.8	SiH$_2$Ph(C$_{10}$H$_7$)	-35.6	-17.2
83	-36.1	SiMeF$_2$Ph[78]	-8.5	-44.6
93	-100.4	SiF$_3$(CH$_2$Ph)[78]	-64.0	-36.4
94	-44.1	SiH$_2$Ph(C$_{10}$H$_7$)	-35.6	-8.5
95	-55.5	SiH$_2$Ph(C$_{10}$H$_7$)	-35.6	-19.9
97	-25.8	SiHMePh(C$_{10}$H$_7$)[78]	-19.8	-6.0

^{29}Si NMR spectroscopy is a useful technique to confirm the coordination between the donor

atom of the ligand and the silicon atom in solution which is evident by a substantial upfield shift

of ^{29}Si resonance. Table 6 lists a comparison of ^{29}Si chemical shift of the coordinated silanes and

their analogues. ^{19}F NMR resonances of Si-F groups and the ^{1}H NMR chemical shift of groups

directly bound to the donor atom of the ligand were also useful in probing these interactions. ^{19}F

NMR spectra of compounds **72** and **93** (collected at 30 °C) as well as **96** (collected at 80 °C) showed

sharp resonance at δ = -142.5, -138.0 and -140.7 ppm respectively. On lowering temperature, these

compounds showed a downfield triplet and up-field doublet which indicated that the F atoms

occupy one axial and two equatorial positions. X-ray crystal structural analysis of **72** also

confirmed its TBP geometry.[80]
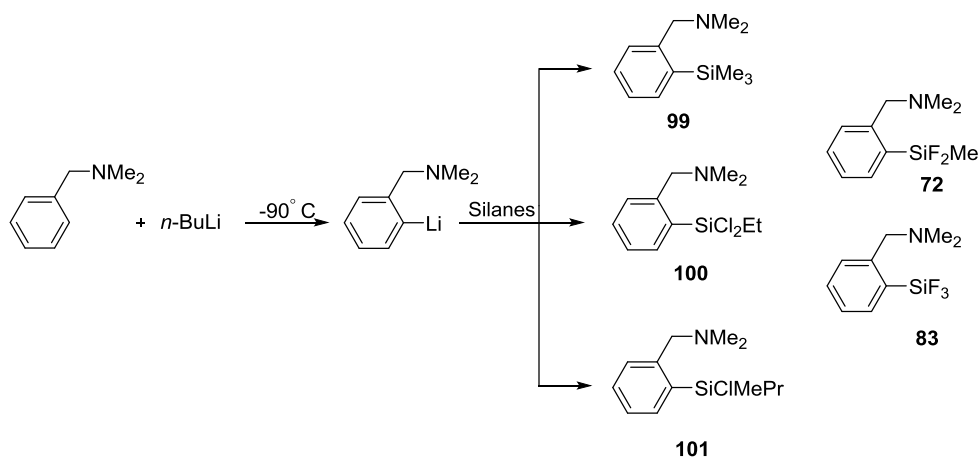
Scheme 8: Synthesis of organosilanes containing *C,N*-chelating ligands.[82]

Kelbe *et al*. synthesized compounds **99**-**101** along with the known compounds **72** and **83** according to Scheme 8. The ^{19}F NMR spectra of fluorosilanes **72** and **83** were obtained at low temperature in non-polar media. Compound **72** showed two peaks of equal intensity (F_a δ = -111 ppm; F_e δ = -154 ppm), while the ^{19}F NMR spectrum of **83** displayed a triplet and a doublet in a 1:2 relative intensity (F_a δ = -128 ppm; F_e δ = -148 ppm) in good agreement with a TBP geometry (having two equatorial and an apical F atoms).[81]
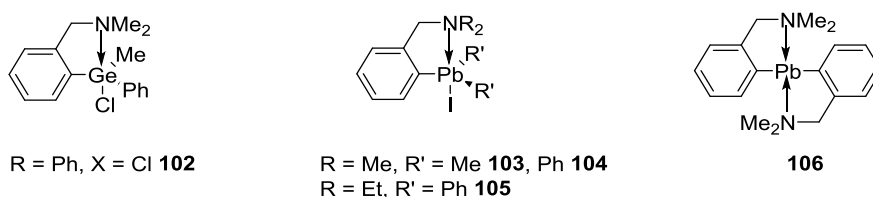
Figure 17: Hypercoordinate organogermanium and organolead compounds.[81,84,85]

Krause and Reissaus[77] reported the synthesis of the first diaryl lead compounds as monomeric species in 1922, but this work could not be reproduced despite attempts by several groups.[87-90] Compound **106** was synthesized by De Wit *et al*.[84] by reacting $PbCl_2$ with two equivalents of [2-(Me_2NCH_2)C_6H_4]Li in THF at -50 °C. In the ^{1}H NMR spectrum of **106**, the $^3J_{207Pb-1H}$ and $^4J_{207Pb-1H}$ coupling constants for Ar-H and benzylic-CH_2, respectively were detected.

The Pb-N interaction is suggested by the presence of a coupling ($^2J_{207Pb-13C} = 28$ Hz) between lead and the carbon atoms of the -N(CH$_3$)$_2$ group.
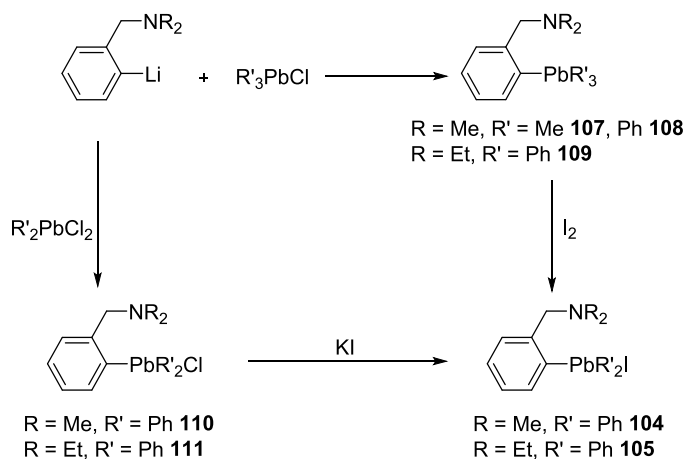
Scheme 9: Synthesis of organolead compounds.[84]

Compounds **104-105** and **107-111** were synthesized by Christea *et al.*[85] by treating [2-(R$_2$NCH$_2$)C$_6$H$_4$]Li with tri- and diorganolead chlorides followed by reaction with I$_2$ and KI respectively. These compounds were characterized by NMR (^{1}H, ^{13}C) spectroscopy, but unfortunately no ^{207}Pb NMR data is available. A crystallographic study of **108** and **110** revealed TBP geometry around the Pb atom and the presence of a Pb-N intramolecular interaction. The distance between Pb and N atoms is 3.051º(9) for **108** and 2.636º(8), 2.646º(9) Å for two distinct molecules of **110** in the unit cell. The bond angle between N-Pb-C for **108** and Cl-Pb-N (*10-Pb-5*) for **110** is 169.1º(3) and 166.11º(19), 167.2º(2) respectively. In the case of compound **108**, the axial positions are occupied by N and the C atom of one of the phenyl groups while equatorial positions were occupied by carbons of the two other phenyl groups and pendant ligand. The Pb-N interaction is much stronger in the case of compound **110** having a Cl atom *trans* to N with Pb as the central atom. In both compounds the C$_3$PbN ring is not planar, thus creating planar chirality. The cleavage of the bond between Pb and phenyl carbon was preferred over cleavage of the Pb and pendant group C, which provides additional evidence to support the intramolecular interaction

between Pb and N. These results suggest that in general, the geometry of pentacoordinated compounds containing later Group 14 elements (Si, Ge, Sn and Pb) is almost exclusively TBP.

1.4 Organotin compounds containing *C,O*-chelating ligands:

Hypervalent compounds of tin are of general interest because of their useful biological activity, reactivity and important industrial and agricultural applications.[91-93] Most compounds having a Sn-O intramolecular interaction are those containing chelating ligands called "Pincer" ligands. There are several publications which report compounds containing *C,O*-chelating ligands. A variety of tin complexes with *C,O*-ligands are shown in Figure 18, 19.
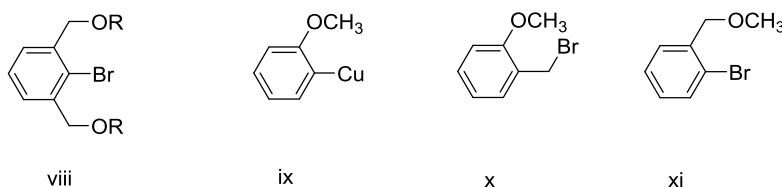
Figure 18: *C,O*-chelating ligands.

R = Me, M = SnPh₃ **119**
R = Me, M = SnPh₂Cl **120**
R = Me, M = SnPhCl₂ **121**
R = Me, M = SnCl₃ **122**
R = Et, M = SnPh₃ **123**
R = Et, M = SnPh₂Cl **124**
R = Et, M = SnPhCl₂ **125**
R = *i*-Pr, M = SnPh₃ **126**
R = *i*-Pr, M = SnPh₂Cl **127**
R = *i*-Pr, M = SnPhCl₂ **128**
R = *i*-Pr, M = SnCl₃ **129**
R = *t*-Bu, M = SnPh₃ **130**
R = *t*-Bu, M = SnPh₂Cl **131**
R = *t*-Bu, M = SnPhCl₂ **132**

R = R' = R" = Ph **112**
R = R' = R" = Me **113**
R = Br , R' = R" = Me **114**

R = R' = R" = Me **115**
R = R = R''' = Ph **116**
R = R' = Ph, R" = Cl **117**
R = Ph, R' = R" = Cl **118**
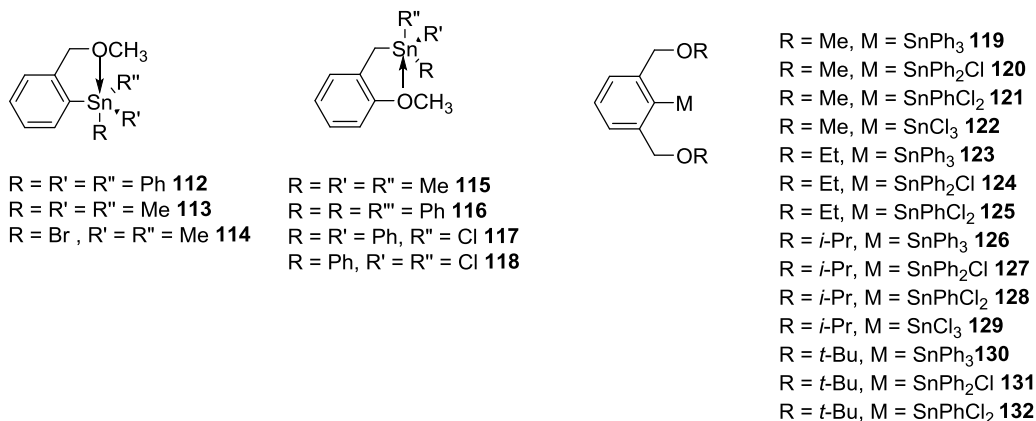
Figure 19: Hypercoordinate tin compounds containing *C,O*-chelating ligands.

1.4.1 Synthesis:

In 1950, Gilman *et al.*[84] reported the synthesis of **112** by reacting [*o*-MeOCH₂C₆H₄]MgBr with Ph₃SnCl which was characterized only by melting point. Compound **113** reported by Reich

et al.[95] was prepared by treating [2-(Me$_2$OCH$_2$)C$_6$H$_4$]Li with Me$_3$SnCl in THF. Compound **114** was synthesized by reacting [2-(Me$_2$OCH$_2$)C$_6$H$_4$]Cu with Me$_2$SnBr$_2$ while **116**-**118** were reported by Pannell *et al.*[96] The synthesis of **115**[96] and **116** was carried out by reacting the *o*-MeOC$_6$H$_4$CH$_2$MgCl Grignard reagent and Me$_3$SnCl or Ph$_3$SnCl respectively, while **117** and **118** were obtained by successive replacement of the phenyl groups in **116** and **117** with chloride by treatment with a solution of HCl/Et$_2$O in C$_6$H$_6$. Compounds **119**-**132** were reported by Jambor *et al.*[92,98] and were obtained by reacting the lithiated ligands with the respective halides at low temperature in hexane.

1.4.2 Structural studies:

The X-ray crystallographic data for compounds **116**-**118** were also reported. It was found that there was a distinctive decrease in Sn-O distance with replacement of the phenyl groups bound to tin with Cl. The substitution of one of the phenyl groups of **116** with Cl reduces the Sn-O bond distance from 3.07 to 2.77 Å. This is likely due to the increase in the Lewis acidity of the central tin atom and the transition from tetrahedral to TBP geometry. Compound **118** exhibited intermolecular interactions *via* Sn-Cl resulting in dimer formation and had pseudo-Oh geometry. A comparison of chemical shift values by solid state and solution ^{119}Sn NMR spectroscopy indicated only minor difference.

Table 7: [119]Sn chemical shifts and Sn-O distances of tin compounds with *C,O*-chelating ligands.

Compounds	δ([119]Sn) ppm	Sn-O distance (Å)
113	-38.2[a]	-
115	2.9	-
116	-144.8	3.07
117	-41.4	2.767
118	-32.7	2.898
119	-163.3	2.908(1), 2.966(1)
120	-144.4	-
121	-208.8	2.619(1), 2.655(1)
122	-270.5	-
123	-159.0	-
124	-140.0	2.454(1), 3.473(1)
125	-197.0	2.447(1), 2.864(1)
126	-153.8	-
127	-136.1	-
128	-177.4	2.475(1), 2.985(2)
129	-238.8	-
130	-154.0	-
131	-121.7	-
132	-148.5	2.775(2), 2.882(2)

[a] Solvent = THF

The [119]Sn chemical shifts and Sn-O bond distances of organotin compounds containing *C,O*-chelating ligands are listed in Table 7. Interestingly, one Sn-O distance in **124** was 2.454(1) Å, while the second Sn-O distance is 3.473(1) Å, indicating that the second interaction is out of the tin coordination sphere.[98] There are only a few literature examples of tetraorganostannanes having mesogenic substituents on the tin which can expand their valence shell by additional coordination or intramolecular interactions between the electronegative O donor atom and tin atom.

133 **134** **135** **136**
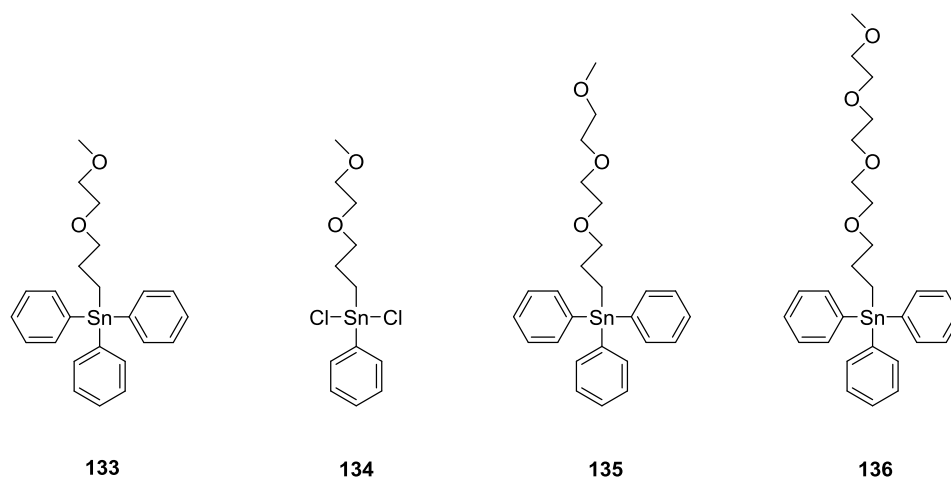
Figure 20: Organotin compounds with an oxa-alkyl side chain.[99]

Compounds **133**-**136** were prepared by reacting Ph₃SnH with the respective oxa-alkenes in the presence of AIBN (Figure 20). Compounds **137**-**150** were synthesized according to the synthetic methodology shown in Scheme 10. It involves the hydrostannation of (4-biphenyloxy)-1-alkenes (**137**-**140**) to produce **141**-**145**. Compounds **141**-**145** were treated with molecular halogens (Br₂ and I₂) to produce the tin dihalides **146**-**150**. The ^{119}Sn chemical shifts and Sn-O distance of organotin compounds **133**-**150** are listed in Table 8.
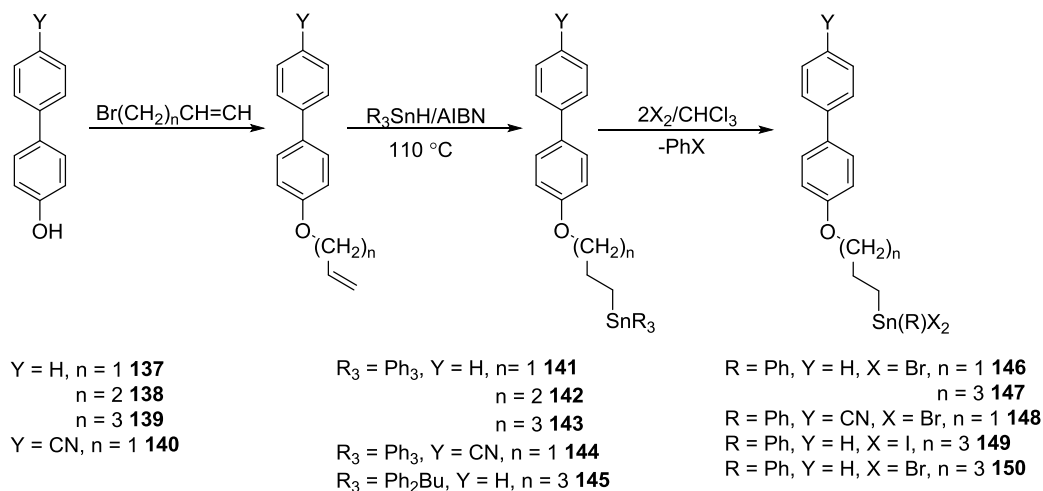
Scheme 10: Synthesis of tin complexes with phenyloxy alkyl side chains.[43]

34

Table 8: [119]Sn chemical shifts and Sn-O distances of tin compounds with *C,O-* chelating ligands.

Compounds	δ([119]Sn) ppm	Sn-O distance (Å)
133[99]	−100.3	-
134[99]	−100.3	-
135[99]	−100.4	-
136[99]	−73.6	2.553(2), 2.540(2)
141[43]	-100.1	-
142[43]	-101.2	-
143[43]	-100.4	-
144[43]	-100.4	-
145[43]	-72.3	-
146[43]	-53.3	2.734(4)
147[43]	3.5	-
148[43]	-47.6	2.918(7)
149[43]	-157.2	-
150[43]	88.6	-

The crystal structure of **134** revealed a hexacoordinated tin atom bonded to two atoms of each of C, Cl and O (Figure 21). The two O and Cl atoms are *cis* to each other and the C atoms are found to occupy axial positions. The Sn-O distances in **134** are 2.553(2) and 2.540(2) Å respectively and are larger than the covalent radii of Sn and O (2.1 Å), but shorter than sum of their van der Waal's radii (3.7 Å).
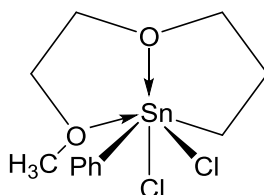
Figure 21: Structure of **134**.[99]

X-ray structure data for compounds **142** and **144** reveal tetrahedral geometries at tin centers having bond angles between 105-113°. Compound **146** exists in a dimeric form and two molecules are linked through Br(1)----Sn(1') and an octahedral sphere was completed by chelation of the ether O with a Sn(1)-O(1) distance 2.734(4) Å. Generally, the Sn-O distance is longer (2.540 - 2.667 Å)[99,100] for diorganotin species with CN = 6 than those with CN = 5 (2.382 – 2.448 Å)[101].

The Sn-O distance is also affected by the presence of an additional electronegative atom which increases the Lewis acidity of tin. In the case of **148**, the Sn-O distance is transoid to Sn-Br bond with an angle of O(1)-Sn(1)-Br(1) = 169.0º(1) with the molecule assuming a TBP structure.[43]

Compounds **151-154** were synthesized by Takeuchi *et al*. using Scheme 11.[102] The line width for germanium compounds were also determined and a broadening of signal was always accompanied by hypervalency. The ^{73}Ge shift for compounds **151**-**153** are -85.0, -85.0 and -84.0 ppm (Ph$_3$GeH δ = -57.0 ppm) with the line widths of 350 Hz. An X-ray crystal structure determination revealed that Ge-O distances for **153** were 3.2773(3), 3.214(3) and 3.703(3) Å. Both crystal structure and NMR data gave evidence for a dative interaction between Ge and O, although it is weaker than between Ge and N.
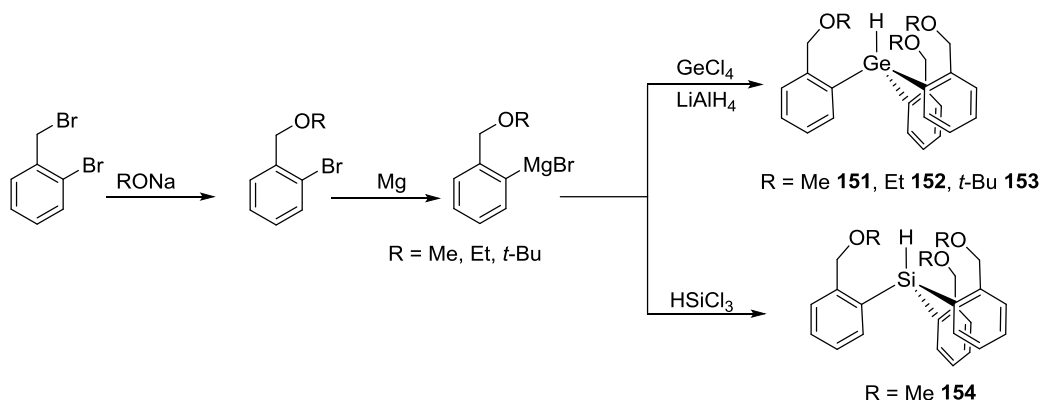
Scheme 11: Synthesis of *C,O*-chelating ligand and the corresponding triarylgermanes and silane.

1.5 *C,S*-chelating ligands containing compounds of Group 14:
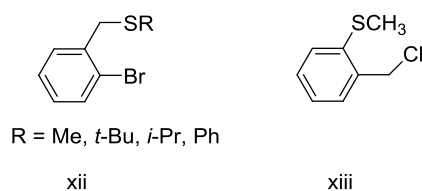
Figure 22: *C,S*-chelating ligands.

C,S-chelating ligands commonly used to hypercoordinate a Group 14 element are listed in Figure 22. There are only a few reports of hypercoordinated Sn-S compounds. Ligands of type xii (R = *n*- Pr, Ph) were synthesized using the methods reported in the literature.[103-105] It is well established that Group 14 elements have the ability to expand their coordination number through dative interactions of Lewis bases of functional groups containing N, P, S and O donor atom).[95] This strategy was used to produce a variety of hypercoordinated compounds of Sn.

R = R' = R" = Ph **155**
R = Cl, R' = R" = Ph **156**   E = Si **158**, Ge **159**, Sn **155**, Pb **160**   **161**
R = R' = Cl, R" = Ph **157**
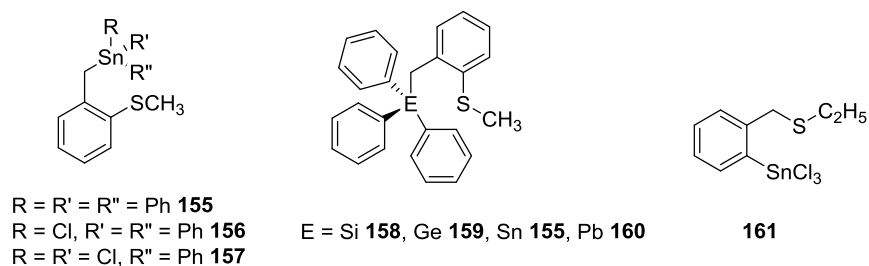
Figure 23: Group 14 compounds containing *C,S*-chelating ligands.

Compound **155** was successfully prepared by using methods shown in Scheme 12. An *in-situ* synthesis of the respective Grignard reagent in the presence of the halide afforded the desired product in a good yield.[96] Two phenyl groups were subsequently substituted with Cl by reacting **155** and **156** with of HCl/Et$_2$O in C$_6$H$_6$ to produce the dihalides **156**-**157** respectively. Compounds **155** and **158**-**160** were synthesized by reacting Group 14 halides with Li metal followed by reaction with *o*-(SCH$_3$C$_6$H$_4$)CH$_2$Cl at low temperature (Scheme 12).[106]

E = Si, Ge, Sn, Pb
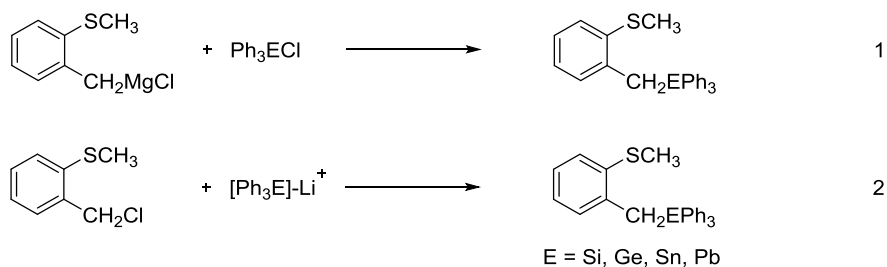
Scheme 12: Group 14 compounds containing a *C,S*-chelating ligand.

The reaction of thiols and NaH followed by the reaction with 1-bromo-2-bromomethylbenzene produced the corresponding sulfides **162**-**164** in good yields (Scheme 13). Lithiation of **162-164** with *n*-BuLi in Et$_2$O at 0 ℃ followed by treatment with SiHCl$_3$ and the subsequent reduction with LiAlH$_4$ afforded silicon dihydrides **165**-**167**. Compounds **170-172** were reported by Berlekamp and synthesized according to Scheme 14.[107] Compounds **173-174** were synthesized by Takeuchi *et al.* using Scheme 15.[102]
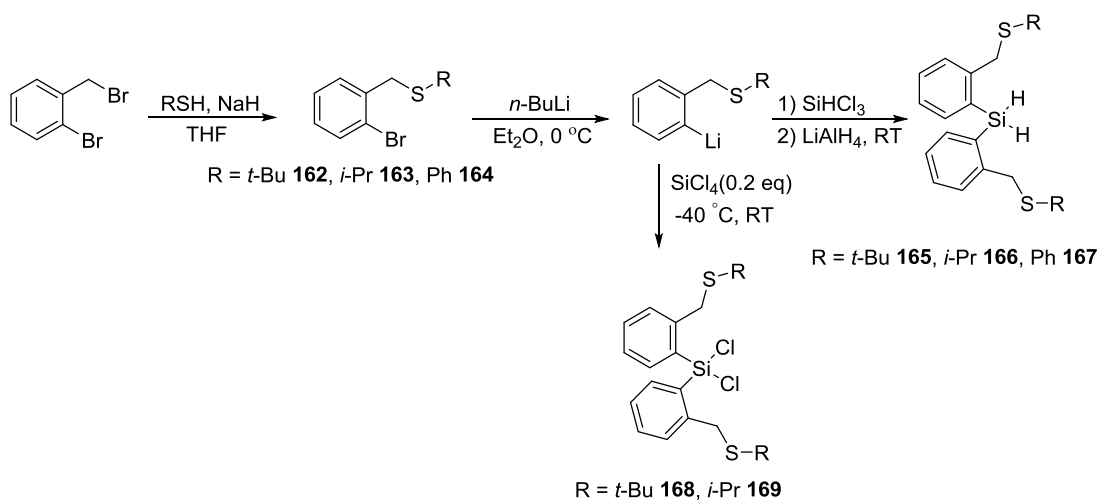
Scheme 13: Synthesis of organosilicon compounds containing a *C,S*-chelating ligand.

^{119}Sn NMR data of compound **155** showed an upfield shift of 70.5 ppm relative to the non-chelating, structurally similar analog, suggestive of substantial S-Sn interaction.[107] The ^{29}Si NMR spectra of dihydrosilanes **165–167** showed small upfield shifts compared to the closely related unsubstituted analogue Ph$_2$SiH$_2$ (δ [29]Si = −34.5 ppm).[108] These small $\Delta\delta$ values suggest that there is only a weak to no Si-S interaction present.
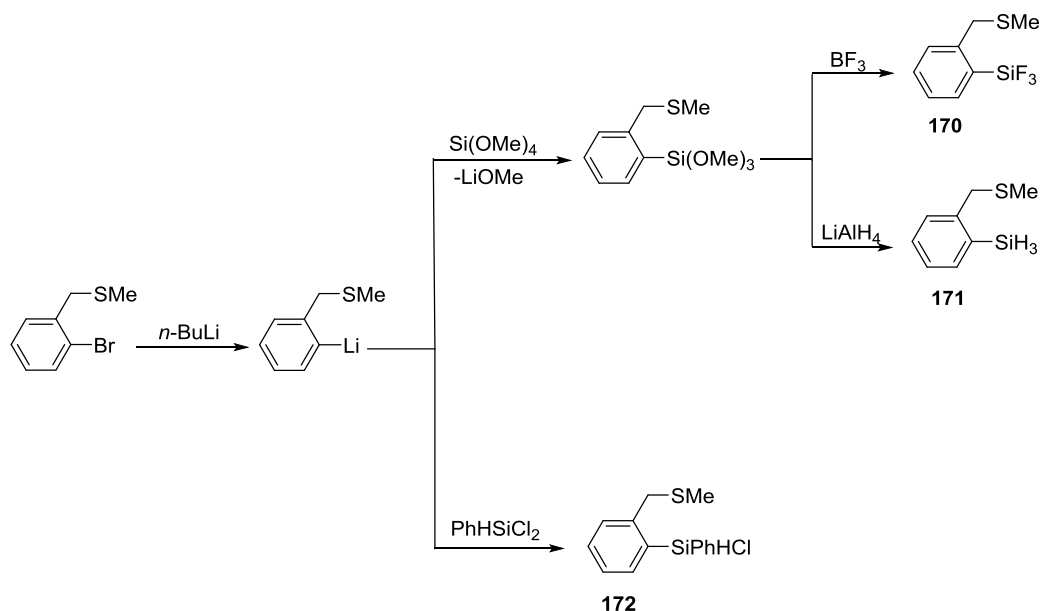
Scheme 14: Synthesis of SiF$_3$, SiH$_3$ and SiPhHCl silanes containing a *C,S*-chelating ligand.

The ^{29}Si NMR data of S-donor containing compounds (**158**, **165**-**174**) give no indication of donor complexation. The observed ^{29}Si resonance for **170** is nearly identical to that of tetrahedral PhSiF$_3$. It was also reported that the tendency of S-donor to form an adduct with SiF$_3$ is negligible compared to N- and O-donors. These results are in accordance with recently published theoretical investigations concerning the adduct formation behaviour of SiF$_4$.[109] Slight upfield shifts of ^{29}Si resonances of 4.9 ppm and 7.0 ppm for compounds **171** and **172** were observed compared to their unsubstituted analogues, again suggestive of only weak Si-S interactions (Table 9).

Table 9: ^{29}Si/^{119}Sn/^{207}Pb chemical shifts and Si/Sn/Pb-S distances of compounds with *C,S*-chelating ligands.

Compound	^{29}Si/^{119}Sn/^{207}Pb δ (ppm)	S-Si/Sn/Pb distance (Å)	Unsubstituted analogue	^{29}Si/^{119}Sn/^{207}Pb δ (ppm)	Δδ ^{29}Si/^{119}Sn/^{20}^{7}Pb (ppm)
155	-115.5	3.699	Ph$_3$SnCl	-45.0	70.5
156	-46.3	3.062	Ph$_2$SnCl$_2$	-32.0	14.3
157	-48.5	2.994	PhSnCl$_3$	-63.0	-14.5
158	-11.9	3.985	Ph$_3$SiCl	1.5	13.4
160	-146.2[a]	3.953	Ph$_3$PbCl	33	179.2
165	-41.3	-	Ph$_2$SiH$_2$	-34.5	6.8
166	-40.8	-	Ph$_2$SiH$_2$	-34.5	6.3
167	-40.1	-	Ph$_2$SiH$_2$	-34.5	5.6
168	-3.6	-	Ph$_2$SiCl$_2$	6.2	9.8
169	-3.2	-	Ph$_2$SiCl$_2$	6.2	-3.0
170	-71.9	-	PhSiF$_3$	-73.2	-1.3
171	-65.0	-	PhSiH$_3$	-60.1	4.9
172	-12.4	-	Ph$_2$SiHCl	-5.4	7.0
174	-33.3	-	Ph$_3$SiH	-21.1	12.2

A comparison of the Sn-S distances in compounds **155**-**157** showed a progressive decrease in Sn-S distances given in Table 9 which corresponds to an increase of the Lewis acidity of the central tin atom. In compounds **156** and **157** the Sn-S bond is *trans* to Sn-Cl bond with angles of 168º and 167º respectively. The transition from tetrahedral to TBP can also be determined from the difference between the sums of equatorial and axial angles.[96] A greater difference is associated with more TBP geometry. In compounds **155** and as well as in **158**-**160**, the E-S (E = Si, Ge, Sn, Pb) distances (Table 9) indicate a progressive change in the structural features of these compounds.
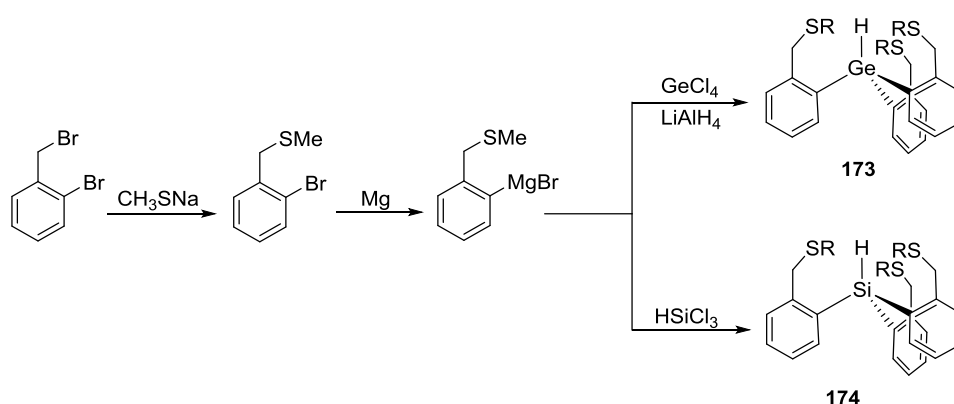
Scheme 15: Synthesis of a *C,S*-chelating ligand and reactions to form a triarylgermane or silanes.

Hypervalency in the case of Ge compound **173** is associated with a large upfield [73]Ge NMR shift (δ = -93.0 ppm vs Ph₃GeH δ = -57.0 ppm) and a significant line broadening. The average distance between Ge and S was 3.778(2) Å. The data obtained from X-ray crystallography and NMR spectroscopy for **173** support the presence of a Ge-S dative interaction, although it is still weaker when compared to similar Ge-N compounds.

1.6 *C,P*-chelating ligand containing compounds of Group 14:

The ability of Sn to expand its coordination number beyond four due to the donor-acceptor interactions with Lewis bases such as N and O has been conclusively established. The intramolecular interactions between Sn and soft phosphine donors are less studied.[102] Higher coordination can be successfully induced by the integration of a donor atom into the side chain of an alkyl or aryl substituent.[99] Dative interaction between Sn-P can be inferred from the upfield shifts of ^{119}Sn NMR resonance signals and short Sn-P distances and the large values of the $J_{119Sn-31P}$ coupling constant compared to tetracoordinated tin compounds.[102,103] The ligands used to obtain the molecules having Sn-P interaction are given in Figure 24.
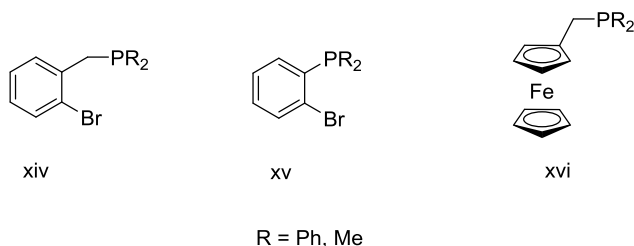
Figure 24: Structure of *C,P*-chelating ligands.

R¹ = R² = R³ = Ph **175**
R¹ = Ph, R² = Me, R³ = *t*-Bu **176**
R¹ = Me, R² = Ph, R³ = Ph **177**
R¹ = Me, R² = Me, R³ = *t*-Bu **178**

R¹ = Ph, R² = Ph, R³ = Cl **179**

R¹ = Me **180**, Cl **181**
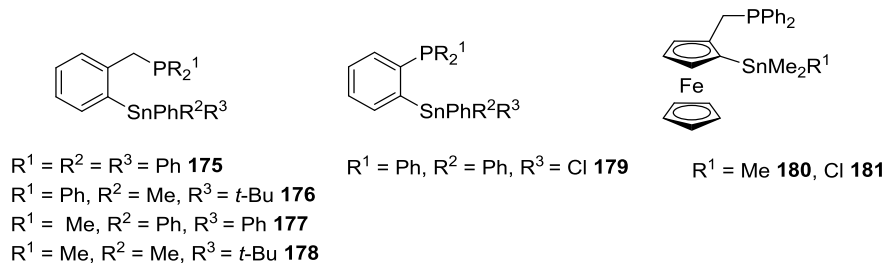
Figure 25: Organotin compounds containing *C,P*-chelating ligands.[110, 112-114]

Compounds **175**-**178** and **179** (Figure 25) were synthesized by von Abicht *et al.*[112] and Lin *et al.*[110] by reacting *o*-(C₆H₄CH₂PPh₂)Li and *o*-(Ph₂P)C₆H₄Li with R₃SnCl and Ph₂SnCl₂ respectively in Et₂O. The ^{31}P NMR resonance at -1.0 ppm for **179** is downfield from -4.0 ppm for Ph₃P, and the ^{119}Sn NMR chemical shift of -101.7 ppm for **179** is significantly upfield compared to Ph₃SnCl (-45.0 ppm). The same observations were obtained in the case of *o*-((*i*-Pr₂P)C₆H₄)₂SnPhCl **179a** which showed ^{119}Sn resonance of -126.4 ppm. X-ray crystallography of both **179** and **179a** showed Sn-P distance of 3.125(4) and 3.120(1) Å which is less than the sum of van der Waals radii (4.2 Å).[110] Therefore, a dative interaction is likely present between Sn and P. The P-Sn-Cl bond angles of 159.76º (1)and 153.92º(1) clearly suggests that the coordination geometry at the tin centers is TBP.

Compound **182** was synthesized by treating *o*-(C₆H₄CH₂PPh₂)Br with Me₂SiHCl. Berlekamp *et al.*[107] reported the synthesis of **183**-**185** by using the route outlined in Scheme 16.
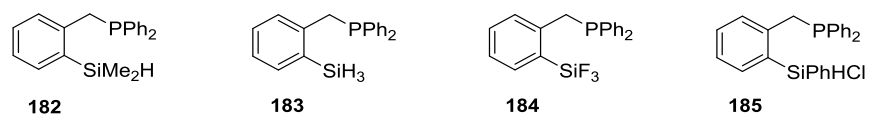
Figure 26: Organosilicon compounds containing *C,P*-chelating ligands.[107, 115]

The ^{29}Si NMR resonances for compounds **183**-**185** are -62.4, -72.0 and -10.1 ppm respectively, which indicate only very small upfield shifts compared to structurally similar non-chelating silanes. This data anticipates the non-coordinating behavior of P in compounds **183**-**185**.
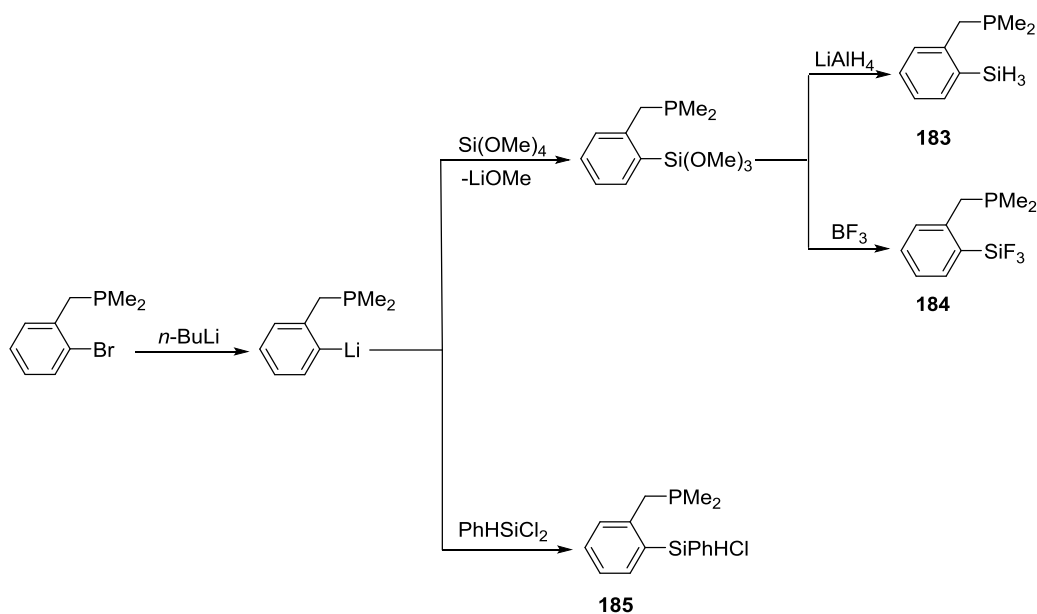
Scheme 16: Synthesis of SiF$_3$, SiH$_3$ and SiPhHCl silanes containing a *C,P*-chelating ligand.

1.7 Polystannanes:

Group 14 elements (E = C, Si, Ge, Sn and Pb) have a unique tendency towards catenation, which decreases significantly from carbon to lead. In the early 1980's, the synthesis of polysilanes introduced a new class of materials with interesting electronic and optical properties due to the presence of significant σ-delocalization[116] along the polymer backbone which also stimulated a similar interest in polystannanes. Polystannanes represent a unique class of polymers having a backbone of covalently bonded metal (Sn) atoms. Polystannane possess extensive σ-delocalization compared to polysilanes because of their more diffuse orbitals, lower band gaps (>390 nm,[116] some 70 nm or more red-shifted vs. Si) and greater metallic character.[43] It was first demonstrated by Dräger et al.[117] that the HOMO-LUMO energy gap of oligostannanes decreased when the number of tin atoms in the chain was increased, and a significantly red shifted absorption maxima in UV spectra was observed. A consequence of catenation in polystannane is longer central Sn-Sn bonds and flatter Sn-Sn-Sn angles. Thus, the term "molecular metal" was proposed by Dräger to describe high molecular weight analogues.[117] The tri-, tetra-, penta- and hexastannanes were isolated and characterized by ^{119}Sn NMR spectroscopy and X-ray analyses.

λmax = 280 nm   λmax = 300 nm   λmax = 330 nm   λmax = 370 nm
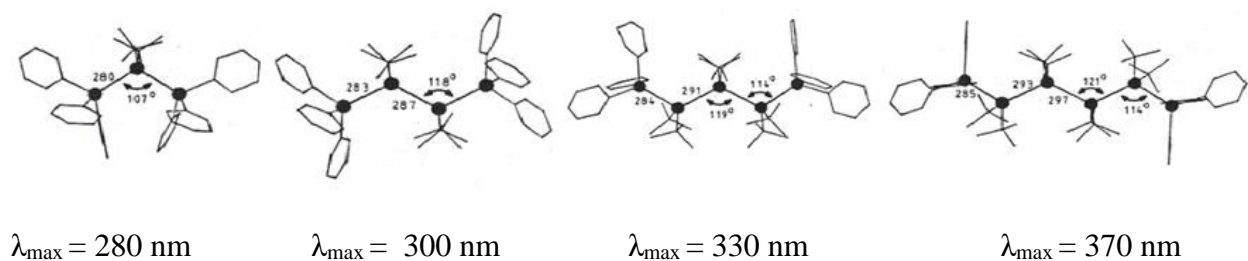
Figure 27: Dräger's oligostannanes with their average Sn-Sn bond lengths (pm), Sn-Sn-Sn bond angles and absorption maxima.[117]

1.7.1 Challenges for polystannanes:

Polystannanes are thermally stable up to 200 ℃ in inert atmosphere as well as in air.[108,110-112] Polystannanes show sensitivity to the ambient environment, have greater stability in the solid state than in solution, and suffer a higher rate of degradation under light exposure compared to dark.[116,118,121-123] Furthermore, it was found that poly(dialkylstannane)s degrade immediately upon exposure to light to five- and six-membered cyclic oligostannanes, whereas poly(diarylstannane)s were stable in the dark in air for at least one week.[119]

Choffat *et al.*[122] reported degradation studies of poly(dialkylstannane)s having alkyl side groups of varying lengths, in the presence of different solvents and dyes. It was demonstrated that the length of the alkyl side chain has no significant influence on the stability of these polymers. It was found that the use of dyes such as Sudan 1, Sudan Black B, or inorganic colloidal platinum, or organic small molecules such as carotene, curcumin and TEMPO reduced the rate of degradation. The reason for the reduction of degradation may be the absorption of light by these species or the reaction with transient radicals or both. Trummer *et al.*[124] reported that the stability of polystannanes in light is dependent on the nature of the organic side groups. The degradation behaviour of two polymers, poly[bis(4-butylphenyl)stannane] and poly(dibutylstannane) were studied, and the diarylpolystannanes were found to be more stable towards light than the dialkyl in THF as well as in DCM. The initial photochemical damage caused by laser flash photolysis is comparable for both polymers. Poly[bis(4-butylphenyl)stannane] "recovered" to 90% during a period of a few seconds after irradiation. The higher recovery of poly[bis(4-butylphenyl)stannane] degraded by photolysis may be the re-formation of polymer chains resulting in an apparent stabilization of this polymer. This type of behaviour was not observed for poly(di-*n*-butylstannane). The degradation mechanism proposed in this study is based on the random homolytic cleavage of Sn-Sn bonds in a polymer chain resulting in two smaller chains ending with

a radical (Figure 28). The enhanced stability of a chain ending with two aromatic groups bonded to a tin atom may be due to the radical delocalization throughout the aromatic ring which decreases the probability of the radical reacting with the polymer chains. This mechanism was further supported by the fact that in the presence of the radical scavenger 2,6-di-tert-butyl-4-methylphenol (BHT) in THF, the degradation rate of polystannanes was slow. In the absence of BHT the degradation of polystannane was rapid.
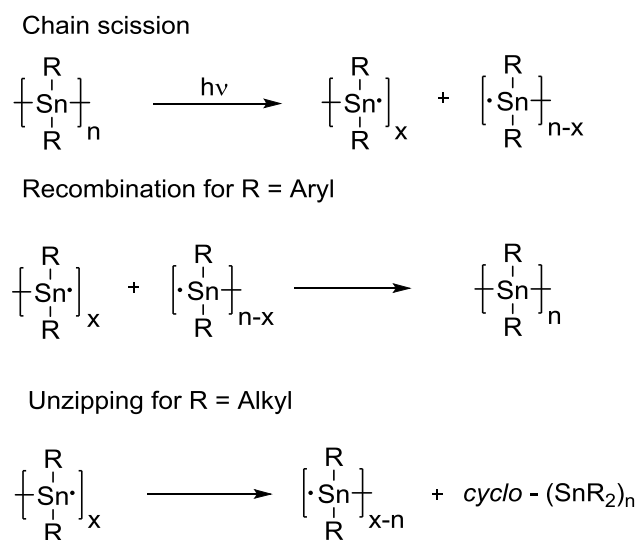
Figure 28: Proposed degradation mechanism of polystannanes.

1.7.2 Synthesis of polystannanes:

The common reductive coupling methods used for the synthesis of polystannanes include Wurtz type, electrochemical and catalytic dehydrogenation in the presence of a transition metal catalyst.

1.7.2.1 Wurtz coupling:

Wurtz coupling was first used to form a C-C bond from the reaction of alkyl halides with sodium metal. Later, investigations by Kipping[125] showed that Wurtz coupling can be used for preparation of materials having only organosilicon units in the backbone. In these Wurtz-type reactions, a dichlorodiorganosilane is reacted with a slight excess of sodium dispersion in a high-

boiling-point solvent such as toluene under reflux. In 1992, Zou *et al.*[126] reported the first synthesis of high molecular weight (~10^4 Da) poly(di-*n*-butylstannane) using a Wurtz-type coupling of (*n*-Bu)$_2$SnCl$_2$ in toluene/heptane in the presence of 15-crown-5.

$$(n\text{-Bu})_2\text{SnCl}_2 \xrightarrow[\substack{15\text{-crown-5} \\ -2\text{NaCl, 14h}}]{2\text{Na, 60 °C}} \left[\begin{array}{c} n\text{-Bu} \\ | \\ \text{Sn} \\ | \\ n\text{-Bu} \end{array} \right]_n$$

186
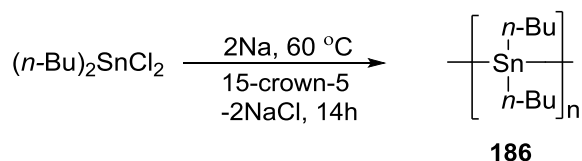
Scheme 17: Wurtz coupling of (*n*-Bu)$_2$SnCl$_2$.

A reinvestigation of this study by Tilley failed to produce the same results and only low molecular weight oligomers were isolated under these conditions.[118] This may have been due to the longer reaction times used, which caused a degradation of the polymer. In a later study by Price *et al.*[127] high molecular weight (10^6 Da) poly(di-*n*-butylstannane) was produced in toluene at 60 °C. It was observed that the optimal yield is achieved in 4h; after that time, degradation of the polymer begins and cyclic oligomers such as (*n*-Bu$_2$Sn)$_5$ and (*n*-Bu$_2$Sn)$_6$ are obtained as a result of "end-biting" and "back-biting" of chains. This demonstrated that reaction time is critical for these types of reactions. In 2003, Molloy *et al.*[43] reported the Wurtz polymerization of RBr$_2$Sn(CH$_2$)$_5$OC$_6$H$_4$C$_6$H$_5$ (R = Ph, *n*-Bu), yielding moderately high molecular weight polystannanes (RR'Sn)$_n$ ($M_w = 3.0 \times 10^5$ Da; PDI = 1.30 and $M_w = 2.5 \times 10^5$ Da; PDI = 1.96 respectively). Foucher *et al.*[128] also successfully synthesized high molecular weight ($M_w = 1.1 \times 10^5$ Da; PDI = 1.40 and $M_w = 1.47 \times 10^5$ Da; PDI = 1.3) fluorinated polystannanes using Wurtz coupling reactions of fluorinated dichlorostannanes.
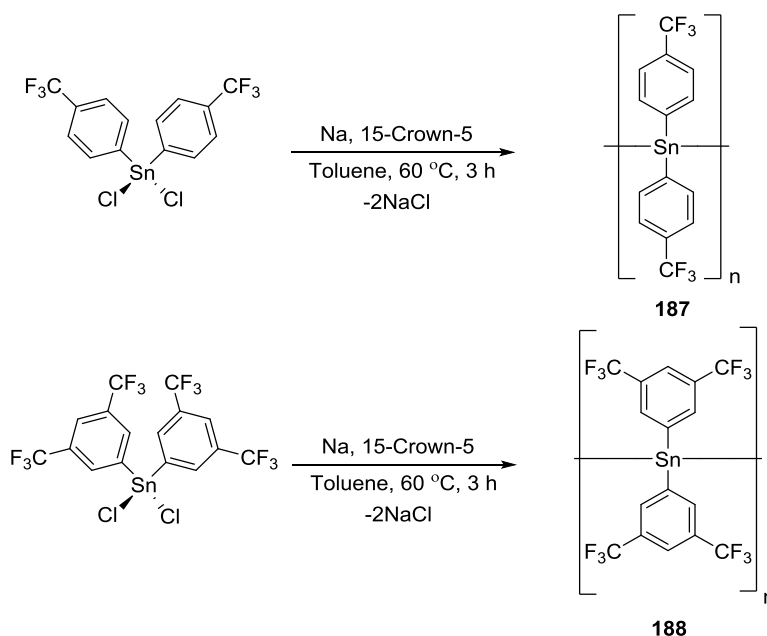
Scheme 18: Wurtz coupling reactions of fluorinated dichlorostannanes.

Recently, Caseri *et al.*[129] reported the polymerization of dichlorodiorganostannanes with Na in 1:2 ratio in liquid NH_3. These reaction conditions afforded the polymerization of (*n*-Bu)$_2$SnCl$_2$ and (*n*-Oct)$_2$SnCl$_2$ to the polystannanes (*n*-Bu$_2$Sn)$_n$ and (*n*-Oct$_2$Sn)$_n$ having molar masses 8.0×10^3 and 6.0×10^3 Da respectively. The material produced from the reaction of Ph$_2$SnCl$_2$ under similar conditions was insoluble in organic solvents at room or elevated temperatures making molecular weight determination impossible; however the elemental composition of the isolated yellow product was in agreement with that of (Ph$_2$Sn)$_n$.[130]

In general, there are several disadvantages of the Wurtz synthetic method; it has limited tolerance to functional groups, the yields are moderate, the reproducibility is poor and it is dangerous due to the pyrophoric nature of Na metal and harsh reaction conditions.[131]

1.7.2.2 Electrochemical synthesis:

Electrochemical polymerization has also been successfully applied to the synthesis of linear and network polystannanes. Okano *et al.*[132] prepared poly(di-*n*-butylstannane) and poly(di-*n*-octylstannane) by this method. The synthesis is completed in a one compartment cell in which 20V is constantly applied between the Pt cathode and Ag anode in DME or THF with tetra *n*-butylammonium perchlorate (TBAP) as the supporting electrolyte.

$$nR_2SnCl_2 \xrightarrow{+ 2ne^-} \left[\begin{array}{c} R \\ | \\ -Sn- \\ | \\ R \end{array} \right]_n + 2nCl^-$$

R = *n*-Bu **186**, *n*-Oct **189**
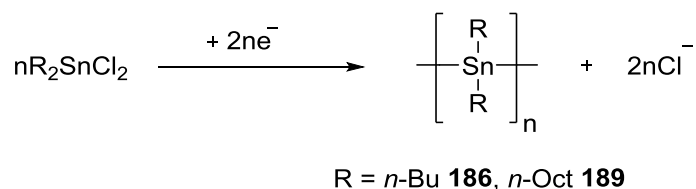
Scheme 19: Electrochemical polymerization dialkyltin dihalides.

Yields for (*n*-Bu$_2$Sn)$_n$ and (*n*-Oct$_2$Sn)$_n$ polymers were between 40-60% and 30-50% respectively. The highest reported molecular weight of (*n*-Bu$_2$Sn)$_n$ and (*n*-Oct$_2$Sn)$_n$ from this method was 1.09×10^4 (PDI = 2.6) and 0.59×10^4 Da (PDI = 1.7) respectively.[124] Kulandainathan *et al.*[133] reported the polymerization of Me$_2$SnCl$_2$ using aluminium rods as the cathode and anode and 0.4 M tetra *n*-butylammonium tetrafluoroborate (TBATFB) in DME as the supporting electrolyte and reaction solvent.

Network polystannanes of methyl-, *n*-butyl-, *n*-octyl-, and phenyl-trichlorostannane were also synthesized by electrochemical reduction reaction. The estimated molar masses of these polymers were $4\text{-}10 \times 10^4$ Da.[134]

$$nRSnCl_3 \xrightarrow{+3ne^-} \left[\begin{array}{c} | \\ -Sn- \\ | \\ R \end{array} \right]_n + 3nCl^-$$

R = Me **190**, *n*-Bu **190a**,
Ph **191**, *n*-Oct **191a**
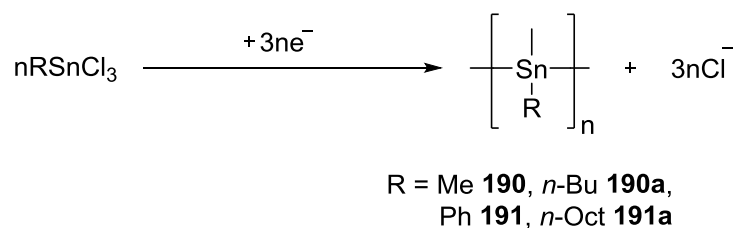
Scheme 20: Electrochemical polymerization alkyltin trihalides.

1.7.2.3 Catalytic dehydrogenation:

Polystannanes are readily synthesized by catalytic dehydrocoupling of alkyl or aryl tin dihydrides. Harrod *et al.*[135] had earlier reported the catalytic dehydrocoupling of silanes (PhSiH$_3$) and germanes (PhGeH$_3$) to oligosilanes and oligogermanes which is facilitated by Group IV metallocene (M = Ti, Zr) catalysts (Cp$_2$MR$_2$ (Cp = η^5-C$_5$H$_5$)). By contrast, transition metal complexes of Ti, Zr, Hf, Cr, Mo, W, Rh, Pt have been employed as catalysts for the dehydropolymerization of primary and secondary stannanes. This method is most successful for the polymerization of secondary stannanes, R$_2$SnH$_2$.

$$R_2SnH_2 \xrightarrow[-H_2]{\text{catalyst}} H\left[\begin{array}{c} R \\ | \\ Sn \\ | \\ R \end{array}\right]_n H \quad + \quad \text{cyclo-}(SnR_2)_m$$

$$m = 5, 6$$
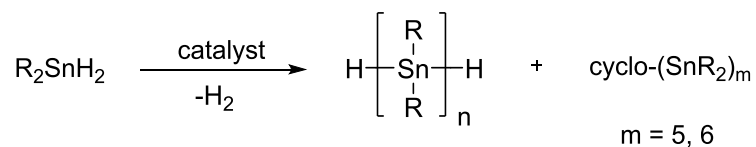
Scheme 21: Catalytic dehydrocoupling of diorganostannanes.

Tilley *et al.*[136] reported the synthesis of high molecular weight ($M_w = 1.7 \times 10^4$ Da) poly(di-*n*-butylstannane) by catalytic dehydrocoupling. Using [Zr(*n*-C$_5$H$_5$)(*n*-C$_5$Me$_5$){Si(SiMe$_3$)$_3$}Me]. Tilley *et al.*[118] also synthesized high molecular weight polystannanes along with cyclic products from the dehydropolymerization of secondary stannanes using the simpler organometallic zirconium catalyst Cp$_2$ZrMe$_2$. The best examples for poly(dialkylstannanes) are **186** ($M_w = 4.6 \times 10^4$ Da) and **187** ($M_w = 9.2 \times 10^4$ Da) and for poly(diarylstannanes) are H[(*p*-Bu^t-C$_6$H$_4$)$_2$Sn]$_n$H ($M_w = 5.6 \times 10^4$ Da) and H[(*p*-Hex-C$_6$H$_4$)$_2$Sn]$_n$H ($M_w = 4.8 \times 10^4$ Da). Sita *et al.*[121] catalyzed the polymerization of (*n*-Bu)$_2$SnH$_2$ utilizing the commercially available carbonyltris(triphenylphosphine)rhodium(I) hydride, HRh(CO)(PPh$_3$)$_3$. The synthesis of high molecular weight **186** ($M_w = 5.0 \times 10^4$ Da) was confirmed by gel permeation chromatography (GPC) along with a small amount of oligomeric or cyclic components. Kim *et al.*[137] investigated the dehydrocoupling of the (*n*-Bu)$_2$SnH$_2$ utilizing a series of early transition metal catalysts

Cp$_2$MCl$_2$/Red-Al (M = Ti, Zr, Hf) and M(CO)$_6$/Red-Al (M = Cr, Mo, W). This produced two phases of polymers, one a cross-linked insoluble material and the other a non cross-linked THF soluble solid. Tilley *et al.*[138] has also used hafnocene stannyl complexes for the dehydropolymerization of secondary stannanes. The catalyst [Me$_2$C(C$_5$H$_4$)$_2$]Hf(SnHMes$_2$)NMe$_2$, produced H(n-Bu$_2$Sn)$_n$H polymer that was isolated as a yellow solid ($M_w = 2.0 \times 10^4$ Da) along with cyclic oligomers.
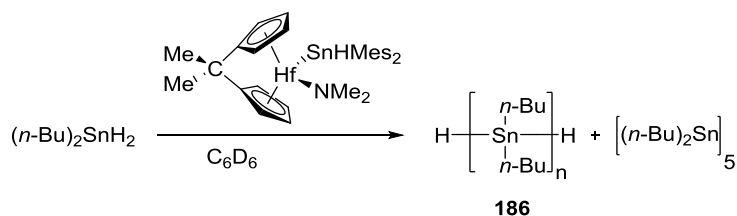
Scheme 22: Hafnocene catalyzed dehydrocoupling of (n-Bu)$_2$SnH$_2$

Schubert *et al.*[139] attempted the dehydrocoupling of stannanes ((n-Bu)$_2$SnH$_2$ and Ph$_2$SnH$_2$) to polystannanes using (PhMe$_2$P)$_2$PtMe$_2$ or [(κ^2-P,N)-Ph$_2$PC$_2$H$_4$NMe$_2$]PtMe$_2$. Soluble poly(di-n-butylstannane) was observed by ^{119}Sn NMR analysis along with the appearance of cyclic and linear oligomers whereas only insoluble material reovered when Ph$_2$SnH$_2$ was polymerized. More recently, Caseri *et al.*[119-120, 140] reported the synthesis of high molecular weight alkylpolystannanes catalyzed by Wilkinson's catalyst, [RhCl(PPh$_3$)$_3$]. The polymers obtained were isolated without the detectable amount of cyclic oligomers. This polymerization is sensitive to the steric bulk of branched dialkylstannanes and the polymerization only proceeds if at least two methylene groups are present between the an aryl carbon and the tin atom.[141]

Samarium diiodide (SmI$_2$) was used to synthesize low molecular weight poly(dialkystannanes) under mild conditions from R$_2$SnCl$_2$ (R = Me-, Et-, n-Hex-).[143,144] SmI$_2$ is a mild one-electron reducing agent of a homogeneous nature and has been applied to the catenation of Group 14 elements. The polymerization was carried out at room temperature using SmI$_2$ (2.0

eq.) in HMPA/THF and a reaction time of 24-120 h. The maximum molecular weight 4.82×10^3 Da was obtained for $(Et_2Sn)_n$.

Beckmann *et al.*[142] prepared first example of a chiral polystannane by catalytic dehydrocoupling following Scheme 23.
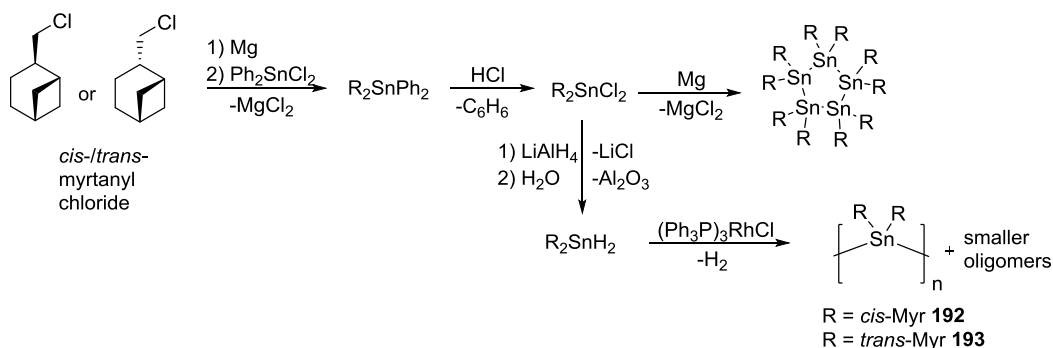
Scheme 23: Synthesis of chiral polystannanes.

Lechner *et al.*[130] more recently reported the preparation of polystannanes by dehydrogenative coupling in the presence of TMEDA. The unsymmetrical polystannanes [*n*-Bu(Ph)Sn]$_n$ and [(4-*n*-BuPh)$_2$Sn]$_n$ were synthesized having molar weights of 1.3×10^4 and 4.6×10^4 Da, while PDI values were 2.0 and 3.2, respectively.
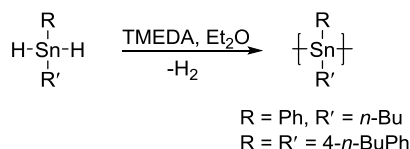
Scheme 24: TMEDA catalyzed dehydrocoupling of stannanes

1.7.3 Properties of polystannanes:

Polystannanes represent an interesting class of organometallic polymers due to their thermal, optical and electronic properties. These polymers are often viscous oils or solids yellow to orange in color. Polystannanes are stable in their oil/solid state but relatively less stable in different solvents, particularly in pentane and THF. However, a major drawback of these polymers is their sensitivity towards light and moisture.

1.7.3.1 Photosensitivity:

The photobleaching of polystannanes in ambient light causes the scission of Sn-Sn bonds resulting in the formation of cyclic oilgomers such as cyclic-$(R_2Sn)_5$ and $(R_2Sn)_6$. Recently,[124] it was demonstrated that the photostability of polystannanes changes with the type of organic side groups. For instance, poly[bis(4-*n*-butylphenyl)stannane] was found to be more stable to light than poly(di-*n*-butyl)stannane in THF and DCM solvents.

1.7.3.2 Thermal properties:

Overall, polystannanes relatively exhibit good thermal stability. Thermogravimetric analysis showed that poly(dialkylstannanes) start decomposition at temperatures > 255-270 °C under N_2 which is slightly lower than for poly(diarylstannanes) at temperature ≈ 300 °C.[116] Differential scanning calorimetry (DSC) is a technique used to measure the heat effects on the phase transitions as a function of temperature. For polystannanes it is routinely used to determine the glass transition (T_g) temperature. In the case of poly(dialkylstannanes) T_g varies between 0 °C to 91 °C depending upon the chain of the length of alkyl chain and for poly(alkylphenylstannane) ranges from -20 °C to -50 °C.[120,140]

1.7.3.3 Conductivity:

Room temperature conductivity studies for a number of neutral polystannanes, such as poly(di(3-propylphenyl)stannanes) found values of approximately ≈ 3 × 10^{-8} S·cm^{-1} which increase with temperature a characteristic of a semi-conducting material.[142] The thin film of H(*n*-$Bu_2Sn)_nH$ and H(*n*-$Oct_2Sn)_nH$ doped with SbF_5 measured at room temperature had conductivity of 10^{-2} and 0.3 S·cm^{-1} respectively.[118]

1.7.3.4 Electronic properties:

A number of electronic studies were conducted on oligostannanes which showed a systematic red shift with an increase in the chain length of the molecule. Drenth *et al.* [145] demonstrated that λ_{max} for Et_3Sn-$(SnEt_2)_n$-$SnEt_3$ (n = 0-4) is red shifted and associated with a σ-σ^* transition from 232-325 nm. Sita *at el.*[146] also observed similar trends for n-Bu_3Sn-$(n$-$Bu_2Sn)_n$-$Sn(n$-$Bu)_2$-CH_2CH_2OEt (n = 0-4) and Drager *et al.*[117] for Ph_3Sn-$(t$-$Bu_2Sn)_n$-$SnPh_3$ (n = 1-4) oligomers.
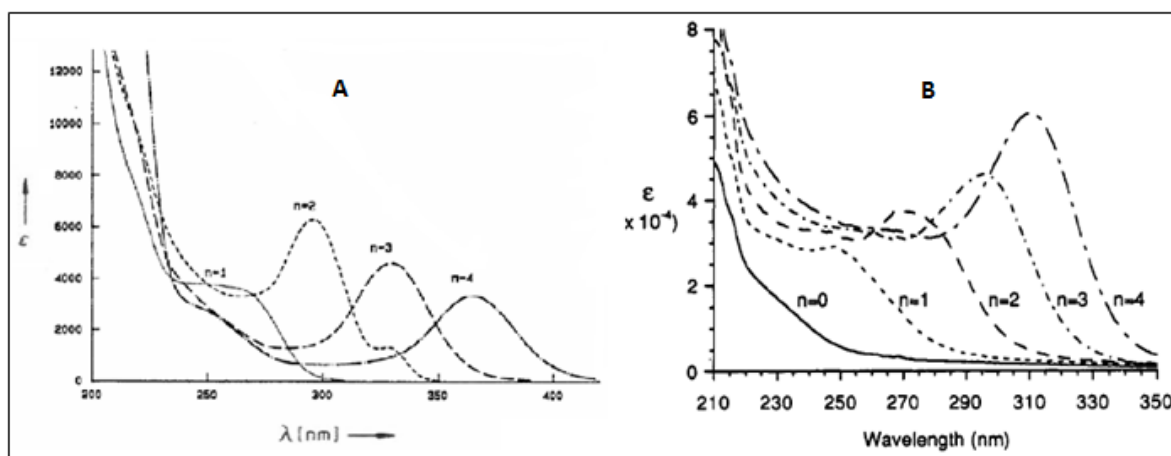
Figure 29: The electronic spectra of (A) (n-$Bu)_3Sn$-$(n$-$Bu_2Sn)_n$-$Sn(n$-$Bu)_2$-$(CH_2)_2OEt$ (n = 0-4)[148], (B) for Ph_3Sn-$((t$-$Bu)_2Sn)_n$-$SnPh_3$ (n = 1-4).[117]

The λ_{max} values of hydrogen terminated poly(dialkylstannane)s are in the range of 380-480 nm. The λ_{max} values depend on a number of factors such as solvent, polymer conformation, molar mass and the amount of cyclics present in the sample. The λ_{max} values of poly(diarylstannane)s (430-506 nm) are significantly red shifted (> 50 nm) compared to poly(dialkylstannane)s, which indicate the presence of σ-π conjugation between aryl substituents and the tin atoms in the backbone of the polymer. The λ_{max} values of polystannanes are listed in Table 10.

Table 10: UV-Visible spectral data and ^{119}Sn NMR chemical shifts for polystannanes.

Polymer	λ_{max} (nm)[a]	^{119}Sn NMR (ppm)	Ref.
$(Et_2Sn)_n$	368	-172.2[c]	120
$(Pr_2Sn)_n$	-	-194.8[d]	120
$(n$-$Bu_2Sn)_n$	390	-189.6[e]	118, 120
$(n$-$Pn_2Sn)_n$	-	-192.0[d]	120
$(n$-$Hex_2Sn)_n$	384	-190.9[e]	118, 120
$(n$-$Oct_2Sn)_n$	388	-190.7[e]	116
$(n$-$Dod_2Sn)_n$	-	-189.0[d]	120
$H[(p$-t-Bu-$C_6H_4)_2Sn]_nH$	432	-197.0[d]	116, 120
$H[(p$-n-Hex-$C_6H_4)_2Sn]_nH$	436[b]	-196.0[d]	116, 118
$H[(p$-n-BuO-$C_6H_4)_2Sn]_nH$	448[b]	-183.0[d]	116, 120
$H[(o$-Et-p-n-BuO-$C_6H_3)_2Sn]_nH$	506[b]	-125.0[d]	116, 120
$[(o$-Et-$C_6H_4)_2Sn)]n$	468[b]	-	116
$[(4$-n-$BuPh)_2Sn]_n$	420[b]	-	116
$[n$-$Bu(Ph)Sn]_n$	410[b]	-	-
$[(PhC_2H_4)_2Sn]_n$	-	-187.0[c]	140
$[(PhC_3H_6)_2Sn]_n$	-	-192.12[c]	140
$[(PhC_4H_8)_2Sn]_n$	-	-190.4[c]	140
$[(p$-$CF_3C_6H_4)_2Sn]_n$	332	-56.7	128
$[(3,5$-$CF_3C_6H_4)_2Sn]_n$	327	-48.9	128

[a] In THF, [b] As film, [c] Measured in dichloromethane-d_2, [d] benzene-d_6, and [e] toluene-d_8

1.7.3.5 ^{119}Sn NMR:

NMR (^{1}H, ^{13}C, ^{119}Sn) spectroscopy is the key instrumental tool for the structural characterization of polystannanes. In particular, ^{119}Sn NMR can easily differentiate between linear polymer and oligomeric chains and cyclic structures. The linear poly(dialkylstannane)s in Table 10 exhibit a single resonance around ~-190 ppm, except for the poly(diethylstannane) which shows a signal at -172.2 ppm. The ^{119}Sn NMR resonance for poly(diarylstannane)s range from -183 to -197 ppm with the exception of $[(o$-Et-p-BuO-$C_6H_3)_2Sn]_n$ which showed an unusual resonance at -125 ppm.

1.7.3.6 Thermochromic properties:

The poly(dialkylstannane)s $(n$-$Hex_2Sn)_n$ and $(n$-$Oct_2Sn)_n$ showed reversible thermochromic behaviour which is evident from the discoloration of these materials upon warming

above room temperature. UV-vis spectrometry revealed a blue shift in the absorption maximum between 384-369 nm for (n-Oct$_2$Sn)$_n$ moving from 30-40 $^{\circ}$C in a toluene solution and from 392-382 nm for a solid film of (n-Hex$_2$Sn)$_n$ in the same temperature range.

1.7.3.7 Molecular weights:

Gel permeation chromatography (GPC) has been used to estimate the molar masses of polystannanes. The molecular weights of polystannanes (Table 11) are determined against polystyrene standards of different known molecular weights in THF as the mobile phase using a RI detector.

Table 11: Molar weights of polystannanes.

Compound	M_w [Da]	M_n [Da]	PDI [M_w/M_n]	Polymerization Method	Ref.
$(Me_2Sn)_n$	1,120		1.49	SmI_2 in HMPA-THF	145
$(Et_2Sn)_n$	31,000	13,000	1.47	catalytic dehydrogenation	120
	4,820		1.21	SmI_2 in HMPA-THF	145
	4,100		1.25	Mg in THF	145
	3,700		1.15	Ca in THF	145
$(Pr_2Sn)_n$	27,000	10,000	1.58	catalytic dehydrogenation	120
$(n\text{-}Bu_2Sn)_n$	91,000	36,000	1.39	catalytic dehydrogenation	120
	17,500	7,800	2.24	catalytic dehydrogenation	118
	46,000	13,900	3.31	catalytic dehydrogenation	118
	10,900		2.26	Electrochemical synthesis	132
$(n\text{-}Pn_2Sn)_n$	48,000	19,000	1.30	catalytic dehydrogenation	120
$(n\text{-}Hex_2Sn)_n$	76,000	31,000	1.32	catalytic dehydrogenation	120
	36,800	15,300	2.4	catalytic dehydrogenation	118
	2,770		1.18	SmI_2 in HMPA-THF	145
$(n\text{-}Oct_2Sn)_n$	97,000	40,000	1.22	catalytic dehydrogenation	120
	95,700	14,300	6.7	catalytic dehydrogenation	118
	92,600	21,700	4.26	catalytic dehydrogenation	118
	5,900		1.7	Electrochemical synthesis	132
$(n\text{-}Dod_2Sn)_n$	28,000	19,000	1.16	catalytic dehydrogenation	120
$H[(p\text{-}^tBu\text{-}C_6H_4)_2Sn]_nH$	56,000	16,700	3.35	catalytic dehydrogenation	116
$H[(p\text{-}^nHex\text{-}C_6H_4)_2Sn]_nH$	48,200	20,000	2.41	catalytic dehydrogenation	116
$H[(p\text{-}^nBuO\text{-}C_6H_4)_2Sn]_nH$	12,000	7,000	1.71	catalytic dehydrogenation	116
$H[(o\text{-}Et\text{-}p\text{-}^nBuO\text{-}C_6H_4)_2Sn]_nH$	4,400	4,000	1.1	catalytic dehydrogenation	144
$[(4\text{-}n\text{-}BuPh)_2Sn]_n$	46,000		3.2	TMEDA	147
$[n\text{-}Bu(Ph)Sn]_n$	13,000		2.0	TMEDA	147

1.8 Thesis objectives:

The main objective of this thesis is to prepare structurally stable 5-coordinate polystannanes having ligands containing different donor atoms such as N, S, P, and O.

The increase in the coordination at Sn is expected to achieve the following:

1) Moderate the Lewis acidity of Sn atoms in the backbone of the polystannanes.

2) Increase steric hindrance around Sn.

3) Reduce susceptibility to nucleophilic attack.

The objectives of this research can be accomplished as follows:

i) Synthesize a series of diorganotin dihalides containing *C,N-*, *C,P-*, *C,O-* and *C,S-* chelating ligands.

ii) Prepare new diorganotin dihydrides by using $LiAlH_4$ or $NaBH_4$ as reducing agents.

iii) Carry out the polymerization by dehydrogenative coupling of dihydrides or by the Wurtz coupling of dihalides.

iv) Characterize all monomers and polymers by ^1H, ^{13}C and ^{119}Sn NMR spectroscopy, UV-vis spectroscopy and X-ray crystallography where applicable.

iv) Finally, investigate the material properties and stability of these new 5-coordinate polystannanes.

2.0 Results and Discussion:

2.1: Synthesis

2.1.1 Phenyloxy vinyl ethers

Vinyl ethers **137** and **194**-**196** were synthesized following methods reported in literature.[43,148,149] These reactions are examples of classic Williamson ether syntheses where an alcohol (4-phenylphenol or phenol), in the presence of a base (K_2CO_3) and an alkyl halide (i.e. allyl bromide) is converted to an ether. The reaction (Scheme 25) procedes by deprotonating the phenol to produce an aryloxide as an intermediate, which attacks the allyl bromide in a nucleophilic substitution (S_N2) fashion producing the desired ethers. Acetone was the preferred solvent as (S_N2) reactions work best in polar aprotic solvents.[148] It was reported that a 1.1 molar equivalence of the base resulted in an optimal yield of **137** and **194**.[149] The target ether species was purified by first redissolving the crude product in DCM, and sequentially washing the organic layer with a 1 M NaOH solution, brine and water respectively to remove unreacted allyl bromide and phenol.[148] After solvent removal compound **137** was obtained as a flaky white coloured solid, whereas compounds **194**-**196** were recovered as yellow coloured viscous oils.

R = H, Y = H **194** (82%)
R = Ph, Y = H **137** (65%)
R = H, Y = CF$_3$ **195** (94%)
R = OCH$_3$, Y = H **196** (89%)
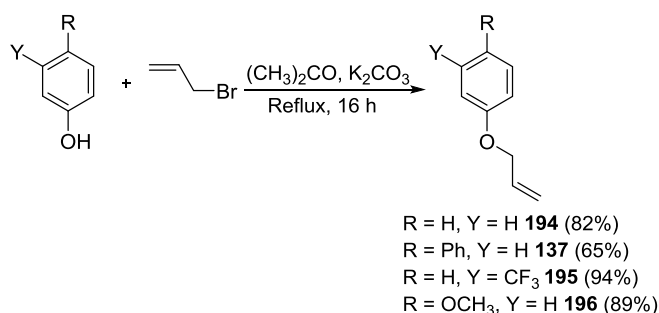
Scheme 25: Williamson's ether synthesis of phenyloxy allyl ethers.

2.1.2: Triphenylphenyloxy propyl tin:

Compounds **141** and **197**-**199** were synthesized via a radical hydrostannylation reaction (Scheme 25) utilizing azobisisobutyronitrile (AIBN) as the radical initiator.[43] When an equimolar

amount of allyl ether (**137** and **194**-**196**) and Ph$_3$SnH were used, a significant amount (>20%) of

the distannane (Ph$_3$SnSnPh$_3$: ^{119}Sn NMR (C$_6$D$_6$) δ = -143 ppm) was always observed. Compounds

141 and **197**-**199** are relatively air and heat stable; as a result, Ph$_3$SnSnPh$_3$ and unreacted starting

material were readily separated from this mixture by vacuum sublimation. Subsequently, the

dissolution of crude **141** in Et$_2$O followed by filtration afforded a pure white coloured solid

product. Compound **197** was purified by an initial wash with hexane to remove Ph$_3$SnSnPh$_3$,

followed by heating under reduced pressure at 75 ºC for 12 h to remove unreacted **194** leaving a

clear, viscous oil. Crude **198** was dissolved in MeOH to remove unreacted **195**, filtered and finally

dried under reduced pressure to afford a white coloured solid. The crude reaction mixture

containing **199** was purified in two steps including sublimation to remove the Ph$_3$SnSnPh$_3$,

followed by silica gel column chromatography using hexane:EtOAc (6:1). The NMR (^{1}H, ^{13}C,

^{119}Sn) analysis of **141** was consistent with reported literature values.[43] Triphenylstannanes **197**-

199 were found to have very similar tin chemical environments (^{119}Sn NMR) to **141**.

R = H, Y = H **197** (79%)
R = Ph, Y = H **141** (70%)
R = H, Y = CF$_3$ **198** (79%)
R = OCH$_3$, Y = H **199** (65%)
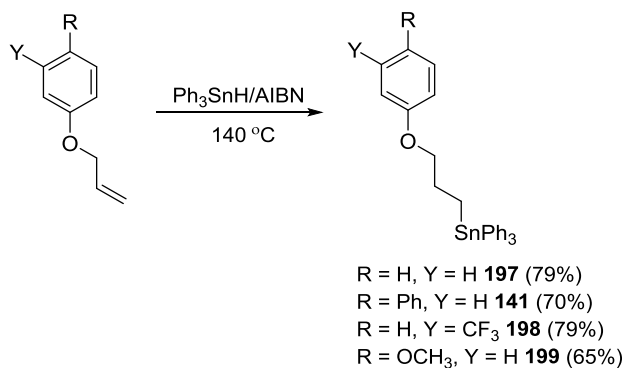
Scheme 26: Synthesis of triphenylphenyloxy propyltin.

2.1.3: Phenylphenyloxy propyltin dichloride:

In the original report by Molloy *et al*., phenyl groups attached to tin were exchanged for

Br by stoichiometric bromination.[43] Despite our best efforts to prepare the desired dibromide **146**,

most synthetic attempts resulted in the formation of a considerable amount of the mono- and

tribromide species that proved difficult to purify. In order to make sufficient quantities of the dihalide materials for polymerization studies, an alternative route to these materials was explored. Compounds **202**-**203** were obtained by stepwise conversion of compounds **197** (Figure 30) and **141** initially to the triorganotin monochlorides (**200**-**201**) and then sequentially to diorganotin dichlorides (**202**-**203**). This method was first reported by Pannell *et al.*[96] for the synthesis of diorganotin dichlorides from triphenyl starting materials. The NMR (^{1}H, ^{13}C, and ^{119}Sn) data obtained for compound **203** showed similar chemical shifts when compared to **202**.
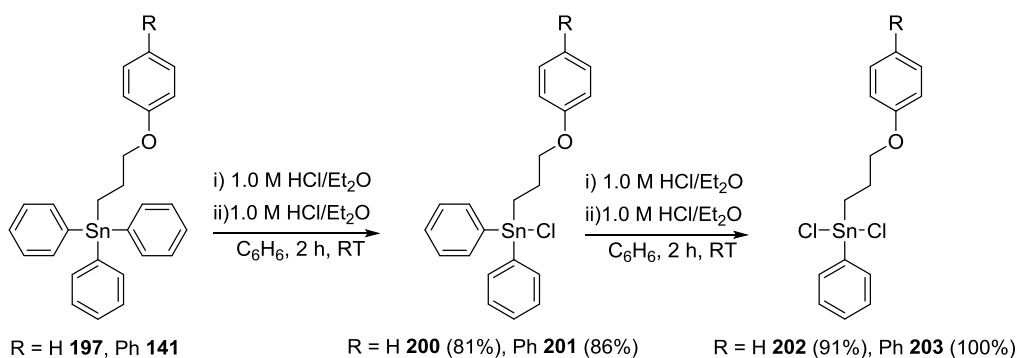
Scheme 27: Stepwise preparation of triorganotin monochlorides and diorganotin dichlorides.

The initial attempt to prepare **200** resulted in a mixture of the starting material **197** and the product monochloride. An essentially pure sample of **200** was obtained by washing the crude product with hot hexane or alternatively by the addition of a stoichiometric aliquot of the 1.0 M HCl solution (calculated on the basis of the amount of starting material from ^{1}H NMR, see Figure 30) required to complete conversion to chloride.

The monochlorides **200** and **201** were not completely converted to their respective dichlorides **202** and **203**. The amount of the unreacted monochloride as calculated on the basis of the comparison of intensities of the ortho phenyl protons (2H, *o*-C$_6$H$_4$O) of the mono- and dichloride by ^{1}H NMR spectroscopy, and the required aliquot of 1.0 M HCl/Et$_2$O added to the solution containing the mixture of mono- and dichlorides. The progressive change from the mono-

and dichlorides (**200**, **202**) are shown in Figure 31 respectively. The percent conversion was calculated from ^{1}H NMR by dividing the integration of the peak for the starting materials **200** and **201** by the peak for the products according to the following formula;[150]

$$\% \text{ Conversion} = (x/2)/((x/2+y/2))$$

where y is the disappearance of peaks (6.53 ppm and 6.61 ppm for **200** and **201**) while x is the appearance of new peak (6.70 ppm and 6.75 ppm for **202** and **203**) respectively. Recrystallization in DCM and hexane afforded single crystals of both **202** and **203**.

The synthesis of the monochloride **201** by this method routinely resulted in the recovery of 10-15% of the unreacted starting material, **141**. Compound **201** was purified by dissolving the crude product in hot hexane, letting it cool to room temperature and placing it into fridge overnight at -20 ℃. A white coloured crystalline product precipitated out of solution after 24 h. The starting material **141** was recovered by first decanting, then removing solvent under reduced pressure. Recrystallization of compounds **200**-**201** using a mixture of DCM and hexane afforded clear, colourless crystals.
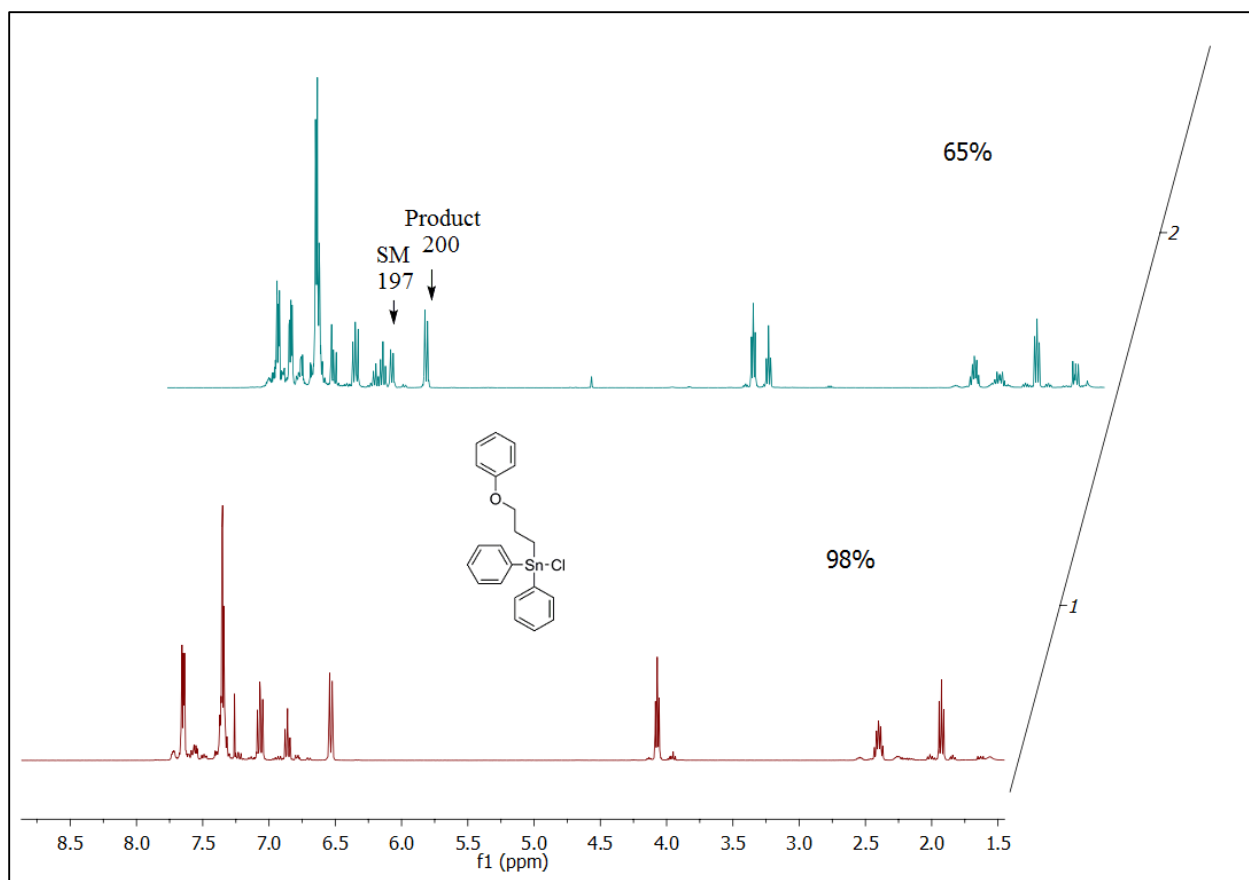
Figure 30: ^{1}H NMR (CDCl$_3$) spectra showing the conversion of **197** to **200**.
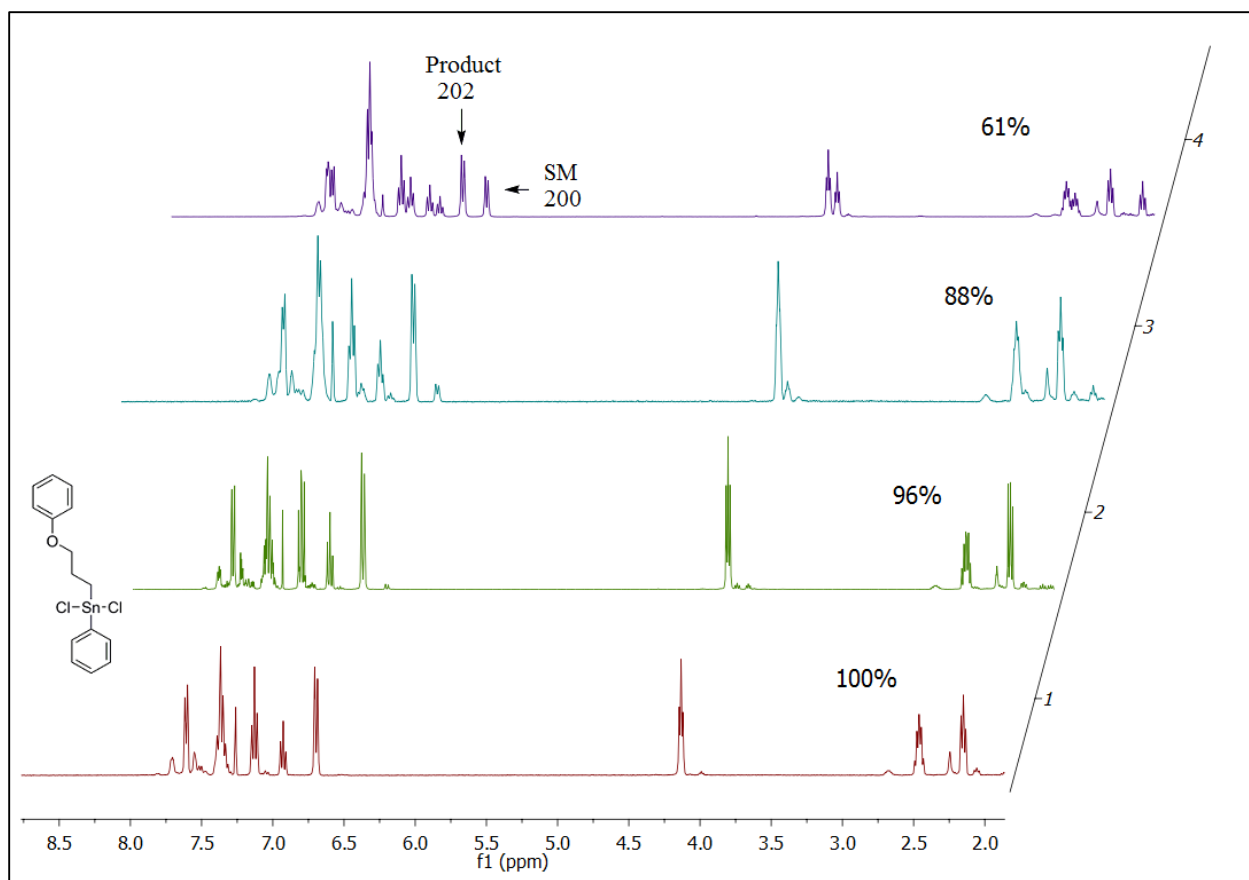
Figure 31: ^{1}H NMR (CDCl$_3$) spectra showing conversion of **200** to **202**.

^{119}Sn NMR chemical shifts, Sn-O distances and yields of compounds **141**, **146** and **197**-**203** are listed in Table 12.

Table 12: ^{119}Sn NMR (CDCl$_3$) chemical shift, Sn-O distances and yields of stannanes.

Compounds	δ ^{119}Sn (ppm) Observed/Literature[43]	Sn··O Distance Å	Yield (%)
141	-99.3/-100.1	-	70
146	-51.3/-53.3	2.73	81
197	-99.9	-	79
198	-99.3	-	79
199	-100.0	-	65
200	-26.6	2.80	81
201	-24.7	2.81	86
202	-21.9	2.72	91
203	-20.3	2.82	100

An attempt to replace the third phenyl group (Scheme 27) with chlorine using Pannell's[96] method for replacing the first and second phenyl groups resulted in the recovery of only clean dichloride starting material. Substitution in this case is likely hindered by the increased dative interaction between Sn-O.
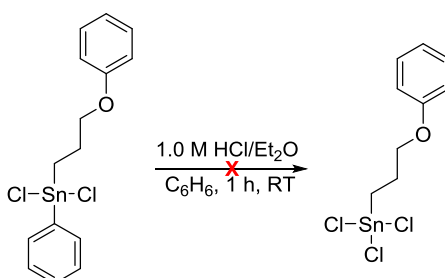
Scheme 28: Attempted synthesis of a tin trihalide.

2.1.4: Synthesis of hydrides:

LiAlH$_4$ was used as a reducing agent for the synthesis of compounds **202**-**205** from their respective halides (Scheme 28).

R = H, R′ = Ph **200**
R = R′ = Ph **201**
R = H, R′ = Cl **202**
R = Ph, R′ = Cl **203**

R = H, R′ = Ph **204** (70%)
R = R′ = Ph **205** (61%)
R = H, R′ = H **206** (81%)
R = Ph, R′ = H **207** (65%)
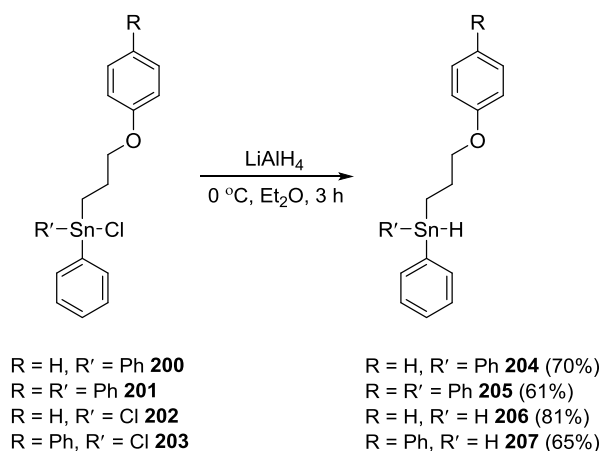
Scheme 29: Preparation of triorganotin hydrides and diorganotin dihydrides.

The ^{1}H NMR (C$_6$D$_6$) resonances for the hydrogen atoms attached to tin in organotin hydrides range from 4.50-7.50 ppm.[65] The spectrum of **207** showed a large $^1J_{117/119Sn-1H}$ coupling constant characteristic of most tin hydrides (Figure 32, Table 13).
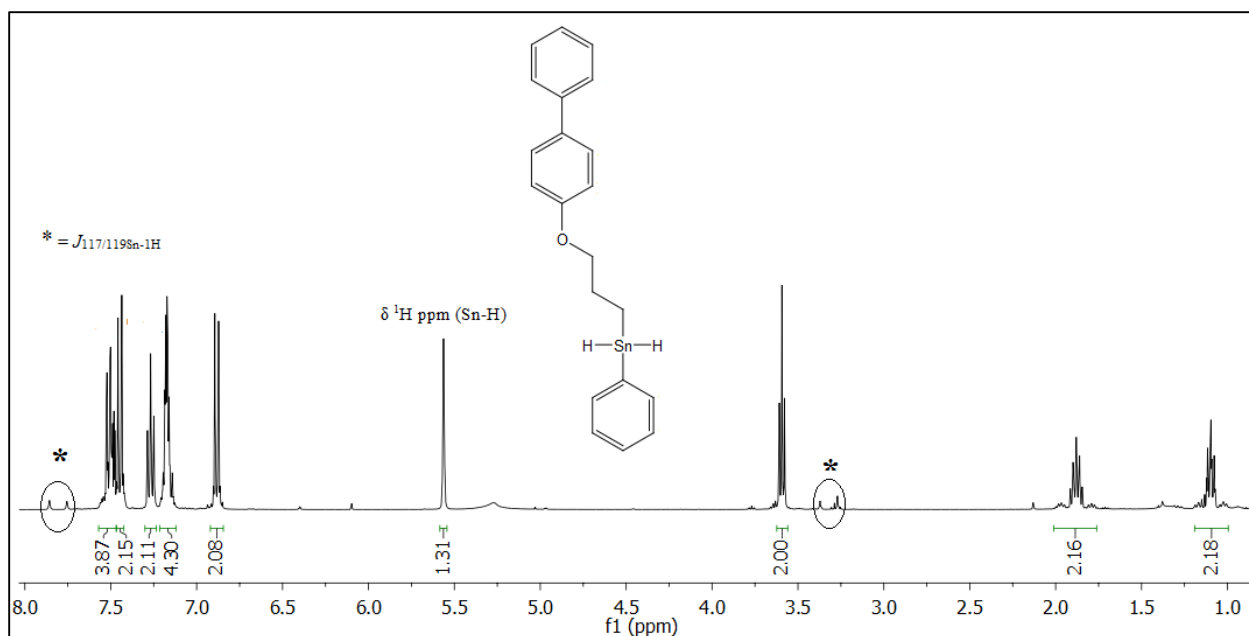
Figure 32: ^{1}H NMR (C$_6$D$_6$) spectrum of **207**.

A comparison of coupling constants in Table 13 suggest that the dative interaction between Sn and O atoms for organotin hydrides causes a slight increase in the magnitude of the coupling constants as compared to dihydrides. The ^{119}Sn and ^{1}H NMR (C$_6$D$_6$) chemical shifts for several tin hydrides (**204**-**207** and **69**, **70**) are listed in Table 13.

Table 13: ^{119}Sn NMR (C$_6$D$_6$) data for organotin hydrides.

Compound	δ ^{119}Sn or δ ^{117}Sn (ppm)	δ ^{1}H(ppm) Sn-H	$J_{119/117Sn-1H}$(Hz)
69	-225.9[a]	6.17-6.04	1615/1703[72] 1987/1883
70	-244.5[a]	6.78-6.64	1940/1853[72] 2155/2059
204	-137.0	6.35	1856/1776
205	-137.0	6.36	1862/1780
206	-215.1	5.59	1837/1754
207	-215.0	5.54	1835/1754

2.1.5: Dimerization of 204 and 205:

Dimerization of **204** and **205** was achieved by catalytic dehydrocoupling using Pd(PPh$_3$)$_4$. The distannane **208** was purified by column chromatography using hexane:EtOAc (1:1) and **209** by extraction with petroleum ether. Similar distannanes having a hypercoordinate donor interaction were previously reported by Rupnicki *et al.*[70]

R = H **204**, Ph **205**   R = H **208**, Ph **209**
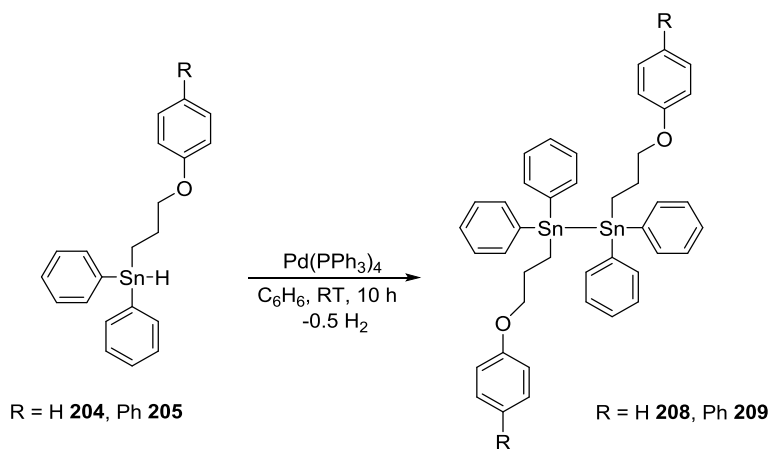
Scheme 30: Synthesis of distannanes **208** and **209**.
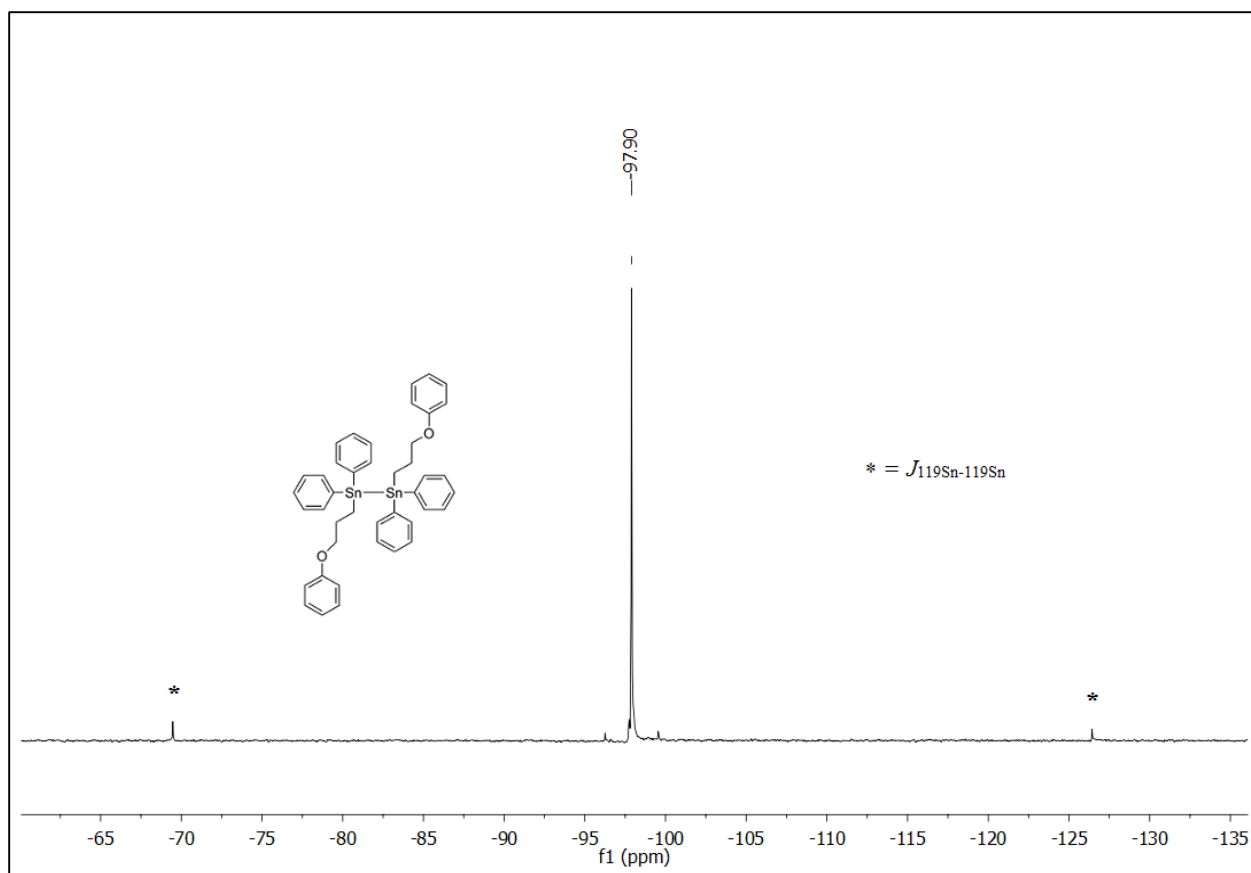
Figure 33: ^{119}Sn NMR (C$_6$D$_6$) spectrum of **208**.

Generally, the value of $J_{119Sn-119Sn}$ couplings increase with an increase of the coordination number at the Sn atom. A comparison of the $J_{119Sn-119Sn}$ coupling of distannanes with and without a potential coordinating ligand is given in Table 14.

Table 14: Comparison of $J_{119Sn-119Sn}$ distannanes with and without a coordinated ligand.

Compound	J^{119}Sn-^{119}Sn (Hz)	Non-coordinated analogue	J^{119}Sn-^{119}Sn (Hz)
208	8527	Ph$_6$Sn$_2$	4470[151]
209	-	Ph$_6$Sn$_2$	4470[151]
210	8925[70]	Ph$_6$Sn$_2$	4470[151]
211	6294[70]	(n-Bu)$_6$Sn$_2$	2748[151]
212	3796[70]	(n-Bu)$_6$Sn$_2$	2748[151]
213	11272[153]	(n-Bu)$_6$Sn$_2$	2748[151]
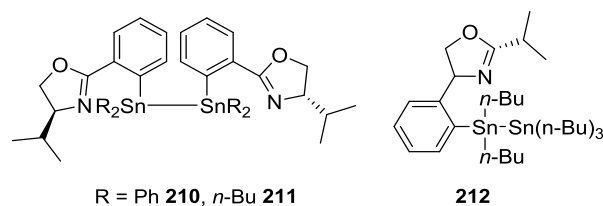
Scheme 31: 5-coordinate distannanes.

The values of $^1J_{119Sn-119Sn}$ couplings for aryl-substituted distannane **208** having Sn-O interactions are distinctly higher than Ph$_6$Sn$_2$. In the case of known distannanes **211** and **212**, replacement of one or two n-butyl groups in (n-Bu)$_6$Sn$_2$ by the 2-(4-isopropyl-2-oxazolinyl)-5-phenyl ligand results in an increase of 1048 and 3500 Hz for the $^1J_{119Sn-119Sn}$ coupling compared ro Ph$_6$Sn$_2$. A remarkable increase of the $^1J_{119Sn-119Sn}$ to 2748 Hz to 11272 was caused by replacement of two n-butyl groups in (n-Bu)$_6$Sn$_2$ with electronegative acetoxy groups due to the Sn-O interactions in n-Bu$_4$Sn$_2$(OAc)$_2$ **213**.[145]

2.1.6: Compounds containing *C,O*-chelating ligand:

2.1.6.1 Benzyl methyl ether:
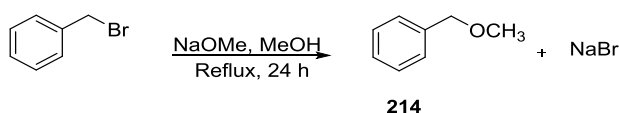
Scheme 32: Synthesis of benzyl methyl ether.

Compound **214** was prepared by reacting benzyl bromide with NaOMe in low yield (34%). This synthetic route was attempted as a means to reduce costs as it is considerably less expensive than bromobenzyl bromide.[152] Due to the low yield of this intermediate, it was abandoned and bromobenzyl bromide was used exclusively for the preparation of all *C,O*-chelating ligands.

2.1.6.2 2-Bromobenzyl methyl ether:
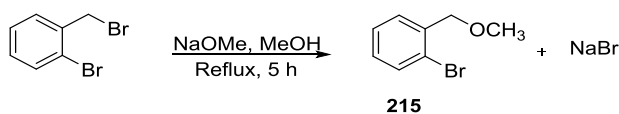
Scheme 33: Synthesis of 2-bromobenzyl methyl ether.

Compound **215** was prepared in good yield (84%) using bromobenzyl bromide and NaOMe (Scheme 33). [95,153] It is a stable compound and was used for further reactions.

2.1.6.3 [2-(MeOCH₂)C₆H₄]Li:
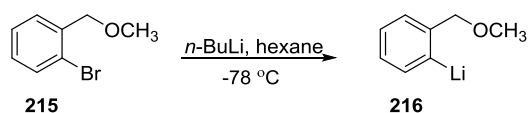
Scheme 34: Lithiation of 2-bromobenzyl methyl ether.

Compound **215** was treated with *n*-BuLi at -78 ℃ in hexane and the reaction mixture stirred overnight. The solvent was decanted in the glove box and the solid washed with additional fresh hexane. The residual solvent was then removed under reduced pressure and the product stored under inert atmosphere for further use. Surprisingly, compound **216** was found to be extremely sensitive and violently decomposed while transferring to a flask (Figure 34) from the weighing dish in the glove box. Thereafter, this product was only prepared *in situ* for use in all further reactions.

Figure 34: Flask containing the decomposed product of **216**.

70

2.1.6.4 2-Trialky/arylstannylbenzyl methyl ether:
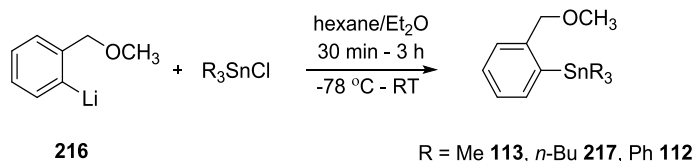
Scheme 35: Synthesis of 2-Trialky/arylstannylbenzyl methyl ether.

Compound **113** was obtained in a 70 % yield and isolated as a clear oil. This yield was somewhat less than that reported for **113** in the literature (84 %).[95] The ^{119}Sn resonance for **113** was -32.5 ppm (CDCl$_3$) and is shifted slightly downfield from the reported value (δ = -38.2 ppm obtained in d^{8}THF at -78 °C). The stannylbenzyl methoxy ethers **112** and **217** were prepared in a manner similar to that used for **113**. Compound **217** was obtained as yellow-brown coloured oil in good yield (65 %) while compound **112** was recovered as a white solid in 73 % yield with a melting point of 95 °C (Scheme 35). Gilman *et al.*[94] had previously synthesized **112** in a 35 % yield by reacting (*o*-MeOCH$_2$C$_6$H$_4$)MgBr with Ph$_3$SnCl. He reported a melting point of 94.5 - 95.5 °C for **112** however no NMR characterization was provided.

2.1.6.5 2-Chloroalkyl/arylstannylbenzyl methoxy ethers:
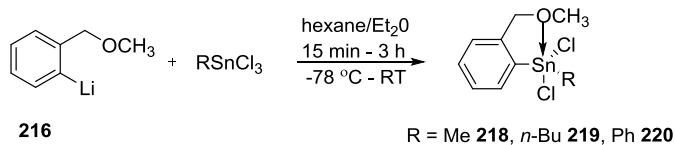
Scheme 36: Synthesis of dichloroalkyl/arylstannylbenzyl methoxy ethers.

Compounds **218**-**220** were prepared as brown coloured oils by addition of **216** to a pre-cooled (-78 °C) hexane/Et$_2$O solution of the appropriate organotin halide. Compounds **218** and **219** were isolated after extraction of their crude mixtures with toluene and hot hexane, respectively. The ^{119}Sn NMR (CDCl$_3$) analysis showed only a single resonance for both **218** (δ = -54 ppm) and **219** (δ = -60.0 ppm). The ^{119}Sn NMR spectrum of **220** revealed two unidentified peaks of small

intensity at $\delta = -48.0$ and -132.0 ppm, along with the main resonance at $\delta = -28.0$ ppm. Purification of compound **220** by hot hexane extraction was unsuccessful even after several attempts. The reported resonance for the closely related compound **118** prepared by Pannell *et al.*[96] was found at $\delta = -32.69$ ppm with the (o-MeOC$_6$H$_4$)CH$_2$ ligand instead of (o-MeOCH$_2$C$_6$H$_4$) used for **220**.
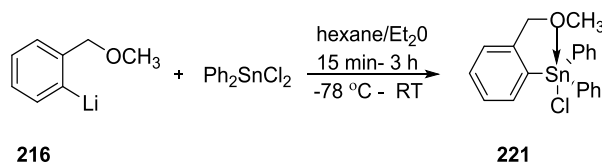
Scheme 37: Synthesis of the chloro(2-(methoxymethyl)phenyl)diphenylstannane **221**.

Compound **221** was obtained as white coloured solid after precipitating the product in hexane at -20 °C. The ^{119}Sn NMR (CDCl$_3$) chemical shift for the recovered monochloride solid **221** was -127.0 ppm (Scheme 37). The soluble fraction from this reaction in hexane displayed a ^{119}Sn NMR chemical shift at -136.0 ppm which is similar to the chemical shift observed for **225** (see page 74). Compound **221** was also obtained by reacting compound **112** in C$_6$H$_6$ with 1.6 M HCl solution in Et$_2$O in a 81% yield; this is considerably higher than in Scheme 38. An attempt to convert the monochloride, **221** to the dichloride by further reaction with the HCl solution was undertaken (Scheme 38). This reaction resulted in only unreacted **221**, which might be due to the presence of a substantial Sn-O interaction in the monochloride. ^{119}Sn NMR chemical shifts, Sn-O bond distances and yields of stannanes **112**-**113** and **217**-**221** are listed in Table 15.
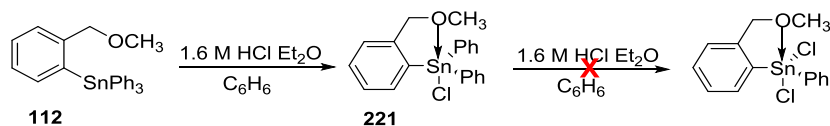
Scheme 38: Alternative route for the synthesis of chloro(2-(methoxymethyl)phenyl)arylstannane.

Table 15: ^{119}Sn NMR chemical shifts of selected stannanes.

Compound	^{119}Sn chemical shift(δ) ppm	Unsubstituted analogue	^{119}Sn chemical shift(δ) ppm	Δ ^{119}Sn chemical shift(δ) ppm
112	-133.0	-	-	-
113	-32.5	-	-	-
217	-40.3	-	-	-
218	-54.0	PhMeSnCl$_2$	55.1[154]	99.1
219	-60.9	Ph(n-Bu)SnCl$_2$	-	-
220	-28.2	Ph$_2$SnCl$_2$	-33.0[22]	-3.8
221	-127.2	Ph$_3$SnCl	-45.0	82.2
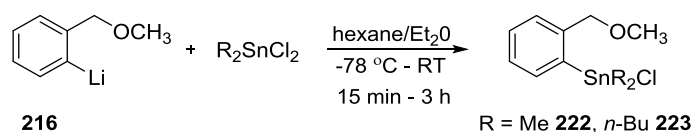
Scheme 39: Attempted synthesis of *o*-chlordialkylstannyl benzyl methyl ether.

The syntheses of **222** and **223** shown in Scheme 39 did not yield clean products. The reaction of **216** with Me$_2$SnCl$_2$ showed five resonances by ^{119}Sn NMR spectroscopy, along with a signal of higher intensity at -71.0 ppm. No assignments of this mixture was made and no further attempts to purify this material were undertaken. Similarly, the reaction of **216** with (n-Bu)$_2$SnCl$_2$ showed six unassigned ^{119}Sn NMR signals and could not be purified by extraction with hexane. The oily reaction mixture was stored in the glove box and after 30 days, an off-white coloured solid material separated from the oil. The solid was then washed with hexane and its ^{119}Sn NMR (CDCl$_3$) spectrum showed two resonances at -91.0 and -138.0 ppm of unequal intensities. This may be due to the exchange of the axial and equatorial positions of Cl atom attached to the tin. When Cl is in axial position, it pulls the electron density from tin and promotes a strong Sn-O interaction which may be absent if the Cl occupies an equatorial position (Figure 35). An accurate mass determination by mass spectrometry was consistent for a structure with a formulae **223**.
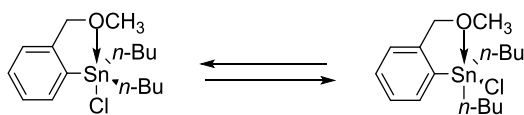
Figure 35: Possible structural isomers of **223**.

Bis-chelate compounds **224**-**225** were synthesized according to Scheme 39. The crude products of these reactions were not successfully purified by extraction techniques, however NMR (^{1}H, ^{13}C, ^{119}Sn) and mass spectrometry of the crude products **224**-**225** were obtained. The ^{119}Sn NMR of both **224** and **225** showed three resonances, along with a signals of higher intensity at -73.0 ppm and -136 ppm respectively.

225   **216**   **224**
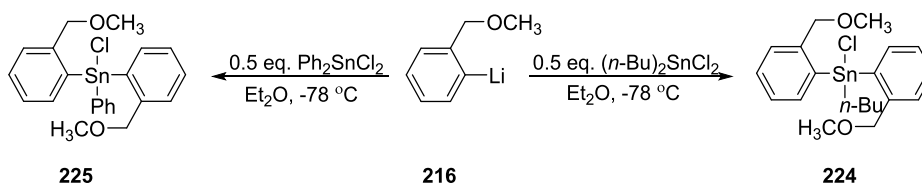
Scheme 40: Attempted synthesis of **224**-**225**.

2.1.6.6 Dihydridoalkylstannylbenzyl methyl ether:

R = Me **218**, *n*-Bu **219**   R = Me **226**, *n*-Bu **227**
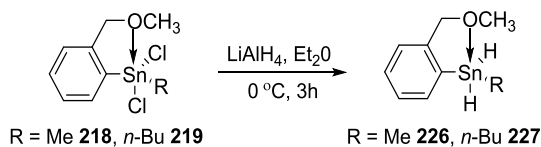
Scheme 41: Synthesis of dihydridoalkylstannyl benzyl methy ethers.

Donor–acceptor interactions between Sn and O in hypervalent compounds have been previously confirmed by small molecule X-ray diffraction techniques as well as by NMR spectroscopy.[45,155-156] Dakternieks *et al*. obtained new triorganotin and tin hydrides containing either the chiral 2-(4-isopropyl-2-oxazolinyl)-5-phenyl or the 2-(4-isopropyl-2-oxazolinyl)-5-(methyl)phenyl ligand.[68] The ^{1}H NMR spectroscopy of **227** (Figure 36) show distinct $^{119/117}$Sn-H coupling constants which are larger than the structurally similar tetracoordinate tin compounds (Table 16).

Table 16: ^{119}Sn NMR data of tin dihydrides with or without coordinating ligand.

Compound	^{119}Sn NMR (ppm)	$^1J_{119/117Sn-1H}$ (Hz)	R$_2$SnH$_2$ analogue	^{119}Sn NMR (ppm)	$^1J_{119Sn-1H}$ (Hz)
226	-221.0	1727	PhMeSnH$_2$	-110[157]	1835
227	-210.0	1770/1677	PhBuSnH$_2$	105[157]	-

To the best of our knowledge, these are the first examples of the organotin dihydrides containing a *C,O*-chelating ligand (Figure 36).
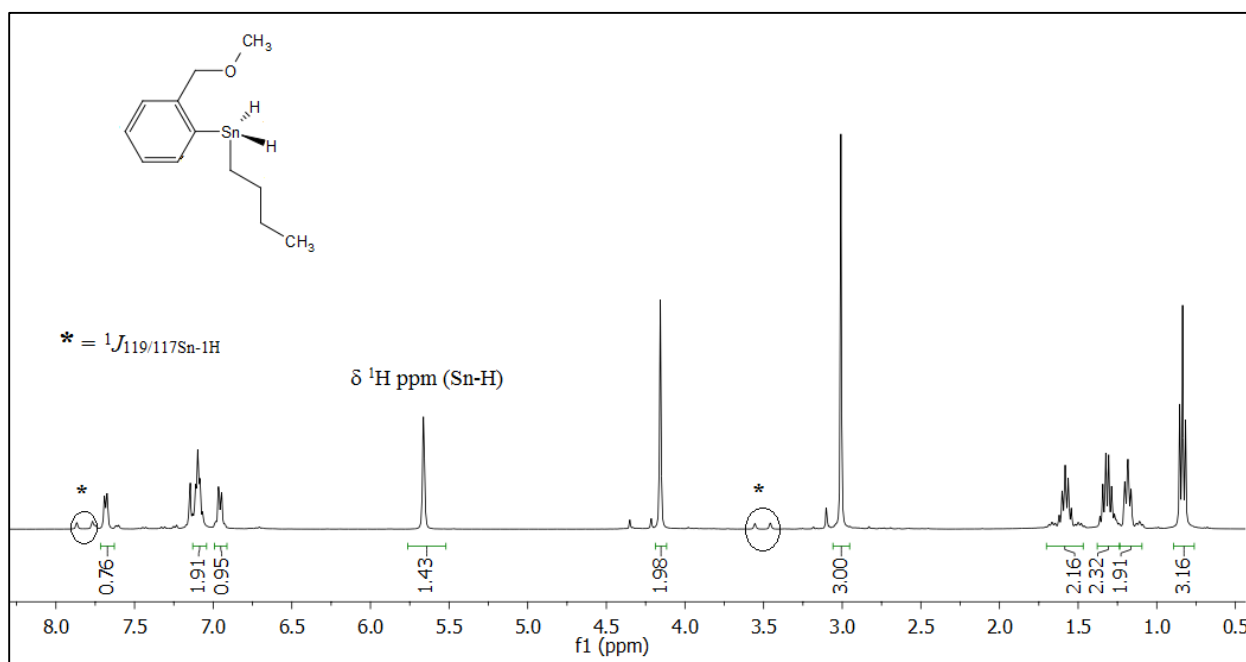
Figure 36: ^{1}H NMR (C$_6$D$_6$) spectrum of **227**.

2.1.7 Organotin compounds containing a *C,N*-chelating ligand

The synthesis of 2-bromo-*N,N*-dimethylbenzylamine (**228**) was unsuccessfully attempted using a literature preparation involving the reaction of 2-bromobenzyl bromide and dimethylamine (1:1.5) at room temperature for 6 h.[158] However, this *C,N*- ligand was prepared in high yield (88%) and purity by heating 2-bromobenzyl bromide with an excess of dimethylamine. The product was recovered by extraction with 3M HCl, 20% NaOH and finally with DCM.[159]

Compounds **33**, **35** and **37** were obtained according to Scheme 42 by reacting **229** with either MeSnCl$_3$, *n*-BuSnCl$_3$ or PhSnCl$_3$ respectively. Compound **33** was previously reported by

van Koten *et al.*[59] from the reaction of $[2\text{-}(Me_2NCH_2)C_6H_4]Cu$ with $MeSnCl_3$ in C_6H_6. Varga *et al.*[45] and Novák *et al.*[29a] reported the synthesis of **37** and **35** by treating **229** with *n*-$BuSnCl_3$ or $PhSnCl_3$ in C_6H_6 and the crude product purified by extraction with hot petroleum ether and hexane respectively. Compound **35** was also prepared by Rippstein *et al.*[48] using Et_2O as a solvent, followed by toluene extraction. The diorganotin dihalides **33, 35** and **37** reproduced in this study were synthesized using Et_2O as a solvent and purified by extraction with hot hexane.
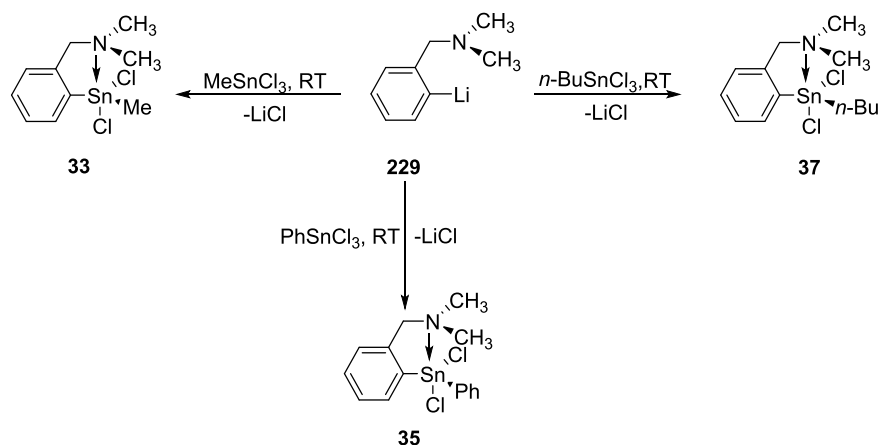
Scheme 42: Preparative routes to compounds **33**, **35**, **37**.

The intramolecular Sn-N interaction and relative change in the Lewis acidity at the Sn center of hypervalent compounds can be monitored by ^{119}Sn and ^{13}C NMR spectroscopy. Three parameters can be used to determine the strength of Sn-N interaction: a distinct upfield shift of ^{119}Sn NMR signals of these compounds as compared to their analogues before ligand substitution, an increase in the coupling constants (^{119}Sn, ^{13}C), and the presence of ($^2J_{119Sn\text{-}CH3}$) coupling constant between the tin and amino methyl group. A distorted TBP geometry was expected for diorganotin dihalides (**33**, **35**, **37**) having an aryl and R group at equatorial positions, while the amino ligand occupies an axial position, leaving one axial and one equatorial position for the two halogen atoms.[33,47,55]

The ^{1}H NMR spectra of compounds **33**, **35**, and **37** display a downfield shift to about 8.2 ppm for the ortho protons of C$_6$H$_4$- ring, which is similar for other known tin TBP compounds.[59] The increase in $^2J_{119Sn-1H}$ coupling constant to 80 Hz for **33** also indicates the existence of TBP geometry. The upfield shift in the ^{119}Sn NMR to -96.4, 169.4, -104.0 ppm (Table 17) for these compounds **33**, **35**, and **37**, as compared to their corresponding unsubstituted analogues (MeSnCl$_3$: 21.0 ppm, PhSnCl$_3$: -63.0 ppm, n-BuSnCl$_3$: 6.0 ppm respectively) provide strong evidence for a substantive Sn-N intramolecular interaction and TBP geometry.

Table 17 : ^{119}Sn NMR (CDCl$_3$) chemical shift values of tin dichlorides containing a *C,N*-chelating ligand.

Compound	^{119}Sn NMR (ppm)		Yield (%)	
	Lit.	Found	Lit.	Found
33	-94[26, 59]	-96.4[a]	96	85
35	-170[29a, 48]	-169.4	68	69
37	104.3[29b, 51, 160]	-104	86	73

[a] d-toluene

The hydrogenation of **33** and **37** was successfully attempted by reaction with LiAlH$_4$ (Scheme 43). Compound **228** could not be hydrogenated using the same technique.

R = Me **33**, *n*-Bu **37**   R = Me **230**, *n*-Bu **231**
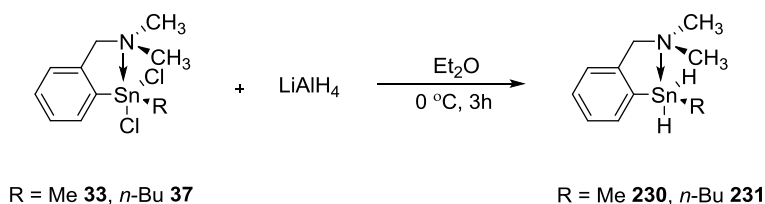
Scheme 43: Preparation of tin dihydrides containing a *C,N*-chelating ligand.

Hydrides **230** and **231** possess a typical ^{1}H NMR resonance shifted downfield (δ = 5.73 ppm and δ = 5.62 ppm) compared to the stannyl dihydrides (n-Bu)$_2$SnH$_2$ (4.78 ppm)[40] and Me$_2$SnH$_2$ (4.46 ppm).[161] Another characteristic of diorganotin hydrides is that the $^1J_{119Sn-1H}$ coupling constants (1760 Hz for **230**, 1860 Hz for **231**) are larger than tetracoordinate diorganotin

hydrides (Me$_2$SnH$_2$ 1758 Hz; (n-Bu)$_2$SnH$_2$ 1675 Hz). The [119]Sn chemical shifts of **230** and **231** are -236 ppm (Figure 37) and -217 ppm respectively, and are significantly shifted upfield when compared to their structurally closest analogs (n-Bu)PhSnH$_2$ at 105 ppm and MePhSnH$_2$ -110 ppm.[157] These results suggest the presence of a stronger intramolecular Sn–N coordination in **230** than in **231**.
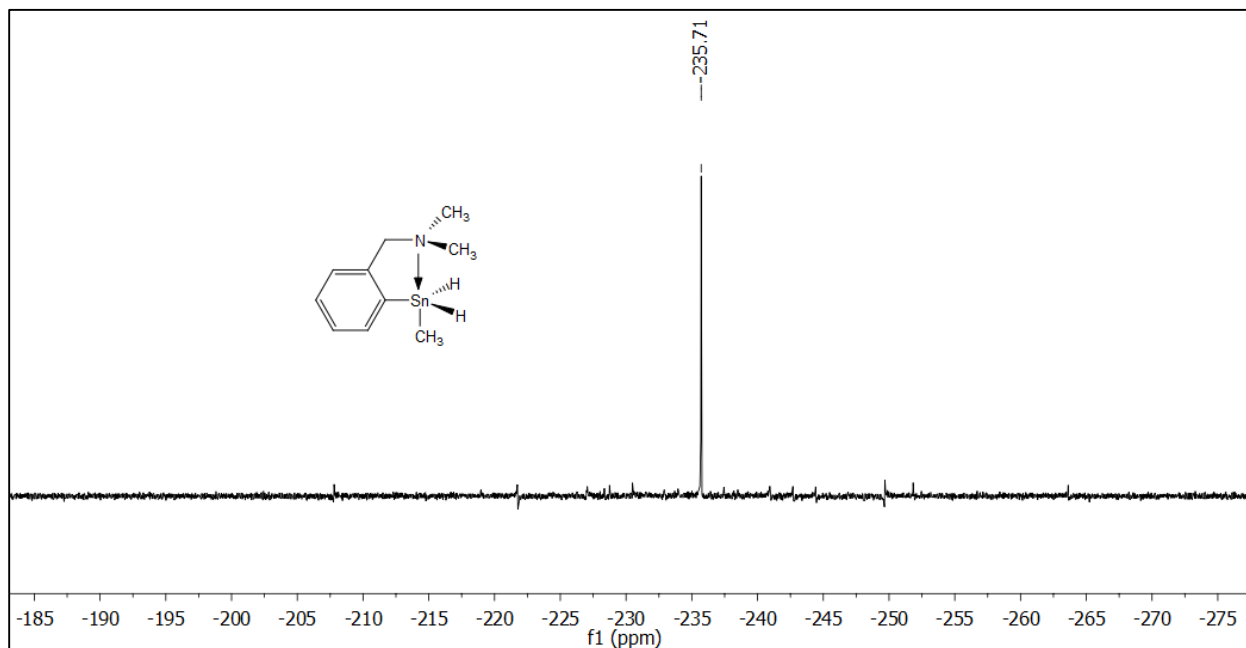
Figure 37: ^{119}Sn NMR(C$_6$D$_6$) spectrum of **230**.

The range of [119]Sn chemical shifts for dihydrides may be explained on the basis of the differing electron donating ability of methyl and n-butyl groups of **230** and **231** respectively. The hydride ligand would likely be more apicophile in **230** than in **231** for these structurally confined pentacoordinated tin centers. Unfortunately, no crystal structure determinations by X-ray crystallography are yet available for these dihydrides to compare with structural information obtained from solution NMR spectroscopy.
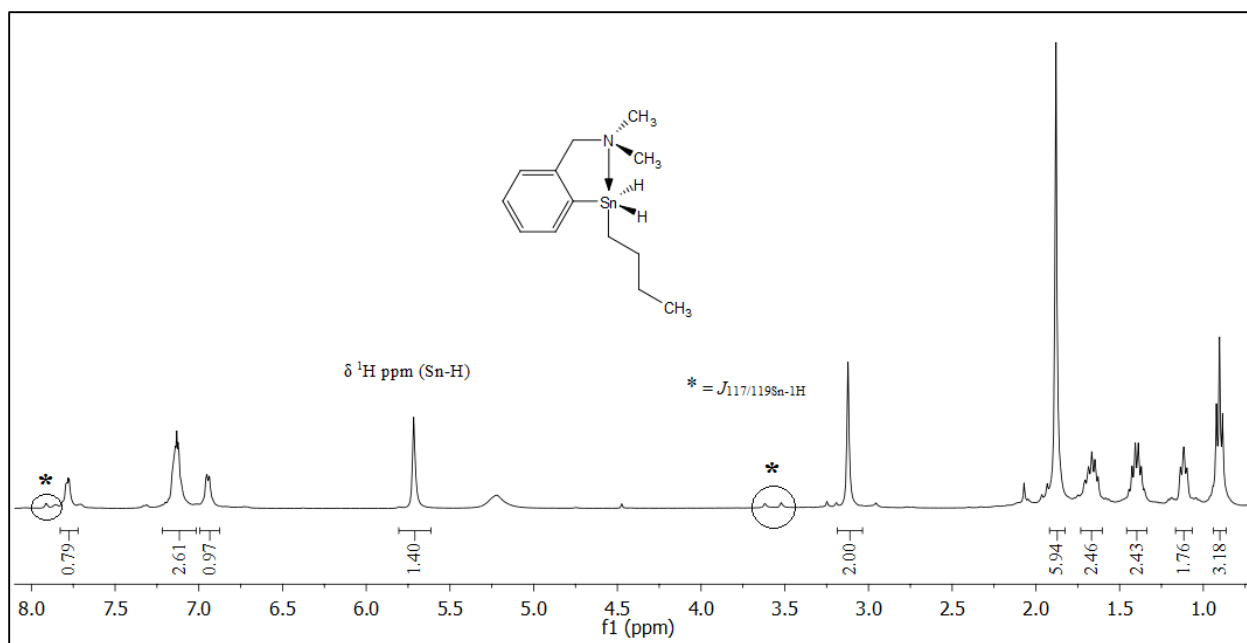
Figure 38: ^{1}H NMR (C$_6$D$_6$) spectrum of **231**.

In the literature there are only two reported examples (**69**, **70**)[72] of stannyl dihydrides with Sn-N interactions. The presence of dative Sn-N coordination is evident from the increase of $^1J_{119Sn\text{-}1H}$ and presence of $^3J_{119Sn\text{-}13C}$ (Sn-CH$_2$) coupling values for **230** and **231** compared to four coordinate analogues.

Table 18: Coupling constant values for tin dihydrides.

Compounds	^{119}Sn NMR ppm	$^1J_{119Sn\text{-}1H}$ (Hz)	Sn-CH$_2$ $^3J_{119Sn\text{-}13C}$ (Hz)
(*n*-Bu)$_2$SnH$_2$	-203	1675[40]	-
PhMeSnH$_2$	-110[157]	1835[73]	-
69[72]	-225.9	1703, 1987	-
70[72]	-244.5	1940, 2155	-
230	-217.5	1860	22.7
231	-236.0	1760	24.3

At temperatures above room temperature, compound **231** evolved gas (presumably H$_2$) and decomposed changing from a light yellow to orange coloured semi-solid. Analysis of these residues by ^{119}Sn NMR revealed the complete absence of the resonance at -217.5 ppm in the orange

product and presence of a mixture of unidentified tin containing species. The use of LiAlH$_4$ as a reducing agent for **35** appeared to favour a redistribution reaction. The ^{119}Sn NMR spectrum of the product showed a resonance at -181 ppm, similar to value reported earlier by Turek *et al.*[66] for **232**. A softer hydrogenating agent, NaBH$_4$, was then used and a yellow coloured oil obtained (Scheme 44). Once again the ^{119}Sn NMR resonance at -181 ppm corresponded to the presence of the redistribution product **232** and a second unidentified resonance at -223 ppm which may be the dihydride. No further characterization of this compound was attempted at this time.

232 **35**
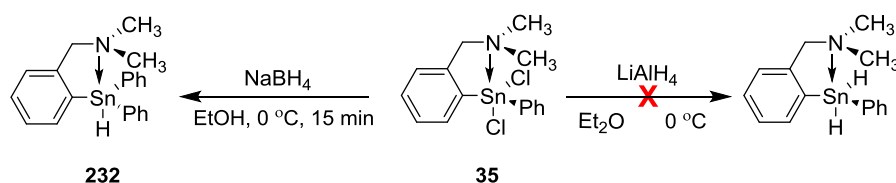
Scheme 44: Attempted synthesis of an aryltin dihydrides containing a *C,N*-ligand.

2.1.8 Compounds containing *C, S*-chelating ligand:

2.1.8.1 1-bromo-2-(*n*-propylthiomethyl) benzene

R = *n*-Pr **233**, Ph **234**
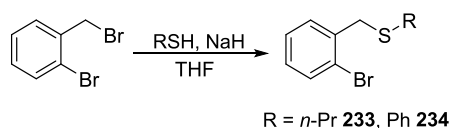
Scheme 45: Synthesis of *C,S*-ligands thiol.

A previously reported method was used for the synthesis of **233** and **234**.[105] Compounds **233** and **234** were obtained after adjustment of the ratios of thiol and 2-bromobenzyl bromide (1.5:1). The use of a 1:1 ratio resulted in a substantial amount of unreacted 2-bromobenzylbromide. Similar types of thiols having R = *i*-Pr, *t*-Bu substituents were also reported in literature.[104,105]

2.1.8.2 Tributylstannylbenzyl thioether:
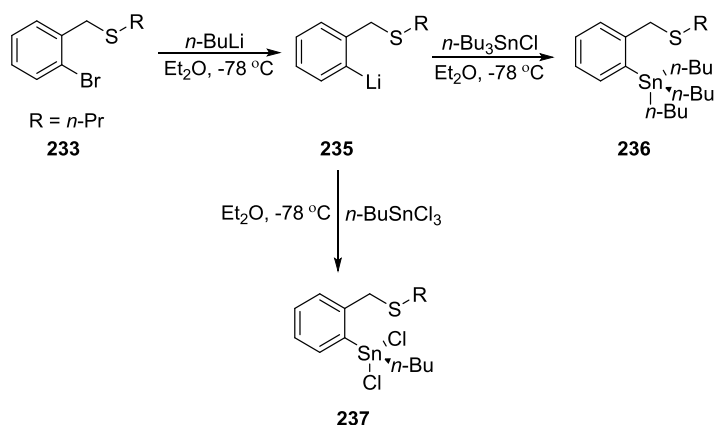
Scheme 46: Synthesis of tributylstannylbenzyl thioether.

An attempt to prepare compounds **236** and **237** by an initial lithiation of **233** followed by the reaction with n-Bu$_3$SnCl and n-BuSnCl$_3$ is shown in Scheme 45. NMR (^{1}H, ^{13}C and ^{119}Sn) spectroscopy revealed the presence of multiple products. The ^{119}Sn spectrum showed three resonances; a chemical shift at $\delta = 140.0$ for the starting material n-Bu$_3$SnCl, and two unassigned resonances at 103.0 and 94.0 ppm (Figure 39). This reaction was also attempted with n-BuSnCl$_3$ under the same conditions; analysis by ^{119}Sn NMR spectroscopy of the reaction mixture gave chemical shifts at -54 and -78 ppm (Figure 40). Both crude reaction mixtures could not be purified using extraction techniques. The alkyl region in both the ^{1}H NMR and ^{13}C NMR spectra of these compounds display extra resonances which have not been assigned. No further characterization of these reaction mixtures was attempted at this time.
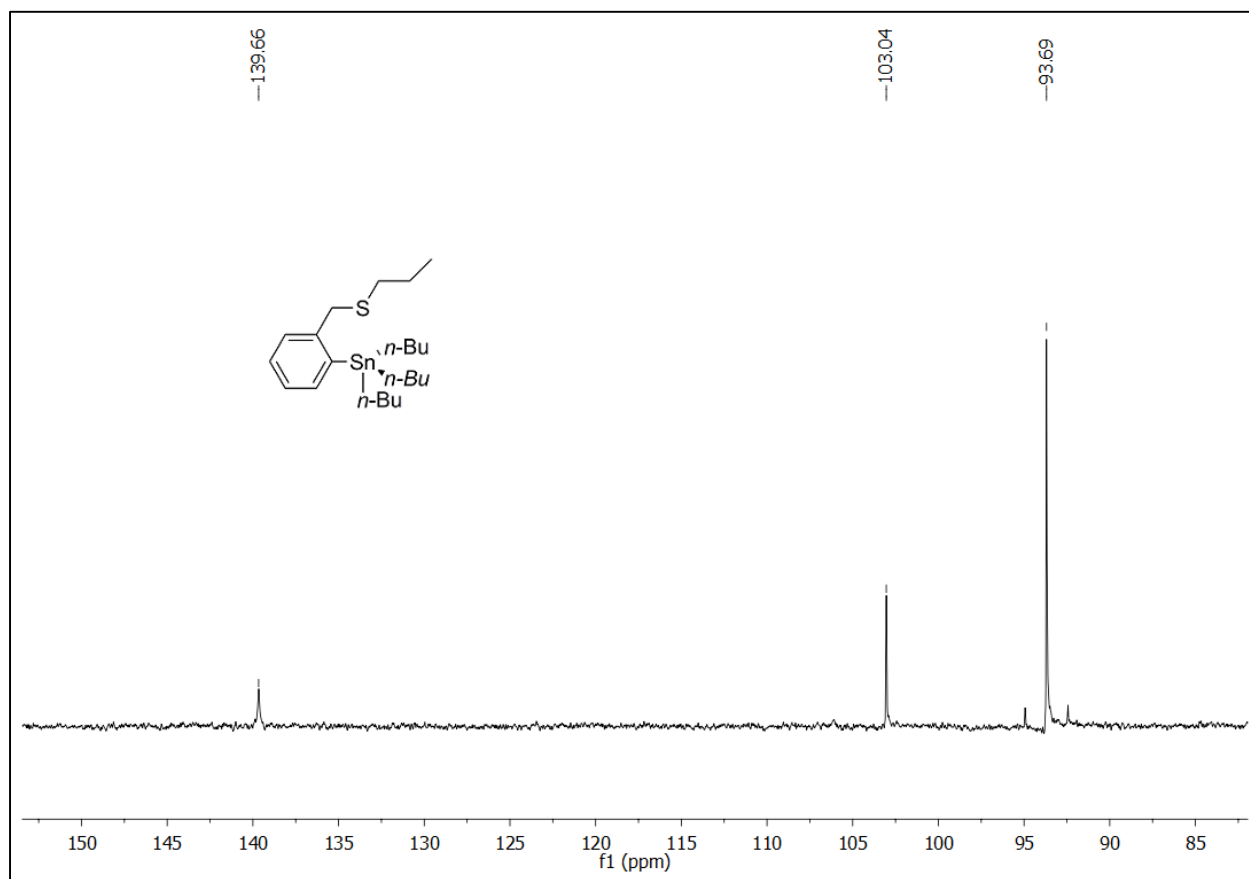
Figure 39: ^{119}Sn (CDCl$_3$) NMR spectrum of **236**.
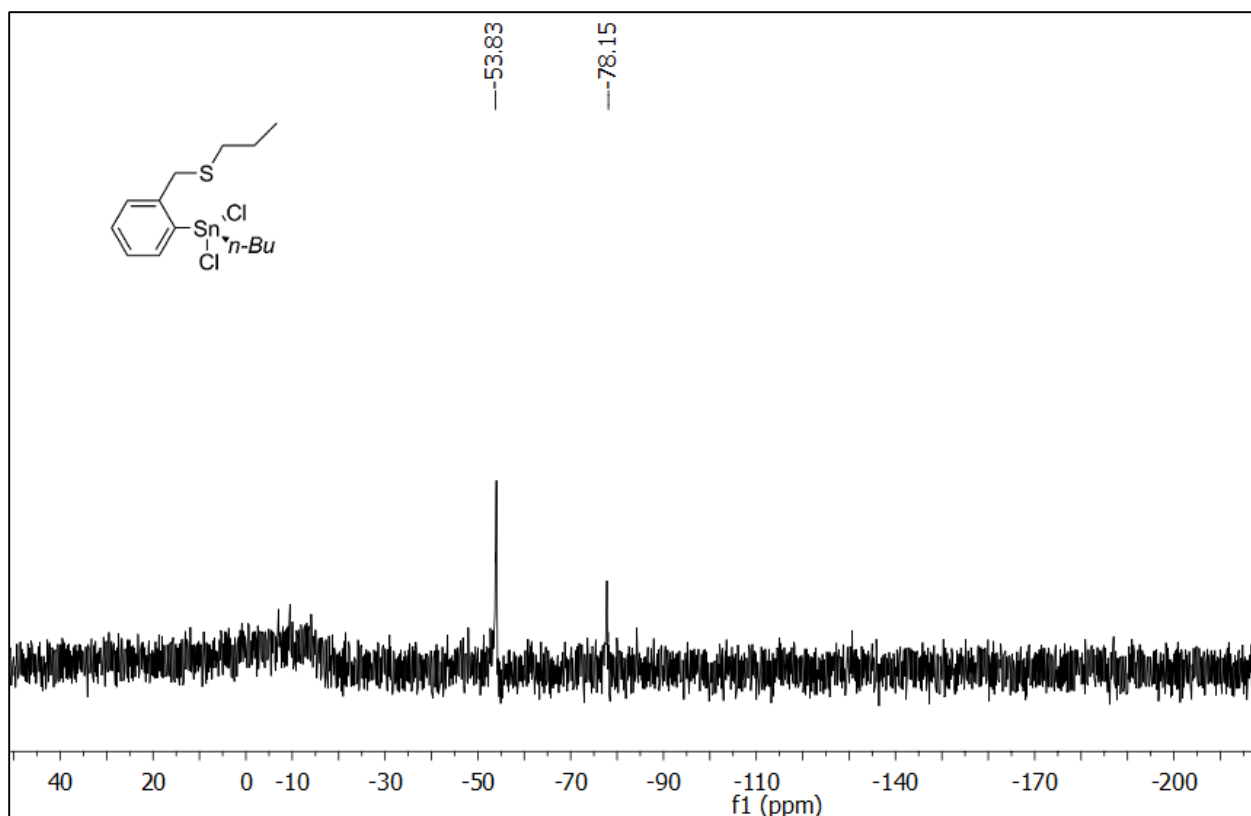
Figure 40: ^{119}Sn (CDCl$_3$) NMR spectrum of **237**.

R = *n*-Pr
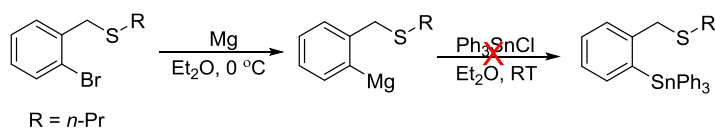
Scheme 47: Synthesis of triphenylstannylbenzyl thioether.

The reaction of Ph$_3$SnCl with the thiobenzyl ether Grignard reagent as shown in Scheme 47 was

unsuccessful. The ^{119}Sn NMR spectroscopy revealed the resonances only for the unreacted starting

material, Ph$_3$SnCl (δ = -45.0 ppm).

2.1.9 Compounds containing *C,P*-chelating ligand:

2.1.9.1 Synthesis of (*o*-bromobenzyl)-diphenylphosphine:
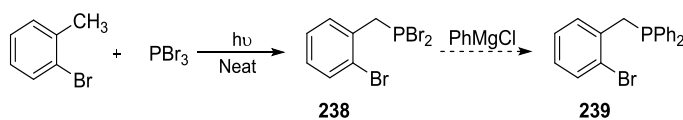
Scheme 48: Attempted route for UV- light catalyzed synthesis of o-(Ph$_2$PCH$_2$)C$_6$H$_4$Br.

The reaction mixture shown in Scheme 48 was irradiated with UV light for 4 h. ^{31}P NMR spectroscopy revealed a resonance at 173 ppm, which was assigned to the target compound **238**. Unreacted PBr$_3$ and four other unidentified peaks (Figure 41) were also observed. The reported yield for this compound is 27%.[162] An attempt to make same product through Grignard synthesis was also tried, but was unsuccessful.
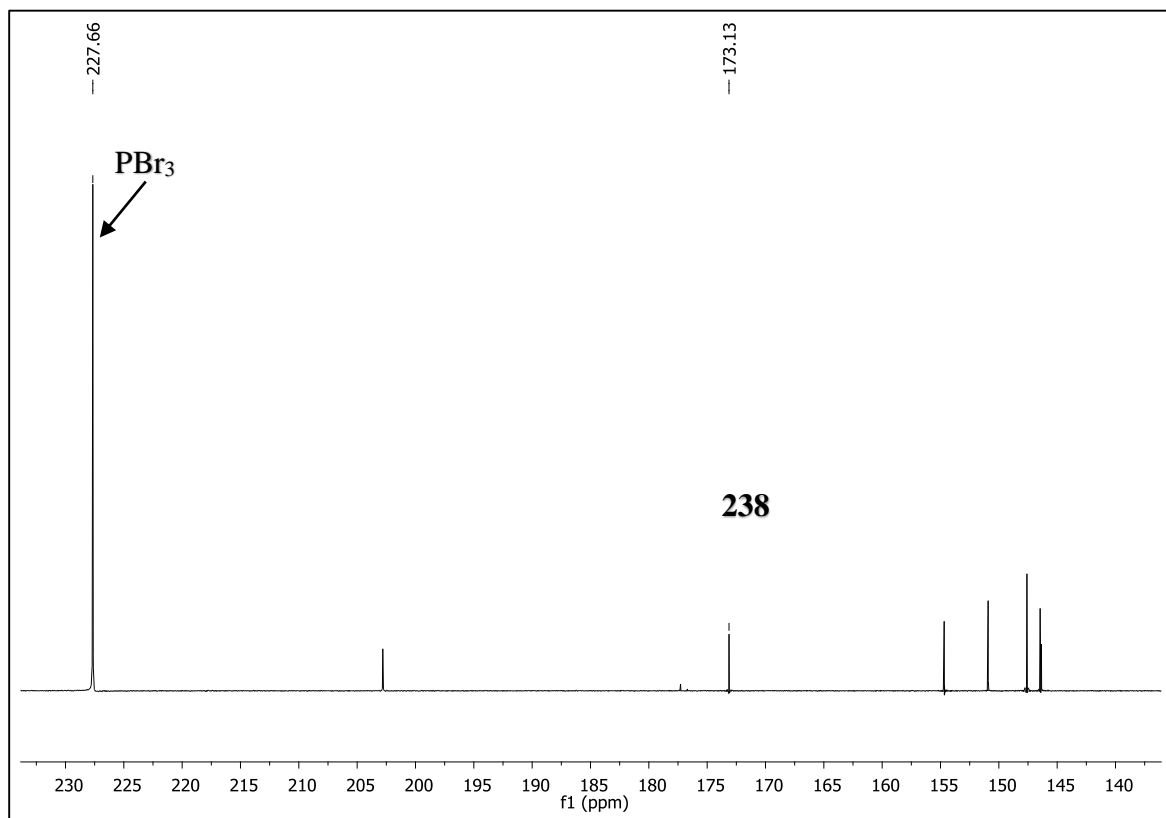
Figure 41: ^{31}P NMR (CDCl$_3$) spectrum of compound **238**.
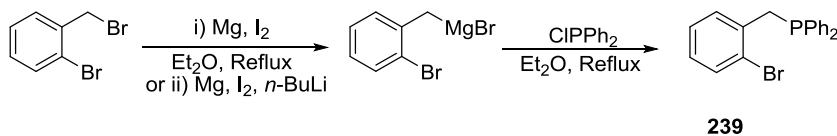
Scheme 49: Synthetic route for the intermediate **239**.

^{31}P NMR spectroscopy showed two resonances at -72.0 ppm and -82.0 ppm (which corresponds to ClPPh$_2$). There was no indication of product formation with a reported ^{31}P NMR resonance for **239** at -12.0 ppm.[163] The crude product was suspended in Et$_2$O and the insoluble component analysis of this residue removed by decantation. The residual solvent was removed under reduced pressure and a ^{31}P NMR analysis of the recovered solid showed a resonance at -14.8 ppm corresponding to the previously reported disubstituted phosphine **240** along with two other unassigned peaks at -21.0 ppm and -40.0 ppm.

240
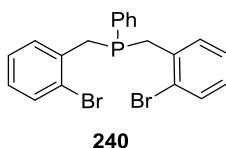
Figure 42: Structure of **240a**.

Compound **239** was successfully prepared by using a method reported by Telleson *et al.*[164] The addition of few drops of *n*-BuLi to activate the Mg is the only difference from Scheme 49. NMR data obtained agreed with that reported in literature (Figure 43).[164]
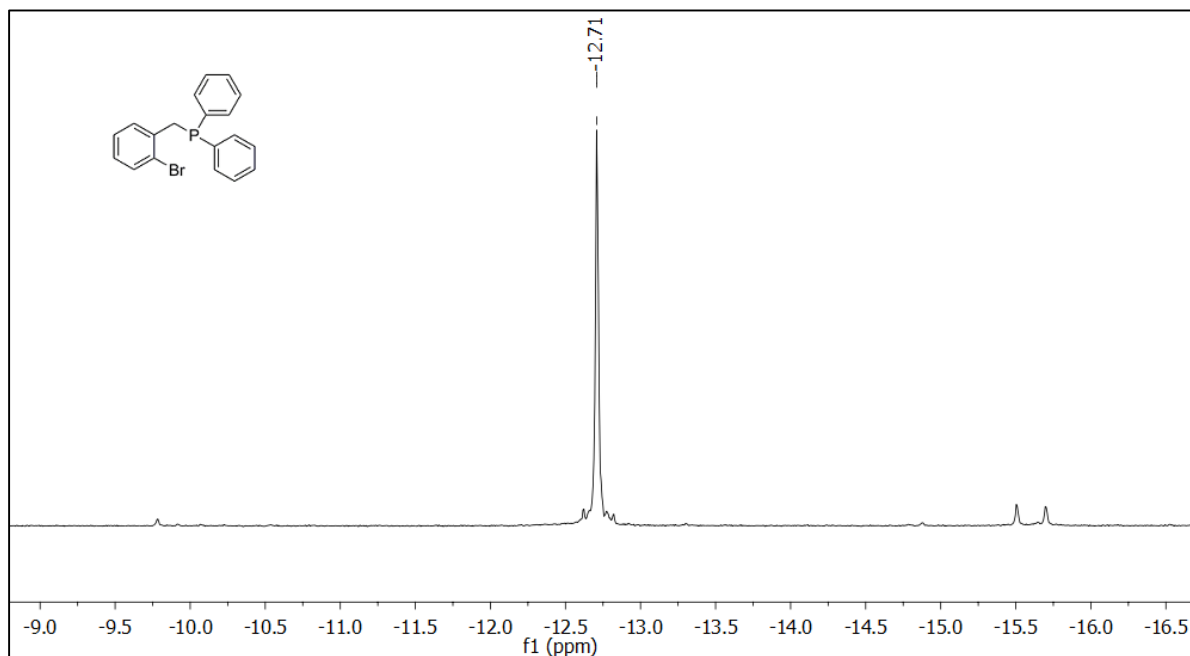
Figure 43: ^{31}P NMR (CDCl$_3$) spectrum of compound **239**.

2.1.9.2 (*o*-(diphenylphosphino)benzyl)stannanes:

The lithiated intermediate **240a** was synthesized by following the method reported by Gossage *et al.*,[115] and isolated as orange-red powder (Scheme 50). After washing with hexane, (*o*-(diphenylphosphino)benzyl) lithium was suspended in dry C_6H_6 and treated with solution of either Ph_3SnCl or $PhSnCl_3$ in C_6H_6 to prepare **241** and **242** respectively. The ^{119}Sn NMR spectrum of **241** showed a single resonance at δ = -85.0 ppm and the ^{31}P NMR spectrum a resonance at δ = -9.8 ppm. Similarly, the reaction of **240a** with $PhSnCl_3$ showed a ^{119}Sn resonance at δ = -27.0 ppm and ^{31}P NMR resonance at δ = 43.0 ppm with four unidentified small impurity peaks. No further characterization of these compounds was attempted at this time.
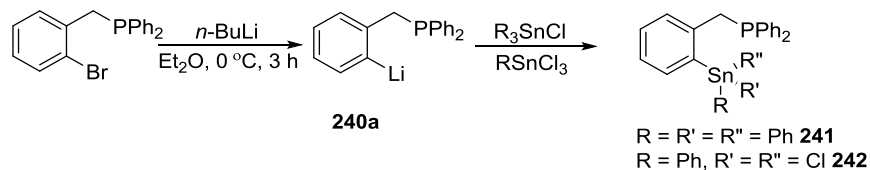
Scheme 50: Synthesis of (*o*-(diphenylphosphino)benzyl)stannanes.

2.2 Characterization and Properties:

Crystal structure data for the dibromostannane **146**, similar to compounds prepared in this study (**200**, **201**, **202**, **203**) was previously reported by Molloy *et al.*[43] Compound **198** was recrystallized in methanol, while **200**, **201**, **202** and **203** were recrystallized using a 1:1 ratio of DCM:hexane. Crystallographic data for compounds **198**, **202**-**203** are listed in Table 19 and in Tables A1-A29 and the ORTEP representation of their unit cell components in Figure 45-48. The crystal structure determination of **198** (Figure 45) revealed a distorted tetrahedral geometry about tin with the central bond angles ranging from 103-117°. The absence of a Sn-O dative interaction in **198** may due to the steric bulk of three phenyl rings at tin. Compounds **200** (Figure 46), **201** (Figure 47), **202** (Figure 48) and **203** (Figure 49) all display a distorted trigonal bipyramidal

geometry around tin with angles ranging from 69.37º-166.3º and 73.22º-170.83º, 97.49º-169.78º, 99.53º-171.02º and 97.10º-168.62º respectively. There are two unique molecules found in the unit cell for **200** with substantially different Sn-O distances (2.72 and 2.89 Å). The distance between the datively bonded Sn and O atoms is 2.80 Å (average) in **200**, 2.81 Å in **201**, 2.72 Å in **202** and 2.82 Å in **203**. These values are smaller than the sum of the van der Waal's radii of oxygen and tin (3.70 Å) and larger than the sum of their covalent radii 2.066 Å.[161] The values reported here represent a medium to strong Sn-O dative interaction. Molloy *et al*. [43] observed a similar Sn-O distance of 2.734(4) Å for the hypercoordinated dibromo compound **146**. The significant increase in Sn-O interaction on replacing the phenyl group by Cl is likely due to a moderation of the Lewis acidity at Sn. In the structures of **200** and **202** the equatorial plane is formed by three carbon atoms while the axial positions are occupied by Cl and O atom. The values of the O-Sn-Cl bond angles are 166.30º(1A) and 170.83º(2A) for **200** and 171.02º for **202**. In **201** and **203** the equatorial plane is formed by one Cl and two carbon atoms while axial positions are occupied by Cl and O atoms and the values of the O-Sn-Cl bond angle are 169.78º for **201** and 168.62º for **203**. The dative interactions between Sn and O are found *trans* to Sn-Cl bond and nearly linear. For compounds **200**-**203** the Sn-C (phenyl) bond lengths are within the sum of covalent radii (2.15 Å) for tin and carbon.[165]

The strength of Sn-O interaction can impact the geometry of these molecules. The difference between the sum of equatorial angles and sum of the axial angles can be used to monitor the transition from tetrahedral to TBP geometry (Figure 43, Table 20).[96,101,166-168] This difference would be zero (Σeq-Σax = 328.5°- 328.5° = 0) for a tetrahedral geometry while for TBP geometry it would be 90°(Σeq - Σax = 360°- 270° = 90); the greater the value of (Σeq – Σax) more TBP the structure.
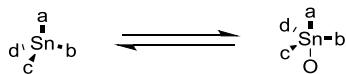
Figure 44: Transition from tetrahedral geometry to TBP.

The bond order is a measure of the strength of such interactions which is calculated using the following equation.[101,169,170]

$$BO = d(Sn\text{-}E_{ave}) + 1 - d(Sn\text{-}E)$$
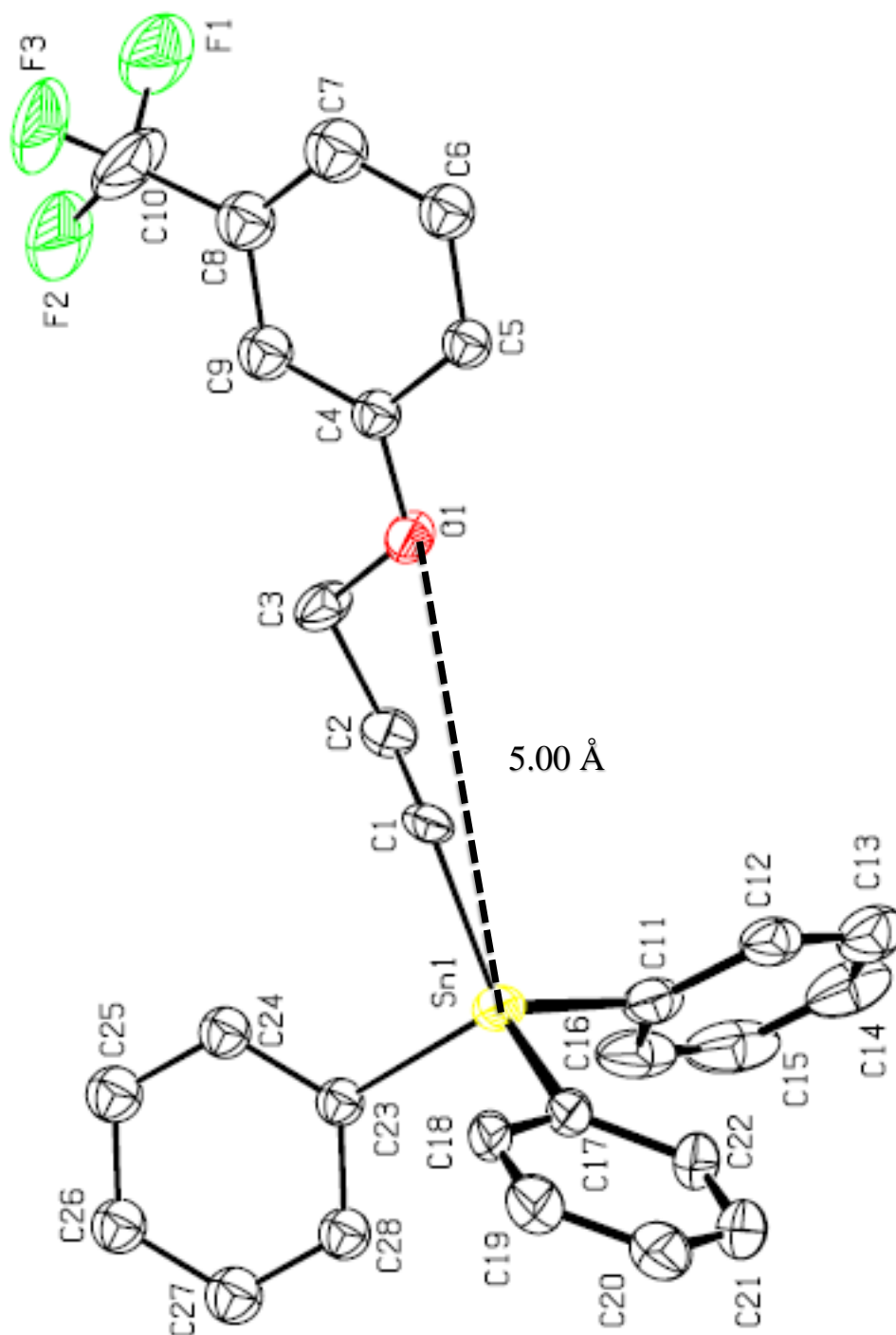
Figure 45: ORTEP representation of the unit cell components for **198**.
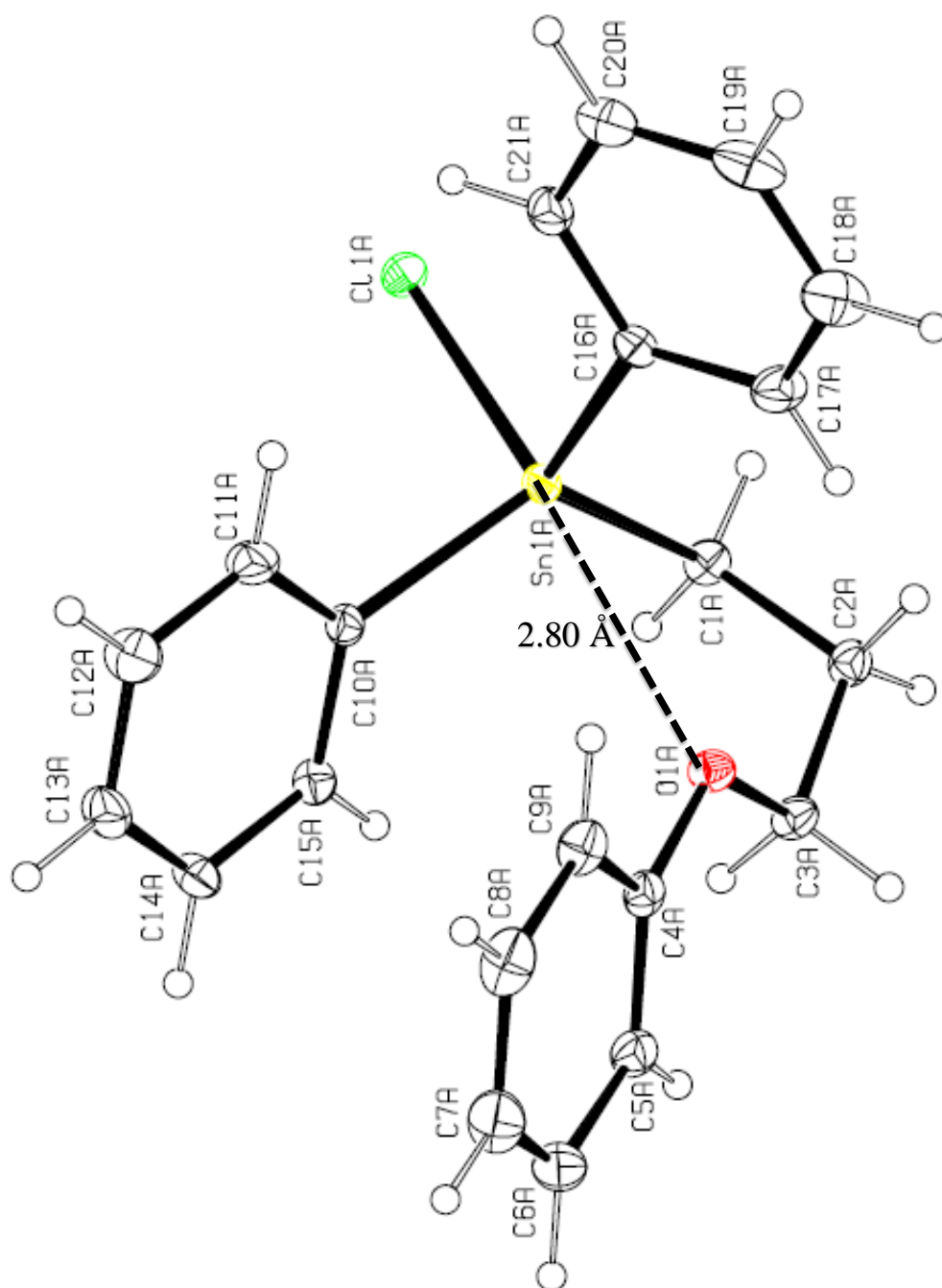
Figure 46: ORTEP representation of the unit cell (A) components for **200**.
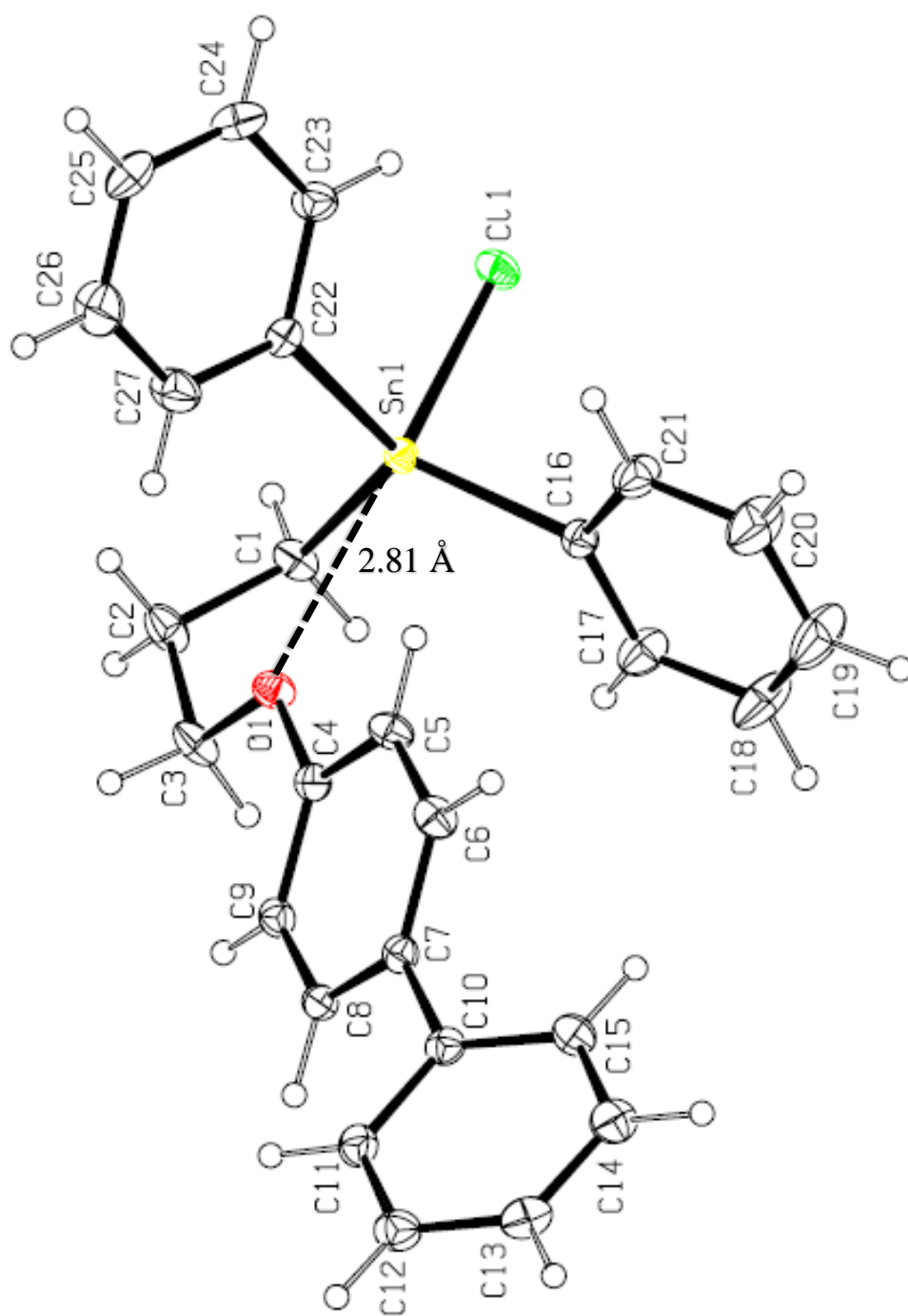
Figure 47: ORTEP representation of the unit cell components for **201**.
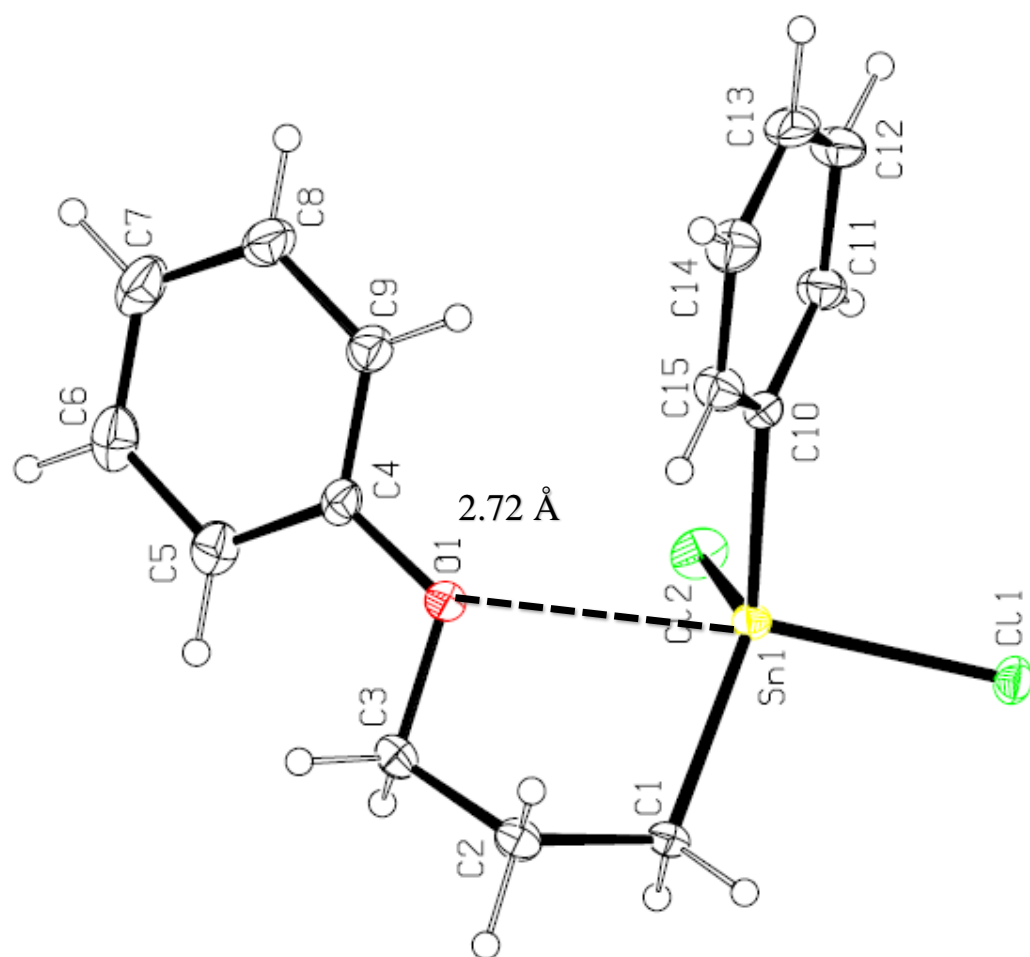
Figure 48: ORTEP representation of the unit cell components for **202**.
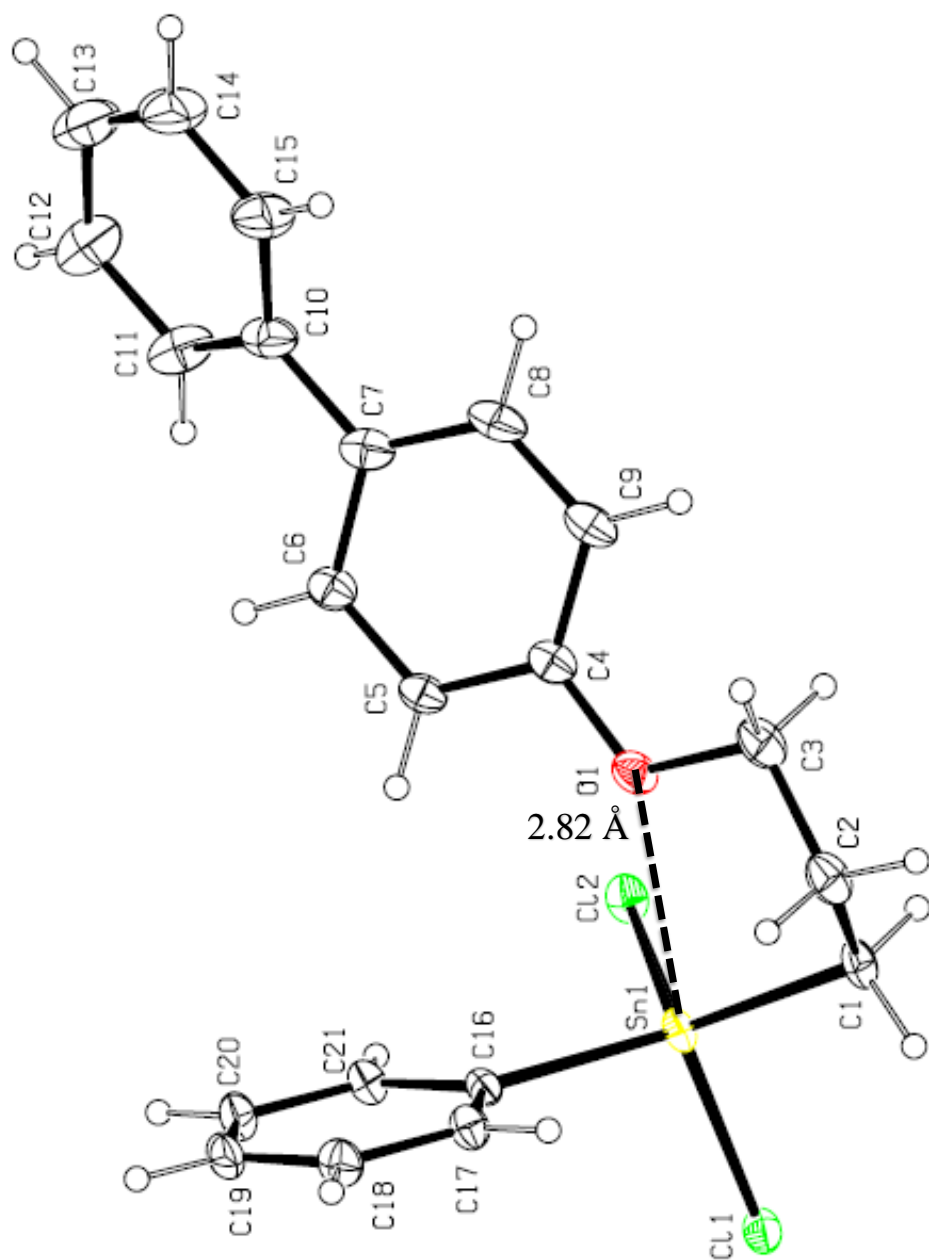
Figure 49: ORTEP representation of the unit cell components for **203**.

Table 19: Crystallographic data and structural refinement for compounds **198**, **200**, **201**, **202**, **203**

	198	200	201	202	203
Empirical formula	$C_{28}H_{25}F_3OSn$	$C_{21}H_{21}ClOSn$	$C_{27}H_{25}ClOSn$	$C_{15}H_{16}Cl_2OSn$	$C_{21}H_{20}Cl_2OSn$
Formula weight	553.17	443.52	519.61	401.87	477.96
Crystal system	Monoclinic	Triclinic	Monoclinic	Monoclinic	477.96
Space group	P 21/n	P – 1	P 21/c	P21	P 21/c
a [Å]	6.4331(31)	10.478(11)	9.7304(4)	6.0761(10)	14.2473(9)
b[Å]	12.192(2)	11.0954(12)	12.9001(5)	8.4920(14)	6.3874(4)
c[Å]	31.554(6)	16.9797(18)	18.5688(7)	15.752(3)	22.0483(13)
α = [deg]	90	89.678(2)	90	90	90
β = [deg]	90.14(3)	79.66(2)	91.177(1)	100.89	93.158
γ = [deg]	90	82.832(2)	90	90	90
Volume Å^3	2486.3(9)	1925.4(4)	2330.32(16)	798.1(2)	2003.4(2)
Z	4	4	4	2	4
Density [Mg/m^3]	1.478	1.530	1.481	1.672	1.585
Crystal size[mm]	$0.34 \times 0.08 \times 0.06$	$0.20 \times 0.09 \times 0.03$	$0.42 \times 0.27 \times 0.24$	$0.35 \times 0.23 \times 0.07$	$0.35 \times 0.12 \times 0.12$
θ range [deg]	2.56 to 25.12	1.219 to 27.481	1.92 to 27.50	2.634 to 27.487	1.431 to 27.536
Reflections collected	15431	63709	21942	12905	32922
Independent reflections, $R_{int.}$	4391, 0.0558	5347, 0.032	5347, 0.032	3126, 0.0171	4602, 0.0374
$T_{max.}$, $T_{min.}$	0.998 and 0.936	0.7456 and 0.6543	0.7456 and 0.6792	0.7456 and 0.6167	0.7456 and 0.6530
Data / restraints / parameters	4391 / 71 / 306	8816 /0 /433	5347 / 0 / 271	3126 / 1 / 172	4602 / 0 / 226
Goodness-of-fit on F^2	1.092	1.020	1.043	1.042	0.985
Final R indices [I>2σ(I)]	R1 = 0.0589 wR2 = 0.1152	R1 = 0.0161 wR2 = 0.0385	R1 = 0.0209 wR2 = 0.0503	R1 = 0.0129 wR2 = 0.0331	R1 = 0.0223 wR2 = 0.0474
R indices (all data)	R1 = 0.1023 wR2 = 0.0530	R1 = 0.0197 wR2 = 0.0402	R1 = 0.0252 wR2 = 0.1344	R1 = 0.0132 wR2 = 0.0333	R1 = 0.0311 wR2 = 0.0506
Largest diff. peak and hole [e.Å^{-3}]	0.679 and -0.988	0.370 and -0.350	0.523 and -0.286	0.503 and -0.360	0.784 and -0.476

Table 20: Data used to obtain the transition from tetrahedral to TBP for compounds **198**, **200**-**203**.

Compound	Sn-O Å	Equatorial angles	Σeq (deg)	Axial angles	Σax (deg)	Σeq- Σax (deg)	BO
198	5.00	C1-Sn-C17 C1-Sn-C11 C11-Sn-C17	330.2	C1-Sn-C17 C1-Sn-C23 C11-Sn-C23	328.8	1.4	-1.87
200	2.81	C1-Sn-Cl1 C1-Sn-C10 C10-Sn-Cl1	325.15	C1-Sn-Cl1 C1-Sn-C16 C10-Sn-C16	325.44	-0.29	0.32
201	2.81	C1-Sn-Cl1 C1-Sn-C22 C22-Sn-Cl1	315.16	C1-Sn-Cl1 C1-Sn-C16 C16-Sn-C22	334.15	-18.99	0.32
202	2.72	C1-Sn-Cl2 C10-Sn-C1 C10-Sn-Cl2	350.65	C1-Sn-Cl1 C10-Sn-C1 Cl1-Sn-Cl2	332.51	17.54	0.41
203	2.82	C16-Sn-Cl2 C16-Sn-C1 C1-Sn-Cl2	347.31	C1-Sn-Cl1 C16-Sn-C1 Cl1-Sn-Cl2	327.78	19.53	0.31

* Calculated using a Sn-O average bond distance of 2.14 Å

2.3 Polymerization and characterization:

2.3.1: Wurtz coupling:

The polymerization of **37** by Wurtz coupling under different conditions produced three products that were identified by ^{119}Sn NMR spectroscopy. The distannane[171] **243**, stannoxane bis-{[2-(*N*,*N*-dimethyaminomethyl)phenyl]*n*-butylchloro}tin oxide[171] **244** and the bis-{[2-(*N*,*N*-dimethyaminomethyl)phenyl]di-*n*-butyltin(IV) **245** were obtained from two reaction.[66] Previous work by Turek *et al.* [171] who prepared **243** by adding a solution (1:1 hexane/C_6H_6) of **37** to a K-mirror at -30 ºC that was stirred for one week at RT produced a single ^{119}Sn NMR resonance at δ = -88.1 ppm. Turek then bubbled oxygen through the solution containing **243** and converted it to **244** generating two ^{119}Sn NMR signals at -134.5 and -137.5 ppm that are presumably two possible stereoisomers **224a** and **244b**.
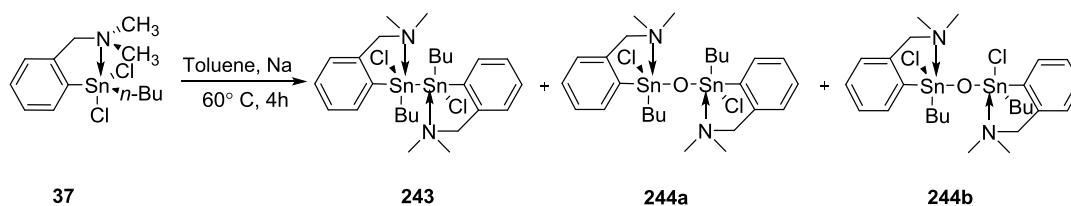
Scheme 51: Wurtz Coupling of **37** for 4 h.
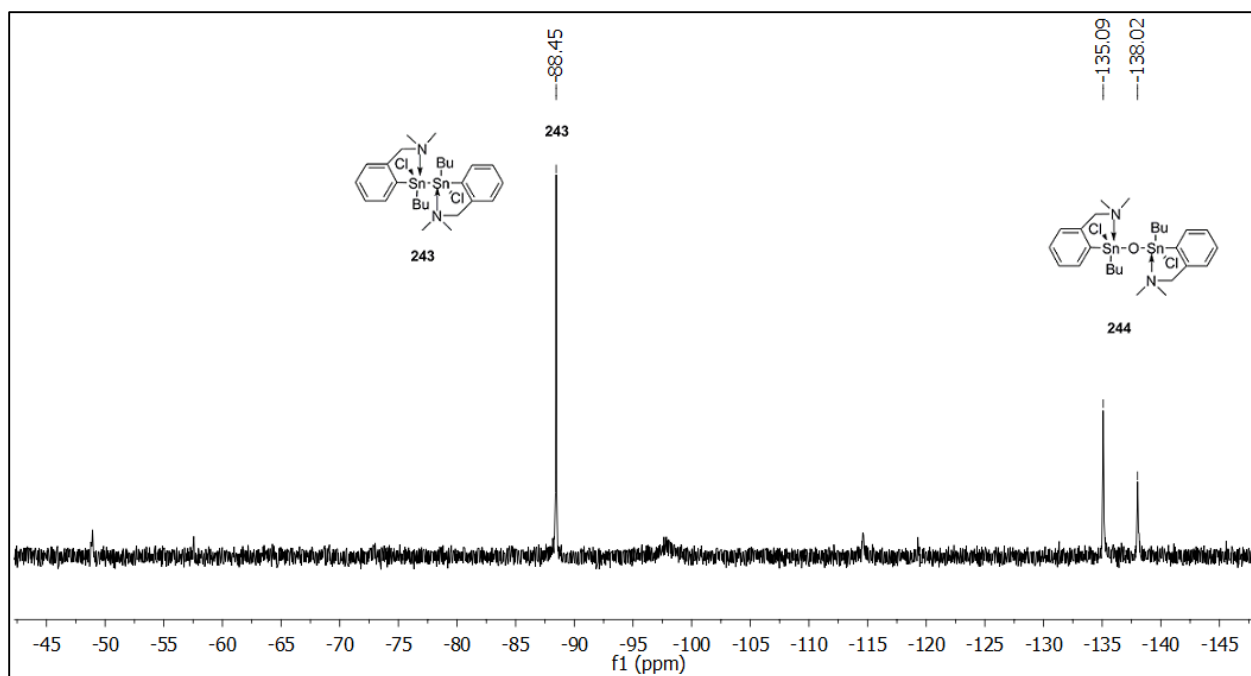
Figure 50: ^{119}Sn NMR (C$_6$D$_6$) spectrum of Wurtz coupling of **37** for 4 h at 60 °C.

For this study the reaction time was increased from 4 h to 4 days and **245** was produced along with other unidentified products. Turek *et al*.[66] also prepared **245** by reacting the K-mirror and L(*n*-Bu)$_2$SnCl in hexane for 5 days.
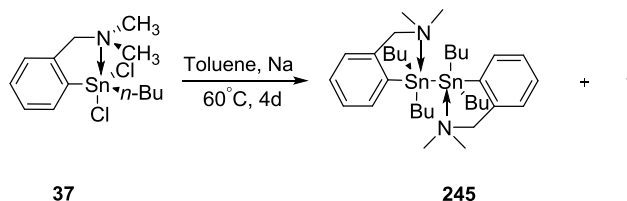
Scheme 52: Wurtz Coupling of **37** for 4 days.

The polymerization of **35** was attempted by the Wurtz method developed by Molloy *et al*.[127] for 4 h. The ^{119}Sn NMR showed resonances at δ = -173.0, -210.6 and -212.2 ppm. The resonance at -173.0 ppm was identified as **247**. After increasing the reaction time from 4h to 8h, ^{119}Sn NMR showed resonances at -145.5 ppm and -173.0 ppm corresponding to **246** and **247** respectively. Turek *et al*.[66] also prepared **246** by reacting the K-mirror and L(Ph)$_2$SnCl in hexane for 5 days at -30° C-room temperature.

Scheme 53: Na Wurtz Coupling of **35**.

Figure 51: ^{119}Sn NMR (C$_6$D$_6$) spectrum of the reaction mixture from the Wurtz coupling of **35**.

Table 21: ^{119}Sn NMR data for distannanes.

Compounds	^{119}Sn δ(ppm)		$^1J_{119Sn-119Sn}$ (Hz)	Ref.
	Literature	Found		
243	-88.1	-88.1	9219 (9221)[a]	171
244	-134.5, -137.5	-134.5, -137.5	-	171
245	-105.7	-105.7	-	66
246	-145.1	**-**145.5	5520 (5158)[a]	66
247	-173.2	-173.0	-	66

[a] Literature values

The results obtained by the Wurtz coupling of **35** and **37** are comparable to the previously reported values. Earlier polystannanes studies showed that the reduction of $(n\text{-Bu})_2\text{SnCl}_2$ using Na in toluene at 60 °C lead to high molecular weight polymer $\text{poly}(\text{Bu}_2\text{Sn})_n$ ($n \approx 4000\text{--}5000$) in addition to five and six membered cyclic oligomers in varying amounts.[127] On the other hand, the reduction of bulkier stannanes, such as $(t\text{-Bu})_2\text{SnCl}_2$, mainly produced smaller oligostannane rings, such as *cyclo*-$(t\text{-Bu}_2\text{Sn})_4$.[172] Beckmann *et al.*[145] reported that the reduction of *cis*-$\text{Myr}_2\text{SnCl}_2$ and *trans*-$\text{Myr}_2\text{SnCl}_2$ (Myr = myrtanyl) under same reaction conditions resulted in a mixture of unidentified products with the ^{119}Sn NMR spectra of the crude reaction mixtures of both revealing more than 10 signals. The reduction of *cis*-$\text{Myr}_2\text{SnCl}_2$ and *trans*-$\text{Myr}_2\text{SnCl}_2$ with Mg resulted in the exclusive formation of five-membered oligostannane rings *cyclo*-(*cis*-$\text{Myr}_2\text{Sn})_5$ and *cyclo*-(*trans*-$\text{Myr}_2\text{Sn})_5$. ^{119}Sn NMR (CDCl$_3$) spectra of *cyclo*-(*cis*-$\text{Myr}_2\text{Sn})_5$ and *cyclo*-(*trans*-$\text{Myr}_2\text{Sn})_5$ showed signals δ = −209.9 and −218.1 ppm which are close to the resonances obtained for the Wurtz coupled of **35** at δ = -210.6 and -212.2 ppm which are likely the 5- and 6-membered cyclics.

2.3.2 Dehydrocoupling:

2.3.2.1: Metal catalyzed dehydrocoupling:

The synthesis of polymers **248**-**250** are based on the metal-catalyzed dehydropolymerization (Scheme 54, 55) of a diarylstannane with different chelating ligands. As the polymerization proceeded, the colour of reaction mixture changed from colourless to yellow to dark orange and finally to dark brown for the solid polymer. Dehydrocoupling of the hypercoordinated compound **231** using Wilkinson's catalyst was unsuccessful. However polymerization did occur in the presence of Cp_2ZrMe_2 in hexane. The reaction was monitored by ^{1}H NMR spectroscopy until the signal for the Sn-H resonance completely disappeared. The solvent was removed under reduced pressure and the ^{119}Sn NMR (C_6D_6) analysis of the crude product

showed resonances at δ = -49.0, 114.0, 162.0 ppm. A portion of the crude product precipitated slightly in hexane and was filtered off. The solid was insoluble in common organic solvents. The ^{119}Sn NMR (C_6D_6) of the hexane soluble fraction was obtained and it revealed a sharp single resonance at -49 ppm (Figure 53).
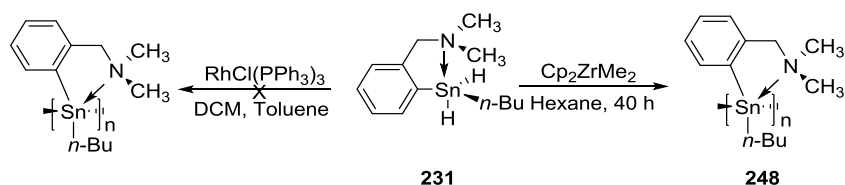
Scheme 54: Polymerization of **231**.
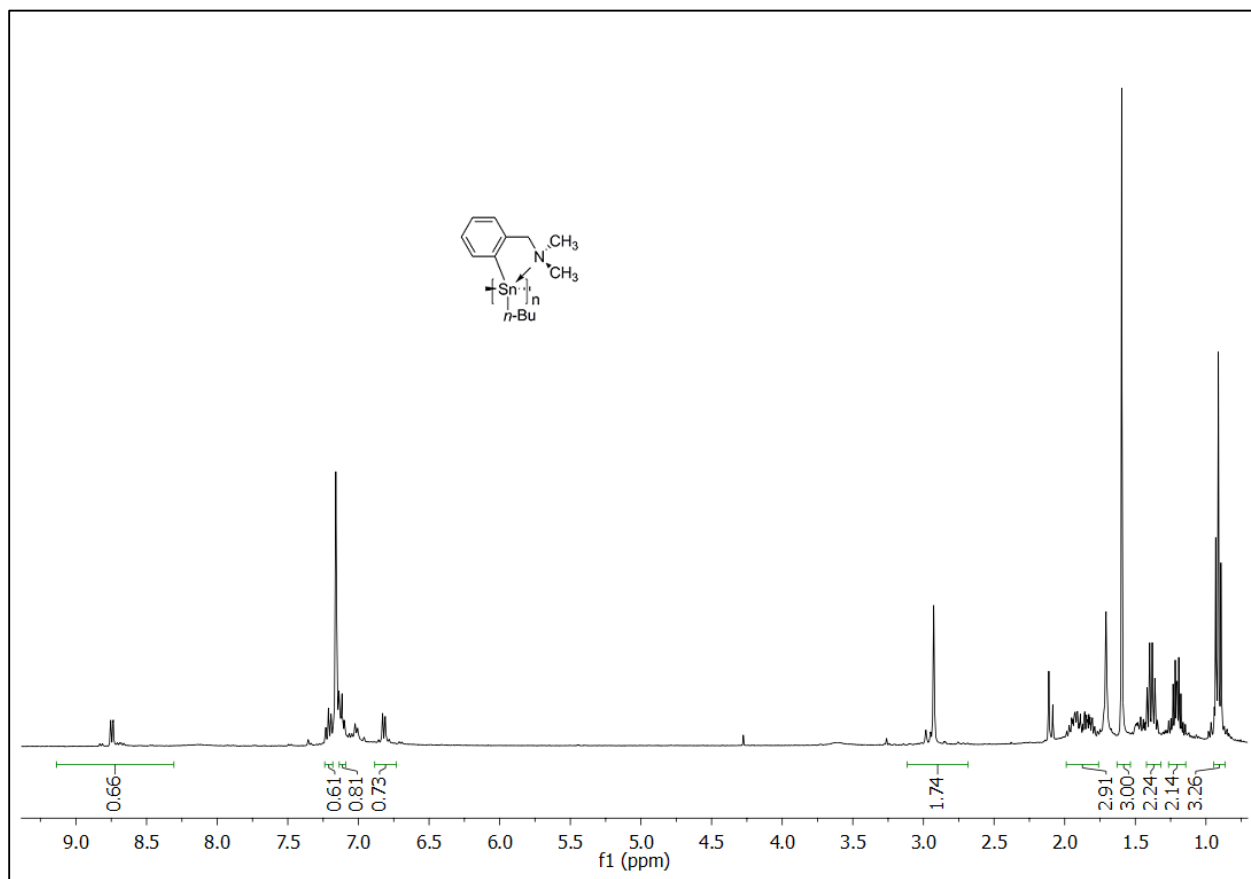
Figure 52: ^1H NMR (C_6D_6) spectrum of **248**.
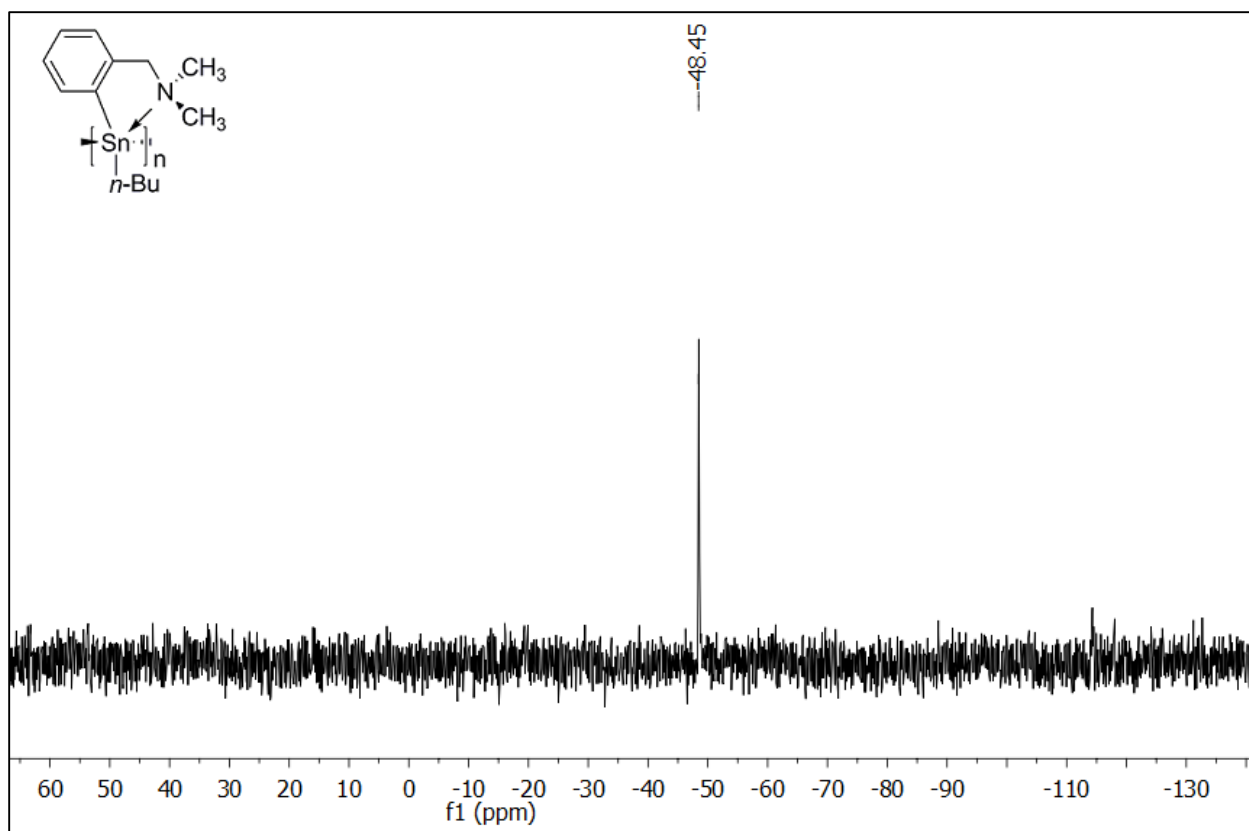
Figure 53: ^{119}Sn NMR (C$_6$D$_6$) spectrum of **248**.

Polymers **249**-**250** were synthesized by catalytic dehydrocoupling of monomers **206**-**207** using Wilkinson's catalyst in toluene. It was suggested by Molloy *et al*.[43] that the Wurtz coupling of the dibromide **146** did not proceed as a result of the sterically hindered 5-coordinate structure at tin from the chelating propylether group. The polymerization of dihydrides **206** and **207** is an indication of the absence of 5-coordinate geometry at tin in these tin dihydrides. The polymers were purified by precipitating THF solutions of the crude mixtures twice in petroleum ether. The gummy orange/yellow coloured polymers remained attached to the walls of the flask. The residual solvent was removed from the purified product by prolonged drying under reduced pressure. The soft gummy polymers were characterized fully by NMR (^{1}H, ^{13}C, ^{119}Sn) spectroscopy.
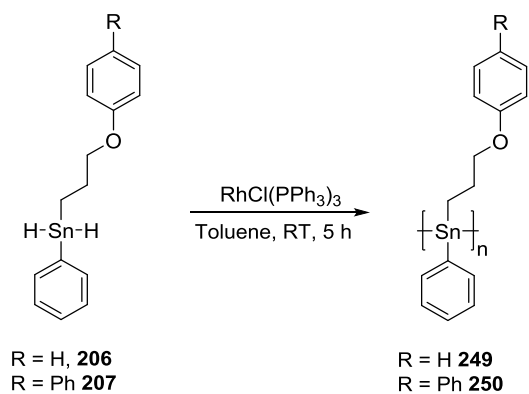
Scheme 55: Transition metal catalyzed synthesis of polymers **249** and **250**.
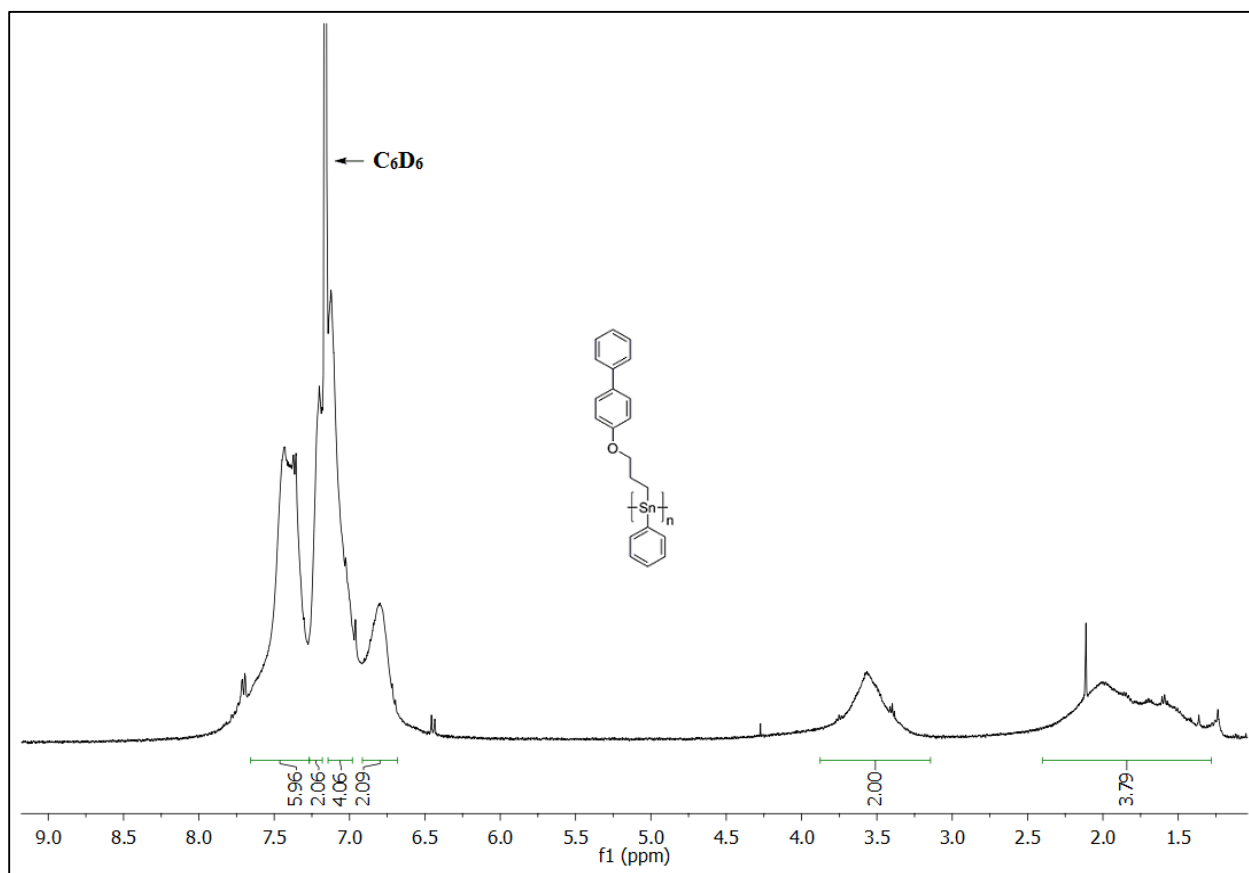
Figure 54: ^{1}H NMR (C$_6$D$_6$) spectrum of polymer **250**.

^{119}Sn NMR revealed a single broad peak at -199 ppm (Figure 55) for **249** and -195 ppm for

250 respectively, which is 16-19 ppm downfield compared to their starting monomers **206**-**207**.

The disappearance of both the monomer signal at ca. δ = -215 ppm in the ^{119}Sn NMR spectrum

and the Sn–H signal (ca. 5.5 ppm) in the ^{1}H NMR spectra reflect a complete monomer conversion. ^{1}H NMR spectroscopy also showed broad peaks (Figure 54) which is typical in case of polymers.
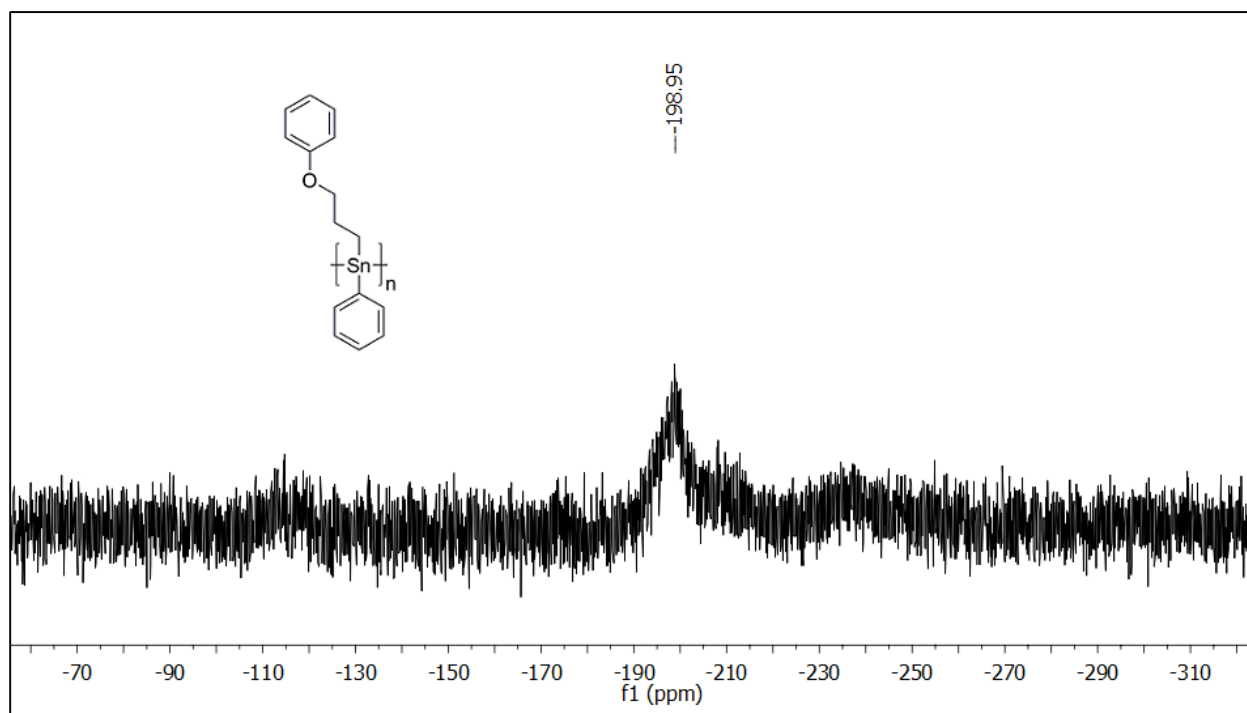
Figure 55: ^{119}Sn NMR (C$_6$D$_6$) spectrum of **249**.

2.3.2.2 Non-metal catalyzed dehydrocoupling:

Catalytic dehydropolymerization of compound **227** was unsuccessfully attempted using Wilkinson's catalyst or Cp$_2$ZrMe$_2$. This may be a result of steric crowding at tin as a result of the *C,O*-chelating ligands. Lechner *et al.*[130] used TMEDA for the polymerization of R$_2$SnH$_2$ (R = *n*-butyl, phenyl, 4-*n*-butylphenyl) to polymers **251** and **252** which gave ^{119}Sn NMR resonance at -197 ppm, a typical region for polystannanes.

251

252
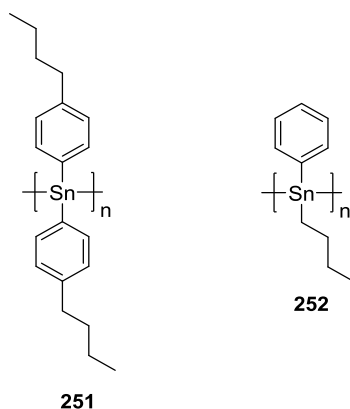
Figure 56: TMEDA catalyzed polymerization of organotin dihyrides.[130]

Dehydrocoupling of **227** in the presence of TMEDA produced the desired polymer **251** in 36 h. This reaction proceeds most likely via a radical process as predicted by Davies *et al.* for the reaction of R_2SnXH with pyridine.[173] The ^{119}Sn NMR resonance for **251** was located at -196 ppm, shifting 13.0 ppm downfield from the monomer chemical shift of the resonance. There are some other peaks upfield of the polymer peak at δ = -198 ppm to -200 ppm, which may be due to the cyclic oligomeric species (Figure 57).
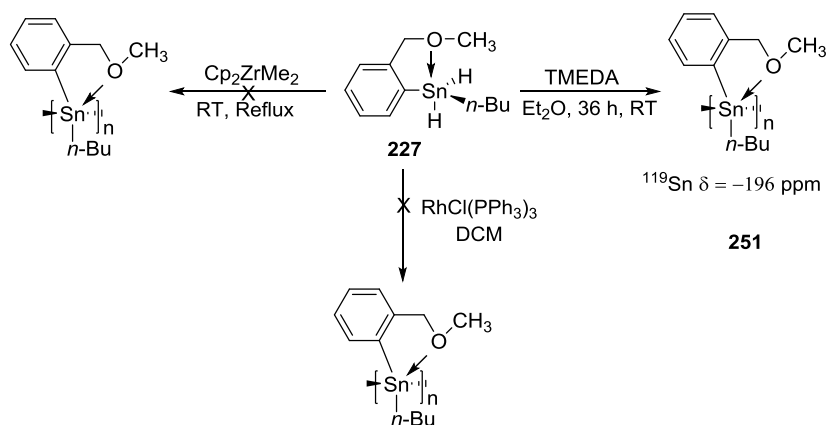
Scheme 56: Synthesis of polymer **251**.
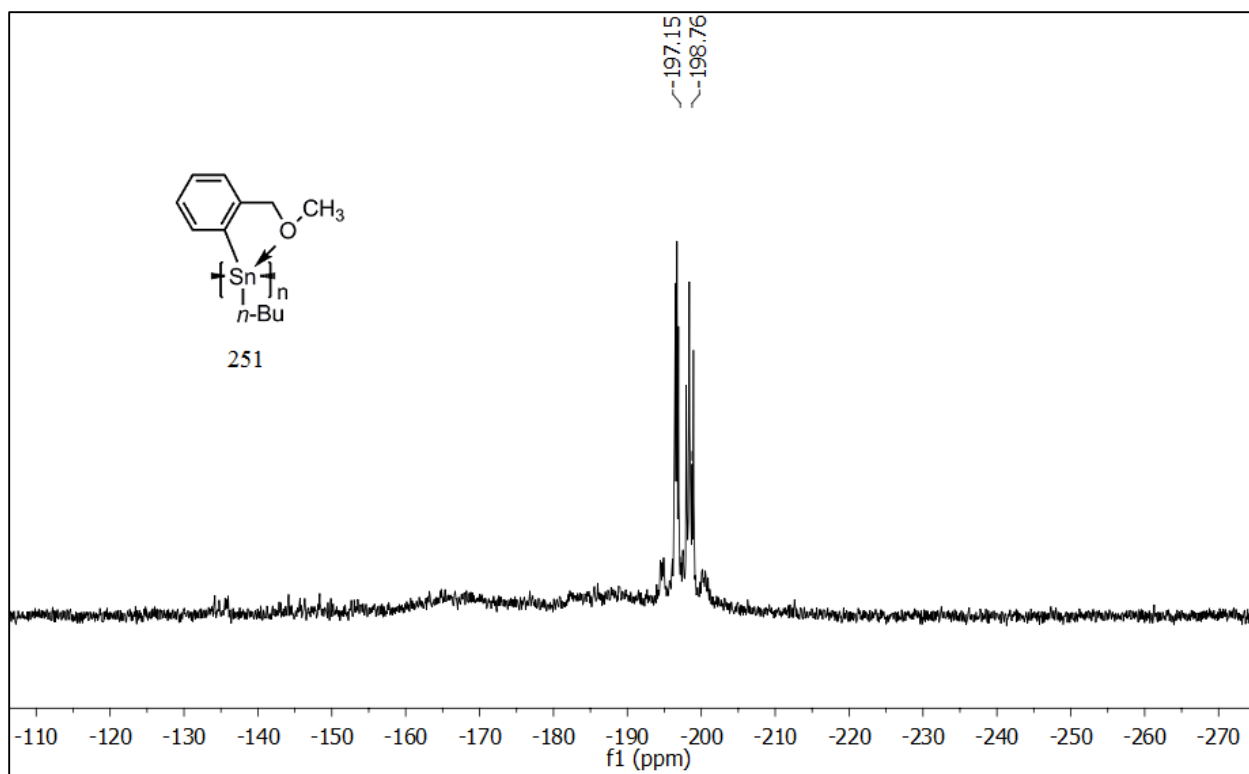
Figure 57: ^{119}Sn NMR (C_6D_6) spectrum of **251**.

2.3.3 Characterization of polymers:

2.3.3.1 GPC Characterization:

Gel permeation chromatography (GPC) is equipped with a triple detection system to determine the absolute molecular weight of polymers. GPC analysis of polystannanes (solution in THF) typically causes chain cleavage or clipping of polymers due to the laser ($\lambda_0 = 670$ nm) used. The analysis of polymers **248**-**250** was attempted using solutions (1×10^{-4} M) of these materials in THF. It was observed that the signal intensity for the right angle and low angle detectors which use the laser source would not appear in the GPC, presumably as a result of photodegradation of the polystannane. This results in the clipping of Sn-Sn bonds in polymer backbone converting polymer to oligomers. If the laser is turned off for the light scattering detector, signal response from both the refractive index (RI) and intrinsic viscometry (IV) are observed. To mitigate this issue, a UV-A photoabsorber was introduced to the THF solutions and exposure minimized.

Compounds **206**-**207** were catalytically dehydrocoupled using Wilkinson's catalyst to polymers **249** and **250**. These gummy yellow coloured materials were readily soluble in common organic solvents such as DCM, THF and C_6H_6. A solution of these polymers in THF was used for molar mass determination. The Mw for **250** was 1.01×10^5 Da with a PDI 1.3. The molar masses of these polymers are in the range of polymer material reported previously by Molloy.[43] The PDI values indicate that the polymers are relatively uniform and contain chains that are essentially monomodal. Similar polymers (**252**, **253**) were synthesized by Molloy *et al.*[43] via Wurtz coupling of dibromides (**147**, **150**) with molar masses 2.50 - 3.00 $\times$ 10^5 Da and with PDI of 1.3 and 2.0 respectively comparable to the values found in this effort. The properties of these polymers are given in Table 22.

R = Ph, n = 3 **252**
R = n-Bu, n =3 **253**
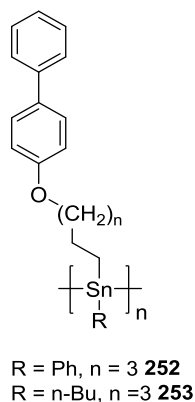
Figure 58: Structure of polymers **252** and **253**

Table 22: molecular weight and [119]Sn chemical data for polystannanes.

Polymer	M_w (Da)	PDI	[119]Sn (δ)	λ_{max} (nm)
248	3.2×10^4	1.8	-49.0	-
249	-	-	-199	263
250	1.01×10^5	1.3	-195	273
251	-	-	-196	380
252[43]	3.0×10^5	1.3	-	255
253[43]	2.5×10^5	2.0	-	255

Polymerization of monomers **227** and **231** using Wilkinson's catalyst was unsuccessful. This may suggest that the presence of bulky groups in close proximity to the tin center such as the chelating ligand containing donor atoms like N and O hindered the polymerization with [$RhCl(PPh_3)_3$]. ^1H and ^{119}Sn NMR spectroscopy of the polymerization attempt did not show any signals attributable to polymers.

Dehydrocoupling of **227** and **231** using TMEDA and Cp_2ZrMe_2 in Et_2O and hexane respectively resulted in polymeric products. The GPC of the crude product **248** in THF produced a molecular weight $Mw = 3.2 \times 10^4$ Da and PDI = 1.8. An attempt to purify the polymer by precipitation of the THF solution in hexane afforded a small amount of a THF insoluble light yellow coloured solid. No further characterization of this insoluble material was undertaken. A gummy yellow coloured polymer of **248** was used for NMR and GPC analysis.
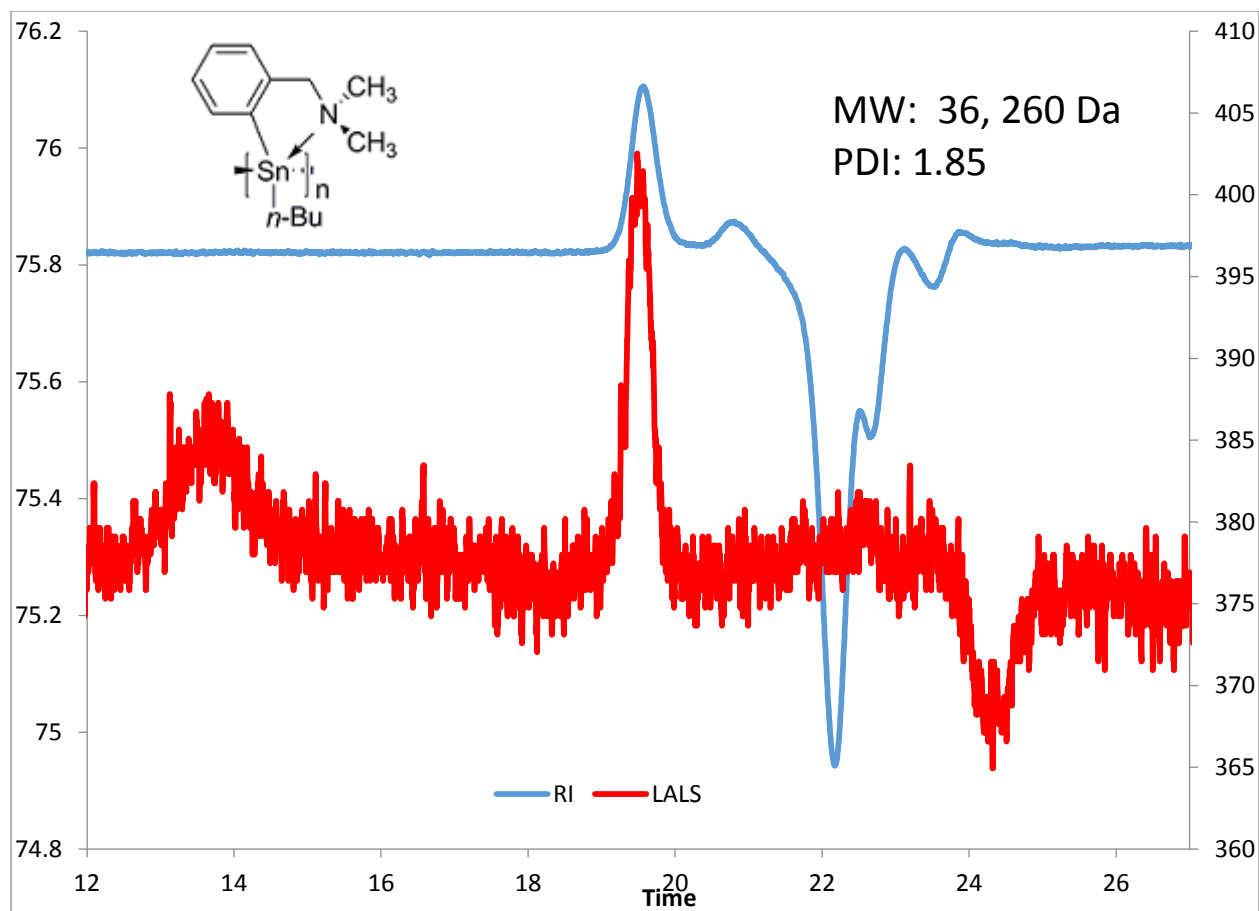
Figure 59: Triple detector GPC trace (THF) of polymer **248**

2.3.3.2 Electronic properties:

The UV-Vis spectroscopy of polystananes **249** and **250** display a strong allowed π-π* transition at 228 nm. A lower intensity σ-σ* transition is found at $\lambda_{max} = 273$ nm for these polymers with tailing to λ_{max} 325 nm. The tailing at 325 nm suggest that the tin atoms of the backbone are delocalized as a result of strong overlap. The strong π-π* transition at $\lambda_{max} = 255$ nm was also reported by Molloy's *et al.*[43] for poly[phenyl5-(4-biphenyloxy)pentyl]tin synthesized by Wurtz coupling which does not hypercoordinate.
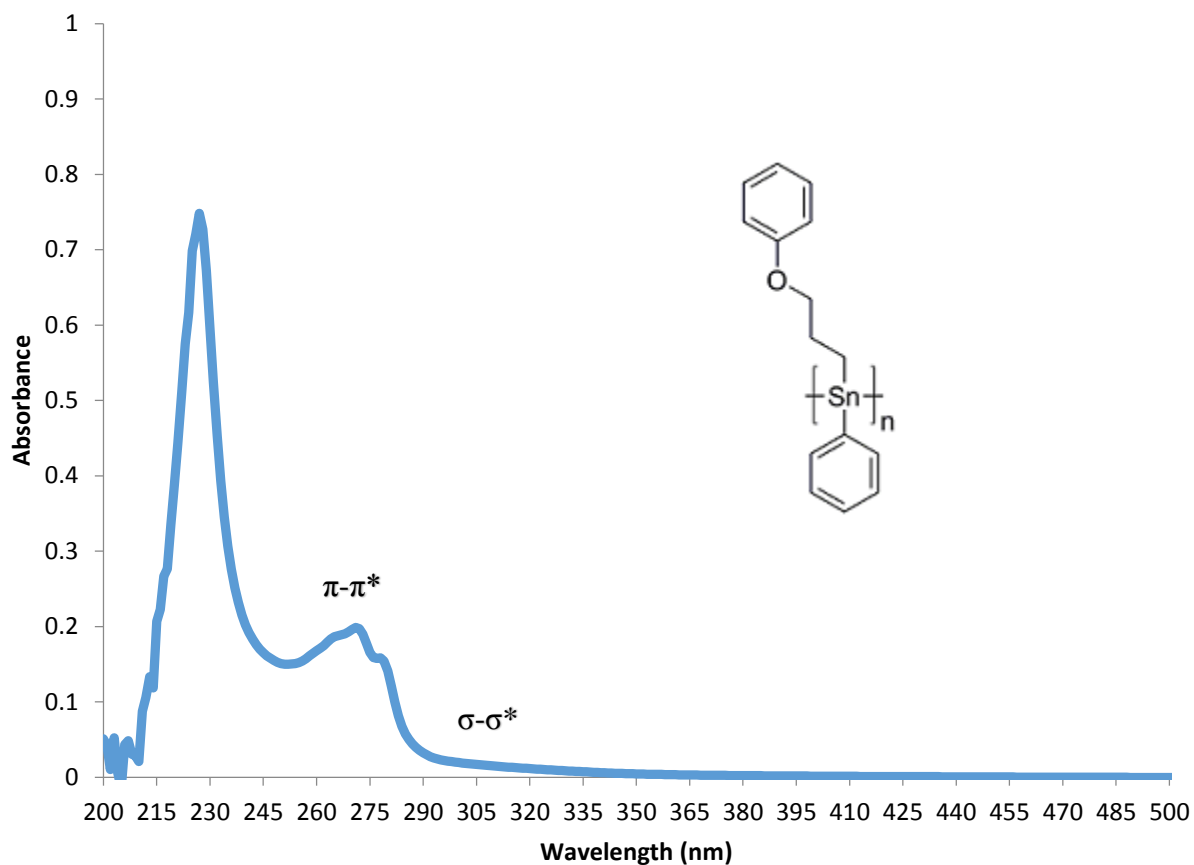
Figure 60: UV-visible spectrum of **249**

2.3.3.3 DSC studies:

Thermal analysis of the polymers **249** and **250** by Differential scanning calorimetry (DSC) in the temperature range between -5 ℃ and 120 ℃ revealed glass transition temperatures (T_g): ca. 65 ℃ and 64 ℃ for **249** and **250** respectively. These T_g values reported for previously found for these polymers fall between for polydialkyl- (0 ℃ to 91 ℃) and polydialkyphenylstannanes (-20 ℃ to -50 ℃).
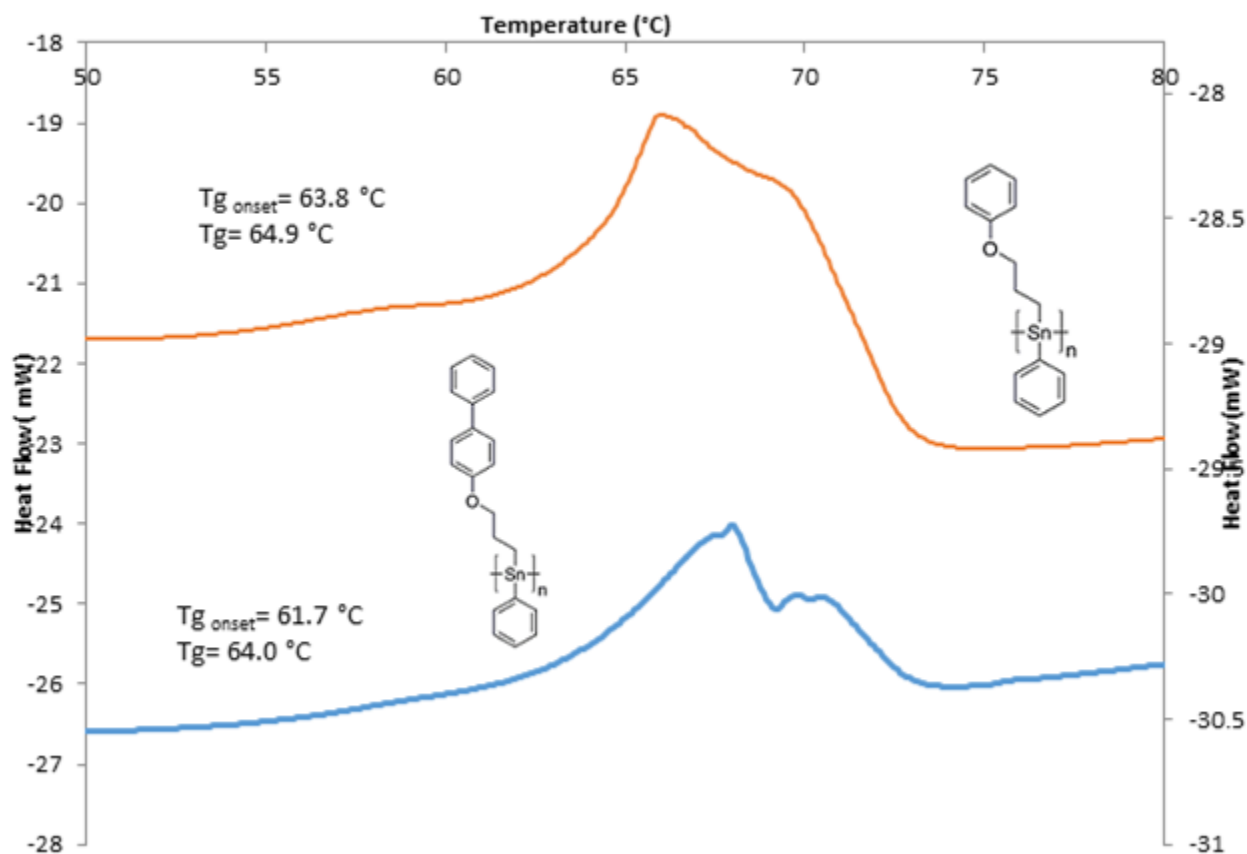
Figure 61: DSC heating thermograms of **249** and **250** (under N_2, heating rate 5 ℃/min)

2.3.3.4 UV-Vis and NMR Stability studies:

Polystannanes **249** and **250** were found to be stable in the solid state under ambient conditions if left in a sealed flask for weeks as concluded after periodic evaluation by NMR (^1H and ^{119}Sn) spectroscopy. NMR solutions (C_6D_6) of these polymers **249** and **250** were also stable in dark and did not show any degradation after one week. However, degradation was observed after 1 day in ambient light and the ^{119}Sn NMR signals characteristic for polymer **250** gradually disappeared with appearance of four new signals with chemical shifts δ = 27.0, -23.0, -34.0, -67.0 and -207 ppm. These new signals continuously increase with continued light exposure and the ^{119}Sn NMR signals characteristic for polymer **250** completely disappeared after 10 days. ^{119}Sn

NMR signals at δ = -207 ppm are similar to that reported by Choffat *et al*. for five and six membered cyclo-oligo(dipropylstannane) at δ = -207.4 and -207.9 ppm respectively.

It was previously shown that poly(dialkylstannane)s exhibit an absorption maximum in the region of 370–410 nm,[118,119, 121,127,136,132] which is caused by delocalization of the σ-electrons of the tin atoms along the polymer backbone. In several reports, the degree of degradation of these materials was evaluated from the UV-Vis spectroscopy.[127,136,132] In this study, the extent of degradation of polymer **250** was investigated in THF solutions at a concentration 5.9×10^{-5} mol/L in the range of 200–500 nm for 5 consecutive scans over intervals of 10 days (1, 10, 20 days). No significant degradation was observed under these conditions as the absorption bands at different intervals are superimposable (Figure 62). The most probable reason of these conflicting solution stability results of ^{119}Sn NMR and UV studies may be the solvent dependence.
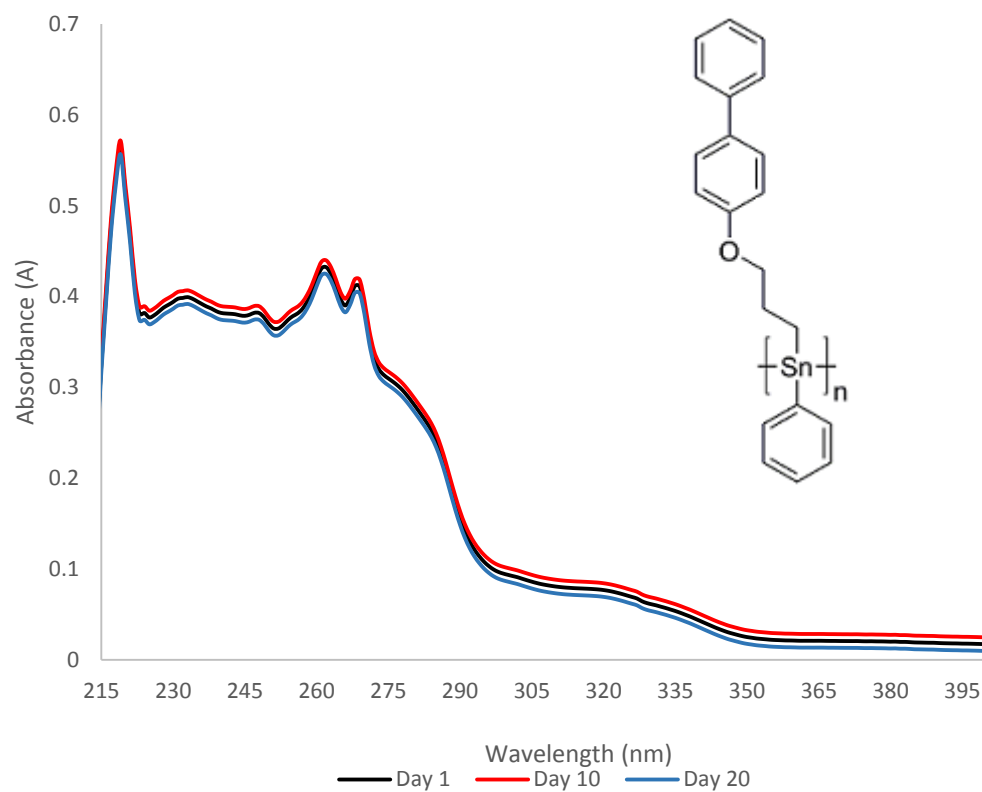
Figure 62: Consecutive UV-visible spectra of **250** at day 1, 10 and 20.

3.0 Conclusion:

A variety of organotin compounds containing potential Sn-E (E = N, O, P and S) interactions were synthesized and characterized using different techniques. Tetraorganotin compounds **141**, **198-199** with tethered phenyloxy moieties were prepared and characterized by NMR spectroscopy (^{1}H, ^{13}C, ^{119}Sn), HRMS spectroscopy or elemental analysis and X-ray crystallography in case of **198**. Triorganotin chlorides **200**-**201** were synthesized from a stepwise replacement of the phenyl groups with HCl and further converted using the same methodology to produce diorganotin dihalides **202**-**203**. These organotin halides **200-203** were structurally characterized to reveal moderate to strong Sn-O interactions. Novel tin hydrides **204**-**207** were prepared by the reduction of organotin halides **200-203** with LiAlH$_4$ and used for polymerization studies. Model hexaorganoditin **208**-**209** were also prepared by dehydrocoupling of triorganotin hydrides **204**-**205**.

Organotin compounds with *C,O*- chelating ligands were also synthesized. Tetraorganotin compounds **112** and **217** were prepared in good or improved yields. Organotin halides **218-219** containing a *C,O*- chelating ligand were synthesized from the reaction of the lithiated salt **216** with RSnCl$_3$ (R = Me, *n*-Bu). An attempt to replace the phenyl group of **112** with chlorine resulted in redistribution product **221**. Reduction of tin dihalides **218** and **219** afforded two novel diorganotin dihydrides **226** and **227**.

Tin dichlorides **33**, **35**, **37** containing a *C,N*-chelating ligand were also synthesized. The hydrogenation of **33** and **35** resulted in the formation of tin dihydrides **230** and **231**. Wurtz coupling of dichlorides **35** and **37** resulted in distannanes **243**-**246** that were previously reported in literature by different methods.

113

Sulfur containing **233** and **234** were prepared using a modified method and investigated for their suitability for organotin compounds containing a *C,S-* chelating ligand. Reaction attempts to produce the organotin compounds with a *C,S-* chelating ligand resulted in the formation of multiple products and the purification attempts were unsuccessful. Compound **239** with a *C,P-* functionality was synthesized and used to produce compound **241**. NMR analysis of **241** revealed a single ^{119}Sn and ^{31}P resonance.

Catalytic dehydropolymerization of diorganotin dihydrides was completed using both metal and non-metal catalysts. Diorganotin dihydrides **206**-**207** catalytically dehydrocoupled in the presence of Wilkinson's catalyst resulted in the formation of polymers **249**-**250**. These polymers were obtained as orange-yellow coloured gums. GPC analysis of **250** in THF yielded a moderate molecular weight polymer ($M_w = 1.1 \times 10^5$ Da, PDI = 1.3). A DSC thermal analysis of of polymers **249** and **250** revealed glass transition temperatures (T_g) of 65 ℃ and 64 ℃ respectively. Dehydrocoupling of compound **231** was successfully completed in the presence of Cp$_2$ZrMe$_2$ in hexane. GPC analysis of **248** in THF yielded a moderate molecular weight polymer ($M_w = 3.2 \times 10^4$ Da, PDI 1.8). Non-metal catalyzed dehydrocoupling of compound **227** in the presence of TMEDA produced the desired polymer **253** which has not been fully characterized. Stability studies of polymer **250** by ^{119}Sn NMR and UV-visible spectroscopies indicated a faster degradation in C$_6$D$_6$ than in THF. Overall, this polymer was considerably more stable than known poly(dialkyl)stannanes.

Our investigation of organotin compounds containing different chelating ligands indicates that substantial intramolecular interactions between Sn-E (E = N, O) are present in monomers that contain at least one halide and adopt TBP geometry. The degree of the Sn-E interaction likely decreases as the halides are converted to hydrides as there is a substantial decrease of

electronegativity at Sn which reduces its ability to draw electron density into a 3c-4e arrangement as well as the lack of orbitals to accommodate the extra electron density. The dative interaction in polystannanes **249**-**251** seems to be completely absent as is evident from their ^{119}Sn NMR chemical shifts (δ = -195 ppm to -199 ppm) which are very similar to most known polystannanes. In the case of **248**, the ^{119}Sn NMR resonance at -49 ppm suggests that the dative interaction between Sn and N atom is likely still present.

4.0 Future work:

In this study asymmetrical polystannanes were prepared from diorganotin dihydrides synthesized from 5-coordinate diorganotin dihalides possess Sn-E (E = N, O) intramolecular interactions. The characterization of these new polystannanes indicated that the hypercoordination geometry is likely not preserved, except perhaps in the polymer with a Sn-N interaction as evident by a dramatic downfield chemical shift. All polymeric materials displayed considerable stability in solid state and in solution in dark. It has been previously established that wavelengths at visible light are harmful for these type of materials and cause photodegradation. Unless the issue of photostability is sufficiently resolved, the utility of polystannanes for applications such as polymeric wires will not be realized.

To overcome this problem we propose the use of light absorbing chromophore side chains. The chromophore has the ability to absorb wavelengths of visible light and reflects or transmit the others. There are some examples of the molecule having side groups such as azobenzene that are currently being developed in our lab. These can be used as starting point to produce the dihydrides and dehydrocoupled to structurally more stable polystannanes. This will not increase the strength of Sn-Sn bonds but should reduce the light exposure of Sn-Sn bonds in the backbone of the polymers.

Further investigation of the geometry in polymers such as **249** and **250** has not been conclusively established. Analysis of the Sn environments by Mössbauer spectroscopy for these polymers would be instructive. Structural characterization by X-ray diffraction would also shed light on the geometry of the new dihydrides. Molecular modelling of monomers, oligomers and polymers could also provide insight into the extent the Lewis acidity at Sn is moderated by chelating ligands. This has not been established for any of the new molecules made in this study.

Finally, a systemic investigation of the polymerization behaviour of structurally hindered tin sites to establish general rules, including solvent and catalyst choices, length of polymerizations, concentrations, to guide optimum polymerization outcomes is required.

5.0 Experimental:

^{1}H NMR, ^{13}C {^{1}H}, ^{119}Sn {^{1}H}, ^{19}F {^{1}H} and ^{31}P {^{1}H} NMR spectra were recorded on a Bruker Avance 400 MHz NMR spectrometer. All chemical shifts are in ppm with respect to Me$_4$Si (^{1}H and ^{13}C), Me$_4$Sn for ^{119}Sn, CFCl$_3$ for ^{19}F and 85% H$_3$PO$_4$ for ^{31}P. UV-Vis measurements were carried out in THF solutions using a Perkin Elmer Lambda 40 spectrometer. Molecular weights of polymers were determined by gel permeation chromatography (GPC) using a Viscotek Triple Model 302 Detector system equipped with a Refractive Index Detector (RI), a four capillary differential viscometer (VISC), a right angle (90°) laser light scattering detector ($\lambda_0 = 670$ nm) and a low angle (7°) laser light scattering detector. GPC columns were calibrated versus polystyrene standards (American Polymer Standards). A flow rate of 1.0 mL min^{-1} was used with ACS grade THF as the eluent. GPC samples were prepared using 3–10 mg of polymers per mL THF, and filtered using a 0.45 μm filter. All samples were run with and without UVA (conc. $\approx$ 0.001 M) for comparison. All reactions were carried out under a nitrogen atmosphere using Schlenk techniques unless otherwise described. A Bruker-Nonius Kappa-CCD diffractometer at the University of Toronto was used to obtain the X-ray diffraction data for crystal structures. High resolution mass spectrometry experiments were carried out using an accuTOF DART-MS at the University of Toronto. Elemental analyses were performed by Atlantic Microlab of Norcross Georgia. 4-phenylphenol, KOH, KI, K$_2$CO$_3$, AIBN, Br$_2$, allyl bromide, LiAlH$_4$ (1.0 M in Et$_2$O), n-BuLi (1.6 M in hexane), anhydrous MgSO$_4$, anhydrous CaCl$_2$ and Wilkinson's catalyst were purchased commercially form Sigma Aldrich and used without further purification. 1.6 M solution of HCl in Et$_2$O was prepared in laboratory. Solvents were dried using MBraun solvent purification system or by standard procedures prior to use.

5.1 Synthesis of (allyloxy)benzene (194):
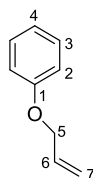
Allyl bromide (13.06 g, 108 mmol) and K_2CO_3 (15.0 g, 108 mmol) were added to a 250 mL dried two neck round bottom flask containing a solution of phenol (10.0 g, 106 mmol) in 60 mL of acetone. The reaction mixture was refluxed for 16 h and cooled to room temperature. Removal of solvent under reduced pressure afforded a white solid. The residue was dissolved in 50 mL DCM and washed sequentially with (15 mL) 1.0 M NaOH, water and brine solution. The organic layer was dried over anhydrous $MgSO_4$ and removal of solvent under reduced pressure afforded a highly viscous clear oil. NMR data (^{1}H, ^{13}C) obtained is essentially the same as reported in the literature.[148,149] Yield: 9.1 g (82%).

^{1}H NMR (400 MHz, CDCl$_3$, δ): 7.36 (2H, H3), 7.0 (m, 3H, H2, H4), 6.13 (m, 1H, H6), 5.50 (dd, 1H, H7, $J_{geminal}$ = 1.6 Hz, J = 16 Hz), 5.35 (dd, 1H, H7, $J_{geminal}$ = 1.6 Hz, J = 12 Hz), 4.60 (d, 2H, H5) ppm; **^{13}C NMR** (100 MHz, CDCl$_3$, δ): 158.6 (C1), 133.4 (C), 129.4 (C), 120.8 (C), 117.6 (C), 114.7 (C), 68.7 (C5) ppm.

5.2 Synthesis of 3-(4-biphenyloxy)-1-propene (137):
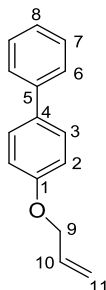
Allyl bromide (3.55 g, 29.4 mmol) and K_2CO_3 (5.1 g, 36.7 mmol) were added to a 250 mL dried two neck round bottom flask containing a solution of 4-phenylphenol (5.0 g, 29.4 mmol) in 100 mL acetone. The reaction mixture was refluxed for 16 h and cooled to room temperature. Removal of solvent under reduced pressure afforded a white coloured solid. The residue was dissolved in 50 mL DCM, washed sequentially with (15 mL) 1.0 M NaOH, water and brine solution. The organic layer was dried over anhydrous $MgSO_4$ and solvent removal under reduced pressure afforded a white solid coloured product. NMR data (^{1}H, ^{13}C) obtained is essentially the same as reported in the literature.[43] Yield: 4.0 g (65%)

^{1}H NMR (400 MHz, CDCl$_3$, δ): 7.63 (m, 4H, H3, H6), 7.50 (t, 2H, H7), 7.39 (m, 1H, H8), 7.05 (d, 2H, H2), 6.17 (m, 1H, H10), 5.52 (d, 1H, *cis*-H11), 5.40 (d, 1H, *trans*-H11), 4.65 (d, 2H, H9) ppm;

^{13}C NMR (100 MHz, CDCl$_3$, δ): 158.2 (C1), 140.8 (C4), 133.9 (C5), 133.3 (C7), 128.7 (C6), 128.1 (C3), 126.7 (C8), 117.7 (C11), 115.6 (C10), 115.0 (C2), 69.2 (C9) ppm.

5.3 Synthesis of of 1-allyloxy-3-trifluoromethylbenzene (195):
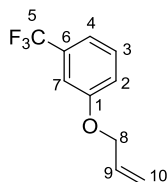
Allyl bromide (1.49 g, 12.3 mmol), K_2CO_3 (3.41 g, 24.7 mmol) was added to a solution of 3-(trifluoromethyl)phenol (2.00 g, 12.3 mmol) in 50 mL of acetone in a 250 mL round bottom flask and refluxed for 16 h. The reaction mixture was then filtered and the solvent removed under reduced pressure. The residue was dissolved in 50 mL of DCM and washed sequentially with (15 mL) 1.0 M NaOH, water and brine solution. The organic layer was dried over anhydrous $MgSO_4$, and solvent removed under reduced pressure. The product was recovered as a yellow oil. NMR data (^{1}H, ^{13}C, ^{19}F) is essentially the same as reported in the literature.[174] Yield = 2.34 g (94%).

^{1}H NMR (400 MHz, CDCl$_3$, δ): 7.40 (t, 1H, H3), 7.22 (d, 1H, H4), 7.15 (br s, 1H, H7), 7.10 (dd, 1H, H2), 6.06 (m, 1H, H9), 5.44 (qd, 1H, *cis*-H10), 5.32 (qd , 1H, *trans*-H10), 4.59 (m, 2H, H8) ppm; **^{13}C NMR** (100 MHz, CDCl$_3$, δ): 158.8 (s, C1), 132.7 (s, C9), 131.9 (q, C6, $^2J_{13C-19F}$ = 30 Hz), 130.0 (s, C3), 124.1 (q, C5, $^1J_{13C-19F}$ = 272 Hz), 118.4 (q, C2, $^4J_{13C-19F}$ = 1.5 Hz), 118.3 (s, C10), 117.6 (q, C7, $^2J_{13C-19F}$ = 4.0 Hz), 111.7 (q, C4, $^2J_{13C-19F}$ = 4.0 Hz), 69.2 (s, C8), ppm; **^{19}F NMR** (376 MHz, CDCl$_3$, δ): -62.7 ppm.

5.4 Synthesis of 1-(allyloxy)-4-methoxybenzene ether (196):
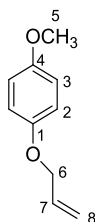
Allyl bromide (3.0 mL, 32.0 mmol) and K$_2$CO$_3$ (9.0 g, 64.0 mmol) were added to a solution of 4-methoxyphenol (4.0 g, 32.0 mmol) in 70 mL of acetone in a 250 mL round bottom flask and refluxed for 16 h. After filtration, solvent was removed under reduced pressure. The residue was dissolved in 50 mL DCM and washed sequentially with (15 mL) 1.0 M NaOH, water and brine solution. The organic layer was dried over anhydrous MgSO$_4$ and removal of solvent under reduced pressure afforded a white coloured solid. NMR data (^{1}H, ^{13}C) obtained is essentially the same as reported in literature.[175] Yield = 4.7g (89%).

^{1}H NMR (400 MHz, CDCl$_3$, δ): 6.82 - 6.88 (m, 4H, H2, H3), 6.06 (m, 1H, H7), 5.41 (dq, 1H, *cis*-H8, ^1J = 17 Hz), 5.28 (dq, 1H, *trans*-H8, ^1J = 10.5 Hz, ^2J = ^3J = 1.5 Hz), 4.49 (dd, 2H, H6, ^1J = 5.3 Hz, ^2J = ^3J = 1.5 Hz), 3.77 (s, 3H, H5) ppm; **^{13}C NMR** (100 MHz, CDCl$_3$, δ): 153.9 (C4), 152.8 (C1), 133.6 (C7), 117.5 (C8), 115.8 (C2), 114.6 (C3), 69.6 (C6), 55.7 (C5) ppm.

5.5 Synthesis of triphenyltin hydride (254):
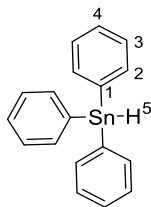
A solution 1.0 M LiAlH$_4$ (11.0 mL, 11.0 mmol) in 20 mL of Et$_2$O was added dropwise to a suspension of Ph$_3$SnCl (10.51 g, 29.85 mmol) in 50 mL of Et$_2$O at 0 ºC. The reaction mixture was stirred for 30 min at this temperature, allowed to warm to room temperature and stirred for an additional 2.5 h. The reaction mixture was then placed in an ice bath and quenched with 25 mL of chilled degassed water. The organic layer was separated and the aqueous fraction extracted with (3 × 15 mL) Et$_2$O. The collected organic layer was then dried over anhydrous MgSO$_4$, filtered and the solvent removed under reduced pressure to yield a colourless viscous product. NMR data (^{1}H, ^{13}C) obtained is essentially the same as reported in literature.[42,64] Yield: 7.63 g (80%).

^{1}H NMR (400 MHz, C$_6$D$_6$, δ): 6.93 (s, 1H, H5, $^1J_{119Sn-1H}$ = 1935 Hz, $^1J_{117Sn-1H}$ = 1849 Hz), 7.13 (m, 9H, H3, H4), 7.52 (m, 6H, H2, $^2J_{119Sn-1H}$ = 8.4 Hz) ppm; **^{13}C NMR** (100 MHz, C$_6$D$_6$, δ): 137.6 (C2, $^2J_{119Sn-13C}$ = 39 Hz), 137.3 (C1, $^1J_{119Sn-13C}$ = 535 Hz, $^1J_{117Sn-13C}$ = 511 Hz), 129.3 (C4, $^4J_{119Sn-13C}$ = 11 Hz), 128.9 (C3, $^3J_{119Sn-13C}$ = 52 Hz) ppm; **^{119}Sn{^{1}H}NMR** (149 MHz, C$_6$D$_6$, δ): -163.1 ppm.

5.6 Synthesis of triphenyl[(3-phenyloxy)propyl]tin (197):
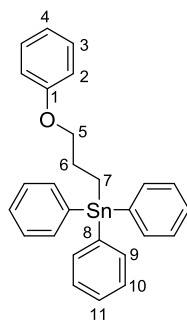
Compound **194** (2.0 g, 14.3 mmol) and **254** (4.24 g, 7.45 mmol) were heated with AIBN (0.05 g, 0.913 mmol) in a dried 100 mL Schlenk flask at 140 ºC for 1 h. The reaction mixture was allowed to cool to room temperature, which resulted in formation of a white coloured gum. The distannane (Ph$_3$SnSnPh$_3$) byproduct was precipitated from the mixture by adding hexane to the crude product and subsequently removed by filtration. Unreacted **194** was removed by heating under reduced pressure at 75 ºC which afforded a colourless, highly viscous oil of **197**. Yield: 5.68 g (79%)

^{1}H NMR (400 MHz, CDCl$_3$, δ): 7.64 (m, 6H, H9), 7.43 (m, 9H, H10, H11), 7.31 (m, 2H, H3), 6.99 (t, 1H, H4), 6.88 (d, 2H, H2), 4.03 (t, 2H, H5), 2.29 (m, 2H, H6), 1.71 (t, 2H, H7) ppm; **^{13}C NMR** (100 MHz, CDCl$_3$, δ): 159.0 (C1), 138.7 (C8, $^1J_{119Sn-13C} = 488$ Hz, $^1J_{117Sn-13C} = 468$ Hz), 137.0 (C9, $^2J_{119Sn-13C} = 36$ Hz), 129.4 (C3), 128.9 (C11, $^3J_{119Sn-13C} = 11$ Hz), 128.5 (C10, $^3J_{119Sn-13C} = 49$ Hz), 120.6 (C4), 114.6 (C2), 70.5 (C5), 26.4 (C6, $^2J_{119Sn-13C} = 19$ Hz), 6.93 (C7, $^1J_{119Sn-13C} = 388$ Hz, $^1J_{117Sn-13C} = 372$ Hz) ppm; **^{119}Sn{^{1}H}NMR** (149 MHz, C$_6$D$_6$, δ): -99.9 ppm. Found: C, 66.64; H, 5.47. Calc. for C$_{27}$H$_{26}$OSn: C, 66.84, H, 5.40%.

5.7 Synthesis of triphenyl[3-(4-biphenyloxy)propyl]tin (141):

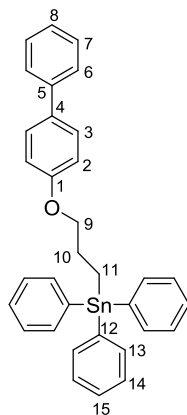Compound **137** (2.78 g, 13.22 mmol) and **254** (4.64 g, 13.18 mmol) were heated with AIBN (0.16 g, 0.973 mmol) in a dried 100 mL Schlenk flask at 140 ºC under inert atmosphere. The reaction mixture was allowed to cool to room temperature. The distannane (Ph$_3$SnSnPh$_3$) produced as a

side-product and unreacted **137** were separated from **141** by sublimation (130 °C for 4 h). The product (a sticky semi-solid) was further purified to remove the trace distannane ($Ph_3SnSnPh_3$) by dissolving in Et_2O followed by filtration. The removal of residual solvent under reduced pressure afforded a white coloured powder. NMR data (^1H, ^{13}C, ^{119}Sn) obtained is essentially the same as previously reported by Molloy *et al.*[43] Yield: 5.1 g (70%).

^1H NMR (400 MHz, $CDCl_3$, δ): 7.55 (m, 6H, H13), 7.46 (m, 2H, H6), 7.40 (m, 3H, H7, H8), 7.37 (m, 9H, H14, H15), 7.30 (d, 2H, H3), 6.85 (dd, 2H, H2), 4.02 (t, 2H, H9), 2.26 (m, 2H, H10), 1.67 (t, 2H, H11) ppm; **^{13}C NMR** (100 MHz, $CDCl_3$, δ): 158.6 (C1), 141.0 (C4), 138.8 (C12), 137.4 (C8), 137.2 (C13), 133.2 (C-Ar), 129.0 (C-Ar), 128.8 (C-Ar), 128.7 (C-Ar), 128.2 (C-Ar), 126.9 (C-Ar), 114.9 (C-Ar), 70.8 (C9), 26.2 (C10), 7.06 (C11) ppm; **$^{119}Sn\{^1H\}$NMR** (149.21 MHz, $CDCl_3$, δ): -99.3 ppm.

5.8 Synthesis of triphenyl [3-(3-trifluromethylphenyloxy)propyl]tin (198):
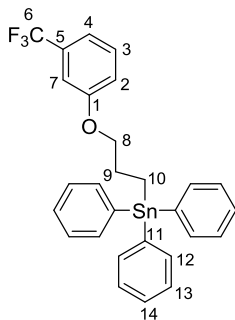
Compound **195** (1.0 g, 4.95 mmol), **254** (1.69 g, 4.83 mmol) and AIBN (0.055 g, 0.99 mmol) were heated at 120 °C for 1 h in a 50 mL Schlenk flask. The crude product was washed with 2×5 mL of MeOH to remove unreacted **195**. The residue was then dissolved in MeOH and after decanting the solvent removed under reduced pressure. The product **198** was recovered as a white coloured powder and recrystallized in MeOH:DCM. Yield: 2.13 g (79%) m.p. 60-65 °C.

¹H NMR (400 MHz, CDCl₃, δ): 7.52-7.56 (m, 6H, H12), 7.33-7.37 (m, 9H, H13, H14), 7.30 (t, $J_{H9\text{-}H8}$ = 8.0 Hz, 1H, H3), 7.15 (m, 1H, H4), 6.98 (s, 1H, H7); 6.90 (dd, 1H, H2, $J_{H10\text{-}H9}$ = 7.6 Hz, $J_{H10\text{-}H8}$ = 2.4 Hz), 3.96 (t, 2H, H8, $J_{H6\text{-}H5}$ = 6.4 Hz), 2.22 (tt, 2H, H9), 1.63 (t, 2H, H10, $J_{H4\text{-}H5}$ = 8.0 Hz, $J_{H4\text{-}Sn}$ = 57 Hz) ppm; **¹³C NMR** (100 MHz, CDCl₃, δ): 159.1 (C1), 138.7 (C11), 137.7 (C-Ar), 137.4 (C-Ar), 137.1 (C13, $^3J_{119Sn\text{-}13C}$ = 36.2), 129.9 (C-Ar), 129.1 (C14, $^4J_{119Sn\text{-}13C}$ = 11 Hz), 128.7 (C12, $^2J_{119Sn\text{-}13C}$ = 50 Hz), 118.1 (q, C6, $J_{13C\text{-}19F}$ = 1.5 Hz), 117.3 (d, C4, $J_{13C\text{-}19F}$ = 4.0 Hz), 111.4 (d, C2, $J_{13C\text{-}19F}$ = 4.0 Hz), 70.8 (C8), 26.3 (C9), 7.06 (C10) ppm; **¹⁹F NMR** (376 MHz, CDCl₃, δ): -62.7 (s, CF₃) ppm; **¹¹⁹Sn{¹H}NMR** (149.21 MHz, CDCl₃, δ): -100.0 ppm. Found: C, 60.38, H, 4.55. Calc. for C₂₇H₂₆OSn: C, 60.79, H, 4.56 %.

5.9 Synthesis of triphenyl [3-(4-methoxyphenyloxy)propyl]tin (199):
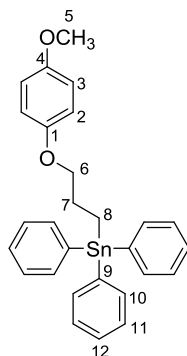
Compound **196** (0.50 g, 3.05 mmol), **254** (1.03 g, 2.93 mmol) and AIBN (0.02 g, 0.36 mmol) were heated at 120 ℃ in a sealed Schlenk flask for 1 h under dynamic N₂. The crude product was sublimed to remove the Ph₃SnSnPh₃ side-product and further purified by silica gel column chromatograph using hexane:EtOAc (6:1). Yield 0.98 g (65%).

¹H NMR (400 MHz, CDCl₃, δ): 7.49-7.61 (m, 6H, H12), 7.36-7.38 (m, 9H, H13, H14), 6.71-80 (m, 4H, H2, H3), 3.90 (t, 2H, H8, ^1J = 6.2 Hz), 3.76 (s, 3H, H5), 2.18 (tt, 2H, H9), 1.64 (t, 2H, H10, J = 8.0 Hz) ppm; **¹³C NMR** (100 MHz, CDCl₃, δ): 153.9 (C4), 153.2 (C1), 138.9 (C9, $J_{119Sn\text{-}}$

$_{13C}$ = 490 Hz $J_{117Sn-13C}$ = 468 Hz), 137.2 (C11, $J_{119Sn-13C}$ = 35 Hz), 129.0 (C12, $J_{119Sn-13C}$ = 11 Hz), 128.7 (C10, $J_{119Sn-13C}$ = 48 Hz) 115.6 (C2), 114.7 (C3), 71.4 (C6, $^3J_{119Sn-13C}$ = 68 Hz), 55.9 (C5), 26.5 (C7, $^2J_{119Sn-13C}$ = 20 Hz), 7.09 (C8, $^1J_{119Sn-13C}$ = 392 Hz, $^1J_{117Sn-13C}$ = 375 Hz) ppm; ^{119}Sn{^{1}H}NMR (149.21 MHz, CDCl$_3$, δ): -99.3 ppm.

5.10 Synthesis of diphenyl[(3-phenyloxy)propyl]tin chloride (200):
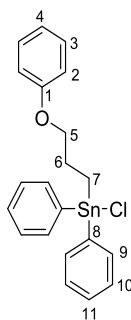
1.0 M solution of HCl (4.5 mL, 4.5 mmol) in Et$_2$O was added dropwise to a solution of **197** (2.06 g, 4.24 mmol) dissolved in 10 mL of dry C$_6$H$_6$ and stirred for 1 h. The removal of solvent under reduced pressure afforded an off-white coloured solid. The crude product was first extracted with hot hexane and filtered. The hexane solution containing the product was kept at -20 ºC overnight, and a white coloured crystalline product recovered. The hexane was decanted and residual solvent was removed under reduced pressure. The product was recrystallized in DCM:hexane (1:1). Yield: 1.52 g (81%), m.p. 63 ºC.

^{1}H NMR (400 MHz, CDCl$_3$, δ): 7.64 (m, 4H, H9), 7.35 (m, 6H, H10, H11), 7.07 (m, 2H, H3), 6.88 (tt, 1H, H4), 6.53 (dd, 2H, H2), 4.07 (t, 2H, H5), 2.40 (m, 2H, H6), 1.93 (t, 2H, H7) ppm; **^{13}C NMR** (100 MHz, CDCl$_3$, δ): 157.7 (C1), 139.7 (C8, $^1J_{119Sn-13C}$ = 592 Hz, $^1J_{117Sn-13C}$ = 569 Hz), 136.1 (C10, $J_{119Sn-13C}$ = 47 Hz), 129.8 (C11, $J_{119Sn-13C}$ = 13 Hz), 129.2 (C3), 128.8 (C9, $J_{119Sn-13C}$ = 61 Hz), 121.7 (C4), 115.3 (C2), 70.2 (C5), 25.8 (C6, $^2J_{119Sn-13C}$ = 27 Hz), 15.0 (C7, $^1J_{119Sn-13C}$ = 460 Hz) ppm; **^{119}Sn{^{1}H}NMR** (149.21 MHz, CDCl$_3$, δ): -26.6 ppm. **HRMS-DART** (m/z): [M$^+$] +

H$_2$O, Calc. for C$_{21}$H$_{23}$ClO$_2$Sn, 462.06637; found 462.06575. Found: C, 56.79, H, 4.78. Calc. for C$_{21}$H$_{21}$ClOSn: C, 56.87, H, 4.77%.

5.11 Synthesis of diphenyl[3-(4-biphenyloxy)propyl]tin chloride (201):

1.0 M solution of HCl (1.0 mL, 1.0 mmol) in Et$_2$O was added dropwise to a solution of compound **141** (0.561 g, 1.0 mmol) dissolved in 5 mL of dry C$_6$H$_6$ and stirred for 1 h. The removal of solvent under reduced pressure afforded white coloured solid. The crude product was purified by washing with hot hexanes. The removal of solvent under reduced afforded a white coloured solid. Yield: 0.45 g (86%), m.p. 82 ºC.

^{1}H NMR (400 MHz, CDCl$_3$, δ): 7.66 (m, 4H, H13), 7.46 (m, 2H, H6), 7.40 (dd, 2H, H3), 7.35 (m, 6H, H13, H14), 7.29 (m, 3H, H7, H8), 6.58 (dd, 2H, H2), 4.11 (t, 2H, H9), 2.42 (m, 2H, H10), 1.94 (t, 2H, H11) ppm; **^{13}C NMR** (100 MHz, CDCl$_3$, δ): 157.3 (C, i-Ar), 140.5 (C- i-Ar), 139.6 (C- i-Ar), 136.1 (C14, $^3J_{119Sn-13C}$ = 47 Hz), 134.6 (C- i-Ar), 129.8 (C15, $^4J_{119Sn-13C}$ = 13 Hz), 128.8 (C13, $^2J_{119Sn-13C}$ = 62 Hz), 128.7 (C- Ar), 127.9 (C- Ar), 126.8 (C- Ar), 126.7 (C- Ar), 115.5 (C2), 70.4 (C9), 25.8 (C10, $^2J_{119Sn-13C}$ = 26 Hz), 15.0 (C11) ppm; **^{119}Sn{^{1}H}NMR** (149.21 MHz, CDCl$_3$, δ): -24.7 ppm. **HRMS-DART** (m/z): [M$^+$], Calc. for C$_{27}$H$_{25}$ClOSn, 520.06; found 520.1.

5.12 Synthesis of phenyl[3-(4-biphenyloxy)propyl]tin dibromide (146):
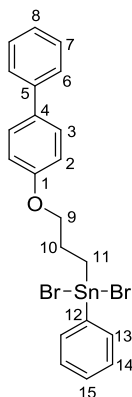
A solution of Br_2 (2.6 g, 32.54 mmol) in 80 mL of DCM was added dropwise to a solution of **141** (4.54 g, 8.08 mmol) in 80 mL of DCM at 0 ºC. The resulting solution was stirred for 24 h. The solvent was removed under reduced pressure. The crude product mixture was kept under reduced pressure at 50 ºC for 12 h to remove the C_6H_5Br byproduct from **146**. A white coloured solid was recovered. NMR data (^1H, ^{13}C, ^{119}Sn) obtained is essentially the same as previously reported in literature.[43] Yield: 3.71 g (81%).

^{1}H NMR (400 MHz, CDCl$_3$, δ): 7.66 (m, 2H, H13), 7.50 (m, 3H, H14, H15), 7.41 (m, 2H, H7), 7.35-7.39 (m, 4H, H3, H6), 7.31 (m, 1H, H8), 6.73 (d, 2H, H2), 4.16 (t, 2H, H9), 2.46 (m, 2H, H10), 2.29 (m, 2H, H11) ppm; **^{13}C NMR** (100 MHz, CDCl$_3$, δ): 157.0 (C- *i*-Ar), 140.5 (C- *i*-Ar), 140.0 (C- *i*-Ar), 134.8 (C- Ar), 134.7 (C- Ar), 130.9 (C- Ar), 129.1 (C- Ar), 128.8 (C- Ar), 127.9 (C- Ar), 126.8 (C- Ar), 126.7 (C- Ar), 116.3 (C2), 70.0 (C9), 25.7 (C10), 23.8 (C11) ppm; **^{119}Sn{^{1}H}NMR** (149.21 MHz, CDCl$_3$, δ): - 51.6 ppm.

5.13 Synthesis of phenyl[(3-phenyloxy)propyl]tin dichloride (202):
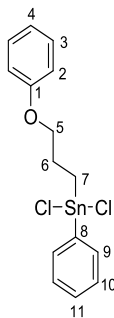
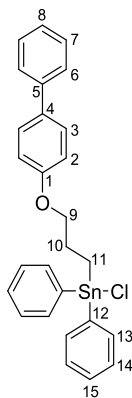A 1.0 M solution of HCl (5.0 mL, 5.0 mmol) in Et$_2$O was added dropwise to a solution of **200** (2.13 g, 4.8 mmol dissolved in 10 mL of dry C$_6$H$_6$) and stirred for 1 h. The removal of solvent under reduced pressure afforded an off-white coloured solid. ^{1}H NMR (CDCl$_3$) revealed a 60% conversion of **200** to **202**. The crude product was re-dissolved in C$_6$H$_6$ and an additional aliquot (1.6 mL) of 1.0 M HCl added. The reaction mixture was stirred for 1 h, and removal of solvent under reduced pressure afforded a white coloured solid. Yield: 1.21 g (91%) m.p. 70 ºC.

^{1}H NMR (400 MHz, CDCl$_3$, δ): 7.62 (dd, 2H, H9), 7.38 (m, 3H, H10, H11), 7.15 (tt, 2H, H3), 6.95 (dt, 1H, H4), 6.70 (dd, 2H, H2), 4.15 (t, 2H, H5), 2.49 (m, 2H, H6), 2.17 (t, 2H, H7) ppm; **^{13}C NMR** (100 MHz, CDCl$_3$, δ): 157.2 (C2), 140.2 (C8), 134.9 (C10, $^3J_{119Sn-13C}$ = 62 Hz), 130.9 (C11, $^4J_{119Sn-13C}$ = 17 Hz), 129.3 (C3), 129.1 (C9, $^2J_{119Sn-13C}$ = 81 Hz), 122.4 (C4), 116.1 (C2), 69.8 (C5), 25.2 (C6), 22.4 (C7) ppm; **^{119}Sn{^{1}H}NMR** (149 MHz, CDCl$_3$, δ): - 21.9 ppm. **HRMS-DART** (m/z): [M$^+$] + H$_2$O, Calc. for C$_{15}$H$_{18}$Cl$_2$O$_2$Sn, 419.99439; found 419.99440. Found: C, 45.01, H, 4.14. Calc. for C$_{27}$H$_{26}$OSn: C, 44.83, H, 4.01%.

5.14 Synthesis of phenyl[3-(4-biphenyloxy)propyl]tin dichloride (203):
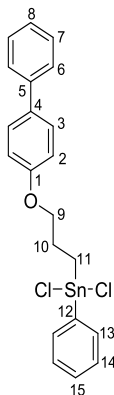
A 1.0 M solution of HCl (3.1 mL, 3.1 mmol) in Et$_2$O was added dropwise to a solution of **201** (1.50 g, 3.1 mmol) dissolved in 10 mL of dry C$_6$H$_6$ and stirred for 1 h. The removal of solvent under reduced pressure afforded an off-white solid. ^{1}H NMR (CDCl$_3$) revealed a 95% conversion of **201** to **203**. The crude mixture was re-dissolved in C$_6$H$_6$ and an additional aliquot (0.2 mL) of 1.0 M HCl added, and the reaction mixture stirred for 1 h. Removal of solvent under reduced pressure afforded a white coloured product. Yield: 1.38 g (100%), m.p. 75 ºC.

^{1}H NMR (400 MHz, CDCl$_3$, δ): 7.63 (m, 2H, H13), 7.47 (m, 2H, H14), 7.36 (m, 7H, H3, H6, H7, H8), 7.30 (m, 1H, H15), 6.75 (dd, 2H, H2), 4.17 (t, 2H, H9), 2.48 (m, 2H, H10), 2.17 (t, 2H, H11) ppm; **^{13}C NMR** (100 MHz, CDCl$_3$, δ): 156.8 (C- *i*-Ar), 140.4 (C- *i*-Ar), 140.3 (C, *i*-Ar), 135.0 (C12, $^1J_{119Sn-13C}$ = 40 Hz), 131.0 (C- Ar), 129.2 (C- Ar), 128.8 (C- Ar), 128.4 (C- Ar), 128.0 (C- Ar), 127.0 (C- Ar), 126.8 (C- Ar), 116.3 (C2), 70.0 (C9), 22.5 (C10), 25.2 (C11) ppm; **^{119}Sn{^{1}H}NMR** (149 MHz, CDCl$_3$, δ): -20.3 ppm. Found: C, 52.95, H, 4.38. Calc. for C$_{21}$H$_{20}$Cl$_2$OSn: C, 52.77, H, 4.22%.

5.15 Synthesis of diphenyl[(3-phenyloxy)propyl]tin (204):
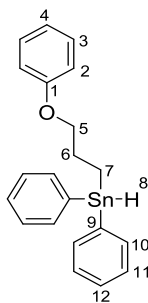
A solution of **200** (0.334 g, 0.75 mmol) in 15 mL of Et_2O was added dropwise to a Schlenk flask containing 1.0 M $LiAlH_4$ (0.8 mL, 0.8 mmol) in 10 mL of Et_2O over 30 min at 0 ℃. The resulting solution was allowed to stir for 3 h at 0 ℃ and the reaction mixture was then quenched with 15 mL of chilled degassed water. The organic layer was washed with water (2×15 mL) and dried over anhydrous $MgSO_4$. The dried organic layer was filtered and the solvent removed under reduced pressure to yield a colourless viscous oil. Yield: 0.22 g (70%).

^{1}H NMR (400 MHz, C_6D_6, δ): 7.49 (m, 4H, H10, $^1J_{119Sn-1H} = 48$ Hz), 7.14 (m, 8H, H3, H11, H12), 6.81 (3H, H2, H4), 6.35 (t, 1H, H8, $^1J_{119Sn-1H} = 1862$ Hz, $^1J_{117Sn-1H} = 1780$ Hz), 3.56 (t, 2H, H5), 1.92 (m, 2H, H6, $^1J_{119Sn-1H} = 64$ Hz), 1.23 (dt, 2H, H7, $^1J_{119Sn-1H} = 56$ Hz), ppm; **^{13}C NMR** (100 MHz, C_6D_6, δ): 159.6 (C1), 138.3 (C9, $^1J_{119Sn-13C} = 494$ Hz, $^1J_{117Sn-13C} = 472$ Hz), 137.5 (C10, $^2J_{119Sn-13C} = 36$ Hz), 129.7 (C11, $J_{119Sn-13C} = 29$ Hz), 129.1 (C12, $J_{119Sn-13C} = 11$ Hz), 128.9 (C3), 120.9 (C4), 114.9 (C2), 70.10 (C5, $^3J_{119Sn-13C} = 60$ Hz), 26.9 (C6, $^2J_{119Sn-13C} = 21$ Hz), 6.67 (C7, $^1J_{119Sn-13C} = 396$ Hz, $^1J_{117Sn-13C} = 378$ Hz) ppm; **^{119}Sn{^{1}H}NMR** (149 MHz, C_6D_6, δ): - 137.1 ppm.

HRMS-DART (m/z): Calcd for $C_{21}H_{21}OSn$ [M$^+$] − H, 409.06025; found 409.06010.

5.16 Synthesis of diphenyl[3-(4-biphenyloxy)propyl]tin (205):
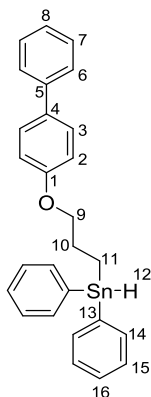
A solution of **201** (0.885 g, 1.7 mmol) in 15 mL of Et_2O was added dropwise to a solution of 1.0

M $LiAlH_4$ (1.0 mL, 1.0 mmol) in 10 mL of Et_2O over 30 min at 0 ℃. The resulting solution was

stirred for further 3 h at 0 ℃ and the reaction mixture was then quenched with 15 mL of chilled

degassed water. The organic layer was washed (2×10 mL) with water, then dried over anhydrous

$MgSO_4$. The dried organic layer was then filtered and the solvent removed under reduced pressure

to afford a colourless viscous oil. Yield: 0.50 g (61%).

^{1}H NMR (400 MHz, C_6D_6, δ): 7.50 (m, 6H, H15, H16), 7.39 (dd, 2H, H3), 7.24 (m, 2H, H6), 7.16

(m, 7H, H6, H7, H8, H14), 6.83 (dd, 2H, H2), 6.38 (t, 1H, H12, $^1J_{119Sn-1H}$ = 1860 Hz, $^1J_{117Sn-1H}$ =

1820 Hz), 3.61 (t, 2H, H9, $^3J_{119Sn-1H}$ = 28 Hz), 1.95 (m, 2H, H10, $^2J_{119Sn-1H}$ = 64 Hz), 1.27 (dt, 2H,

H11, $^1J_{119Sn-1H}$ = 56 Hz) ppm; **^{13}C NMR** (100 MHz, C_6D_6, δ): 159.0 (C- i-Ar), 141.4 (C- i-Ar),

138.3 (C13, $^1J_{119Sn-13C}$ = 495 Hz, $^1J_{117Sn-13C}$ = 472 Hz), 137.5 (C14, $^2J_{119Sn-13C}$ = 36 Hz), 134.1 (C-

i-Ar), 129.1 (C- Ar), 129.1 (C- Ar), 128.9 (C- Ar), 128.5 (C- Ar), 127.1 (C- Ar), 126.9 (C- Ar),

115.2 (C2), 70.3 (C9, $^3J_{119Sn-13C}$ = 60 Hz), 26.9 (C10, $^2J_{119Sn-13C}$ = 21 Hz), 6.67 (C11, $^1J_{119Sn-13C}$ =

396 Hz , $^1J_{117Sn-13C}$ = 378 Hz) ppm; **^{119}Sn{^{1}H}NMR** (149 MHz, C_6D_6, δ): - 137.0 ppm. **HRMS-**

**DART** (m/z): calcd for $C_{27}H_{25}OSn$ [M$^+$] − H, 485.09325; found 485.09336.

5.17 Synthesis of phenyl[(3-phenyloxy)propyl]tin (206):
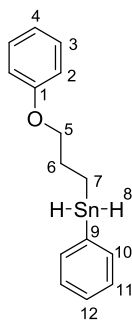
A solution of **202** (1.36 g, 3.38 mmol) in 30 mL of Et$_2$O was added dropwise to a solution of 1.0 M LiAlH$_4$ (4.0 mL, 4.0 mmol) in 15 mL of Et$_2$O cooled to 0 °C over 30 min and the resulting mixture stirred for further 3 h at 0 °C. The reaction was quenched with 20 mL of chilled degassed water. The aqueous layer was extracted with (3×15 mL) Et$_2$O. The organic layers were dried over anhydrous MgSO$_4$, filtered and solvent removed under reduced pressure to afford a colourless, viscous oil. Yield: 0.89 g (81%).

^{1}H NMR (400 MHz, C$_6$D$_6$, δ): 7.48 (m, 2H, H10), 7.19 (m, 5H, H3, H11, H12), 6.88 (3H, H2, H4), 5.57 (t, 2H, H8, $^1J_{119Sn-1H}$ = 1836 Hz, $^1J_{117Sn-1H}$ = 1752 Hz), 3.59 (t, 2H, H5), 1.88 (m, 2H, H6, $^1J_{119Sn-1H}$ = 64 Hz), 1.10 (tt, 2H, H7, $^1J_{119Sn-1H}$ = 56 Hz) ppm; **^{13}C NMR** (100 MHz, C$_6$D$_6$, δ): 159.4 (C1), 137.8 (C10, $^2J_{119Sn-C}$ = 38 Hz), 136.7 (C9, $^1J_{119Sn-13C}$ = 499 Hz, $^1J_{117Sn-13C}$ = 476 Hz), 129.7 (C12), 128.9 (C11, $^3J_{119Sn-13C}$ = 11 Hz), 120.9 (C4), 128.8 (C3), 114.9 (C2), 69.9 (C5, $^3J_{119Sn-13C}$ = 56 Hz), 27.4 (C6, $^2J_{119Sn-13C}$ = 24 Hz), 5.04 (C7, $^1J_{119Sn-13C}$ = 406 Hz , $^1J_{117Sn-13C}$ = 387 Hz) ppm; **^{119}Sn{^{1}H}NMR** (149 MHz, C$_6$D$_6$, δ): -215.1 ppm. **HRMS-DART** (m/z): [M$^+$] calculated for C$_{15}$H$_{17}$OSn, 333.02937; found 333.03014.

5.18 Synthesis of phenyl[3-(4-biphenyloxy)propyl]tin (207):
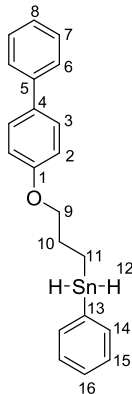
Method 1:

A solution of **203** (0.912 g, 1.6 mmol) in 20 mL of Et$_2$O was added dropwise to a solution of 1.0 M LiAlH$_4$ (4.27 mL, 4.27 mmol) in 15 mL Et$_2$O at 0 °C over 30 min and the mixture stirred for further 2 h at 0 °C. The reaction was quenched with 7.0 mL of chilled degassed water. The organic layer was separated and the aqueous layer extracted with (2 × 30 mL) Et$_2$O. The combined organic layers were dried over MgSO$_4$. After filtration, the solvent was removed under reduced pressure to yield a light yellow coloured oil. Yield: 0.54 g (84%). **HRMS-DART:** [M$^+$], Calc. for C$_{21}$H$_{22}$OSn 409.0614; found 409.0613.

Method 2:

A suspension of NaBH$_4$ (0.228 g, 6.16 mmol) in 20 mL of EtOH was added to **146** (0.25 g, 0.445 mmol) suspended in 10 mL of EtOH at 0 °C. The resulting solution was stirred for an additional 30 min at same temperature. The reaction was quenched with 1.0 mL of chilled degassed water and product extracted with (2 × 15 mL) hexane. The collected organic layers were dried over MgSO$_4$. After filtration and solvent removal under reduced pressure, a light yellow coloured oil was recovered. Yield: 0.15 g (81%).

Method 3:

A solution of compound **146** (0.24 g, 0.586 mmol) in 15 mL of Et_2O was added dropwise to a suspension of 1.0 M $LiAlH_4$ (0.6 mL, 0.6 mmol) in 10 mL of Et_2O at 0 ºC over 30 min and the mixture stirred for a further 3 h at 0 ºC. The reaction mixture was then quenched with 10 mL of chilled degassed water. The organic layer was separated and the aqueous layer extracted with (3 × 15 mL) Et_2O. The combined organic layers were dried over anhydrous $CaCl_2$. The solution was filtered and solvent removed under reduced pressure to yield a colourless viscous oil. Yield: 0.13 g (65%).

¹H NMR (400 MHz, C_6D_6, δ): 7.48 (m, 4H, H4, H10), 7.42 (m, 2H, H11), 7.23 (m, 2H, H5, H12), 7.15 (m, 4H, H2, H3), 6.88 (2H, H1), 5.56 (t, 2H, H9, $^1J_{119Sn-1H}$ = 1837 Hz, $^1J_{117Sn-1H}$ = 1754 Hz), 3.57 (t, 2H, H6), 1.88 (m, 2H, H7, $^2J_{119Sn-1H}$ = 72 Hz), 1.10 (tt, 2H, H8, $^1J_{119Sn-1H}$ = 60 Hz) ppm;

¹³C NMR (100 MHz, C_6D_6, δ): 158.9 (C- *i*-Ar), 141.5 (C- *i*-Ar), 137.80 (C14, $^2J_{119Sn-13C}$ = 38 Hz), 136.6 (C13, $^1J_{119Sn-13C}$ = 493 Hz , $^1J_{117Sn-13C}$ = 474 Hz), 134.1 (C- *i*-Ar), 129.1 (C- Ar), 129.0 (C-*i*-Ar), 128.8 (C- Ar), 128.5 (C- Ar), 127.1 (C- Ar), 126.9 (C- Ar), 115.2 (C2), 70.1 (C9, $^3J_{119Sn-13C}$ = 57 Hz), 27.4 (C10, $^2J_{119Sn-13C}$ = 23 Hz), 5.01 (C11, $^1J_{119Sn-13C}$ = 404 Hz, $^1J_{117Sn-13C}$ = 387 Hz) ppm; **¹¹⁹Sn{¹H}NMR** (149 MHz, C_6D_6, δ): - 215.1 ppm.

5.19 Dimerization of diphenyl[(3-phenyloxy)propyl]tin (208):
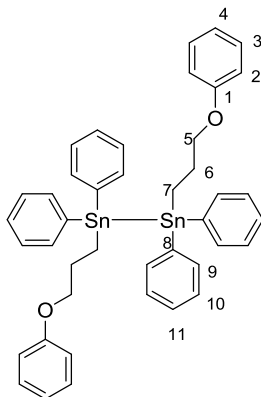
A solution of $Pd(PPh_3)_4$ (0.027 g, 0.035 mmol) in 5 mL of dry C_6H_6 was added slowly to a solution of **204** (0.105 g, 0.26 mmol) in 5 mL of C_6H_6 under inert atmosphere. The mixture was stirred for 2 h at room temperature and then at 50 ℃ overnight. The product was purified by column chromatography on silica gel (hexanes:EtOAc (1:1)). Yield: 0.03 g (53%).

¹H NMR (400 MHz, C_6D_6, δ): 7.55 (m, 4H, H9), 7.36 (m, 6H, H10, H11), 7.23 (m, 2H, H3), 6.91 (m, 1H, H4), 6.79 (dd, 2H, H2), 3.94 (t, 2H, H5), 2.2 (m, 2H, H6), 1.62 (m, 2H, H7) ppm; **¹³C NMR** (100 MHz, C_6D_6, δ): 159.2 (C1), 138.7 (C8, $^1J_{119Sn-13C}$ = 488 Hz), 137.1 (C10, $^3J_{119Sn-13C}$ = 36 Hz), 129.30 (C9, $^2J_{119Sn-13C}$ = 480 Hz), 128.8 (C11, $^4J_{119Sn-13C}$ = 10 Hz), 128.6 (C3), 120.4 (C4), 114.5 (C2), 70.0 (C5), 26.3 (C6, $^2J_{119Sn-13C}$ = 20 Hz), 6.77 (C7, $^1J_{119Sn-13C}$ = 390 Hz) ppm; **¹¹⁹Sn{¹H}NMR** (149 MHz, C_6D_6, δ): -98.0 ($J_{119Sn-117Sn}$ = 8480 Hz) ppm.

5.20 Dimerization of diphenyl[3-(4-biphenyloxy)propyl]tin (209):
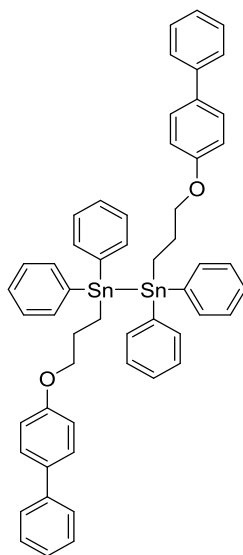
A solution of Pd(PPh$_3$)$_4$ (0.035 g, 0.045 mmol) in 5 mL of C$_6$H$_6$ was added slowly to a solution of 0.172 g (0.35 mmol) of **205** in 5 mL C$_6$H$_6$ under an inert atmosphere. The mixture was stirred overnight at room temperature. The crude reaction mixture was extracted with petroleum ether. An attempt to purify the remaining reaction mixture by column chromatography on silica gel (hexanes/EtOAc) was unsuccessful. The ^{1}H NMR spectrum show unidentified resonance additional resonances.

^{1}**H NMR** (400 MHz, C$_6$D$_6$, δ):7.67-7.73 (m, 10H), 7.55-7.61 (m, 5H), 7.47-7.51 (m, 7H), 7.37-7.42 (m, 11H), 6.92 (m, 1H), 6.80 (m, 1H), 3.97 (t, 2H,), 2.22 (m, 2H,), 1.65 (t, 2H,) ppm:

^{119}**Sn{^{1}H}NMR** (149 MHz, C$_6$D$_6$, δ): -98.0 ppm.

5.21 Polymeriztion of phenyl[(3-phenyloxy)propyl]tin (249):
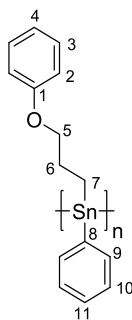
A solution of **206** (0.295 g, 0.9 mmol) in 10 mL of dry toluene was added by syringe to a solution of Wilkinson's catalyst (0.035 g, 0.038 mmol) in 10 mL of toluene in a Schlenk flask wrapped in aluminium foil. The reaction mixture was allowed to stirr for 5 h. The solvent was removed under reduced pressure. The product was redissolved in fresh toluene, filtered and added dropwise to an excess of petroleum ether. The precipitated product was recovered as an orange/yellow coloured gum. Yield: 0.22 g (75%).

^{1}H NMR (400 MHz, C$_6$D$_6$, δ): 7.29-7.76 (m, 2H, H$_{aryl}$), 6.95-7.25 (bm, 5H, H$_{aryl}$), 6.67-6.2 (s, 3H, H aryl), 3.12-3.97 (bs, 2H, H5), 1.04-2.44 (bs, 4H, H6, H7) ppm; **^{13}C NMR** (100 MHz, C$_6$D$_6$, δ): 159.6 (C1), 138.1 (C8), 136.6 (C9), 132.5 (C11), 129.7 (C10), 128.9 (C3), 120.7 (C4), 114.9 (C2), 70.6 (C5), 30.1 (C6), 21.9 (C7) ppm; **^{119}Sn{^{1}H}NMR** (149 MHz, C$_6$D$_6$, δ): -199.0 ppm. Found: C, 56.68; H, 4.82. Calc. for C$_{27}$H$_{26}$OSn: C, 54.43, H, 4.87 %

5.22 Polymerization of phenyl[3-(4-biphenyloxy)propyl]tin (250):
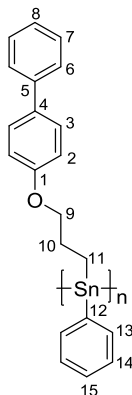
A solution of **207** (0.333 g, 1.0 mmol in 10 mL of toluene) was added with a syringe to a solution

of Wilkinson's catalyst (0.040 g, 0.043 mmol in 5 mL of toluene) in a Schlenk flask wrapped in

aluminium foil stirred for 5 h. The solvent was removed under reduced pressure. The product was

dissolved in a minimum amount of fresh toluene, filtered and added dropwise into petroleum ether.

The precipitated product was recovered as an orange/yellow coloured gum. Yield: 0.23 g (68%).

^{1}H NMR (400 MHz, C_6D_6, δ): 7.28-7.66 (br m, 6H, H_{aryl}), 7.2 (s, 2H, H_{aryl}), 6.97-7.13 (br m, 4H,

H_{aryl}), 6.67-6.90 (br s, 2H, H2), 3.13-3.88 (br s, 2H, H9), 1.29-2.39 (br s, 4H, H10, H11), ppm; **^{13}C**

NMR (100 MHz, C_6D_6, δ): 158.8 (C- i-Ar), 140.9 (C- i-Ar), 138.0 (C- i-Ar), 137.3 (C- i-Ar), 133.6

(C- Ar), 129.0 (C- Ar), 128.7 (C- Ar), 128.2 (C- Ar), 126.7 (C- Ar), 126.5 (C- Ar), 125.3 (C- Ar),

114.9 (C2), 70.0 (C9), 22.4 (C10), 21.1(C11) ppm; **^{119}Sn{^{1}H}NMR** (149 MHz, C_6D_6, δ): -195.0

ppm. Found: C, 50.50, H, 4.75. Calc. for $C_{27}H_{26}OSn$: C, 61.96, H, 4.95%.

5.23 Synthesis of Benzyl methyl ether (214):
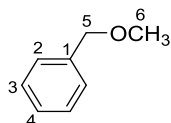
NaOCH$_3$ (1.6 g, mmol) was dissolved in 50 mL of CH$_3$OH and added to benzyl bromide (5.0 g,

mmol) in a two neck round bottom flask equipped with a condenser and heated to reflux for 24 h.

The solution was cooled to room temperature and solvent removed under reduced pressure. 60 mL

of EtOAc was added to the flask and the organic layer washed with (2×50 mL) water, and dried

over $MgSO_4$. The solvent was removed under reduced pressure to obtain a colourless oil of **214**.

NMR data (^{1}H, ^{13}C) was comparable to that reported in the literature.[152] Yield: 10.6 g (34%).

^{1}H NMR (400 MHz, $CDCl_3$, δ): 7.39-7.41 (m, 4H, H2, H3), 7.32 (m, 1H, H4), 4.51 (s, 2H, H5),

3.44 (s, 3H, H6) ppm; **^{13}C NMR** (100 MHz, $CDCl_3$, δ): 138.3 (C1), 128.4 (C), 127.8 (C), 127.7

(C), 74.7 (C5), 58.1 (C6) ppm.

5.24 Synthesis of 2-Bromobenzyl methyl ether (215):
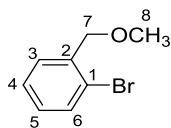
$NaOCH_3$ (3.39 g, 62.75 mmol) was dissolved in 40 mL of CH_3OH and added to 2-bromobenzyl

bromide (15.6 g, 62.41 mmol) in a two neck round bottom flask equipped with a condenser and

heated to reflux for 5 h. The reaction mixture was cooled to room temperature and the solvent

removed under reduced pressure. A mixture of 100 mL of hexane and Et_2O (1:1) was added to

flask. The organic layer was washed with (2×50 mL) water and (2×50 mL) of brine, and finally

dried over $MgSO_4$. The solvent was removed under reduced pressure to obtain a colorless oil of 1-

bromo-2-(methoxymethyl)benzene. NMR data (^{1}H, ^{13}C) was comparable to that reported in the

literature.[95] Yield: 10.6 g (84%).

^{1}H NMR (400 MHz, $CDCl_3$, δ): 7.57 (dd, $J = $ 8.0 Hz, 1H) 7.55 (dd, $J = $ 7.6 Hz, 1H), 7.33 (td, J

$= 7.6$ Hz, 1H), 7.15 (td, $J = 8.0$ Hz, 1H), 4.55 (s, 2H), 3.49 (s, 3H) ppm; **^{13}C NMR** (100 MHz,

$CDCl_3$, δ): 137.6 (C2), 132.5 (C3), 129.0 (C6), 128.9 (C4), 127.4 (C5), 122.7 (C1), 73.9 (C7), 58.6

(C8) ppm.

5.25 Synthesis of [2-(MeOCH$_2$)C$_6$H$_4$]Li (216):

1.6 M solution of *n*-BuLi (26.0 mL, 41.6 mmol) in hexane was added dropwise to a solution of 2-bromobenzyl methyl ether (8.37 g, 41.64 mmol) in 40 mL of hexane at -78 ℃ over 30 min. The solution became yellow and hazy with the addition of *n*-BuLi. A yellow tinged white coloured solid began to precipitate from solution after 1h and the reaction mixture allowed to stir overnight. The solid product was separated by filtration through glass frit and washed with hexane. The remaining residual solvent was removed under reduced pressure to give an off white coloured solid. Yield: 5.16 g (97%).

Warning: [2-(MeOCH$_2$)C$_6$H$_4$]Li should be used *in situ* and not isolated due to its pyrophoric nature. This compound is shock sensitive and can detonate even in glove box. Therefore, avoid isolation.

5.26 Synthesis of 2-Trimethylstannylbenzyl methyl ether (113):
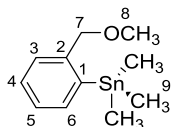
Compound **215** (2.0 g, 9.95 mmol) and 20 mL of hexane were added to a dry 100 mL Schlenk flask equipped with a magnetic stirrer and septum. 1.6 M *n*-BuLi in hexane (6.3 mL, 10.1 mmol) was added slowly at -78 ℃. The cooling bath was removed for 15 min and the *in situ* generated lithium benzyl methyl ether allowed to react with a solution of Me$_3$SnCl (1.98 g, 9.94 mmol in 10 mL hexane/Et$_2$O (1:1)) at -78 ℃. The reaction mixture was warmed to room temperature and stirred for 3 h. The solvent was removed under reduced pressure and the recovered crude product taken up in 1:1 Et$_2$O/hexanes (80 mL), washed with (2 × 100 mL) water and (2 × 50 mL) brine. The organic layer was dried over MgSO$_4$, filtered, and solvent removed under reduced pressure to

give a colourless oil. NMR data (^{1}H, ^{13}C, ^{119}Sn) is essentially the same as previously reported in the literature.[95] Yield: 1.98 g (70%).

^{1}H NMR (400 MHz, CDCl$_3$, δ): 7.6 (m, 1H, H6), 7.31-7.35 (m, 3H, H3, H4, H5), 4.51 (s, H7), 3.41 (s, 3H, H8), 0.34 (s, 9H, H9, $^1J_{119Sn\text{-}1H}$ = 56 Hz) ppm; **^{13}C NMR** (100 MHz, CDCl$_3$, δ): 144.6 (C2, ^2J = 27 Hz), 141.5 (C1, $^1J_{119Sn\text{-}13C}$ = 476 Hz), 136.6 (C6, ^2J = 44 Hz), 128.2 (C3, $^3J_{119Sn\text{-}13C}$ = 6.0 Hz), 127.7 (C5, $^3J_{119Sn\text{-}13C}$ = 11 Hz), 127.2 (C4), 76.3 (C7, $^3J_{119Sn\text{-}13C}$ = 19 Hz), 57.8 (C8), 8.06 (C9, $^1J_{119Sn\text{-}13C}$ = 175 Hz) ppm; **^{119}Sn{^{1}H}NMR** (149 MHz, CDCl$_3$, δ): -32.5 ppm.

5.27 Synthesis of 2-Tributylstannylbenzyl methyl ether (217):

Compound **215** (2.0 g, 9.95 mmol) in 20 mL of hexanes was added to a 100 mL dry Schlenk flask equipped with a magnetic stirrer and septum. 1.6 M *n*-BuLi in hexanes (6.2 mL, 9.92 mmol) was added at -78 ºC. After addition of *n*-BuLi the cooling bath was removed for 15 minutes and the lithiated reagent allowed to react with the *n*-Bu$_3$SnCl (3.22 g, 9.9 mmol) in 10 mL hexane/Et$_2$O (1:1) at -78 ºC added slowly to the flask. The reaction mixture was stirred for 3 h and solvent removed under reduced pressure. The remaining solution was taken up in 1:1 Et$_2$O/hexanes (80 mL), washed with (2 × 100 mL) water and (2 × 50 mL) brine. The organic layer dried over MgSO$_4$, filtered, and solvent removed under reduced pressure to give a clear, yellow-brown coloured oil. Yield: 2.64 g (65%).

^{1}H NMR (400 MHz, CDCl$_3$, δ): 7.55 (d, 1H, H6), 7.31 (m, 3H, H3, H4, H5), 4.46 (s, 2H, H7), 3.41 (s, 3H, H8), 1.60 (m, 6H, H10), 1.39 (m, 6H, H11), 1.14 (m, 6H, H9), 1.11 (t, 9H, H12) ppm; **^{13}C NMR** (100 MHz, CDCl$_3$, δ): 144.7 (C2, $^2J_{119Sn13C}$ = 25 Hz), 141.6 (C1, $^1J_{119Sn\text{-}13C}$ = 390 Hz,

$^1J_{119Sn-13C}$ = 370 Hz), 137.2 (C6, $^2J_{119Sn13C}$ = 30 Hz), 128.0 (C4), 127.9 (C3, $^3J_{119Sn13C}$ = 14 Hz), 127.0 (C-5, $^3J_{119Sn13C}$ = 40 Hz), 76.8 (C7, $^2J_{119Sn13C}$ = 18 Hz), 57.9 (C8), 29.2 (C11, $^3J_{SnC}$ = 20 Hz), 27.5 (C10, $^2J_{119Sn13C}$ = 60 Hz), 13.7 (C12), 10.4 (C9, $^1J_{119Sn13C}$ = 344 Hz, $^1J_{119Sn13C}$ = 325 Hz) ppm; **^{119}Sn{^{1}H}NMR** (149 MHz, CDCl$_3$, δ): -40.3 ppm. **HRMS-DART** (m/z): [M$^+$], Calc. for C$_{20}$H$_{37}$OSn 413.18664; found 413.18728.

5.28 Synthesis of 2-Triphenylstannylbenzyl methyl ether (112):
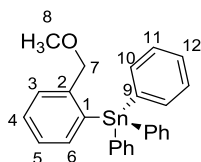
1.6 M solution of *n*-BuLi (3.1 mL, 4.97 mmol) was added dropwise at -78 ºC to a solution of **215** (1.0 g, 4.97 mmol) in 25 mL hexane. The resulting yellow solution was stirred for an additional 2 h at RT, then added dropwise to a suspension of Ph$_3$SnCl (1.87 g, 4.85 mmol) in 30 mL of hexane, followed by stirring for further 3 h. The resulting solid was filtered and washed with 15 mL of *n*-hexane and the filtrate concentrated to 15 mL. Cooling to -20 ºC afforded **112** as a white coloured solid. Yield: 0.80 g (73%), m.p. 95 ºC.[94]

^{1}H NMR (400 MHz, CDCl$_3$, δ): 7.59 (m, 6H, H10), 7.48 (d, 1H, H6), 7.36 (m, 9H, H11,12), 7.30 (m, 2H, H4, H5), 7.24 (m, 1H, H3), 4.37 (s, 2H, H7, $^3J_{119Sn-1H}$ = 269 Hz), 2.80 (s, 3H, H8) ppm; **^{13}C NMR** (100 MHz, CDCl$_3$, δ): 145.2 (C2, $^2J_{119Sn-13C}$ = 33 Hz), 140.3 (C9, $^1J_{119Sn-13C}$ = 543 Hz), 138.6 (C11, $^3J_{119Sn-13C}$ = 38 Hz), 137.2 (C10, $^2J_{119Sn-13C}$ = 40 Hz), 136.5 (C12), 129.0 (C3, $^3J_{119Sn-13C}$ = 12 Hz), 128.5 (C5, $^3J_{119Sn-13C}$ = 12 Hz), 128.3 (C4), 127.5 (C1, $^1J_{119Sn-13C}$ = 56 Hz), 127.3 (C6, $^2J_{119Sn-13C}$ = 46 Hz), 75.2 (C7, $^3J_{119Sn-13C}$ = 20 Hz), 57.3 (C8) ppm; **^{119}Sn{^{1}H}NMR** (149 MHz, CDCl$_3$, δ): -133.0 ppm. Found: C, 65.74, H, 5.11. Calc. for C$_{27}$H$_{26}$OSn: C, 66.28, H, 5.13%**.**

5.29 Synthesis of [2-(MeOCH₂)C₆H₄]MeSnCl₂ (218):

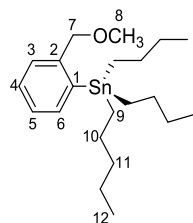**5.29 Synthesis of [2-(MeOCH$_2$)C$_6$H$_4$]MeSnCl$_2$ (218):**
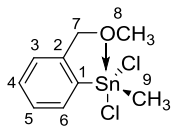
Compound **215** (0.5 g, 2.48 mmol) in 20 mL of hexane was added to a 100 mL dry Schlenk flask equipped with a magnetic stirrer and septum. 1.6 M *n*-BuLi in hexane (1.55 mL, 2.48 mmol) was slowly added at -78 ℃. The cooling bath was removed for 30 min, and the lithiated reagent allowed to react with a solution of MeSnCl$_3$ (0.58 g, 2.08 mmol) in 10 mL of hexane/Et$_2$O (1:1) at -78 ℃ added slowly to the reaction mixture. The reaction mixture was warmed to room temperature and stirred stirred for 3 h and solvent removed under reduced pressure. The residue was taken up in toluene (20 mL), decanted and the solvent removed under reduced pressure to give clear, brown oil. Yield: 0.67 g (98%).

¹H NMR (400 MHz, CDCl$_3$, δ): 8.12 (m, 1H, H6), 7.46 (m, 2H, H4, H5), 7.21 (m, 1H, H3), 4.77 (s, 2H, H7, $^3J_{119Sn-1H}$ = 9.0 Hz), 3.42 (s, 3H, H8), 1.26 (s, 3H, H9, $^1J_{119Sn-1H}$ = 83 Hz, $^1J_{117Sn-1H}$ = 79 Hz) ppm; **¹³C NMR** (100 MHz, CDCl$_3$, δ): 141.7 (C2), 136.3 (C4), 134.6 (C1), 131.1 (C3), 128.6 (C5), 125.2 (C6), 73.9 (C8), 58.8 (C7), 8.42 (C9) ppm; **¹¹⁹Sn{¹H}NMR** (149 MHz, CDCl$_3$, δ): -54.0 ppm. **HRMS-DART** (m/z): [M$^+$] + H$_2$O calculated for C$_9$H$_{12}$Cl$_2$OSn 343.96309; found 343.96336.

5.30 Synthesis of [2-(MeOCH₂)C₆H₄]BuSnCl₂ (219):

5.30 Synthesis of [2-(MeOCH$_2$)C$_6$H$_4$]BuSnCl$_2$ (219):
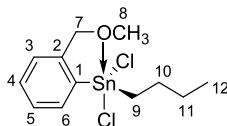
Compound **215** (2.0 g, 9.95 mmol) in 30 mL of hexane was added to a 100 mL dry Schlenk flask equipped with a magnetic stirrer and septum. The solution was cooled to -78 ℃ and 1.6 M *n*-BuLi in hexane (6.2 mL, 9.92 mmol) was then added. The cooling bath was removed after 30 min and

the lithiated reagent allowed to react with a solution of n-BuSnCl$_3$ (2.75 g, 9.75 mmol) in 15 mL

hexane/Et$_2$O (1:1) at 0 °C that was slowly added to the reaction mixture and stirred for 3 h. The

solvent was removed under reduced pressure and the residue taken up in toluene (25 mL) and

decanted. The solvent was removed under reduced pressure to give a clear, orange-brown coloured

oil. The product was further purified by extraction with hot hexanes. Yield: 2.9 g (81%).

^{1}H NMR (400 MHz, CDCl$_3$, δ): 8.11 (d, 1H, H6), 7.41-7.47 (m, 2H, H4, H5), 7.22 (m, 1H, H3),

4.75 (s, 2H, H7), 3.65(s, 3H, H8), 1.85 (m, 4H, H10, H11), 1.43 (t, 2H, H9), 0.95 (t, 3H, H12)

ppm; **^{13}C NMR** (100 MHz, CDCl$_3$, δ): 141.8 (C2, $^2J_{119Sn-13C}$ = 48 Hz), 136.0 (C5, $^3J_{119Sn-13C}$ = 55

Hz), 134.9 (C3), 130.8 (C4), 128.3 (C1, $^1J_{119Sn-13C}$ = 81 Hz, $^1J_{117Sn-13C}$ = 78 Hz), 125.2 (C6, $^2J_{119Sn-13C}$ = 74 Hz, $^2J_{117Sn-13C}$ = 70 Hz), 73.8 (C7, $^3J_{119Sn-13C}$ = 18 Hz), 59.0 (C8), 27.9 (C9, $^1J_{119Sn-13C}$ = 652 Hz, $^1J_{117Sn-13C}$ = 624 Hz), 27.1 (C11, $^3J_{119Sn-13C}$ = 40 Hz), 26.0 (C10, $^2J_{119Sn-13C}$ = 106 Hz, $^2J_{119Sn-13C}$ = 102 Hz) 13.6 (C12) ppm; **^{119}Sn{^{1}H}NMR** (149 MHz, CDCl$_3$, δ): -61.0 ppm. **HRMS-DART** (m/z): [M$^+$] + H$_2$O calculated for C$_{12}$H$_{22}$Cl$_2$O$_2$Sn 386.00907; found 386.00918. Found: C, 39.36, H, 4.93. Calc. for C$_{27}$H$_{26}$OSn: C, 39.18, H, 4.93%.

5.31 Synthesis of [2-(MeOCH$_2$)C$_6$H$_4$]PhSnCl$_2$ (220):

Compound **215** (1.0 g, 4.98 mmol) in 30 mL of hexanes was added to a 100 mL dry Schlenk flask

equipped with a magnetic stirrer and septum. The solution was cooled to -78 °C and 1.6 M n-BuLi

in hexane (3.1 mL, 4.96 mmol) was then added. The cooling bath was removed for 30 min and the

lithiated C,O-ligand was allowed to react with a solution of PhSnCl$_3$ (1.46 g, 4.83 mmol) in 15 mL

hexane/Et$_2$O (1:1) at -78 °C. The reaction mixture was stirred for 3 h and solvent removed under

reduced pressure. The product was extracted with hot hexanes and precipitated as a white coloured

powder at -30 °C. The yield of this product was not obtained due to the presence of a minor impurity found in the ^{119}Sn NMR spectrum.

^{1}H NMR (400 MHz, CDCl$_3$, δ): 7.76 (m, 3H, H6, H10), 7.59 (m, 3H, H11, H12), 7.52 (m, 1H, H4), 7.36 (m, 1H, H5), 7.18 (td, 1H, H3), 4.58 (s, 2H, H7), 3.45 (s, 3H, H8) ppm; **^{13}C NMR** (100 MHz, CDCl$_3$, δ): 137.6 (C2), 137.0 (C1, $J_{119Sn-13C}$ = 72 Hz), 135.1 (C10, $J_{119Sn-13C}$ = 64 Hz, $^{1}J_{117Sn-13C}$ = 60 Hz), 132.6 (C5), 131.9 (C6, $J_{119Sn-13C}$ = 20 Hz), 129.8 (C9, $J_{119Sn-13C}$ = 86 Hz, $J_{117Sn-13C}$ = 82 Hz), 129.1 (C4), 129.0 (C12), 127.5 (C3), 122.8 (C11), 73.9 (C7), 58.6 (C8) ppm; **^{119}Sn{^{1}H}NMR** (149 MHz, CDCl$_3$, δ): -28.2 ppm (-48.2 ppm, impurity)

5.32 Synthesis of [2-(MeOCH$_2$)C$_6$H$_4$]Ph$_2$SnCl (221):
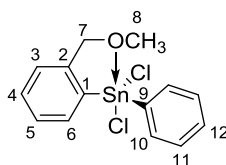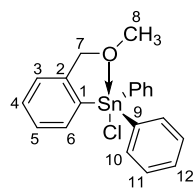

Method 1: Compound **215** (2.0 g, 9.95 mmol) in 20 mL of hexane was added to a 100 mL dry Schlenk flask equipped with a magnetic stirrer and septum. The solution was cooled to -78 °C and 1.6 M *n*-BuLi in hexane (1.55 mL, 9.92 mmol) was then added. The cooling bath was removed after 30 min and the lithiated *C,O*-ligand was allowed to react with a solution of Ph$_2$SnCl$_2$ (3.17 g, 9.22 mmol) in 10 mL hexane/Et$_2$O (1:1) at -78 °C. The reaction mixture was stirred for further 3 h and solvent removed under reduced pressure. The residue was taken up in toluene (20 mL). After decanting, the solvent was removed under reduced pressure to give a mixed semi-solid product. Hexane was added to the mixture of products and a solid product separated by filtration. The residual solvent was removed to obtain a white solid of (**221**). Yield: 1.5 g (38%) m.p. 155 °C.

Method 2: A 1.0 M HCl solution in Et$_2$O (0.43 mL, 0.43 mmol) was added to a solution of **112** (0.21 g, 0.44 mmol) in 25 mL of dry C$_6$H$_6$. The resulting yellow coloured solution was stirred for

30 min. The solvent was removed under reduced pressure and the crude product extracted with hot hexane. The solution was cooled to -20º C and a white coloured solid precipitated overnight. Yield: 0.15 g (81%), m.p. 155 ºC.

^{1}H NMR (400 MHz, CDCl$_3$, δ): 8.35 (d, 1H, H6), 7.72 (m, 4H, H11), 7.50 (m, 6H, H10,12), 7.4 (m, 2H, H3, H4), 7.24 (m, 1H, H5), 4.74 (s, 2H, H7, $^3J_{119Sn-1H}$ = 11 Hz), 3.13 (s, 3H, H8) ppm; **^{13}C NMR** (100 MHz, CDCl$_3$, δ): 142.8 (C9, $^1J_{119Sn13C}$ = 42 Hz), 141.0 (C2), 137.7 (C1, $^1J_{119Sn13C}$ = 41 Hz), 135.7 (C5, $^3J_{119Sn-13C}$ = 50 Hz, $^3J_{117Sn-13C}$ = 47 Hz), 133.1 (C4), 129.8 (C3, $^3J_{119Sn13C}$ = 14 Hz), 129.5 (C12, $^4J_{119Sn13C}$ = 15 Hz), 128.7 (C10, $^2J_{119Sn-13C}$ = 70 Hz, $J_{117Sn-13C}$ = 67 Hz), 128.2 (C6, $^2J_{119Sn13C}$ = 68 Hz), 124.8 (C11, $^3J_{119Sn13C}$ = 63 Hz), 74.4 (C7), 58.4 (C8) ppm; **^{119}Sn{^{1}H}NMR** (149 MHz, CDCl$_3$, δ): -127.0 ppm. **HRMS-DART** (m/z): [M$^+$] + H$_2$O calculated for C$_{20}$H$_{21}$ClO$_2$Sn 448.05085; found 448.05098.

### 5.33 Synthesis of [2-(MeOCH$_2$)C$_6$H$_4$]*n*-Bu$_2$SnCl (223):
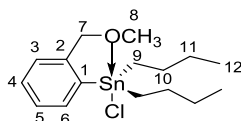
Compound **215** (1.0 g, 4.98 mmol) in 30 mL of hexanes was added to a 100 mL dry Schlenk flask equipped with a magnetic stirrer and septum. The solution was cooled to -78 ºC and 1.6 M *n*-BuLi in hexane (3.1 mL, 4.96 mmol) was then added. The cooling bath was removed for 30 min and the lithiated *C,O*-ligand was allowed to react with a solution of *n*-Bu$_2$SnCl$_2$ (1.47 g, 4.83 mmol) in 15 mL hexane/Et$_2$O (1:1) at -78 ºC. The reaction mixture was stirred for 3 h and solvent removed under reduced pressure. The ^{119}Sn NMR of the crude product showed six resonances. An attempt to purify the crude product by extraction with hot hexanes was unsuccessful. The product was stored in glove box and solid material separated out of the oil. No yield was recorded. NMR chemical shift resonances attributable to 223 are listed below.

¹H NMR (400 MHz, CDCl₃, δ): 8.27 (m, 1H, H6), 7.58 (dd, 1H, H5), 7.36 (m, 1H, H4), 7.15 (m, 1H, H3), 4.71 (s, 2H, H7), 3.60 (s, 3H, H8), 1.79 (m, 8H, H10, H11), 1.43 (m, 4H, H9), 0.98 (m, 6H, H12) ppm; **¹³C NMR** (100 MHz, CDCl₃, δ): 141.7 (C2), 137.3 (C1), 132.6 (C6), 128.8 (C4), 127.5 (C5), 124.1 (C3), 75.1 (C7), 58.5 (C8), 32.9(C9, isomer 1), 32.3 (C9, isomer 2), 27.3 (C10, isomer 1), 27.1 (C10, isomer 2), 26.6 (C11, isomer 1), 26.3 (C11, isomer 2), 13.6 (C12) ppm; **¹¹⁹Sn{¹H}NMR** (149 MHz, CDCl₃, δ): -91.0, -127.0 ppm. **HRMS-DART** (m/z): calcd for C₁₆H₂₇ClOSn 390.08, Found [M+H₂O] 408.1

5.34 Synthesis of [(2-(MeOCH₂)C₆H₄)₂]*n*-BuSnCl (224):

An equimolar amount of 3.1 mL of *n*-BuLi (3.1 mL, 4.97 mmol) was added dropwise at -78 ℃ to a solution of **215** (1.0 g, 4.97 mmol) in 15 mL of Et₂O and stirred for an additional 2 h. The resulting solution was added dropwise to a suspension of *n*-BuSnCl₃ (0.686 g, 2.43 mmol) in 20 mL of hexane/Et₂O at 0 ℃, followed by stirring for further 3 h. Purification of the crude product was unsuccessful. There are unassigned chemical shifts in ¹H and ¹³C NMR spectrum indicating the presence of impurities.

¹H NMR (400 MHz, CDCl₃, δ): 7.74 (d, 1H, H6), 7.43 (dd, 1H, H5), 7.28 (m, 2H, H3), 7.45 (m, 1H, H4), 3.052-3.45 (4s, 3H, H8), 4.38-4.64 (5s, 2H, H7) 2.15- 1.2 (m, 6H, H9, H10, H11), 1.1-0.8 (m, 3H, H12) ppm; **³C NMR** (100 MHz, CDCl₃, δ): 142.9 (C1, $^{1}J_{119Sn\text{-}13C}$ = 370 Hz), 139.9 (C2), 136.3 (C6, $J_{119Sn\text{-}13C}$ = 43 Hz), 132.5 (C5), 129.1 (C3, $J_{119Sn\text{-}13C}$ = 13 Hz), 128.9 (C4), [128.4, 127.6, 127.4, 126.6 impurities], 75.6 (C7), 58.1 (C8), 27.8 (C10, $^{2}J_{119Sn\text{-}13C}$ = 93 Hz), 26.6 (C11,

$^3J_{119Sn-13C}$ = 30 Hz), 20.8 (C9, $^1J_{119Sn-13C}$ = 549 Hz, $J_{117Sn-13C}$ = 525 Hz), 13.7 (C12) ppm;

^{119}Sn{^{1}H}NMR (149 MHz, CDCl$_3$, δ): -73.0 ppm.

5.35 Synthesis of [(2-(MeOCH$_2$)C$_6$H$_4$)$_2$]PhSnCl (225):
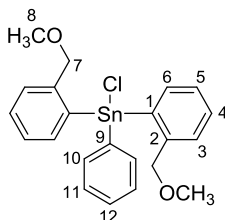
An equimolar amount of 3.1 mL of *n*-BuLi (3.1 mL, 4.97 mmol) was added dropwise at -78 °C to

a solution of **215** (1.0 g, 4.97 mmol) in 15 mL of Et$_2$O and stirred for an additional 2 h. The

resulting solution was added dropwise to a suspension of PhSnCl$_3$ (0.734 g, 2.43 mmol) in 20 mL

of hexane/Et$_2$O at room temperature, followed by stirring for further 3 h. An attempt to purify the

crude product was attempted by washing with hexane, but was unsuccessful.

^{1}H NMR (400 MHz, CDCl$_3$, δ): 7.89 (dd, 1H, H$_{aryl}$), 7.73 (br s, 1H, H$_{aryl}$), 7.65 (br s, 1H, H$_{aryl}$),

7.58 (br s, 3H, H$_{aryl}$), 7.39 (m, 7H, H$_{aryl}$), 4.31 (s, 2H, H7), 2.81 (s, 3H, H8) ppm; **^{13}C NMR** (100

MHz, CDCl$_3$, δ): 144.9 (C1, $J_{119Sn-13C}$ = 29 Hz), 140.2 (C2), 138.0 (C9, $J_{119Sn-13C}$ = 40 Hz), 137.2

(C11), 135.0 (C12), 131.8 (C10, $^2J_{119Sn-13C}$ = 18 Hz), 129.7 (C4), 128.6(C6, $J_{119Sn-13C}$ = 11 Hz),

128.1 (C3), 127.3 (C5), 75.9 (C7, $^3J_{119Sn-13C}$ = 23 Hz), 57.5 (C8) ppm; **^{119}Sn{^{1}H}NMR** (149 MHz,

CDCl$_3$, δ): -136.0 ppm.

5.36 Synthesis of [2-(MeOCH$_2$)C$_6$H$_4$]MeSnH$_2$ (226):
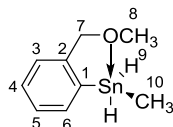
A solution of **218** (0.52 g, 1.6 mmol in 15 mL of Et$_2$O) was added dropwise to a suspension of

LiAlH$_4$ (0.34 g, 3.0 mmol in 15 mL of Et$_2$O), and stirred at 0 °C for 3 h. The reaction was quenched

with 10 mL of degassed and chilled water. The organic layer was separated and the aqueous layer

extracted with Et$_2$O (3 × 10 mL). The combined organic layers were dried over anhydrous MgSO$_4$.

The solvent was removed under reduced pressure to yield **226** as a yellow coloured oil. Yield: 0.35

g (85%). The product start decomposing as soon as the temperature start rising after the removal

of solvent. The ^{1}H and ^{13}C NMR of **226** is not included. The ^{119}Sn NMR data and mass

spectrometry are listed below.

^{119}Sn{^{1}H}NMR (149 MHz, C$_6$D$_6$, δ): -221.0 ppm. **HRMS-DART** (m/z): [M$^+$] - H calculated for

C$_9$H$_{13}$OSn 256.99967; found 256.99884.

5.37 Synthesis of [2-(MeOCH$_2$)C$_6$H$_4$]n-BuSnH$_2$ (227):
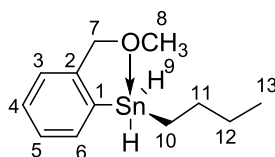
A solution of **219** (0.5 g, 1.35 mmol in 15 mL of Et$_2$O) was added dropwise to a suspension of

LiAlH$_4$ (0.114 g, 7.0 mmol in 15 mL of Et$_2$O), and stirred at 0 ℃ for 3 h. The reaction was

quenched with 5 mL of degassed and chilled water. The organic layer was separated and the

aqueous layer extracted with Et$_2$O (3 × 10 mL). The combined organic layers were dried over

anhydrous MgSO$_4$. The solvent was removed under reduced pressure to yield **225** as a yellow

coloured oil. Yield: 0.28 g (70%).

^{1}H NMR (400 MHz, CDCl$_3$, δ): 7.80 (m, 1H, H6), 7.21 (m, 2H, H4, H5), 7.06 (m, 1H, H3), 5.78

(s, 2H, H9, $^1J_{119Sn-1H}$ = 1727 Hz, $^1J_{117Sn-1H}$ = 1677 Hz), 4.27 (s, 2H, H7), 3.12 (s, 3H, H8), 1.70 (m,

2H, H11), 1.42 (m, 2H, H10), 1.30 (m, 2H, H12), 0.96 (t, 3H, H13) ppm; **^{13}C NMR** (100 MHz,

CDCl$_3$, δ): 145.0 (C2, $^2J_{119Sn-13C}$ = 26 Hz), 139.3 (C6, $^2J_{119Sn-13C}$ = 39 Hz), 137.2 (C1, $^1J_{119Sn-13C}$ =

522 Hz, $^1J_{117Sn-13C}$ = 498 Hz), 128.7 (C5, $^3J_{119Sn-13C}$ = 12 Hz), 127.7 (C4), 127.4 (C3), 76.1 (C7,

$^2J_{119Sn-13C}$ = 19 Hz), 57.1 (C8), 30.6 (C11, $^2J_{119Sn-13C}$ = 22 Hz), 27.1 (C10, $^1J_{119Sn-13C}$ = 67 Hz), 13.9

(C12), 10.2 (C13) ppm; **^{119}Sn{^{1}H}NMR** (149.21 MHz, C$_6$D$_6$, δ): -210.0 ppm. **HRMS-DART** (m/z): [M$^+$] calculated for ^{12}C$_{12}$^{1}H$_{19}$^{16}O^{116}Sn 295.04534; found 295.04595.

5.38 Polymerization of 227:

TMEDA (0.16 mL, 0.124 g1.07 mmol) was added to a solution of **227** (0.32 g, mmol) in 10 mL of Et$_2$O. The reaction mixture turned yellow in colour and was stirred for 36 h. The product was unsuccesfuly precipitated in hexane, petroleum ether. Limited analysis was undertaken.

^{119}Sn{^{1}H}NMR (149 MHz, C$_6$D$_6$, δ): -196.0.

5.39 Synthesis of 2-Bromo-*N,N*-dimethylbenzylamine (228):
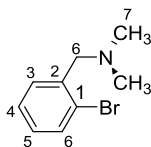
16.0 mL of a 33% dimethylamine solution (120.0 mmol) was added dropwise to 4.0 g (16.0 mmol) of 2-bromo-benzylbromide dissolved in 30 mL of DCM in 100 mL Schlenk flask. The reaction mixture was heated at 42 ºC under N$_2$ in a closed system for 7 h. The product was extracted with 3 M HCl (3 × 30 mL) and the extract neutralized with an alkaline solution containing 20% NaOH. The basic product was isolated by extraction with DCM. NMR data (^{1}H, ^{13}C) agreed well with the reported literature.[158] Yield: 3.0 g (87%).

^{1}H NMR (400 MHz, CDCl$_3$, δ): 7.53 (d, 1H, H3), 7.42 (d, 1H, H6), 7.27 (m, 1H, H4), 7.11 (m, 1H, H5), 3.52 (s, 2H, H6), 2.30 (s, 6H, H7) ppm; **^{13}C NMR** (100 MHz, CDCl$_3$, δ): 138.1 (C2), 132.7 (C3), 130.9 (C6), 128.4 (C5), 127.2 (C4), 124.7 (C1), 63.3 (C6), 45.5 (C7) ppm.

5.40 Synthesis of [2-(Me$_2$NCH$_2$)C$_6$H$_4$]Li (229):[176]

63.0 mL (100.0 mmol) of 1.6 M solution of *n*-BuLi in hexane was added dropwise to a solution of 13.52 g (100.0 mmol) of **228** in 150 mL Et$_2$O. The solution became yellow and hazy during the

addition of *n*-BuLi. The white solid started to precipitate after 1 h. The reaction mixture was stirred overnight. The solid product was separated by decantation and the remaining residual solvent was removed under reduced pressure. Yield: 12.1 g (87%).

5.41 Synthesis of [2-(Me₂NCH₂)C₆H₄]MeSnCl₂ (33):
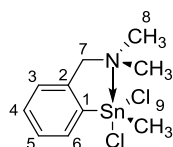
A suspension of **229** (0.294 g, 2.08 mmol) in 30 mL Et₂O was added dropwise over 30 min to a solution of MeSnCl₃ (0.500 g, 2.08 mmol) in 20 mL Et₂O at -78 ℃. The reaction mixture was stirred for 3 h at room temperature. The salt was removed by decantation in the glove box, and the solvent removed under reduced pressure. The product was purified by extraction with toluene. The product was white coloured solid. NMR data (^{1}H, ^{13}C, ^{119}Sn) agreed with the reported literature.[26] Yield: 0.35 g (85%)

^{1}H NMR (400 MHz, CDCl₃, δ): 8.18 (m, 1H, H6, $^2J_{119Sn-1H}$ = 100 Hz, $^2J_{117Sn-1H}$ = 98.0 Hz), 7.44 (m, 2H, H4, H5), 7.20 (m, 1H, H3), 3.76 (s, 2H, H7), 2.43 (s, 6H, H8), 1.26 (s, 3H, H9, $^1J_{119Sn-1H}$ = 84 Hz, $^1J_{117Sn-1H}$ = 76 Hz) ppm; **^{13}C NMR** (100 MHz, CDCl₃, δ): 141.9 (C2, $^2J_{119Sn-13C}$ = 52 Hz, $^2J_{117Sn-13C}$ = 49 Hz), 138.5 (C1), 137.0 (C3, $^3J_{119Sn-13C}$ = 67 Hz, $^2J_{117Sn-13C}$ = 65 Hz), 131.2 (C4), 128.7 (C6, $^2J_{119Sn-13C}$ = 94 Hz), 127.4 (C5, $^3J_{119Sn-13C}$ = 79 Hz, $^3J_{117Sn-13C}$ = 76 Hz), 63.2 (C7, $^3J_{119Sn-13C}$ = 39 Hz), 44.9 (C8), 8.0 (C9, $^1J_{119Sn-13C}$ = 696 Hz, $^1J_{117Sn-13C}$ = 669 Hz) ppm; **^{119}Sn{^{1}H}NMR** (149 MHz, CDCl₃, δ): -96.4 ppm.

5.42 Synthesis of [2-(Me₂NCH₂)C₆H₄]*n*-BuSnCl₂ (37):
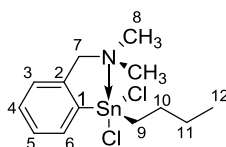
A suspension of **229** (2.0 g, 14.2 mmol) in 30 mL Et$_2$O was added dropwise over 30 min to solution of *n*-BuSnCl$_3$ (4.0 g, 14.2 mmol) in 20 mL Et$_2$O at 0 ℃. The reaction mixture was stirred overnight. The crude product was separated by decantation in the glove box. The solvent was removed under reduced pressure. The product was extracted with hot hexane and a white solid product obtained. NMR data (^{1}H, ^{13}C, ^{119}Sn) agreed with the reported literature.[29b,51] Yield: 3.9 g (73%).

^{1}H NMR (400 MHz, CDCl$_3$, δ): 8.18 (m, 1H, H6), 7.41 (m, 2H, H4, H5), 7.20 (m, 1H, H3), 3.74 (s, 2H, H7), 2.43 (s, 6H, H8), 1.92 (m, 2H, H10), 1.80 (t, 2H, H9), 1.45 (sex, 2H, H11), 0.95 (t, 3H, H12) ppm; **^{13}C NMR** (100 MHz, CDCl$_3$, δ): 141.1 (C2, $^2J_{119Sn-13C}$ = 48 Hz), 139.6 (C1), 137.0 (C6, $^2J_{119Sn-13C}$ = 65 Hz, $^2J_{117Sn-13C}$ = 63 Hz), 130.9 (C4, $^4J_{119Sn-13C}$ = 16 Hz), 128.6 (C5, $^3J_{119Sn-13C}$ = 89 Hz, $^3J_{119Sn-13C}$ = 85 Hz), 127.4 (C3, $^3J_{119Sn-13C}$ = 74 Hz, $^3J_{117Sn-13C}$ = 72 Hz), 63.4 (C7, $^3J_{119Sn-13C}$ = 34 Hz), 45.1 (C8), 27.4 (C11, $^3J_{119Sn-13C}$ = 44 Hz, $^3J_{117Sn-13C}$ = 42 Hz), 27.2 (C9, $^1J_{119Sn-13C}$ = 694 Hz, $^1J_{117Sn-13C}$ = 664 Hz), 26.3 (C10, $^2J_{119Sn-13C}$ = 120 Hz, $^2J_{117Sn-13C}$ = 115 Hz), 13.7 (C12) ppm; **^{119}Sn{^{1}H}NMR** (149 MHz, CDCl$_3$, δ): -104.0 ppm.

5.43 Synthesis of [2-(Me$_2$NCH$_2$)C$_6$H$_4$]PhSnCl$_2$ (35):
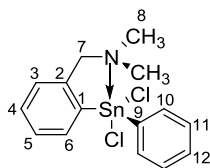
A suspension of **229** (0.467 g, 3.1 mmol) in 30 mL Et$_2$O was added dropwise over 30 min to a solution of PhSnCl$_3$ (1.0 g, 3.1 mmol) in 20 mL Et$_2$O at 0 ℃. With the addition of **229** a white precipitate formed. The reaction mixture was stirred for 3 h at room temperature. The solid by-product was separated by decantation in the glove box. The solvent was removed under reduced pressure. The crude product was purified by extraction with toluene and the solvent was removed

under reduced pressure, and a white coloured powder recovered. NMR data (^{1}H, ^{13}C, ^{119}Sn) agreed with the reported literature.[26,29a,35] Yield: 1.1 g (69%).

^{1}H NMR (400 MHz, CDCl$_3$, δ): 8.36 (d, 1H, H6, $^3J_{119Sn-1H}$ = 101 Hz), 7.68 (d, 2H, H10), 7.50 (m, 2H, H4, H5), 7.46 (m, 3H, H1, H12), 7.26 (d, 1H, H3), 3.72 (s, 2H, H7), 2.19 (s, 6H, H8) ppm;

^{13}C NMR (100 MHz, CDCl$_3$, δ): 141.6 (C2), 141.5 (C1, $^1J_{119Sn-13C}$ = 56 Hz), 137.9 (C11, $^1J_{119Sn-13C}$ = 66 Hz), 136.8 (C4), 133.8 (C6, $^2J_{119Sn-13C}$ = 65 Hz), 131.6 (C3, $^3J_{119Sn-13C}$ = 17 Hz), 130.5 (C5, $^3J_{119Sn-13C}$ = 20 Hz), 129.4 (C9, $^1J_{119Sn-13C}$ = 95 Hz), 129.0 (C10, $^1J_{119Sn-13C}$ = 94 Hz), 127.8 (C10, $^2J_{119Sn-13C}$ = 83 Hz), 63.2 (C7, $^3J_{119Sn-13C}$ = 44 Hz), 45.4 (C8) ppm; **^{119}Sn{^{1}H}NMR** (149 MHz, CDCl$_3$, δ): -168.0 ppm.

5.44 Synthesis of [2-(Me$_2$NCH$_2$)C$_6$H$_4$]MeSnH$_2$ (230):
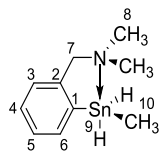
A suspension of **33** (0.240 g, 0.71 mmol) in 20 mL Et$_2$O was added dropwise to 1.0 M LiAlH$_4$ (1.5 mL, 1.5 mmol) in 30 mL of Et$_2$O at 0 ℃. The reaction mixture was stirred for 3 h at 0 ℃. The reaction was quenched with 10 mL of degassed and chilled water. The organic layer was separated and dried over anhydrous MgSO$_4$, and the solvent removed under reduced pressure to give a yellow coloured oil was obtained. It is relatively stable at low temperature. Yield = 0.15 g (76%).

^{1}H NMR (400 MHz, C$_6$D$_6$, δ): 7.78 (m, 1H, H6), 7.15 (m, 2H, H4, H5), 6.95 (m, 1H, H3), 5.63 (q, 2H, H9, $^1J_{119Sn-1H}$ = 1824 Hz, $^1J_{117Sn-1H}$ = 1756 Hz), 3.13 (s, 2H, H7), 1.87(s, 6H, H8), 0.35 (t, 3H, H10, $^1J_{119Sn-1H}$ = 60 Hz) ppm; **^{13}C NMR** (100 MHz, C$_6$D$_6$, δ): 145.0 (C2, $^2J_{119Sn-13C}$ = 27 Hz), 138.85 (C1), 138.5 (C6, $^2J_{119Sn-13C}$ = 47 Hz), 128.6 (C5, $^3J_{119Sn-13C}$ = 12 Hz), 127.8 (C4), 127.2 (C3), 64.9 (C7, $^3J_{119Sn-13C}$ = 24 Hz), 43.6 (C8), -11.3 (C9, $^1J_{119Sn-13C}$ = 392 Hz, $^1J_{117Sn-13C}$ = 382 Hz) ppm;

^{119}Sn{^{1}H}NMR (149.21 MHz, C$_6$D$_6$, δ): -236.0 ppm. **HRMS-DART** (m/z): [M$^+$] - H calculated for C$_{10}$H$_{16}$NSn = 270.03; found = 270.03.

5.45 Synthesis of [2-(Me$_2$NCH$_2$)C$_6$H$_4$]*n*-BuSnH$_2$ (231):
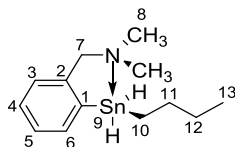
A solution of **37** (1.59 g, 4.16 mmol) in 30 mL Et$_2$O was added dropwise to 1.0 M LiAlH$_4$ (5.0 mL, 5.0 mmol) in 50 mL of Et$_2$O at 0 ℃. The reaction mixture was stirred for 3 h at 0 ℃. The reaction was quenched with 15.0 mL of degassed and chilled water. The organic layer was separated and dried over anhydrous MgSO$_4$. After filtration, the solvent was removed under reduced pressure. A yellow coloured oil was recovered. The product **230** is relatively stable at low temperature. Yield: 1.05 g (81%).

^{1}H NMR (400 MHz, C$_6$D$_6$, δ): 7.78 (m, 1H, H6), 7.13 (m, 2H, H4, H5), 6.94 (m, 1H, H3), 5.72 (s, 2H, H9, $^1J_{119Sn-1H}$ = 1760 Hz, $^1J_{117Sn-1H}$ = 1680 Hz), 3.12 (s, 2H, H7), 1.88 (s, 6H, H8), 1.70 (m, 2H, H11), 1.62 (m, 2H, H10), 1.14 (m, 2H, H12), 0.90 (t, 3H, H13) ppm; **^{13}C NMR** (100 MHz, C$_6$D$_6$, δ): 145.4 (C2, $^2J_{119Sn-13C}$ = 24 Hz), 139.5 (C1), 139.2 (C6, $^2J_{119Sn-13C}$ = 44 Hz), 128.8 (C3, $^3J_{119Sn-13C}$ = 11 Hz), 128.1 (C5, $^3J_{119Sn-13C}$ = 69 Hz), 127.5 (C4), 65.4 (C7, $^3J_{119Sn-13C}$ = 33 Hz), 44.0 (C8), 30.9 (C12, $^3J_{119Sn-13C}$ = 21 Hz), 27.3 (C11, $^2J_{119Sn-13C}$ = 65 Hz), 14.0 (C13), 10.4 (C10, $^1J_{119Sn-13C}$ = 434 Hz, $^1J_{117Sn-13C}$ = 415 Hz) ppm; **^{119}Sn{^{1}H}NMR** (149 MHz, C$_6$D$_6$, δ) -217.0. **HRMS-DART** (m/z): [M+H]$^+$ calculated for C$_{13}$H$_{22}$NSn, 314.09346; found 314.09338.

5.46 Wurtz coupling of 37:

Compound **37** (1.0 g, 2.61 mmol) was dissolved in 5 mL of toluene in a Schlenk flask and 15-crown-5-ether (12 mg, 0.054 mmol) added. In a separate 3-neck flask equipped with reflux condenser, a dispersion of Na (0.130 g, 5.65 mmol) in 5 mL toluene was prepared by reflux at 110

ºC for 1 h. The Na dispersion was allowed to cool to room temperature and the flask wrapped in aluminium foil to protect the reaction from light. The solution of **37** was added dropwise to the stirring sodium dispersion with a syringe. The reaction mixture was heated for 4 h at 60 ºC. The reaction mixture filtered through a frit into aluminium foil wrapped Schlenk flask. The solvent was removed under reduced pressure to produce a light yellow coloured viscous product. **^{119}Sn{^{1}H}NMR** (149 MHz, C$_6$D$_6$, δ): -88.4 ppm (**243**), -135.0 and -138.0 ppm (**244**). By NMR spectra the percentages of (**243**) and (**244**) are 60% and 40% respectively.

Following the above procedure the reaction time was increased from 4 h to 4 days. **^{119}Sn{^{1}H}NMR** (149 MHz, C$_6$D$_6$, δ): -105.7 ppm (**245**).

5.47 Wurtz coupling of 35:

Compound **35** (0.50 g, 1.27 mmol) was dissolved in 5 mL of toluene in a Schlenk flask and 15-crown-5-ether (0.012 mg, 0.054 mmol) added. In a separate 3-neck flask equipped with reflux condenser, Na (0.060 g, 2.61 mmol) dispersion was prepared in 5 mL of toluene by reflux at 110 ºC for 1h. The Na dispersion was allowed to cool to room temperature and flask was then wrapped in aluminium foil to protect the reaction products from light. The solution of **35** added dropwise to the stirring sodium dispersion with a syringe and the reaction mixture was heated for 8h at 60 ºC. The reaction mixture filtered through a frit into aluminium foil wrapped Schlenk flask. The solvent was removed under reduced pressure to produce a yellow coloured product.

^{119}Sn{^{1}H}NMR (149 MHz, C$_6$D$_6$, δ): -145.5 (**246**), -173.0 (**247**), -210.6, -212.2 ppm (cyclo-oligostannane).

5.48 Catalytic dehydrocoupling of 230 using Cp$_2$ZrMe$_2$:
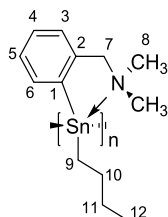
Cp$_2$ZrMe$_2$ (0.005 g, 0.019 mmol) was added to a solution of **230** (0.30 g, mmol) in 10 mL of hexane. The reaction mixture was stirred for 44 h. The solvent was removed under reduced pressure. The product was isolated as brown gummy solid. The crude product was unsuccessfully purified using hexane and MeOH. Some insoluble precipitate was filtered off. The hexane soluble product was used to obtain the NMR data.

^{1}H NMR (400 MHz, CDCl$_3$, δ): 8.74 (1H, H6), 7.21 (1H, H4), 7.0 (1H, H5), 6.83 (1H, H3), 2.92 (2H, H7), 1.60 (3H, H8), 1.88 (m, 2H, H10), 1.40 (m, 2H, H11), 1.19 (m, 2H, H9), 0.91 (t, 3H, H12) ppm; **^{13}C NMR** (100 MHz, CDCl$_3$, δ): 142.3 (C2, $^2J_{119Sn-13C}$ = 16 Hz), 141.4 (C1), 138.6 (C6, $^2J_{119Sn-13C}$ = 19 Hz), 128.9 (C3. $^3J_{119Sn-13C}$ = 15 Hz), 128.1 (C5), 126.4 (C4), 64.9 (C7, $^3J_{119Sn-13C}$ = 18 Hz), 44.6 (C8), 28.3 (C11, $^3J_{119Sn-13C}$ = 30 Hz), 26.9 (C10, $^2J_{119Sn-13C}$ = 82 Hz), 18.1 (C9, $^1J_{119Sn-13C}$ = 494 Hz, $^1J_{117Sn-13C}$ = 472 Hz), 13.5 (C12) ppm; **^{119}Sn{^{1}H}NMR** (149 MHz, C$_6$D$_6$, δ): -49.0 ppm.

5.49 1-Bromo-2-(*n*-propylthiomethyl) benzene (233):
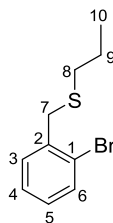
A solution of NaH (0.33 g, 13.13 mmol) in 10 mL of THF was slowly added at 0 °C to a solution of 1-propanethiol (1.0 g, 13.13 mmol) in 60 mL of THF. The reaction mixture was stirred for an additional 2 h and a solution of 2-bromobenzylbromide (2.18 g, 8.73 mmol) in 10 mL of THF added. The resulting mixture was refluxed for 16 h overnight. After the solution was cooled to room temperature, a saturated NH_4Cl solution (100 mL) was added and the organic phase separated. The water phase was extracted with Et_2O (3 × 30 mL). The combined organic layers were dried over anhydrous $MgSO_4$. A clear yellow coloured oil was obtained after the removal of solvent under reduced pressure. Yield: 1.8 g (84%).

^{1}H NMR (400 MHz, CDCl$_3$, δ): 7.56 (dd, 1H, H6), 7.40 (dd, 1H, H3), 7.28 (dt, 1H, H5), 7.12 (dt, 1H, H6), 3.85 (s, H7), 2.49 (t, 2H, H8), 1.64 (sex, 2H, H9), 1.0 (t, 3H, H10) ppm; **^{13}C NMR** (100 MHz, CDCl$_3$, δ): 138.2 (C2), 133.1 (C6), 130.8 (C3), 128.5 (C5), 127.4 (C4), 124.5 (C1), 36.8 (C7), 33.9 (C8), 22.8 (C9), 13.6 (C10) ppm.

5.50 1-Bromo-2-(phenylthiomethyl) benzene (234):
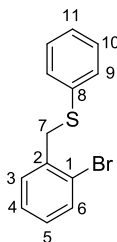
A solution of NaH (0.22 g, 9.07 mmol) in 10 mL of THF was slowly added at 0 ºC to a solution of thiophenol (1.0 g, 9.07 mmol) in 60 mL of THF and the reaction mixture stirred for 1 h. A solution of 2-bromobenzylbromide (1.51 g, 6.04 mmol) in 10 mL of THF was then added and the resulting mixture refluxed for 16 h. The solution was cooled to room temperature, a saturated NH_4Cl solution (100 mL) added, and the organic phase separated. The aqueous phase was extracted with Et_2O (3 × 30 mL). The combined organic layers were dried over anhydrous $MgSO_4$.

A clear yellow coloured oil was obtained after the removal of solvent under reduced pressure. The NMR data agreed with the literature.[105] Yield: 1.05 g (63%).

^{1}H NMR (400 MHz, CDCl$_3$, δ): 7.62 (dd, 1H, H3), 7.41 (dd, 2H, H4, H5), 7.32 (m, 5H, H9, H10, H11), 7.15(dd, 1H, H6), 4.30 (s, 2H, H7), ppm; **^{13}C NMR** (100 MHz, CDCl$_3$, δ): 136.9 (s, C2) 135.9 (C8), 133.0 (C6), 130.7 (d, C3), 130.5 (C9), 129.2 (d, C10), 128.9 (d, C5), 127.5 (d, C11), 126.8 (C1), 125.7(C4), 35.8 (C7) ppm.

5.51 (2-bromobenzyl)diphenylphosphane (237):
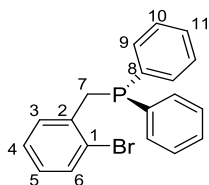
To 3-neck 250 mL round bottom flask containing magnesium turnings (0.5 g, 20.6 mmol) in 30 mL of Et$_2$O, a few crystals of I$_2$ and a few drops of *n*-BuLi (1.6 M) were added. A solution of 1-bromo-2-(bromomethyl)benzene (4.68 g, 18.72 mmol) in 20 mL of Et$_2$O was added dropwise. After the addition the reaction was refluxed for an additional 30 min. ClPPh$_2$ (3.0 mL, 16.24 mmol) in 20 mL of Et$_2$O was added dropwise to the stirred Grignard solution. The reaction mixture was refluxed for an additional hour and then cooled to room temperature and quenched with aqueous 10% NH$_4$Cl under nitrogen. The organic layer was washed with water and dried using MgSO4. After filtration, the solvent was removed under reduced pressure to obtain white solid. NMR data agreed with literature.[163,164] Yield: 3.55 g (57%).

^{1}H NMR (400 MHz, CDCl$_3$, δ): 7.57 (m, 1H), 7.48 (m, 4H), 7.39 (m, 6H), 7.07 (s, 2H), 6.86 (s, 1H), 3.6 (s, 2H, CH_2PPh$_2$) ppm; **^{13}C NMR** (100 MHz, CDCl$_3$, δ): 138.0 (d, C9, $^2J_{31P-13C}$ = 15 Hz), 137.0 (d, C10, $^2J_{31P-13C}$ = 8.0 Hz), 133.2 (d, C8, $^1J_{31P-13C}$ = 19 Hz), 132.9 (C5, $^5J_{31P-13C}$ = 2.0 Hz), 131.2 (C2, $^2J_{31P-13C}$ = 8.0 Hz), 128.9 (C11), 128.5 (C3, $^3J_{31P-13C}$ = 6.0 Hz), 127.7 (C6, $^4J_{31P-13C}$ =

2.0 Hz), 127.2 (C4), 125.1 (d, C1, $^3J_{31P-13C}$ = 5.0 Hz), 36.5 (d, C7, $^1J_{31P-13C}$ =17 Hz) ppm; ^{31}P

NMR(161.9 MHz, CDCl$_3$, δ): -12.7 ppm.

4.52 diphenyl(2-(triphenylstannyl)benzyl)phosphine (241):
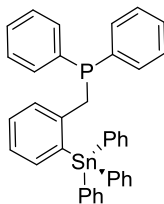
1.6 M solution of *n*-BuLi (1.46 mL, 2.73 mmol) in hexane was added dropwise to a solution **237**

(0.97 g, 2.73mmo) in Et$_2$O at 0 ºC. Reaction mixture was stirred for 3 h and removal of solvent

under reduced pressure afforded an orange-red coloured powder which was washed with hexane

and the residual solvent removed under reduced pressure. This lithiated species (0.153 g, 5.42

mmol) was suspended in dry C$_6$H$_6$ and a solution of Ph$_3$SnCl (0.209 g, 5.42mmol) in C$_6$H$_6$ added

at room temperature. The reaction mixture was stirred for 3 h and after filtration in glove box, the

solvent was removed under reduced pressure. The crude product was dissolved in benzene and

filtered. The removal of solvent under reduced pressure afforded a light yellow coloured semi-

solid. No yield was recorded.

^{119}Sn{^{1}H}**NMR** (149 MHz, CDCl$_3$, δ):-85.0 ppm; ^{31}**P NMR** (161.9 MHz, CDCl$_3$, δ): -9.8 ppm.

4.53 (2-(chlordiphenylstannyl)benzyl)diphenylphosphine (242):
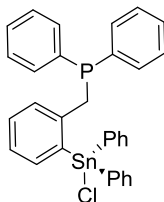
To a suspension of lithiated **241** (0.619 g, mmol) in dry C$_6$H$_6$, a solution PhSnCl$_3$ (0.662 g, mmol)

in dry C$_6$H$_6$ added at room temperature. The reaction mixture was stirred for 3 h and solvent was

removed under reduced pressure after filtration in glove box. The crude product was dissolved in benzene and filtered. The removal of solvent under reduced pressure afforded a yellow brown coloured semisolid. No yield was recorded.

^{119}**Sn{^{1}H}NMR** (149 MHz, CDCl$_3$, δ):-27.0 ppm; ^{31}**P NMR** (161.9 MHz, CDCl$_3$, δ): 43.2 ppm.

6.0 Appendices

List of Appendix tables

List of Appendix Figures

Table A 1. Crystal data and structure refinement for 198.

Identification code	k11250a
Empirical formula	$C_{28}H_{25}F_3OSn$
Formula weight	553.17
Temperature	200(1) K
Wavelength	0.71073 Å
Crystal system	Monoclinic
Space group	P 21/n
Unit cell dimensions	a = 6.4631(13) Å $\alpha = 90°$.
	b = 12.192(2) Å $\beta = 90.14(3)°$.
	c = 31.554(6) Å $\gamma = 90°$.
Volume	2486.3(9) $Å^3$
Z	4
Density (calculated)	1.478 Mg/m^3
Absorption coefficient	1.067 mm^{-1}
F(000)	1112
Crystal size	$0.34 \times 0.08 \times 0.06$ mm^3
Theta range for data collection	2.56 to 25.12°.
Index ranges	-7<=h<=7, -14<=k<=14, -37<=l<=36
Reflections collected	15431
Independent reflections	4391 [R(int) = 0.0558]
Completeness to theta = 25.12°	98.6 %
Absorption correction	Semi-empirical from equivalents
Max. and min. transmission	0.998 and 0.936
Refinement method	Full-matrix least-squares on F^2
Data / restraints / parameters	4391 / 71 / 306
Goodness-of-fit on F^2	1.092
Final R indices [I>2sigma(I)]	R1 = 0.0589, wR2 = 0.1152
R indices (all data)	R1 = 0.1023, wR2 = 0.1344
Largest diff. peak and hole	0.679 and -0.988 e.$Å^{-3}$

Table A 2. Atomic coordinates (x 10^4) and equivalent isotropic displacement parameters ($\text{Å}^2 \times 10^3$) for 198.

	x	y	z	U(eq)
Sn(1)	60(1)	8785(1)	1562(1)	73(1)
F(1)	10730(13)	5463(8)	-541(3)	135(3)
F(2)	7737(16)	4942(7)	-354(3)	138(3)
F(3)	8194(17)	5626(8)	-965(3)	146(3)
F(1A)	9470(30)	5134(12)	-463(5)	139(3)
F(2A)	6471(18)	5357(10)	-725(5)	141(3)
F(3A)	9090(30)	6011(11)	-1038(4)	143(3)
O(1)	5369(15)	8166(8)	436(3)	58(3)
C(1)	1690(20)	8535(11)	967(4)	57(5)
C(2)	3222(15)	7595(9)	1006(3)	56(3)
C(3)	4292(19)	7242(8)	601(3)	59(3)
O(1A)	4540(20)	8471(10)	293(5)	61(5)
C(1A)	2490(18)	8340(20)	1116(5)	54(7)
C(2A)	1410(20)	8137(15)	696(4)	44(4)
C(3A)	2970(20)	7686(13)	382(6)	56(5)
C(4)	6632(11)	7989(6)	103(2)	43(3)
C(5)	7811(12)	8875(5)	-32(2)	43(3)
C(6)	9337(11)	8725(6)	-336(3)	55(3)
C(7)	9685(12)	7689(7)	-505(2)	72(4)
C(8)	8505(13)	6803(5)	-370(3)	62(4)
C(9)	6979(12)	6952(5)	-66(2)	54(3)
C(4A)	6055(15)	8167(8)	24(3)	43(4)
C(5A)	7268(17)	9043(6)	-109(3)	32(4)
C(6A)	8773(16)	8885(7)	-417(3)	38(4)
C(7A)	9065(16)	7851(9)	-592(3)	51(5)
C(8A)	7851(17)	6975(7)	-460(3)	36(4)
C(9A)	6347(16)	7133(7)	-152(3)	37(4)
C(10)	8725(12)	5760(8)	-556(3)	132(6)
C(10A)	8260(20)	5901(10)	-648(4)	132(6)
C(11)	1894(11)	9015(5)	2121(2)	66(2)
C(12)	3340(11)	9854(5)	2151(3)	65(2)

169

C(13)	4564(13)	9997(6)	2509(3)	77(2)
C(14)	4322(15)	9264(8)	2842(3)	91(3)
C(15)	2921(17)	8423(8)	2819(4)	103(4)
C(16)	1720(14)	8305(7)	2466(4)	89(3)
C(17)	-1741(11)	10240(6)	1467(2)	63(2)
C(18)	-3139(12)	10337(7)	1130(2)	69(2)
C(19)	-4313(13)	11264(8)	1072(3)	81(2)
C(20)	-4123(12)	12132(7)	1349(3)	77(2)
C(21)	-2754(12)	12068(6)	1685(3)	71(2)
C(22)	-1588(11)	11141(6)	1739(2)	65(2)
C(23)	-1701(12)	7295(4)	1708(3)	41(3)
C(24)	-1440(12)	6394(6)	1444(3)	48(3)
C(25)	-2756(13)	5497(5)	1477(3)	57(4)
C(26)	-4335(12)	5500(5)	1776(3)	54(3)
C(27)	-4597(12)	6401(6)	2040(3)	59(5)
C(28)	-3280(13)	7298(5)	2007(3)	48(4)
C(23A)	-2252(11)	7464(6)	1549(3)	38(3)
C(24A)	-2273(13)	6689(7)	1226(3)	50(4)
C(25A)	-3553(15)	5776(7)	1255(3)	62(5)
C(26A)	-4812(13)	5638(5)	1608(4)	53(4)
C(28A)	-4790(13)	6412(7)	1931(3)	41(4)
C(27A)	-3510(13)	7325(6)	1902(3)	41(4)

Table A 3.   Bond lengths [Å] and angles [°] for 198.

Sn(1)-C(11)	2.141(8)
Sn(1)-C(17)	2.143(8)
Sn(1)-C(1A)	2.178(9)
Sn(1)-C(1)	2.179(9)
Sn(1)-C(23)	2.193(4)
Sn(1)-C(23A)	2.197(4)
F(1)-C(10)	1.346(5)
F(2)-C(10)	1.346(5)
F(3)-C(10)	1.345(5)
F(1A)-C(10A)	1.351(5)
F(2A)-C(10A)	1.352(5)
F(3A)-C(10A)	1.352(5)
O(1)-C(4)	1.350(6)
O(1)-C(3)	1.423(9)
C(1)-C(2)	1.518(7)
C(1)-H(1A)	0.9900
C(1)-H(1B)	0.9900
C(2)-C(3)	1.517(7)
C(2)-H(2A)	0.9900
C(2)-H(2B)	0.9900
C(3)-H(3A)	0.9900
C(3)-H(3B)	0.9900
O(1A)-C(4A)	1.351(6)
O(1A)-C(3A)	1.424(9)
C(1A)-C(2A)	1.517(7)
C(1A)-H(1AA)	0.9900
C(1A)-H(1AB)	0.9900
C(2A)-C(3A)	1.517(7)
C(2A)-H(2AA)	0.9900
C(2A)-H(2AB)	0.9900
C(3A)-H(3AA)	0.9900
C(3A)-H(3AB)	0.9900
C(4)-C(5)	1.3900

C(4)-C(9)	1.3900
C(5)-C(6)	1.3900
C(5)-H(5A)	0.9500
C(6)-C(7)	1.3900
C(6)-H(6A)	0.9500
C(7)-C(8)	1.3900
C(7)-H(7A)	0.9500
C(8)-C(9)	1.3900
C(8)-C(10)	1.407(11)
C(9)-H(9A)	0.9500
C(4A)-C(5A)	1.3900
C(4A)-C(9A)	1.3900
C(5A)-C(6A)	1.3900
C(5A)-H(5AA)	0.9500
C(6A)-C(7A)	1.3900
C(6A)-H(6AA)	0.9500
C(7A)-C(8A)	1.3900
C(7A)-H(7AA)	0.9500
C(8A)-C(9A)	1.3900
C(8A)-C(10A)	1.462(13)
C(9A)-H(9AA)	0.9500
C(11)-C(12)	1.389(9)
C(11)-C(16)	1.395(11)
C(12)-C(13)	1.389(11)
C(12)-H(12A)	0.9500
C(13)-C(14)	1.388(11)
C(13)-H(13A)	0.9500
C(14)-C(15)	1.369(13)
C(14)-H(14A)	0.9500
C(15)-C(16)	1.364(13)
C(15)-H(15A)	0.9500
C(16)-H(16A)	0.9500
C(17)-C(22)	1.396(9)
C(17)-C(18)	1.399(10)
C(18)-C(19)	1.373(11)
C(18)-H(18A)	0.9500

C(19)-C(20)	1.379(11)
C(19)-H(19A)	0.9500
C(20)-C(21)	1.380(10)
C(20)-H(20A)	0.9500
C(21)-C(22)	1.369(10)
C(21)-H(21A)	0.9500
C(22)-H(22A)	0.9500
C(23)-C(24)	1.3900
C(23)-C(28)	1.3900
C(24)-C(25)	1.3900
C(24)-H(24A)	0.9500
C(25)-C(26)	1.3900
C(25)-H(25A)	0.9500
C(26)-C(27)	1.3900
C(26)-H(26A)	0.9500
C(27)-C(28)	1.3900
C(27)-H(27A)	0.9500
C(28)-H(28A)	0.9500
C(23A)-C(24A)	1.3900
C(23A)-C(27A)	1.3900
C(24A)-C(25A)	1.3900
C(24A)-H(24B)	0.9500
C(25A)-C(26A)	1.3900
C(25A)-H(25B)	0.9500
C(26A)-C(28A)	1.3900
C(26A)-H(26B)	0.9500
C(28A)-C(27A)	1.3900
C(28A)-H(28B)	0.9500
C(27A)-H(27B)	0.9500
C(11)-Sn(1)-C(17)	107.8(3)
C(11)-Sn(1)-C(1A)	99.6(4)
C(17)-Sn(1)-C(1A)	120.4(7)
C(11)-Sn(1)-C(1)	117.4(4)
C(17)-Sn(1)-C(1)	105.0(4)
C(1A)-Sn(1)-C(1)	19.4(5)

C(11)-Sn(1)-C(23)	102.8(3)
C(17)-Sn(1)-C(23)	115.7(3)
C(1A)-Sn(1)-C(23)	107.9(7)
C(1)-Sn(1)-C(23)	108.6(5)
C(11)-Sn(1)-C(23A)	119.1(3)
C(17)-Sn(1)-C(23A)	103.6(3)
C(1A)-Sn(1)-C(23A)	107.4(6)
C(1)-Sn(1)-C(23A)	102.3(5)
C(23)-Sn(1)-C(23A)	17.0(3)
C(4)-O(1)-C(3)	117.1(8)
C(2)-C(1)-Sn(1)	110.6(7)
C(2)-C(1)-H(1A)	109.5
Sn(1)-C(1)-H(1A)	109.5
C(2)-C(1)-H(1B)	109.5
Sn(1)-C(1)-H(1B)	109.5
H(1A)-C(1)-H(1B)	108.1
C(3)-C(2)-C(1)	116.3(9)
C(3)-C(2)-H(2A)	108.2
C(1)-C(2)-H(2A)	108.2
C(3)-C(2)-H(2B)	108.2
C(1)-C(2)-H(2B)	108.2
H(2A)-C(2)-H(2B)	107.4
O(1)-C(3)-C(2)	107.9(7)
O(1)-C(3)-H(3A)	110.1
C(2)-C(3)-H(3A)	110.1
O(1)-C(3)-H(3B)	110.1
C(2)-C(3)-H(3B)	110.1
H(3A)-C(3)-H(3B)	108.4
C(4A)-O(1A)-C(3A)	117.4(11)
C(2A)-C(1A)-Sn(1)	105.9(8)
C(2A)-C(1A)-H(1AA)	110.6
Sn(1)-C(1A)-H(1AA)	110.6
C(2A)-C(1A)-H(1AB)	110.6
Sn(1)-C(1A)-H(1AB)	110.6
H(1AA)-C(1A)-H(1AB)	108.7
C(1A)-C(2A)-C(3A)	109.1(12)

C(1A)-C(2A)-H(2AA)	109.9
C(3A)-C(2A)-H(2AA)	109.9
C(1A)-C(2A)-H(2AB)	109.9
C(3A)-C(2A)-H(2AB)	109.9
H(2AA)-C(2A)-H(2AB)	108.3
O(1A)-C(3A)-C(2A)	111.1(11)
O(1A)-C(3A)-H(3AA)	109.4
C(2A)-C(3A)-H(3AA)	109.4
O(1A)-C(3A)-H(3AB)	109.4
C(2A)-C(3A)-H(3AB)	109.4
H(3AA)-C(3A)-H(3AB)	108.0
O(1)-C(4)-C(5)	116.6(6)
O(1)-C(4)-C(9)	122.9(6)
C(5)-C(4)-C(9)	120.0
C(4)-C(5)-C(6)	120.0
C(4)-C(5)-H(5A)	120.0
C(6)-C(5)-H(5A)	120.0
C(5)-C(6)-C(7)	120.0
C(5)-C(6)-H(6A)	120.0
C(7)-C(6)-H(6A)	120.0
C(8)-C(7)-C(6)	120.0
C(8)-C(7)-H(7A)	120.0
C(6)-C(7)-H(7A)	120.0
C(7)-C(8)-C(9)	120.0
C(7)-C(8)-C(10)	121.3(6)
C(9)-C(8)-C(10)	118.6(6)
C(8)-C(9)-C(4)	120.0
C(8)-C(9)-H(9A)	120.0
C(4)-C(9)-H(9A)	120.0
O(1A)-C(4A)-C(5A)	113.0(8)
O(1A)-C(4A)-C(9A)	126.7(8)
C(5A)-C(4A)-C(9A)	120.0
C(6A)-C(5A)-C(4A)	120.0
C(6A)-C(5A)-H(5AA)	120.0
C(4A)-C(5A)-H(5AA)	120.0
C(7A)-C(6A)-C(5A)	120.0

C(7A)-C(6A)-H(6AA)	120.0
C(5A)-C(6A)-H(6AA)	120.0
C(6A)-C(7A)-C(8A)	120.0
C(6A)-C(7A)-H(7AA)	120.0
C(8A)-C(7A)-H(7AA)	120.0
C(9A)-C(8A)-C(7A)	120.0
C(9A)-C(8A)-C(10A)	122.4(8)
C(7A)-C(8A)-C(10A)	117.6(8)
C(8A)-C(9A)-C(4A)	120.0
C(8A)-C(9A)-H(9AA)	120.0
C(4A)-C(9A)-H(9AA)	120.0
F(3)-C(10)-F(2)	104.3(6)
F(3)-C(10)-F(1)	104.1(6)
F(2)-C(10)-F(1)	104.0(6)
F(3)-C(10)-C(8)	118.9(8)
F(2)-C(10)-C(8)	115.0(8)
F(1)-C(10)-C(8)	109.0(8)
F(1A)-C(10A)-F(3A)	103.3(6)
F(1A)-C(10A)-F(2A)	103.3(6)
F(3A)-C(10A)-F(2A)	103.2(6)
F(1A)-C(10A)-C(8A)	123.2(11)
F(3A)-C(10A)-C(8A)	110.8(11)
F(2A)-C(10A)-C(8A)	111.0(11)
C(12)-C(11)-C(16)	117.4(8)
C(12)-C(11)-Sn(1)	121.6(6)
C(16)-C(11)-Sn(1)	121.0(6)
C(13)-C(12)-C(11)	122.0(8)
C(13)-C(12)-H(12A)	119.0
C(11)-C(12)-H(12A)	119.0
C(14)-C(13)-C(12)	118.0(9)
C(14)-C(13)-H(13A)	121.0
C(12)-C(13)-H(13A)	121.0
C(15)-C(14)-C(13)	121.2(10)
C(15)-C(14)-H(14A)	119.4
C(13)-C(14)-H(14A)	119.4
C(16)-C(15)-C(14)	119.8(10)

C(16)-C(15)-H(15A)	120.1
C(14)-C(15)-H(15A)	120.1
C(15)-C(16)-C(11)	121.6(9)
C(15)-C(16)-H(16A)	119.2
C(11)-C(16)-H(16A)	119.2
C(22)-C(17)-C(18)	116.4(7)
C(22)-C(17)-Sn(1)	121.9(6)
C(18)-C(17)-Sn(1)	121.7(5)
C(19)-C(18)-C(17)	121.7(7)
C(19)-C(18)-H(18A)	119.1
C(17)-C(18)-H(18A)	119.1
C(18)-C(19)-C(20)	120.0(8)
C(18)-C(19)-H(19A)	120.0
C(20)-C(19)-H(19A)	120.0
C(19)-C(20)-C(21)	119.9(8)
C(19)-C(20)-H(20A)	120.0
C(21)-C(20)-H(20A)	120.0
C(22)-C(21)-C(20)	119.6(7)
C(22)-C(21)-H(21A)	120.2
C(20)-C(21)-H(21A)	120.2
C(21)-C(22)-C(17)	122.3(8)
C(21)-C(22)-H(22A)	118.8
C(17)-C(22)-H(22A)	118.8
C(24)-C(23)-C(28)	120.0
C(24)-C(23)-Sn(1)	117.6(4)
C(28)-C(23)-Sn(1)	121.5(4)
C(25)-C(24)-C(23)	120.0
C(25)-C(24)-H(24A)	120.0
C(23)-C(24)-H(24A)	120.0
C(24)-C(25)-C(26)	120.0
C(24)-C(25)-H(25A)	120.0
C(26)-C(25)-H(25A)	120.0
C(27)-C(26)-C(25)	120.0
C(27)-C(26)-H(26A)	120.0
C(25)-C(26)-H(26A)	120.0
C(26)-C(27)-C(28)	120.0

C(26)-C(27)-H(27A)	120.0
C(28)-C(27)-H(27A)	120.0
C(27)-C(28)-C(23)	120.0
C(27)-C(28)-H(28A)	120.0
C(23)-C(28)-H(28A)	120.0
C(24A)-C(23A)-C(27A)	120.0
C(24A)-C(23A)-Sn(1)	121.1(5)
C(27A)-C(23A)-Sn(1)	118.3(5)
C(23A)-C(24A)-C(25A)	120.0
C(23A)-C(24A)-H(24B)	120.0
C(25A)-C(24A)-H(24B)	120.0
C(26A)-C(25A)-C(24A)	120.0
C(26A)-C(25A)-H(25B)	120.0
C(24A)-C(25A)-H(25B)	120.0
C(28A)-C(26A)-C(25A)	120.0
C(28A)-C(26A)-H(26B)	120.0
C(25A)-C(26A)-H(26B)	120.0
C(26A)-C(28A)-C(27A)	120.0
C(26A)-C(28A)-H(28B)	120.0
C(27A)-C(28A)-H(28B)	120.0
C(28A)-C(27A)-C(23A)	120.0
C(28A)-C(27A)-H(27B)	120.0
C(23A)-C(27A)-H(27B)	120.0

Symmetry transformations used to generate equivalent atoms:

Table A 4. Anisotropic displacement parameters ($\mathring{A}^2 \times 10^3$) for 198. The anisotropic displacement factor exponent takes the form: $-2p^2[\, h^2\, a^{*2}U^{11} + ... + 2\, h\, k\, a^*\, b^*\, U^{12}\,]$

	U^{11}	U^{22}	U^{33}	U^{23}	U^{13}	U^{12}
Sn(1)	70(1)	44(1)	105(1)	-27(1)	50(1)	-22(1)
F(1)	165(8)	60(5)	180(7)	-33(5)	54(6)	-8(5)
F(2)	180(7)	52(4)	182(6)	-36(4)	41(5)	-27(4)
F(3)	201(8)	62(5)	173(6)	-58(5)	29(5)	-37(5)
F(1A)	177(8)	58(4)	182(6)	-33(5)	44(6)	-14(5)
F(2A)	189(8)	57(4)	177(6)	-51(5)	34(5)	-34(4)
F(3A)	202(9)	59(6)	168(7)	-57(5)	36(6)	-43(6)
O(1)	79(6)	45(6)	51(6)	-10(4)	30(5)	-22(5)
C(1)	29(8)	46(9)	95(13)	-16(8)	20(8)	-5(6)
C(2)	57(7)	58(8)	54(8)	1(6)	17(5)	-12(6)
C(3)	81(8)	35(6)	62(8)	-3(5)	36(7)	-4(6)
O(1A)	101(12)	30(8)	52(10)	-7(6)	37(9)	-20(7)
C(1A)	26(12)	46(13)	89(16)	-18(12)	14(11)	2(10)
C(2A)	44(10)	49(11)	40(11)	8(8)	11(8)	1(8)
C(3A)	69(12)	37(10)	63(13)	1(8)	10(9)	0(8)
C(10)	179(13)	62(8)	158(13)	-49(8)	86(11)	-8(8)
C(10A)	179(13)	62(8)	158(13)	-49(8)	86(11)	-8(8)
C(11)	68(4)	42(4)	88(6)	-7(4)	39(4)	-2(3)
C(12)	67(5)	40(4)	87(6)	1(4)	34(4)	2(3)
C(13)	84(6)	56(5)	92(7)	-5(5)	24(5)	13(4)
C(14)	105(7)	85(7)	82(7)	8(5)	34(5)	41(6)
C(15)	105(8)	72(7)	131(10)	35(6)	67(7)	36(6)
C(16)	83(6)	51(5)	133(9)	18(6)	62(6)	9(4)
C(17)	65(4)	57(4)	67(5)	-23(4)	32(4)	-30(3)
C(18)	71(5)	74(6)	61(5)	-32(4)	31(4)	-40(4)
C(19)	75(5)	85(6)	82(6)	-16(5)	19(4)	-28(5)
C(20)	68(5)	69(6)	93(7)	-4(5)	18(5)	-13(4)
C(21)	71(5)	52(5)	89(6)	-21(4)	13(5)	-12(4)
C(22)	69(5)	54(4)	71(5)	-22(4)	13(4)	-18(4)

Table A 5. **Hydrogen coordinates (x 10^4) and isotropic displacement parameters (Å^2 × 10^3) for 198.**

	x	y	z	U(eq)
H(1A)	685	8372	739	68
H(1B)	2443	9215	889	68
H(2A)	4297	7807	1215	67
H(2B)	2480	6953	1123	67
H(3A)	5275	6638	661	71
H(3B)	3259	6978	393	71
H(1AA)	3504	8948	1089	65
H(1AB)	3225	7676	1213	65
H(2AA)	814	8830	587	53
H(2AB)	269	7605	736	53
H(3AA)	3606	7014	500	68
H(3AB)	2244	7485	116	68
H(5A)	7574	9583	84	51
H(6A)	10143	9331	-428	65
H(7A)	10728	7587	-713	87
H(9A)	6173	6346	26	65
H(5AA)	7069	9750	11	38
H(6AA)	9602	9484	-507	46
H(7AA)	10093	7743	-803	61
H(9AA)	5517	6534	-61	44
H(12A)	3496	10345	1920	78
H(13A)	5538	10579	2526	92
H(14A)	5143	9346	3090	109
H(15A)	2787	7923	3048	123
H(16A)	740	7725	2454	107
H(18A)	-3280	9745	936	83
H(19A)	-5256	11306	841	97
H(20A)	-4934	12774	1310	92
H(21A)	-2621	12664	1877	85
H(22A)	-640	11110	1969	78
H(24A)	-361	6392	1240	57

H(25A)	-2577	4882	1296	68
H(26A)	-5235	4887	1799	65
H(27A)	-5675	6403	2244	71
H(28A)	-3459	7913	2188	57
H(24B)	-1413	6784	985	60
H(25B)	-3568	5247	1034	75
H(26B)	-5686	5014	1628	63
H(28B)	-5650	6317	2172	49
H(27B)	-3496	7854	2123	50

Table A 6. Crystal data and structure refinement for 200.

Identification code	d13211
Empirical formula	$C_{21}H_{21}ClOSn$
Formula weight	443.52
Temperature	147(2) K
Wavelength	0.71073 Å
Crystal system	Triclinic
Space group	P -1

Unit cell dimensions
$a = 10.4728(11)$ Å $\alpha = 89.678(2)°$.
$b = 11.0954(12)$ Å $\beta = 79.636(2)°$.
$c = 16.9797(18)$ Å $\gamma = 82.832(2)°$.

Volume	1925.4(4) Å^3
Z	4
Density (calculated)	1.530 Mg/m^3
Absorption coefficient	1.470 mm^{-1}
F(000)	888
Crystal size	$0.200 \times 0.090 \times 0.030$ mm^3
Theta range for data collection	1.219 to 27.481°.
Index ranges	-13<=h<=13, -14<=k<=14, -21<=l<=22
Reflections collected	63709
Independent reflections	8816 [R(int) = 0.0236]
Completeness to theta = 25.242°	99.8 %
Absorption correction	Semi-empirical from equivalents
Max. and min. transmission	0.7456 and 0.6543
Refinement method	Full-matrix least-squares on F^2
Data / restraints / parameters	8816 / 0 / 433
Goodness-of-fit on F^2	1.020
Final R indices [I>2sigma(I)]	R1 = 0.0161, wR2 = 0.0385
R indices (all data)	R1 = 0.0197, wR2 = 0.0402
Extinction coefficient	n/a
Largest diff. peak and hole	0.370 and -0.350 e.Å^{-3}

Table A 7. Atomic coordinates (x 10^4) and equivalent isotropic displacement parameters ($Å^2 \times 10^3$) for 200.

	x	y	z	U(eq)
Sn(1A)	3605(1)	5501(1)	2673(1)	18(1)
Cl(1A)	3448(1)	5998(1)	1311(1)	25(1)
O(1A)	4348(1)	4535(1)	4132(1)	23(1)
C(1A)	5688(1)	5211(2)	2558(1)	23(1)
C(2A)	6212(2)	5218(2)	3340(1)	25(1)
C(3A)	5744(1)	4227(2)	3890(1)	24(1)
C(4A)	3690(2)	3722(2)	4620(1)	24(1)
C(5A)	4261(2)	2579(2)	4796(1)	28(1)
C(6A)	3497(2)	1817(2)	5276(1)	38(1)
C(7A)	2195(2)	2192(2)	5573(1)	44(1)
C(8A)	1637(2)	3336(2)	5396(1)	41(1)
C(9A)	2377(2)	4111(2)	4923(1)	31(1)
C(10A)	2382(1)	4100(1)	2901(1)	21(1)
C(11A)	1028(2)	4435(2)	3015(1)	33(1)
C(12A)	176(2)	3581(2)	3244(1)	41(1)
C(13A)	656(2)	2399(2)	3380(1)	34(1)
C(14A)	1993(2)	2055(1)	3268(1)	27(1)
C(15A)	2850(2)	2901(1)	3024(1)	23(1)
C(16A)	2591(1)	7116(1)	3275(1)	22(1)
C(17A)	2891(2)	7528(2)	3987(1)	33(1)
C(18A)	2192(2)	8576(2)	4373(1)	44(1)
C(19A)	1185(2)	9211(2)	4058(1)	38(1)
C(20A)	874(2)	8816(2)	3357(1)	33(1)
C(21A)	1569(2)	7779(2)	2966(1)	28(1)
Sn(1B)	3075(1)	-288(1)	7735(1)	18(1)
Cl(1B)	2376(1)	-923(1)	6528(1)	24(1)
O(1B)	4184(1)	549(1)	8925(1)	25(1)
C(1B)	4961(1)	143(2)	7187(1)	26(1)
C(2B)	5867(2)	286(2)	7784(1)	28(1)
C(3B)	5232(2)	1134(2)	8472(1)	28(1)

C(4B)	3515(2)	1122(2)	9630(1)	25(1)
C(5B)	3592(2)	2319(2)	9824(1)	32(1)
C(6B)	2867(2)	2817(2)	10545(1)	37(1)
C(7B)	2089(2)	2136(2)	11060(1)	37(1)
C(8B)	2026(2)	935(2)	10862(1)	38(1)
C(9B)	2738(2)	426(2)	10147(1)	32(1)
C(10B)	2835(2)	-1890(1)	8413(1)	21(1)
C(11B)	1711(2)	-2446(1)	8414(1)	26(1)
C(12B)	1512(2)	-3487(2)	8855(1)	33(1)
C(13B)	2445(2)	-3990(2)	9287(1)	35(1)
C(14B)	3565(2)	-3452(2)	9287(1)	32(1)
C(15B)	3762(2)	-2403(2)	8856(1)	26(1)
C(16B)	1682(1)	1233(1)	8152(1)	20(1)
C(17B)	1844(2)	2378(1)	7832(1)	25(1)
C(18B)	1030(2)	3405(2)	8158(1)	31(1)
C(19B)	37(2)	3302(2)	8803(1)	34(1)
C(20B)	-147(2)	2172(2)	9121(1)	35(1)
C(21B)	678(2)	1144(2)	8802(1)	27(1)

Table A 8. Bond lengths [Å] and angles [°] for 200.

Sn(1A)-C(10A)	2.1249(15)
Sn(1A)-C(16A)	2.1304(15)
Sn(1A)-C(1A)	2.1383(15)
Sn(1A)-Cl(1A)	2.4047(4)
Sn(1A)-O(1A)	2.8894(11)
O(1A)-C(4A)	1.3842(18)
O(1A)-C(3A)	1.4432(18)
C(1A)-C(2A)	1.526(2)
C(1A)-H(1AA)	0.9900
C(1A)-H(1AB)	0.9900
C(2A)-C(3A)	1.510(2)
C(2A)-H(2AA)	0.9900
C(2A)-H(2AB)	0.9900
C(3A)-H(3AA)	0.9900
C(3A)-H(3AB)	0.9900
C(4A)-C(5A)	1.388(2)
C(4A)-C(9A)	1.393(2)
C(5A)-C(6A)	1.395(2)
C(5A)-H(5AA)	0.9500
C(6A)-C(7A)	1.378(3)
C(6A)-H(6AA)	0.9500
C(7A)-C(8A)	1.384(3)
C(7A)-H(7AA)	0.9500
C(8A)-C(9A)	1.386(3)
C(8A)-H(8AA)	0.9500
C(9A)-H(9AA)	0.9500
C(10A)-C(15A)	1.388(2)
C(10A)-C(11A)	1.400(2)
C(11A)-C(12A)	1.388(2)
C(11A)-H(11A)	0.9500
C(12A)-C(13A)	1.378(3)
C(12A)-H(12A)	0.9500
C(13A)-C(14A)	1.383(2)
C(13A)-H(13A)	0.9500

C(14A)-C(15A)	1.390(2)
C(14A)-H(14A)	0.9500
C(15A)-H(15A)	0.9500
C(16A)-C(17A)	1.396(2)
C(16A)-C(21A)	1.402(2)
C(17A)-C(18A)	1.392(2)
C(17A)-H(17A)	0.9500
C(18A)-C(19A)	1.381(3)
C(18A)-H(18A)	0.9500
C(19A)-C(20A)	1.376(3)
C(19A)-H(19A)	0.9500
C(20A)-C(21A)	1.386(2)
C(20A)-H(20A)	0.9500
C(21A)-H(21A)	0.9500
Sn(1B)-C(16B)	2.1216(15)
Sn(1B)-C(10B)	2.1294(15)
Sn(1B)-C(1B)	2.1365(15)
Sn(1B)-Cl(1B)	2.4322(4)
Sn(1B)-O(1B)	2.7254(11)
O(1B)-C(4B)	1.3866(19)
O(1B)-C(3B)	1.4439(19)
C(1B)-C(2B)	1.528(2)
C(1B)-H(1BA)	0.9900
C(1B)-H(1BB)	0.9900
C(2B)-C(3B)	1.506(2)
C(2B)-H(2BA)	0.9900
C(2B)-H(2BB)	0.9900
C(3B)-H(3BA)	0.9900
C(3B)-H(3BB)	0.9900
C(4B)-C(5B)	1.386(2)
C(4B)-C(9B)	1.387(2)
C(5B)-C(6B)	1.396(3)
C(5B)-H(5BA)	0.9500
C(6B)-C(7B)	1.374(3)
C(6B)-H(6BA)	0.9500
C(7B)-C(8B)	1.388(3)

C(7B)-H(7BA)	0.9500
C(8B)-C(9B)	1.387(3)
C(8B)-H(8BA)	0.9500
C(9B)-H(9BA)	0.9500
C(10B)-C(11B)	1.395(2)
C(10B)-C(15B)	1.396(2)
C(11B)-C(12B)	1.390(2)
C(11B)-H(11B)	0.9500
C(12B)-C(13B)	1.386(3)
C(12B)-H(12B)	0.9500
C(13B)-C(14B)	1.380(3)
C(13B)-H(13B)	0.9500
C(14B)-C(15B)	1.390(2)
C(14B)-H(14B)	0.9500
C(15B)-H(15B)	0.9500
C(16B)-C(21B)	1.393(2)
C(16B)-C(17B)	1.397(2)
C(17B)-C(18B)	1.388(2)
C(17B)-H(17B)	0.9500
C(18B)-C(19B)	1.382(3)
C(18B)-H(18B)	0.9500
C(19B)-C(20B)	1.384(3)
C(19B)-H(19B)	0.9500
C(20B)-C(21B)	1.391(2)
C(20B)-H(20B)	0.9500
C(21B)-H(21B)	0.9500
C(10A)-Sn(1A)-C(16A)	108.37(6)
C(10A)-Sn(1A)-C(1A)	124.01(6)
C(16A)-Sn(1A)-C(1A)	117.83(6)
C(10A)-Sn(1A)-Cl(1A)	101.90(4)
C(16A)-Sn(1A)-Cl(1A)	100.34(4)
C(1A)-Sn(1A)-Cl(1A)	99.24(4)
C(10A)-Sn(1A)-O(1A)	79.62(4)
C(16A)-Sn(1A)-O(1A)	91.96(5)
C(1A)-Sn(1A)-O(1A)	69.37(4)

Cl(1A)-Sn(1A)-O(1A)	166.30(2)
C(4A)-O(1A)-C(3A)	116.94(12)
C(4A)-O(1A)-Sn(1A)	124.73(8)
C(3A)-O(1A)-Sn(1A)	101.75(8)
C(2A)-C(1A)-Sn(1A)	115.69(10)
C(2A)-C(1A)-H(1AA)	108.4
Sn(1A)-C(1A)-H(1AA)	108.4
C(2A)-C(1A)-H(1AB)	108.4
Sn(1A)-C(1A)-H(1AB)	108.4
H(1AA)-C(1A)-H(1AB)	107.4
C(3A)-C(2A)-C(1A)	111.78(13)
C(3A)-C(2A)-H(2AA)	109.3
C(1A)-C(2A)-H(2AA)	109.3
C(3A)-C(2A)-H(2AB)	109.3
C(1A)-C(2A)-H(2AB)	109.3
H(2AA)-C(2A)-H(2AB)	107.9
O(1A)-C(3A)-C(2A)	106.56(12)
O(1A)-C(3A)-H(3AA)	110.4
C(2A)-C(3A)-H(3AA)	110.4
O(1A)-C(3A)-H(3AB)	110.4
C(2A)-C(3A)-H(3AB)	110.4
H(3AA)-C(3A)-H(3AB)	108.6
O(1A)-C(4A)-C(5A)	123.69(14)
O(1A)-C(4A)-C(9A)	115.56(14)
C(5A)-C(4A)-C(9A)	120.74(15)
C(4A)-C(5A)-C(6A)	118.98(16)
C(4A)-C(5A)-H(5AA)	120.5
C(6A)-C(5A)-H(5AA)	120.5
C(7A)-C(6A)-C(5A)	120.61(18)
C(7A)-C(6A)-H(6AA)	119.7
C(5A)-C(6A)-H(6AA)	119.7
C(6A)-C(7A)-C(8A)	119.91(17)
C(6A)-C(7A)-H(7AA)	120.0
C(8A)-C(7A)-H(7AA)	120.0
C(7A)-C(8A)-C(9A)	120.55(18)
C(7A)-C(8A)-H(8AA)	119.7

C(9A)-C(8A)-H(8AA)	119.7
C(8A)-C(9A)-C(4A)	119.22(17)
C(8A)-C(9A)-H(9AA)	120.4
C(4A)-C(9A)-H(9AA)	120.4
C(15A)-C(10A)-C(11A)	118.50(14)
C(15A)-C(10A)-Sn(1A)	123.36(11)
C(11A)-C(10A)-Sn(1A)	117.78(11)
C(12A)-C(11A)-C(10A)	120.48(16)
C(12A)-C(11A)-H(11A)	119.8
C(10A)-C(11A)-H(11A)	119.8
C(13A)-C(12A)-C(11A)	120.24(16)
C(13A)-C(12A)-H(12A)	119.9
C(11A)-C(12A)-H(12A)	119.9
C(12A)-C(13A)-C(14A)	119.91(15)
C(12A)-C(13A)-H(13A)	120.0
C(14A)-C(13A)-H(13A)	120.0
C(13A)-C(14A)-C(15A)	120.06(15)
C(13A)-C(14A)-H(14A)	120.0
C(15A)-C(14A)-H(14A)	120.0
C(10A)-C(15A)-C(14A)	120.78(14)
C(10A)-C(15A)-H(15A)	119.6
C(14A)-C(15A)-H(15A)	119.6
C(17A)-C(16A)-C(21A)	118.28(15)
C(17A)-C(16A)-Sn(1A)	121.94(12)
C(21A)-C(16A)-Sn(1A)	119.76(11)
C(18A)-C(17A)-C(16A)	120.41(17)
C(18A)-C(17A)-H(17A)	119.8
C(16A)-C(17A)-H(17A)	119.8
C(19A)-C(18A)-C(17A)	120.29(17)
C(19A)-C(18A)-H(18A)	119.9
C(17A)-C(18A)-H(18A)	119.9
C(20A)-C(19A)-C(18A)	120.06(16)
C(20A)-C(19A)-H(19A)	120.0
C(18A)-C(19A)-H(19A)	120.0
C(19A)-C(20A)-C(21A)	120.18(17)
C(19A)-C(20A)-H(20A)	119.9

C(21A)-C(20A)-H(20A)	119.9
C(20A)-C(21A)-C(16A)	120.78(16)
C(20A)-C(21A)-H(21A)	119.6
C(16A)-C(21A)-H(21A)	119.6
C(16B)-Sn(1B)-C(10B)	114.56(6)
C(16B)-Sn(1B)-C(1B)	115.02(6)
C(10B)-Sn(1B)-C(1B)	121.92(6)
C(16B)-Sn(1B)-Cl(1B)	103.19(4)
C(10B)-Sn(1B)-Cl(1B)	98.65(4)
C(1B)-Sn(1B)-Cl(1B)	97.74(5)
C(16B)-Sn(1B)-O(1B)	79.85(4)
C(10B)-Sn(1B)-O(1B)	87.73(5)
C(1B)-Sn(1B)-O(1B)	73.22(5)
Cl(1B)-Sn(1B)-O(1B)	170.83(3)
C(4B)-O(1B)-C(3B)	117.13(12)
C(4B)-O(1B)-Sn(1B)	125.83(9)
C(3B)-O(1B)-Sn(1B)	101.51(8)
C(2B)-C(1B)-Sn(1B)	113.60(11)
C(2B)-C(1B)-H(1BA)	108.8
Sn(1B)-C(1B)-H(1BA)	108.8
C(2B)-C(1B)-H(1BB)	108.8
Sn(1B)-C(1B)-H(1BB)	108.8
H(1BA)-C(1B)-H(1BB)	107.7
C(3B)-C(2B)-C(1B)	112.62(13)
C(3B)-C(2B)-H(2BA)	109.1
C(1B)-C(2B)-H(2BA)	109.1
C(3B)-C(2B)-H(2BB)	109.1
C(1B)-C(2B)-H(2BB)	109.1
H(2BA)-C(2B)-H(2BB)	107.8
O(1B)-C(3B)-C(2B)	106.60(12)
O(1B)-C(3B)-H(3BA)	110.4
C(2B)-C(3B)-H(3BA)	110.4
O(1B)-C(3B)-H(3BB)	110.4
C(2B)-C(3B)-H(3BB)	110.4
H(3BA)-C(3B)-H(3BB)	108.6
C(5B)-C(4B)-C(9B)	120.52(16)

C(5B)-C(4B)-O(1B)	123.39(15)
C(9B)-C(4B)-O(1B)	116.09(14)
C(4B)-C(5B)-C(6B)	118.96(17)
C(4B)-C(5B)-H(5BA)	120.5
C(6B)-C(5B)-H(5BA)	120.5
C(7B)-C(6B)-C(5B)	120.94(18)
C(7B)-C(6B)-H(6BA)	119.5
C(5B)-C(6B)-H(6BA)	119.5
C(6B)-C(7B)-C(8B)	119.61(17)
C(6B)-C(7B)-H(7BA)	120.2
C(8B)-C(7B)-H(7BA)	120.2
C(9B)-C(8B)-C(7B)	120.31(18)
C(9B)-C(8B)-H(8BA)	119.8
C(7B)-C(8B)-H(8BA)	119.8
C(4B)-C(9B)-C(8B)	119.67(17)
C(4B)-C(9B)-H(9BA)	120.2
C(8B)-C(9B)-H(9BA)	120.2
C(11B)-C(10B)-C(15B)	118.93(14)
C(11B)-C(10B)-Sn(1B)	118.74(11)
C(15B)-C(10B)-Sn(1B)	122.33(12)
C(12B)-C(11B)-C(10B)	120.49(15)
C(12B)-C(11B)-H(11B)	119.8
C(10B)-C(11B)-H(11B)	119.8
C(13B)-C(12B)-C(11B)	119.88(16)
C(13B)-C(12B)-H(12B)	120.1
C(11B)-C(12B)-H(12B)	120.1
C(14B)-C(13B)-C(12B)	120.21(16)
C(14B)-C(13B)-H(13B)	119.9
C(12B)-C(13B)-H(13B)	119.9
C(13B)-C(14B)-C(15B)	120.20(16)
C(13B)-C(14B)-H(14B)	119.9
C(15B)-C(14B)-H(14B)	119.9
C(14B)-C(15B)-C(10B)	120.28(16)
C(14B)-C(15B)-H(15B)	119.9
C(10B)-C(15B)-H(15B)	119.9
C(21B)-C(16B)-C(17B)	118.48(14)

C(21B)-C(16B)-Sn(1B)   121.21(11)
C(17B)-C(16B)-Sn(1B)   119.95(11)
C(18B)-C(17B)-C(16B)   120.76(15)
C(18B)-C(17B)-H(17B)   119.6
C(16B)-C(17B)-H(17B)   119.6
C(19B)-C(18B)-C(17B)   120.10(16)
C(19B)-C(18B)-H(18B)   119.9
C(17B)-C(18B)-H(18B)   119.9
C(18B)-C(19B)-C(20B)   119.87(16)
C(18B)-C(19B)-H(19B)   120.1
C(20B)-C(19B)-H(19B)   120.1
C(19B)-C(20B)-C(21B)   120.14(16)
C(19B)-C(20B)-H(20B)   119.9
C(21B)-C(20B)-H(20B)   119.9
C(20B)-C(21B)-C(16B)   120.63(16)
C(20B)-C(21B)-H(21B)   119.7
C(16B)-C(21B)-H(21B)   119.7

_____

Symmetry transformations used to generate equivalent atoms:

Table A 9. **Anisotropic displacement parameters ($Å^2$ x 10^3) for 200. The anisotropic** displacement factor exponent takes the form: $-2p^2[\,h^2\,a^{*2}U^{11} + ... \ + 2\,h\,k\,a^*\,b^*\,U^{12}\,]$

	U^{11}	U^{22}	U^{33}	U^{23}	U^{13}	U^{12}
Sn(1A)	21(1)	17(1)	17(1)	0(1)	-3(1)	-4(1)
Cl(1A)	33(1)	28(1)	16(1)	3(1)	-7(1)	-7(1)
O(1A)	21(1)	24(1)	22(1)	4(1)	-2(1)	-2(1)
C(1A)	22(1)	28(1)	20(1)	2(1)	-1(1)	-3(1)
C(2A)	21(1)	29(1)	25(1)	2(1)	-5(1)	-6(1)
C(3A)	20(1)	28(1)	24(1)	3(1)	-5(1)	-1(1)
C(4A)	27(1)	30(1)	15(1)	2(1)	-5(1)	-9(1)
C(5A)	31(1)	32(1)	23(1)	4(1)	-8(1)	-7(1)
C(6A)	50(1)	37(1)	32(1)	13(1)	-14(1)	-16(1)
C(7A)	49(1)	58(1)	30(1)	13(1)	-5(1)	-27(1)
C(8A)	29(1)	65(1)	28(1)	2(1)	0(1)	-15(1)
C(9A)	28(1)	41(1)	22(1)	-1(1)	-2(1)	-5(1)
C(10A)	23(1)	22(1)	18(1)	1(1)	-6(1)	-6(1)
C(11A)	25(1)	28(1)	48(1)	10(1)	-12(1)	-2(1)
C(12A)	18(1)	38(1)	66(1)	10(1)	-10(1)	-4(1)
C(13A)	26(1)	31(1)	45(1)	7(1)	-6(1)	-13(1)
C(14A)	29(1)	19(1)	33(1)	1(1)	-4(1)	-4(1)
C(15A)	20(1)	24(1)	25(1)	-2(1)	-3(1)	-2(1)
C(16A)	23(1)	19(1)	22(1)	1(1)	-1(1)	-5(1)
C(17A)	46(1)	28(1)	23(1)	-1(1)	-9(1)	2(1)
C(18A)	72(1)	33(1)	22(1)	-6(1)	-3(1)	0(1)
C(19A)	47(1)	23(1)	35(1)	0(1)	15(1)	4(1)
C(20A)	22(1)	28(1)	45(1)	7(1)	3(1)	0(1)
C(21A)	24(1)	26(1)	33(1)	2(1)	-5(1)	-6(1)
Sn(1B)	17(1)	17(1)	21(1)	0(1)	-4(1)	-2(1)
Cl(1B)	26(1)	28(1)	21(1)	-1(1)	-8(1)	-2(1)
O(1B)	25(1)	24(1)	28(1)	-3(1)	-6(1)	-7(1)
C(1B)	20(1)	27(1)	29(1)	1(1)	-1(1)	-3(1)
C(2B)	18(1)	28(1)	38(1)	-3(1)	-3(1)	-5(1)
C(3B)	22(1)	26(1)	38(1)	-2(1)	-7(1)	-9(1)
C(4B)	24(1)	29(1)	25(1)	-1(1)	-12(1)	-3(1)

C(5B)	36(1)	28(1)	33(1)	-3(1)	-12(1)	-4(1)
C(6B)	44(1)	32(1)	37(1)	-9(1)	-16(1)	1(1)
C(7B)	34(1)	51(1)	28(1)	-10(1)	-13(1)	2(1)
C(8B)	34(1)	52(1)	29(1)	-1(1)	-8(1)	-13(1)
C(9B)	34(1)	34(1)	32(1)	-3(1)	-10(1)	-11(1)
C(10B)	27(1)	18(1)	19(1)	-2(1)	-4(1)	-1(1)
C(11B)	27(1)	23(1)	28(1)	1(1)	-3(1)	-2(1)
C(12B)	34(1)	25(1)	35(1)	0(1)	7(1)	-7(1)
C(13B)	53(1)	21(1)	22(1)	3(1)	9(1)	2(1)
C(14B)	48(1)	28(1)	18(1)	1(1)	-6(1)	8(1)
C(15B)	32(1)	25(1)	22(1)	-2(1)	-9(1)	-1(1)
C(16B)	18(1)	21(1)	22(1)	-2(1)	-7(1)	-1(1)
C(17B)	24(1)	25(1)	26(1)	1(1)	-4(1)	-1(1)
C(18B)	33(1)	22(1)	38(1)	-1(1)	-9(1)	0(1)
C(19B)	29(1)	29(1)	43(1)	-12(1)	-5(1)	5(1)
C(20B)	27(1)	38(1)	35(1)	-9(1)	5(1)	-3(1)
C(21B)	26(1)	27(1)	29(1)	0(1)	-2(1)	-5(1)

Table A 10.   Hydrogen coordinates (x 10^4) and isotropic displacement parameters ($\mathring{A}^2 \times 10^3$) for 200.

	x	y	z	U(eq)
H(1AA)	6011	4420	2282	28
H(1AB)	6058	5849	2211	28
H(2AA)	7180	5105	3220	29
H(2AB)	5922	6016	3615	29
H(3AA)	5944	3429	3607	29
H(3AB)	6177	4183	4364	29
H(5AA)	5159	2320	4593	34
H(6AA)	3877	1033	5400	46
H(7AA)	1681	1666	5898	53
H(8AA)	739	3593	5601	49
H(9AA)	1994	4899	4807	37
H(11A)	688	5252	2935	40
H(12A)	-742	3812	3308	49
H(13A)	71	1821	3550	40
H(14A)	2325	1239	3358	33
H(15A)	3767	2655	2940	27
H(17A)	3576	7091	4211	39
H(18A)	2409	8855	4854	52
H(19A)	706	9922	4326	46
H(20A)	182	9255	3142	40
H(21A)	1349	7514	2481	33
H(1BA)	5380	-508	6795	31
H(1BB)	4851	908	6891	31
H(2BA)	6133	-521	7996	34
H(2BB)	6667	601	7501	34
H(3BA)	5875	1279	8812	33
H(3BB)	4883	1923	8271	33
H(5BA)	4131	2794	9472	38
H(6BA)	2912	3637	10682	45
H(7BA)	1598	2485	11548	45
H(8BA)	1492	461	11217	45

H(9BA)	2695	-397	10013	39
H(11B)	1077	-2111	8112	32
H(12B)	738	-3854	8861	39
H(13B)	2314	-4706	9584	41
H(14B)	4203	-3801	9583	39
H(15B)	4530	-2032	8862	31
H(17B)	2518	2454	7385	30
H(18B)	1157	4180	7939	37
H(19B)	-518	4006	9027	41
H(20B)	-838	2099	9558	42
H(21B)	556	373	9030	33

Table A 11. Torsion angles [°] for 200.

Sn(1A)-C(1A)-C(2A)-C(3A)	60.90(16)
C(4A)-O(1A)-C(3A)-C(2A)	177.59(12)
Sn(1A)-O(1A)-C(3A)-C(2A)	38.27(12)
C(1A)-C(2A)-C(3A)-O(1A)	-66.84(16)
C(3A)-O(1A)-C(4A)-C(5A)	-8.7(2)
Sn(1A)-O(1A)-C(4A)-C(5A)	120.36(14)
C(3A)-O(1A)-C(4A)-C(9A)	172.45(13)
Sn(1A)-O(1A)-C(4A)-C(9A)	-58.49(16)
O(1A)-C(4A)-C(5A)-C(6A)	-178.12(14)
C(9A)-C(4A)-C(5A)-C(6A)	0.7(2)
C(4A)-C(5A)-C(6A)-C(7A)	-0.1(3)
C(5A)-C(6A)-C(7A)-C(8A)	-0.2(3)
C(6A)-C(7A)-C(8A)-C(9A)	0.0(3)
C(7A)-C(8A)-C(9A)-C(4A)	0.6(3)
O(1A)-C(4A)-C(9A)-C(8A)	177.99(14)
C(5A)-C(4A)-C(9A)-C(8A)	-0.9(2)
C(15A)-C(10A)-C(11A)-C(12A)	-0.2(3)
Sn(1A)-C(10A)-C(11A)-C(12A)	-173.52(15)
C(10A)-C(11A)-C(12A)-C(13A)	1.5(3)
C(11A)-C(12A)-C(13A)-C(14A)	-1.6(3)
C(12A)-C(13A)-C(14A)-C(15A)	0.4(3)
C(11A)-C(10A)-C(15A)-C(14A)	-1.0(2)
Sn(1A)-C(10A)-C(15A)-C(14A)	171.94(12)
C(13A)-C(14A)-C(15A)-C(10A)	0.9(2)
C(21A)-C(16A)-C(17A)-C(18A)	-0.4(3)
Sn(1A)-C(16A)-C(17A)-C(18A)	-178.81(14)
C(16A)-C(17A)-C(18A)-C(19A)	0.7(3)
C(17A)-C(18A)-C(19A)-C(20A)	-0.5(3)
C(18A)-C(19A)-C(20A)-C(21A)	0.1(3)
C(19A)-C(20A)-C(21A)-C(16A)	0.2(2)
C(17A)-C(16A)-C(21A)-C(20A)	0.0(2)
Sn(1A)-C(16A)-C(21A)-C(20A)	178.40(12)
Sn(1B)-C(1B)-C(2B)-C(3B)	-50.53(17)
C(4B)-O(1B)-C(3B)-C(2B)	175.17(13)

Sn(1B)-O(1B)-C(3B)-C(2B)	-43.97(13)
C(1B)-C(2B)-C(3B)-O(1B)	66.51(17)
C(3B)-O(1B)-C(4B)-C(5B)	14.9(2)
Sn(1B)-O(1B)-C(4B)-C(5B)	-115.33(14)
C(3B)-O(1B)-C(4B)-C(9B)	-165.17(14)
Sn(1B)-O(1B)-C(4B)-C(9B)	64.56(17)
C(9B)-C(4B)-C(5B)-C(6B)	-0.6(2)
O(1B)-C(4B)-C(5B)-C(6B)	179.28(15)
C(4B)-C(5B)-C(6B)-C(7B)	0.2(3)
C(5B)-C(6B)-C(7B)-C(8B)	0.2(3)
C(6B)-C(7B)-C(8B)-C(9B)	-0.3(3)
C(5B)-C(4B)-C(9B)-C(8B)	0.6(2)
O(1B)-C(4B)-C(9B)-C(8B)	-179.34(15)
C(7B)-C(8B)-C(9B)-C(4B)	-0.1(3)
C(15B)-C(10B)-C(11B)-C(12B)	0.6(2)
Sn(1B)-C(10B)-C(11B)-C(12B)	-179.40(12)
C(10B)-C(11B)-C(12B)-C(13B)	-1.0(2)
C(11B)-C(12B)-C(13B)-C(14B)	0.7(3)
C(12B)-C(13B)-C(14B)-C(15B)	0.2(2)
C(13B)-C(14B)-C(15B)-C(10B)	-0.6(2)
C(11B)-C(10B)-C(15B)-C(14B)	0.3(2)
Sn(1B)-C(10B)-C(15B)-C(14B)	-179.77(12)
C(21B)-C(16B)-C(17B)-C(18B)	0.6(2)
Sn(1B)-C(16B)-C(17B)-C(18B)	-172.59(12)
C(16B)-C(17B)-C(18B)-C(19B)	-0.7(3)
C(17B)-C(18B)-C(19B)-C(20B)	-0.1(3)
C(18B)-C(19B)-C(20B)-C(21B)	1.0(3)
C(19B)-C(20B)-C(21B)-C(16B)	-1.1(3)
C(17B)-C(16B)-C(21B)-C(20B)	0.3(2)
Sn(1B)-C(16B)-C(21B)-C(20B)	173.41(13)

Symmetry transformations used to generate equivalent atoms:

Table A 12. Crystal data and structure refinement for 201.

Identification code	d1362
Empirical formula	$C_{27}H_{25}ClOSn$
Formula weight	519.61
Temperature	147(2) K
Wavelength	0.71073 Å
Crystal system	Monoclinic
Space group	P 21/c
Unit cell dimensions	a = 9.7304(4) Å α = 90°.
	b = 12.9001(5) Å β = 91.177(1)°.
	c = 18.5688(7) Å γ = 90°.
Volume	2330.32(16) Å^3
Z	4
Density (calculated)	1.481 Mg/m^3
Absorption coefficient	1.227 mm^{-1}
F(000)	1048
Crystal size	$0.42 \times 0.27 \times 0.24$ mm^3
Theta range for data collection	1.92 to 27.50°.
Index ranges	-12<=h<=12, -14<=k<=16, -24<=l<=24
Reflections collected	21942
Independent reflections	5347 [R(int) = 0.0321]
Completeness to theta = 27.50°	99.9 %
Absorption correction	Semi-empirical from equivalents
Max. and min. transmission	0.7456 and 0.6792
Refinement method	Full-matrix least-squares on F^2
Data / restraints / parameters	5347 / 0 / 271
Goodness-of-fit on F^2	1.043
Final R indices [I>2sigma(I)]	R1 = 0.0209, wR2 = 0.0503
R indices (all data)	R1 = 0.0252, wR2 = 0.0530
Largest diff. peak and hole	0.523 and -0.286 e.Å^{-3}

Table A 13. Atomic coordinates (x 10^4) and equivalent isotropic displacement parameters ($\text{Å}^2 \times 10^3$) for 201.

	x	y	z	U(eq)
Sn(1)	1969(1)	4361(1)	1534(1)	20(1)
Cl(1)	2120(1)	6230(1)	1516(1)	29(1)
O(1)	1309(1)	2238(1)	1634(1)	26(1)
C(1)	-1(2)	4157(2)	1999(1)	28(1)
C(2)	-71(2)	3178(2)	2461(1)	35(1)
C(3)	37(2)	2201(2)	2020(1)	31(1)
C(4)	1574(2)	1405(1)	1184(1)	23(1)
C(5)	2780(2)	1459(2)	799(1)	27(1)
C(6)	3110(2)	662(2)	332(1)	28(1)
C(7)	2271(2)	-209(1)	251(1)	23(1)
C(8)	1076(2)	-250(1)	652(1)	24(1)
C(9)	717(2)	552(1)	1113(1)	25(1)
C(10)	2640(2)	-1078(2)	-238(1)	25(1)
C(11)	2397(2)	-2102(2)	-39(1)	29(1)
C(12)	2759(2)	-2921(2)	-483(1)	33(1)
C(13)	3360(2)	-2722(2)	-1141(1)	34(1)
C(14)	3591(2)	-1713(2)	-1348(1)	35(1)
C(15)	3246(2)	-892(2)	-902(1)	30(1)
C(16)	2246(2)	4046(1)	427(1)	23(1)
C(17)	1160(2)	3829(2)	-42(1)	36(1)
C(18)	1394(2)	3655(2)	-766(1)	52(1)
C(19)	2705(3)	3694(3)	-1022(1)	61(1)
C(20)	3803(3)	3886(3)	-558(1)	56(1)
C(21)	3575(2)	4065(2)	162(1)	37(1)
C(22)	3749(2)	4077(1)	2200(1)	23(1)
C(23)	4742(2)	4844(2)	2282(1)	31(1)
C(24)	5892(2)	4696(2)	2724(1)	38(1)
C(25)	6057(2)	3784(2)	3097(1)	37(1)
C(26)	5095(2)	3022(2)	3019(1)	46(1)
C(27)	3948(2)	3158(2)	2570(1)	39(1)

Table A 14.   Bond lengths [Å] and angles [°] for 201.

Sn(1)-C(16)	2.1171(17)
Sn(1)-C(1)	2.1348(18)
Sn(1)-C(22)	2.1391(17)
Sn(1)-Cl(1)	2.4155(5)
O(1)-C(4)	1.389(2)
O(1)-C(3)	1.443(2)
C(1)-C(2)	1.530(3)
C(1)-H(1A)	0.9900
C(1)-H(1B)	0.9900
C(2)-C(3)	1.508(3)
C(2)-H(2A)	0.9900
C(2)-H(2B)	0.9900
C(3)-H(3A)	0.9900
C(3)-H(3B)	0.9900
C(4)-C(9)	1.385(3)
C(4)-C(5)	1.388(2)
C(5)-C(6)	1.387(3)
C(5)-H(5A)	0.9500
C(6)-C(7)	1.394(3)
C(6)-H(6A)	0.9500
C(7)-C(8)	1.394(2)
C(7)-C(10)	1.491(3)
C(8)-C(9)	1.392(3)
C(8)-H(8A)	0.9500
C(9)-H(9A)	0.9500
C(10)-C(11)	1.394(3)
C(10)-C(15)	1.398(2)
C(11)-C(12)	1.390(3)
C(11)-H(11A)	0.9500
C(12)-C(13)	1.389(3)
C(12)-H(12A)	0.9500
C(13)-C(14)	1.376(3)
C(13)-H(13A)	0.9500
C(14)-C(15)	1.390(3)

C(14)-H(14A)	0.9500
C(15)-H(15A)	0.9500
C(16)-C(17)	1.384(3)
C(16)-C(21)	1.393(3)
C(17)-C(18)	1.388(3)
C(17)-H(17A)	0.9500
C(18)-C(19)	1.371(3)
C(18)-H(18A)	0.9500
C(19)-C(20)	1.380(3)
C(19)-H(19A)	0.9500
C(20)-C(21)	1.380(3)
C(20)-H(20A)	0.9500
C(21)-H(21A)	0.9500
C(22)-C(27)	1.382(3)
C(22)-C(23)	1.389(3)
C(23)-C(24)	1.388(3)
C(23)-H(23A)	0.9500
C(24)-C(25)	1.372(3)
C(24)-H(24A)	0.9500
C(25)-C(26)	1.363(3)
C(25)-H(25A)	0.9500
C(26)-C(27)	1.390(3)
C(26)-H(26A)	0.9500
C(27)-H(27A)	0.9500
C(16)-Sn(1)-C(1)	120.18(7)
C(16)-Sn(1)-C(22)	114.20(6)
C(1)-Sn(1)-C(22)	117.90(7)
C(16)-Sn(1)-Cl(1)	99.77(5)
C(1)-Sn(1)-Cl(1)	100.60(5)
C(22)-Sn(1)-Cl(1)	97.49(5)
C(4)-O(1)-C(3)	116.43(14)
C(2)-C(1)-Sn(1)	112.34(13)
C(2)-C(1)-H(1A)	109.1
Sn(1)-C(1)-H(1A)	109.1
C(2)-C(1)-H(1B)	109.1

Sn(1)-C(1)-H(1B)	109.1
H(1A)-C(1)-H(1B)	107.9
C(3)-C(2)-C(1)	112.40(16)
C(3)-C(2)-H(2A)	109.1
C(1)-C(2)-H(2A)	109.1
C(3)-C(2)-H(2B)	109.1
C(1)-C(2)-H(2B)	109.1
H(2A)-C(2)-H(2B)	107.9
O(1)-C(3)-C(2)	108.21(15)
O(1)-C(3)-H(3A)	110.1
C(2)-C(3)-H(3A)	110.1
O(1)-C(3)-H(3B)	110.1
C(2)-C(3)-H(3B)	110.1
H(3A)-C(3)-H(3B)	108.4
C(9)-C(4)-C(5)	120.33(17)
C(9)-C(4)-O(1)	123.52(15)
C(5)-C(4)-O(1)	116.15(16)
C(6)-C(5)-C(4)	119.57(17)
C(6)-C(5)-H(5A)	120.2
C(4)-C(5)-H(5A)	120.2
C(5)-C(6)-C(7)	121.43(17)
C(5)-C(6)-H(6A)	119.3
C(7)-C(6)-H(6A)	119.3
C(8)-C(7)-C(6)	117.79(17)
C(8)-C(7)-C(10)	120.68(16)
C(6)-C(7)-C(10)	121.53(16)
C(9)-C(8)-C(7)	121.50(17)
C(9)-C(8)-H(8A)	119.2
C(7)-C(8)-H(8A)	119.2
C(4)-C(9)-C(8)	119.36(16)
C(4)-C(9)-H(9A)	120.3
C(8)-C(9)-H(9A)	120.3
C(11)-C(10)-C(15)	118.19(17)
C(11)-C(10)-C(7)	120.51(16)
C(15)-C(10)-C(7)	121.30(17)
C(12)-C(11)-C(10)	121.14(17)

C(12)-C(11)-H(11A)	119.4
C(10)-C(11)-H(11A)	119.4
C(13)-C(12)-C(11)	119.85(19)
C(13)-C(12)-H(12A)	120.1
C(11)-C(12)-H(12A)	120.1
C(14)-C(13)-C(12)	119.61(18)
C(14)-C(13)-H(13A)	120.2
C(12)-C(13)-H(13A)	120.2
C(13)-C(14)-C(15)	120.76(18)
C(13)-C(14)-H(14A)	119.6
C(15)-C(14)-H(14A)	119.6
C(14)-C(15)-C(10)	120.42(19)
C(14)-C(15)-H(15A)	119.8
C(10)-C(15)-H(15A)	119.8
C(17)-C(16)-C(21)	118.92(17)
C(17)-C(16)-Sn(1)	122.57(13)
C(21)-C(16)-Sn(1)	118.51(13)
C(16)-C(17)-C(18)	120.27(19)
C(16)-C(17)-H(17A)	119.9
C(18)-C(17)-H(17A)	119.9
C(19)-C(18)-C(17)	120.2(2)
C(19)-C(18)-H(18A)	119.9
C(17)-C(18)-H(18A)	119.9
C(18)-C(19)-C(20)	120.3(2)
C(18)-C(19)-H(19A)	119.8
C(20)-C(19)-H(19A)	119.8
C(19)-C(20)-C(21)	119.8(2)
C(19)-C(20)-H(20A)	120.1
C(21)-C(20)-H(20A)	120.1
C(20)-C(21)-C(16)	120.56(19)
C(20)-C(21)-H(21A)	119.7
C(16)-C(21)-H(21A)	119.7
C(27)-C(22)-C(23)	117.77(17)
C(27)-C(22)-Sn(1)	122.58(14)
C(23)-C(22)-Sn(1)	119.63(14)
C(24)-C(23)-C(22)	121.19(19)

C(24)-C(23)-H(23A)	119.4
C(22)-C(23)-H(23A)	119.4
C(25)-C(24)-C(23)	120.0(2)
C(25)-C(24)-H(24A)	120.0
C(23)-C(24)-H(24A)	120.0
C(26)-C(25)-C(24)	119.46(19)
C(26)-C(25)-H(25A)	120.3
C(24)-C(25)-H(25A)	120.3
C(25)-C(26)-C(27)	120.9(2)
C(25)-C(26)-H(26A)	119.6
C(27)-C(26)-H(26A)	119.6
C(22)-C(27)-C(26)	120.6(2)
C(22)-C(27)-H(27A)	119.7
C(26)-C(27)-H(27A)	119.7

Symmetry transformations used to generate equivalent atoms:

Table A 15. **Anisotropic displacement parameters (Å$^2 \times 10^3$) for 201. The anisotropic**
displacement factor exponent takes the form: $-2p^2[\, h^2\, a^{*2}U^{11} + ... \; + 2\, h\, k\, a^*\, b^*\, U^{12}\,]$

	U^{11}	U^{22}	U^{33}	U^{23}	U^{13}	U^{12}
Sn(1)	19(1)	19(1)	21(1)	1(1)	1(1)	1(1)
Cl(1)	29(1)	19(1)	38(1)	4(1)	0(1)	0(1)
O(1)	22(1)	25(1)	31(1)	-2(1)	4(1)	-2(1)
C(1)	26(1)	22(1)	37(1)	-1(1)	9(1)	1(1)
C(2)	40(1)	27(1)	39(1)	2(1)	18(1)	0(1)
C(3)	30(1)	24(1)	42(1)	4(1)	15(1)	-1(1)
C(4)	23(1)	21(1)	25(1)	2(1)	-2(1)	3(1)
C(5)	20(1)	23(1)	38(1)	2(1)	0(1)	-1(1)
C(6)	20(1)	30(1)	35(1)	3(1)	4(1)	2(1)
C(7)	22(1)	23(1)	24(1)	3(1)	-2(1)	2(1)
C(8)	24(1)	24(1)	25(1)	4(1)	-4(1)	-4(1)
C(9)	20(1)	29(1)	25(1)	5(1)	0(1)	-2(1)
C(10)	21(1)	27(1)	26(1)	1(1)	-4(1)	2(1)
C(11)	32(1)	29(1)	27(1)	3(1)	-2(1)	1(1)
C(12)	34(1)	27(1)	39(1)	0(1)	-4(1)	0(1)
C(13)	27(1)	36(1)	38(1)	-11(1)	-1(1)	3(1)
C(14)	27(1)	43(1)	34(1)	-4(1)	6(1)	-3(1)
C(15)	26(1)	30(1)	34(1)	1(1)	4(1)	-2(1)
C(16)	24(1)	22(1)	24(1)	1(1)	0(1)	2(1)
C(17)	22(1)	50(1)	35(1)	-7(1)	-3(1)	5(1)
C(18)	38(1)	80(2)	36(1)	-18(1)	-14(1)	11(1)
C(19)	54(2)	102(2)	27(1)	-19(1)	4(1)	5(2)
C(20)	37(1)	95(2)	36(1)	-17(1)	12(1)	-6(1)
C(21)	27(1)	52(1)	30(1)	-7(1)	1(1)	-7(1)
C(22)	22(1)	25(1)	21(1)	-2(1)	0(1)	5(1)
C(23)	33(1)	24(1)	37(1)	0(1)	-6(1)	-1(1)
C(24)	33(1)	37(1)	44(1)	-11(1)	-10(1)	-2(1)
C(25)	31(1)	48(1)	30(1)	-8(1)	-10(1)	9(1)
C(26)	43(1)	44(1)	52(1)	17(1)	-14(1)	6(1)
C(27)	35(1)	31(1)	52(1)	10(1)	-10(1)	-3(1)

Table A 16. **Hydrogen coordinates ($\times 10^4$) and isotropic displacement parameters (Å^2 $\times$ 10^3) for 201.**

	x	y	z	U(eq)
H(1A)	-210	4768	2301	34
H(1B)	-709	4117	1610	34
H(2A)	685	3191	2826	42
H(2B)	-951	3171	2720	42
H(3A)	26	1586	2338	38
H(3B)	-751	2151	1676	38
H(5A)	3376	2038	855	33
H(6A)	3925	710	61	34
H(8A)	493	-838	609	29
H(9A)	-108	515	1377	30
H(11A)	1976	-2243	407	35
H(12A)	2597	-3615	-337	40
H(13A)	3609	-3278	-1447	40
H(14A)	3991	-1577	-1800	42
H(15A)	3423	-201	-1049	36
H(17A)	250	3798	134	43
H(18A)	645	3509	-1086	62
H(19A)	2858	3589	-1520	73
H(20A)	4713	3894	-735	67
H(21A)	4331	4202	480	44
H(23A)	4632	5480	2030	38
H(24A)	6564	5227	2770	46
H(25A)	6836	3685	3406	44
H(26A)	5209	2389	3275	56
H(27A)	3295	2615	2518	47

Table A 17. Torsion angles [°] for 201.

C(16)-Sn(1)-C(1)-C(2)	104.65(15)
C(22)-Sn(1)-C(1)-C(2)	-42.96(16)
Cl(1)-Sn(1)-C(1)-C(2)	-147.38(13)
Sn(1)-C(1)-C(2)-C(3)	-66.9(2)
C(4)-O(1)-C(3)-C(2)	-178.78(15)
C(1)-C(2)-C(3)-O(1)	57.4(2)
C(3)-O(1)-C(4)-C(9)	-2.3(2)
C(3)-O(1)-C(4)-C(5)	178.24(16)
C(9)-C(4)-C(5)-C(6)	1.2(3)
O(1)-C(4)-C(5)-C(6)	-179.29(16)
C(4)-C(5)-C(6)-C(7)	-1.5(3)
C(5)-C(6)-C(7)-C(8)	0.6(3)
C(5)-C(6)-C(7)-C(10)	-178.55(17)
C(6)-C(7)-C(8)-C(9)	0.6(3)
C(10)-C(7)-C(8)-C(9)	179.76(16)
C(5)-C(4)-C(9)-C(8)	-0.1(3)
O(1)-C(4)-C(9)-C(8)	-179.50(16)
C(7)-C(8)-C(9)-C(4)	-0.9(3)
C(8)-C(7)-C(10)-C(11)	-38.0(3)
C(6)-C(7)-C(10)-C(11)	141.14(19)
C(8)-C(7)-C(10)-C(15)	142.55(18)
C(6)-C(7)-C(10)-C(15)	-38.3(3)
C(15)-C(10)-C(11)-C(12)	0.7(3)
C(7)-C(10)-C(11)-C(12)	-178.74(17)
C(10)-C(11)-C(12)-C(13)	-0.8(3)
C(11)-C(12)-C(13)-C(14)	0.0(3)
C(12)-C(13)-C(14)-C(15)	0.8(3)
C(13)-C(14)-C(15)-C(10)	-0.8(3)
C(11)-C(10)-C(15)-C(14)	0.1(3)
C(7)-C(10)-C(15)-C(14)	179.55(18)
C(1)-Sn(1)-C(16)-C(17)	8.1(2)
C(22)-Sn(1)-C(16)-C(17)	156.88(16)
Cl(1)-Sn(1)-C(16)-C(17)	-100.28(17)
C(1)-Sn(1)-C(16)-C(21)	-172.22(15)

C(22)-Sn(1)-C(16)-C(21)	-23.49(19)
Cl(1)-Sn(1)-C(16)-C(21)	79.36(16)
C(21)-C(16)-C(17)-C(18)	-1.4(3)
Sn(1)-C(16)-C(17)-C(18)	178.24(19)
C(16)-C(17)-C(18)-C(19)	0.2(4)
C(17)-C(18)-C(19)-C(20)	1.3(5)
C(18)-C(19)-C(20)-C(21)	-1.7(5)
C(19)-C(20)-C(21)-C(16)	0.5(4)
C(17)-C(16)-C(21)-C(20)	1.0(4)
Sn(1)-C(16)-C(21)-C(20)	-178.6(2)
C(16)-Sn(1)-C(22)-C(27)	-95.88(17)
C(1)-Sn(1)-C(22)-C(27)	53.61(18)
Cl(1)-Sn(1)-C(22)-C(27)	159.84(16)
C(16)-Sn(1)-C(22)-C(23)	85.54(15)
C(1)-Sn(1)-C(22)-C(23)	-124.97(14)
Cl(1)-Sn(1)-C(22)-C(23)	-18.74(14)
C(27)-C(22)-C(23)-C(24)	-0.4(3)
Sn(1)-C(22)-C(23)-C(24)	178.25(15)
C(22)-C(23)-C(24)-C(25)	-0.6(3)
C(23)-C(24)-C(25)-C(26)	0.9(3)
C(24)-C(25)-C(26)-C(27)	-0.2(4)
C(23)-C(22)-C(27)-C(26)	1.1(3)
Sn(1)-C(22)-C(27)-C(26)	-177.47(17)
C(25)-C(26)-C(27)-C(22)	-0.9(4)

Symmetry transformations used to generate equivalent atoms:

Table A 18. Crystal data and structure refinement for 202.

Identification code	d13230
Empirical formula	$C_{15}H_{16}Cl_2OSn$
Formula weight	401.87
Temperature	147(2) K
Wavelength	0.71073 Å
Crystal system	Monoclinic
Space group	P 21
Unit cell dimensions	a = 6.0761(10) Å $\quad$ $\alpha = 90°$.
	b = 8.4920(14) Å $\quad$ $\beta = 100.891(3)°$.
	c = 15.752(3) Å $\quad$ $\gamma = 90°$.
Volume	798.1(2) $Å^3$
Z	2
Density (calculated)	1.672 Mg/m^3
Absorption coefficient	1.925 mm^{-1}
F(000)	396
Crystal size	$0.350 \times 0.230 \times 0.070$ mm^3
Theta range for data collection	2.634 to 27.487°.
Index ranges	-7<=h<=7, -9<=k<=11, -20<=l<=20
Reflections collected	12905
Independent reflections	3126 [R(int) = 0.0171]
Completeness to theta = 25.242°	99.9 %
Absorption correction	Semi-empirical from equivalents
Max. and min. transmission	0.7456 and 0.6167
Refinement method	Full-matrix least-squares on F^2
Data / restraints / parameters	3126 / 1 / 172
Goodness-of-fit on F^2	1.042
Final R indices [I>2sigma(I)]	R1 = 0.0129, wR2 = 0.0331
R indices (all data)	R1 = 0.0132, wR2 = 0.0333
Absolute structure parameter	0.031(7)
Extinction coefficient	n/a
Largest diff. peak and hole	0.503 and -0.360 $e.Å^{-3}$

Table A 19. Atomic coordinates (× 10^4) and equivalent isotropic displacement parameters (Å^2 × 10^3) for 202.

	x	y	z	U(eq)
Sn(1)	4179(1)	2458(1)	1450(1)	18(1)
Cl(1)	3012(1)	130(1)	638(1)	28(1)
Cl(2)	8006(1)	2309(1)	1357(1)	33(1)
O(1)	5332(3)	5358(2)	2137(1)	27(1)
C(1)	2457(4)	4164(4)	597(2)	23(1)
C(2)	2128(5)	5729(4)	1023(2)	32(1)
C(3)	4326(5)	6443(4)	1466(2)	34(1)
C(4)	7240(4)	5878(3)	2688(2)	26(1)
C(5)	8516(4)	7139(4)	2500(2)	35(1)
C(6)	10407(4)	7589(6)	3106(2)	43(1)
C(7)	10994(5)	6791(5)	3884(2)	45(1)
C(8)	9709(5)	5531(4)	4055(2)	41(1)
C(9)	7835(4)	5055(4)	3461(2)	33(1)
C(10)	4162(4)	1706(3)	2728(2)	23(1)
C(11)	5717(5)	559(4)	3075(2)	30(1)
C(12)	5770(5)	-35(5)	3898(2)	38(1)
C(13)	4284(5)	552(4)	4389(2)	40(1)
C(14)	2738(5)	1700(4)	4057(2)	39(1)
C(15)	2663(4)	2277(5)	3224(2)	29(1)

Table A 20.   Bond lengths [Å] and angles [°] for 202.

Sn(1)-C(1)	2.114(3)
Sn(1)-C(10)	2.114(2)
Sn(1)-Cl(2)	2.3610(6)
Sn(1)-Cl(1)	2.3887(8)
O(1)-C(4)	1.383(3)
O(1)-C(3)	1.448(3)
C(1)-C(2)	1.519(4)
C(1)-H(1A)	0.9900
C(1)-H(1B)	0.9900
C(2)-C(3)	1.512(4)
C(2)-H(2A)	0.9900
C(2)-H(2B)	0.9900
C(3)-H(3A)	0.9900
C(3)-H(3B)	0.9900
C(4)-C(5)	1.386(4)
C(4)-C(9)	1.392(4)
C(5)-C(6)	1.401(4)
C(5)-H(5A)	0.9500
C(6)-C(7)	1.387(6)
C(6)-H(6A)	0.9500
C(7)-C(8)	1.380(5)
C(7)-H(7A)	0.9500
C(8)-C(9)	1.390(4)
C(8)-H(8A)	0.9500
C(9)-H(9A)	0.9500
C(10)-C(15)	1.393(4)
C(10)-C(11)	1.394(4)
C(11)-C(12)	1.385(4)
C(11)-H(11A)	0.9500
C(12)-C(13)	1.389(5)
C(12)-H(12A)	0.9500
C(13)-C(14)	1.386(5)
C(13)-H(13A)	0.9500
C(14)-C(15)	1.394(4)

C(14)-H(14A)	0.9500
C(15)-H(15A)	0.9500
C(1)-Sn(1)-C(10)	136.18(10)
C(1)-Sn(1)-Cl(2)	111.85(8)
C(10)-Sn(1)-Cl(2)	103.02(7)
C(1)-Sn(1)-Cl(1)	99.53(9)
C(10)-Sn(1)-Cl(1)	101.87(8)
Cl(2)-Sn(1)-Cl(1)	96.80(3)
C(4)-O(1)-C(3)	116.3(2)
C(2)-C(1)-Sn(1)	114.17(18)
C(2)-C(1)-H(1A)	108.7
Sn(1)-C(1)-H(1A)	108.7
C(2)-C(1)-H(1B)	108.7
Sn(1)-C(1)-H(1B)	108.7
H(1A)-C(1)-H(1B)	107.6
C(3)-C(2)-C(1)	112.1(2)
C(3)-C(2)-H(2A)	109.2
C(1)-C(2)-H(2A)	109.2
C(3)-C(2)-H(2B)	109.2
C(1)-C(2)-H(2B)	109.2
H(2A)-C(2)-H(2B)	107.9
O(1)-C(3)-C(2)	107.2(3)
O(1)-C(3)-H(3A)	110.3
C(2)-C(3)-H(3A)	110.3
O(1)-C(3)-H(3B)	110.3
C(2)-C(3)-H(3B)	110.3
H(3A)-C(3)-H(3B)	108.5
O(1)-C(4)-C(5)	123.3(2)
O(1)-C(4)-C(9)	115.9(3)
C(5)-C(4)-C(9)	120.8(3)
C(4)-C(5)-C(6)	119.0(3)
C(4)-C(5)-H(5A)	120.5
C(6)-C(5)-H(5A)	120.5
C(7)-C(6)-C(5)	120.6(4)
C(7)-C(6)-H(6A)	119.7

C(5)-C(6)-H(6A)	119.7
C(8)-C(7)-C(6)	119.4(3)
C(8)-C(7)-H(7A)	120.3
C(6)-C(7)-H(7A)	120.3
C(7)-C(8)-C(9)	121.1(3)
C(7)-C(8)-H(8A)	119.5
C(9)-C(8)-H(8A)	119.5
C(8)-C(9)-C(4)	119.2(3)
C(8)-C(9)-H(9A)	120.4
C(4)-C(9)-H(9A)	120.4
C(15)-C(10)-C(11)	119.4(3)
C(15)-C(10)-Sn(1)	123.3(2)
C(11)-C(10)-Sn(1)	117.30(19)
C(12)-C(11)-C(10)	121.0(3)
C(12)-C(11)-H(11A)	119.5
C(10)-C(11)-H(11A)	119.5
C(11)-C(12)-C(13)	119.2(3)
C(11)-C(12)-H(12A)	120.4
C(13)-C(12)-H(12A)	120.4
C(14)-C(13)-C(12)	120.5(3)
C(14)-C(13)-H(13A)	119.7
C(12)-C(13)-H(13A)	119.7
C(13)-C(14)-C(15)	120.1(3)
C(13)-C(14)-H(14A)	119.9
C(15)-C(14)-H(14A)	119.9
C(10)-C(15)-C(14)	119.8(3)
C(10)-C(15)-H(15A)	120.1
C(14)-C(15)-H(15A)	120.1

Symmetry transformations used to generate equivalent atoms:

Table A 21.   Anisotropic displacement parameters ($Å^2 \times 10^3$) for 202. The anisotropic displacement factor exponent takes the form: $-2\pi^2[\, h^2\, a^{*2}U^{11} + ... + 2\, h\, k\, a^*\, b^*\, U^{12}\,]$

	U^{11}	U^{22}	U^{33}	U^{23}	U^{13}	U^{12}
Sn(1)	17(1)	20(1)	18(1)	1(1)	3(1)	2(1)
Cl(1)	30(1)	22(1)	31(1)	-6(1)	1(1)	1(1)
Cl(2)	17(1)	46(1)	36(1)	-1(1)	7(1)	1(1)
O(1)	31(1)	22(1)	25(1)	1(1)	-1(1)	2(1)
C(1)	25(1)	21(2)	21(1)	4(1)	1(1)	3(1)
C(2)	32(1)	25(2)	34(2)	2(1)	-3(1)	7(1)
C(3)	42(2)	20(2)	36(2)	3(1)	-4(1)	4(1)
C(4)	25(1)	23(1)	29(1)	-8(1)	3(1)	6(1)
C(5)	34(1)	34(3)	37(1)	-5(1)	6(1)	-1(1)
C(6)	33(1)	35(2)	60(2)	-11(2)	7(1)	-3(2)
C(7)	34(2)	44(2)	53(2)	-17(2)	-8(1)	4(1)
C(8)	44(2)	38(2)	35(2)	-6(1)	-7(1)	11(1)
C(9)	35(1)	30(2)	31(1)	-5(1)	1(1)	3(1)
C(10)	25(1)	23(1)	19(1)	0(1)	1(1)	-3(1)
C(11)	30(1)	31(2)	27(1)	3(1)	2(1)	4(1)
C(12)	40(1)	38(2)	32(1)	11(2)	-5(1)	1(1)
C(13)	51(2)	46(2)	20(1)	8(1)	2(1)	-12(1)
C(14)	47(2)	44(2)	28(1)	-3(1)	15(1)	-5(1)
C(15)	32(1)	31(2)	27(1)	2(1)	9(1)	4(1)

Table A 22.   Hydrogen coordinates ($\times 10^4$) and isotropic displacement parameters ($\text{Å}^2 \times 10^3$) for 202.

	x	y	z	U(eq)
H(1A)	3301	4350	127	27
H(1B)	969	3738	331	27
H(2A)	1359	6471	579	38
H(2B)	1155	5570	1453	38
H(3A)	5328	6601	1045	41
H(3B)	4064	7477	1720	41
H(5A)	8114	7689	1968	42
H(6A)	11295	8449	2983	51
H(7A)	12268	7108	4296	55
H(8A)	10111	4981	4587	49
H(9A)	6972	4179	3582	39
H(11A)	6756	180	2742	36
H(12A)	6811	-835	4123	46
H(13A)	4328	164	4958	47
H(14A)	1727	2094	4398	46
H(15A)	1594	3057	2994	35

Table A 23. Torsion angles [°] for 202.

Sn(1)-C(1)-C(2)-C(3)	57.0(3)
C(4)-O(1)-C(3)-C(2)	-172.7(2)
C(1)-C(2)-C(3)-O(1)	-61.8(3)
C(3)-O(1)-C(4)-C(5)	-17.4(4)
C(3)-O(1)-C(4)-C(9)	162.5(2)
O(1)-C(4)-C(5)-C(6)	179.2(3)
C(9)-C(4)-C(5)-C(6)	-0.8(4)
C(4)-C(5)-C(6)-C(7)	-0.2(5)
C(5)-C(6)-C(7)-C(8)	0.7(6)
C(6)-C(7)-C(8)-C(9)	-0.2(5)
C(7)-C(8)-C(9)-C(4)	-0.8(5)
O(1)-C(4)-C(9)-C(8)	-178.7(3)
C(5)-C(4)-C(9)-C(8)	1.3(4)
C(15)-C(10)-C(11)-C(12)	1.0(5)
Sn(1)-C(10)-C(11)-C(12)	-177.9(3)
C(10)-C(11)-C(12)-C(13)	-1.6(5)
C(11)-C(12)-C(13)-C(14)	1.1(5)
C(12)-C(13)-C(14)-C(15)	-0.1(5)
C(11)-C(10)-C(15)-C(14)	0.1(5)
Sn(1)-C(10)-C(15)-C(14)	178.9(2)
C(13)-C(14)-C(15)-C(10)	-0.5(5)

Symmetry transformations used to generate equivalent atoms:

Table A 24. Crystal data and structure refinement for 203.

Identification code	d1409
Empirical formula	$C_{21}H_{20}Cl_2OSn$
Formula weight	477.96
Temperature	147(2) K
Wavelength	0.71073 Å
Crystal system	Monoclinic
Space group	P 21/c
Unit cell dimensions	a = 14.2473(9) Å $\alpha = 90°$.
	b = 6.3874(4) Å $\beta = 93.158(2)°$.
	c = 22.0483(13) Å $\gamma = 90°$.
Volume	2003.4(2) $Å^3$
Z	4
Density (calculated)	1.585 Mg/m^3
Absorption coefficient	1.548 mm^{-1}
F(000)	952
Crystal size	$0.350 \times 0.120 \times 0.120$ mm^3
Theta range for data collection	1.431 to 27.536°.
Index ranges	-18<=h<=18, -8<=k<=8, -28<=l<=28
Reflections collected	32922
Independent reflections	4602 [R(int) = 0.0374]
Completeness to theta = 25.242°	99.9 %
Absorption correction	Semi-empirical from equivalents
Max. and min. transmission	0.7456 and 0.6530
Refinement method	Full-matrix least-squares on F^2
Data / restraints / parameters	4602 / 0 / 226
Goodness-of-fit on F^2	0.985
Final R indices [I>2sigma(I)]	R1 = 0.0223, wR2 = 0.0474
R indices (all data)	R1 = 0.0311, wR2 = 0.0506
Extinction coefficient	n/a
Largest diff. peak and hole	0.784 and -0.476 e.$Å^{-3}$

Table A 25. Atomic coordinates ($\times 10^4$) and equivalent isotropic displacement parameters ($\text{Å}^2 \times 10^3$) for 203.

	x	y	z	U(eq)
Sn(1)	4277(1)	11560(1)	907(1)	23(1)
Cl(1)	5931(1)	12098(1)	870(1)	30(1)
Cl(2)	4299(1)	7894(1)	828(1)	31(1)
O(1)	2327(1)	10875(2)	697(1)	32(1)
C(1)	3752(2)	13117(3)	104(1)	30(1)
C(2)	2742(2)	13849(4)	128(1)	36(1)
C(3)	2063(2)	12066(4)	160(1)	38(1)
C(4)	1767(2)	9208(4)	832(1)	30(1)
C(5)	1965(2)	8229(3)	1388(1)	30(1)
C(6)	1426(2)	6557(4)	1565(1)	32(1)
C(7)	671(2)	5808(4)	1195(1)	34(1)
C(8)	493(2)	6808(4)	640(1)	41(1)
C(9)	1028(2)	8482(4)	450(1)	38(1)
C(10)	89(2)	4026(4)	1389(1)	40(1)
C(11)	479(2)	2384(4)	1728(1)	46(1)
C(12)	-65(2)	718(5)	1912(2)	57(1)
C(13)	-1016(2)	673(6)	1743(2)	66(1)
C(14)	-1413(2)	2282(7)	1412(2)	74(1)
C(15)	-876(2)	3970(6)	1237(1)	60(1)
C(16)	3964(1)	12137(3)	1820(1)	22(1)
C(17)	3602(2)	14058(4)	1993(1)	28(1)
C(18)	3393(2)	14410(4)	2591(1)	34(1)
C(19)	3530(2)	12836(4)	3016(1)	35(1)
C(20)	3889(2)	10922(4)	2850(1)	35(1)
C(21)	4113(2)	10564(4)	2253(1)	28(1)

Table A 26. Bond lengths [Å] and angles [°] for 203.

Sn(1)-C(16)	2.1184(19)
Sn(1)-C(1)	2.1289(19)
Sn(1)-Cl(2)	2.3483(6)
Sn(1)-Cl(1)	2.3868(6)
O(1)-C(4)	1.373(3)
O(1)-C(3)	1.441(3)
C(1)-C(2)	1.517(3)
C(1)-H(1A)	0.9900
C(1)-H(1B)	0.9900
C(2)-C(3)	1.498(3)
C(2)-H(2A)	0.9900
C(2)-H(2B)	0.9900
C(3)-H(3A)	0.9900
C(3)-H(3B)	0.9900
C(4)-C(9)	1.390(3)
C(4)-C(5)	1.391(3)
C(5)-C(6)	1.383(3)
C(5)-H(5A)	0.9500
C(6)-C(7)	1.399(3)
C(6)-H(6A)	0.9500
C(7)-C(8)	1.390(4)
C(7)-C(10)	1.485(4)
C(8)-C(9)	1.391(4)
C(8)-H(8A)	0.9500
C(9)-H(9A)	0.9500
C(10)-C(11)	1.387(4)
C(10)-C(15)	1.398(3)
C(11)-C(12)	1.390(4)
C(11)-H(11A)	0.9500
C(12)-C(13)	1.385(4)
C(12)-H(12A)	0.9500
C(13)-C(14)	1.366(5)
C(13)-H(13A)	0.9500
C(14)-C(15)	1.388(5)

C(14)-H(14A)	0.9500
C(15)-H(15A)	0.9500
C(16)-C(17)	1.392(3)
C(16)-C(21)	1.395(3)
C(17)-C(18)	1.386(3)
C(17)-H(17A)	0.9500
C(18)-C(19)	1.379(3)
C(18)-H(18A)	0.9500
C(19)-C(20)	1.382(3)
C(19)-H(19A)	0.9500
C(20)-C(21)	1.391(3)
C(20)-H(20A)	0.9500
C(21)-H(21A)	0.9500
C(16)-Sn(1)-C(1)	128.74(8)
C(16)-Sn(1)-Cl(2)	104.36(6)
C(1)-Sn(1)-Cl(2)	114.21(6)
C(16)-Sn(1)-Cl(1)	105.49(5)
C(1)-Sn(1)-Cl(1)	101.94(6)
Cl(2)-Sn(1)-Cl(1)	97.10(2)
C(4)-O(1)-C(3)	117.35(17)
C(2)-C(1)-Sn(1)	113.95(14)
C(2)-C(1)-H(1A)	108.8
Sn(1)-C(1)-H(1A)	108.8
C(2)-C(1)-H(1B)	108.8
Sn(1)-C(1)-H(1B)	108.8
H(1A)-C(1)-H(1B)	107.7
C(3)-C(2)-C(1)	112.5(2)
C(3)-C(2)-H(2A)	109.1
C(1)-C(2)-H(2A)	109.1
C(3)-C(2)-H(2B)	109.1
C(1)-C(2)-H(2B)	109.1
H(2A)-C(2)-H(2B)	107.8
O(1)-C(3)-C(2)	107.46(18)
O(1)-C(3)-H(3A)	110.2
C(2)-C(3)-H(3A)	110.2

O(1)-C(3)-H(3B)	110.2
C(2)-C(3)-H(3B)	110.2
H(3A)-C(3)-H(3B)	108.5
O(1)-C(4)-C(9)	123.9(2)
O(1)-C(4)-C(5)	116.57(18)
C(9)-C(4)-C(5)	119.5(2)
C(6)-C(5)-C(4)	120.5(2)
C(6)-C(5)-H(5A)	119.8
C(4)-C(5)-H(5A)	119.8
C(5)-C(6)-C(7)	121.4(2)
C(5)-C(6)-H(6A)	119.3
C(7)-C(6)-H(6A)	119.3
C(8)-C(7)-C(6)	116.9(2)
C(8)-C(7)-C(10)	121.9(2)
C(6)-C(7)-C(10)	121.2(2)
C(7)-C(8)-C(9)	122.8(2)
C(7)-C(8)-H(8A)	118.6
C(9)-C(8)-H(8A)	118.6
C(4)-C(9)-C(8)	118.9(2)
C(4)-C(9)-H(9A)	120.6
C(8)-C(9)-H(9A)	120.6
C(11)-C(10)-C(15)	118.0(3)
C(11)-C(10)-C(7)	121.5(2)
C(15)-C(10)-C(7)	120.5(3)
C(10)-C(11)-C(12)	121.5(3)
C(10)-C(11)-H(11A)	119.2
C(12)-C(11)-H(11A)	119.2
C(13)-C(12)-C(11)	119.4(3)
C(13)-C(12)-H(12A)	120.3
C(11)-C(12)-H(12A)	120.3
C(14)-C(13)-C(12)	119.9(3)
C(14)-C(13)-H(13A)	120.1
C(12)-C(13)-H(13A)	120.1
C(13)-C(14)-C(15)	121.0(3)
C(13)-C(14)-H(14A)	119.5
C(15)-C(14)-H(14A)	119.5

C(14)-C(15)-C(10)	120.2(3)
C(14)-C(15)-H(15A)	119.9
C(10)-C(15)-H(15A)	119.9
C(17)-C(16)-C(21)	119.48(18)
C(17)-C(16)-Sn(1)	120.97(15)
C(21)-C(16)-Sn(1)	119.54(15)
C(18)-C(17)-C(16)	120.4(2)
C(18)-C(17)-H(17A)	119.8
C(16)-C(17)-H(17A)	119.8
C(19)-C(18)-C(17)	119.8(2)
C(19)-C(18)-H(18A)	120.1
C(17)-C(18)-H(18A)	120.1
C(18)-C(19)-C(20)	120.4(2)
C(18)-C(19)-H(19A)	119.8
C(20)-C(19)-H(19A)	119.8
C(19)-C(20)-C(21)	120.2(2)
C(19)-C(20)-H(20A)	119.9
C(21)-C(20)-H(20A)	119.9
C(20)-C(21)-C(16)	119.7(2)
C(20)-C(21)-H(21A)	120.2
C(16)-C(21)-H(21A)	120.2

Symmetry transformations used to generate equivalent atoms:

Table A 27.   Anisotropic displacement parameters ($\text{Å}^2 \times 10^3$) for 203. The anisotropic displacement factor exponent takes the form: $-2\pi^2[\,h^2\,a^{*2}U^{11} + ... \; + 2\,h\,k\,a^*\,b^*\,U^{12}\,]$

	U^{11}	U^{22}	U^{33}	U^{23}	U^{13}	U^{12}
Sn(1)	31(1)	23(1)	16(1)	-1(1)	0(1)	5(1)
Cl(1)	31(1)	36(1)	23(1)	1(1)	3(1)	2(1)
Cl(2)	42(1)	23(1)	28(1)	-3(1)	4(1)	5(1)
O(1)	33(1)	32(1)	30(1)	3(1)	-8(1)	2(1)
C(1)	44(1)	26(1)	18(1)	3(1)	-1(1)	7(1)
C(2)	46(1)	32(1)	30(1)	5(1)	-8(1)	10(1)
C(3)	41(1)	40(1)	33(1)	6(1)	-12(1)	10(1)
C(4)	26(1)	32(1)	32(1)	-5(1)	-3(1)	8(1)
C(5)	24(1)	33(1)	32(1)	-4(1)	-6(1)	4(1)
C(6)	25(1)	36(1)	35(1)	-3(1)	-2(1)	5(1)
C(7)	24(1)	35(1)	43(1)	-12(1)	0(1)	5(1)
C(8)	30(1)	49(2)	42(1)	-13(1)	-12(1)	3(1)
C(9)	36(1)	42(1)	34(1)	-5(1)	-12(1)	6(1)
C(10)	27(1)	46(2)	46(1)	-16(1)	3(1)	-3(1)
C(11)	32(1)	34(1)	74(2)	-14(1)	15(1)	0(1)
C(12)	54(2)	40(2)	79(2)	-15(2)	29(2)	-3(1)
C(13)	57(2)	68(2)	75(2)	-28(2)	26(2)	-30(2)
C(14)	37(2)	113(3)	72(2)	-13(2)	0(2)	-28(2)
C(15)	32(1)	86(2)	60(2)	-3(2)	-6(1)	-13(2)
C(16)	22(1)	27(1)	18(1)	-2(1)	0(1)	2(1)
C(17)	30(1)	30(1)	24(1)	1(1)	1(1)	5(1)
C(18)	35(1)	37(1)	30(1)	-9(1)	7(1)	4(1)
C(19)	34(1)	52(2)	19(1)	-6(1)	5(1)	-3(1)
C(20)	39(1)	43(1)	22(1)	5(1)	-1(1)	0(1)
C(21)	33(1)	30(1)	22(1)	0(1)	-1(1)	3(1)

Table A 28.   Hydrogen coordinates ($\times 10^4$) and isotropic displacement parameters ($\mathring{A}^2 \times 10^3$) for 203.

	x	y	z	U(eq)
H(1A)	4156	14344	33	36
H(1B)	3798	12156	-245	36
H(2A)	2685	14756	488	44
H(2B)	2574	14698	-237	44
H(3A)	1414	12603	181	46
H(3B)	2091	11174	-206	46
H(5A)	2473	8712	1648	36
H(6A)	1573	5905	1945	39
H(8A)	-15	6327	380	49
H(9A)	890	9119	66	46
H(11A)	1133	2398	1838	55
H(12A)	212	-379	2151	68
H(13A)	-1391	-476	1858	79
H(14A)	-2066	2247	1299	89
H(15A)	-1166	5090	1013	72
H(17A)	3498	15134	1700	34
H(18A)	3157	15731	2709	41
H(19A)	3375	13069	3424	42
H(20A)	3983	9849	3146	42
H(21A)	4367	9253	2141	34

Table A 29. Torsion angles [°] for 203.

Sn(1)-C(1)-C(2)-C(3)	-65.4(2)
C(4)-O(1)-C(3)-C(2)	176.96(18)
C(1)-C(2)-C(3)-O(1)	59.0(2)
C(3)-O(1)-C(4)-C(9)	6.9(3)
C(3)-O(1)-C(4)-C(5)	-172.61(19)
O(1)-C(4)-C(5)-C(6)	178.96(19)
C(9)-C(4)-C(5)-C(6)	-0.6(3)
C(4)-C(5)-C(6)-C(7)	-0.2(3)
C(5)-C(6)-C(7)-C(8)	0.6(3)
C(5)-C(6)-C(7)-C(10)	-179.4(2)
C(6)-C(7)-C(8)-C(9)	-0.1(4)
C(10)-C(7)-C(8)-C(9)	179.9(2)
O(1)-C(4)-C(9)-C(8)	-178.5(2)
C(5)-C(4)-C(9)-C(8)	1.0(3)
C(7)-C(8)-C(9)-C(4)	-0.7(4)
C(8)-C(7)-C(10)-C(11)	145.2(3)
C(6)-C(7)-C(10)-C(11)	-34.8(3)
C(8)-C(7)-C(10)-C(15)	-35.4(4)
C(6)-C(7)-C(10)-C(15)	144.6(3)
C(15)-C(10)-C(11)-C(12)	0.4(4)
C(7)-C(10)-C(11)-C(12)	179.8(2)
C(10)-C(11)-C(12)-C(13)	1.2(4)
C(11)-C(12)-C(13)-C(14)	-1.5(5)
C(12)-C(13)-C(14)-C(15)	0.3(5)
C(13)-C(14)-C(15)-C(10)	1.3(5)
C(11)-C(10)-C(15)-C(14)	-1.6(4)
C(7)-C(10)-C(15)-C(14)	179.0(3)
C(21)-C(16)-C(17)-C(18)	0.1(3)
Sn(1)-C(16)-C(17)-C(18)	179.46(16)
C(16)-C(17)-C(18)-C(19)	-1.1(3)
C(17)-C(18)-C(19)-C(20)	1.1(4)
C(18)-C(19)-C(20)-C(21)	-0.3(4)
C(19)-C(20)-C(21)-C(16)	-0.7(3)
C(17)-C(16)-C(21)-C(20)	0.8(3)

Sn(1)-C(16)-C(21)-C(20)   -178.59(16)

Symmetry transformations used to generate equivalent atoms:
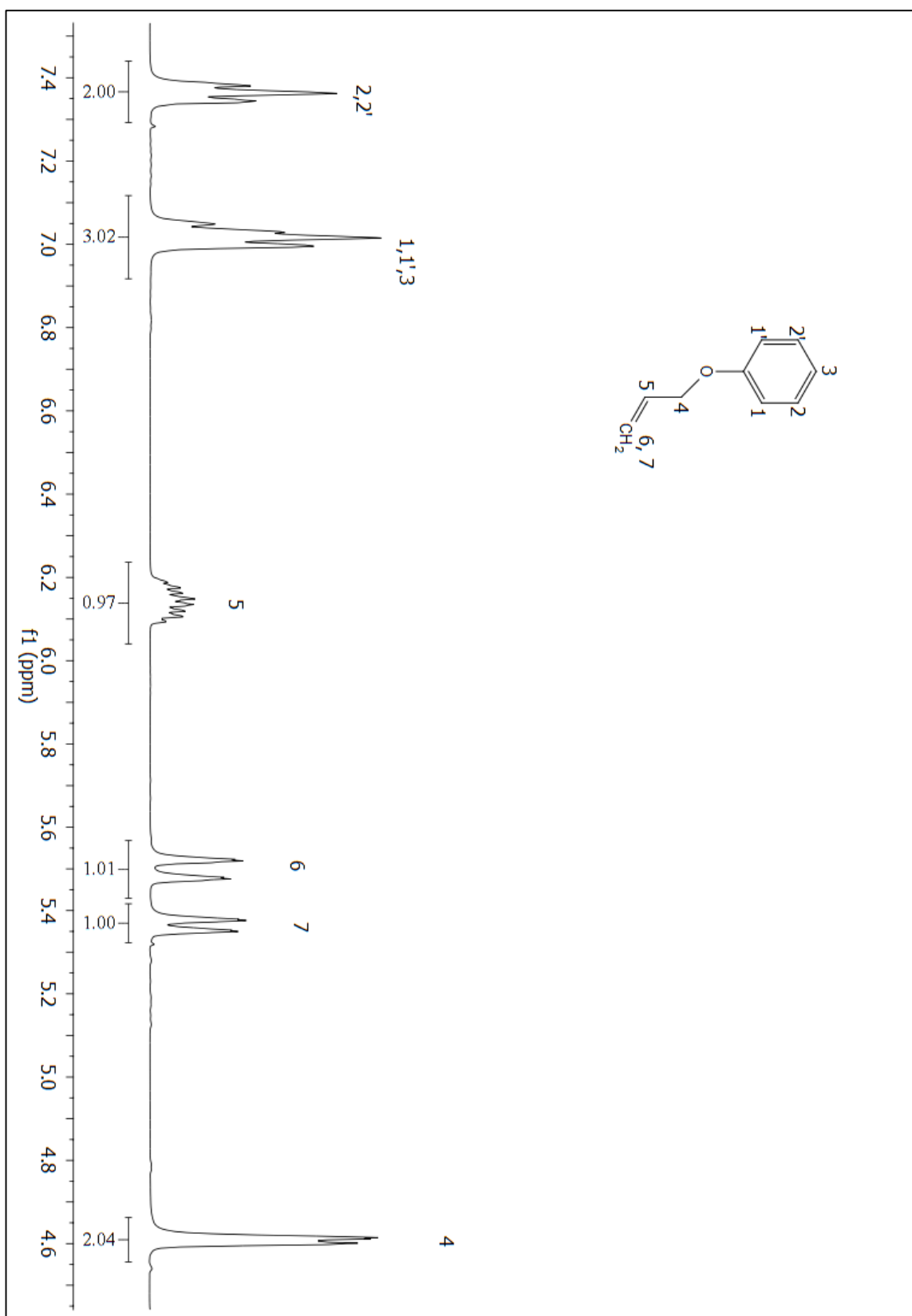
Figure A 1: ¹H NMR (CDCl₃) spectrum of compound 194.
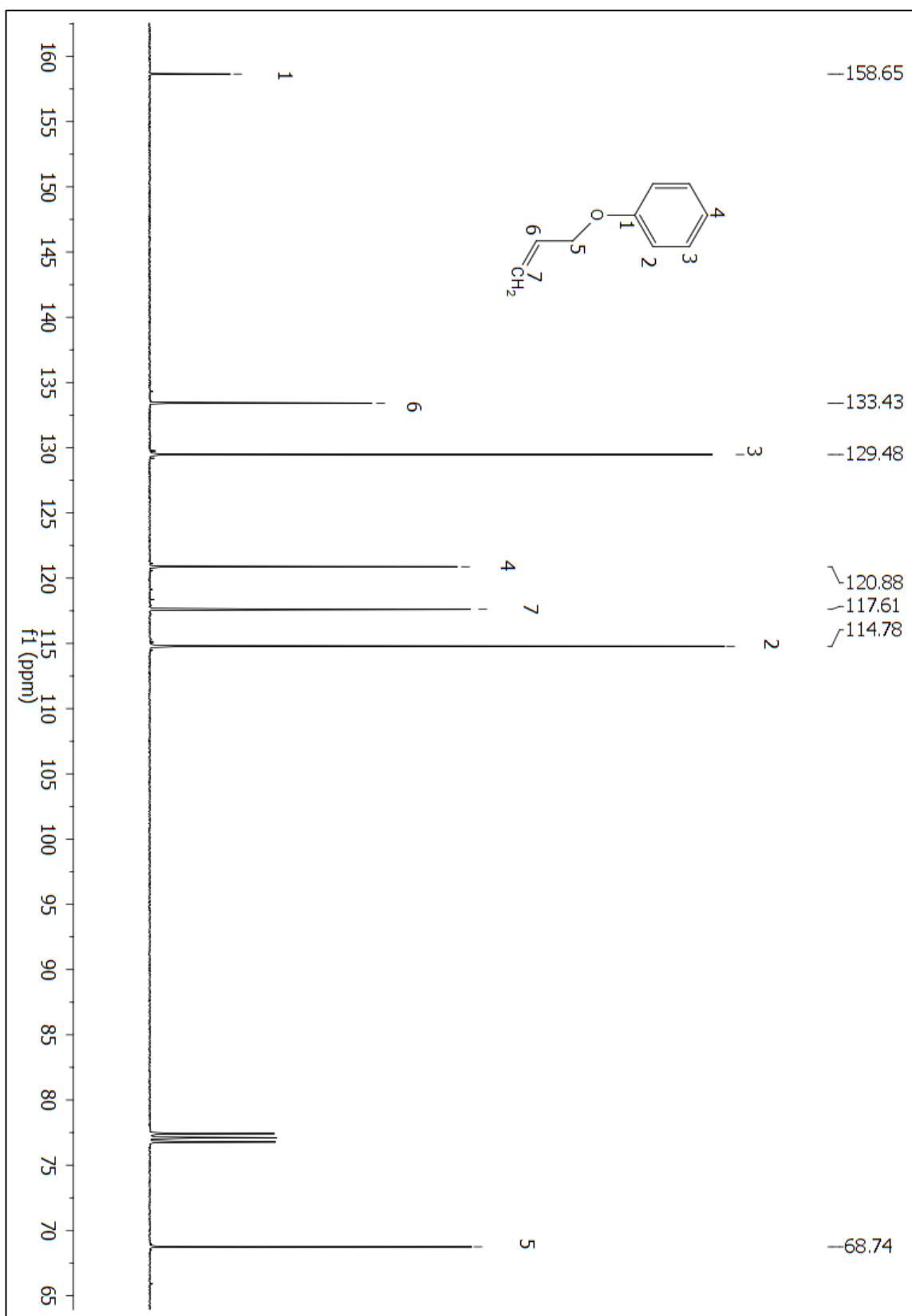
Figure A 2: ^{13}C NMR (CDCl$_3$) spectrum of compound **194.**
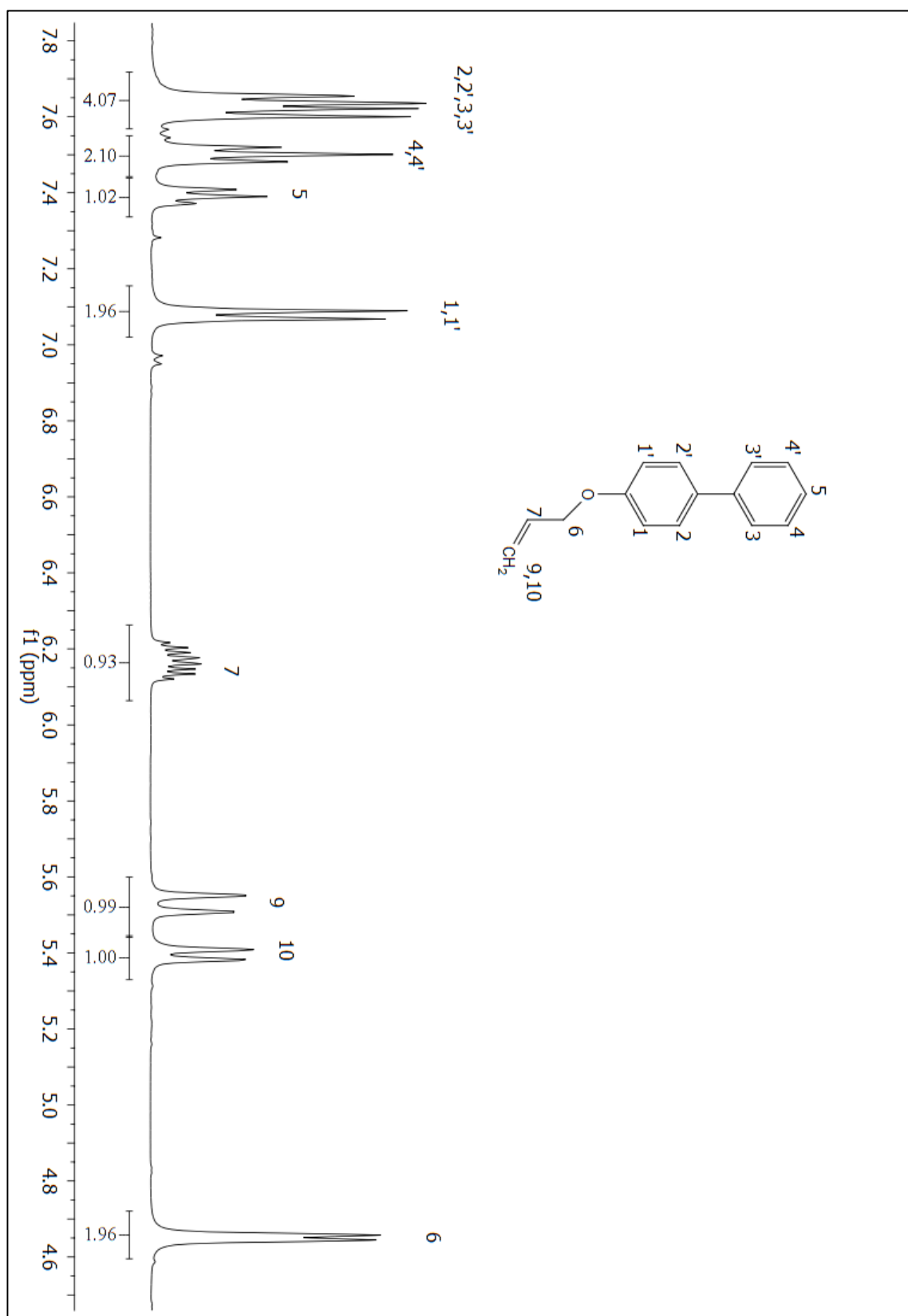
Figure A 3: ¹H NMR (CDCl₃) spectrum of compound 137.
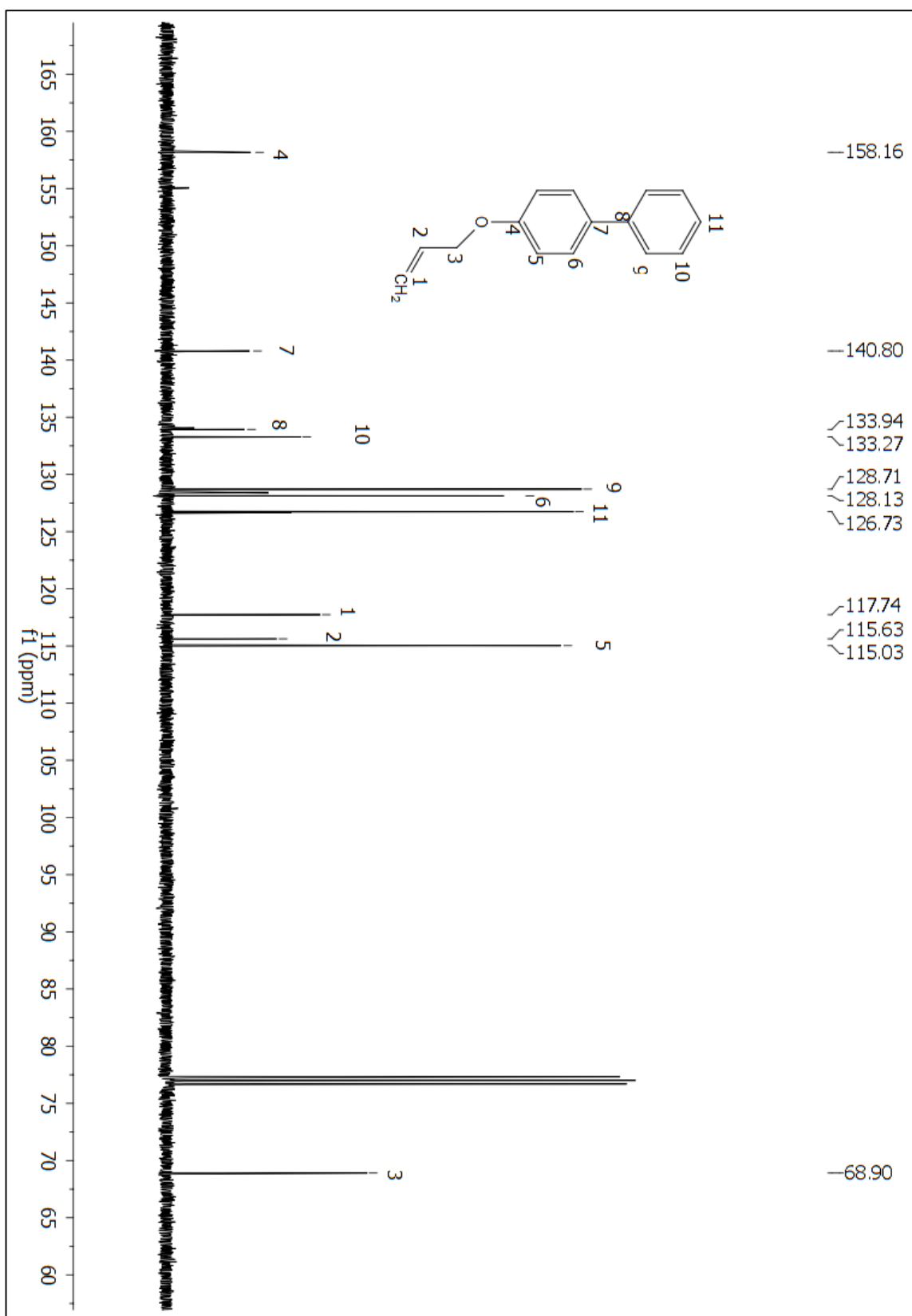
Figure A 4: ^{13}C NMR (CDCl$_3$) spectrum of compound 137.
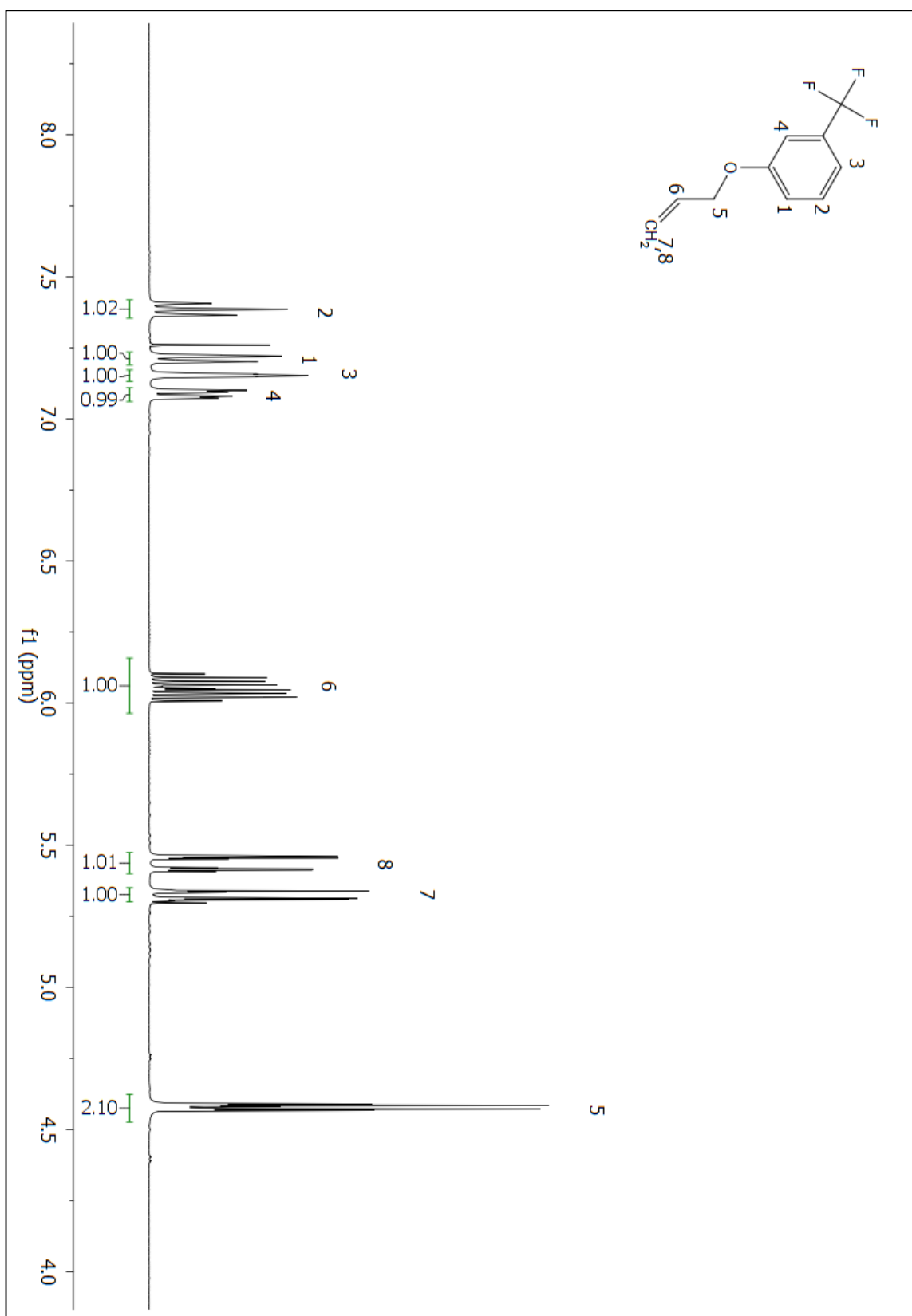
Figure A 5: ¹H NMR (CDCl₃) spectrum of compound in 195.

Figure A 6: ^{13}C NMR (CDCl$_3$) spectrum of compound **195.**
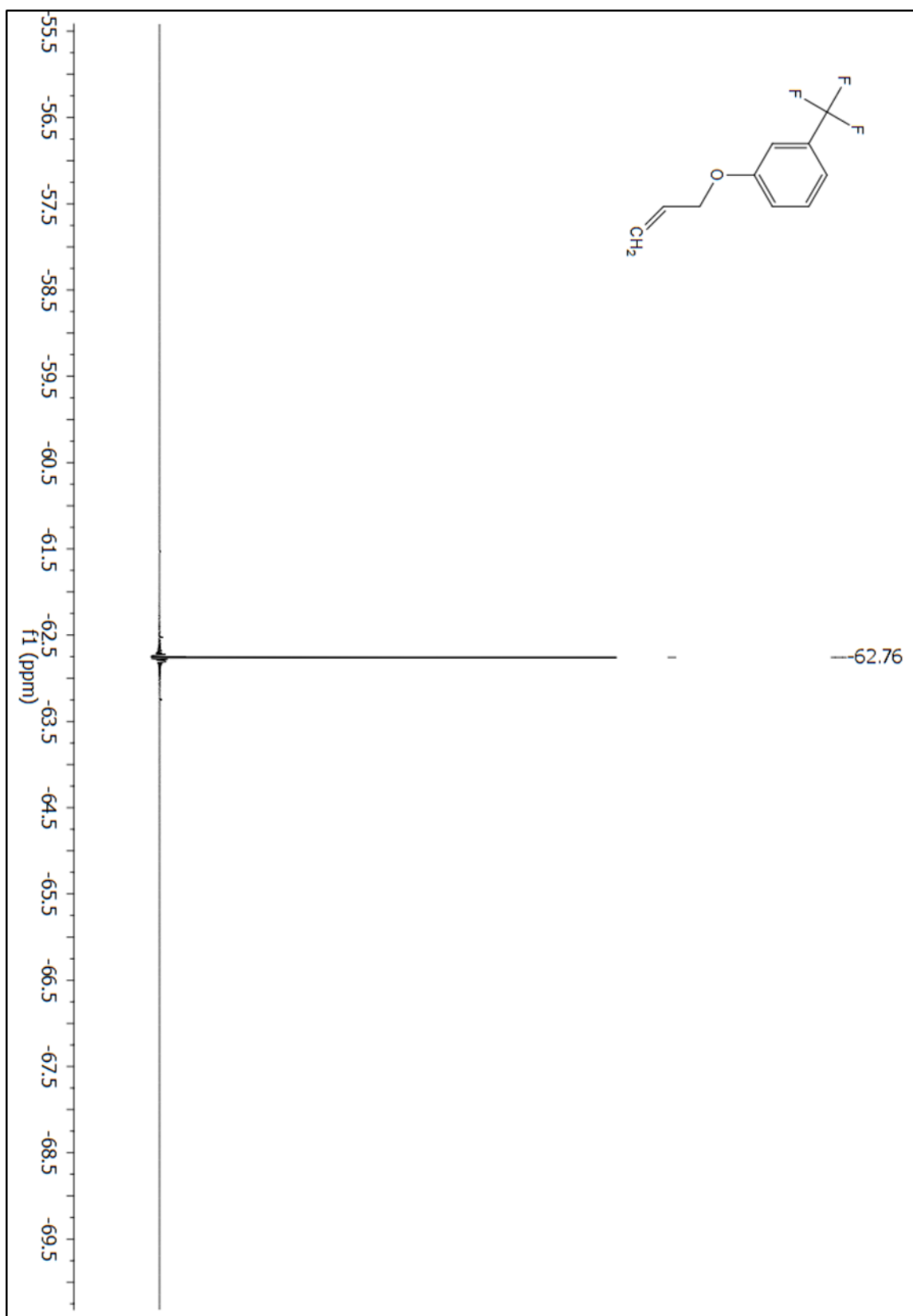
Figure A 7: ^{19}F NMR (CDCl$_3$) spectrum of compound 195.
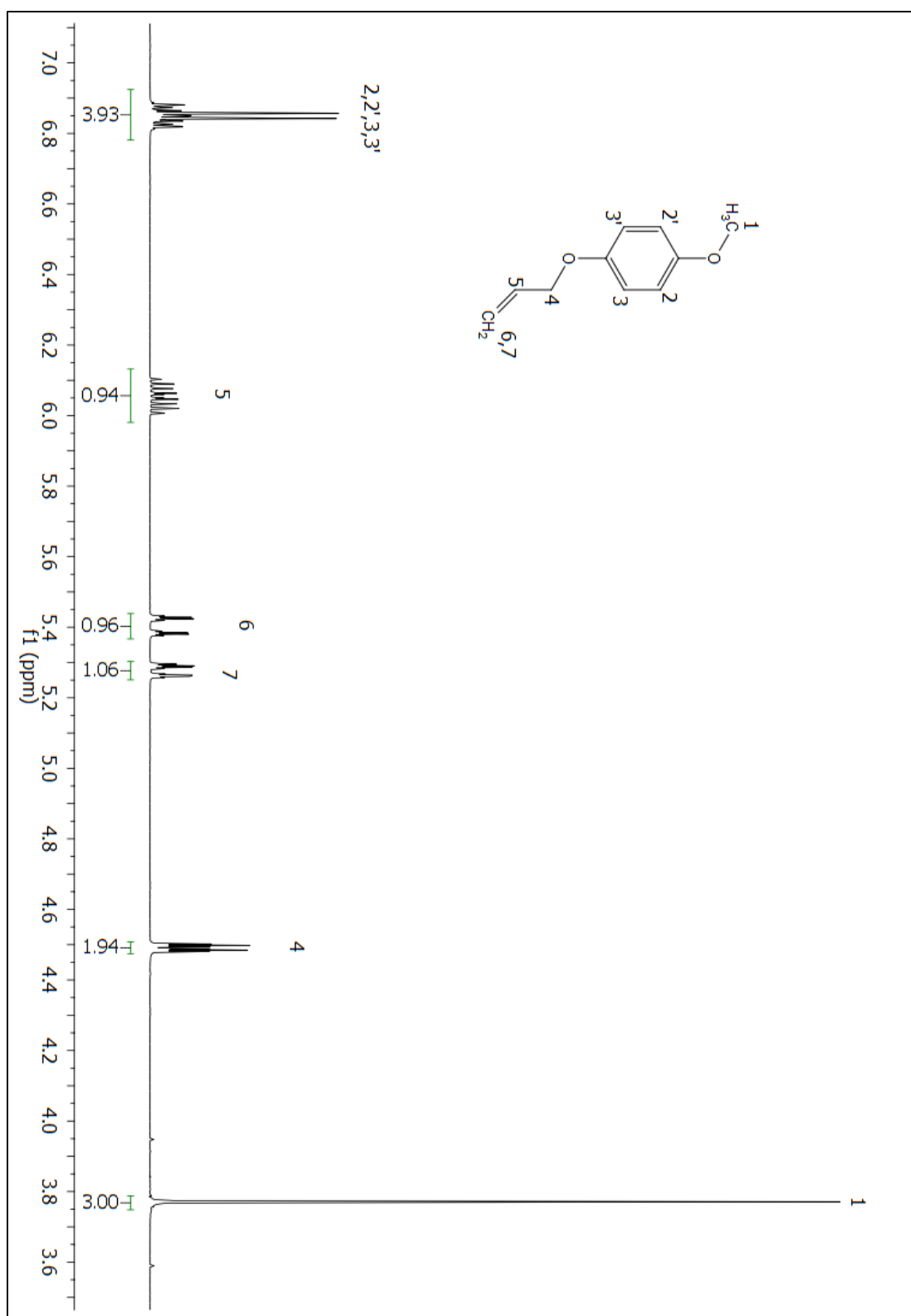
Figure A 8: ¹H NMR (CDCl₃) spectrum of compound 196.
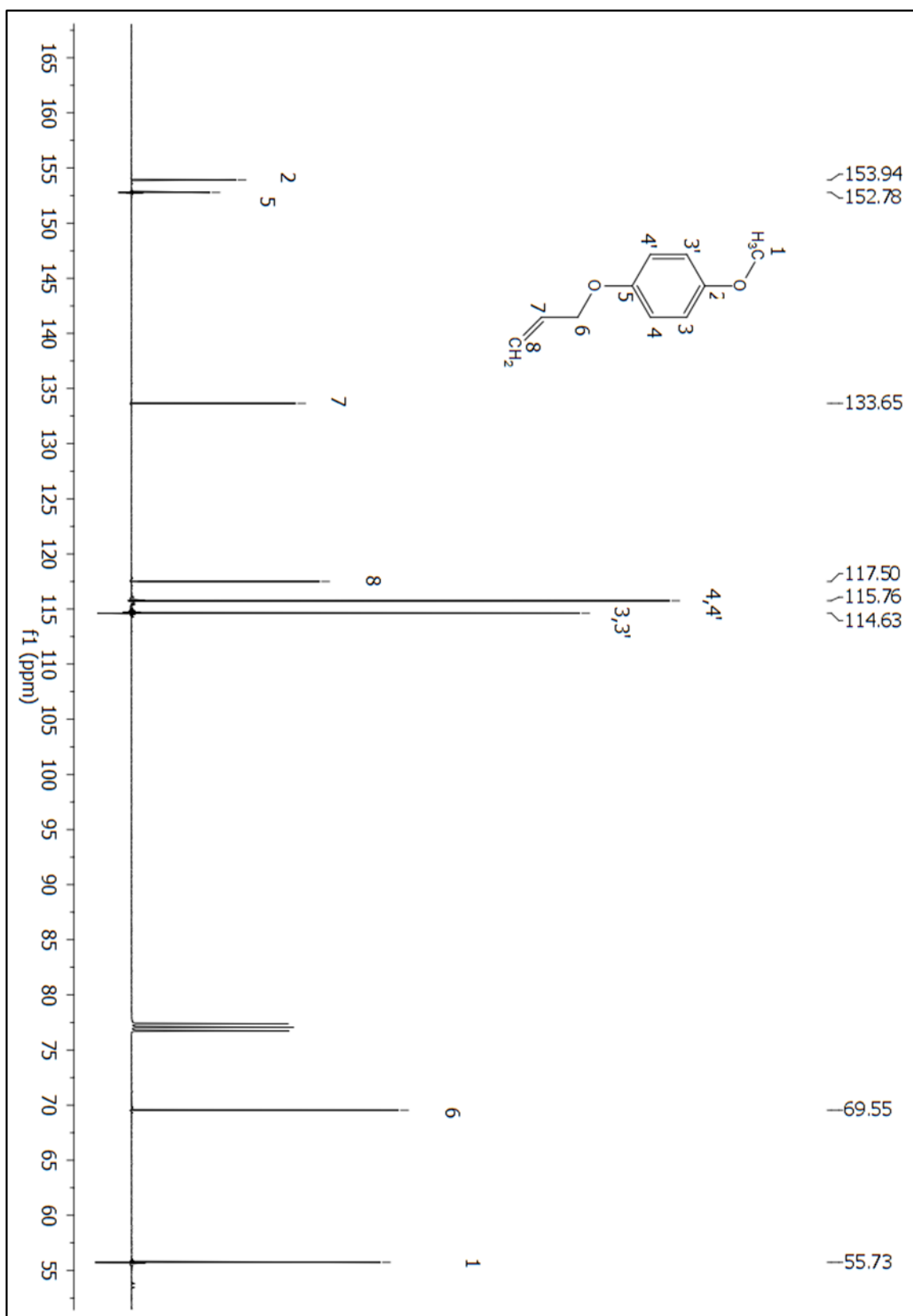
Figure A 9: ^{13}C NMR (CDCl$_3$) spectrum of compound 196.
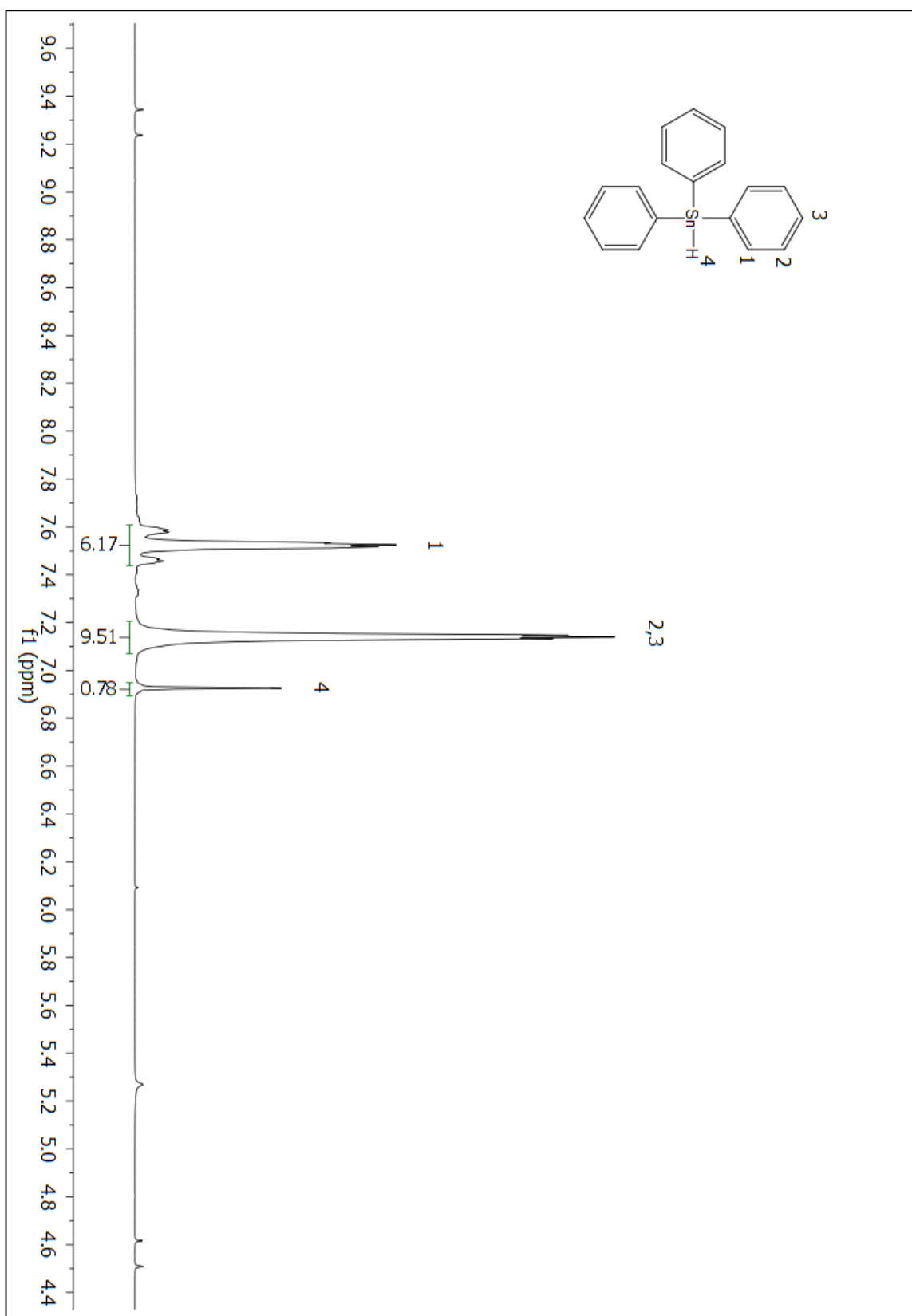
Figure A 10: ¹H NMR (CDCl₃) spectrum of compound 254.
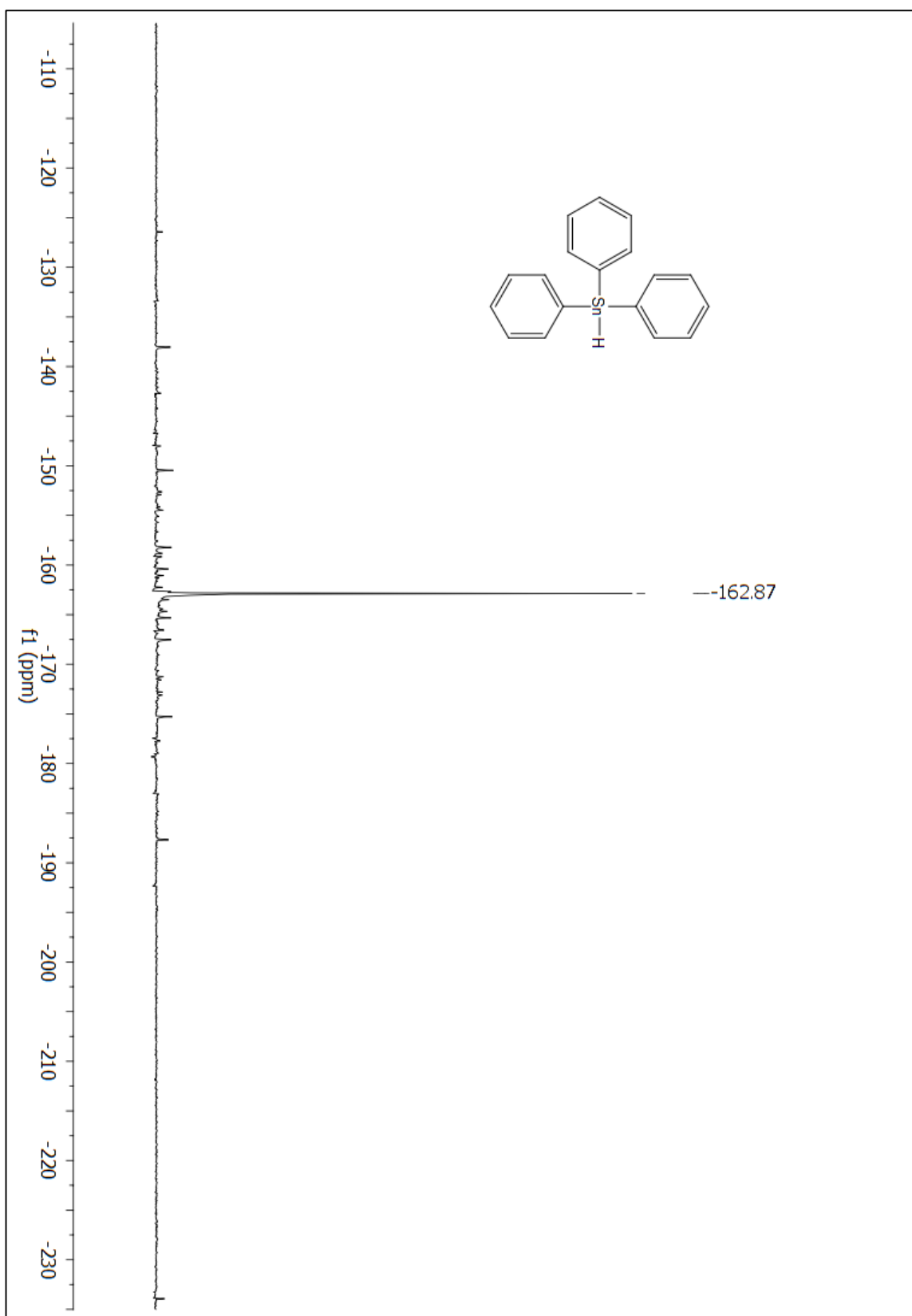
Figure A 11: ^{119}Sn NMR (CDCl$_3$) spectrum of compound 254.
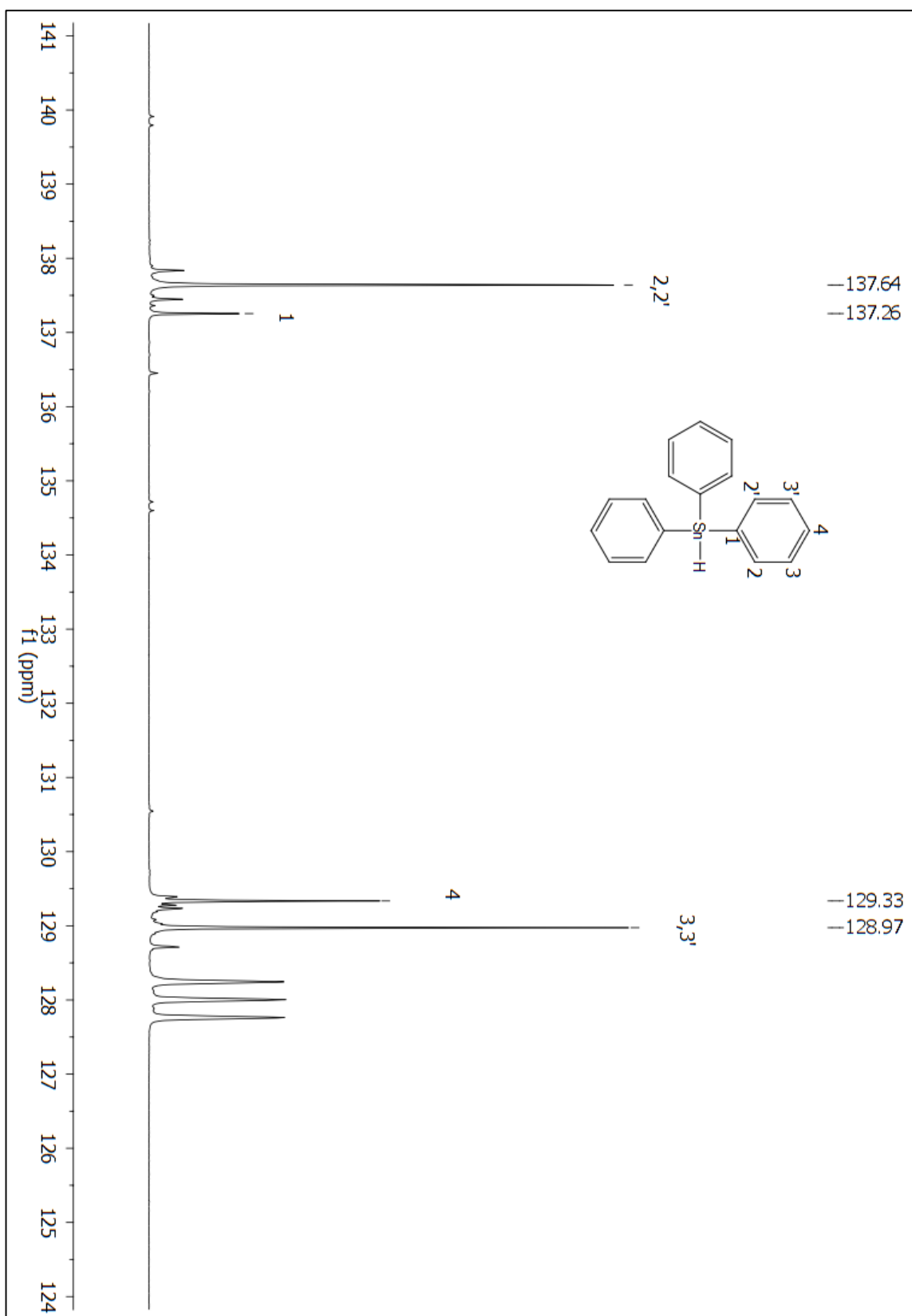
Figure A 12: ^{13}C NMR (C$_6$D$_6$) spectrum of compound 254.
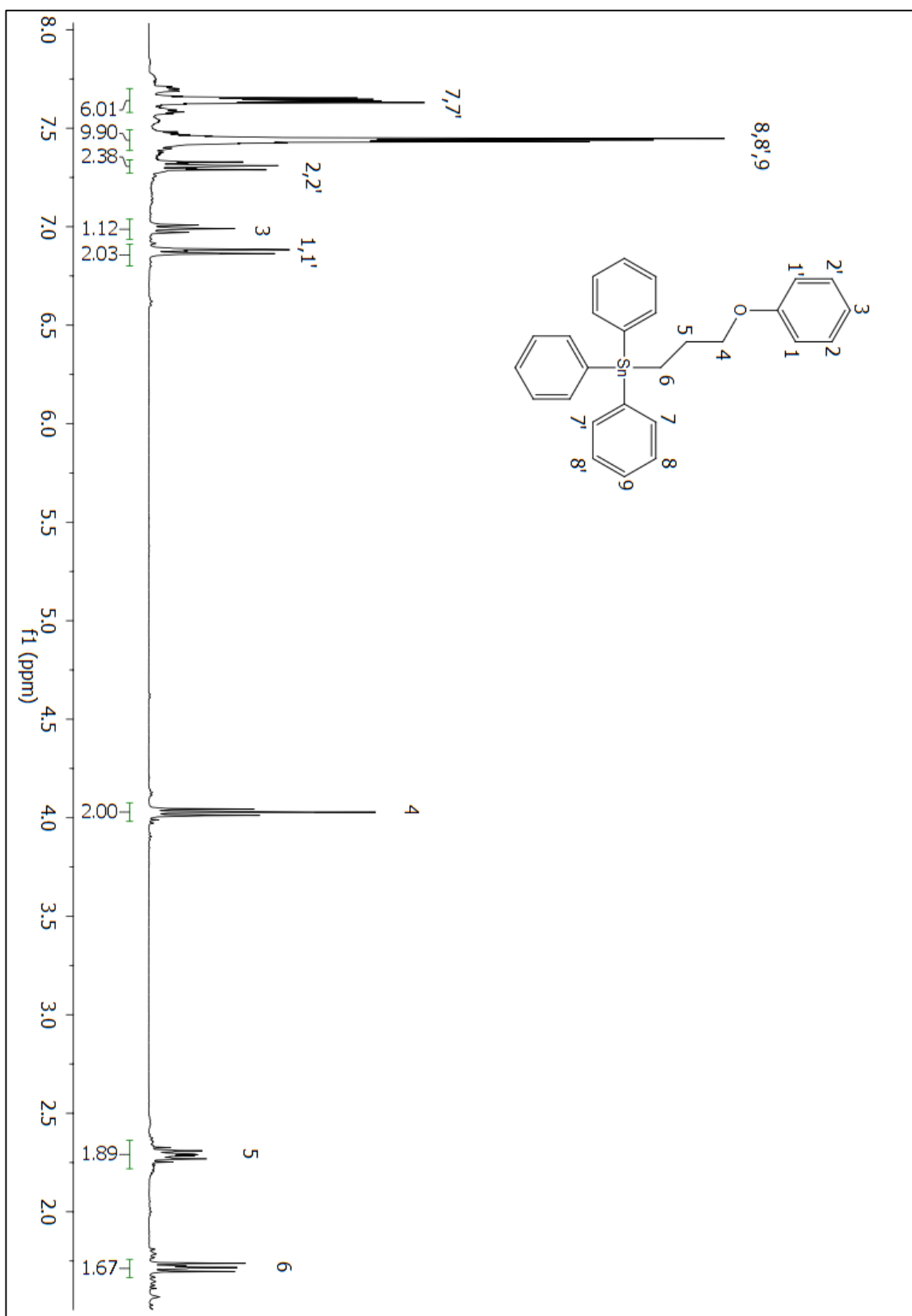
Figure A 13: ^{1}H NMR (C$_6$D$_6$) spectrum of compound 197.
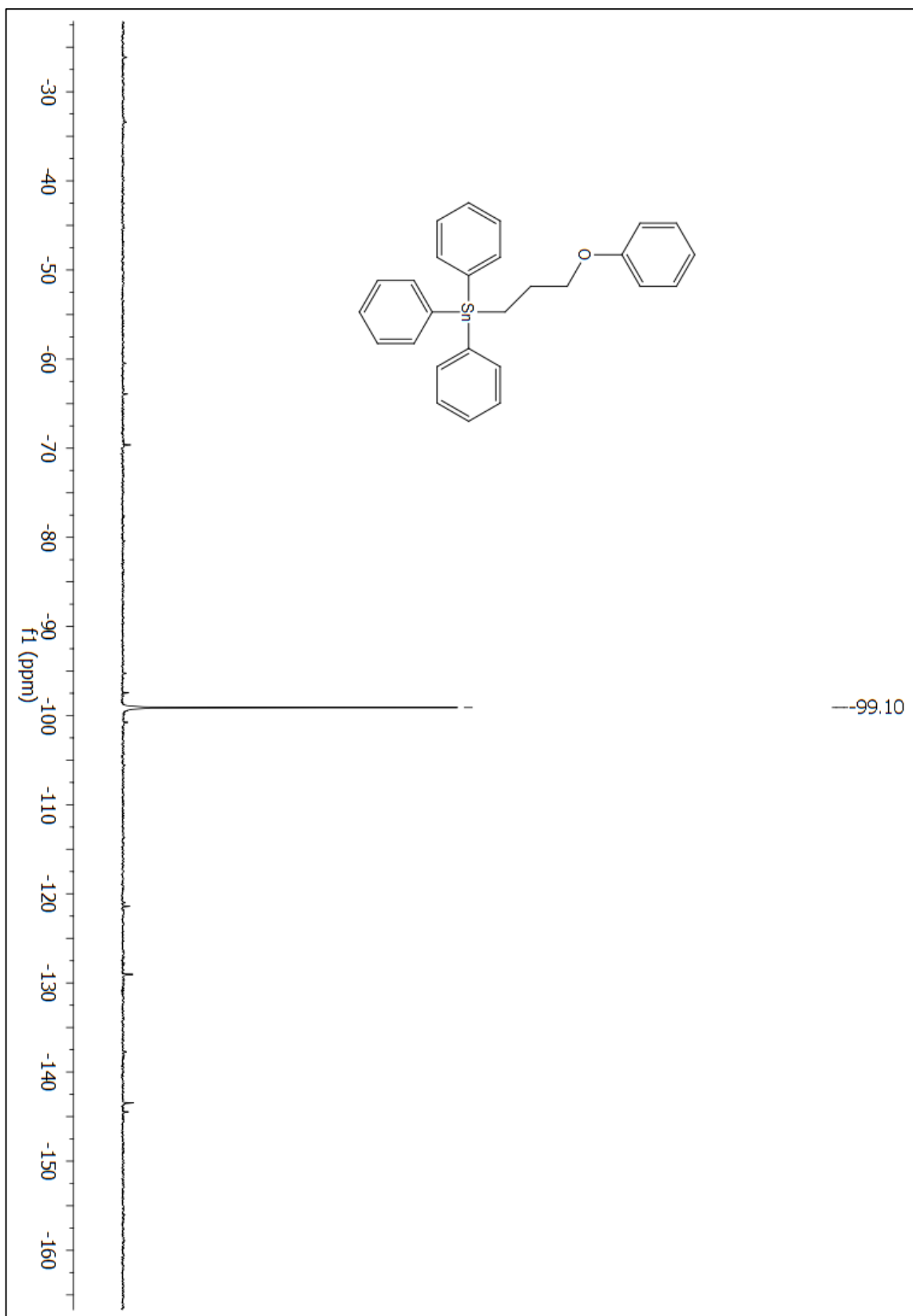
Figure A 14: ^{119}Sn NMR (CDCl$_3$) spectrum of compound 197.
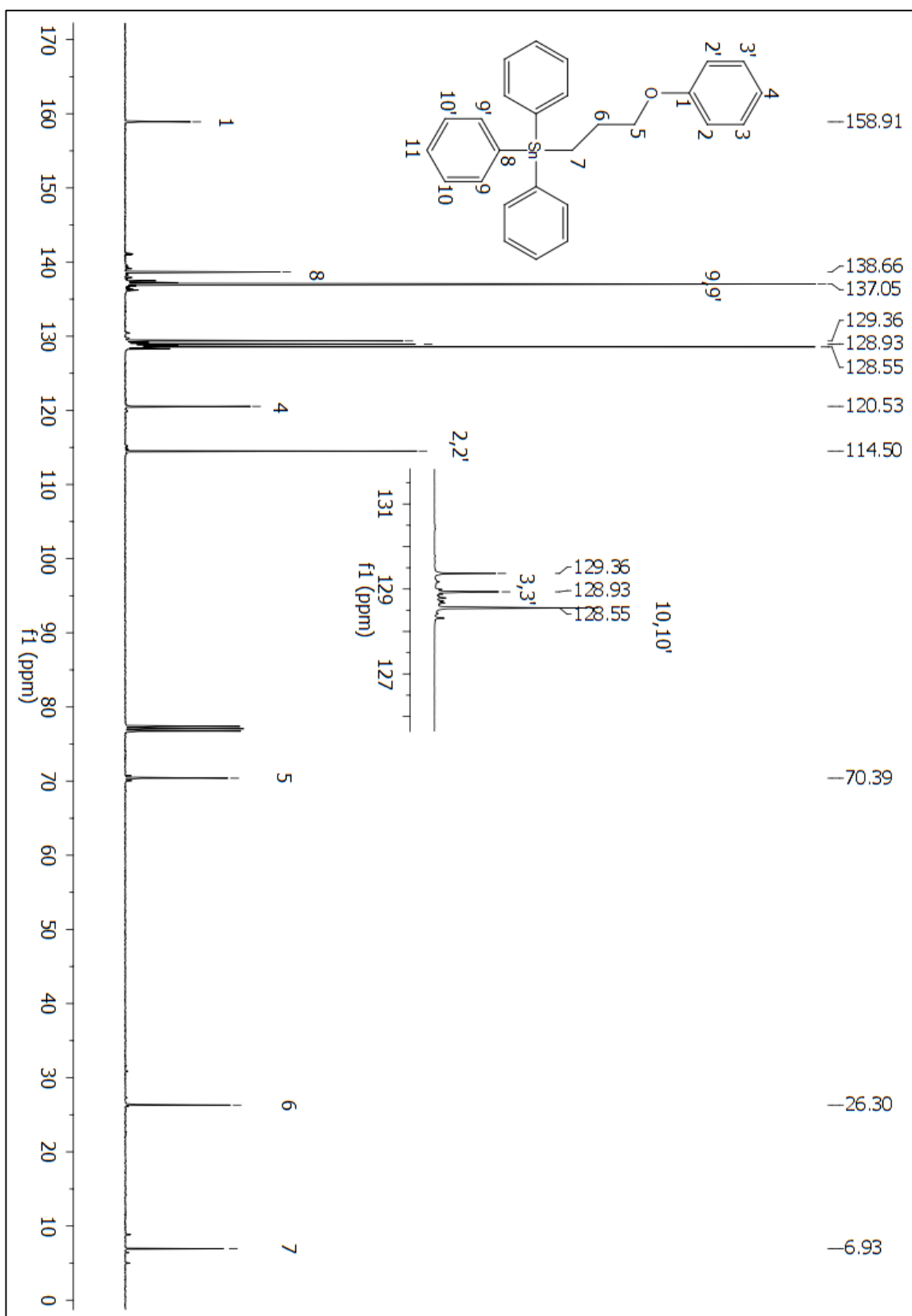
Figure A 15: ^{13}C NMR (CDCl$_3$) spectrum of compound 197.
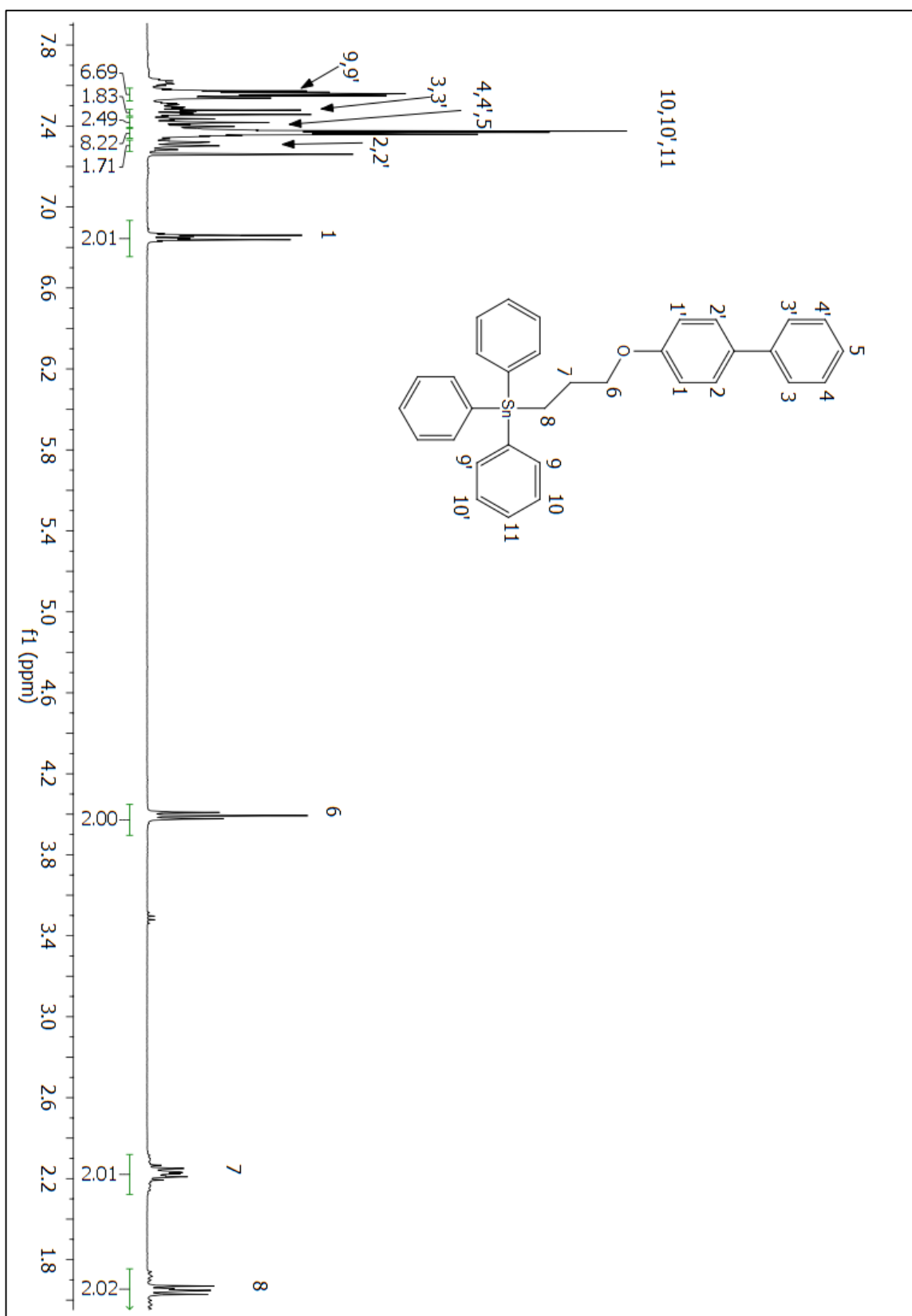
Figure A 16: ¹H NMR (CDCl₃) spectrum of compound 141.
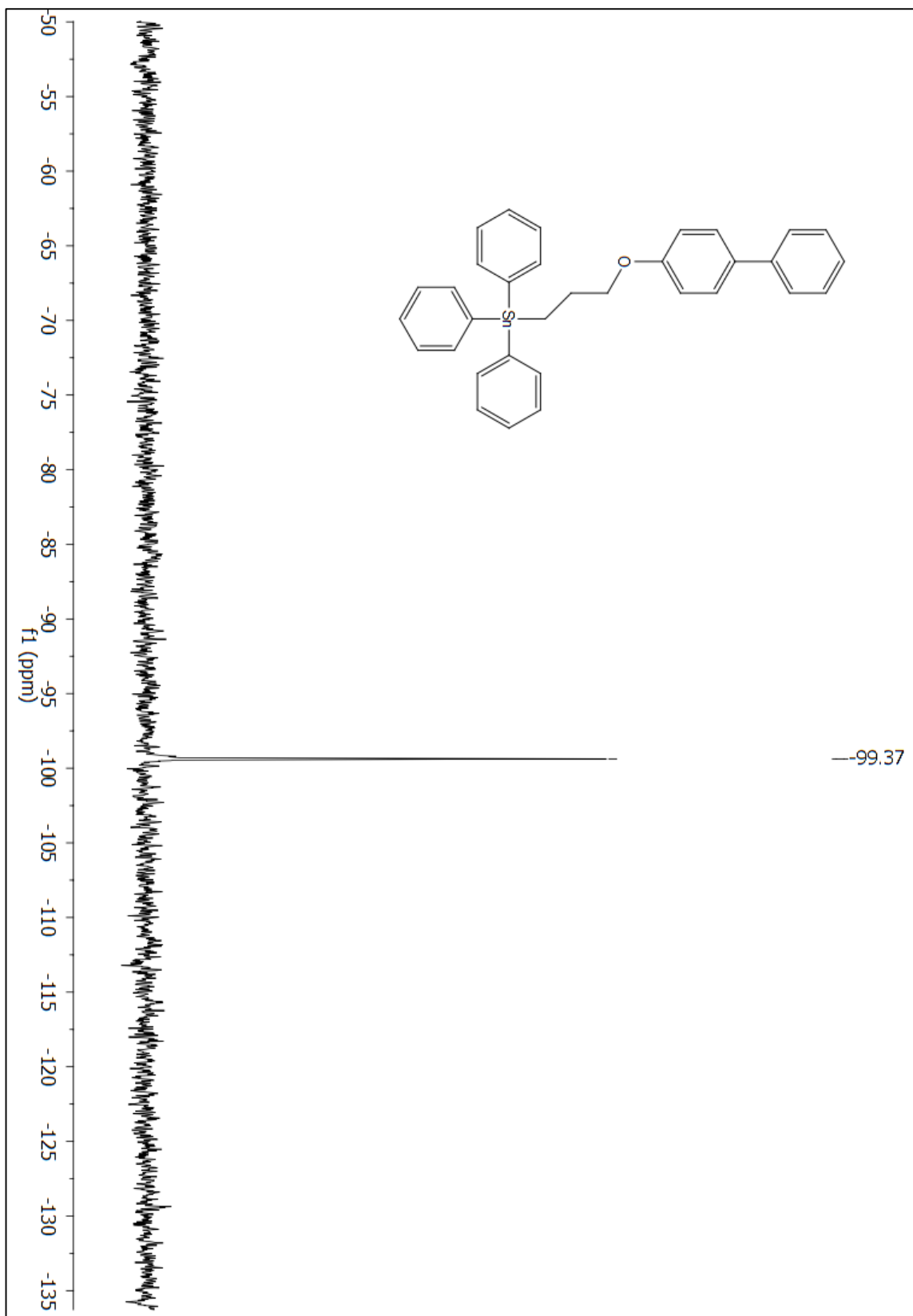
Figure A 17: ^{119}Sn NMR (CDCl$_3$) spectrum of compound 141.
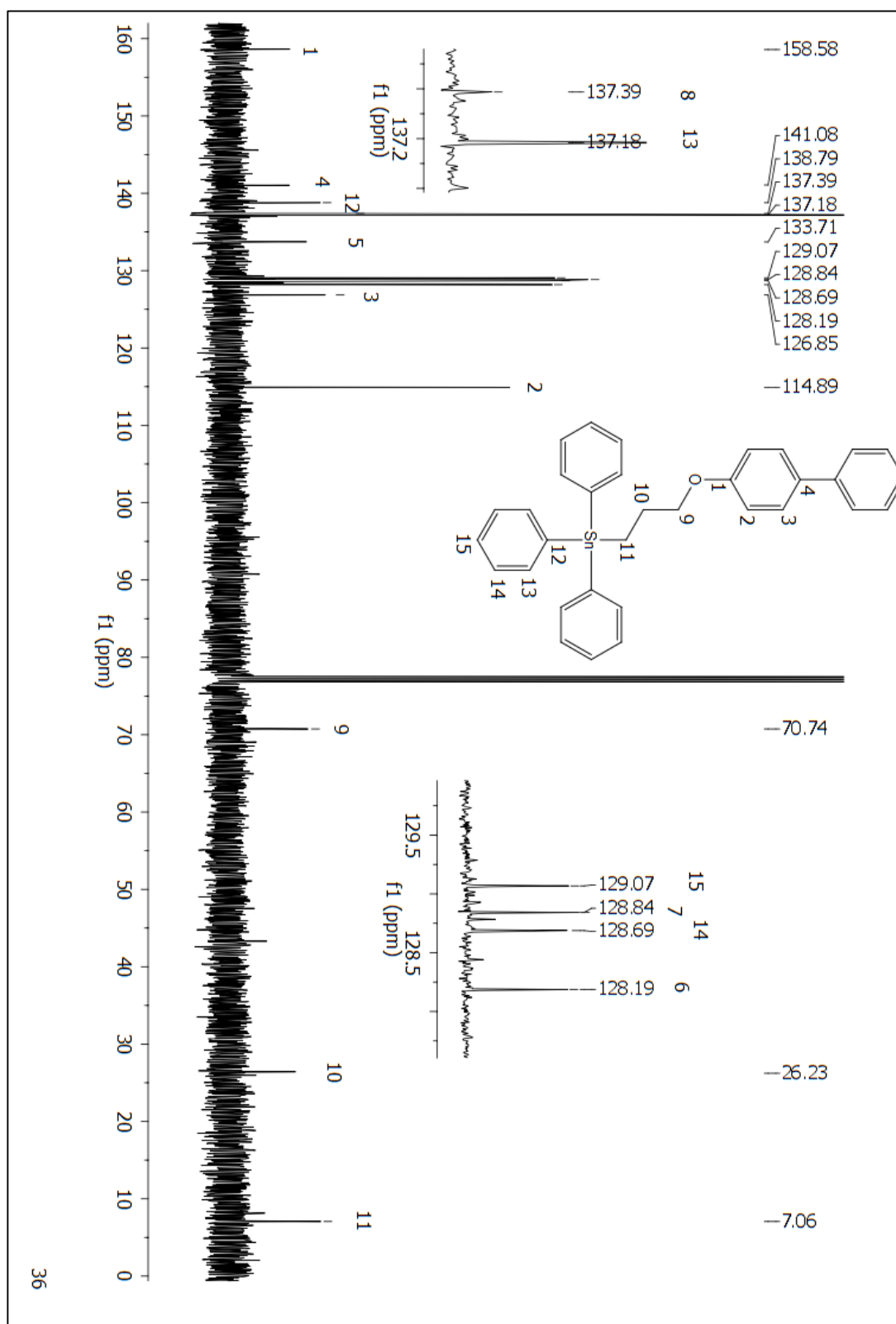
Figure A 18: ^{13}C NMR (CDCl$_3$) spectrum of compound **141**
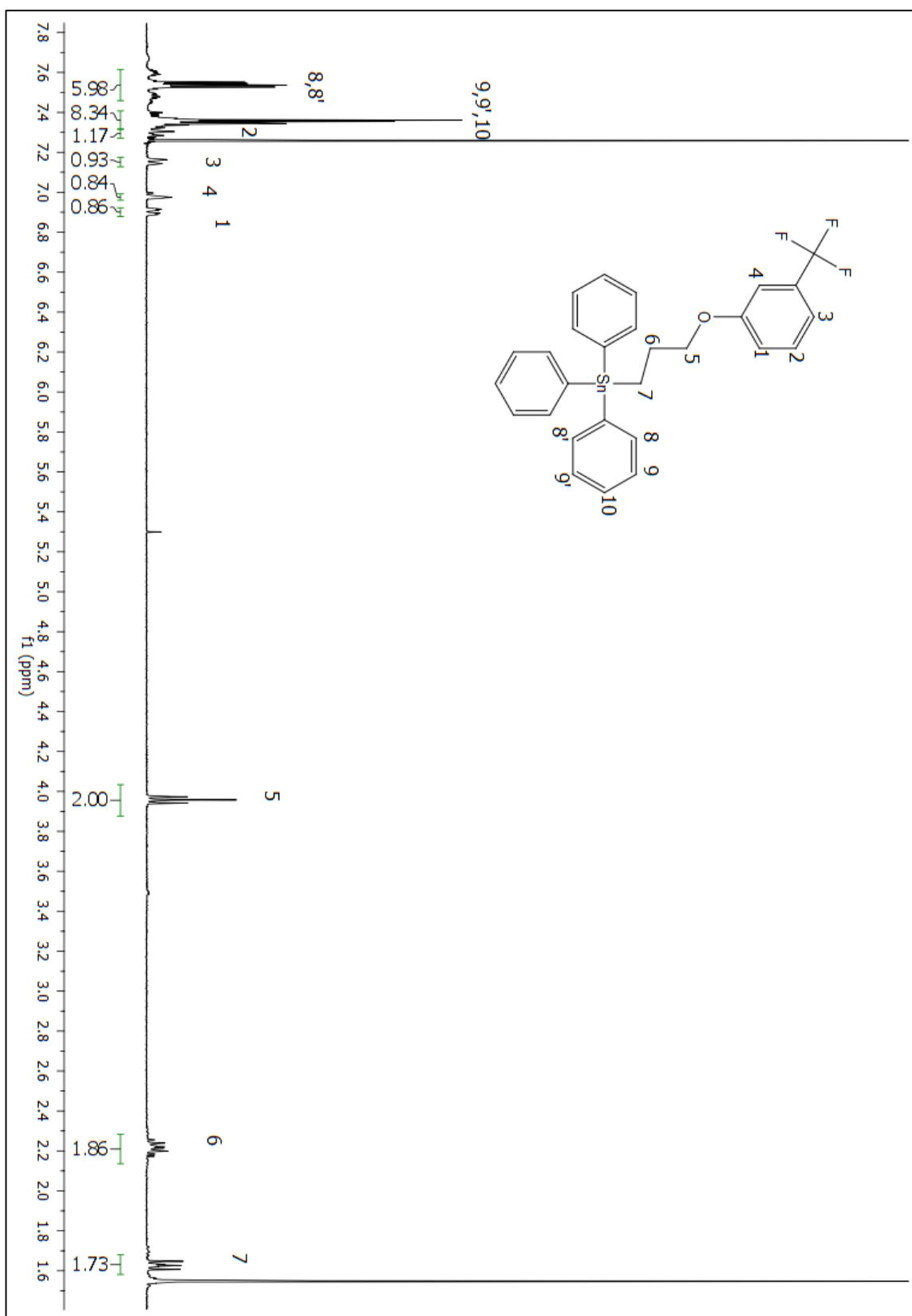
Figure A 19: ¹H NMR (CDCl₃) spectrum of compound 198.
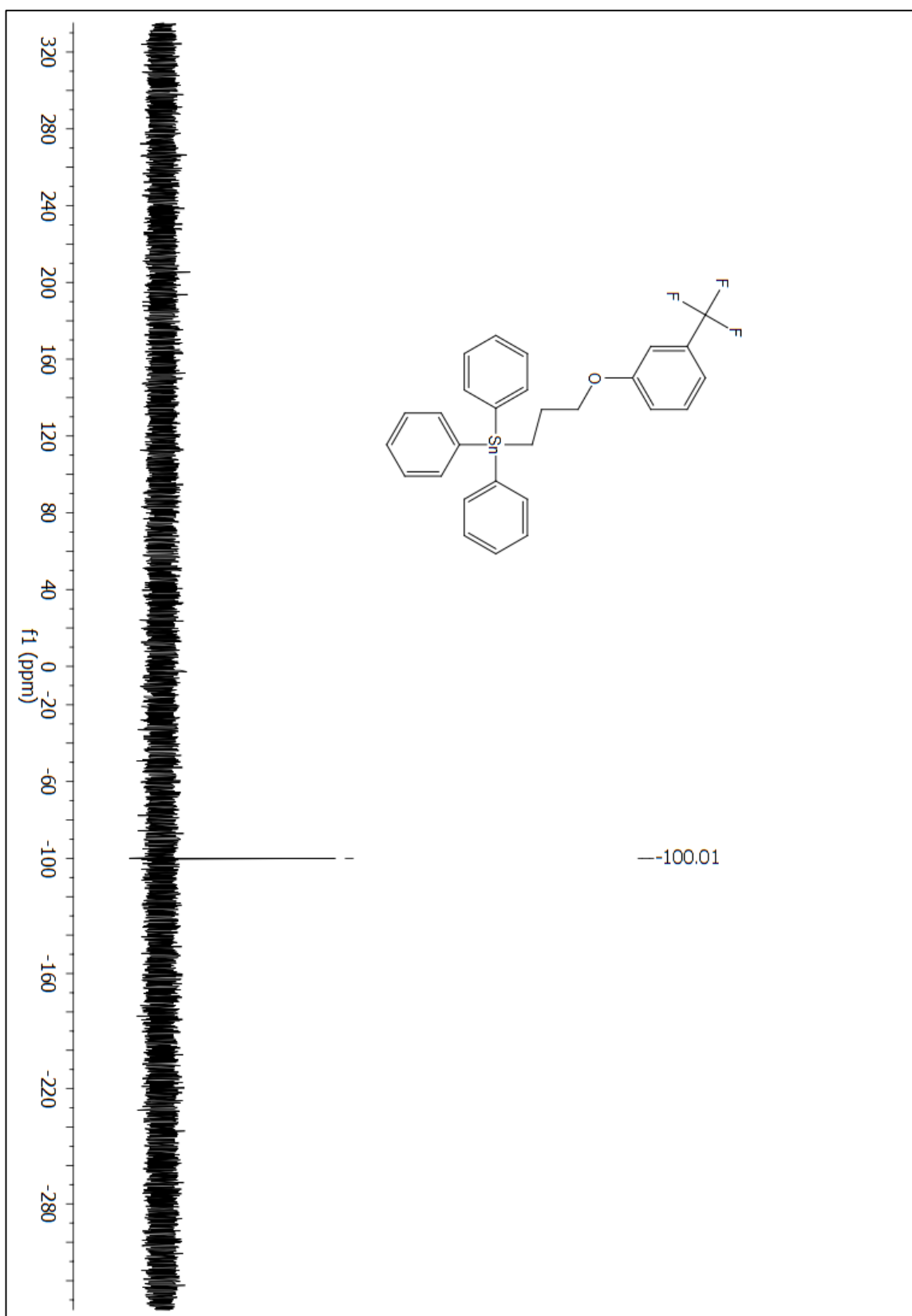
Figure A 20: ^{119}Sn NMR (CDCl$_3$) spectrum of compound 198.
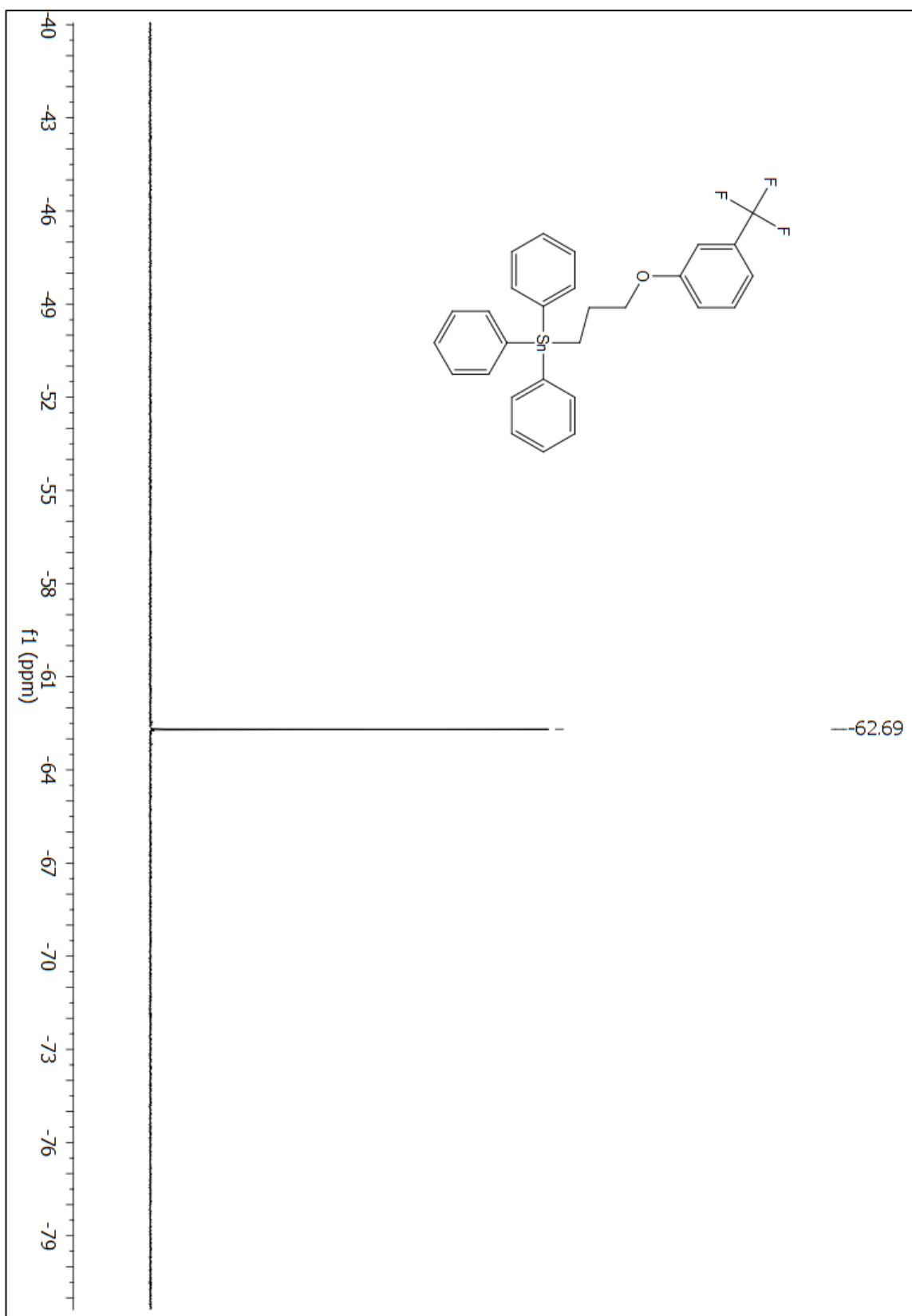
Figure A 21: ¹⁹F NMR (CDCl₃) spectrum of compound 198.
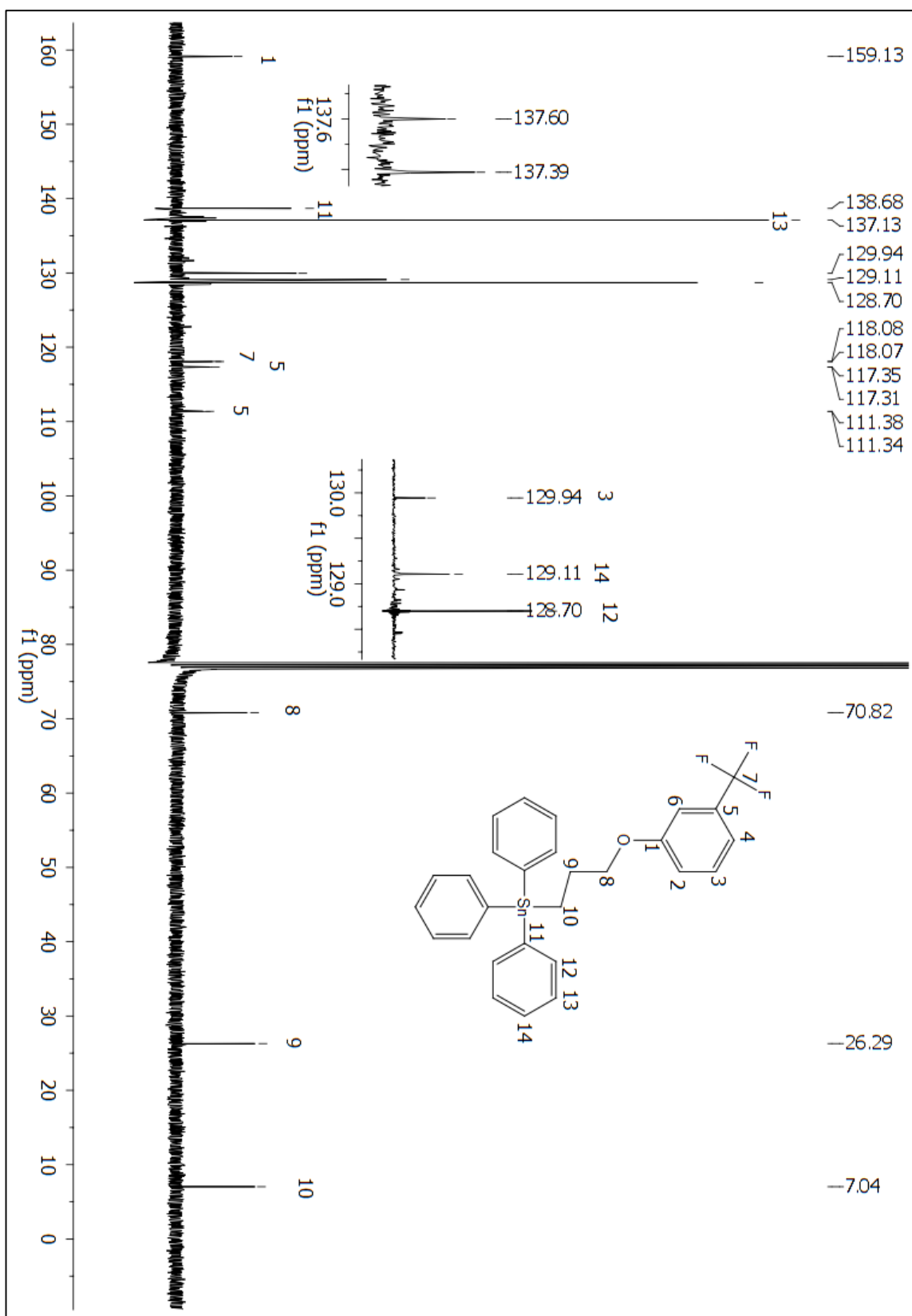
Figure A 22: ^{13}C NMR (CDCl$_3$) spectrum of compound 198
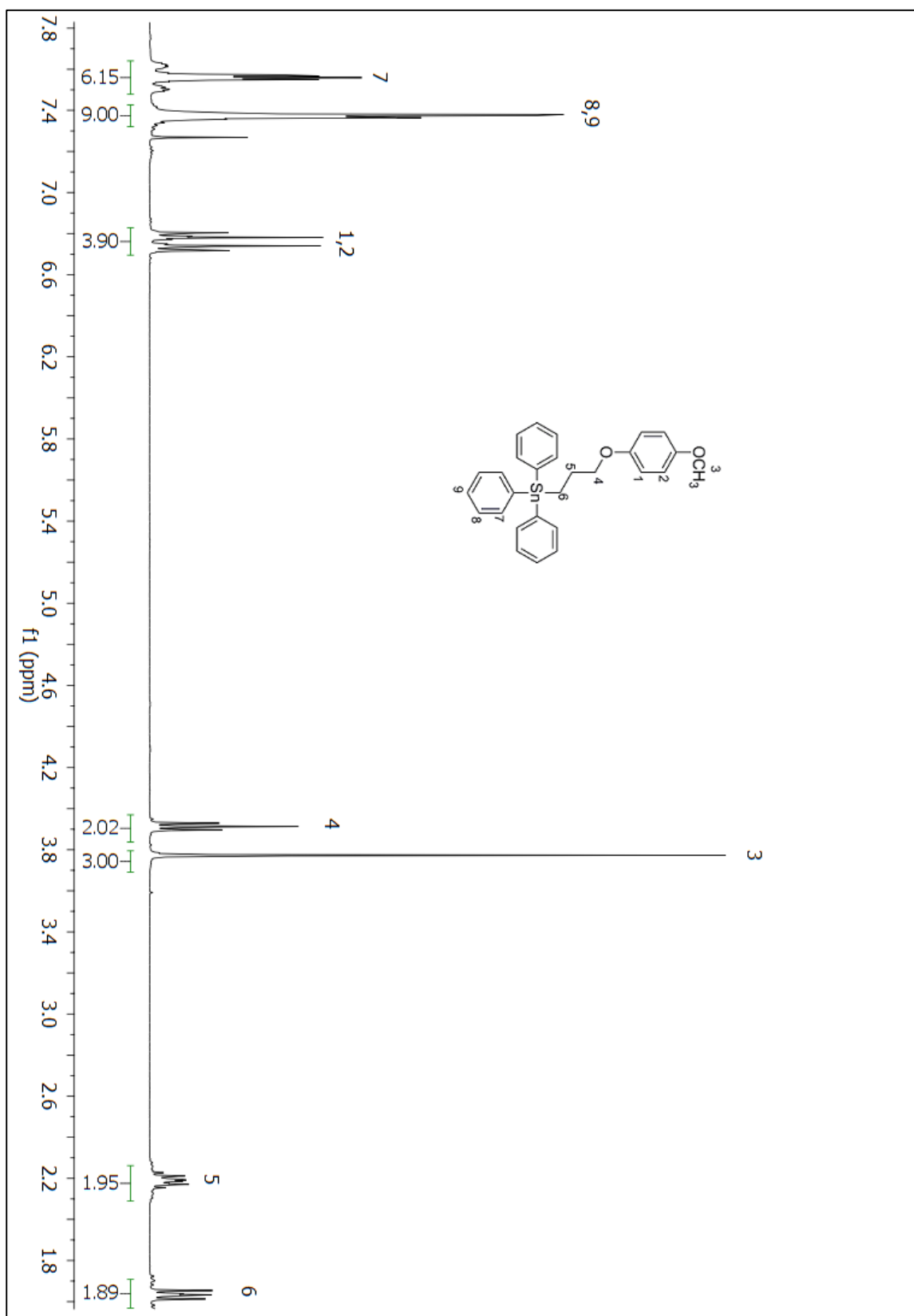
Figure A 23: ¹H NMR (CDCl₃) spectrum of compound 199.
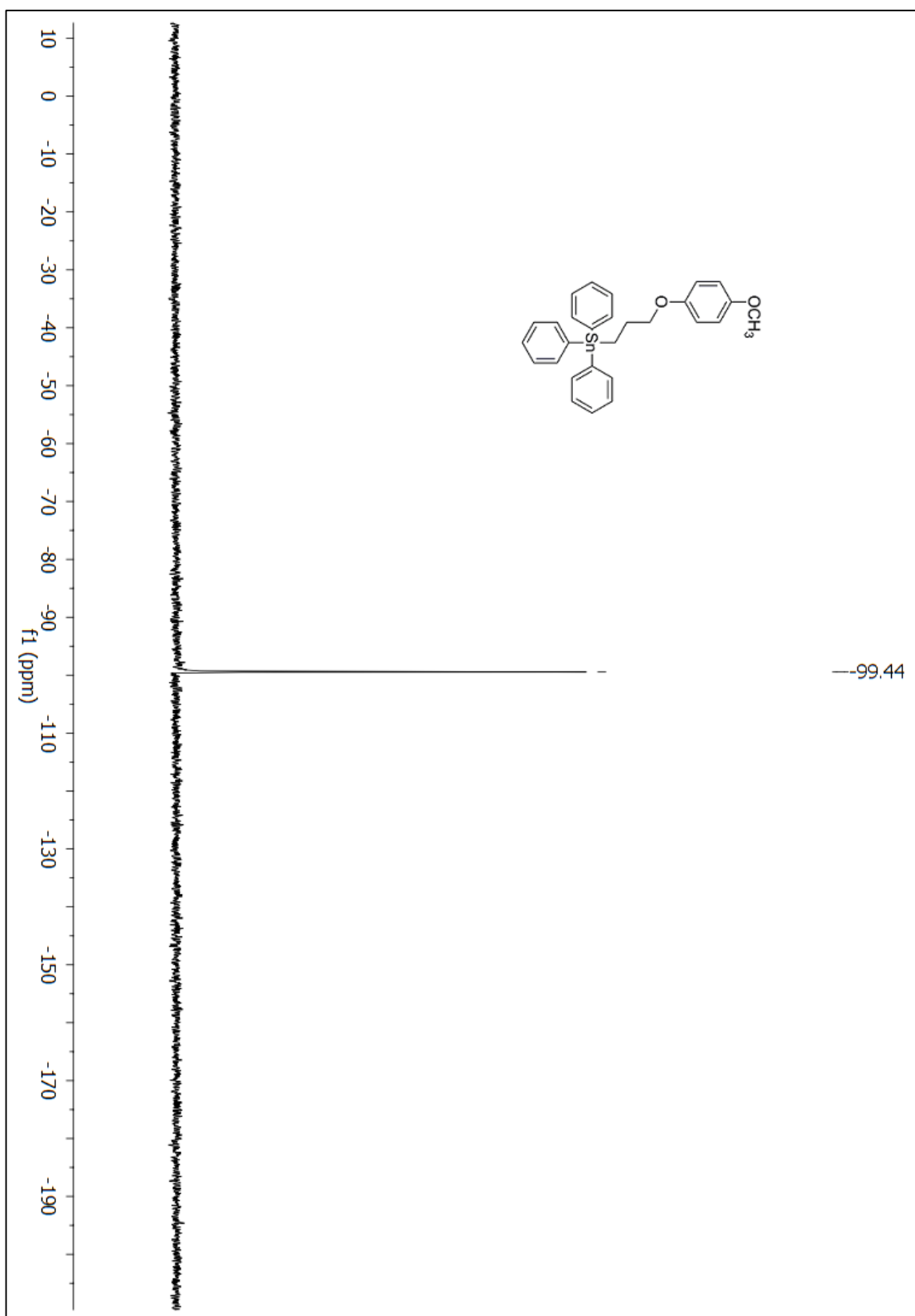
Figure A 24: ^{119}Sn NMR (CDCl$_3$) spectrum of compound 199.
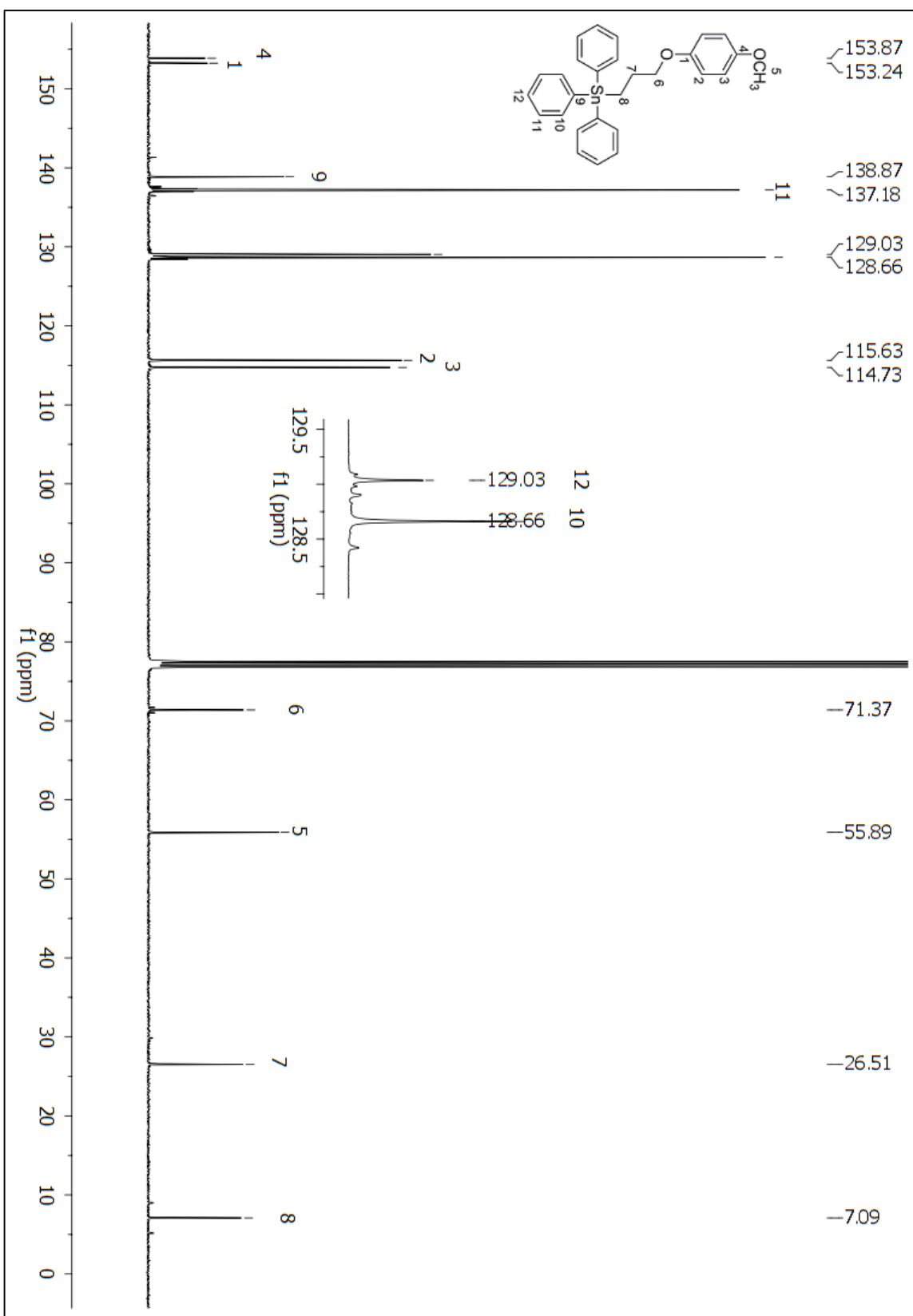
Figure A 25: ^{13}C NMR (CDCl$_3$) spectrum of compound 199.
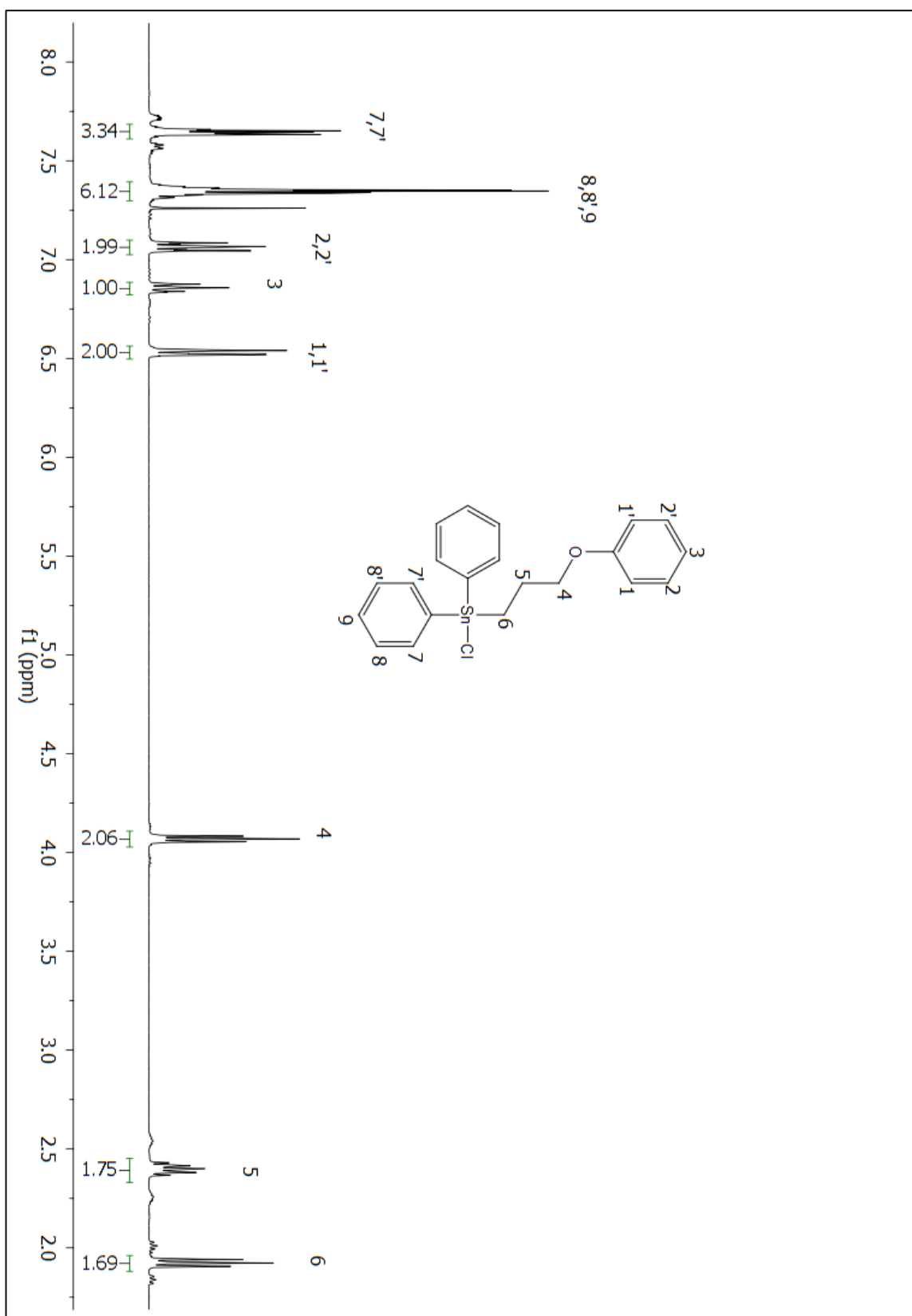
Figure A 26: ^{1}H NMR (CDCl$_3$) spectrum of compound 200.
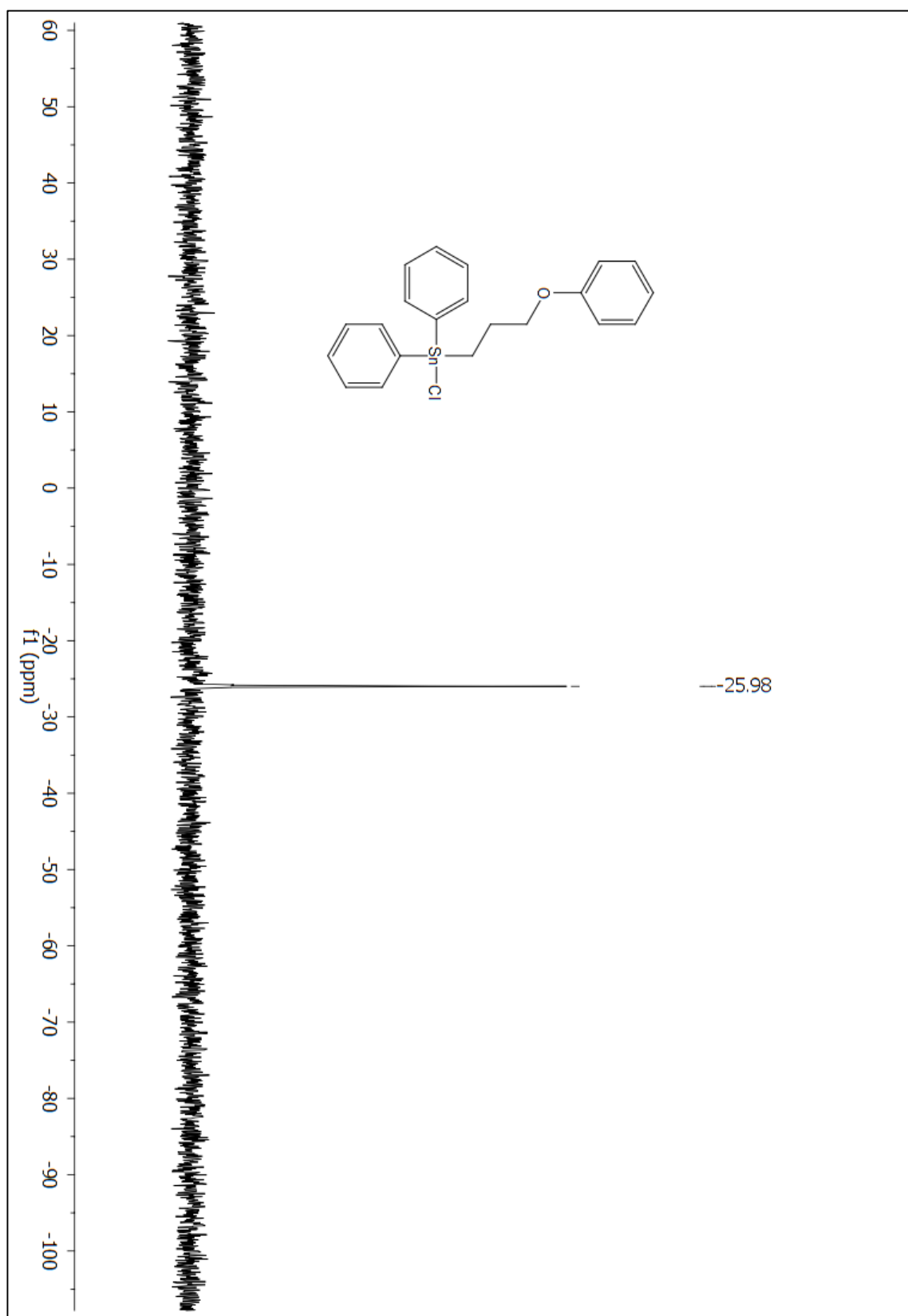
Figure A 27: ^{119}Sn NMR (CDCl$_3$) spectrum of compound 200.
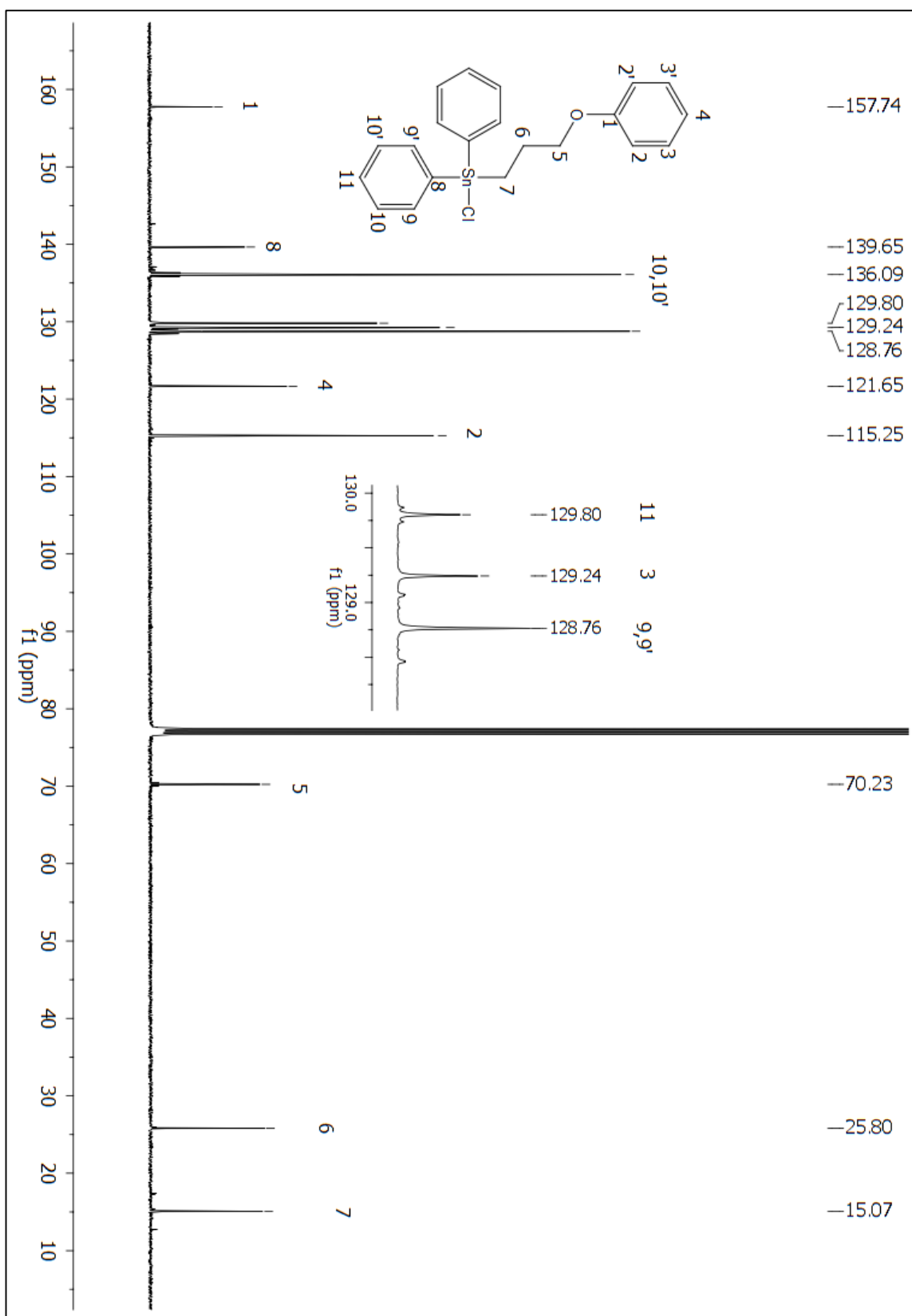
Figure A 28: ^{13}C NMR (CDCl$_3$) spectrum of compound 200.
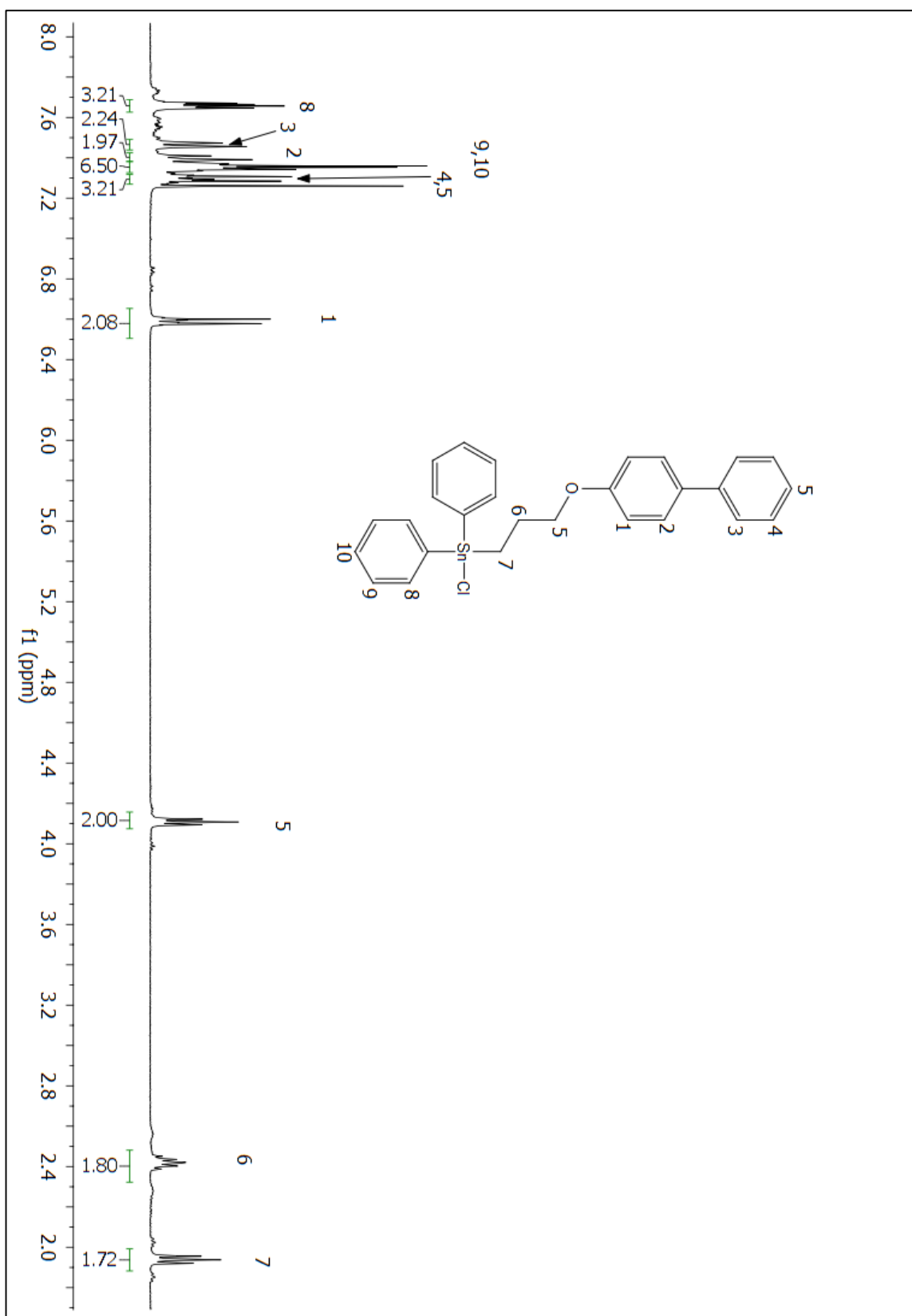
Figure A 29: ^{1}H NMR (CDCl$_3$) spectrum of compound 201.
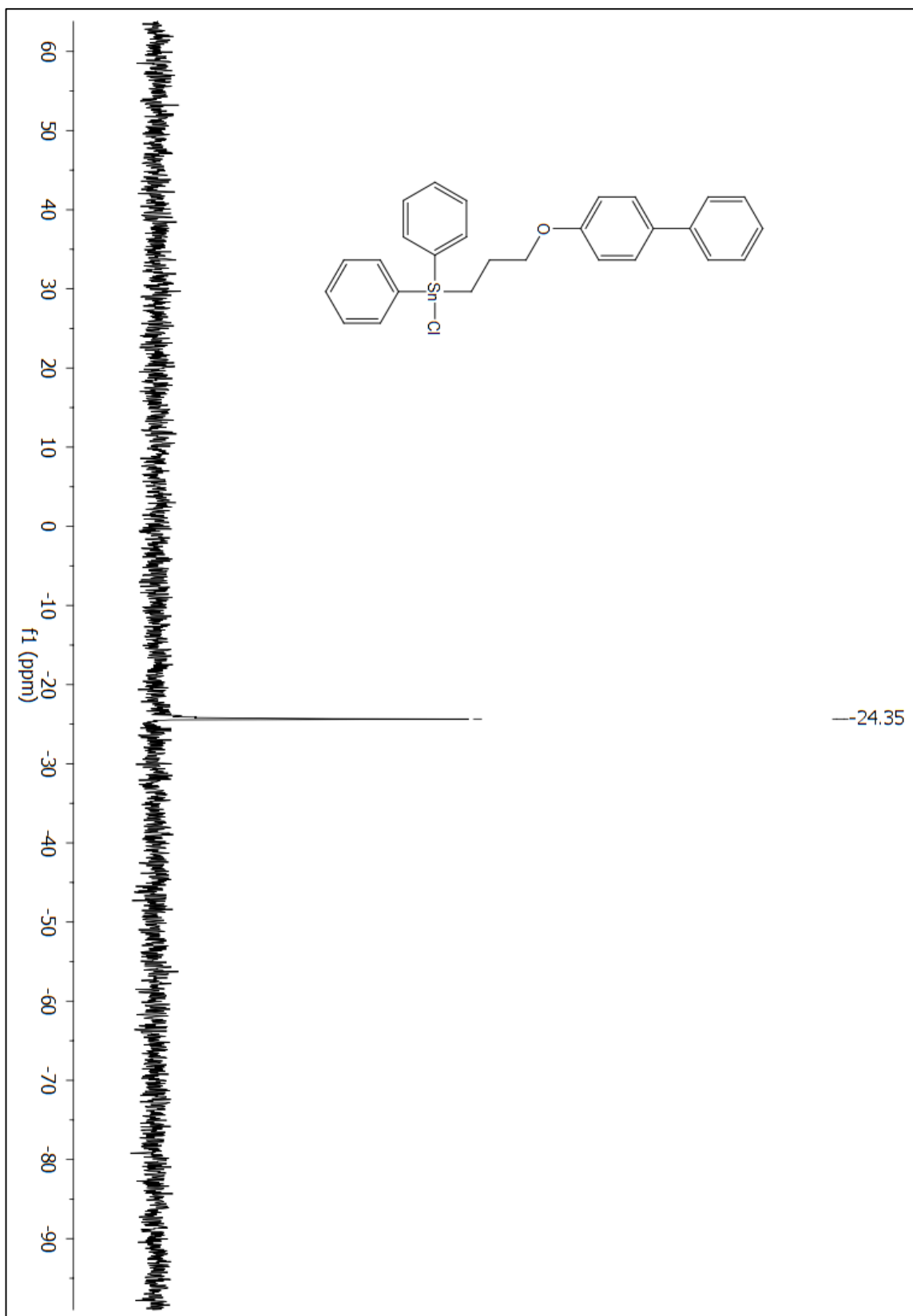
Figure A 30: ^{119}Sn NMR (CDCl$_3$) spectrum of compound 201.
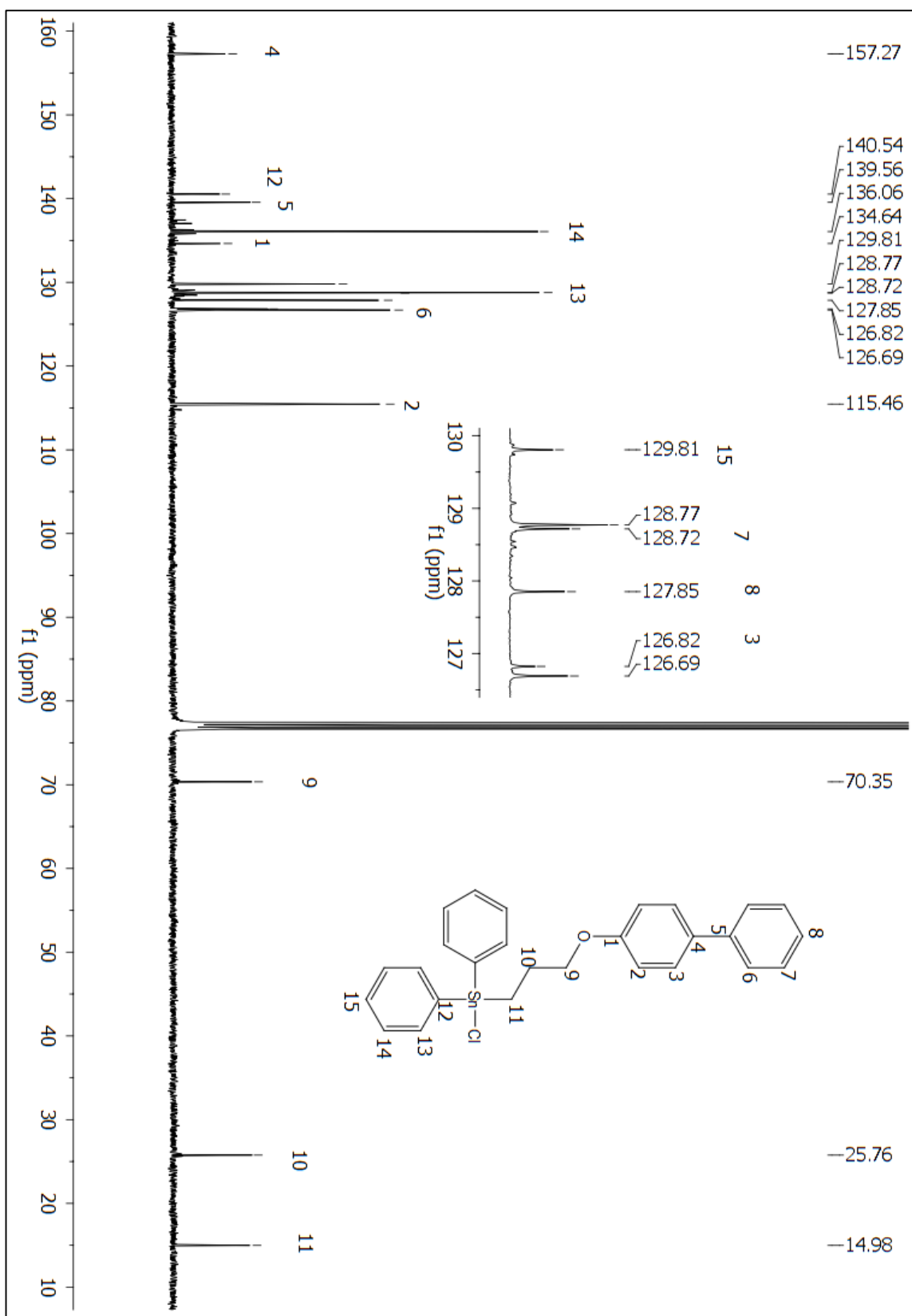
Figure A 31: ^{13}C NMR (CDCl$_3$) spectrum of compound 201.
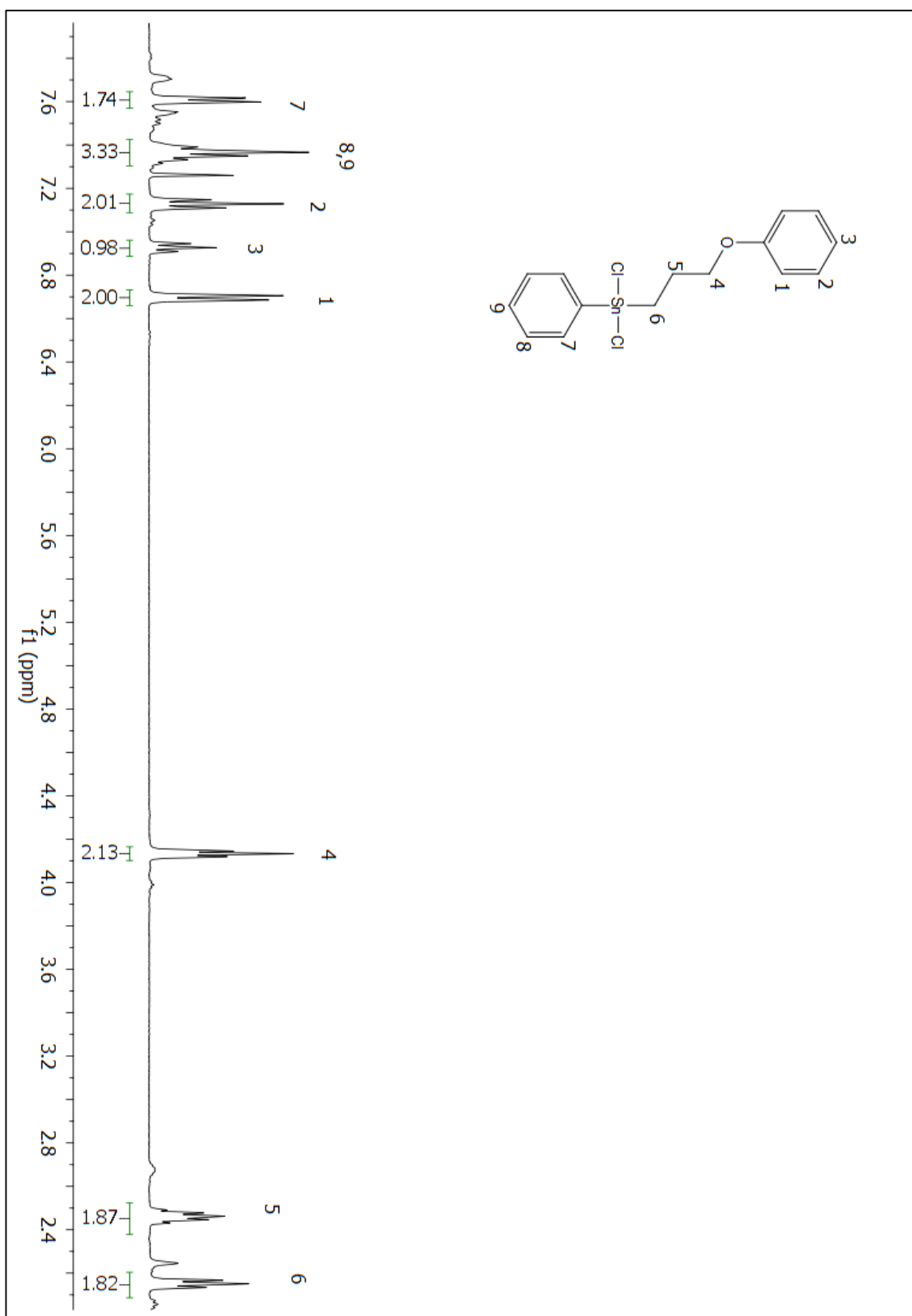
Figure A 32: ¹H NMR (CDCl₃) spectrum of compound 202.
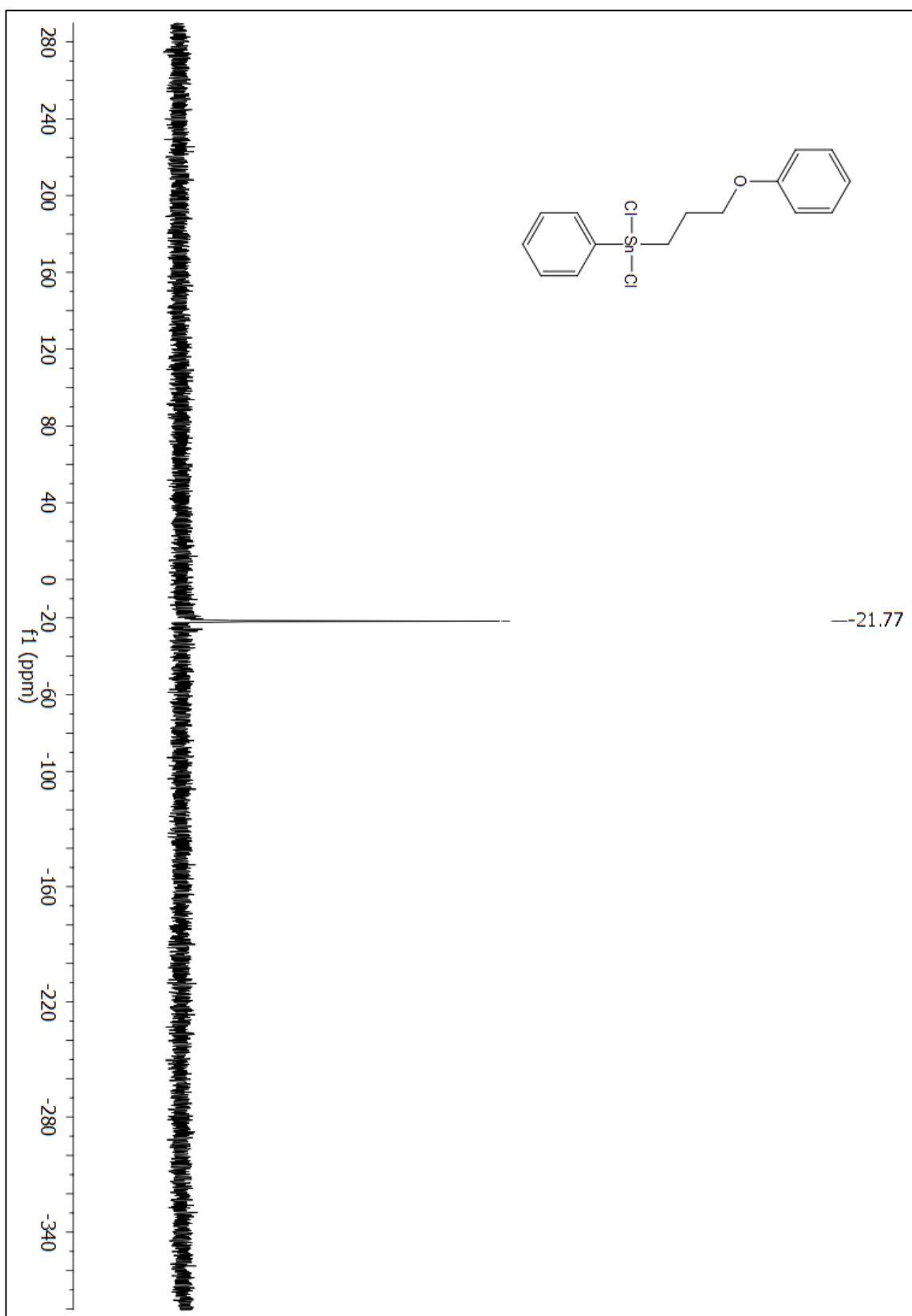
Figure A 33: ^{119}Sn NMR (CDCl$_3$) spectrum of compound **202**.
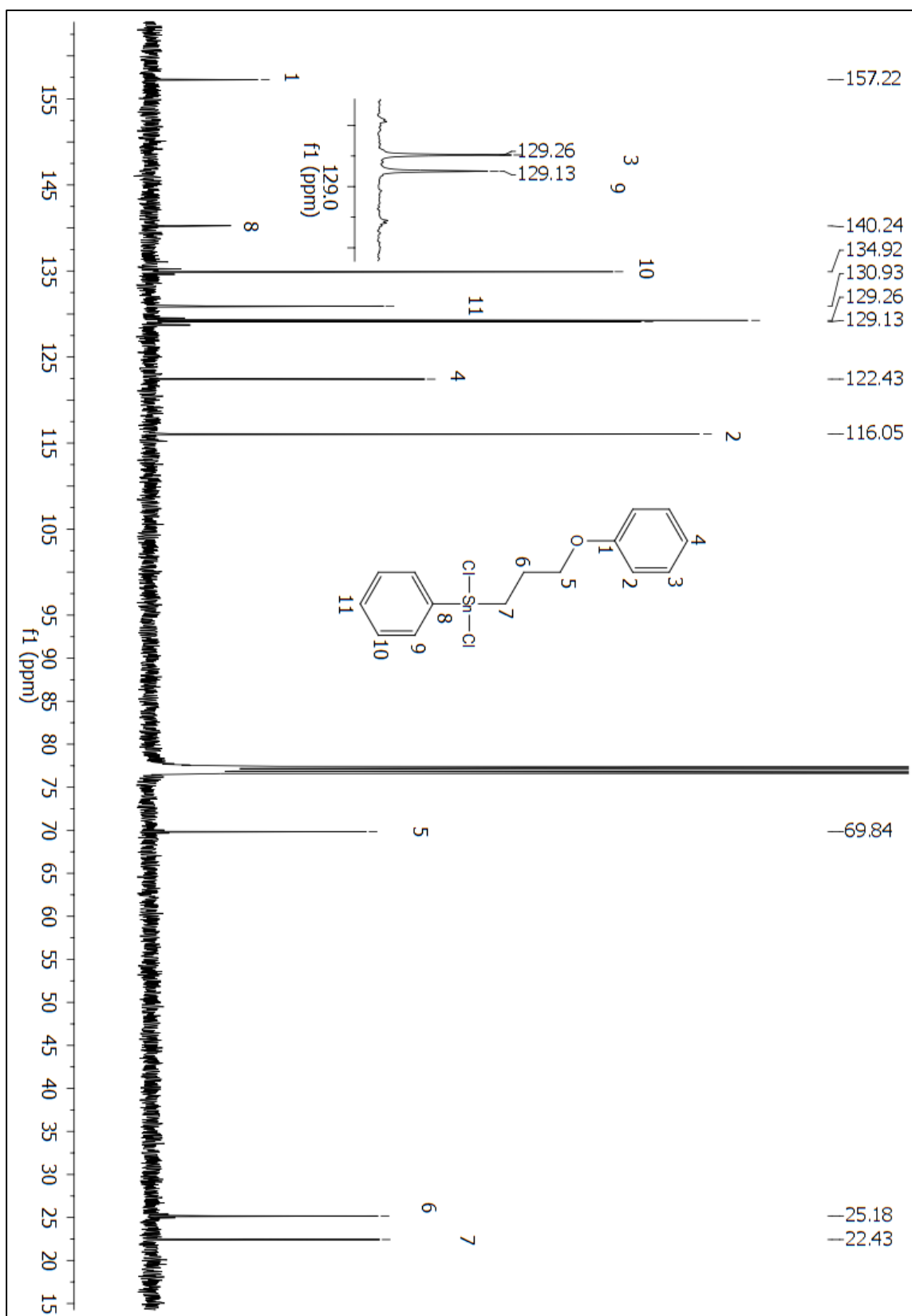
Figure A 34: ^{13}C NMR (CDCl$_3$) spectrum of compound 202.
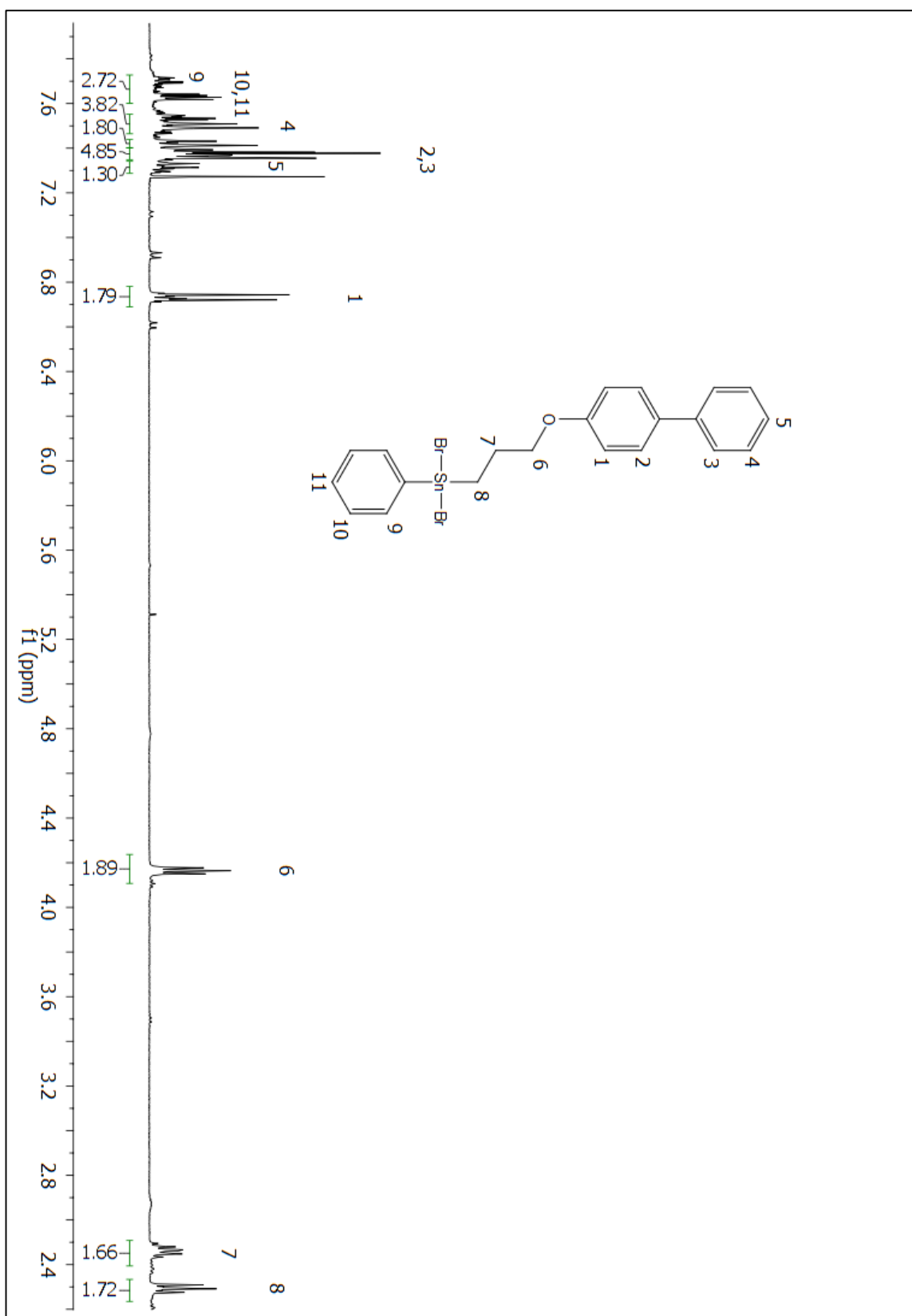
Figure A 35: ¹H NMR (CDCl₃) spectrum of compound 146.
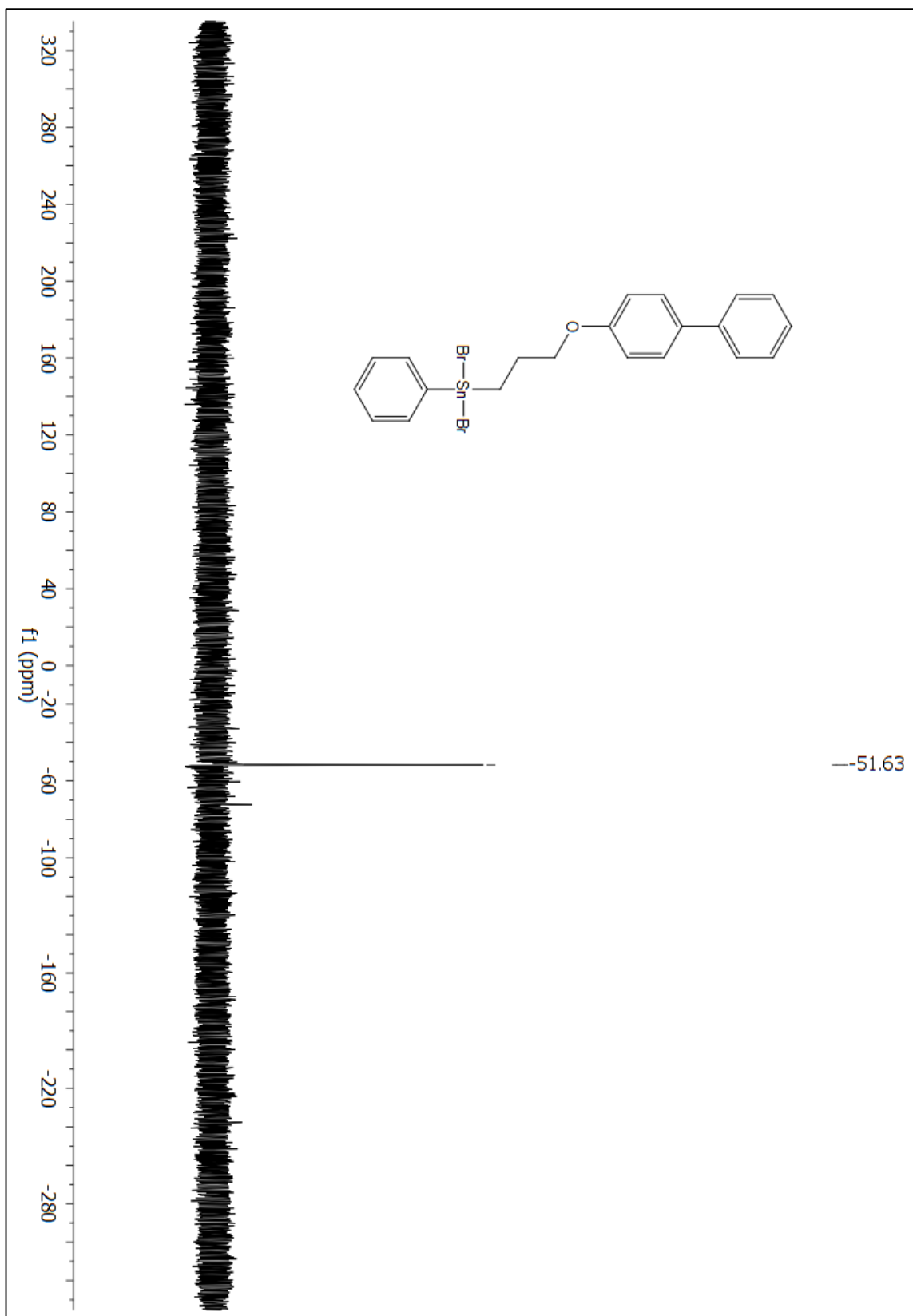
Figure A 36: ^{119}Sn NMR (CDCl$_3$) spectrum of compound 146.
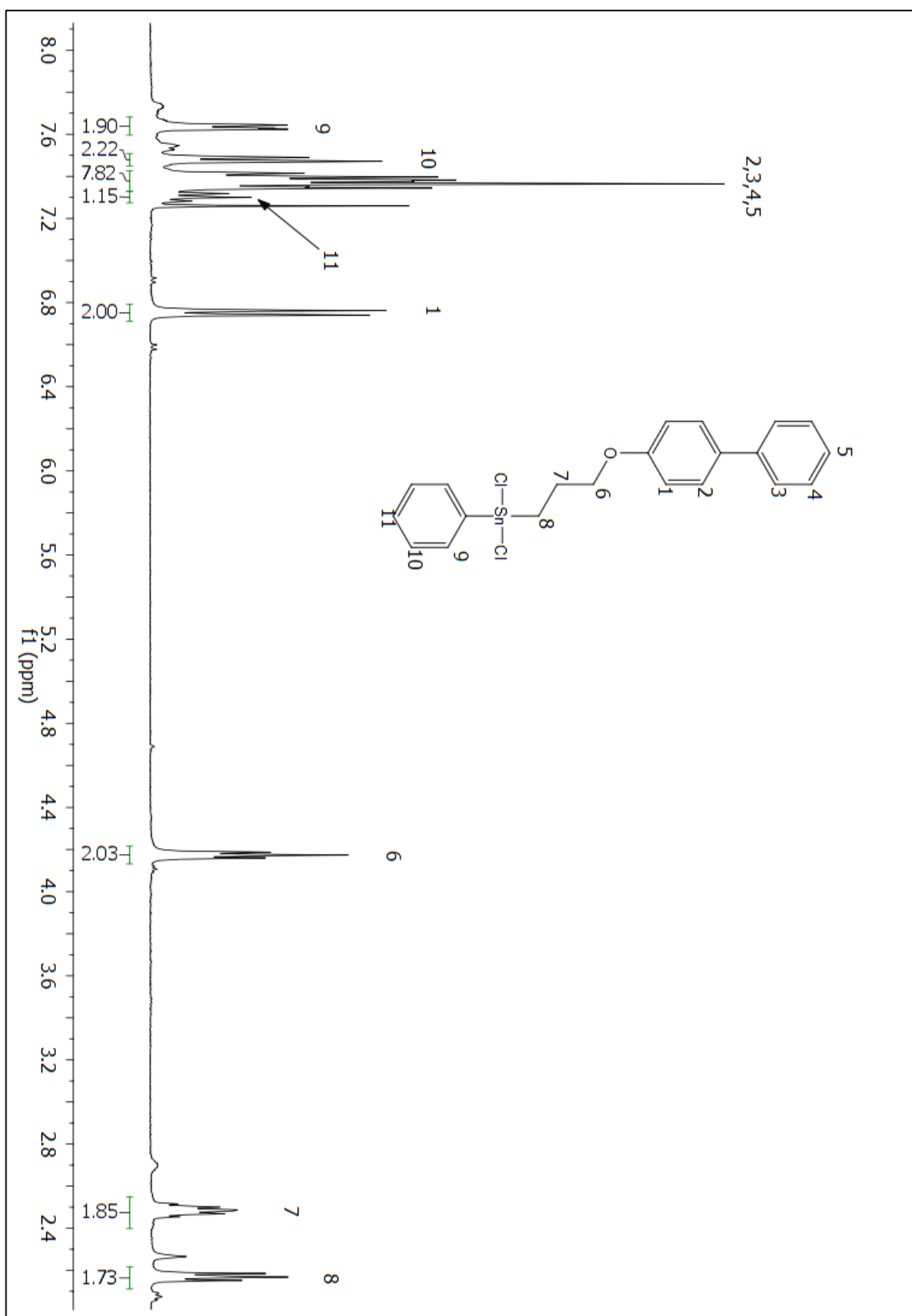
Figure A 37: ¹H NMR (CDCl₃) spectrum of compound 203.
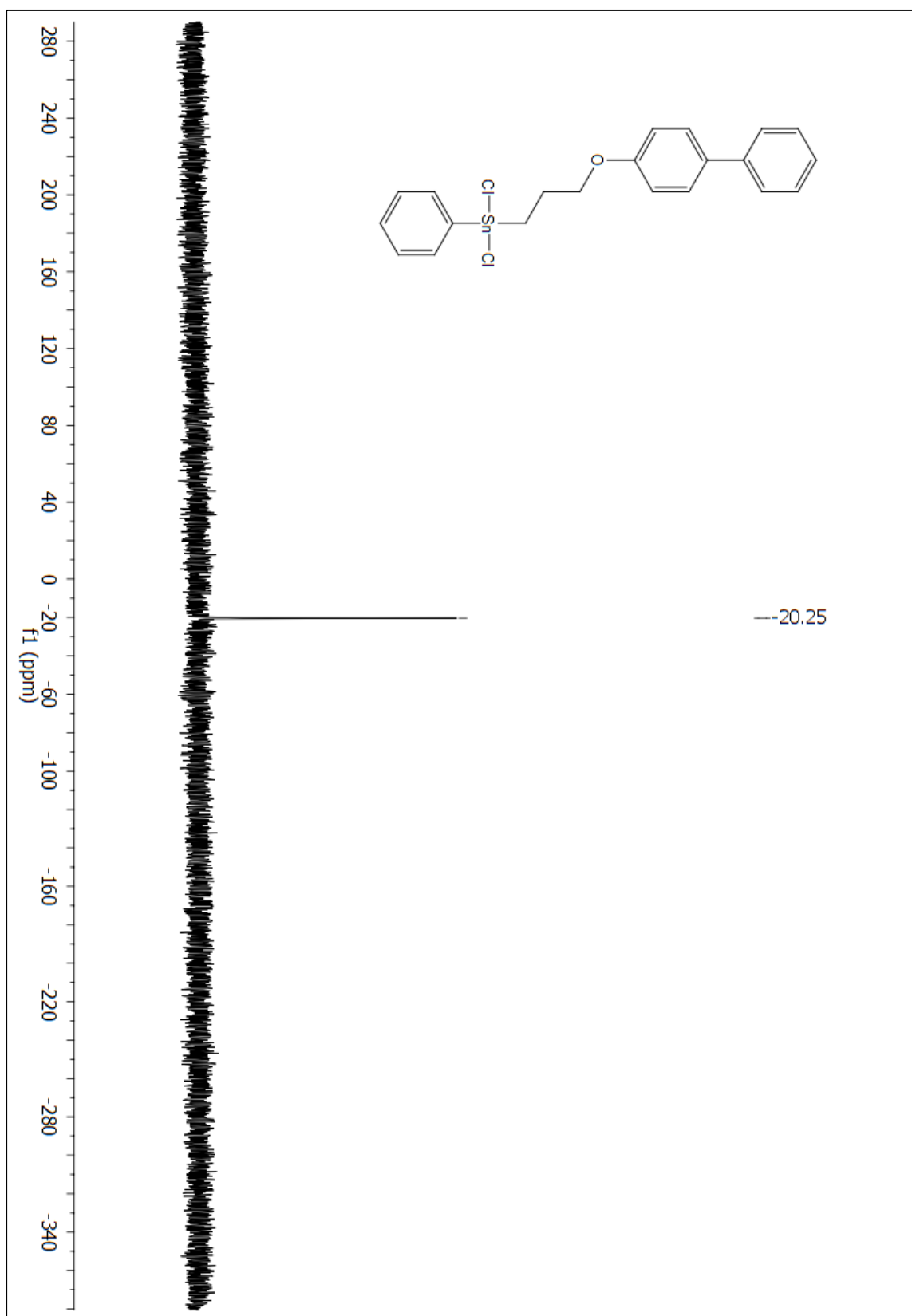
Figure A 38: ^{119}Sn NMR (CDCl$_3$) spectrum of compound 203.
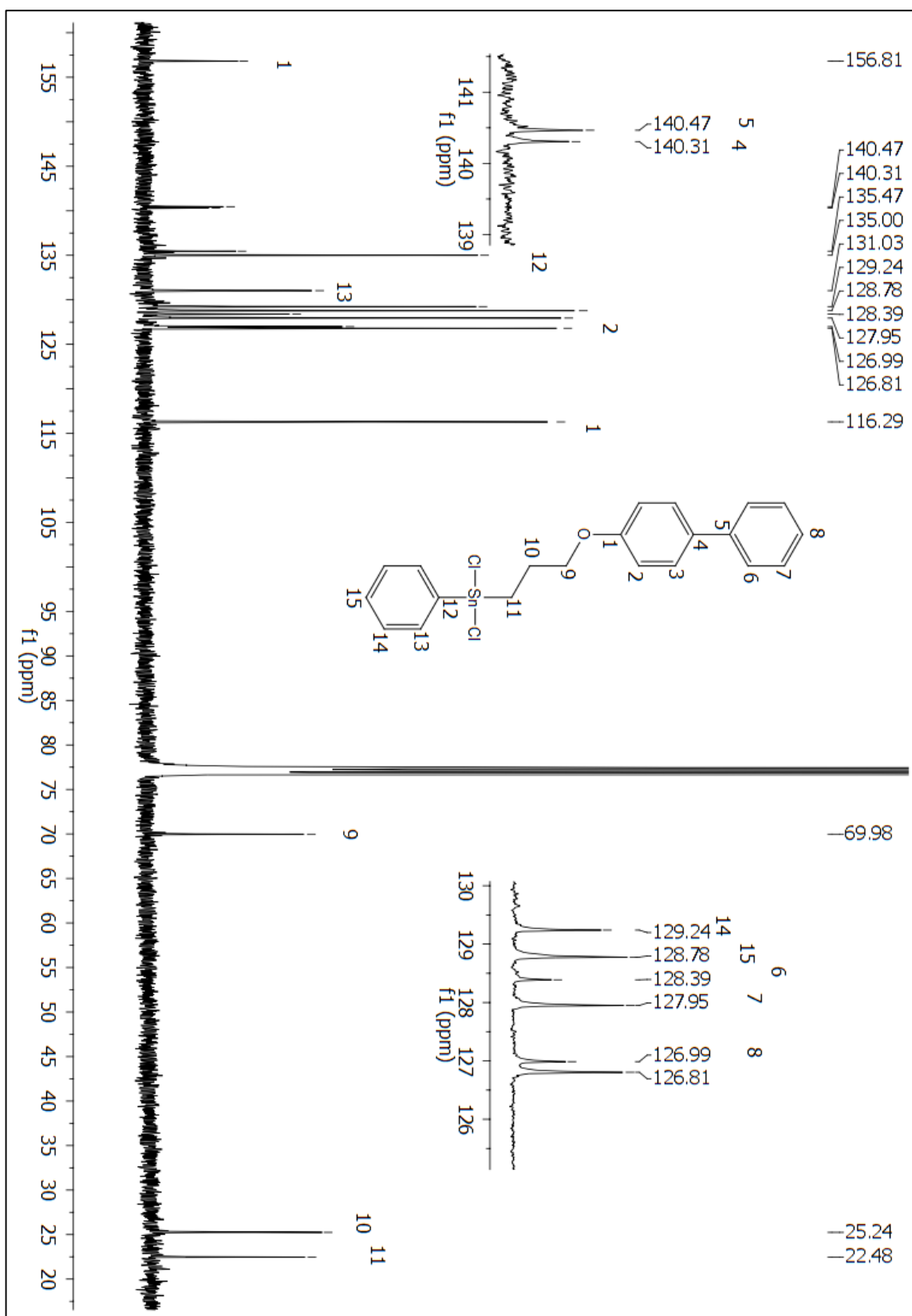
Figure A 39: ^{13}C NMR (CDCl$_3$) spectrum of compound 203.
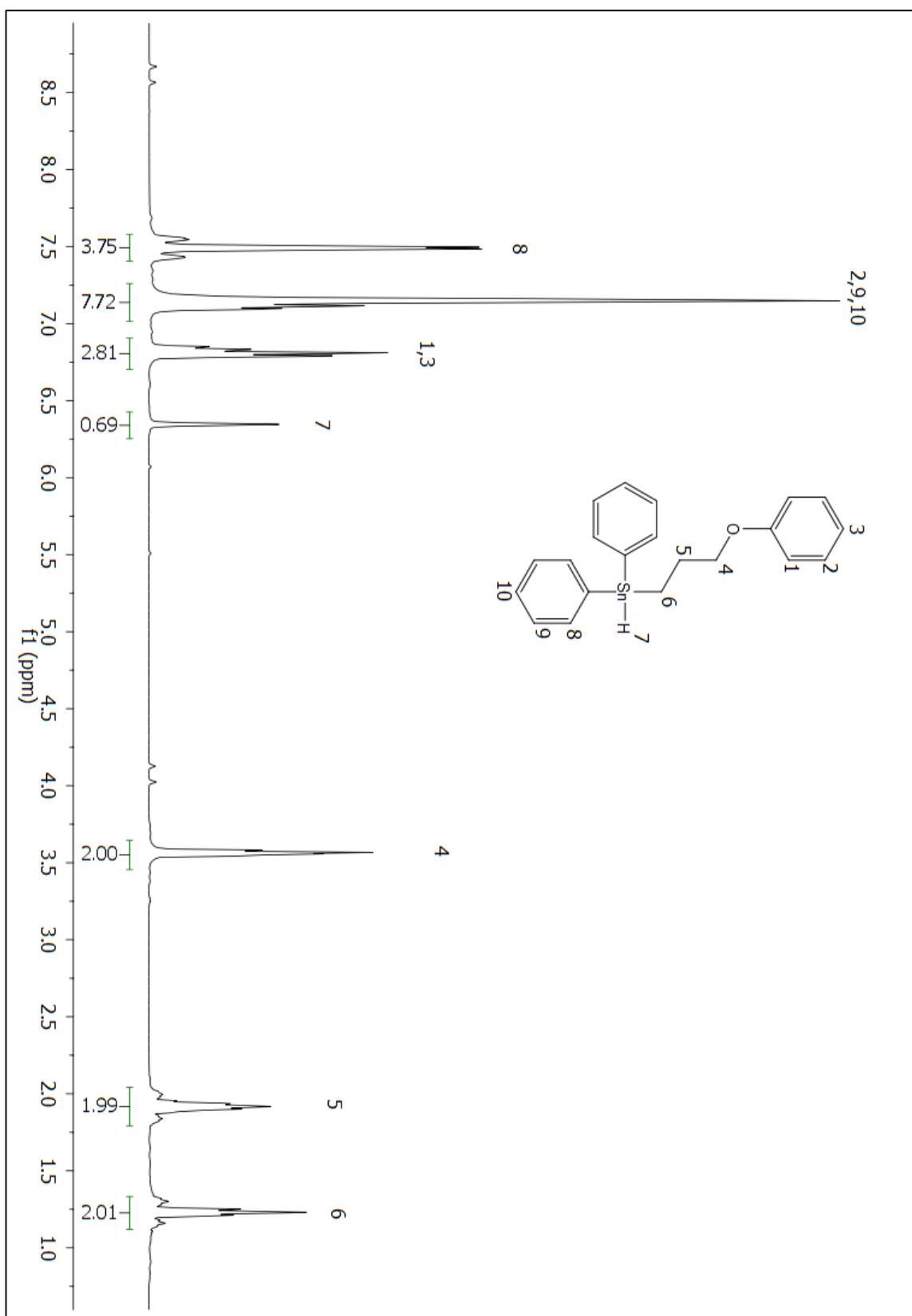
Figure A 40: ^{1}H NMR (C$_6$D$_6$) spectrum of compound 204.
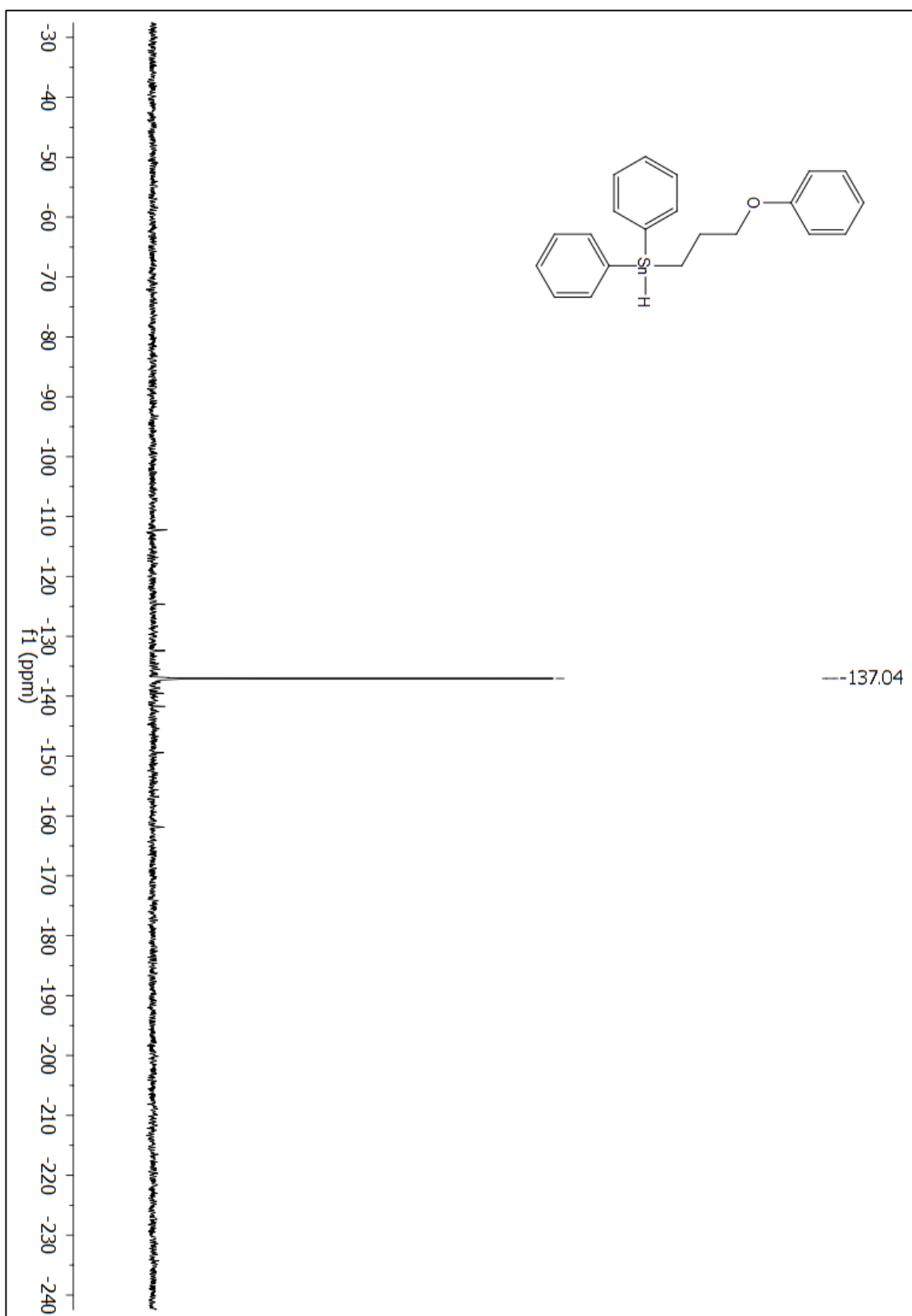
Figure A 41: ^{119}Sn NMR (C$_6$D$_6$) spectrum of compound 204.
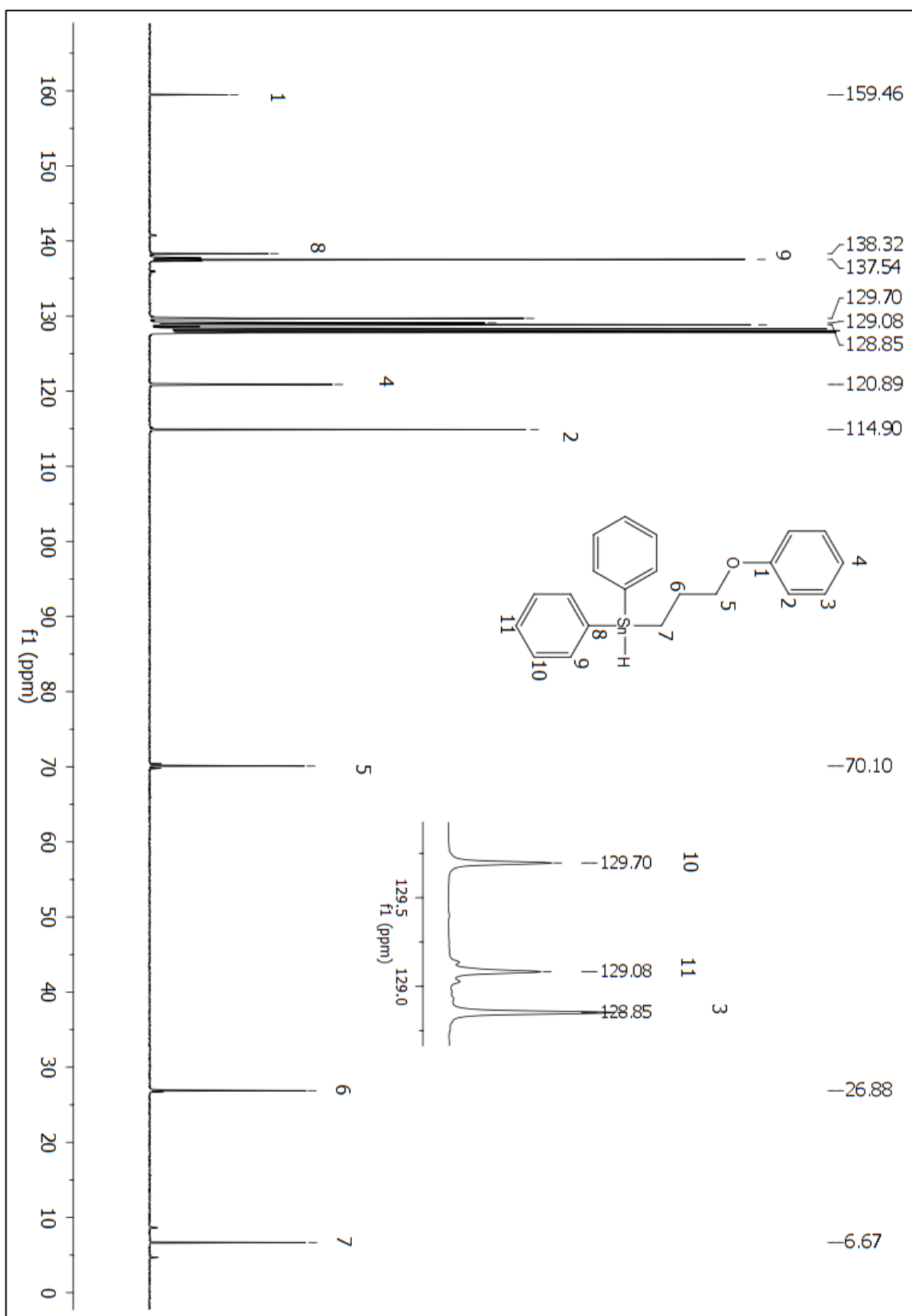
Figure A 42: ^{13}C NMR (C_6D_6) spectrum of compound **204.**
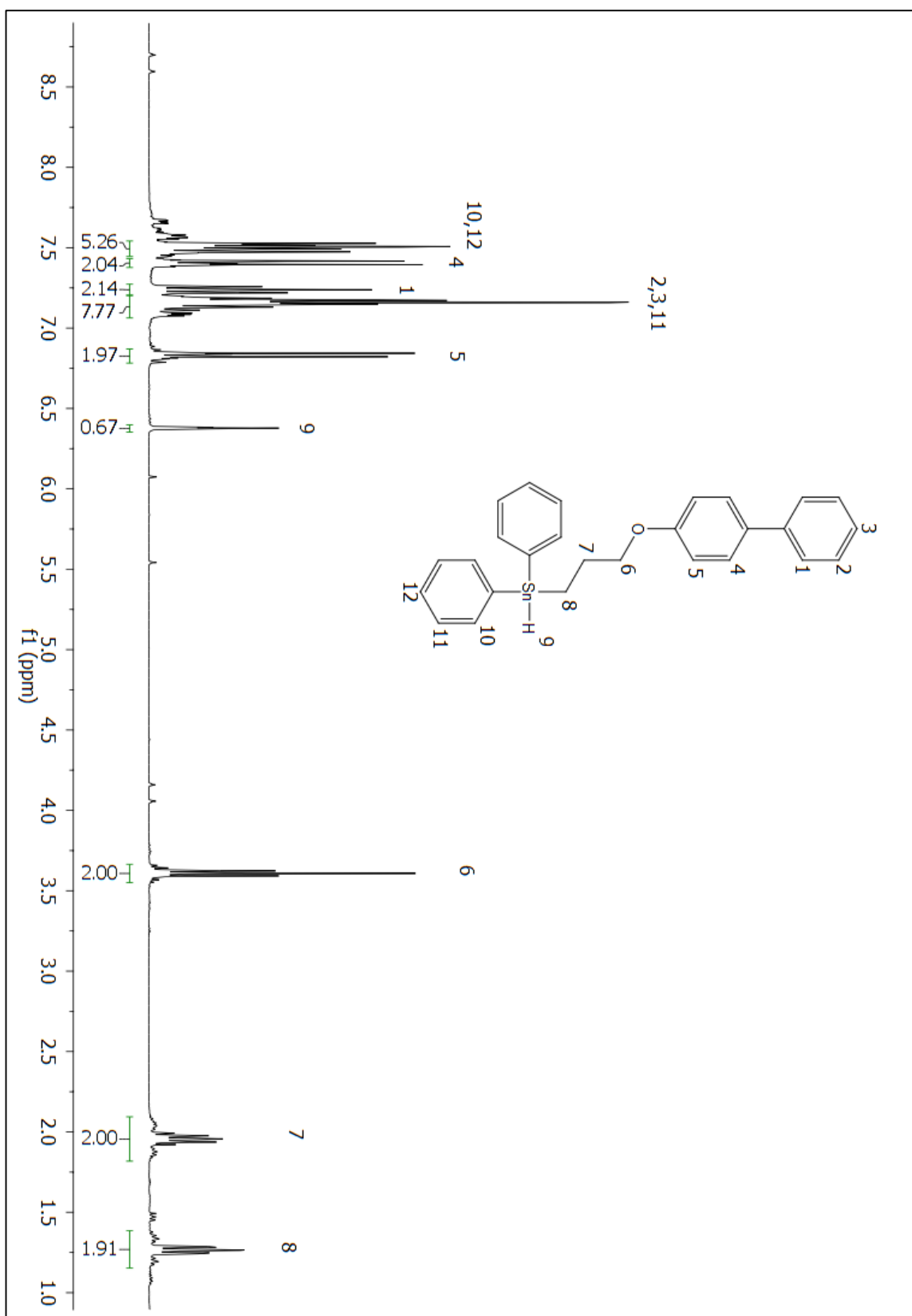
Figure A 43: ¹H NMR (C₆D₆) spectrum of compound 205.
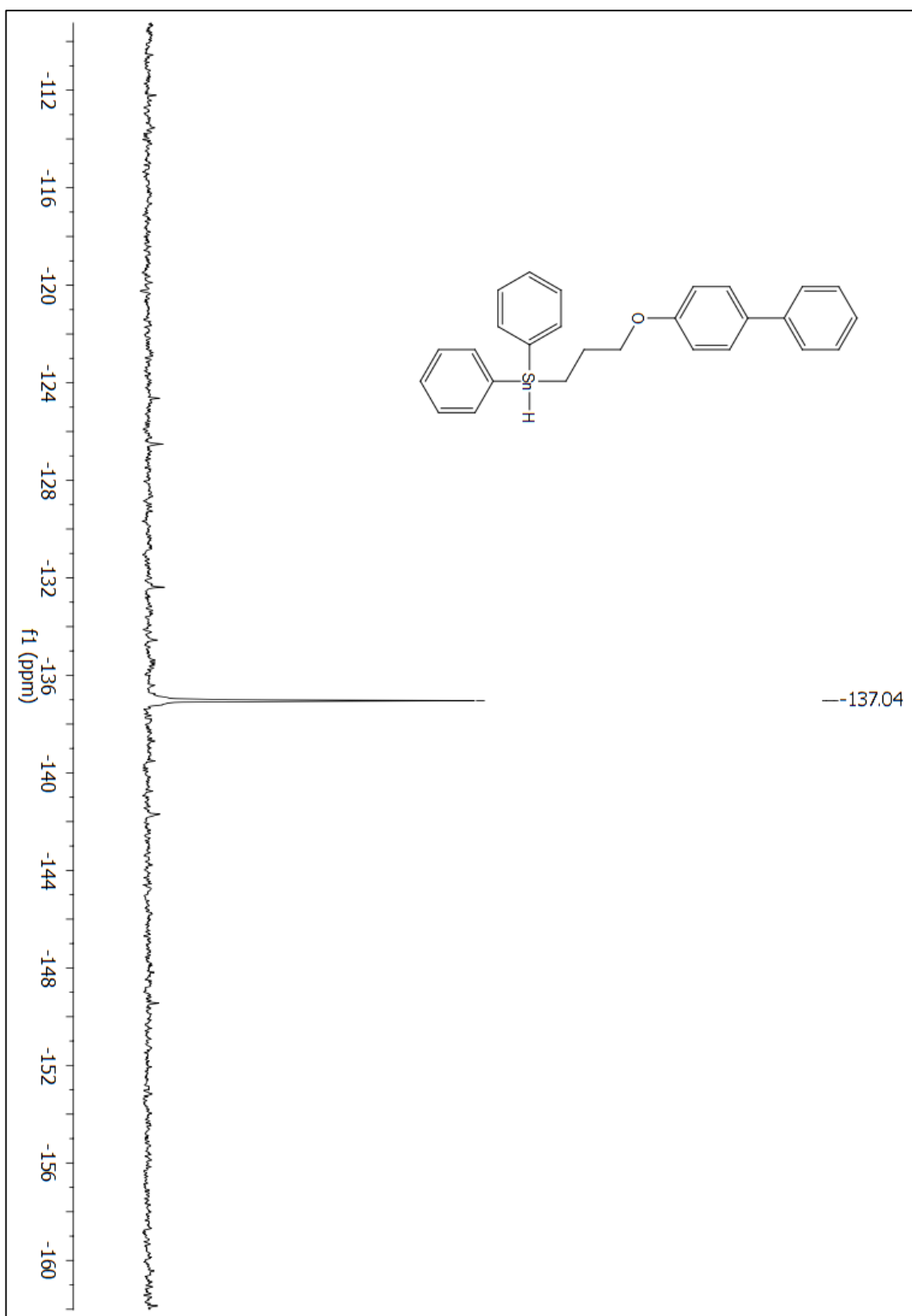
Figure A 44: ^{119}Sn NMR (C$_6$D$_6$) spectrum of compound 205.
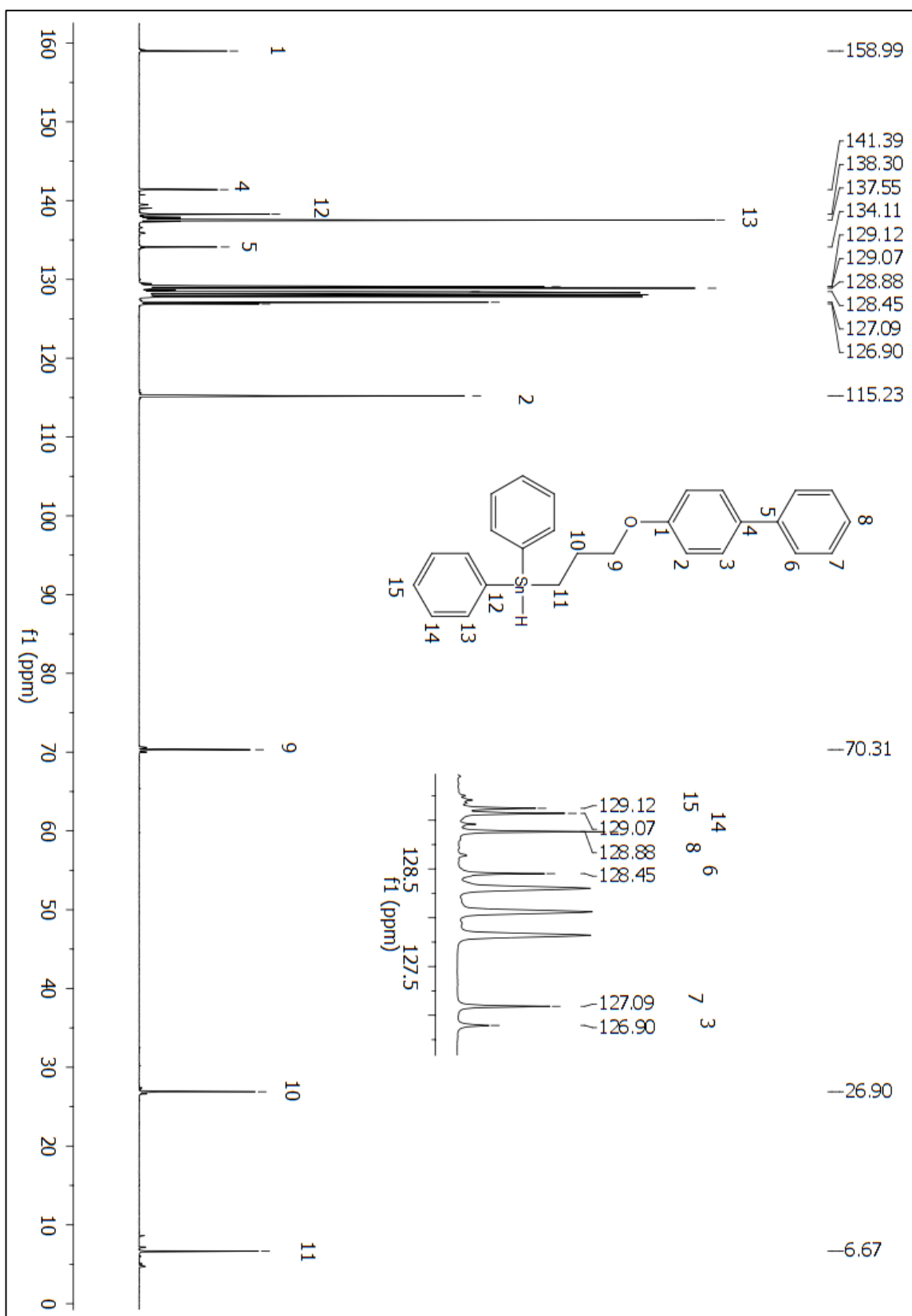
Figure A 45: ^{13}C NMR (C$_6$D$_6$) spectrum of compound 205.

Figure A 46: ¹H NMR (C₆D₆) spectrum of compound 206.
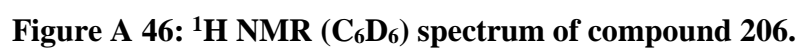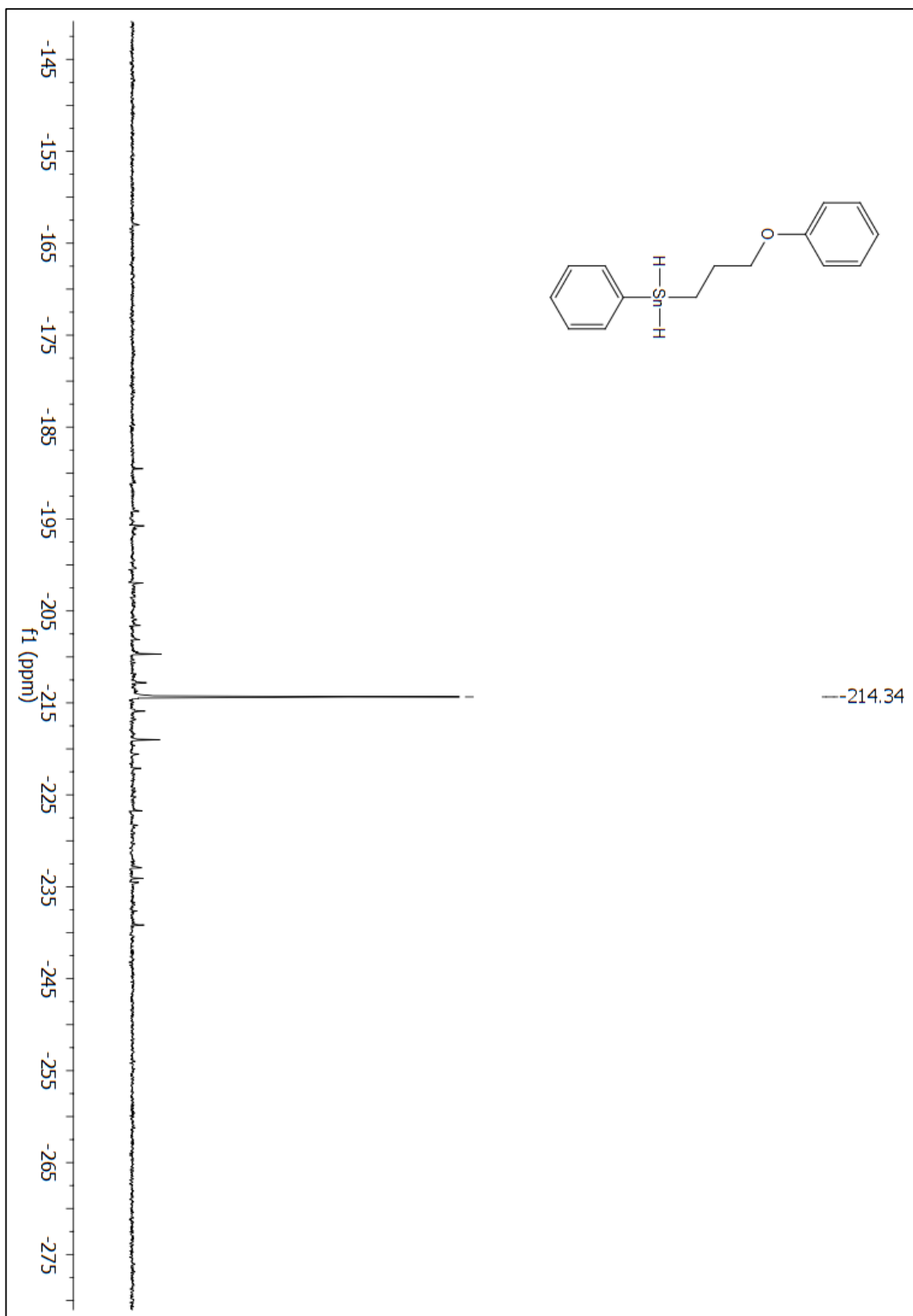
Figure A 47: ^{119}Sn NMR (C$_6$D$_6$) spectrum of compound 206.
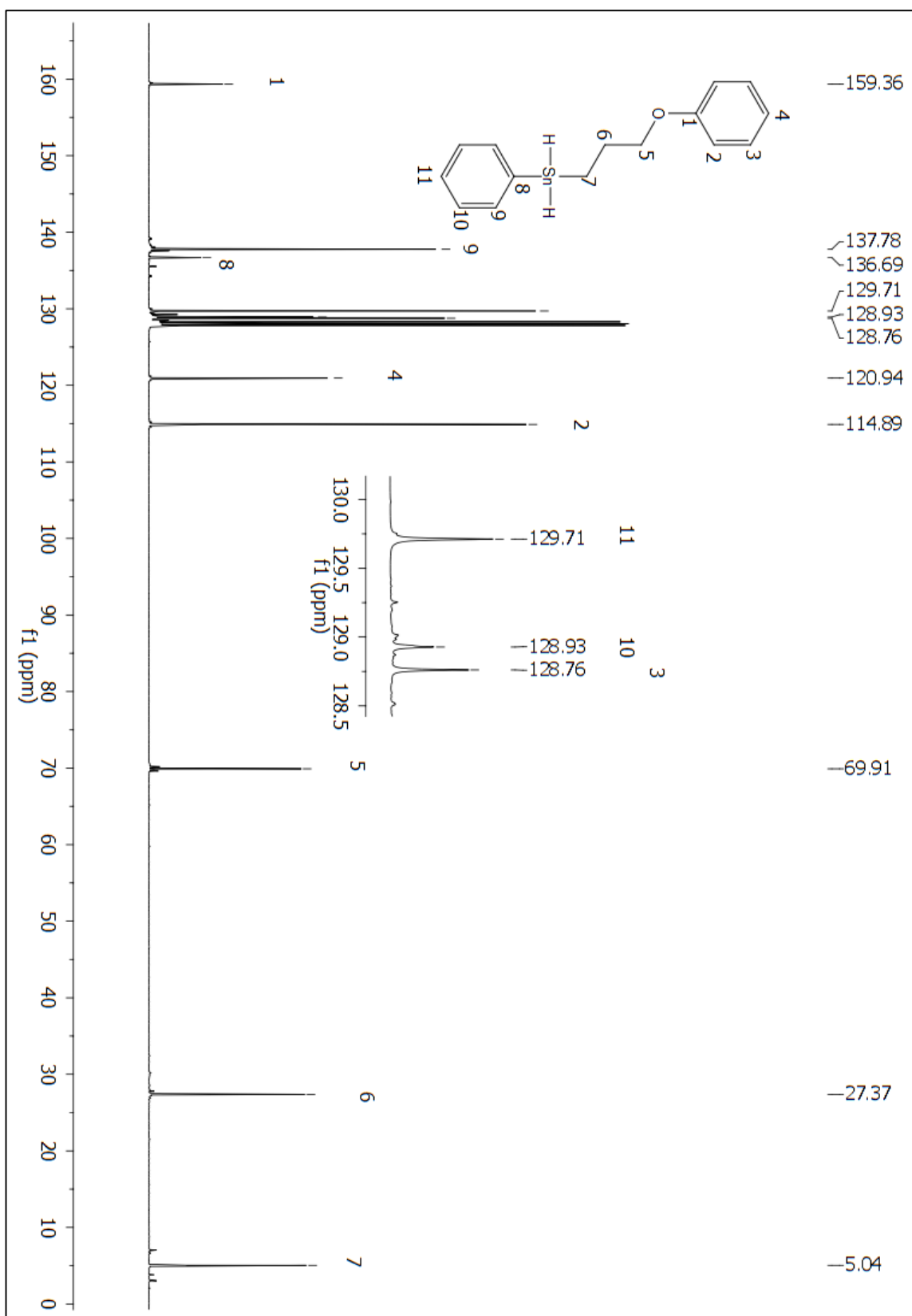
Figure A 48: ^{13}C NMR (C_6D_6) spectrum of compound **206.**
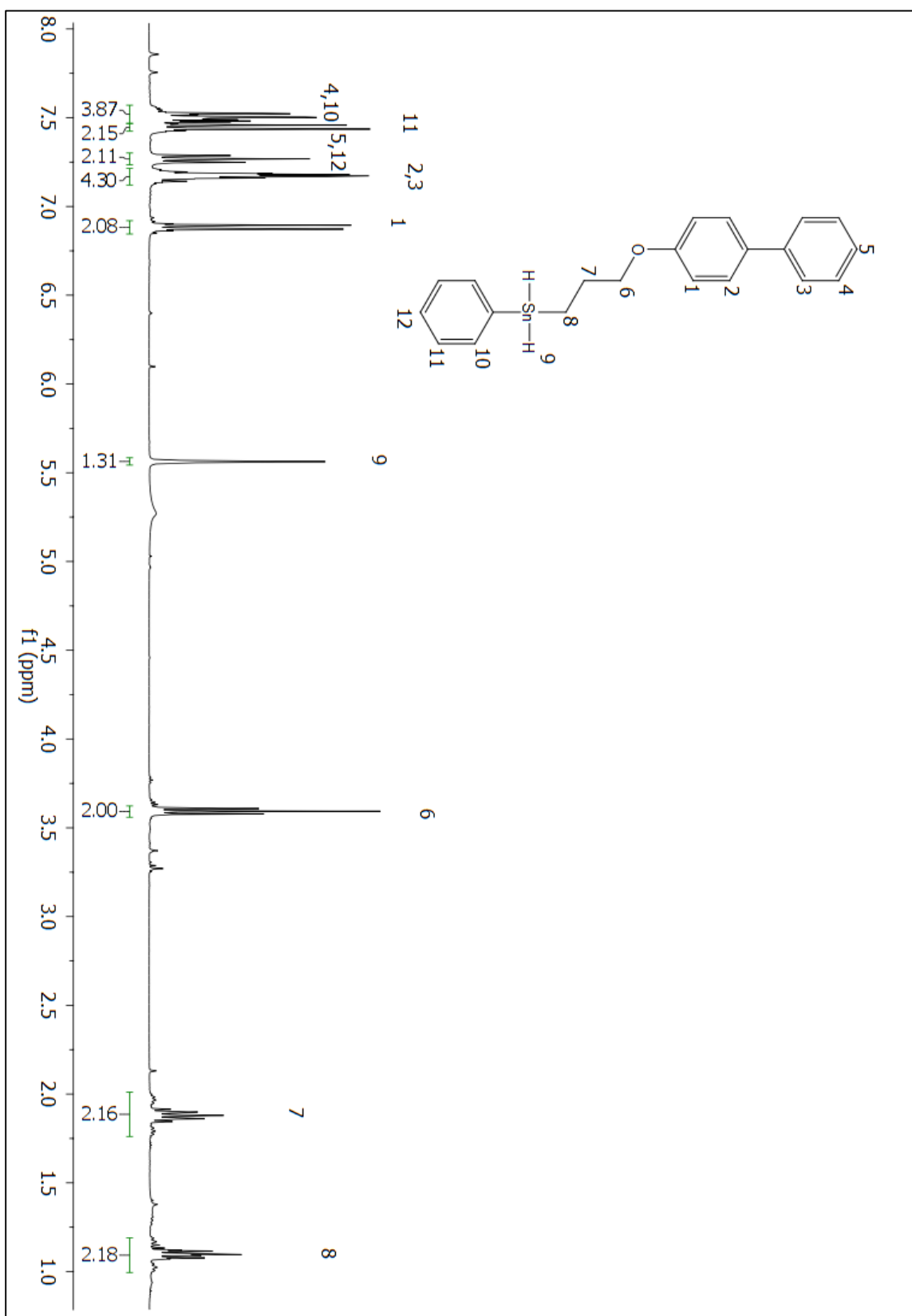
Figure A 49: ¹H NMR (C₆D₆) spectrum of compound 207.
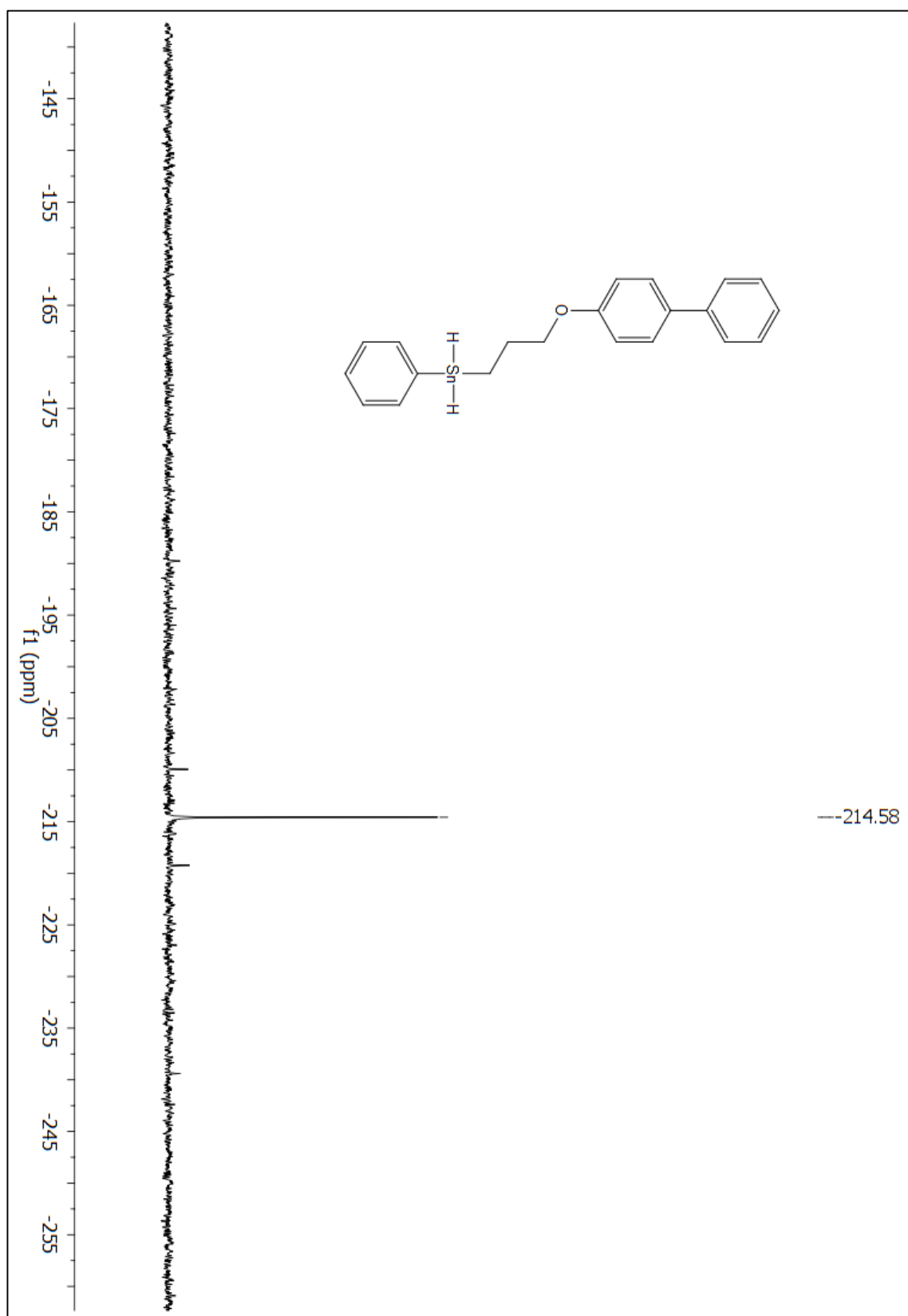
Figure A 50: ^{119}Sn NMR (C$_6$D$_6$) spectrum of compound 207.
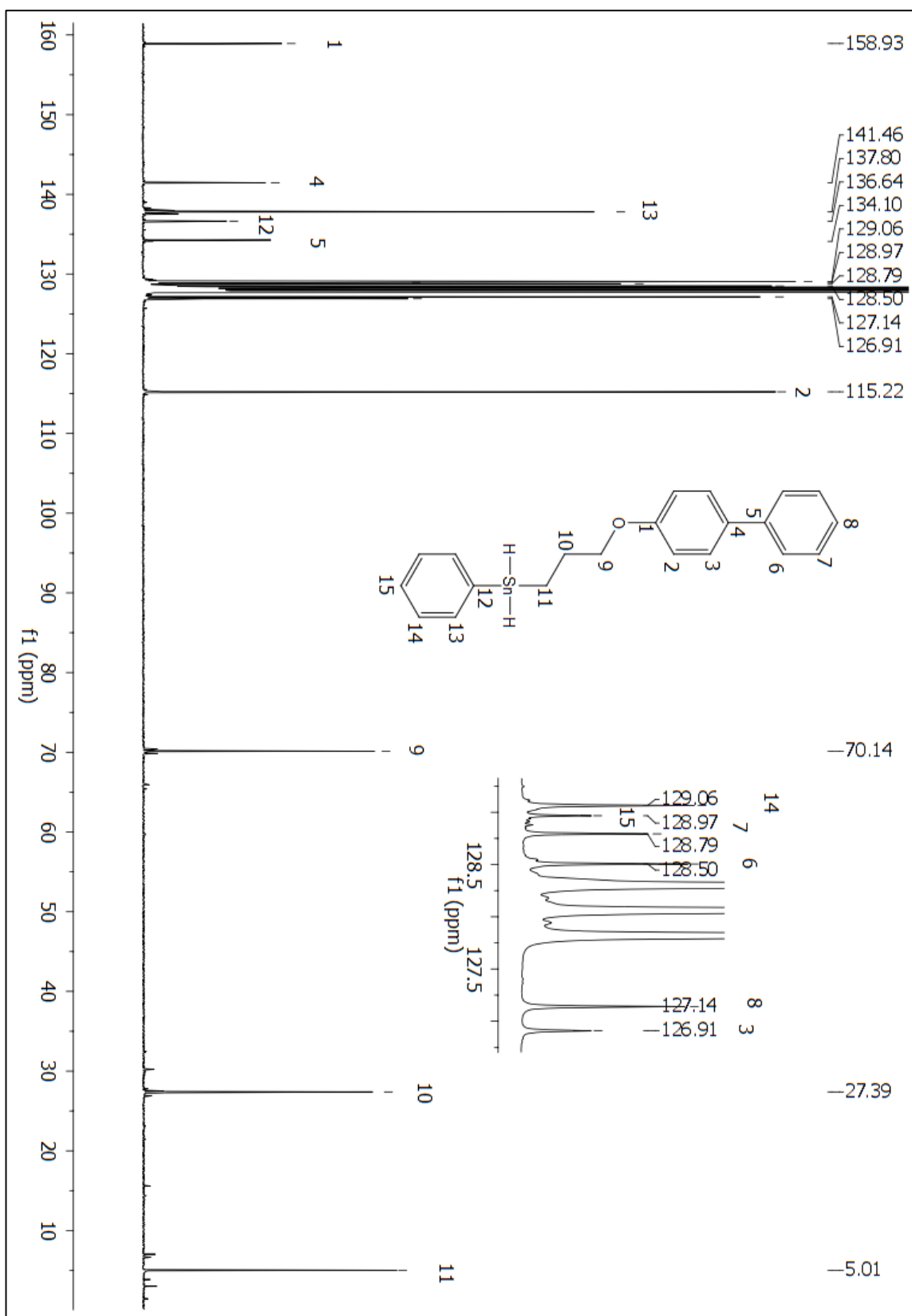
Figure A 51: ^{13}C NMR (C_6D_6) spectrum of compound 207.
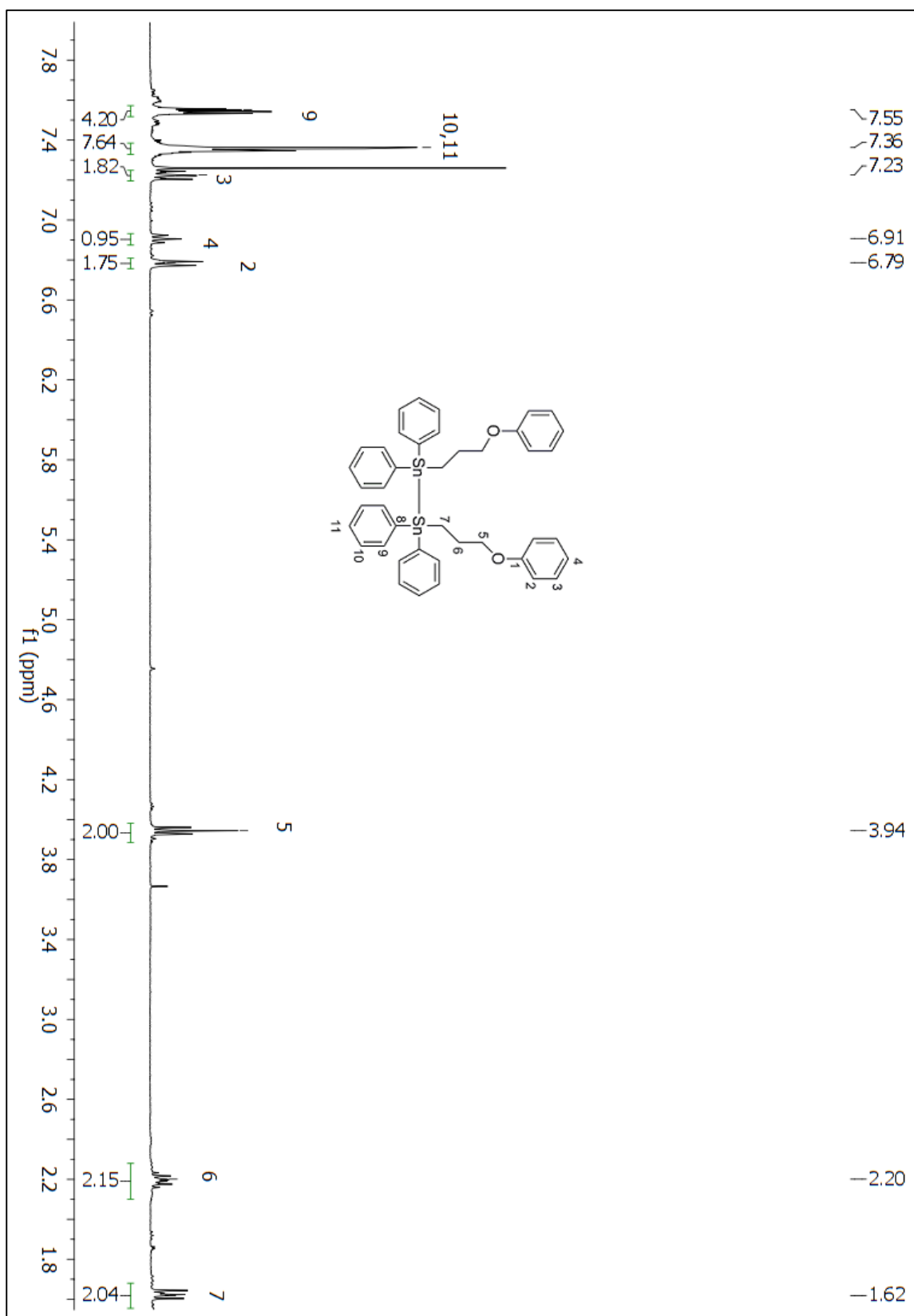
Figure A 52: ^{1}H NMR (C$_6$D$_6$) spectrum of compound 208.
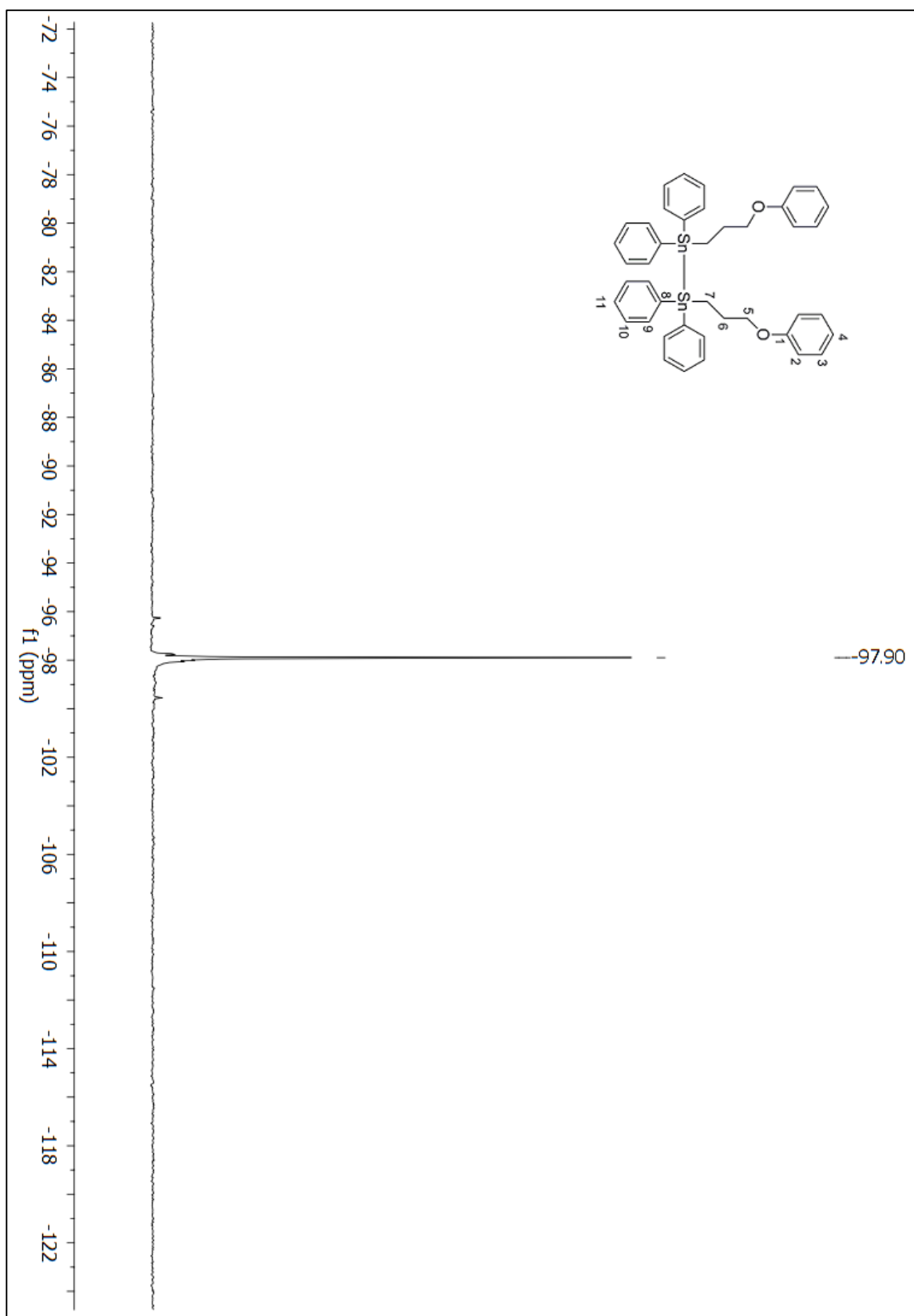
Figure A 53: ^{119}Sn NMR (C$_6$D$_6$) spectrum of compound 208.
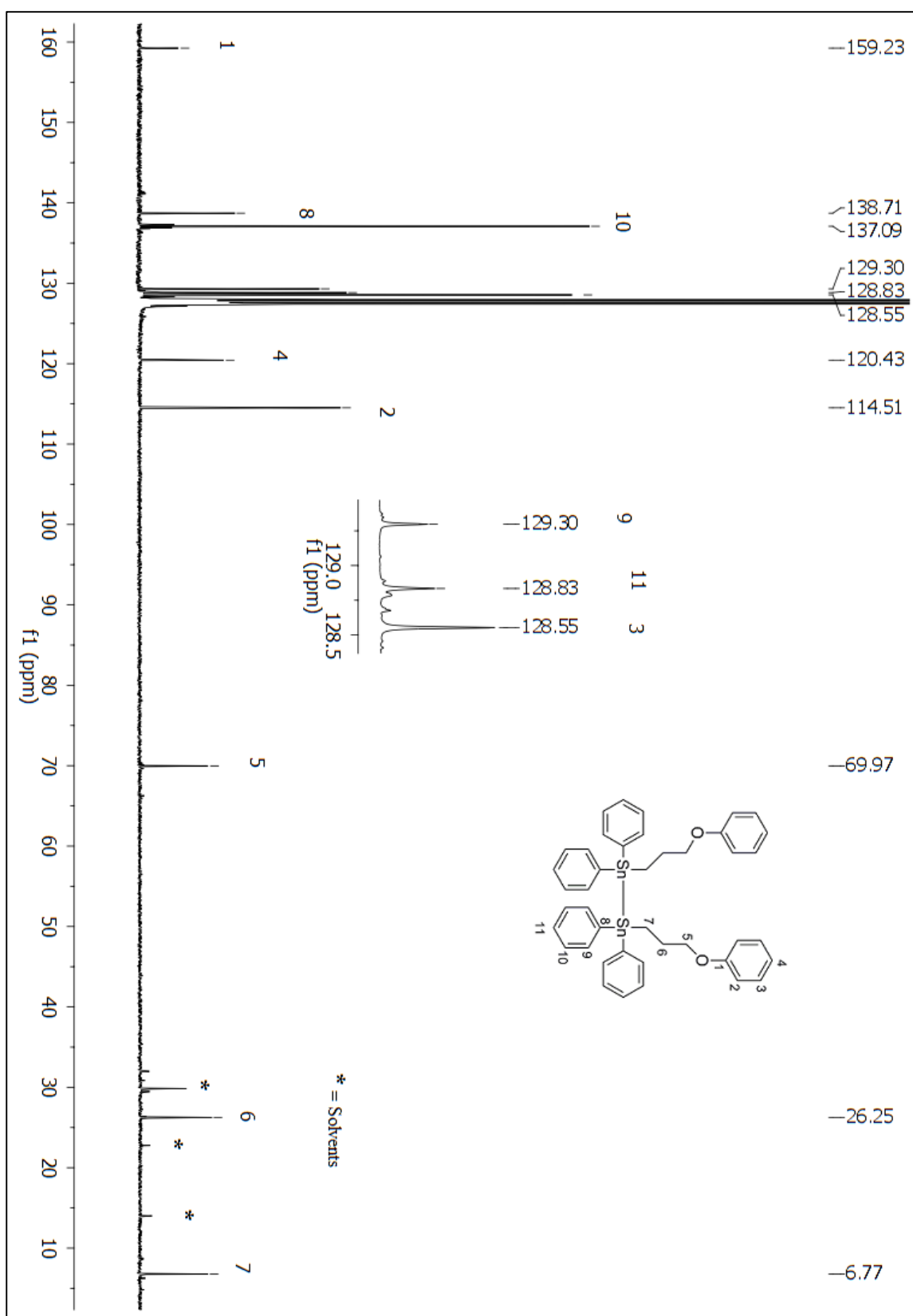
Figure A 54: ^{13}C NMR (C_6D_6) spectrum of compound 208.
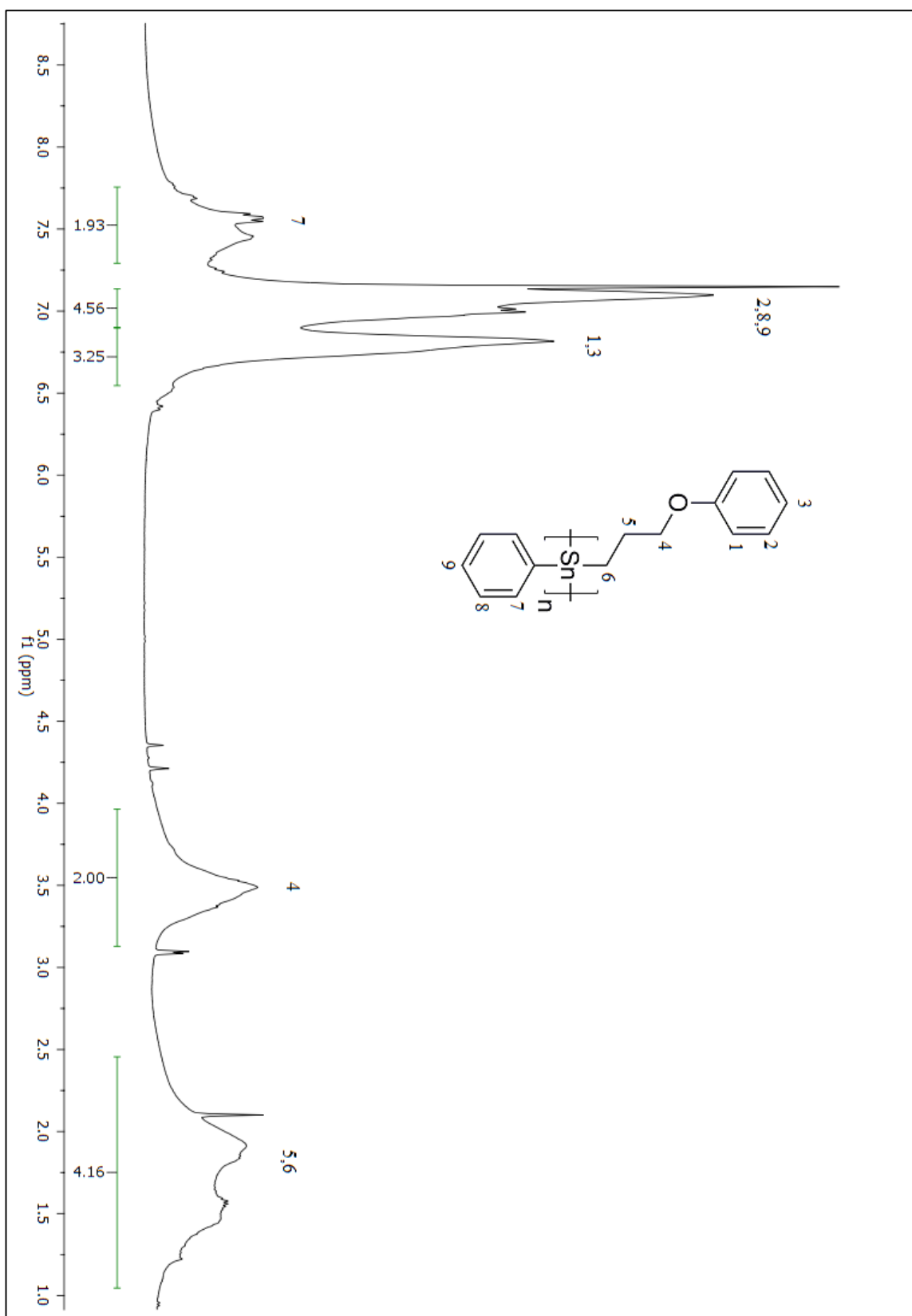
Figure A 55: ^{1}H NMR (C${}_6$D${}_6$) spectrum of compound 249.
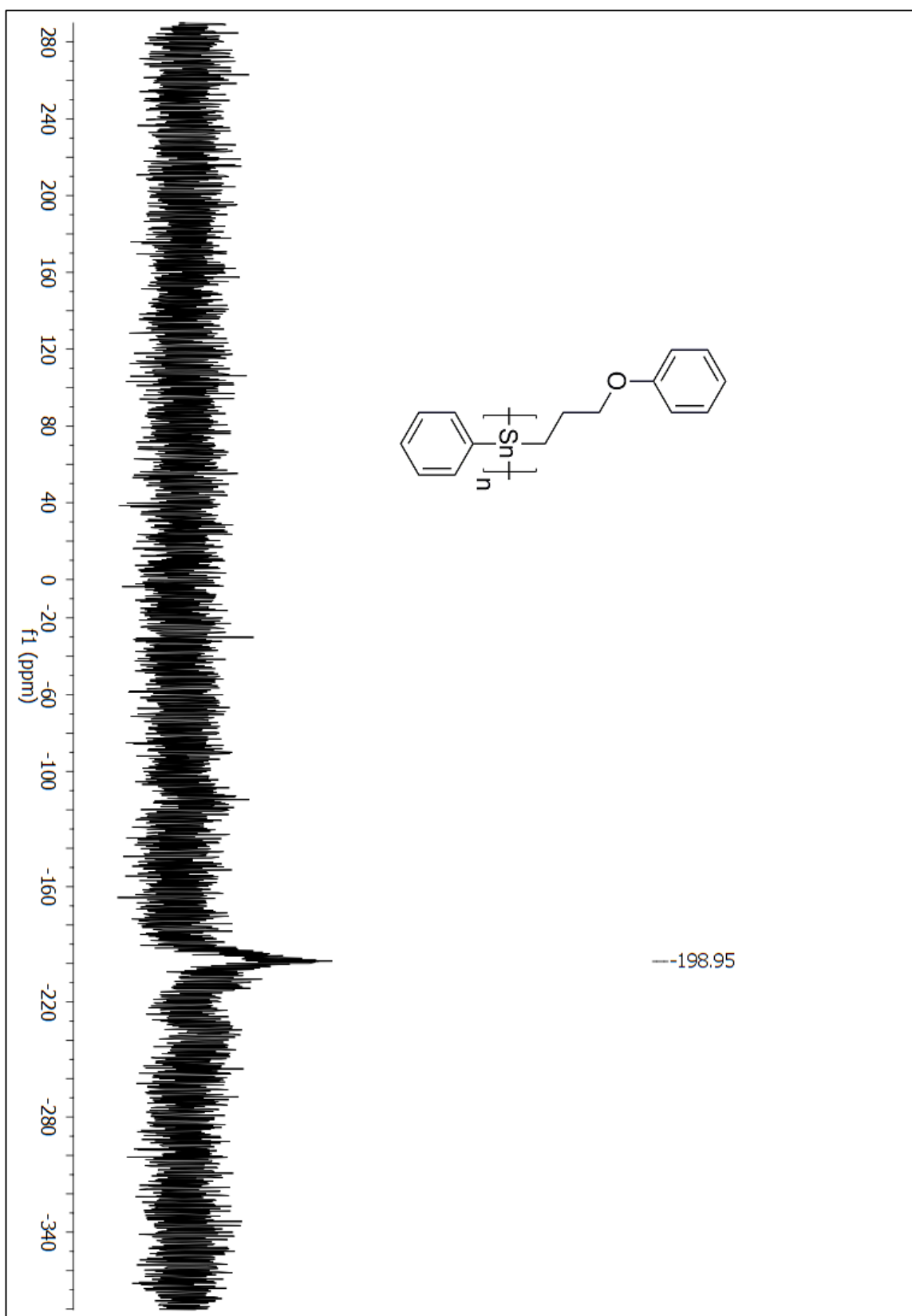
Figure A 56: ^{119}Sn NMR (C_6D_6) spectrum of compound 249.

—-198.95
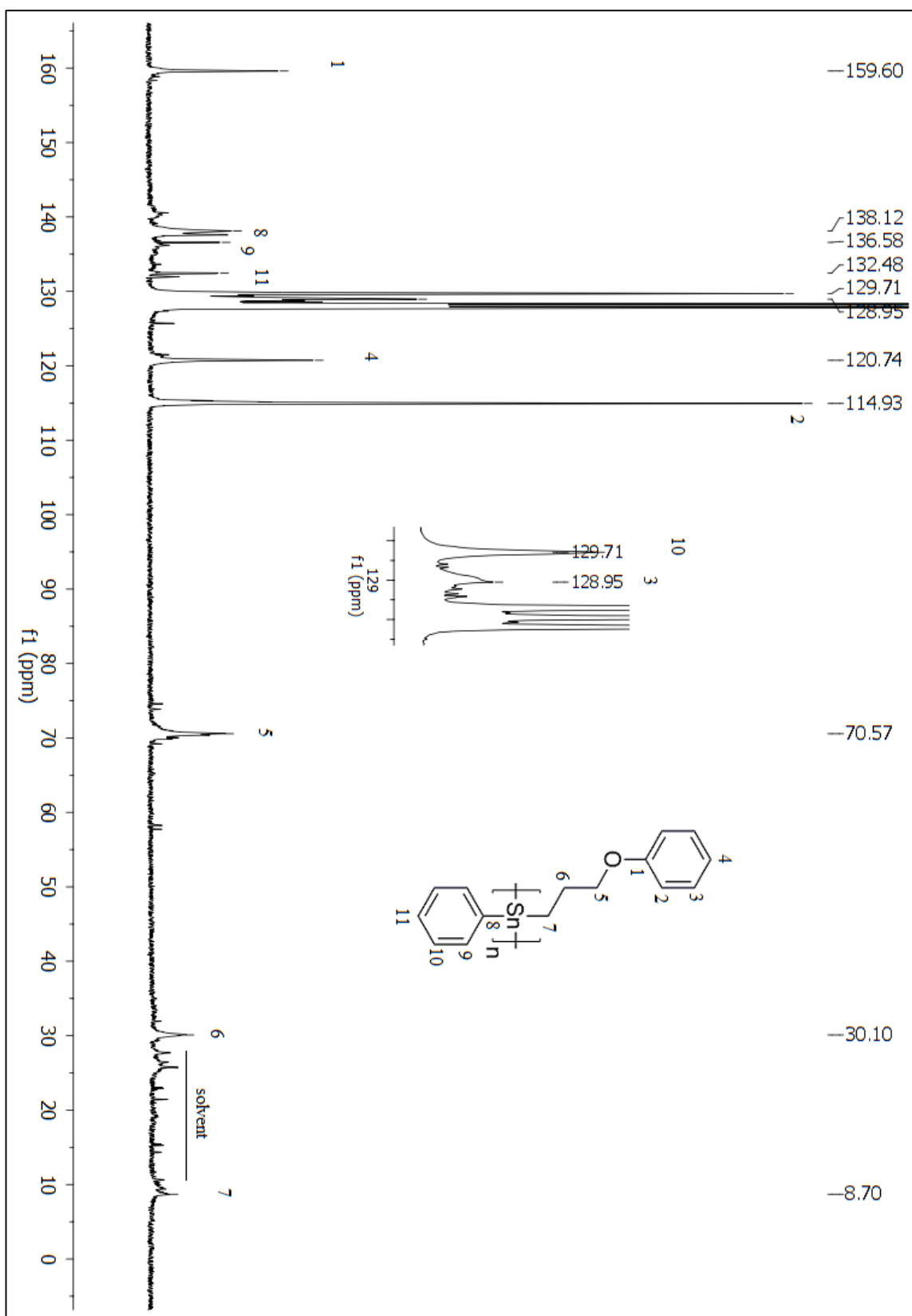
Figure A 57: ^{13}C NMR (C_6D_6) spectrum of compound 249.
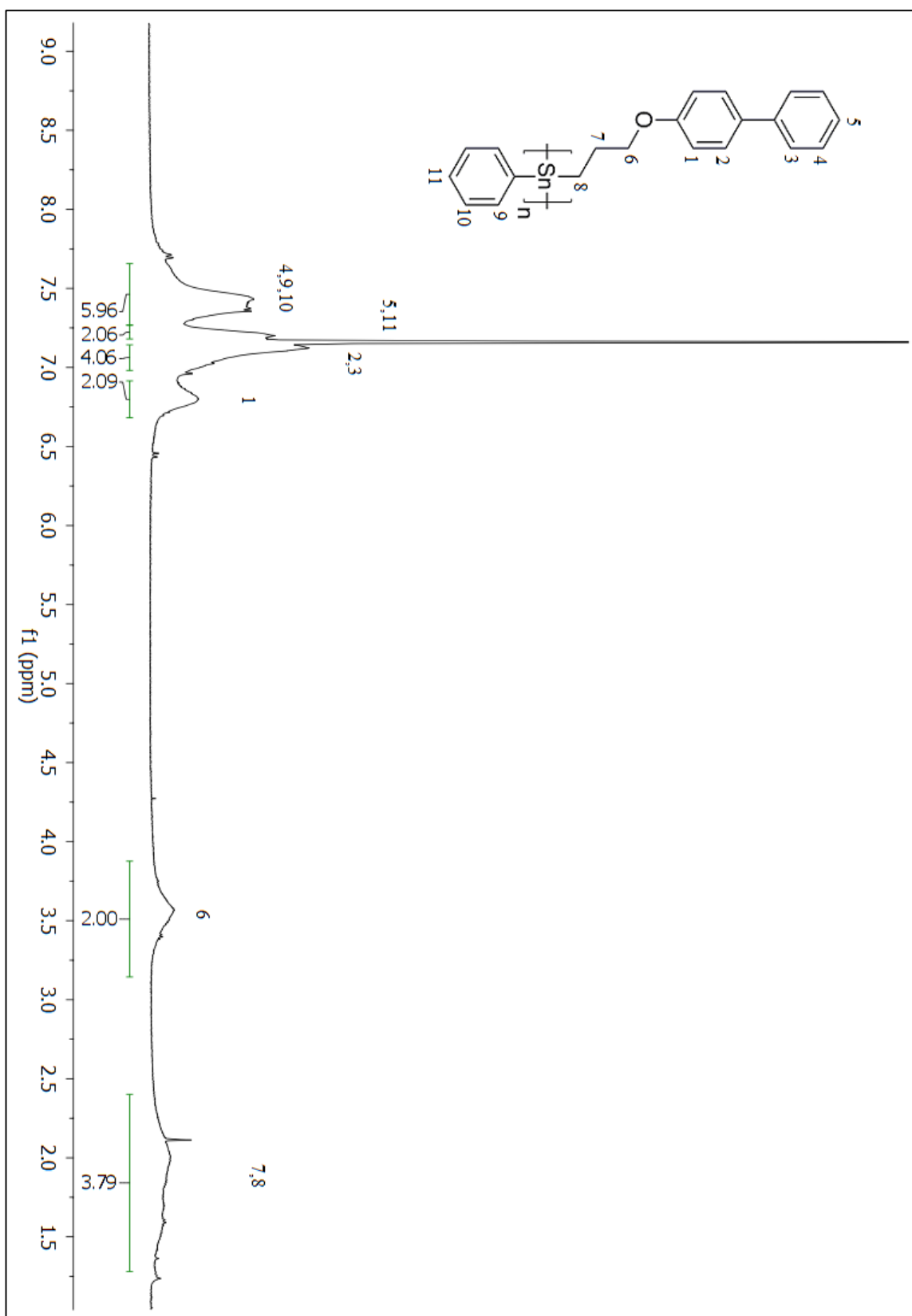
Figure A 58: ^{1}H NMR (C$_6$D$_6$) spectrum of compound 250.
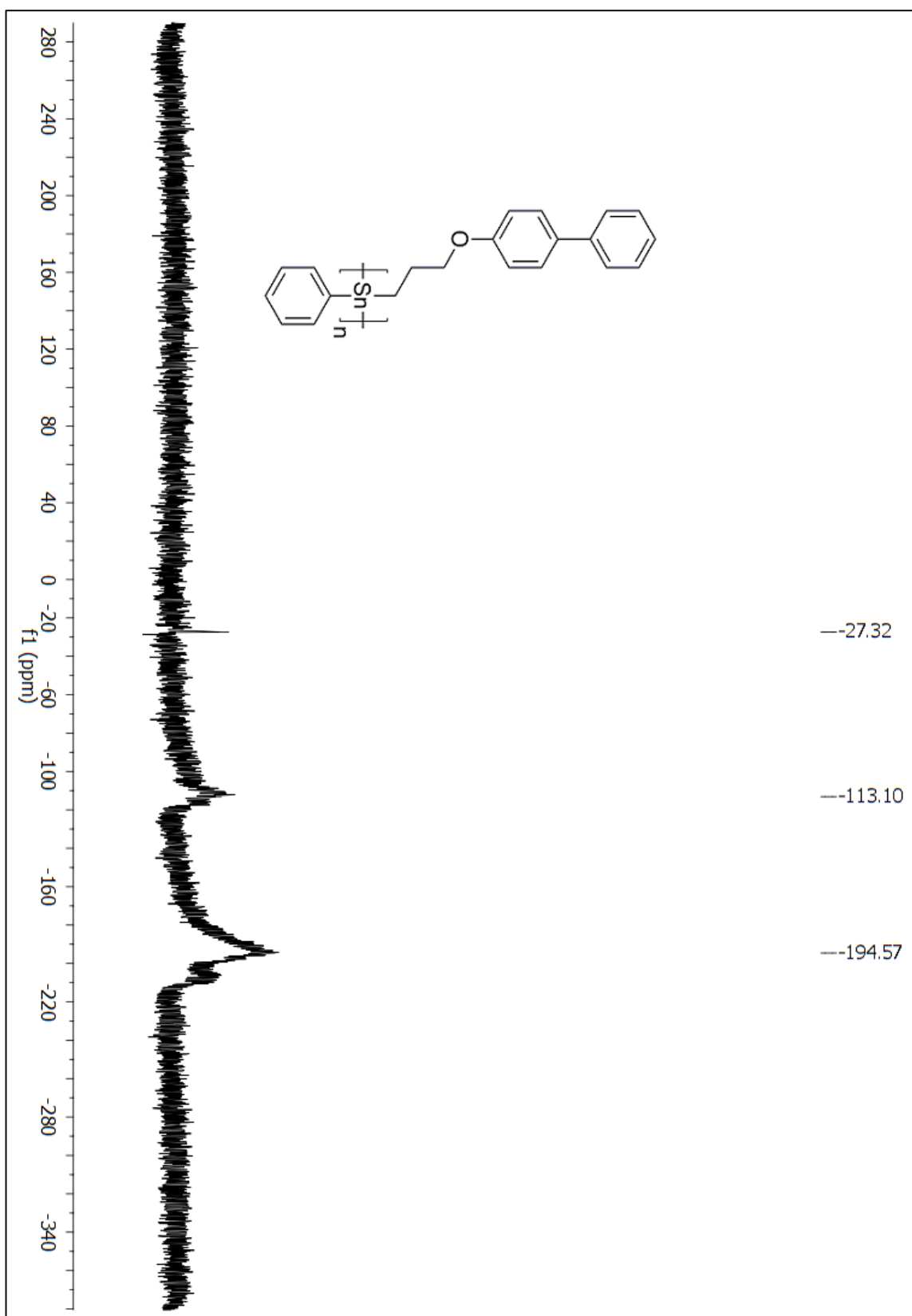
Figure A 59: ^{119}Sn NMR (C_6D_6) spectrum of compound 250.
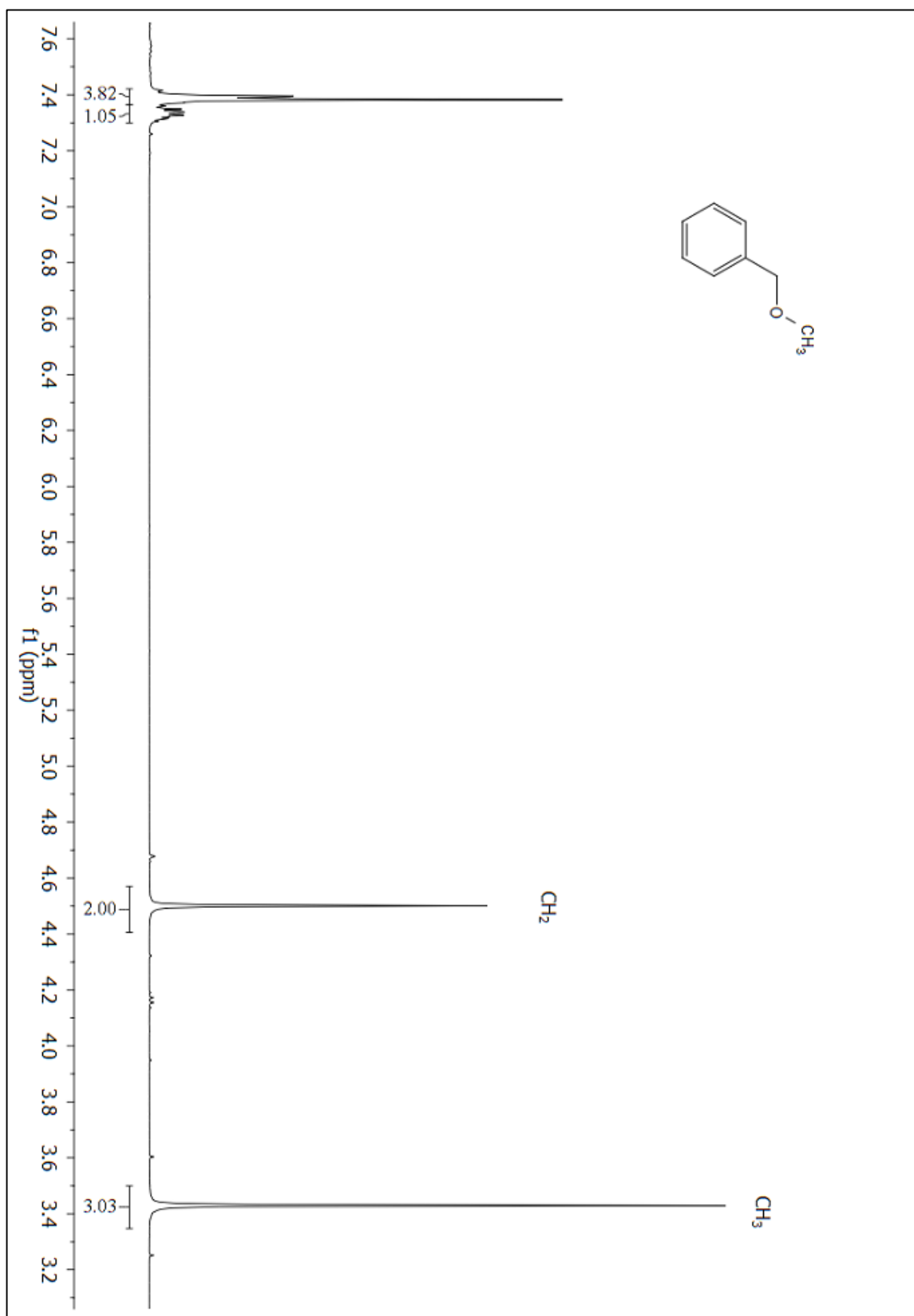
Figure A 60: ¹H NMR (CDCl₃) spectrum of compound 214.
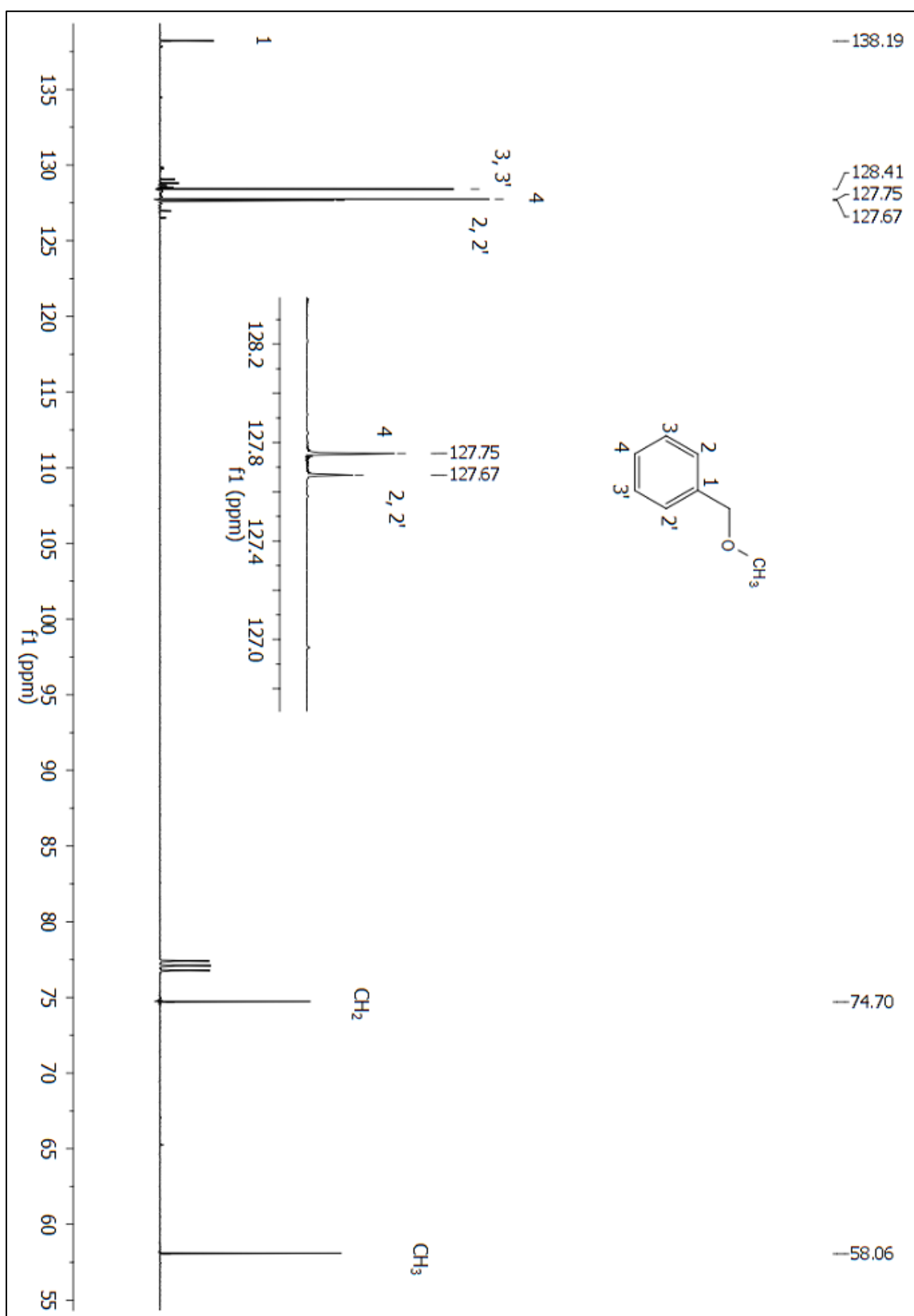
Figure A 61: ^{13}C NMR (CDCl$_3$) spectrum of compound 214.
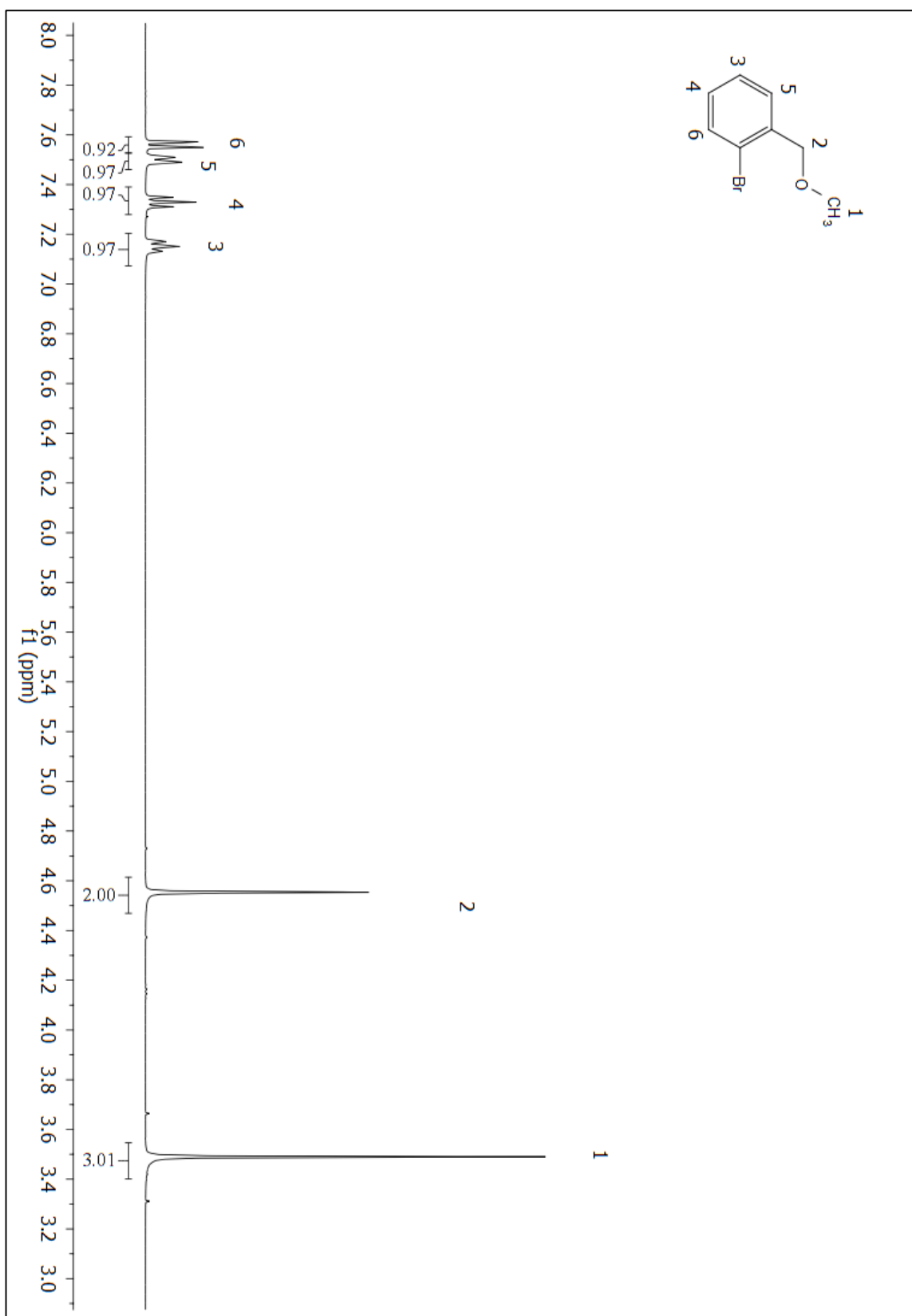
Figure A 62: ^{1}H NMR (CDCl$_3$) spectrum of compound 215.
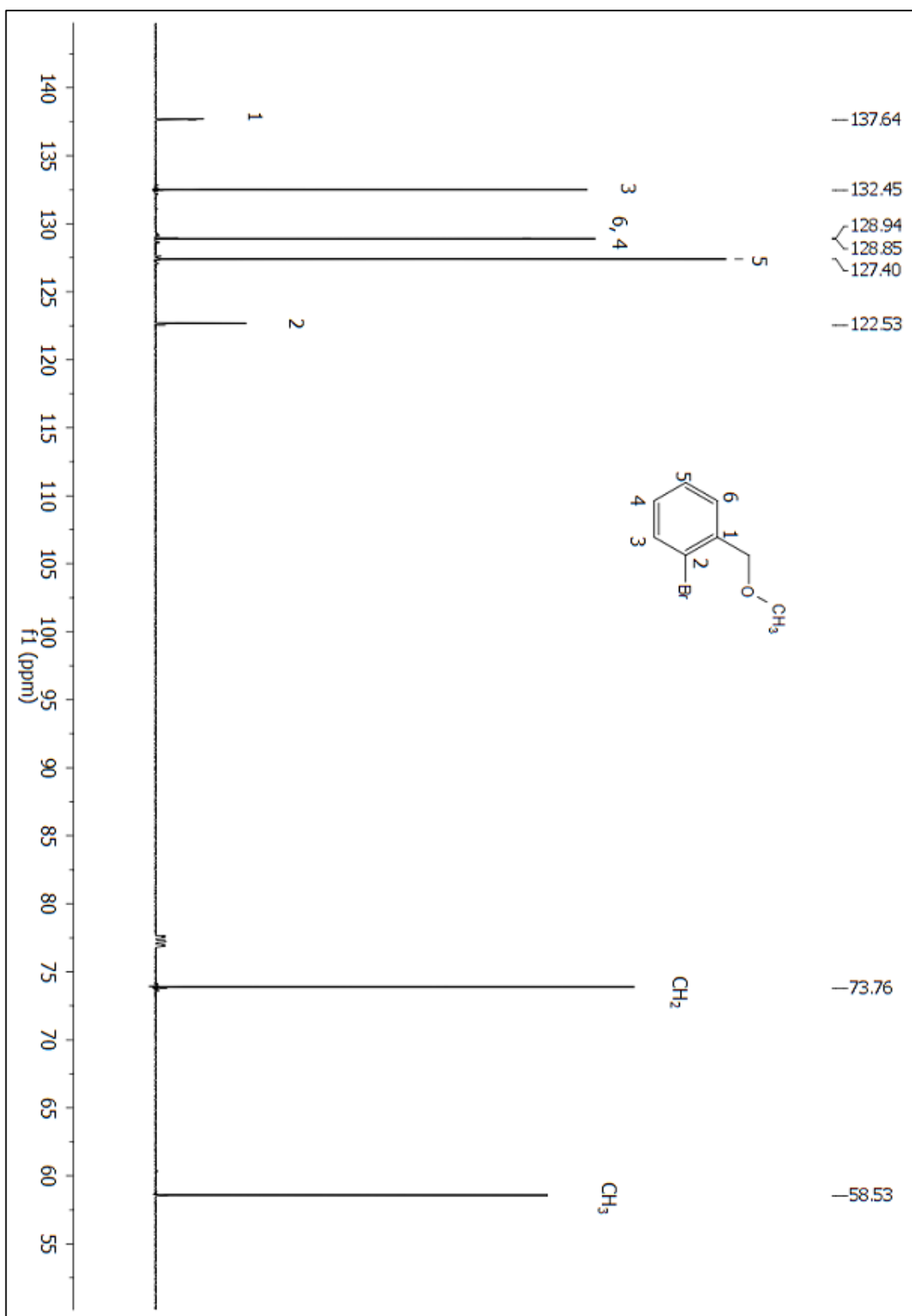
Figure A 63: ^{13}C NMR (CDCl$_3$) spectrum of compound 215.
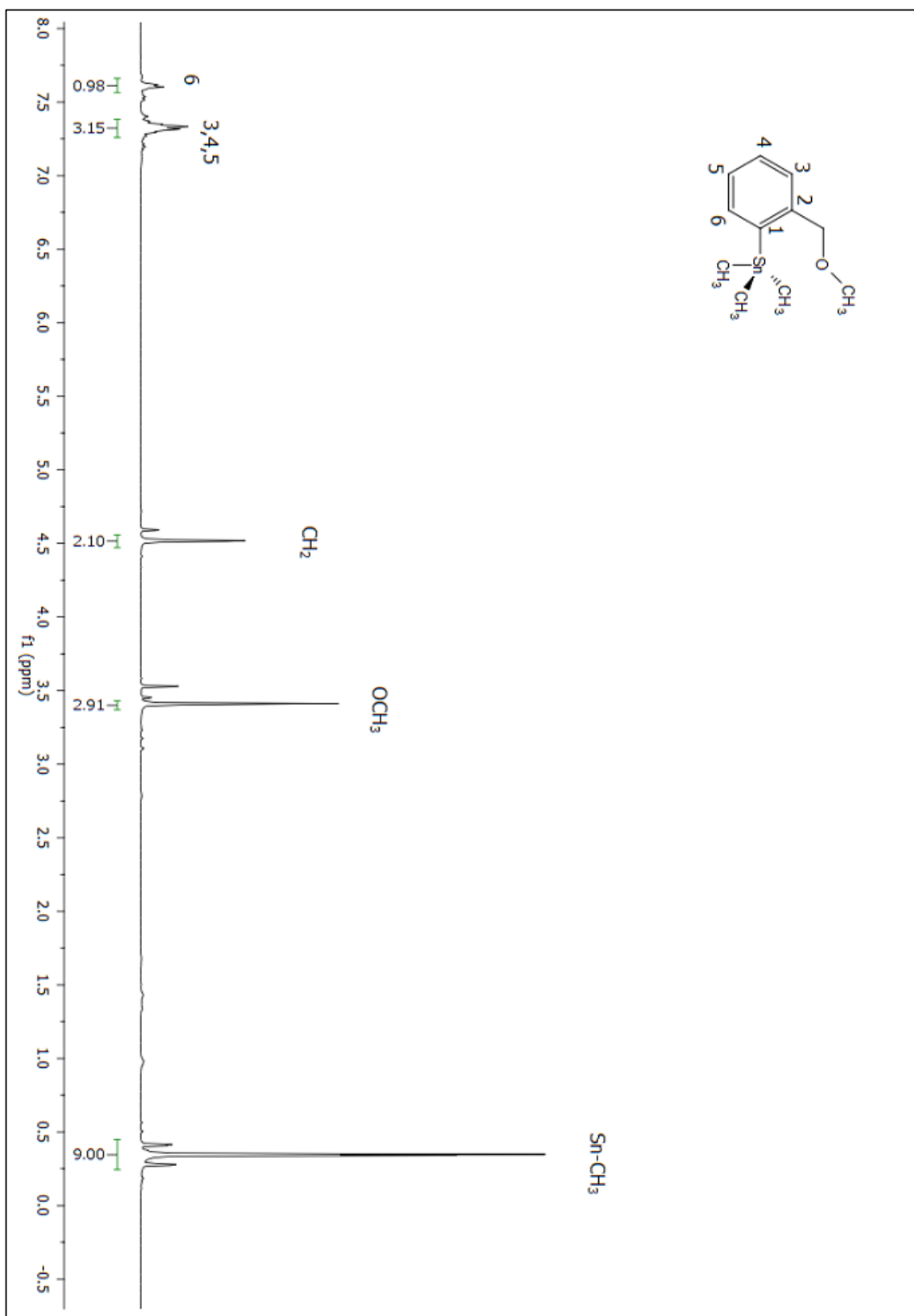
Figure A 64: ¹H NMR (CDCl₃) spectrum of compound 113.
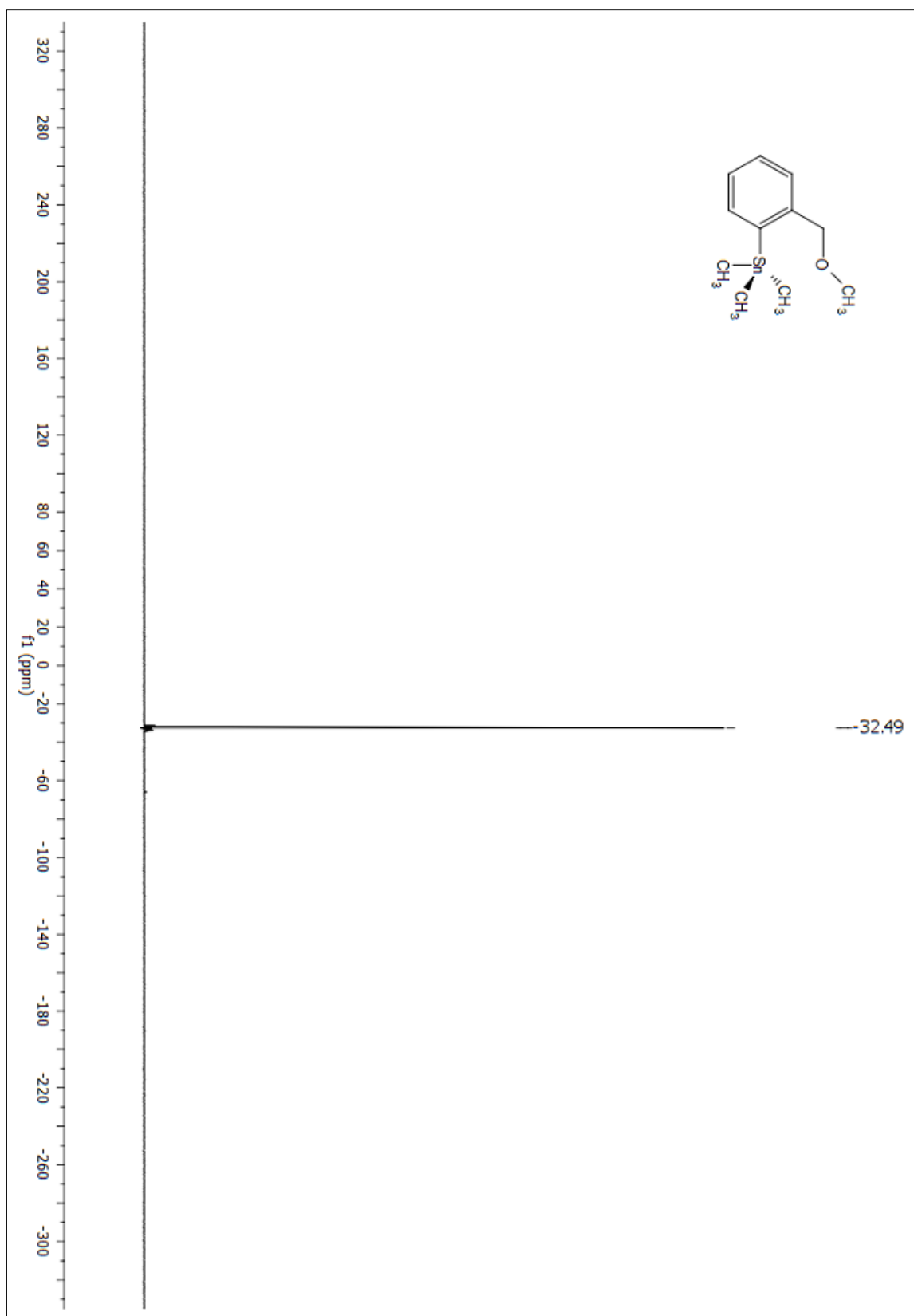
Figure A 65: ^{119}Sn NMR (CDCl₃) spectrum of compound 113.

Figure A 66: ^{13}C NMR (CDCl$_3$) of spectrum compound 113.
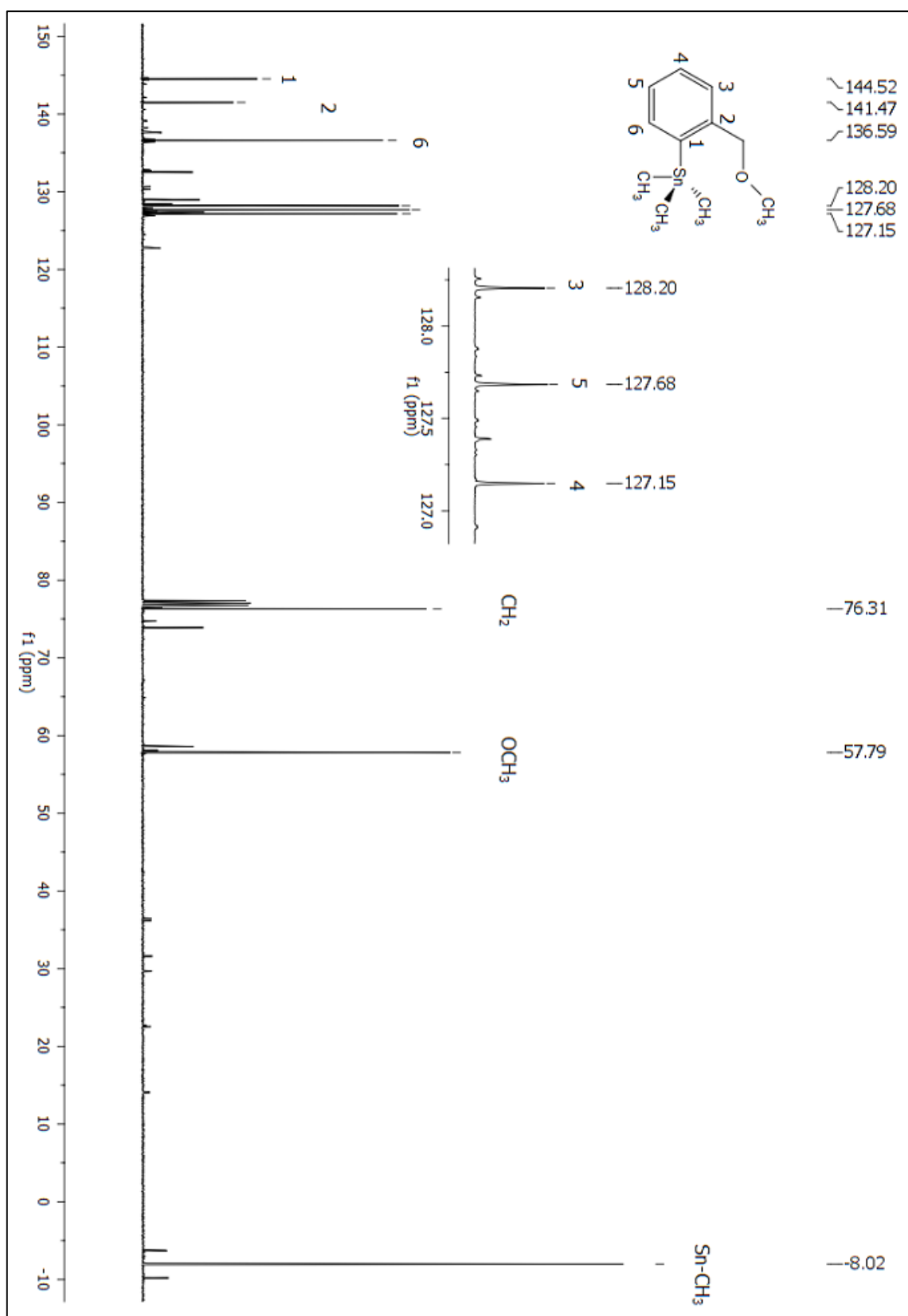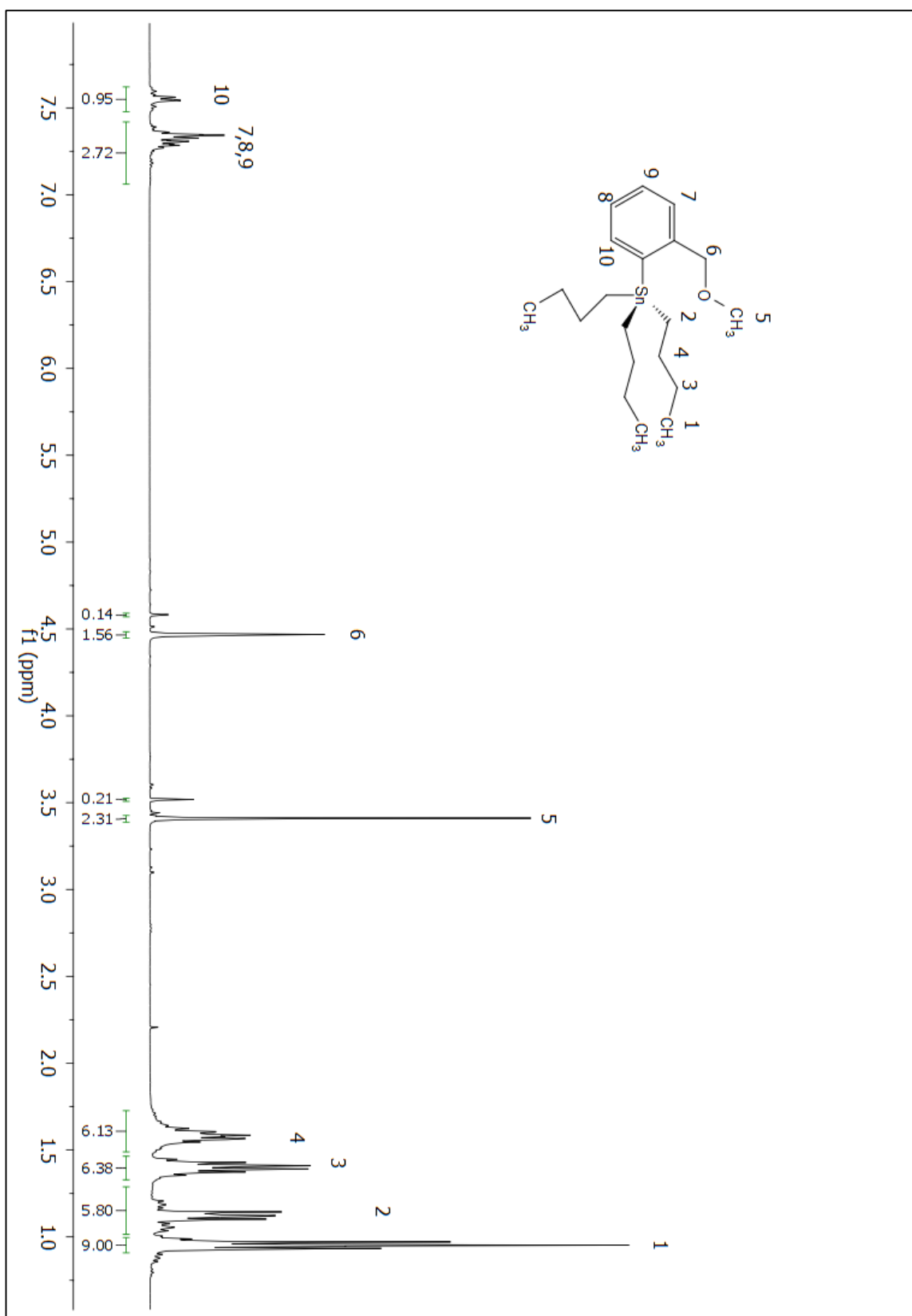
Figure A 67: ^{1}H NMR (CDCl$_3$) spectrum of compound **217**.
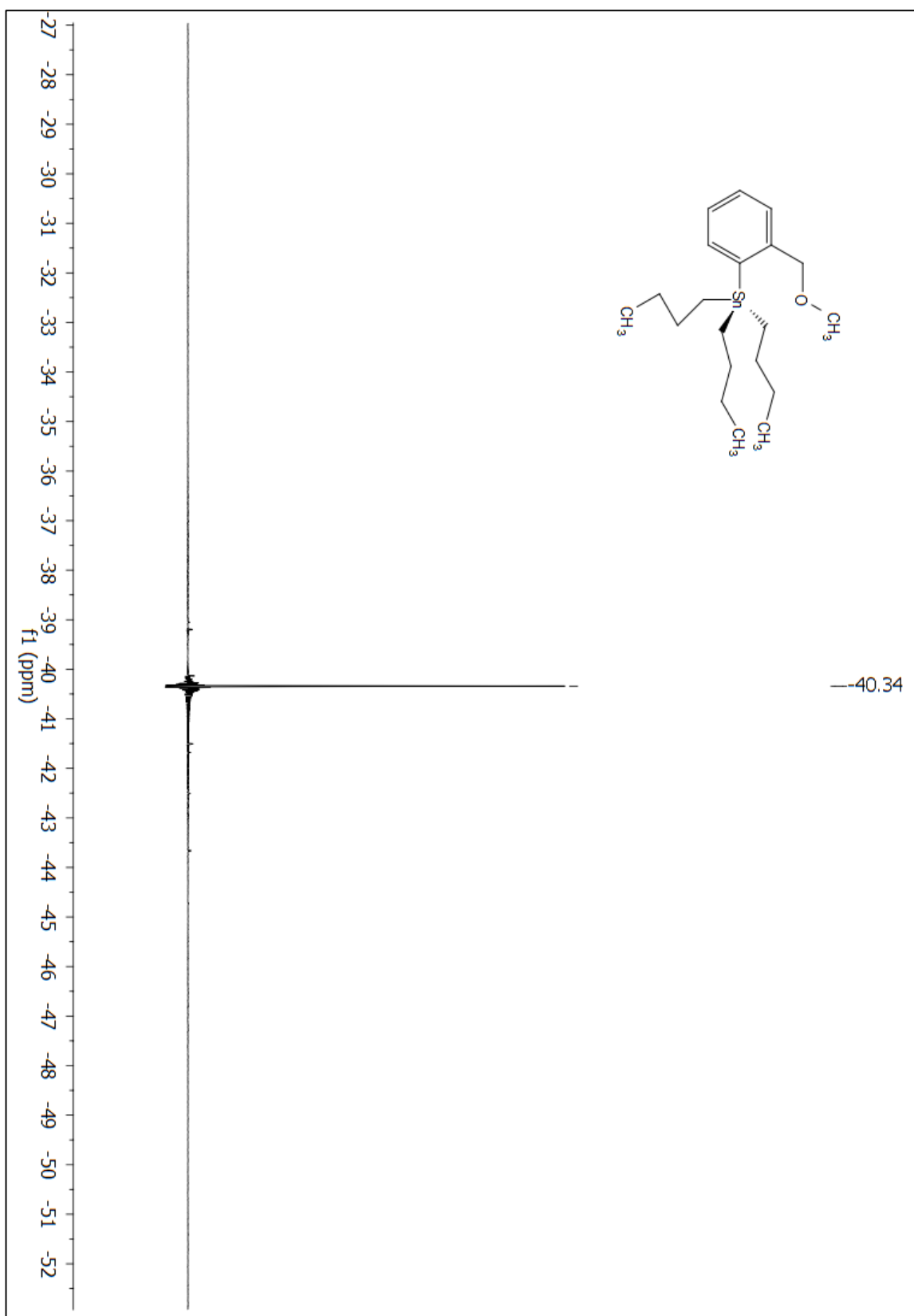
Figure A 68: ^{119}Sn NMR (CDCl$_3$) spectrum of compound 217.

Figure A 69: ^{13}C NMR (CDCl$_3$) spectrum of compound 217.
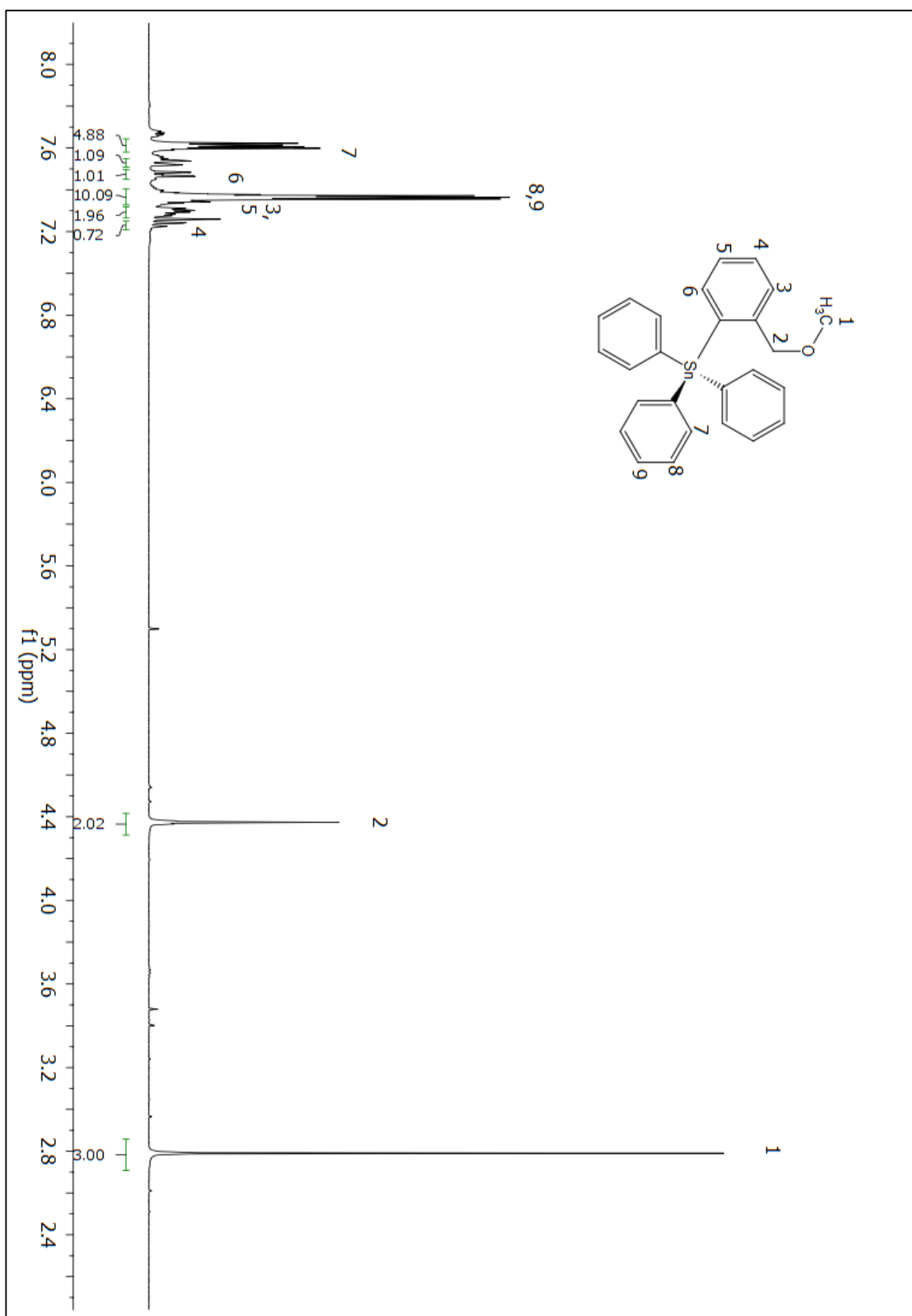
Figure A 70: ¹H NMR (CDCl₃) spectrum of compound 112.
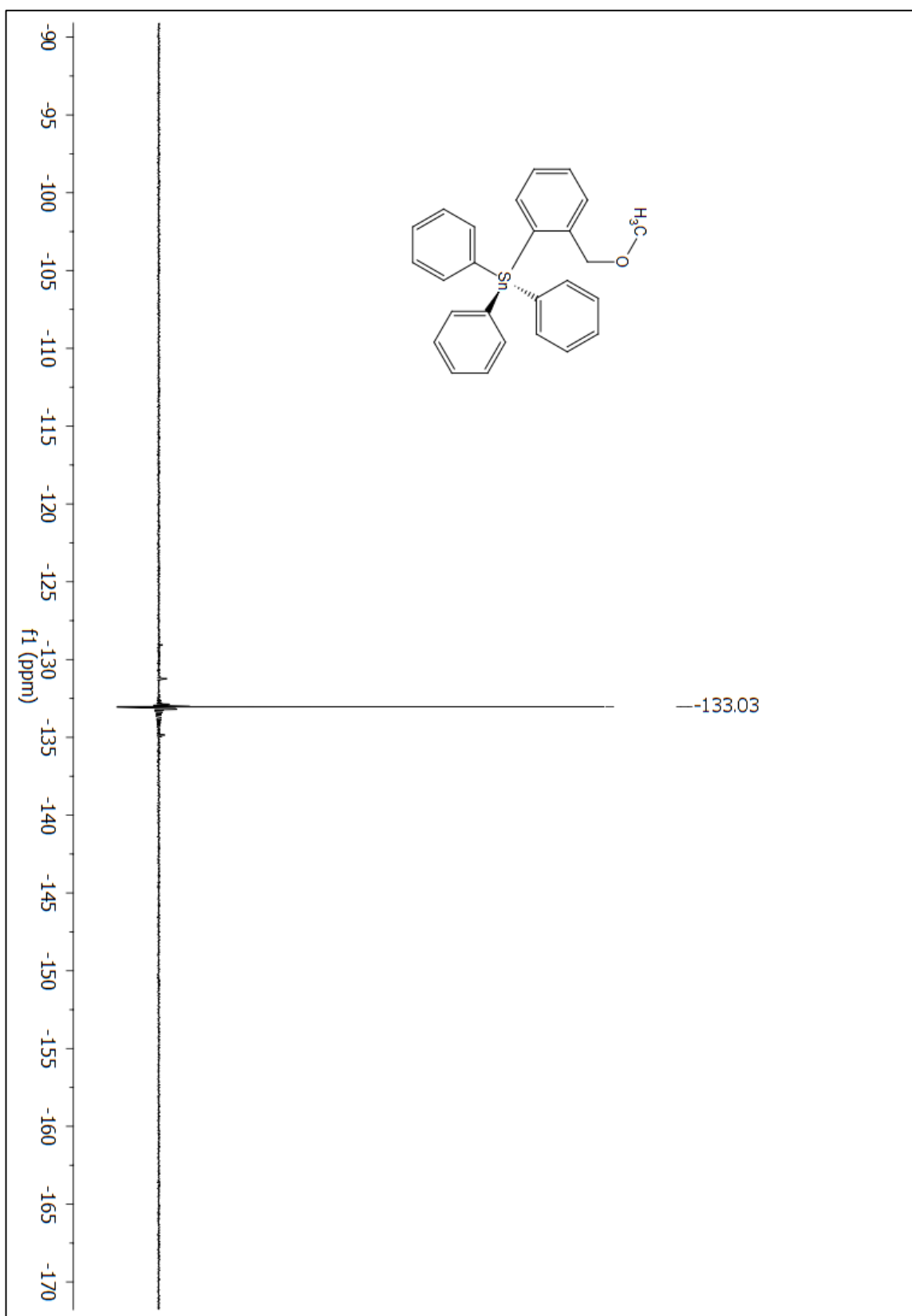
Figure A 71: ^{119}Sn NMR (CDCl$_3$) spectrum of compound 112.
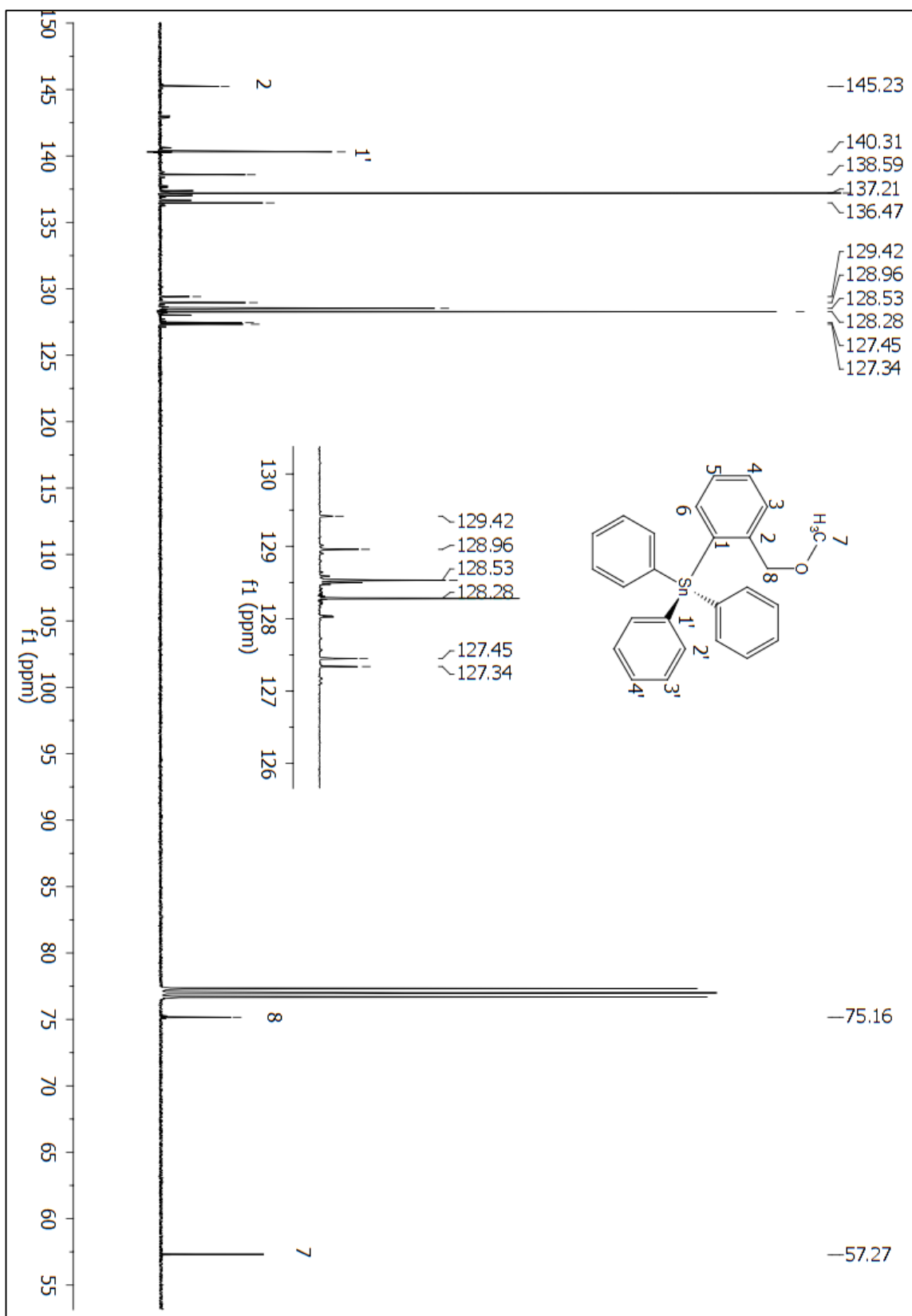
Figure A 72: ^{13}C NMR (CDCl$_3$) spectrum of compound **112.**
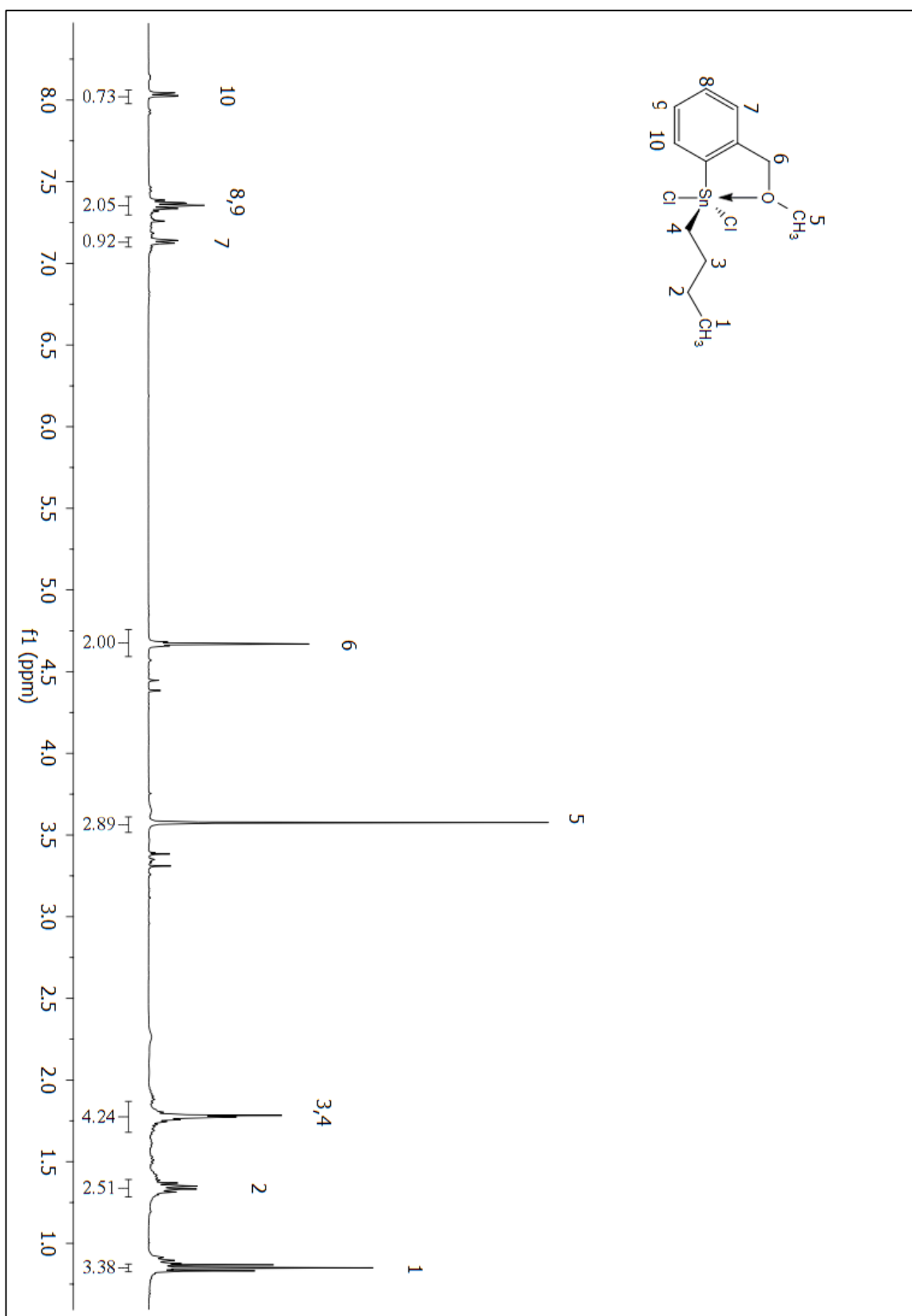
Figure A 73: ¹H NMR (CDCl₃) spectrum of compound 219.
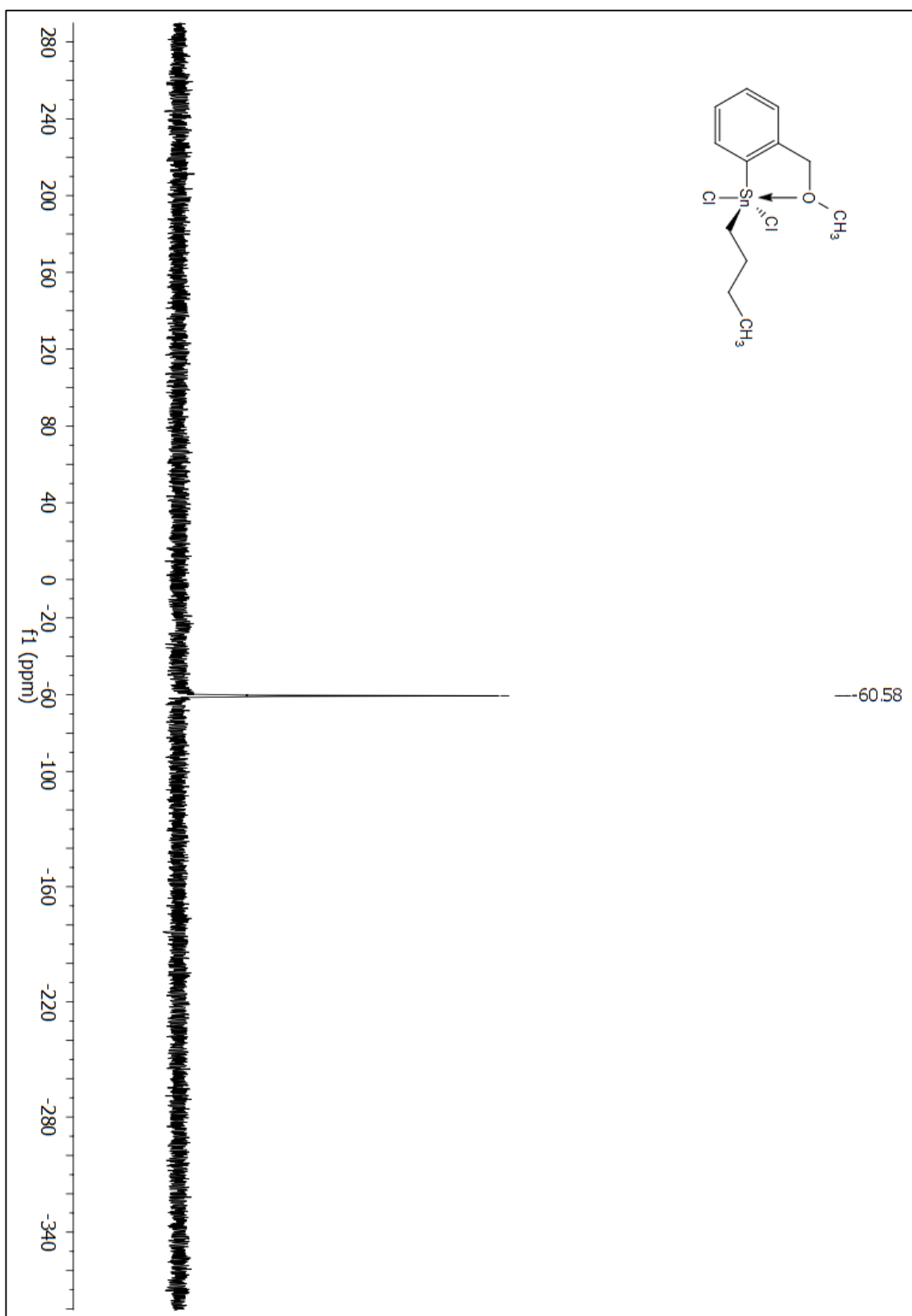
Figure A 74: ^{119}Sn NMR (CDCl$_3$) spectrum of compound 219.
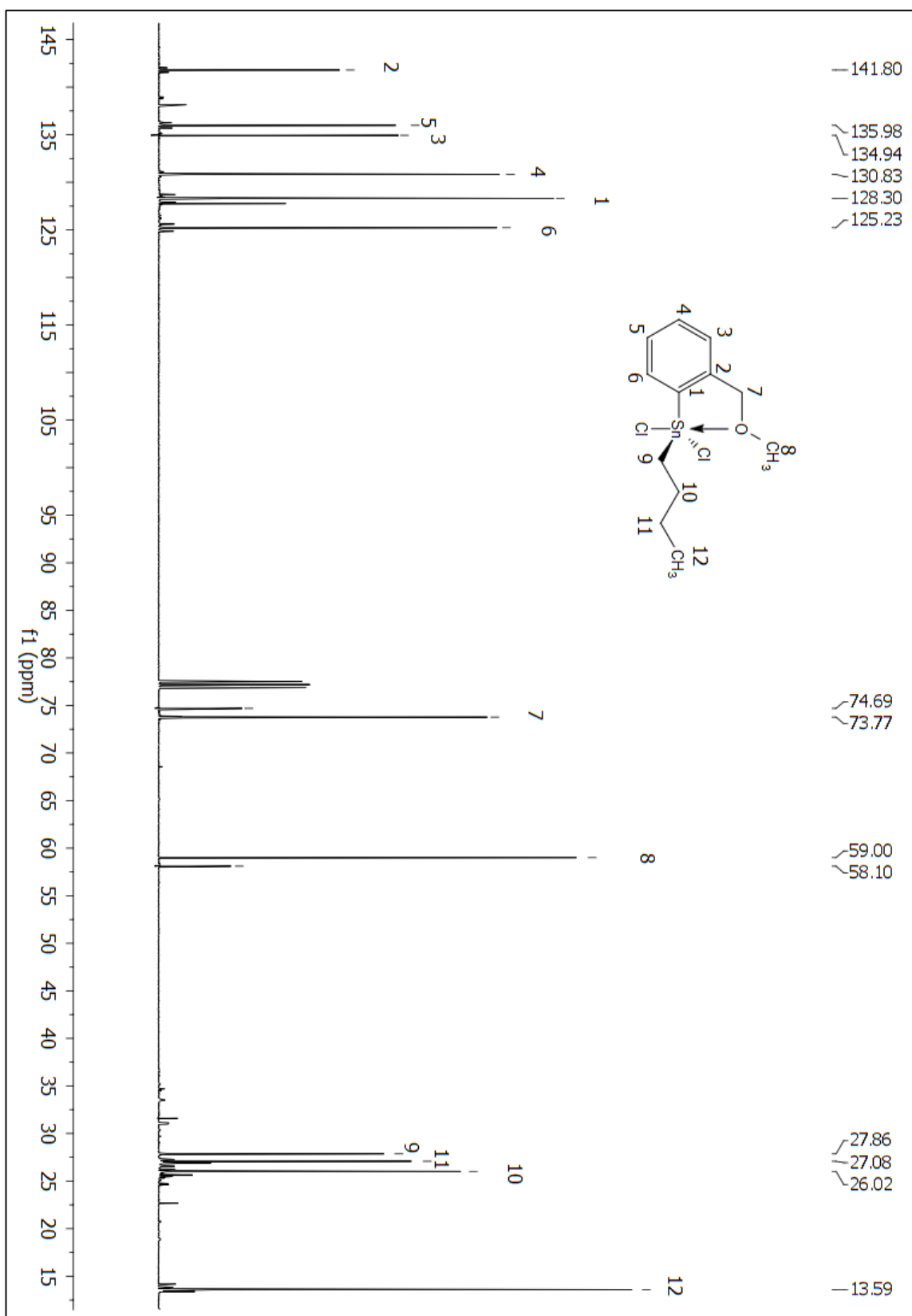
Figure A 75: ^{13}C NMR (CDCl$_3$) spectrum of compound 219.
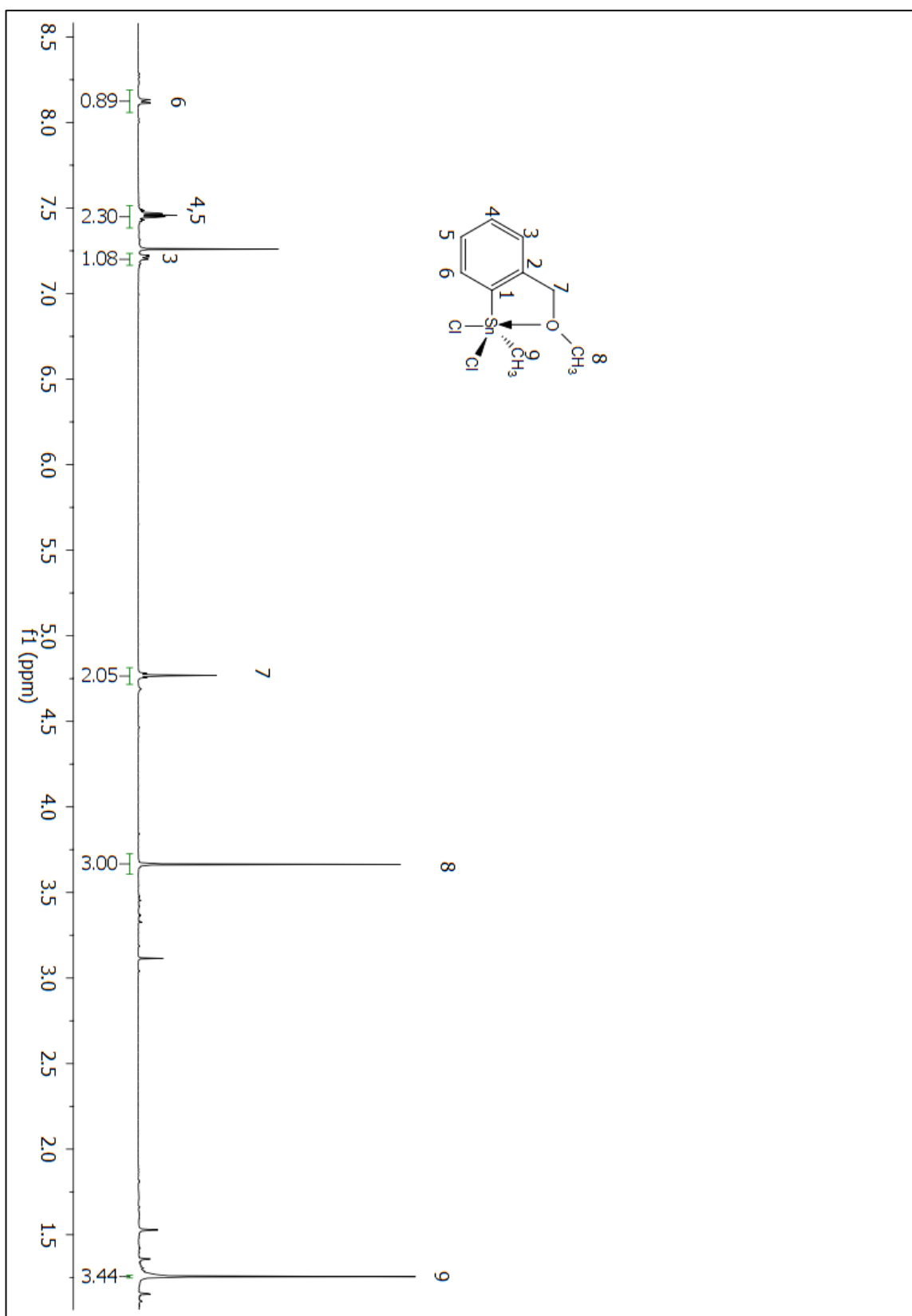
Figure A 76: ^{1}H NMR (CDCl$_3$) spectrum of compound 218.
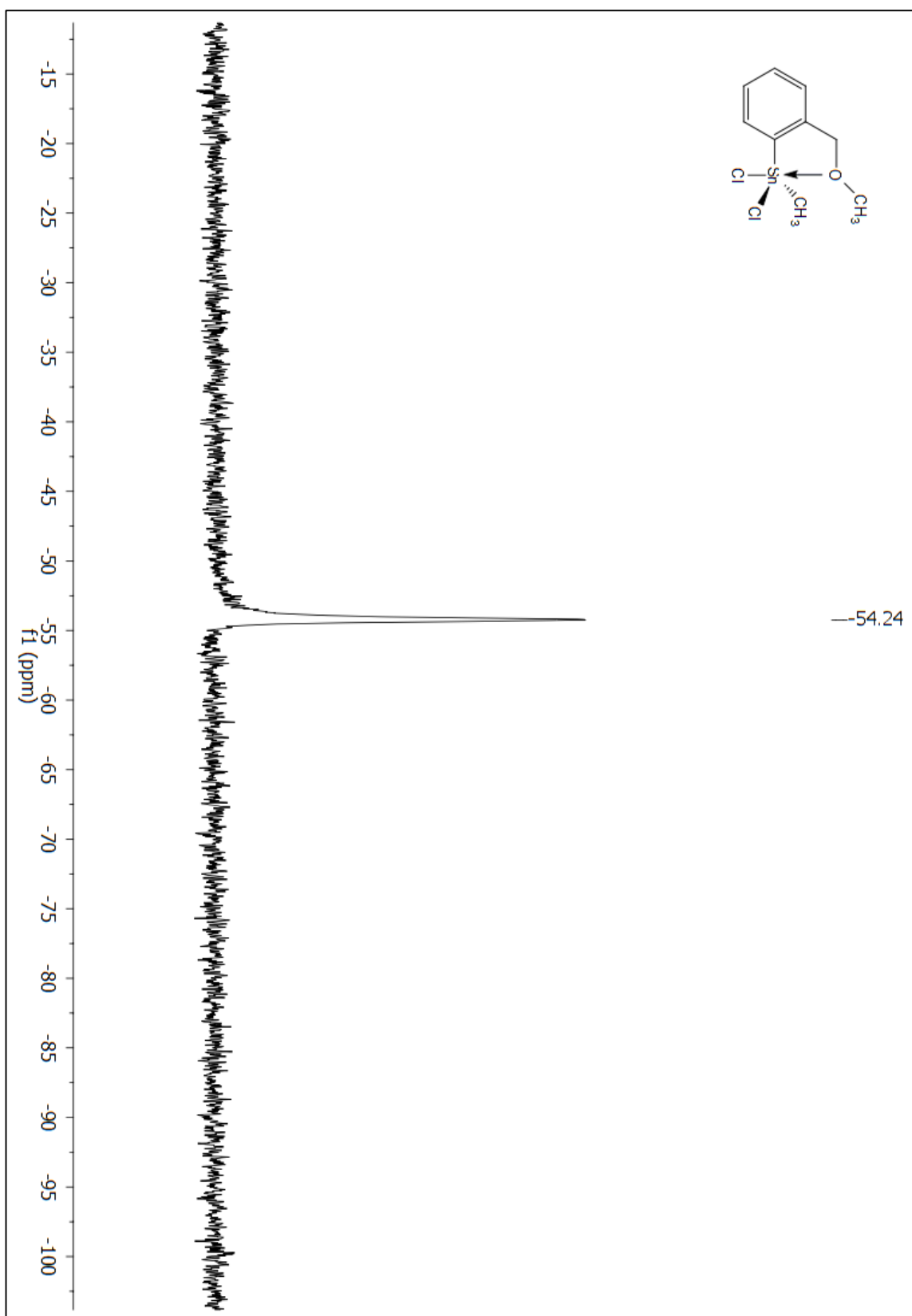
Figure A 77: ^{119}Sn NMR (CDCl$_3$) spectrum of compound 218.
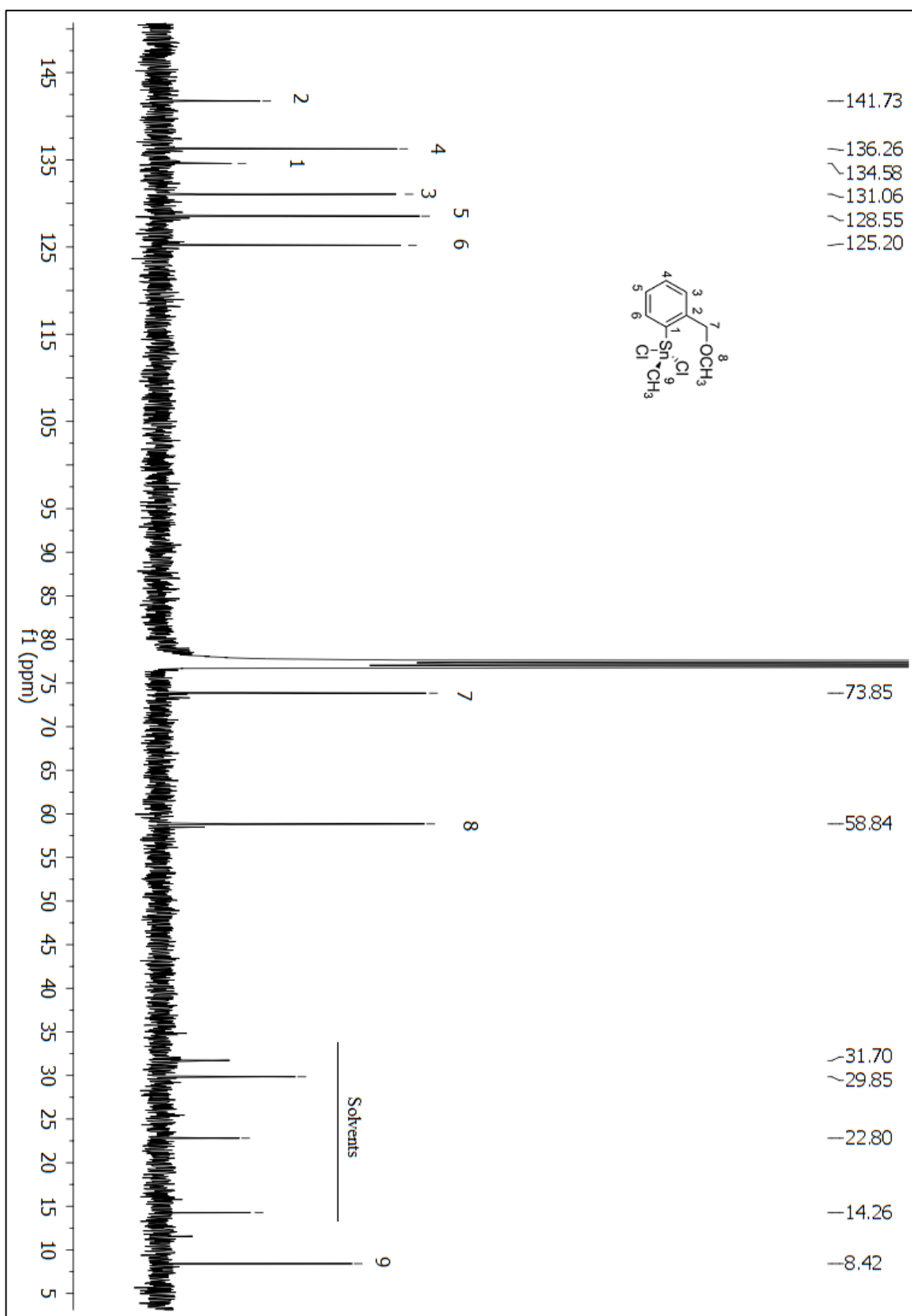
Figure A 78: ^{13}C NMR (CDCl$_3$) spectrum of compound 218.
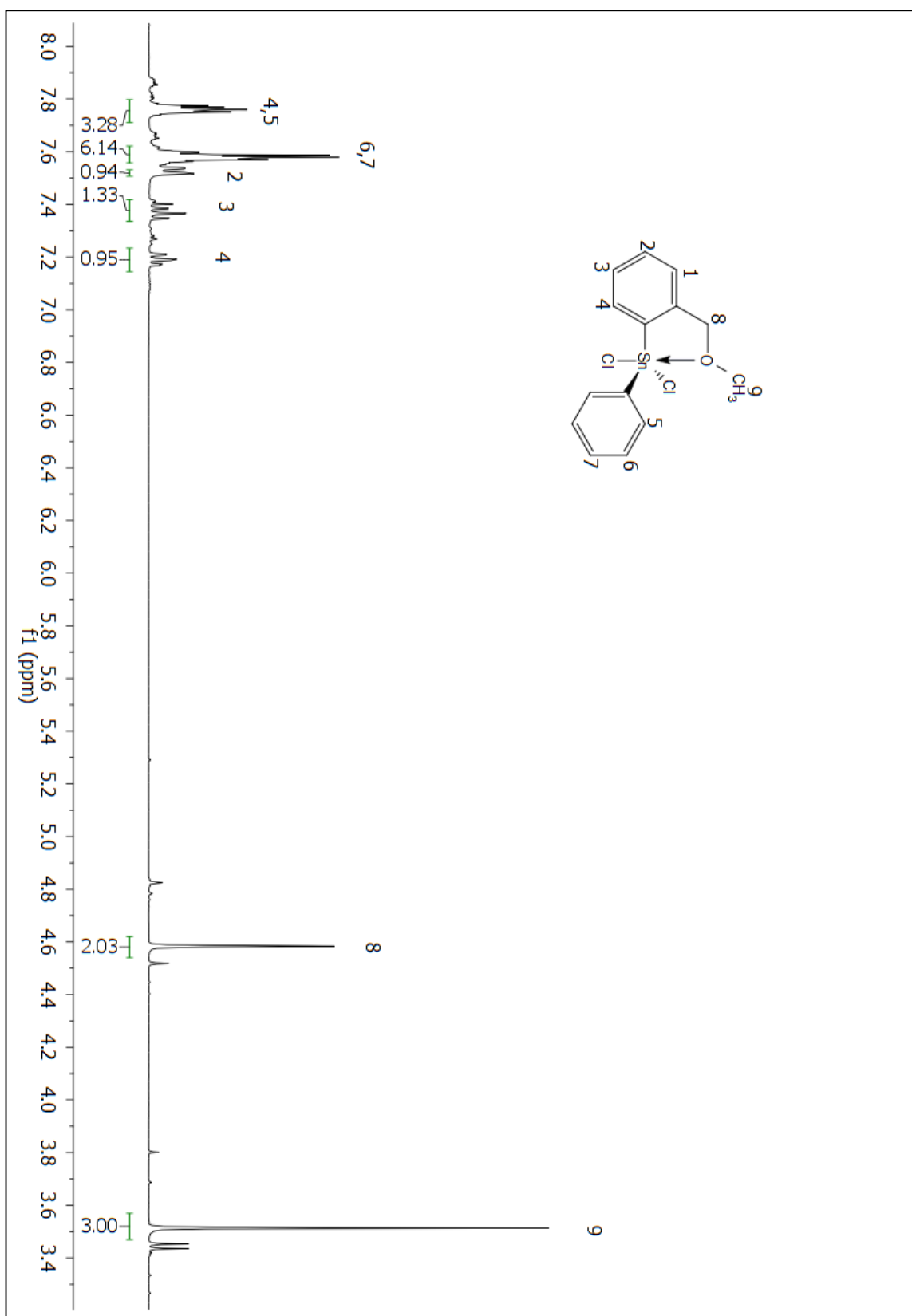
Figure A 79: ¹H NMR (CDCl₃) spectrum of compound 220.
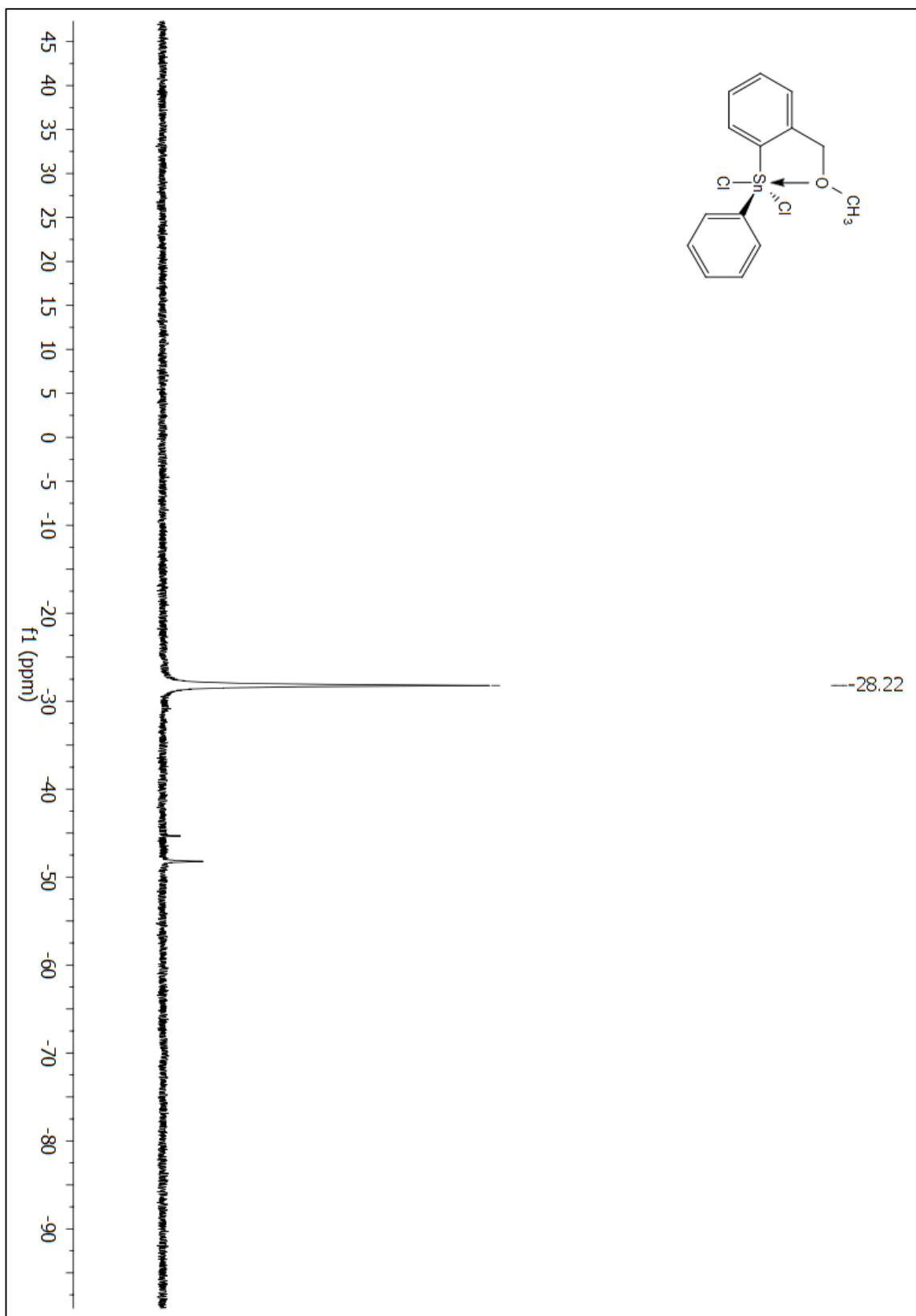
Figure A 80: ^{119}Sn NMR (CDCl$_3$) spectrum of compound 220.
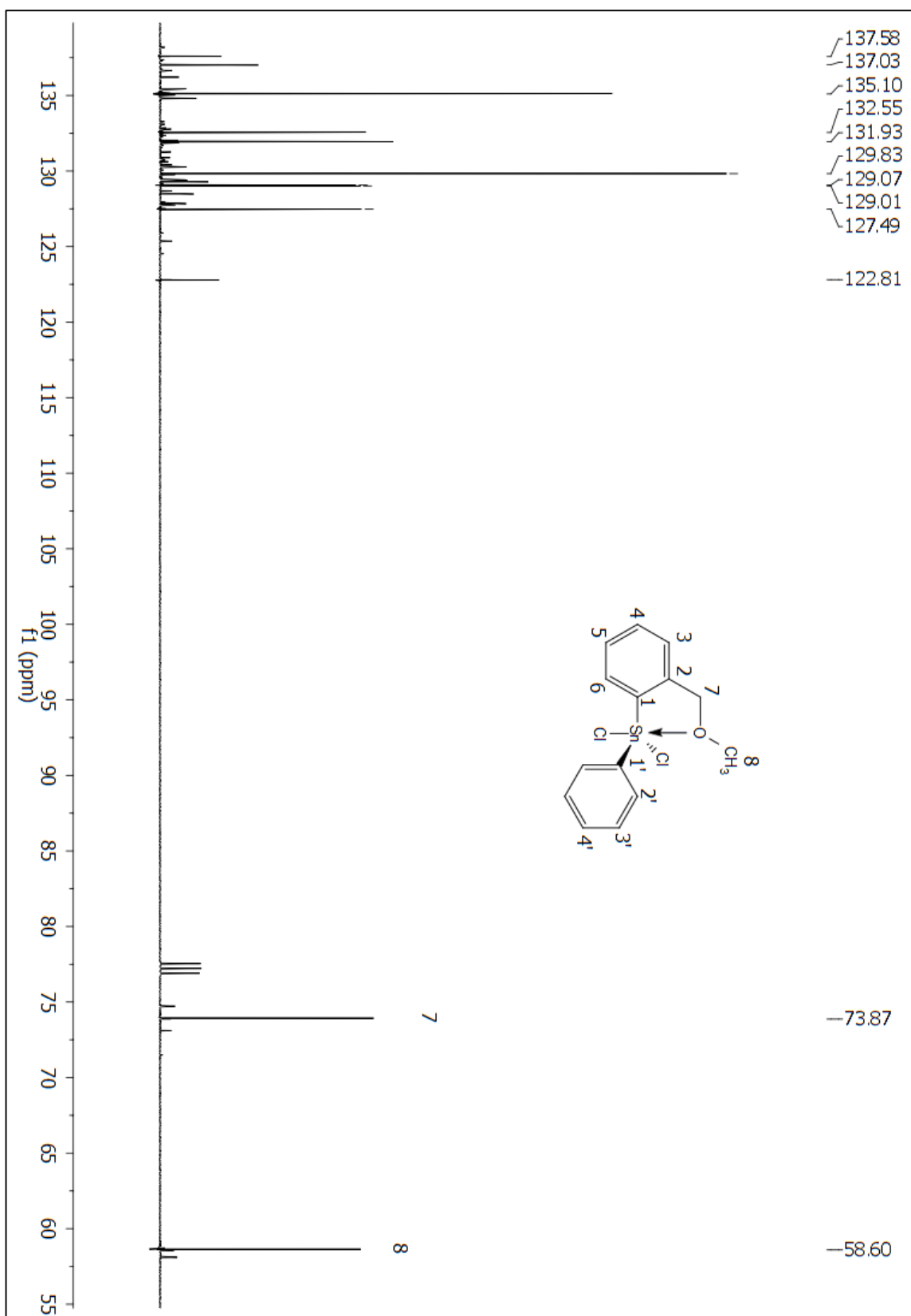
Figure A 81: ^{13}C NMR (CDCl$_3$) spectrum of compound **220.**
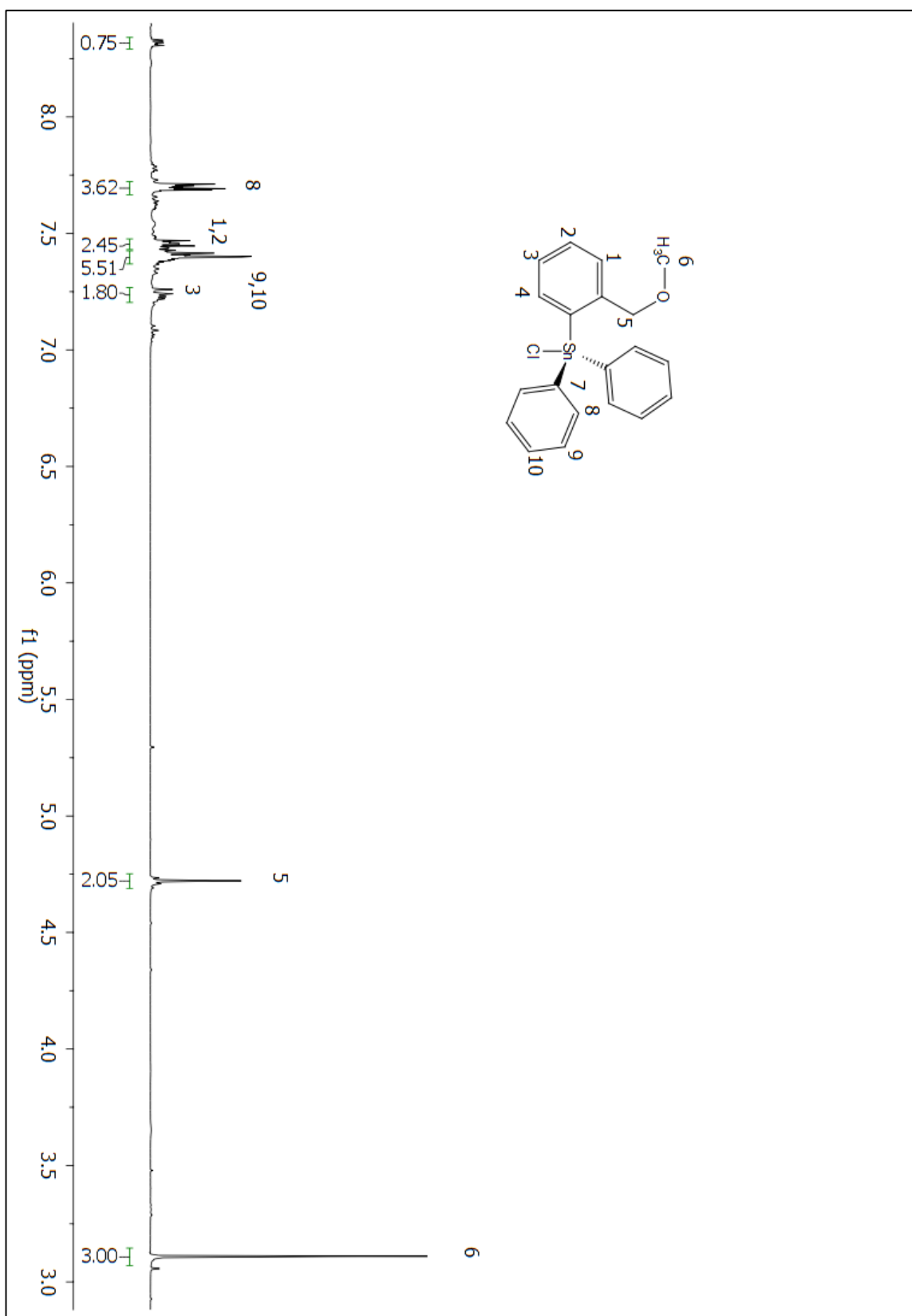
Figure A 82: ^{1}H NMR (CDCl$_3$) spectrum of compound 221.
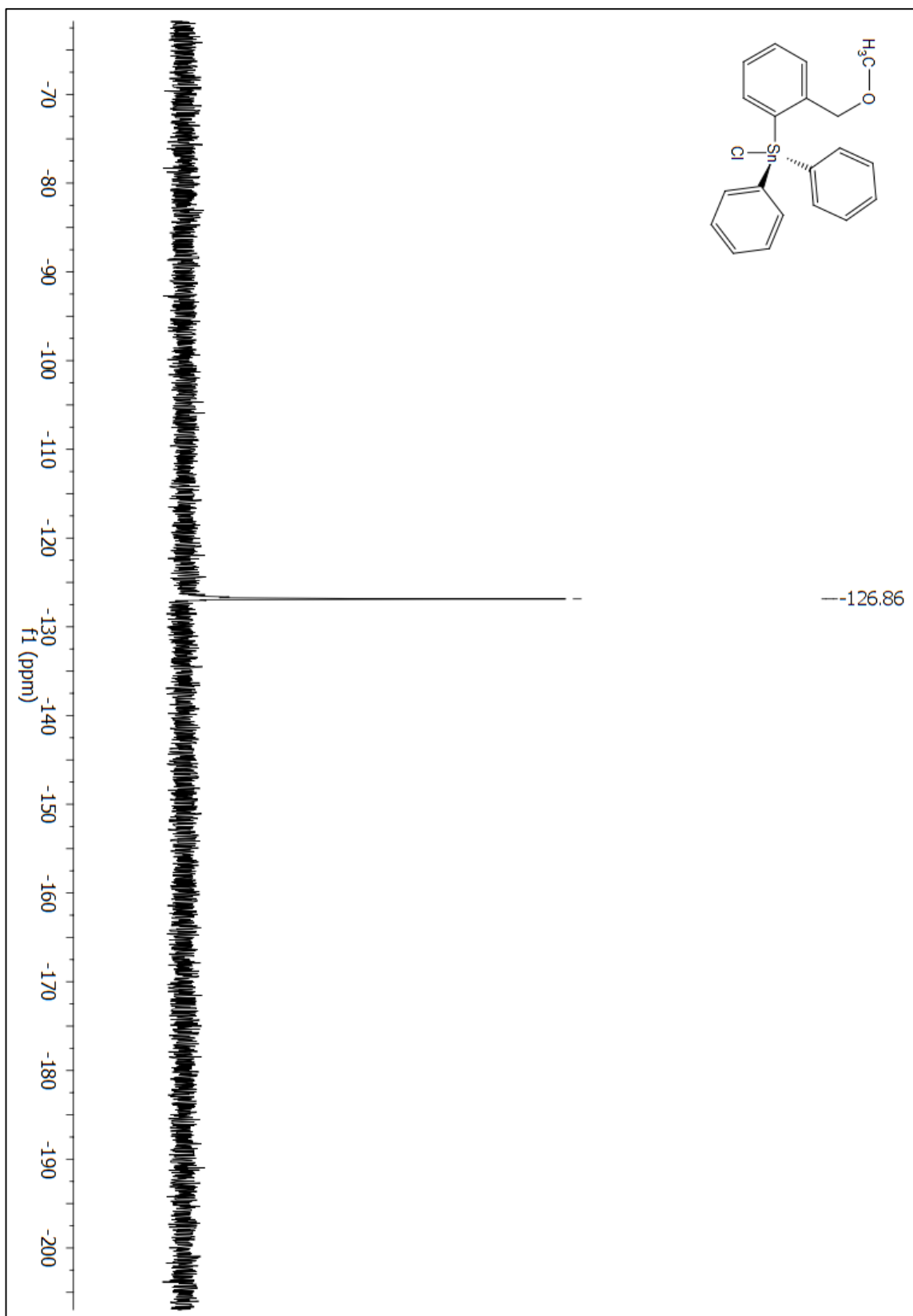
Figure A 83: ^{119}Sn NMR (CDCl$_3$) spectrum of compound **221.**
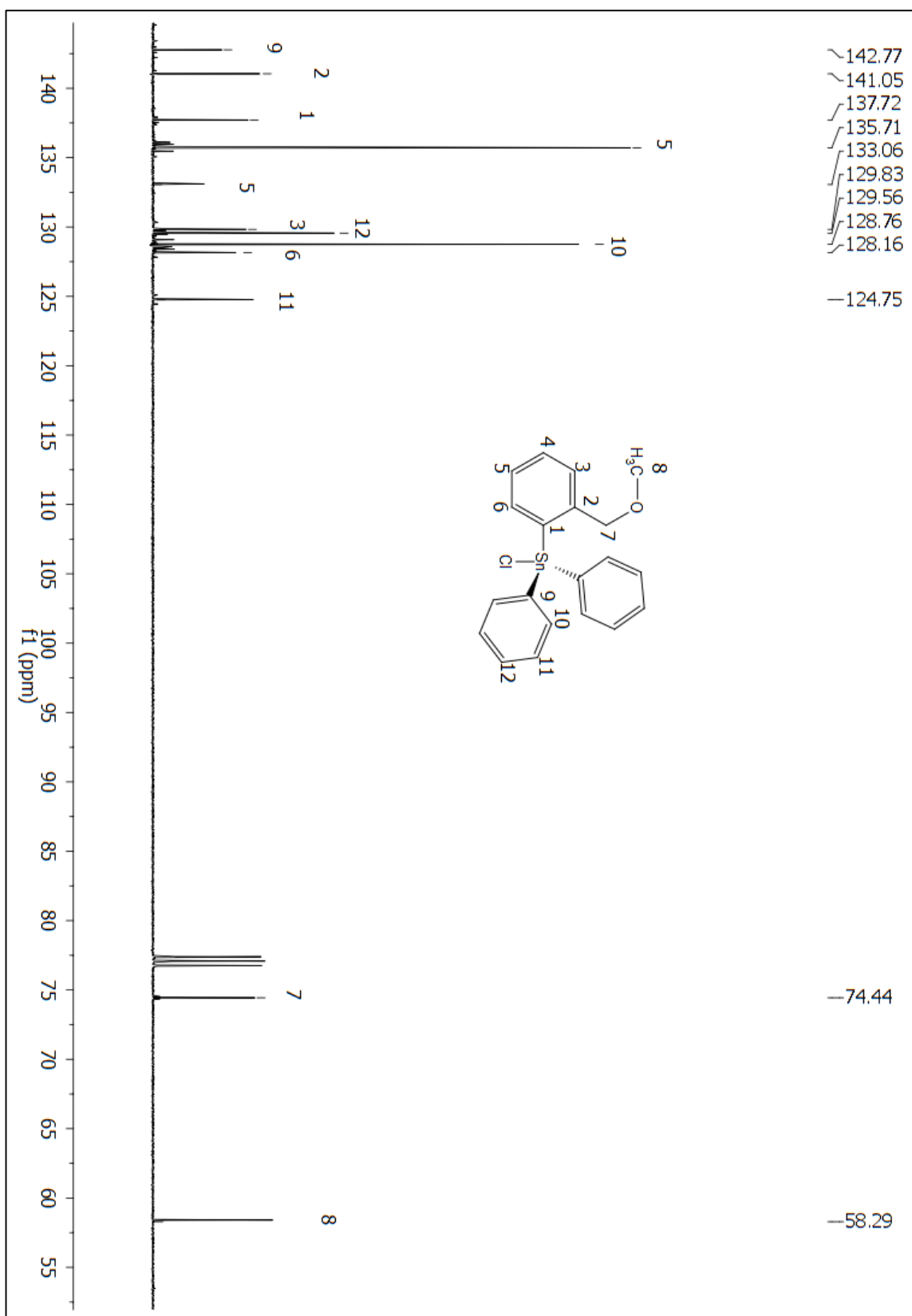
Figure A 84: ^{13}C NMR (CDCl$_3$) spectrum of compound **221.**
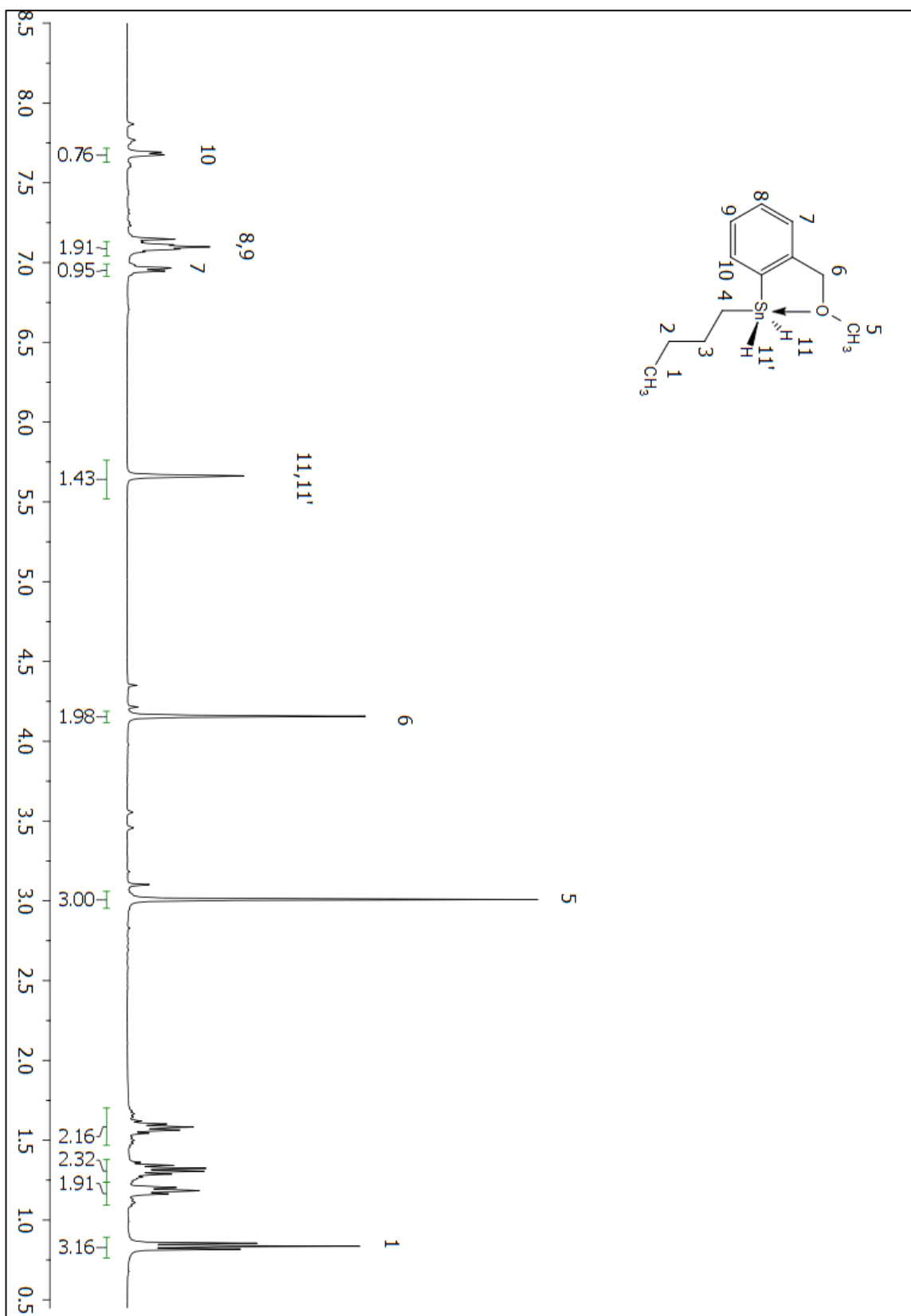
Figure A 85: ¹H NMR (C₆D₆) spectrum of compound 227.
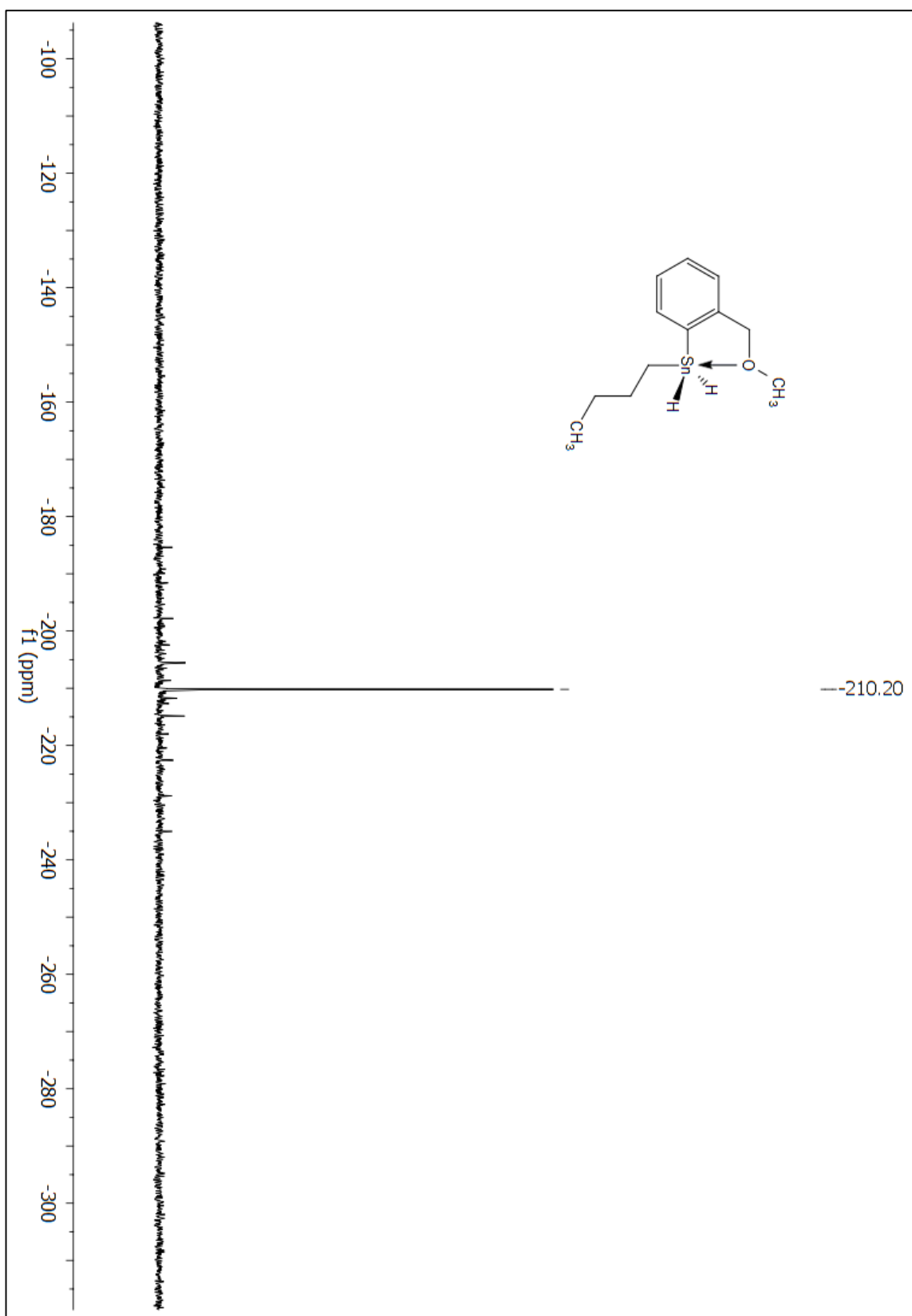
Figure A 86: ^{119}Sn NMR (C$_6$D$_6$) spectrum of compound **227.**
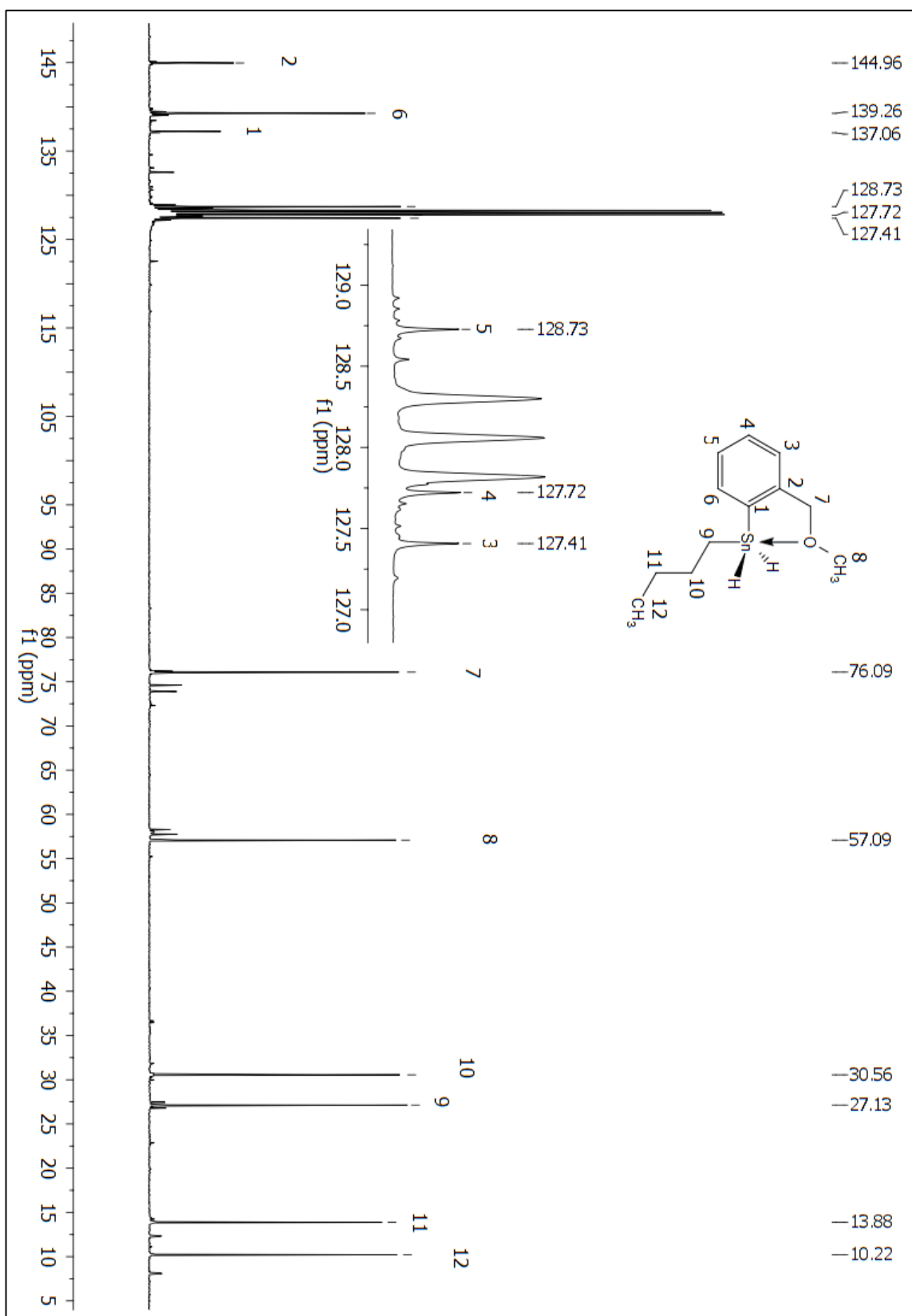
Figure A 87: ^{13}C NMR (C$_6$D$_6$) spectrum of compound **227**.

314
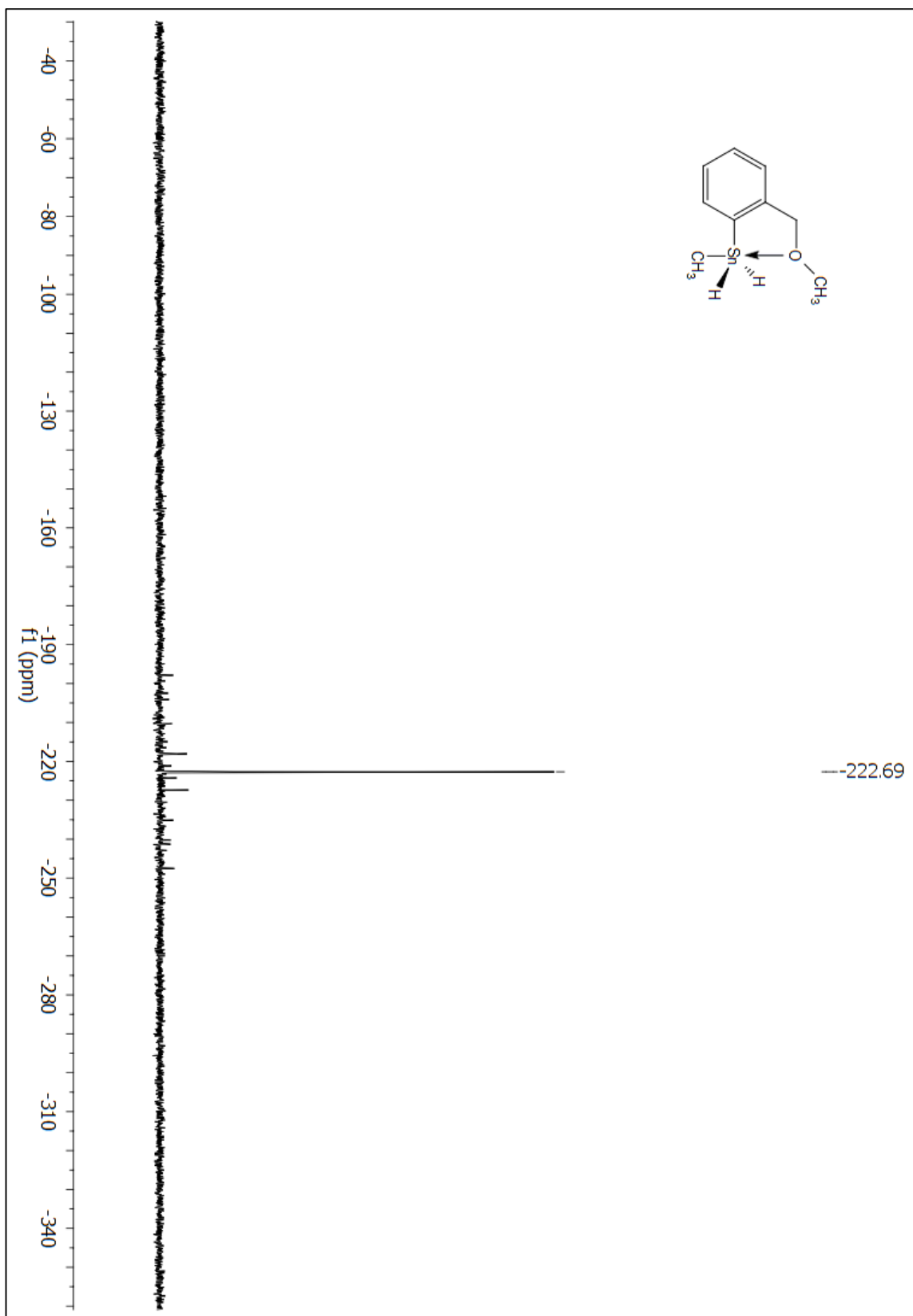
Figure A 88: ^{119}Sn NMR (C$_6$D$_6$) spectrum of compound 226.

---222.69
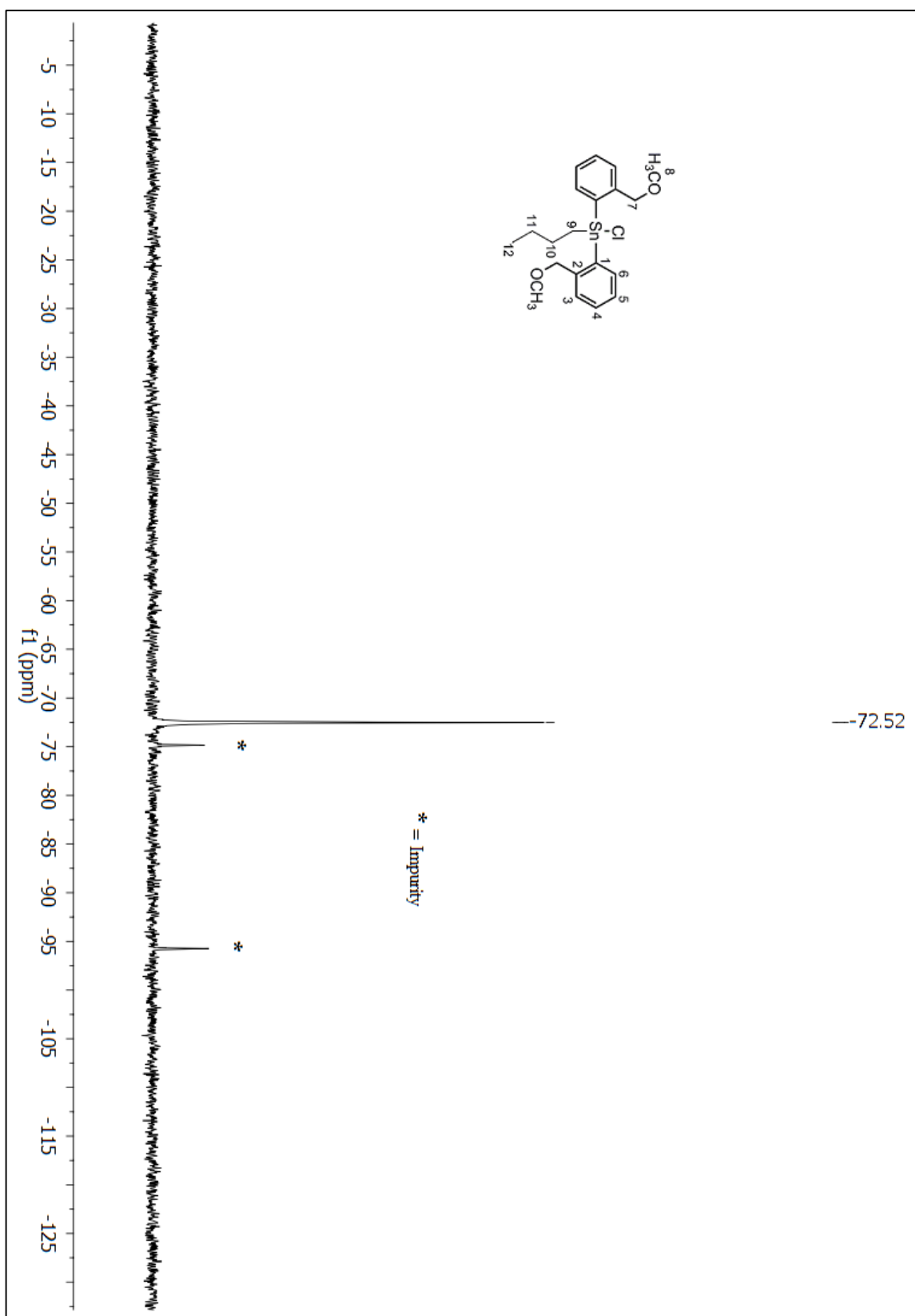
Figure A 89: ^{119}Sn NMR (CDCl$_3$) spectrum of compound **224**

Figure A 90: ^{1}H NMR (CDCl$_3$) spectrum of compound 225
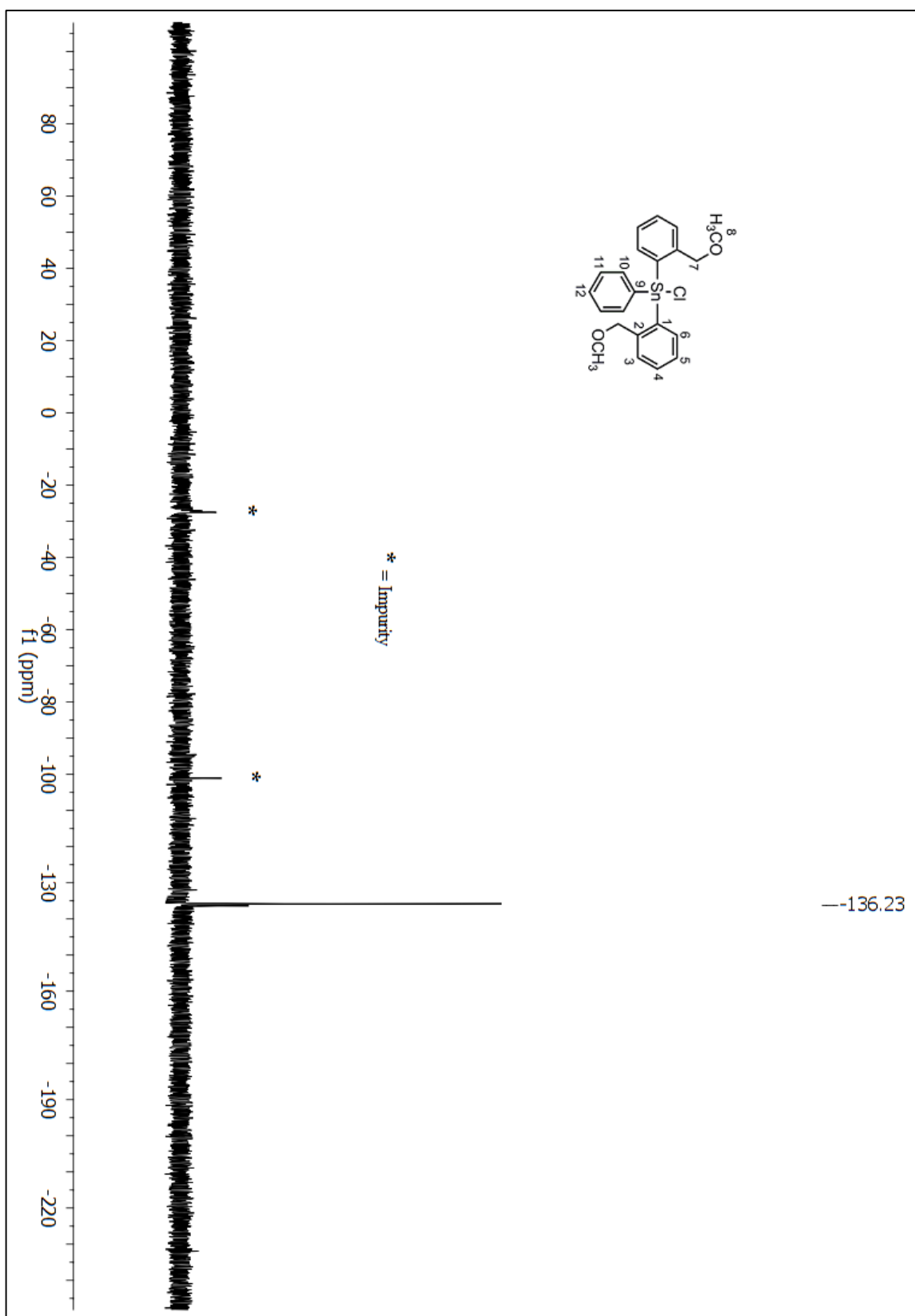
Figure A 91: ^{119}Sn NMR (CDCl$_3$) spectrum of compound **225**
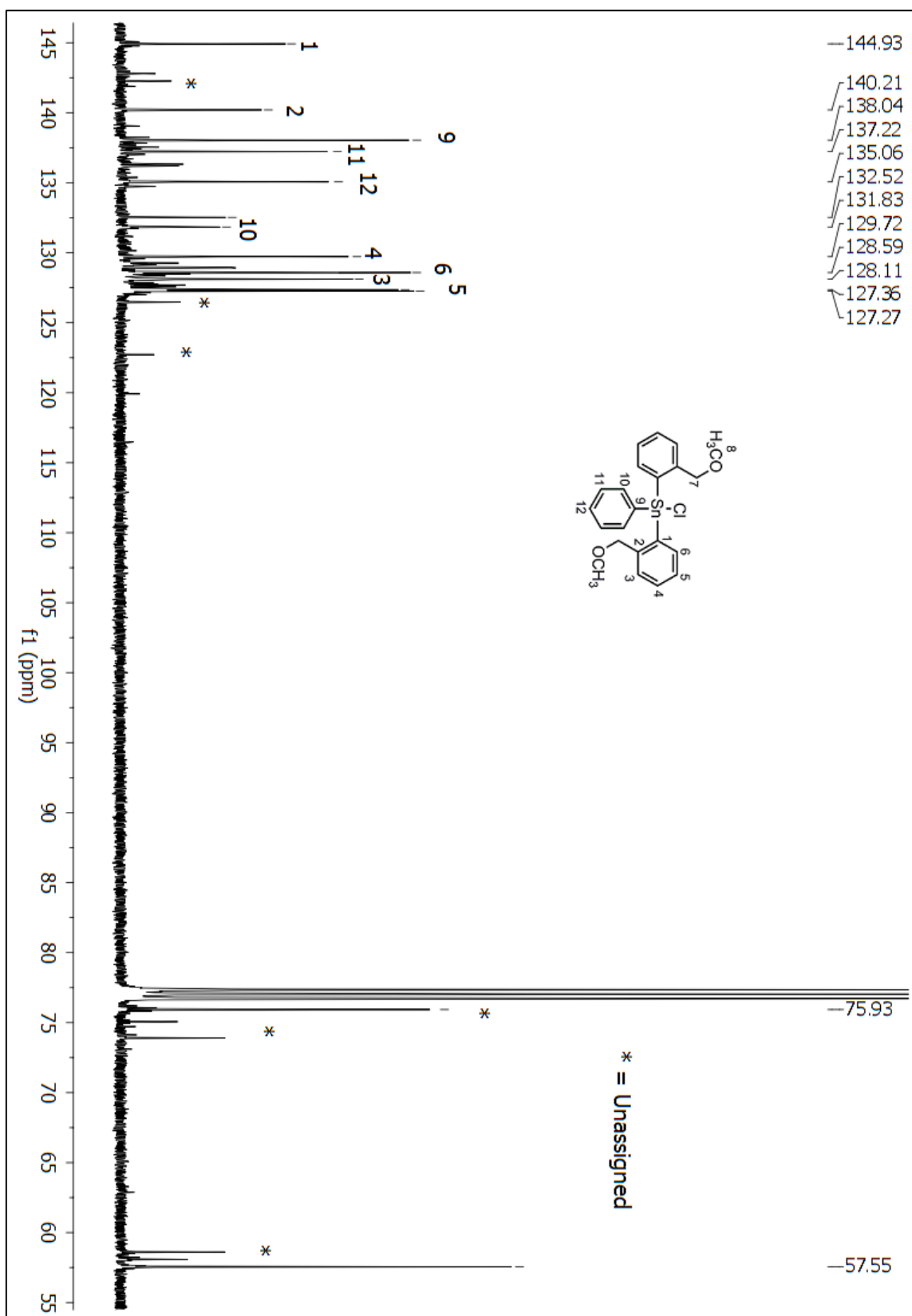
Figure A 92: ^{13}C NMR (CDCl$_3$) spectrum of compound 225
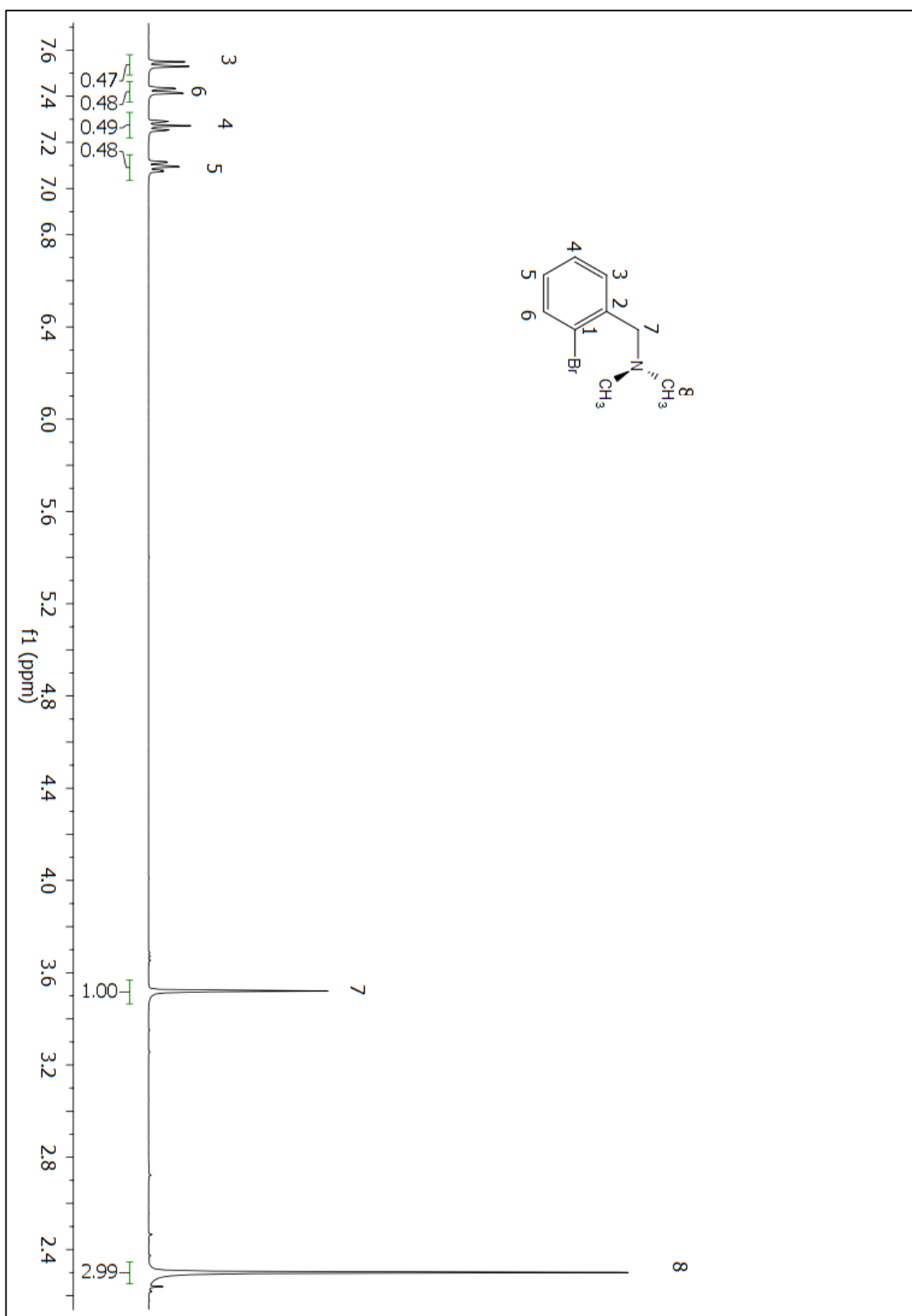
Figure A 93: ^{1}H NMR CDCl$_3$ spectrum of compound **228**
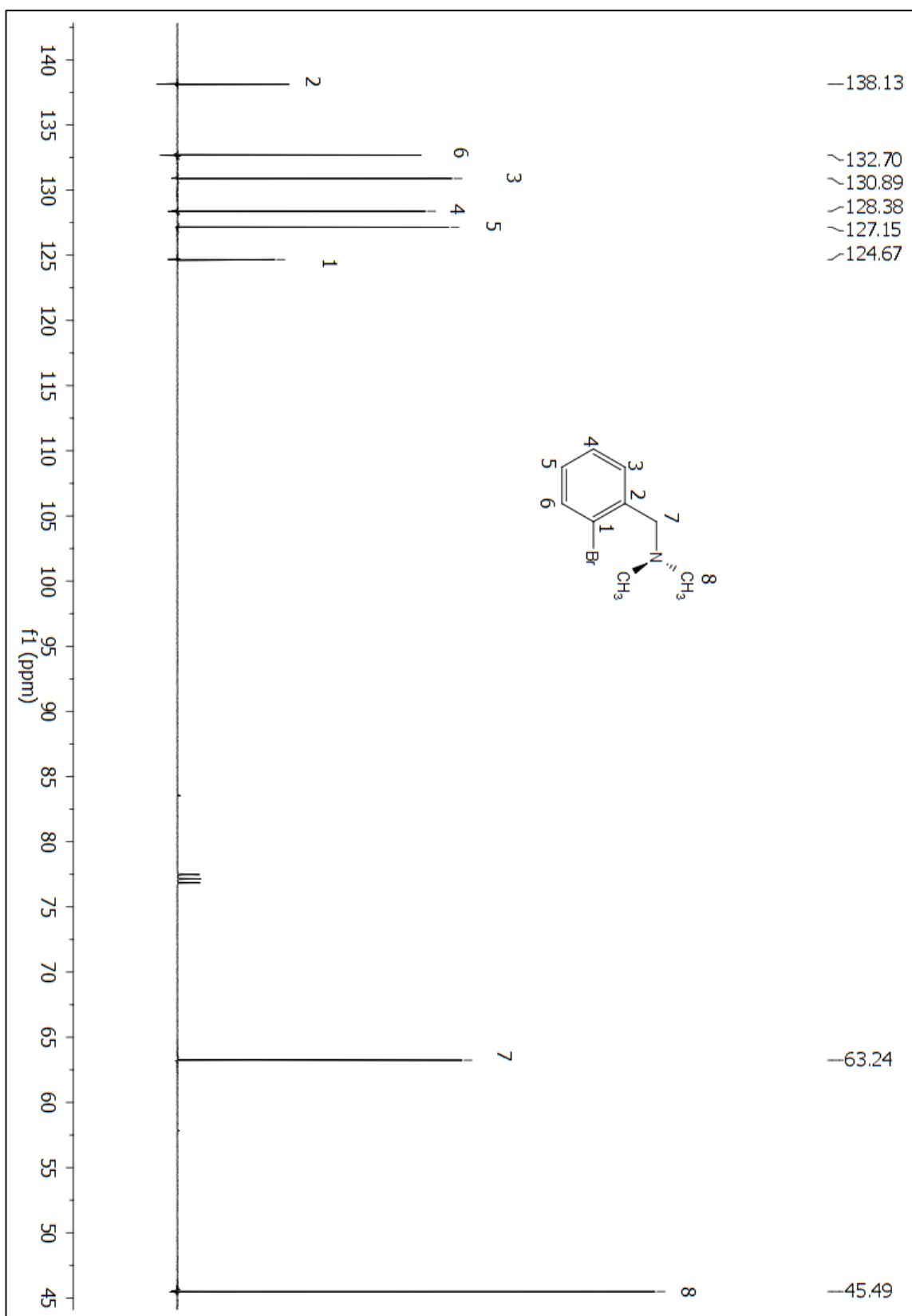
Figure A 94: ^{13}C (CDCl$_3$) NMR spectrum of compound **228**
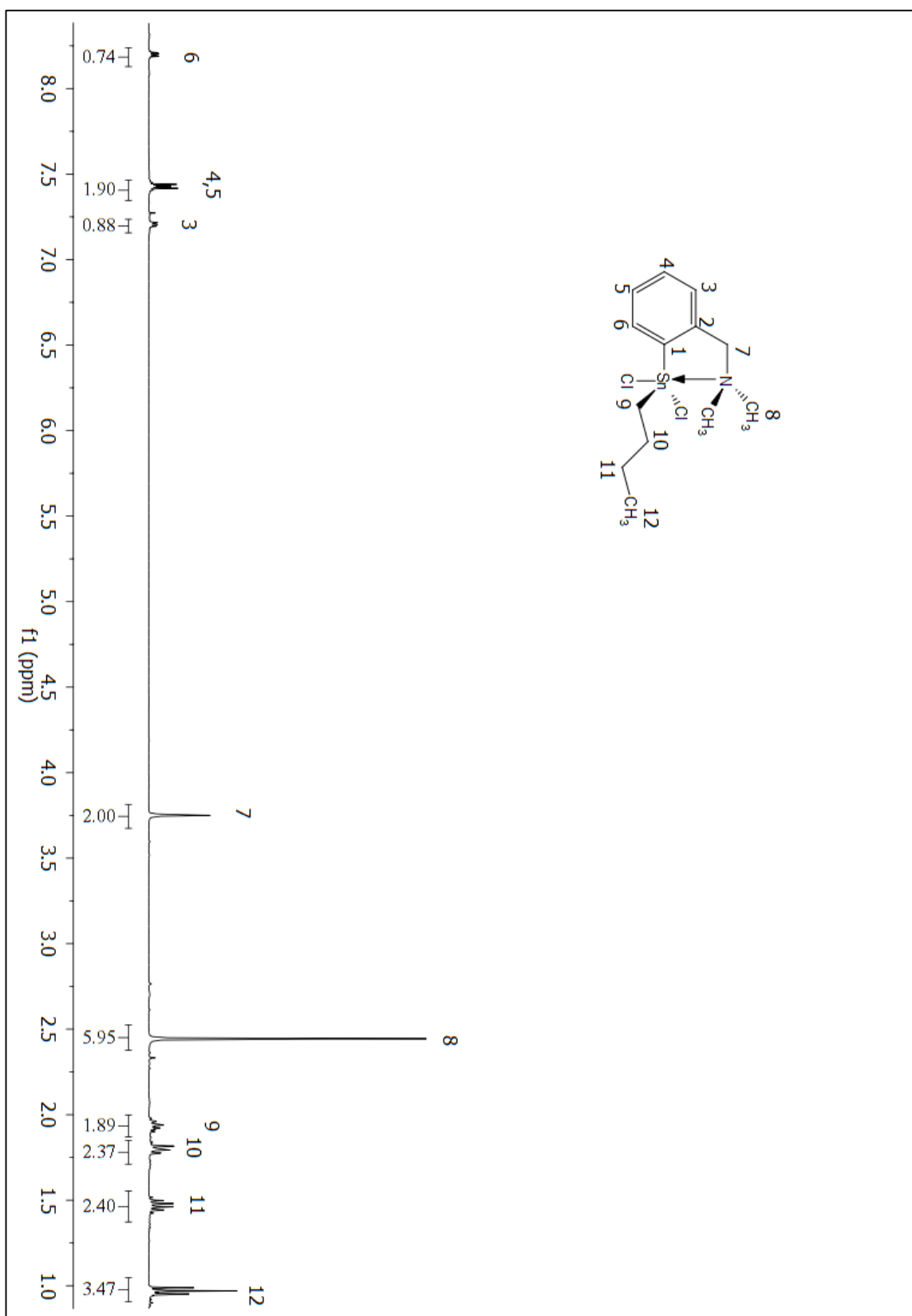
Figure A 95: ¹H NMR (CDCl₃) spectrum of compound 37.
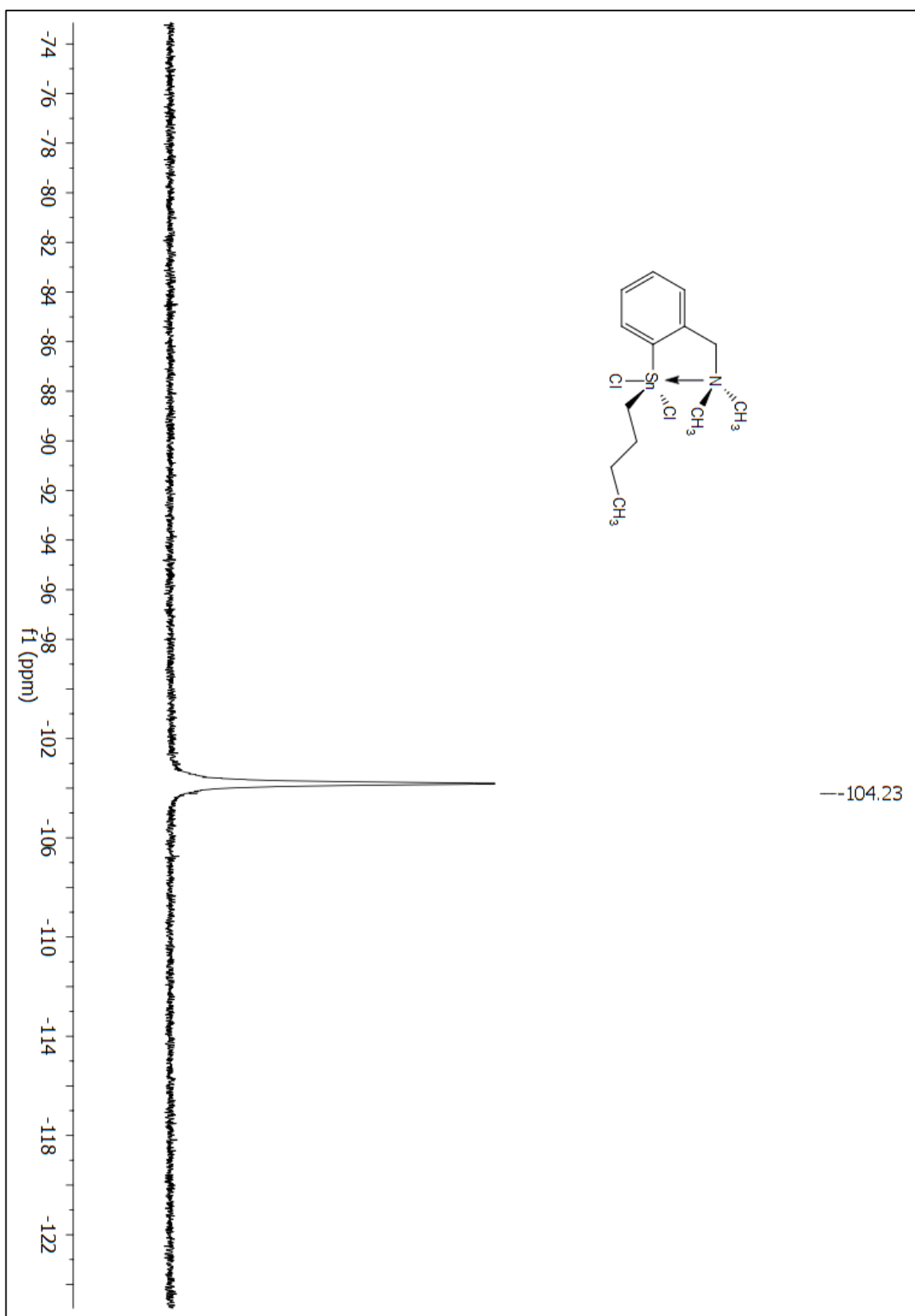
Figure A 96: ^{119}Sn NMR (CDCl$_3$) spectrum of compound 37.
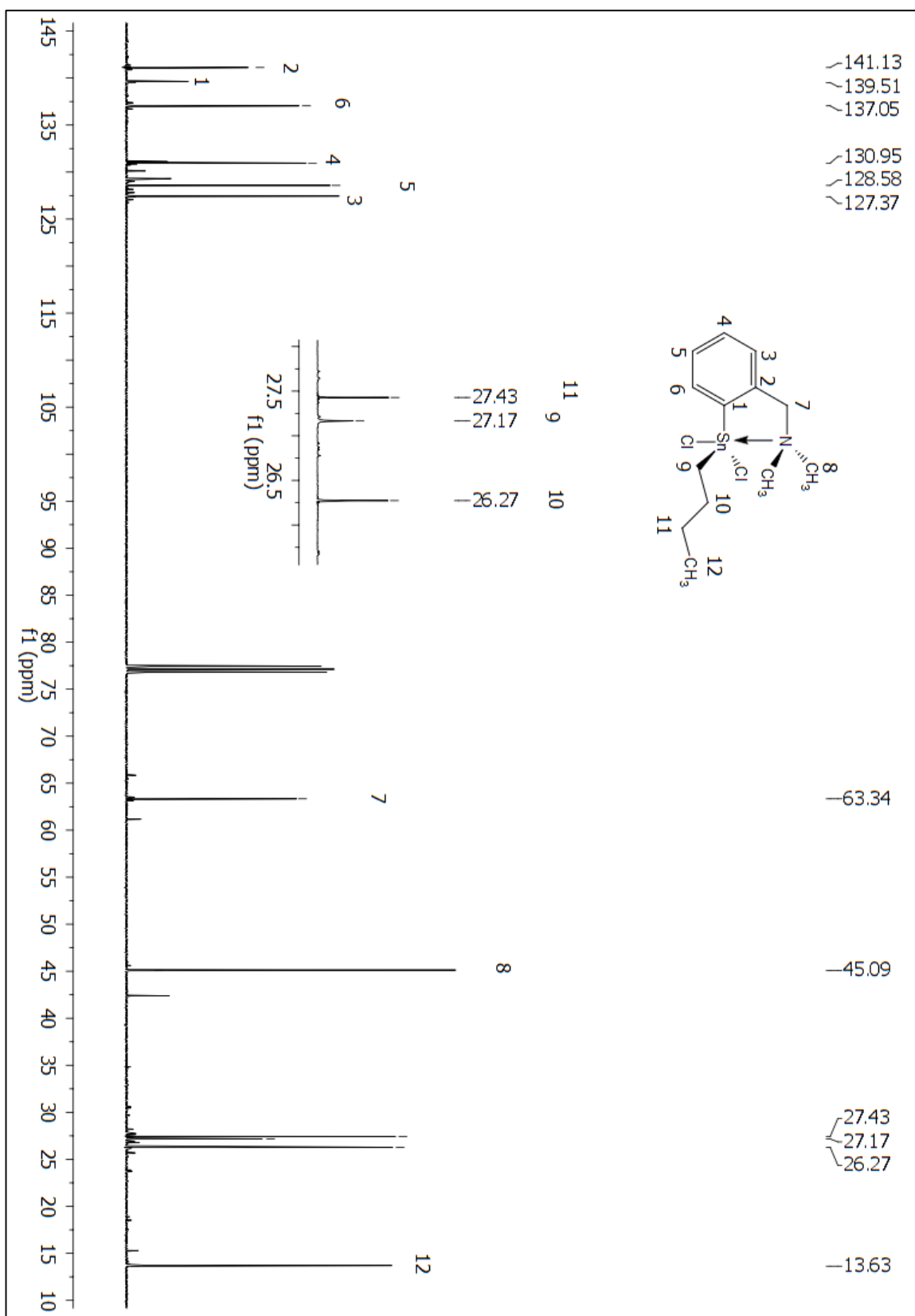
Figure A 97: ^{13}C NMR (CDCl$_3$) of compound **37**.
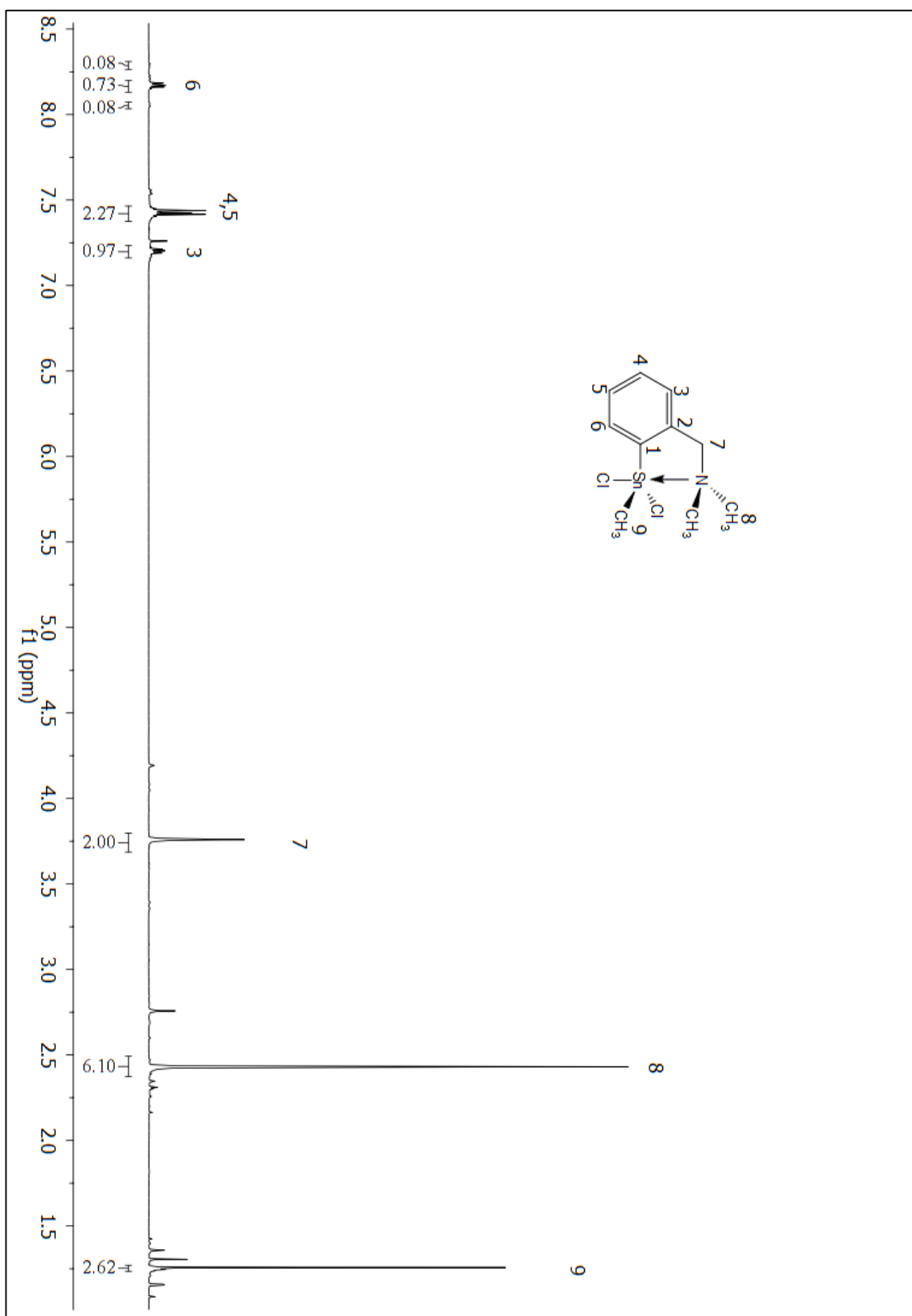
Figure A 98: ^{1}H NMR (CDCl$_3$) spectrum of compound 33.
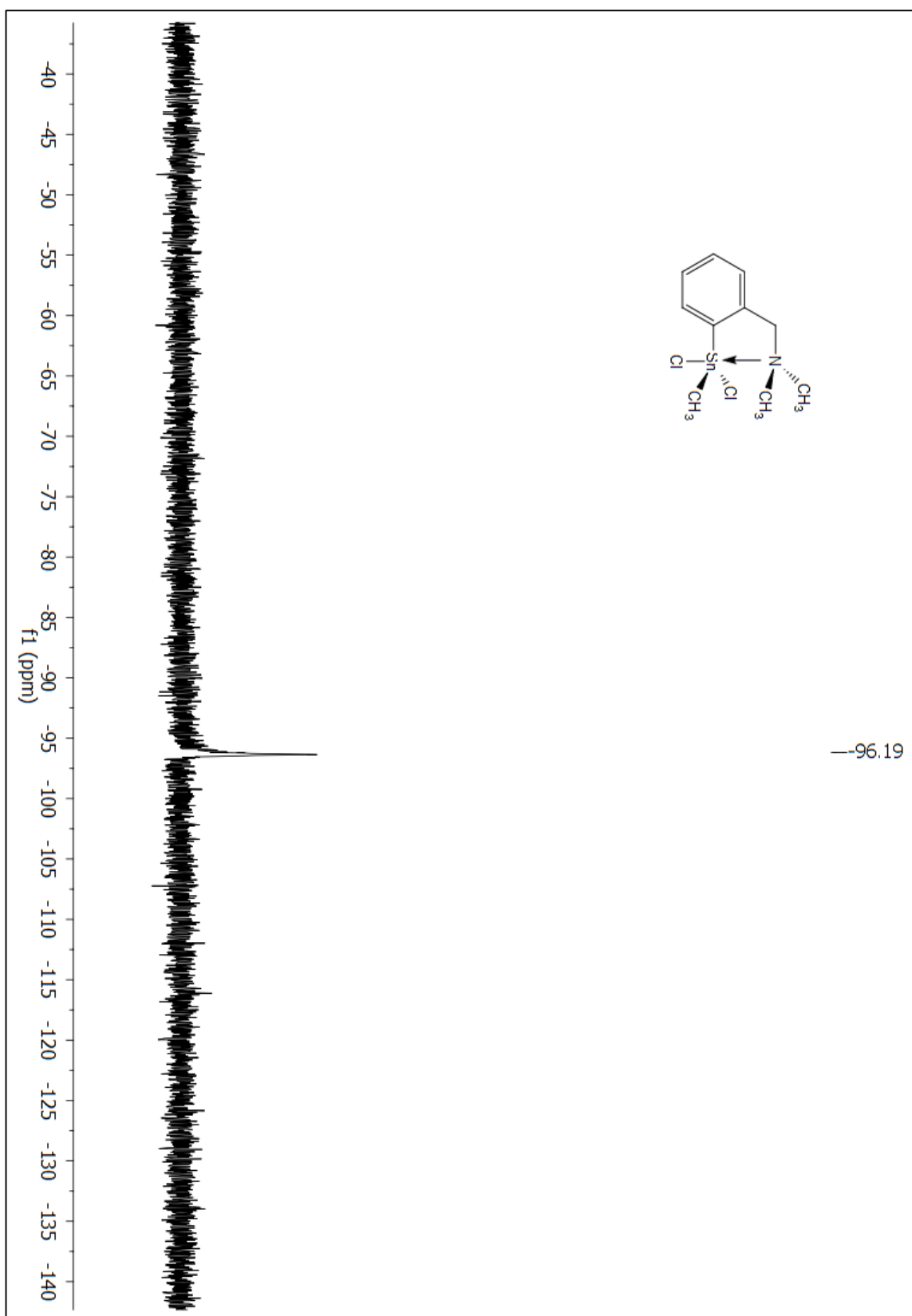
Figure A 99: ^{119}Sn NMR (CDCl$_3$) spectrum of compound 33.

—96.19
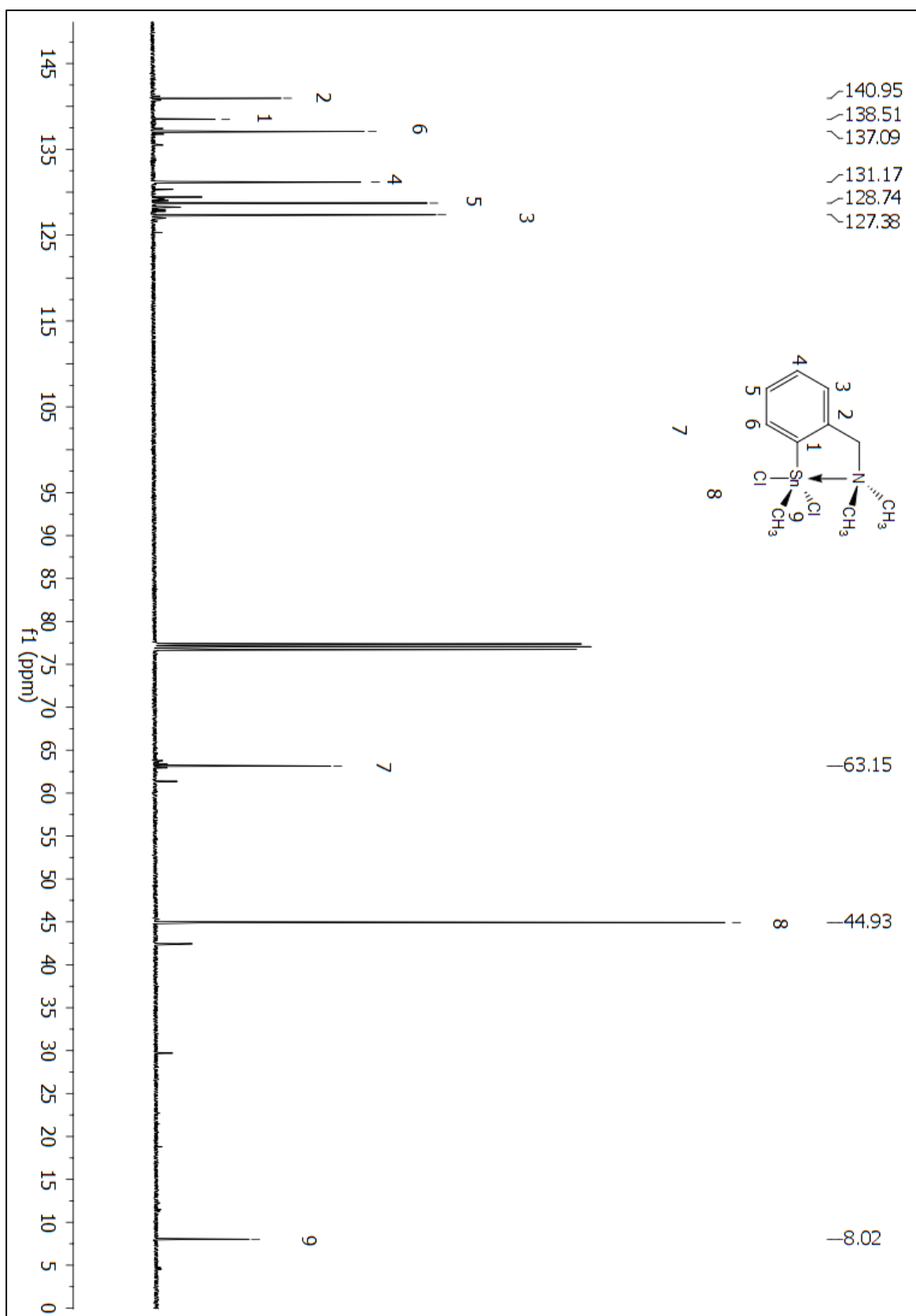
Figure A 100: ^{13}C NMR (CDCl$_3$) spectrum of compound 33.

Figure A 101: ^{1}H NMR (CDCl$_3$) spectrum of compound 35.
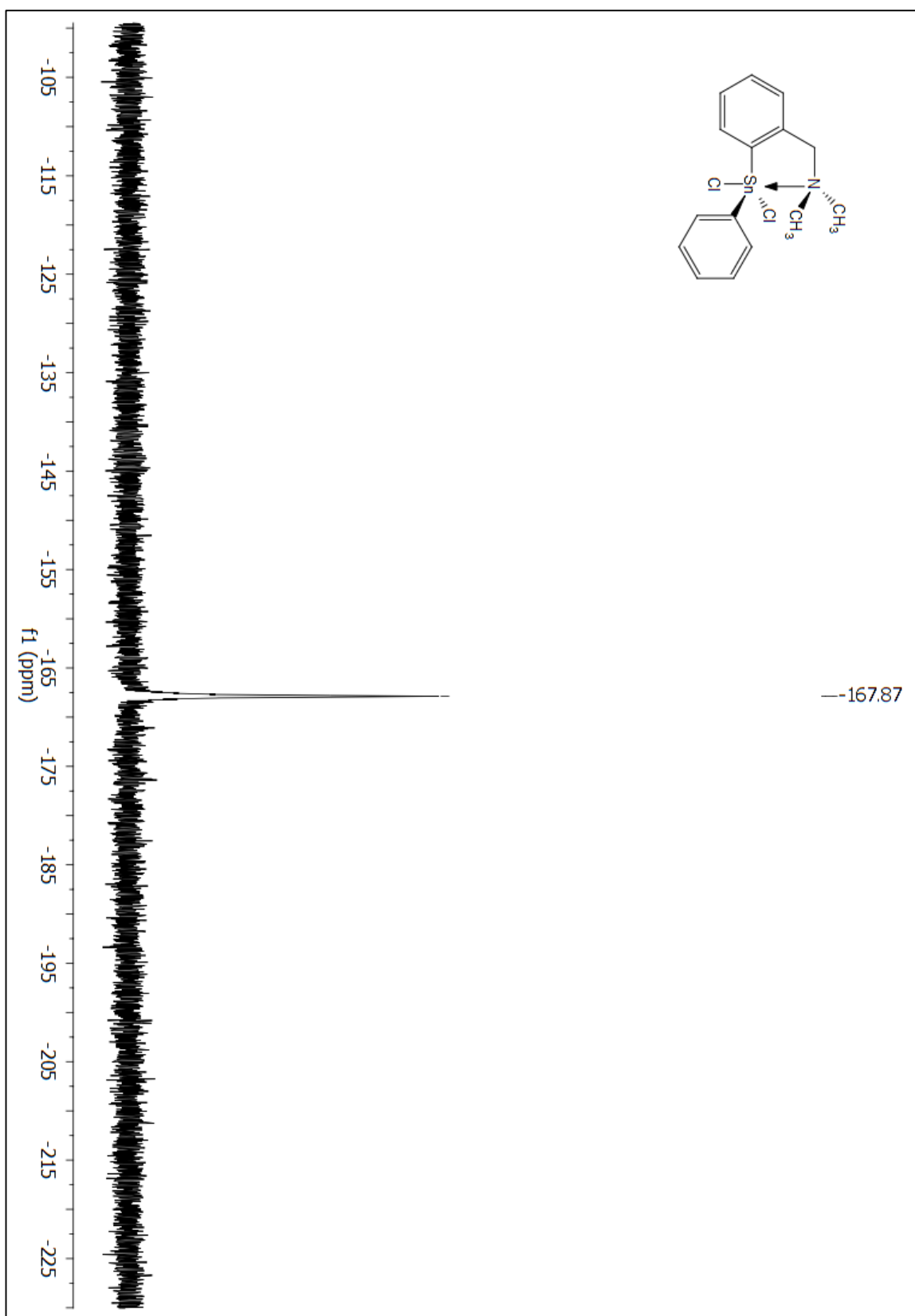
Figure A 102: ^{119}Sn NMR (CDCl$_3$) spectrum of compound 35.
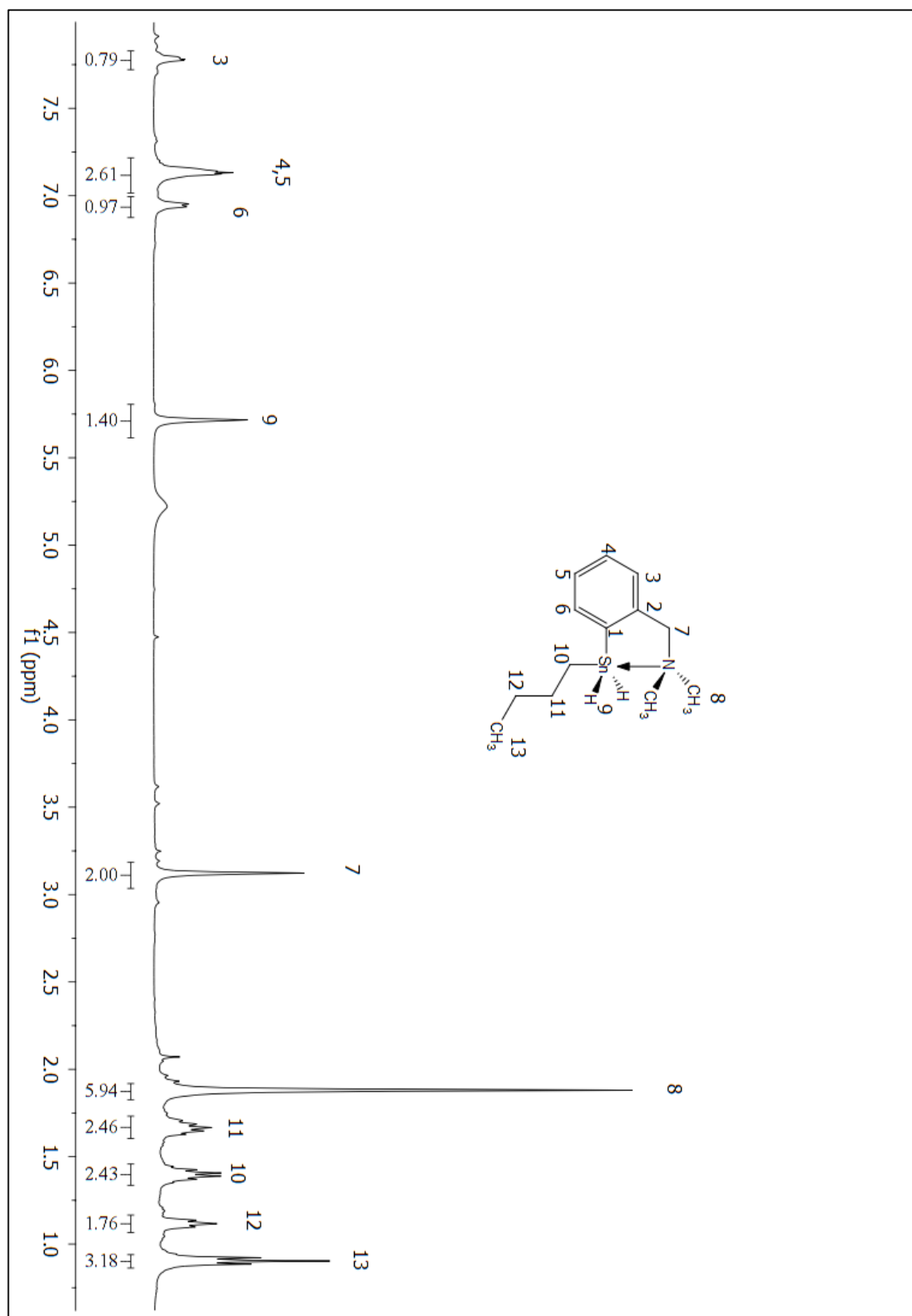
Figure A 103: ^{1}H NMR (C$_6$D$_6$) spectrum of compound 231.
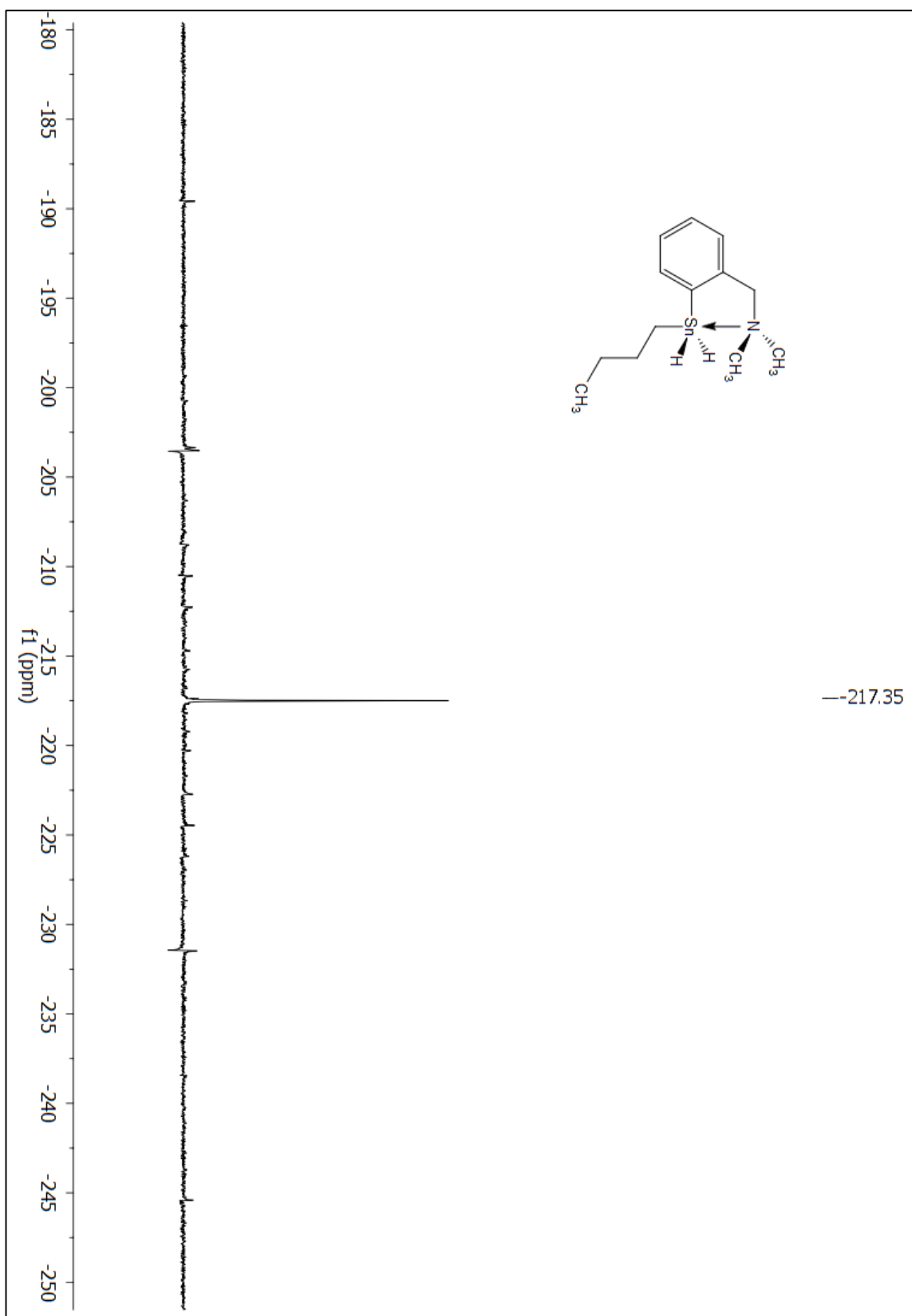
Figure A 104: ^{119}Sn NMR (C$_6$D$_6$) spectrum of compound 231.
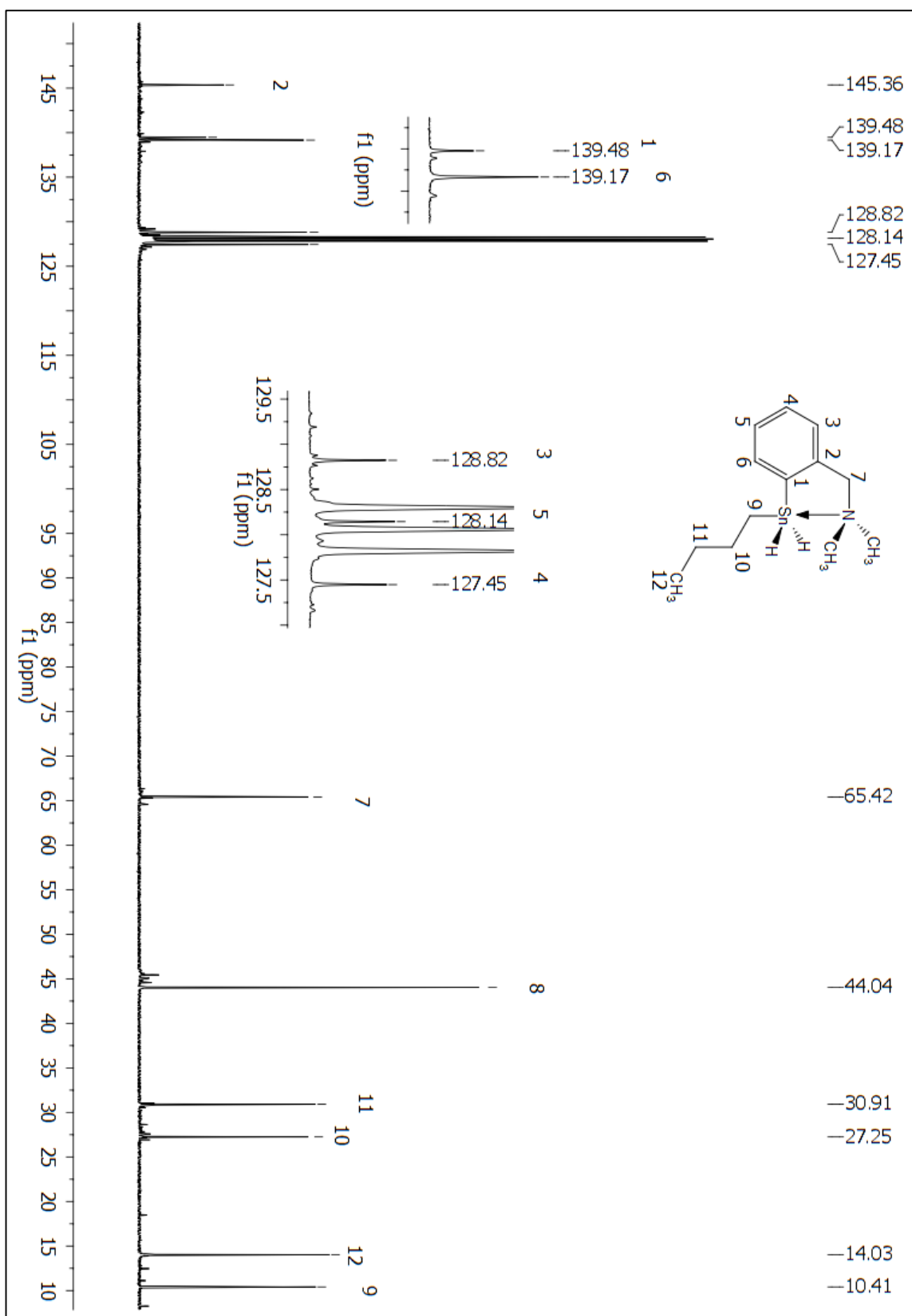
Figure A 105: ^{13}C NMR (C_6D_6) spectrum of compound **231.**
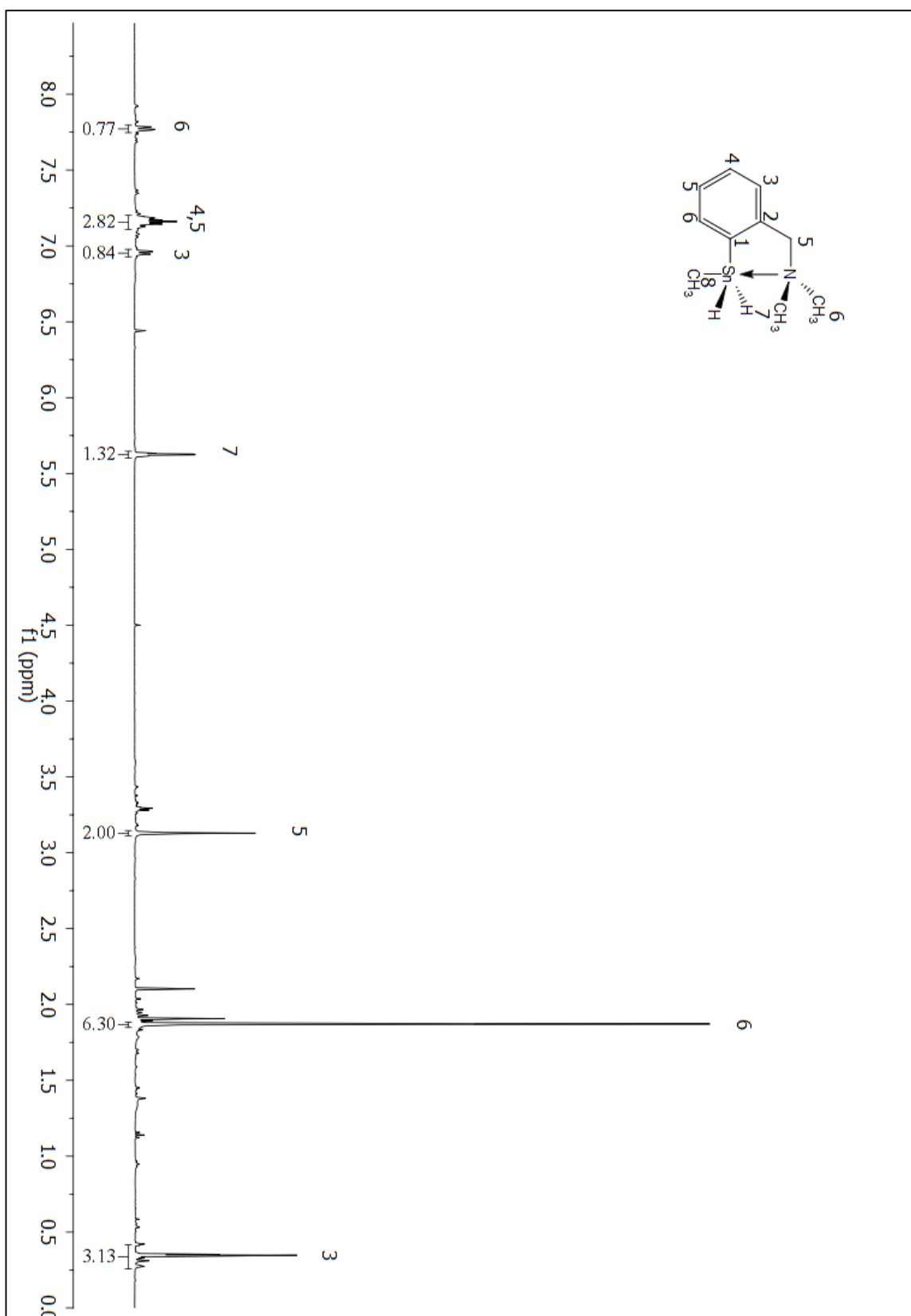
Figure A 106: ^{1}H NMR (C$_6$D$_6$) spectrum of compound 230.
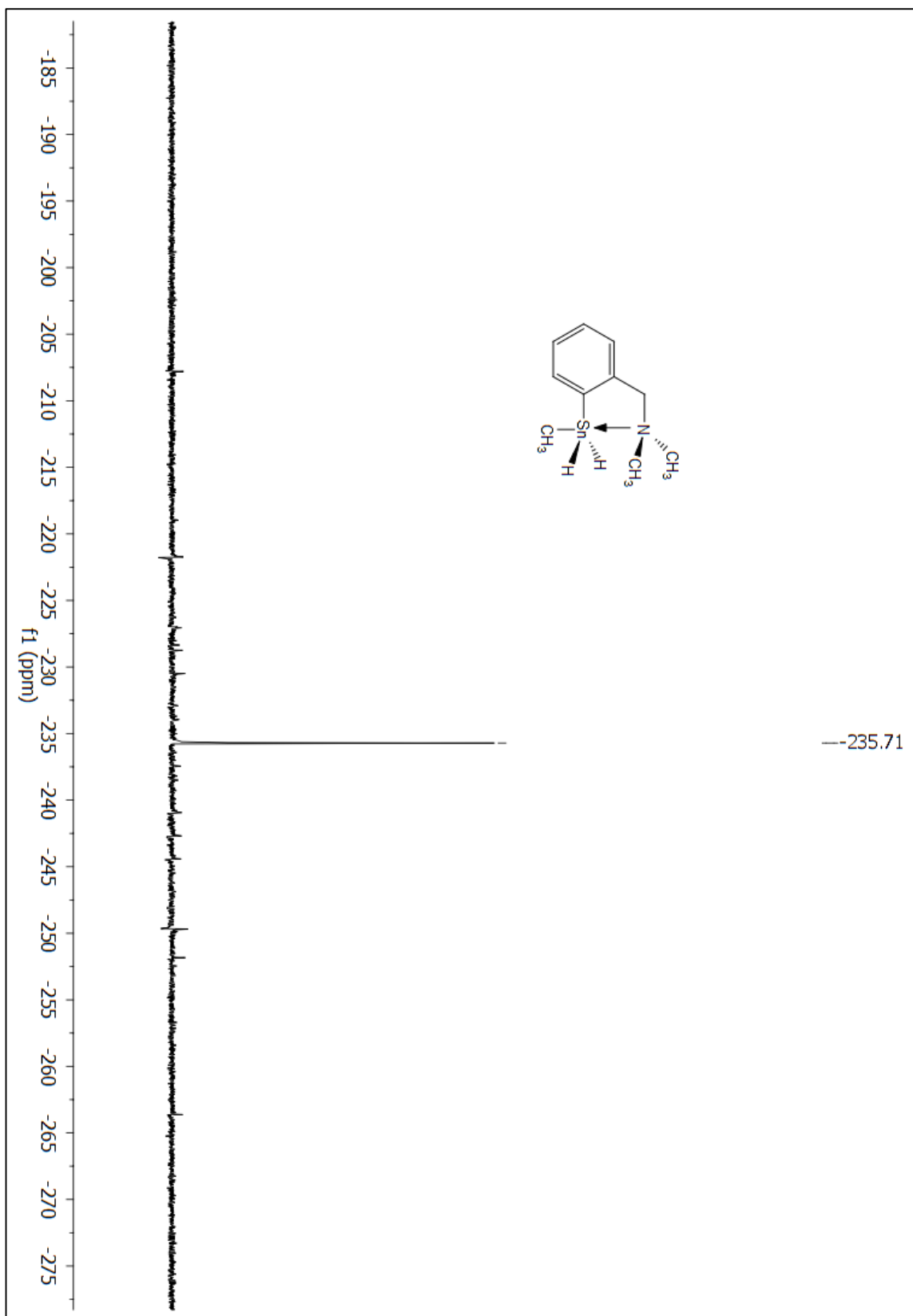
Figure A 107: ^{119}Sn NMR (C$_6$D$_6$) spectrum of compound 230.
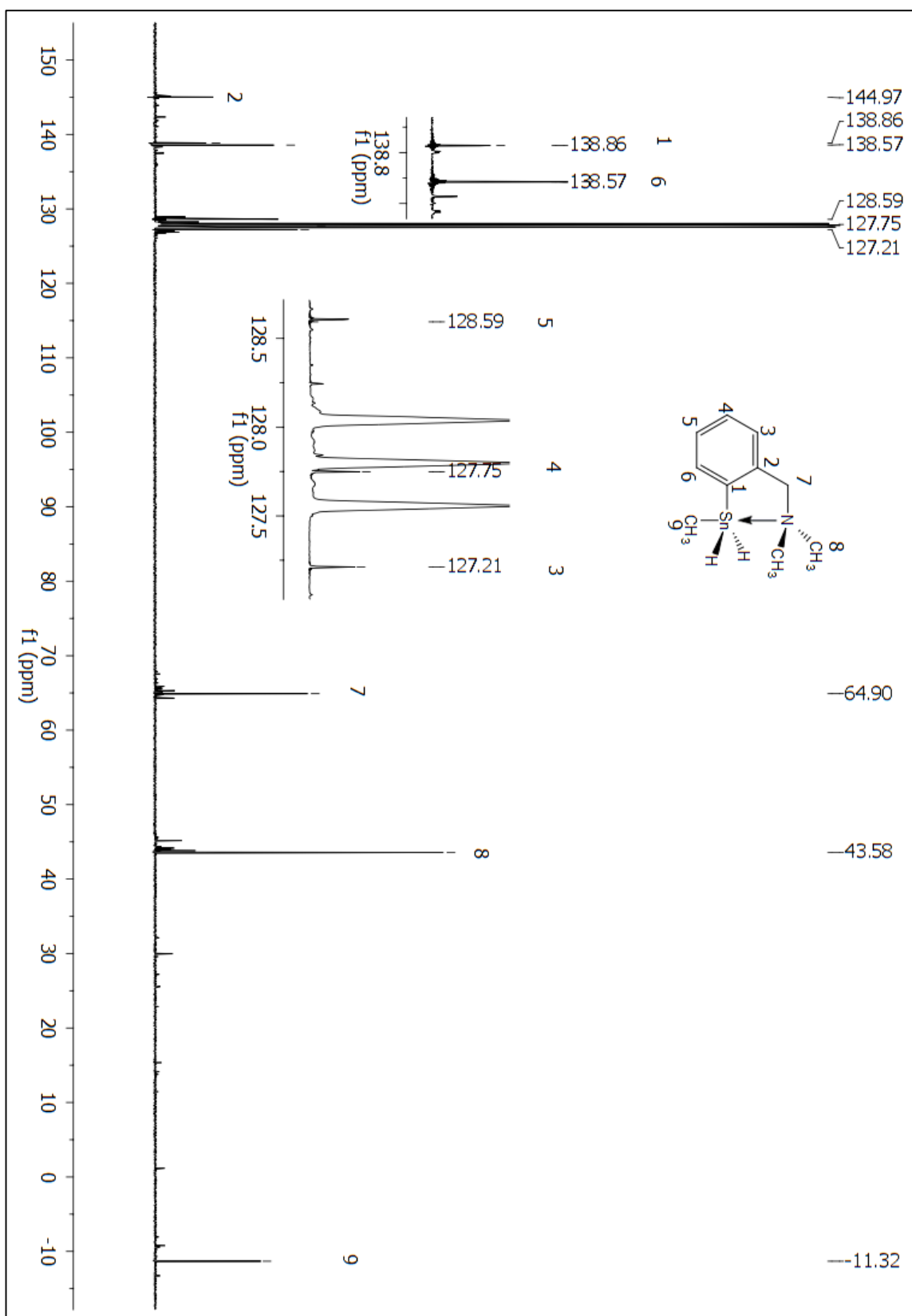
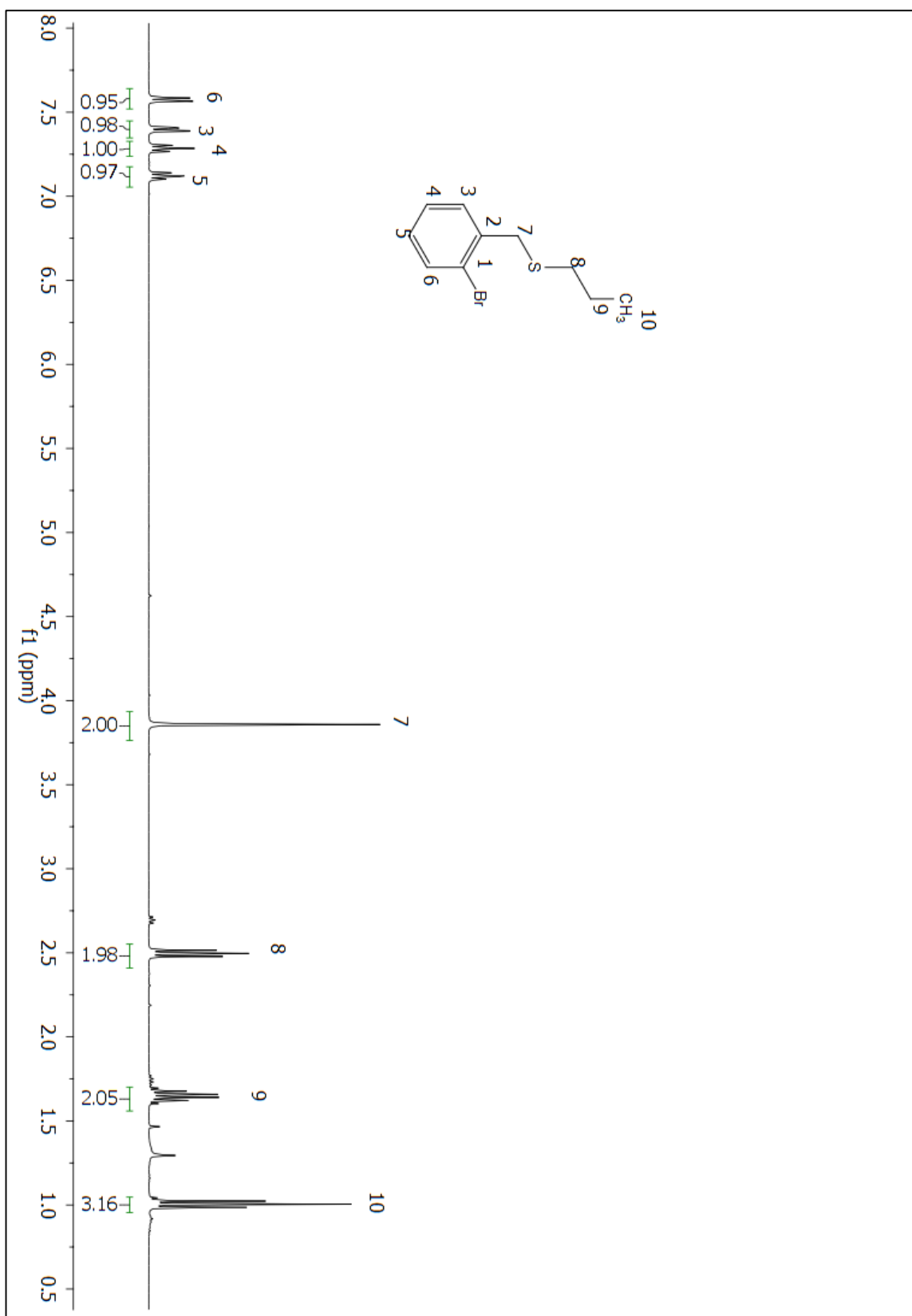**Figure A 108: ^{13}C NMR (C$_6$D$_6$) spectrum of compound 230.**

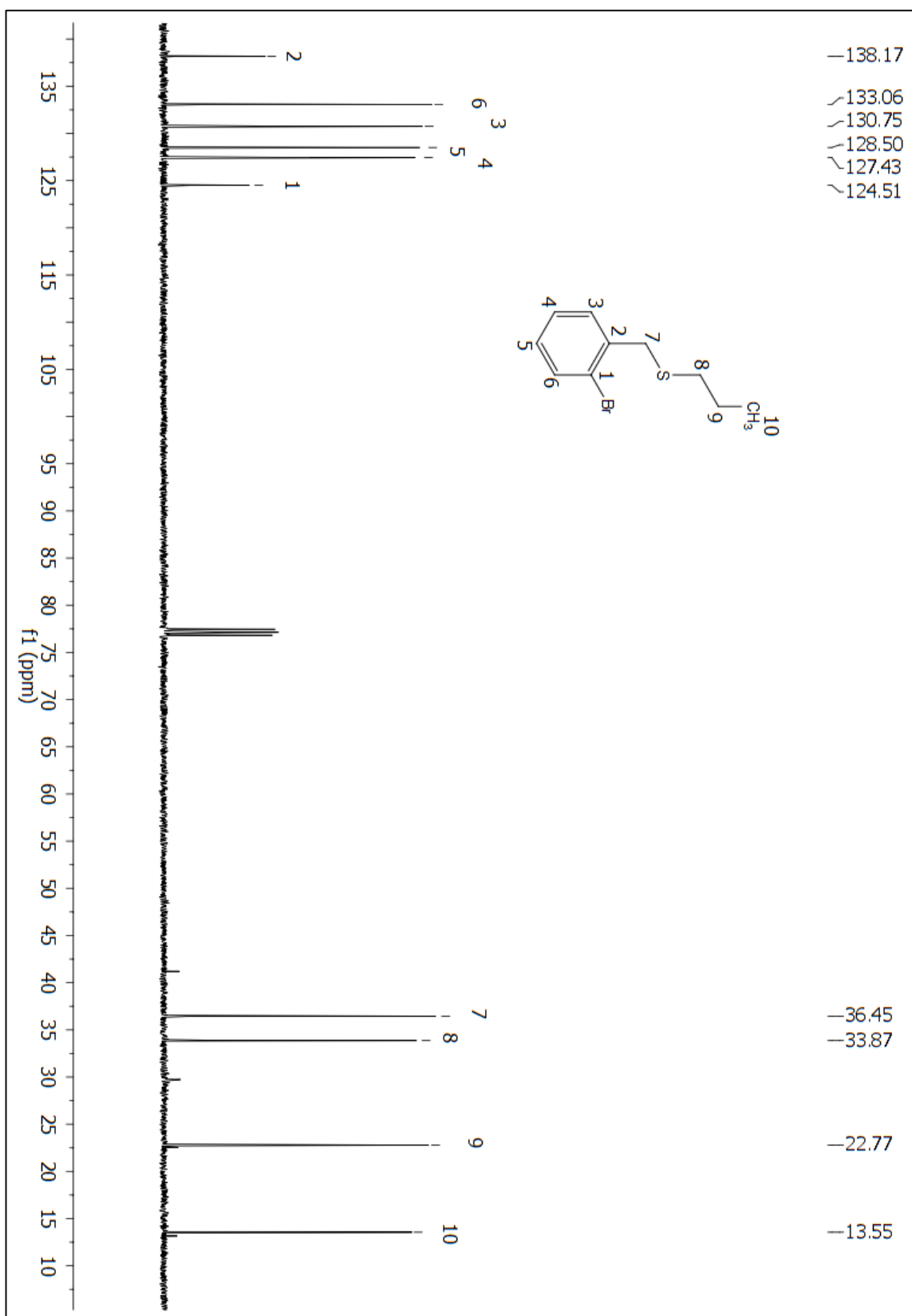**Figure A 109:** ^{1}H NMR (CDCl$_3$) spectrum of compound 233.

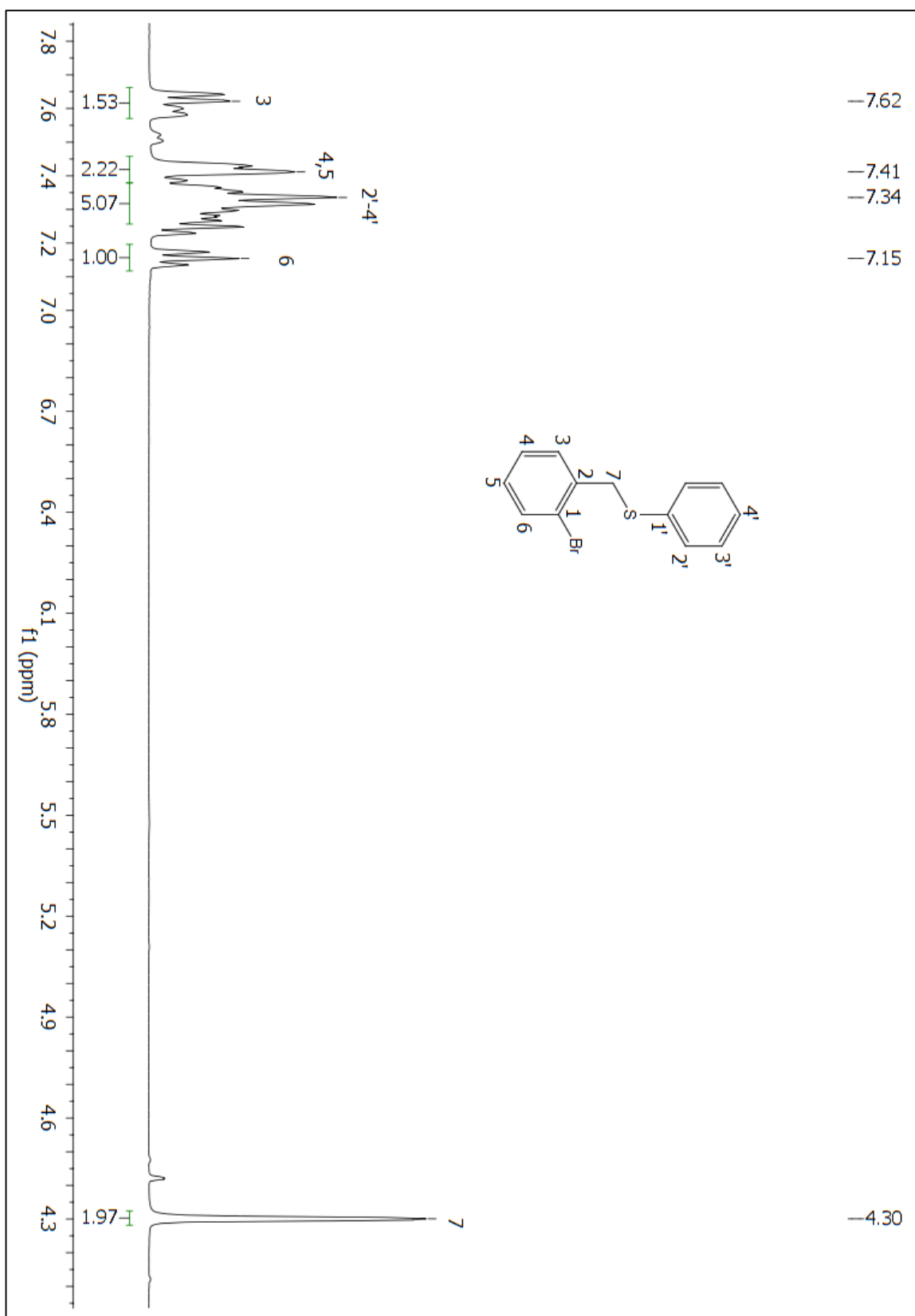**Figure A 110:** ^{13}C NMR (CDCl$_3$) spectrum of compound 233.

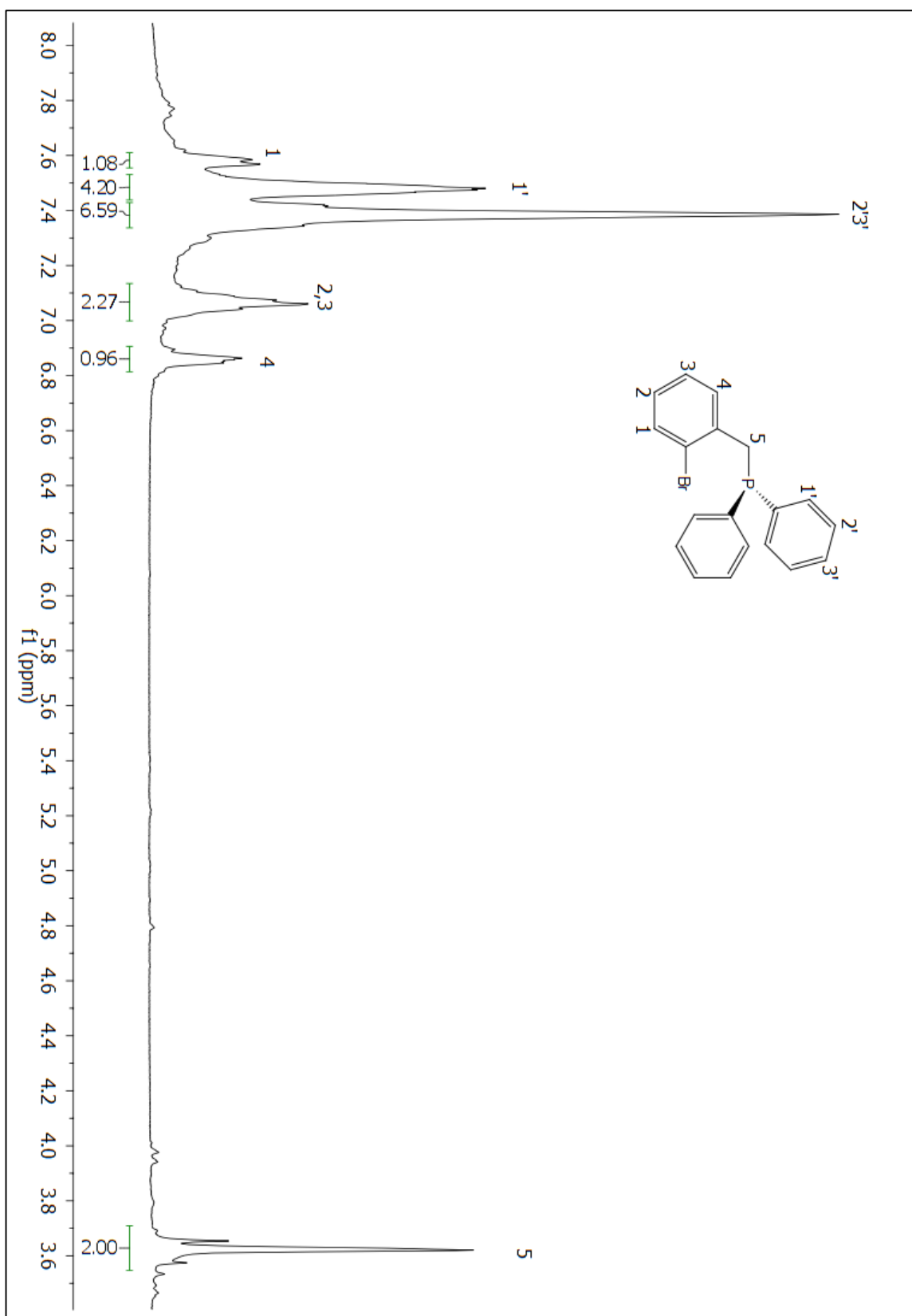**Figure A 111: ^{1}H NMR (CDCl$_3$) spectrum of compound 234.**

Figure A 112: ¹H NMR (CDCl₃) spectrum of compound 237.
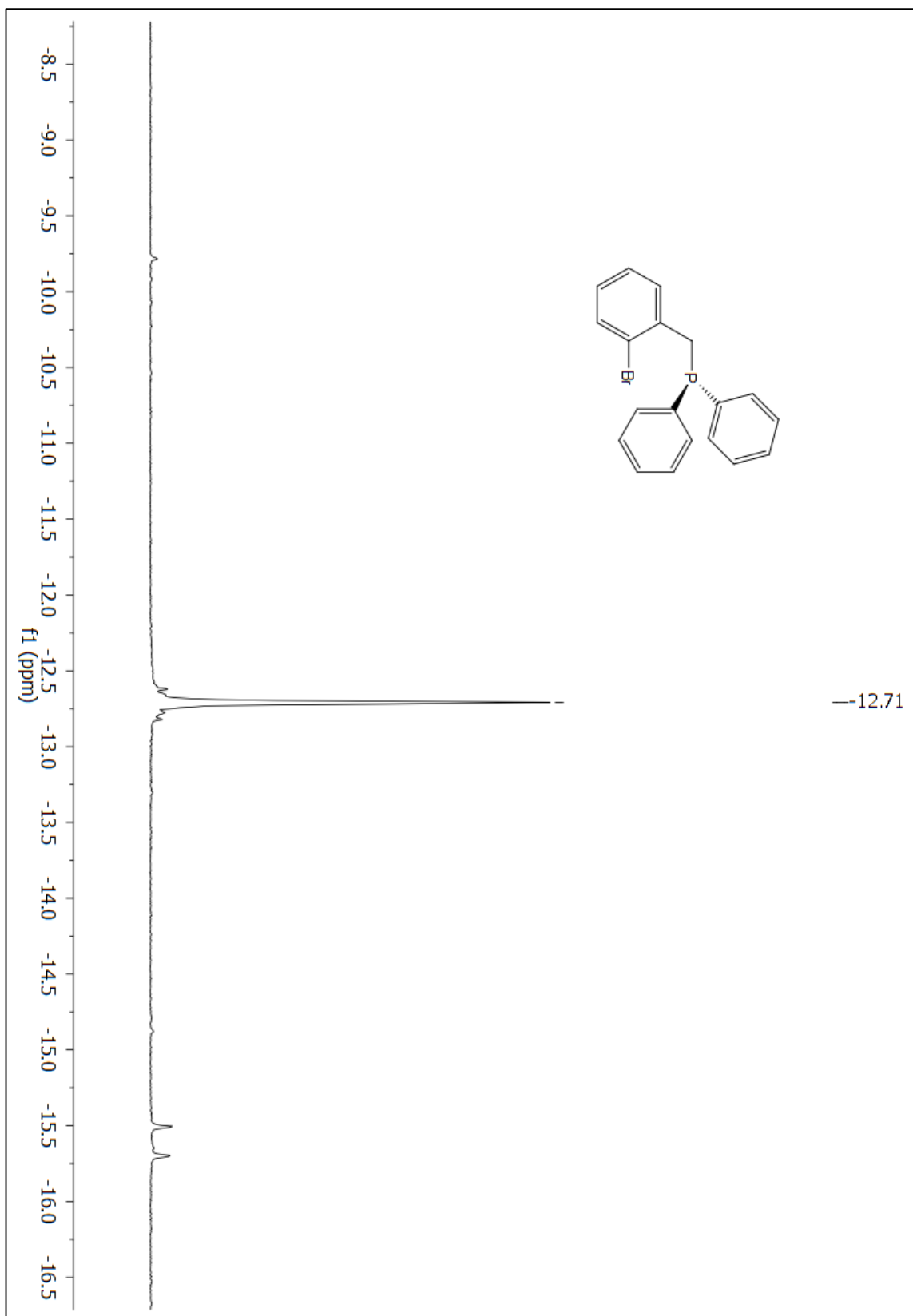
Figure A 113: ^{31}P NMR (CDCl$_3$) spectrum of compound 237.
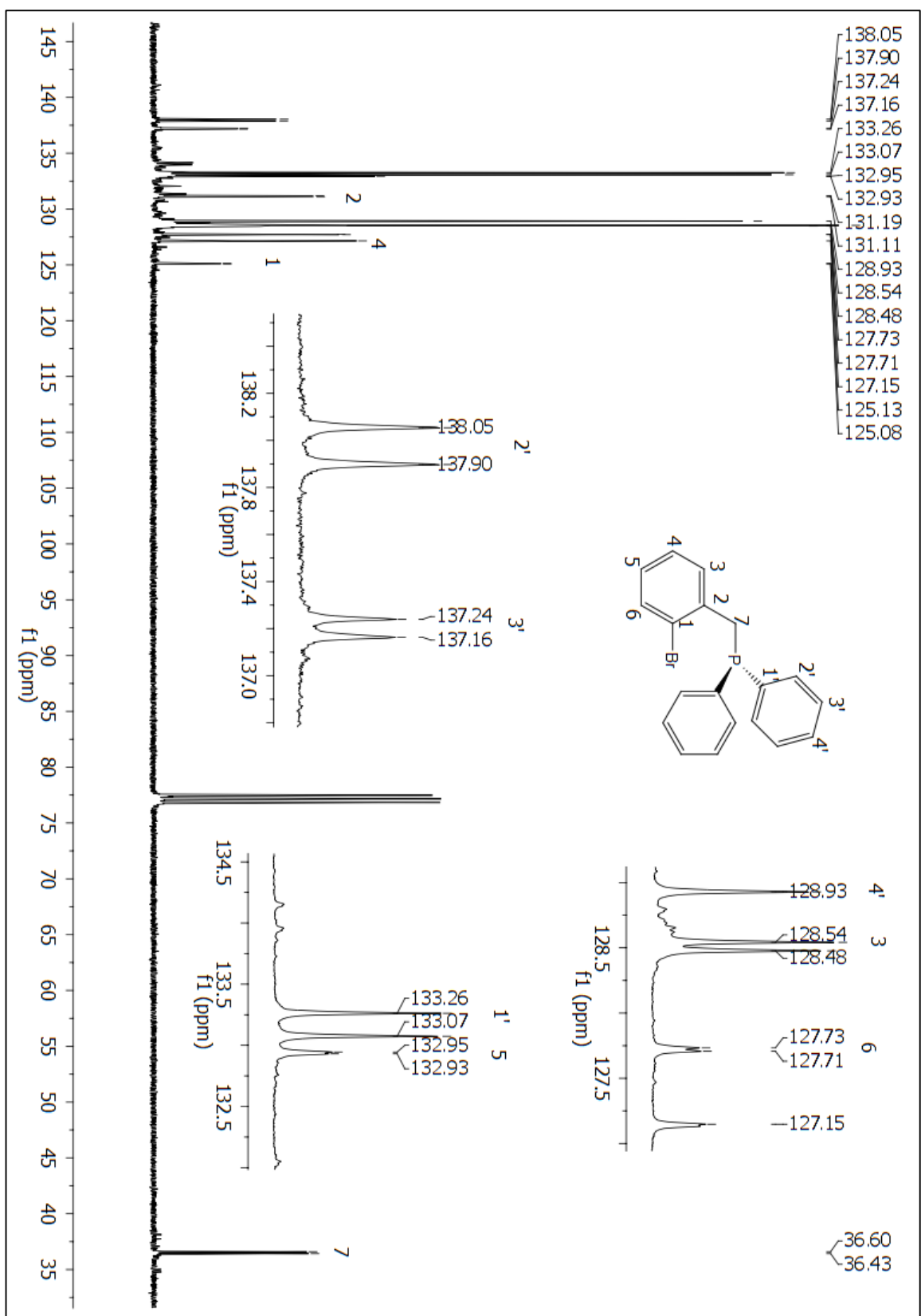
Figure A 114: ^{13}C NMR (CDCl$_3$) spectrum of compound 237.
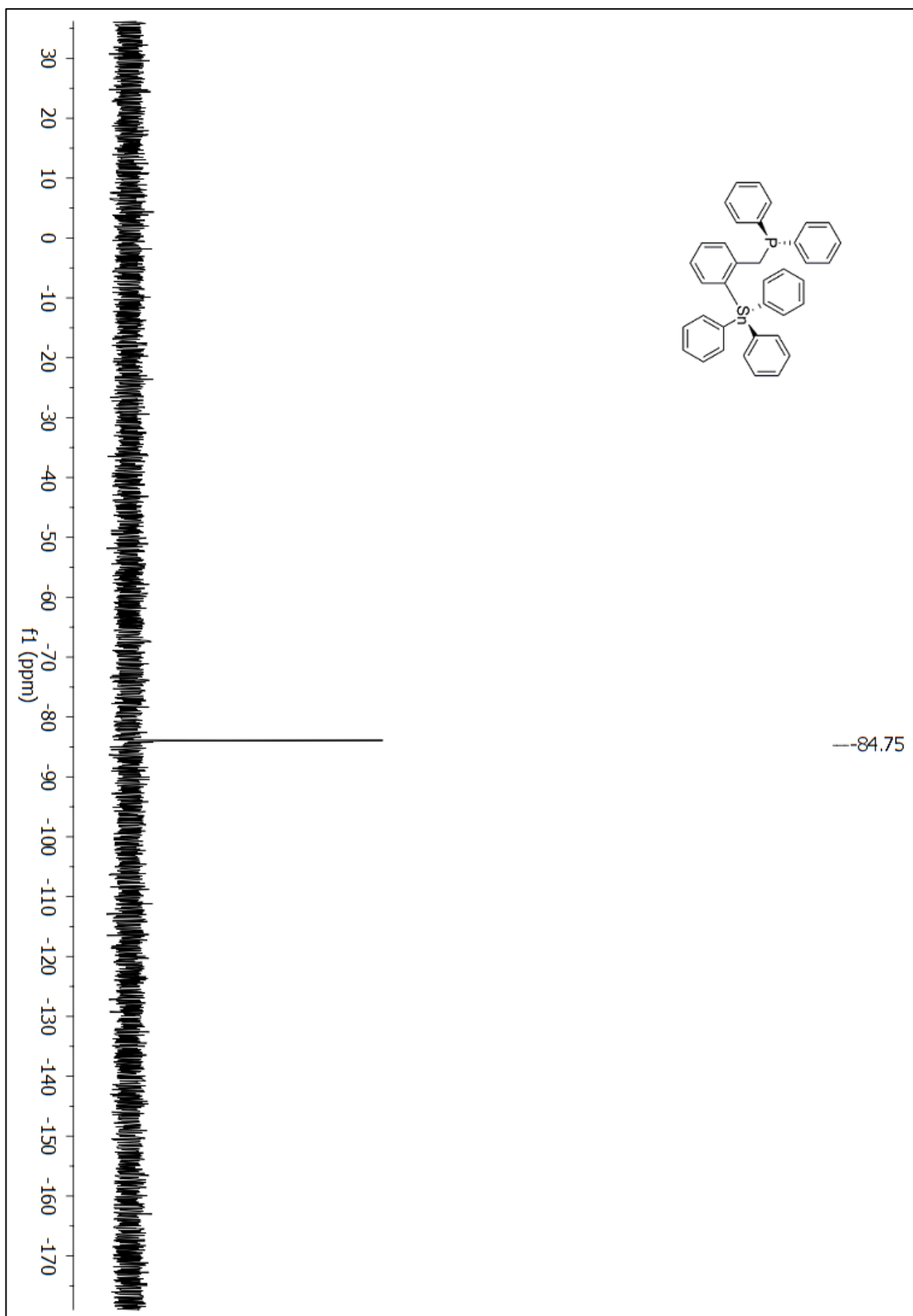
Figure A 115: ^{119}Sn NMR (CDCl$_3$) spectrum of compound 241.

--84.75
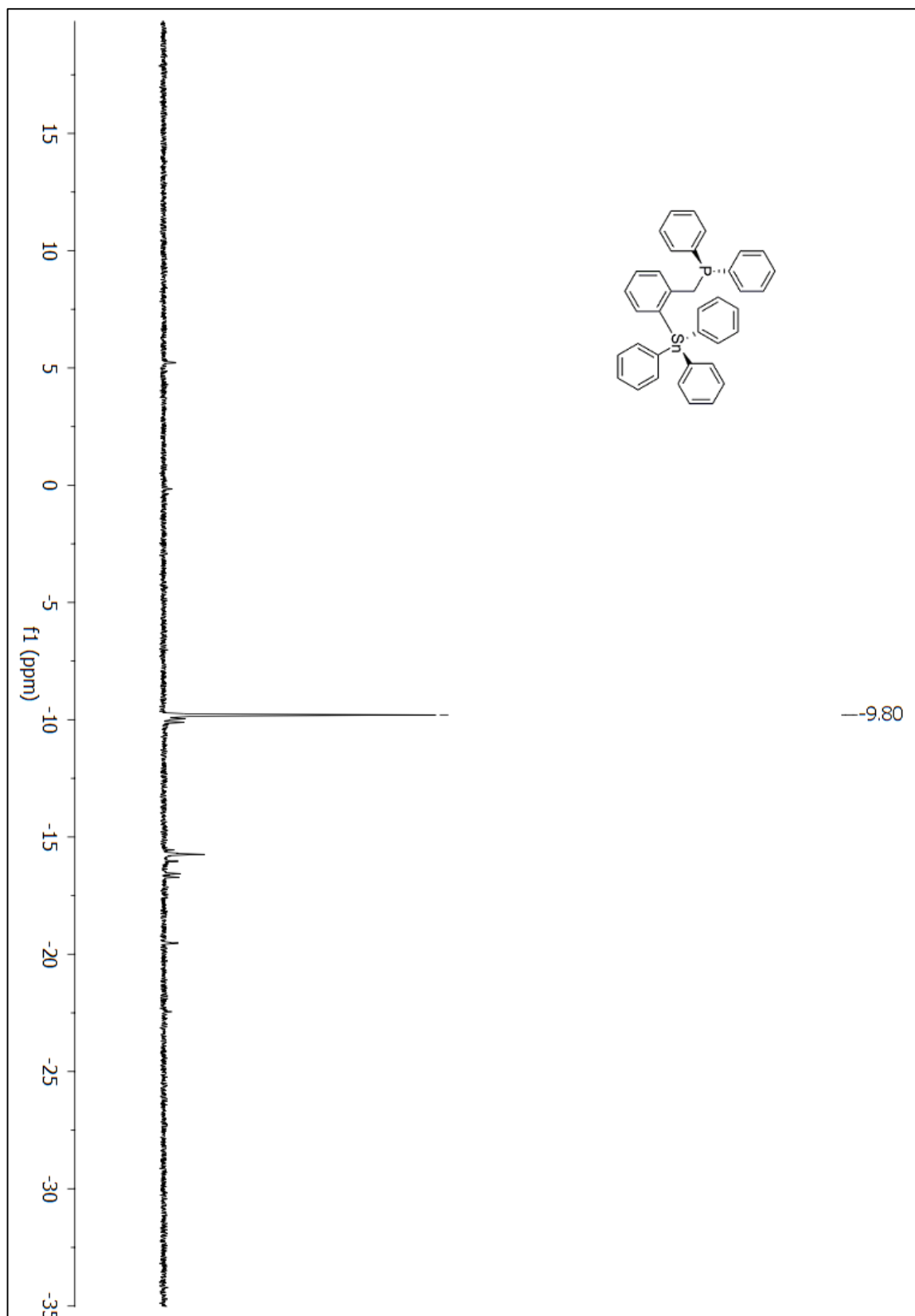
Figure A 116: ^{31}P NMR (CDCl$_3$) spectrum of compound **241.**
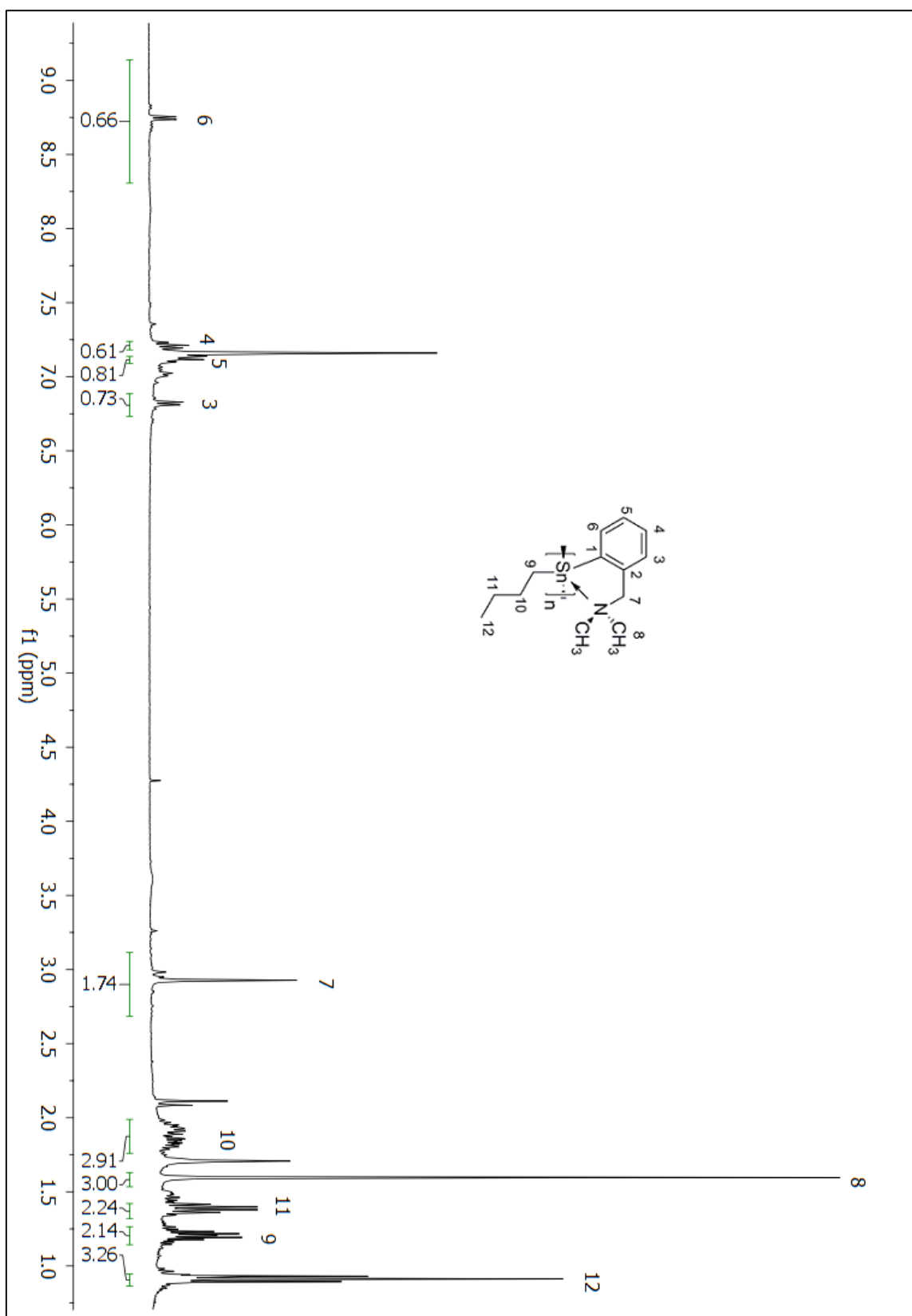
Figure A 117: ^{1}H NMR (C$_6$D$_6$) spectrum of compound 248
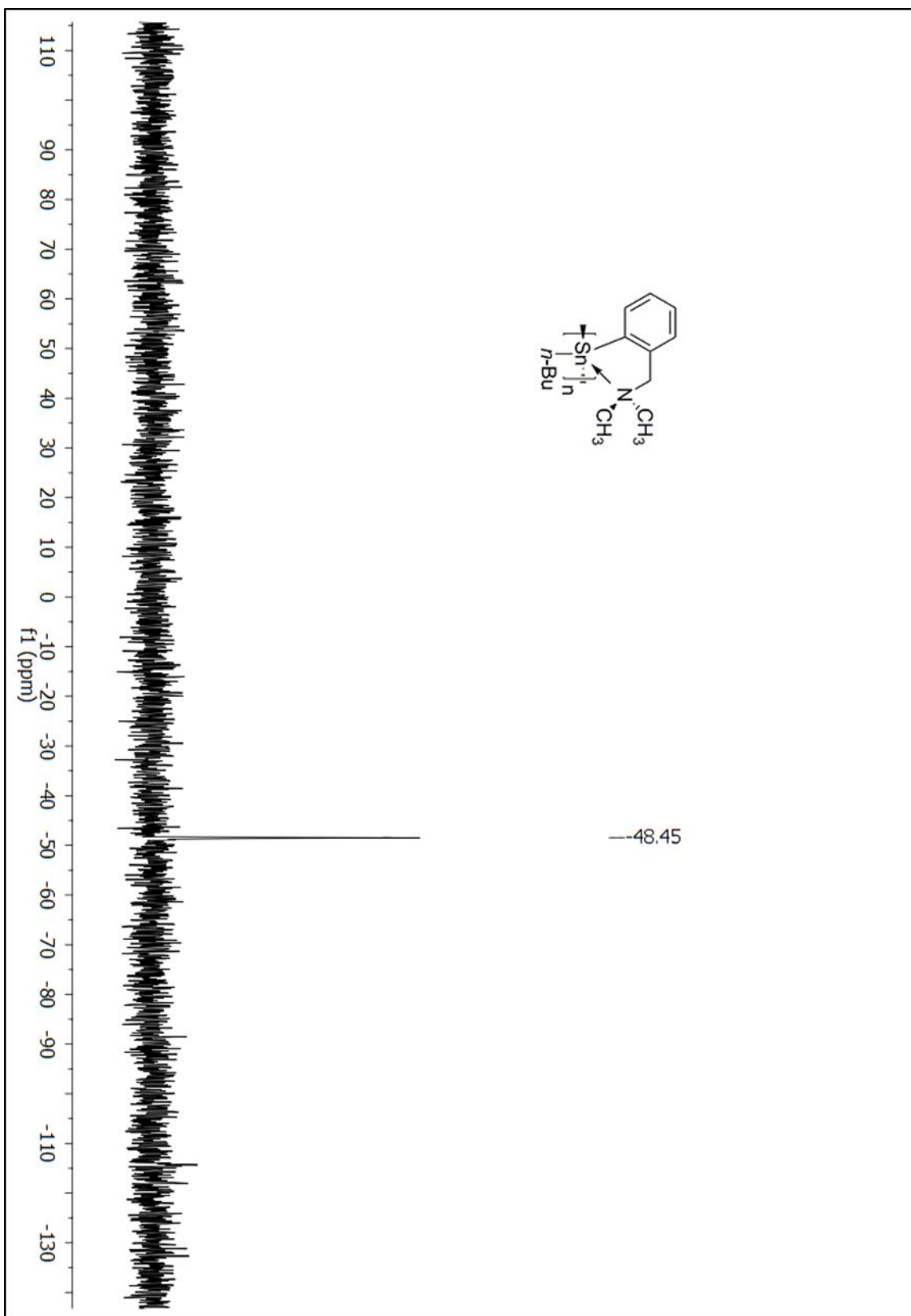
Figure A 118: ^{119}Sn NMR (C$_6$D$_6$) spectrum of compound **248**
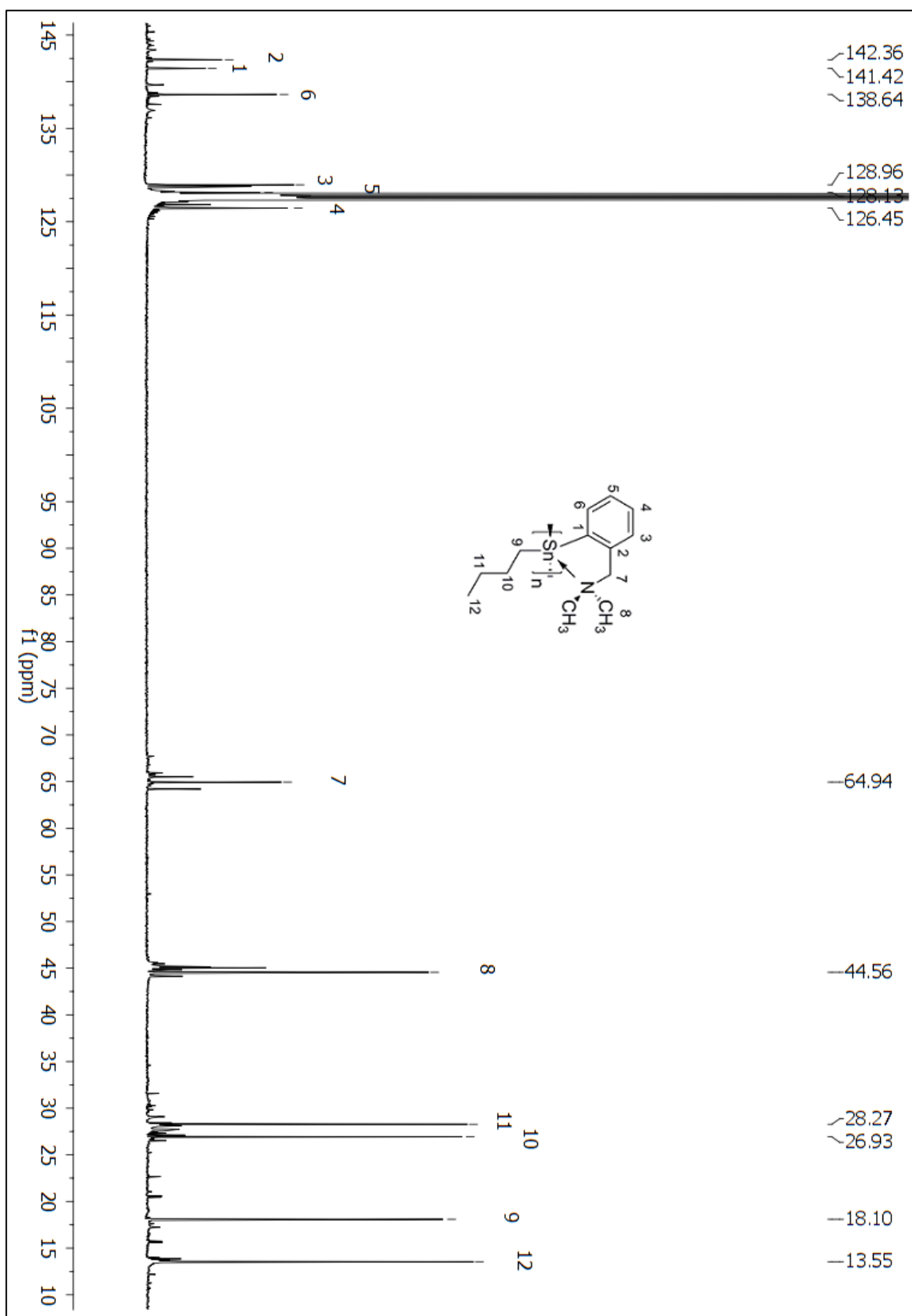
Figure A 119: ^{13}C NMR (C$_6$D$_6$) spectrum of compound 248

Figure A 120: DART spectrum of compound 197

Figure A 121: DART spectrum of compound 198

Figure A 122: HRMS-DART spectrum of compound 200

Figure A 123: DART spectrum of compound 202

Figure A 124: HRMS-DART spectrum of compound 202

Figure A 125: DART spectrum of compound 204

Figure A 126: HRMS-DART spectrum of compound 204

Figure A 127: DART spectrum of compound 205

Figure A 128: HRMS-DART spectrum of compound 205

Figure A 129: DART spectrum of compound 206

Figure A 130: HRMS-DART spectrum of compound 206
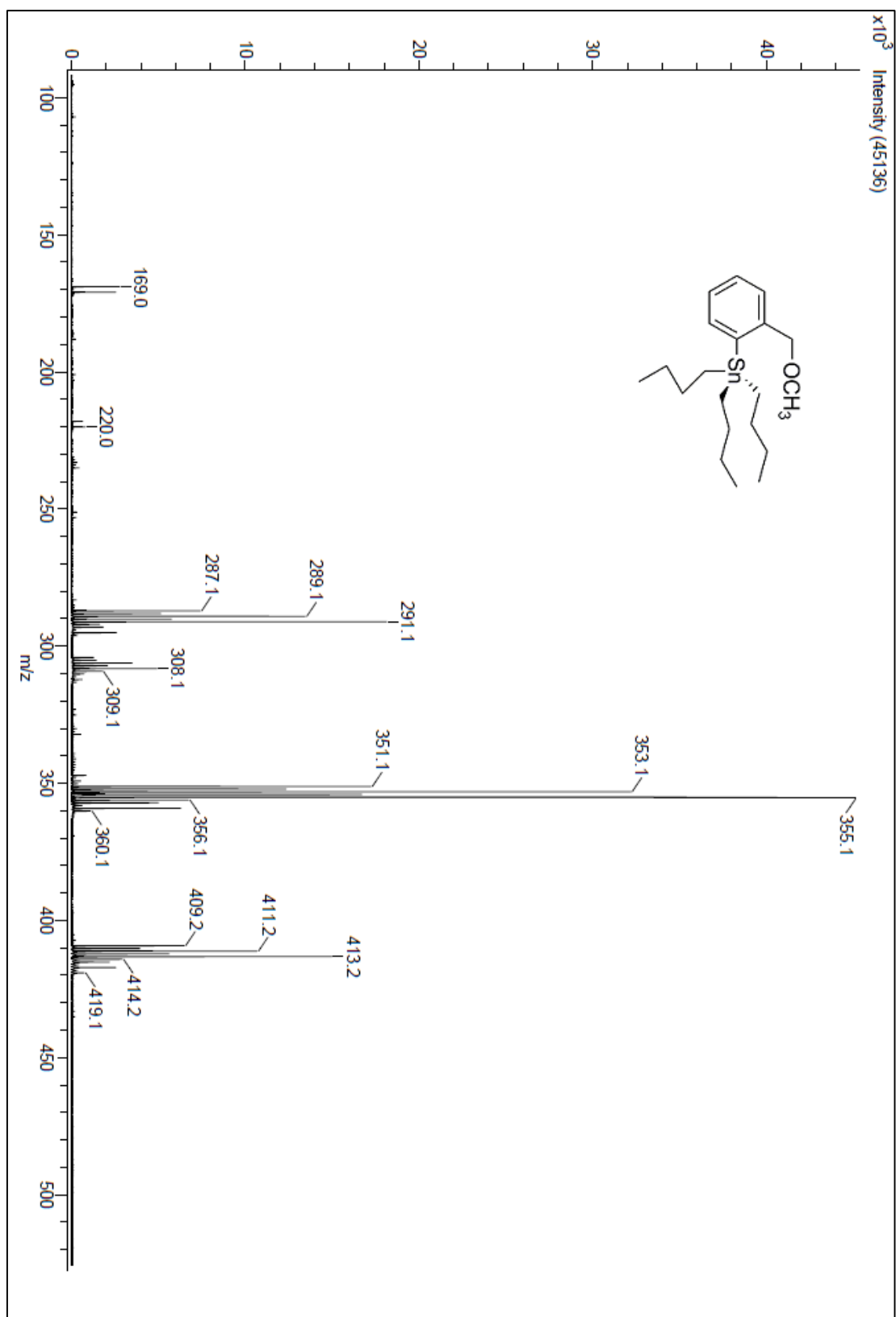
Figure A 131: DART spectrum of compound 217
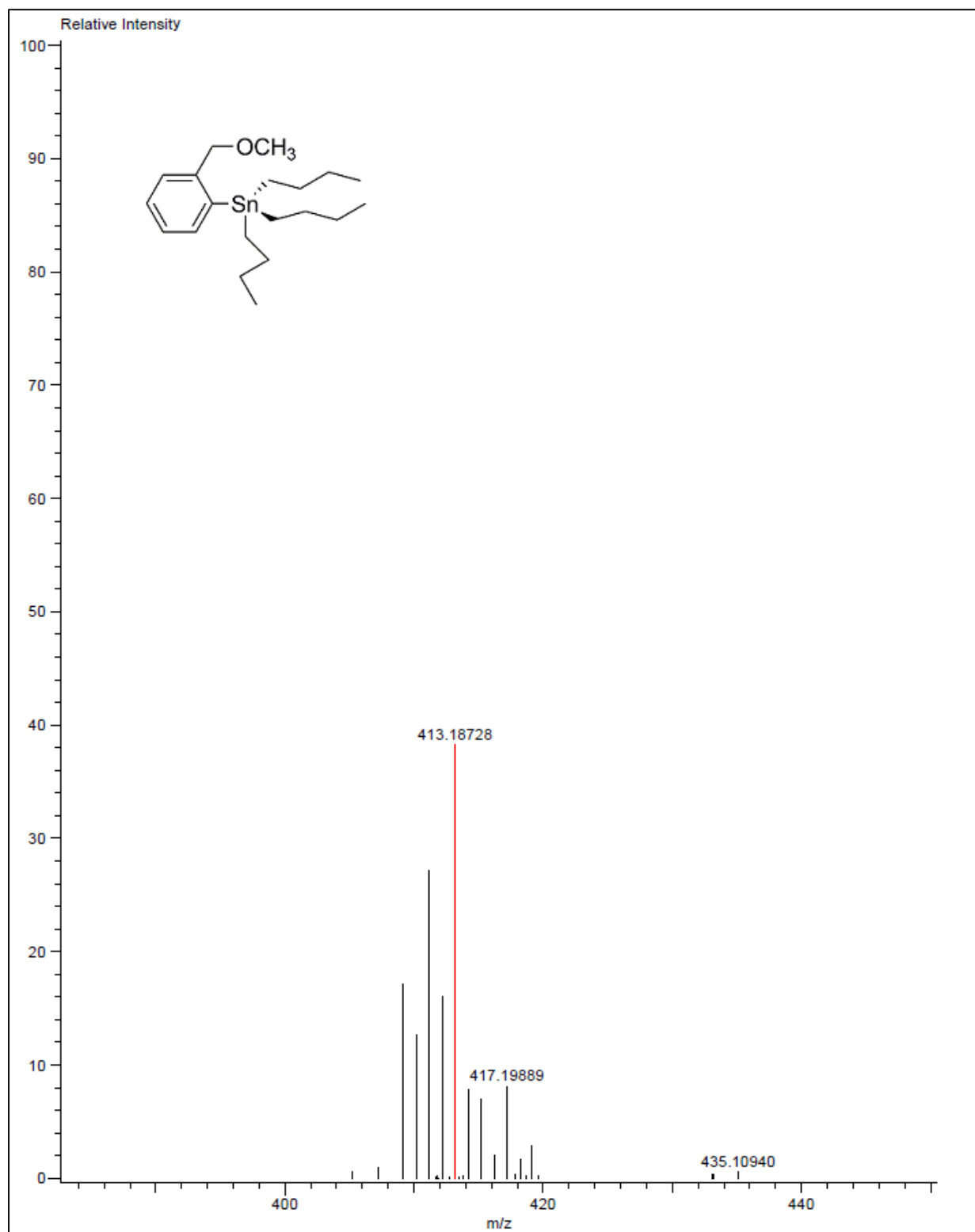
Figure A 132: HRMS-DART spectrum of compound 217
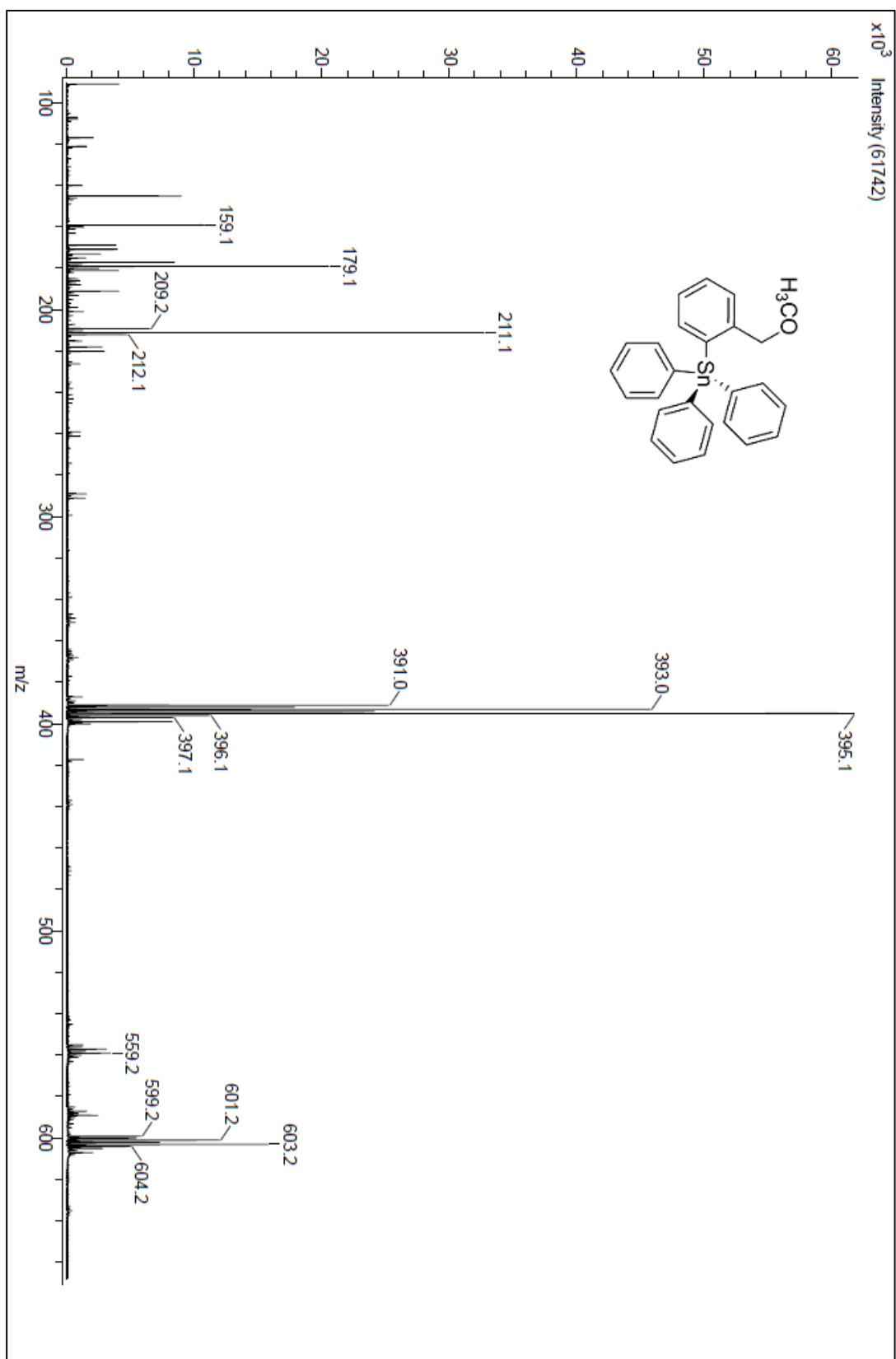
Figure A 133: DART spectrum of compound 112
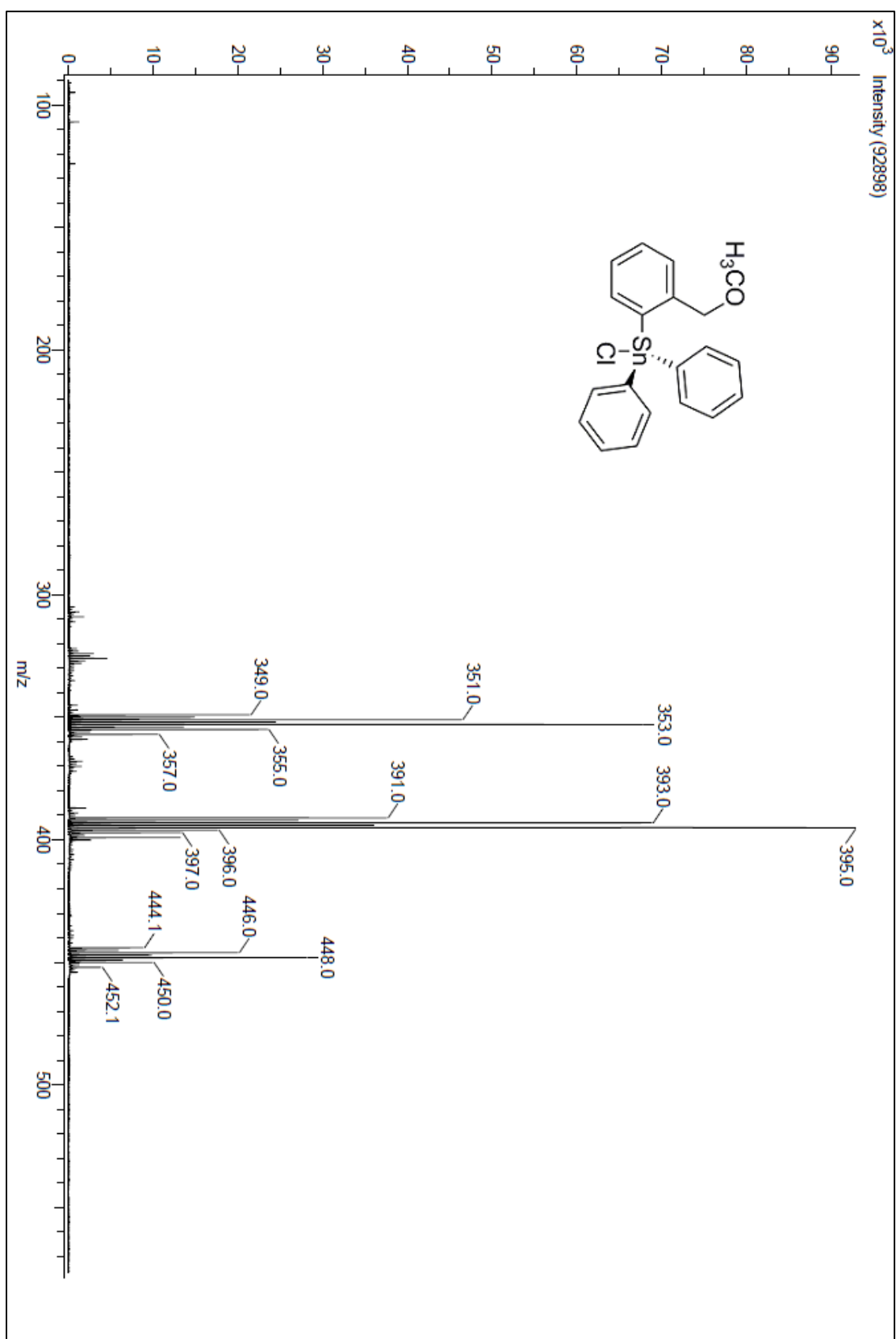
Figure A 134: DART spectrum of compound 112
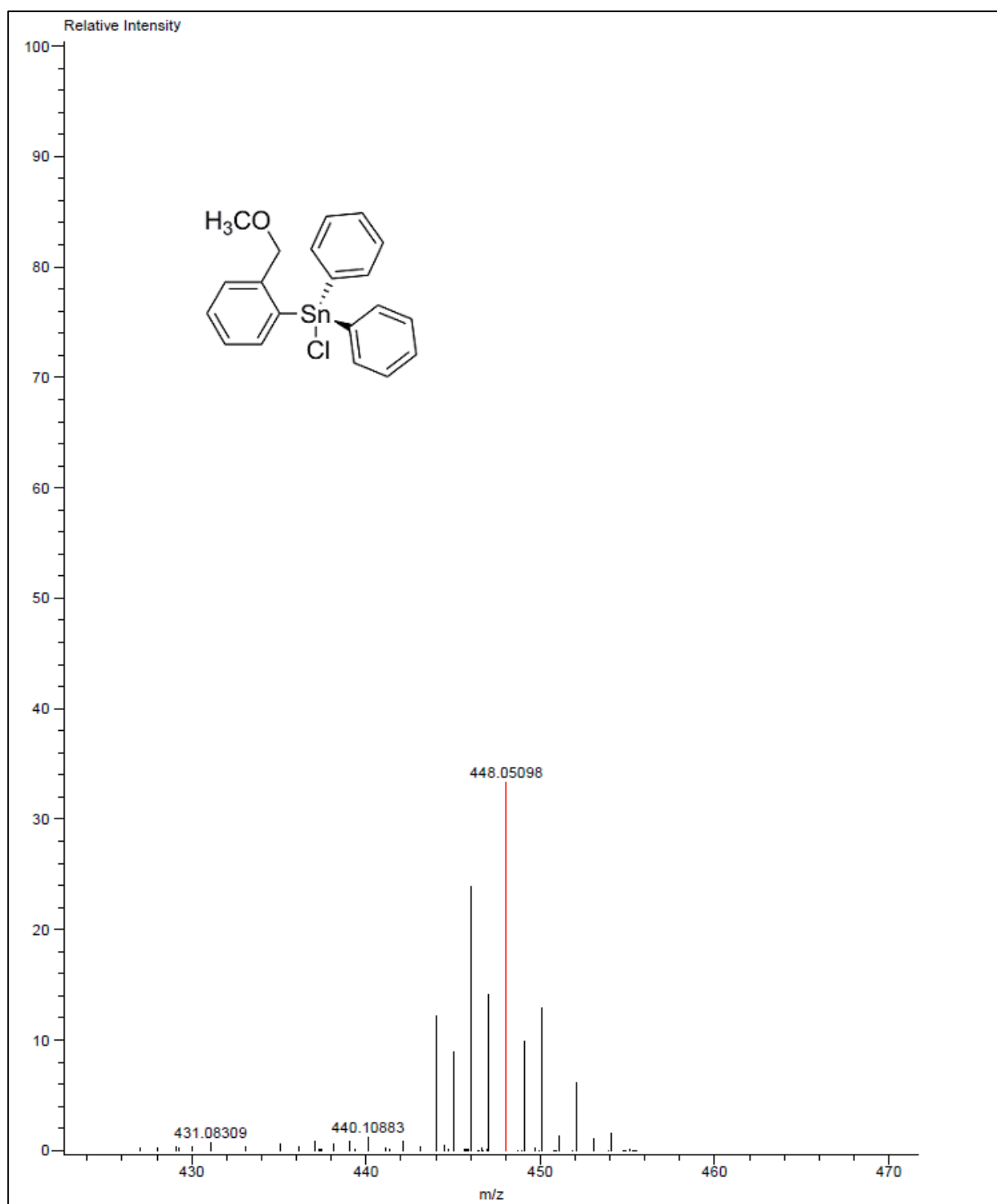
Figure A 135: HRMS-DART spectrum of compound 112
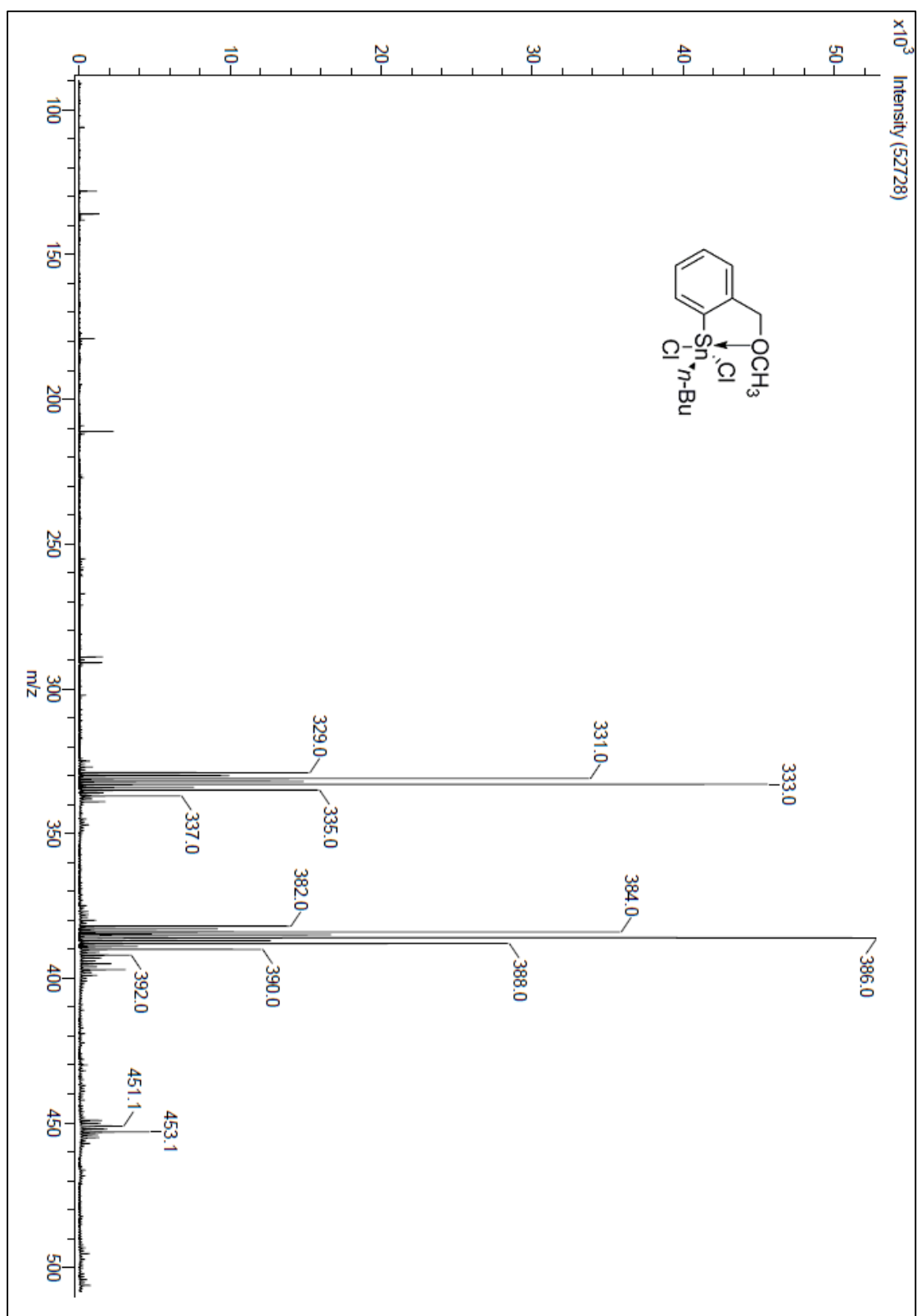
Figure A 136: DART spectrum of compound 219
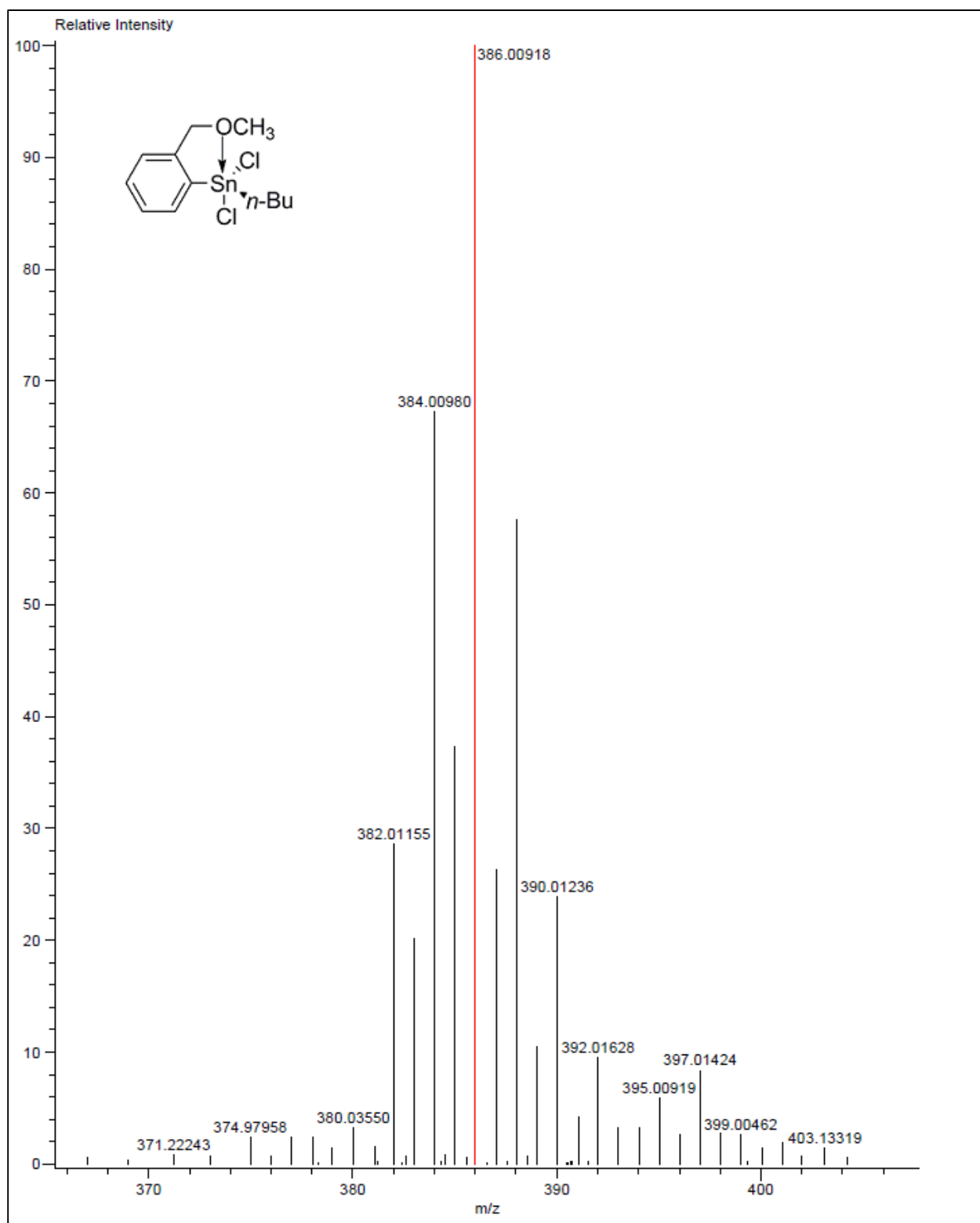
Figure A 137: HRMS-DART spectrum of compound 219
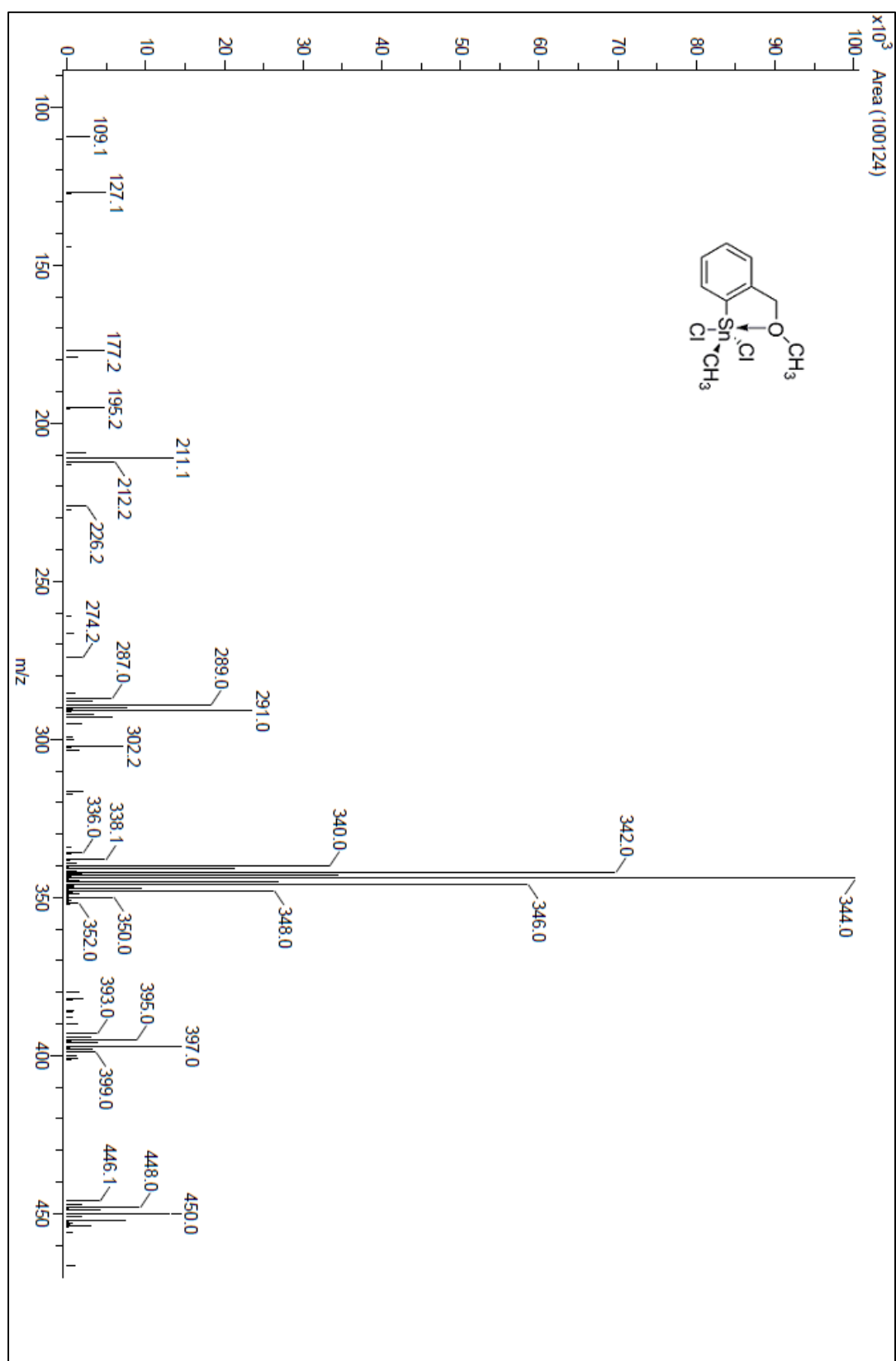
Figure A 138: DART spectrum of compound 218
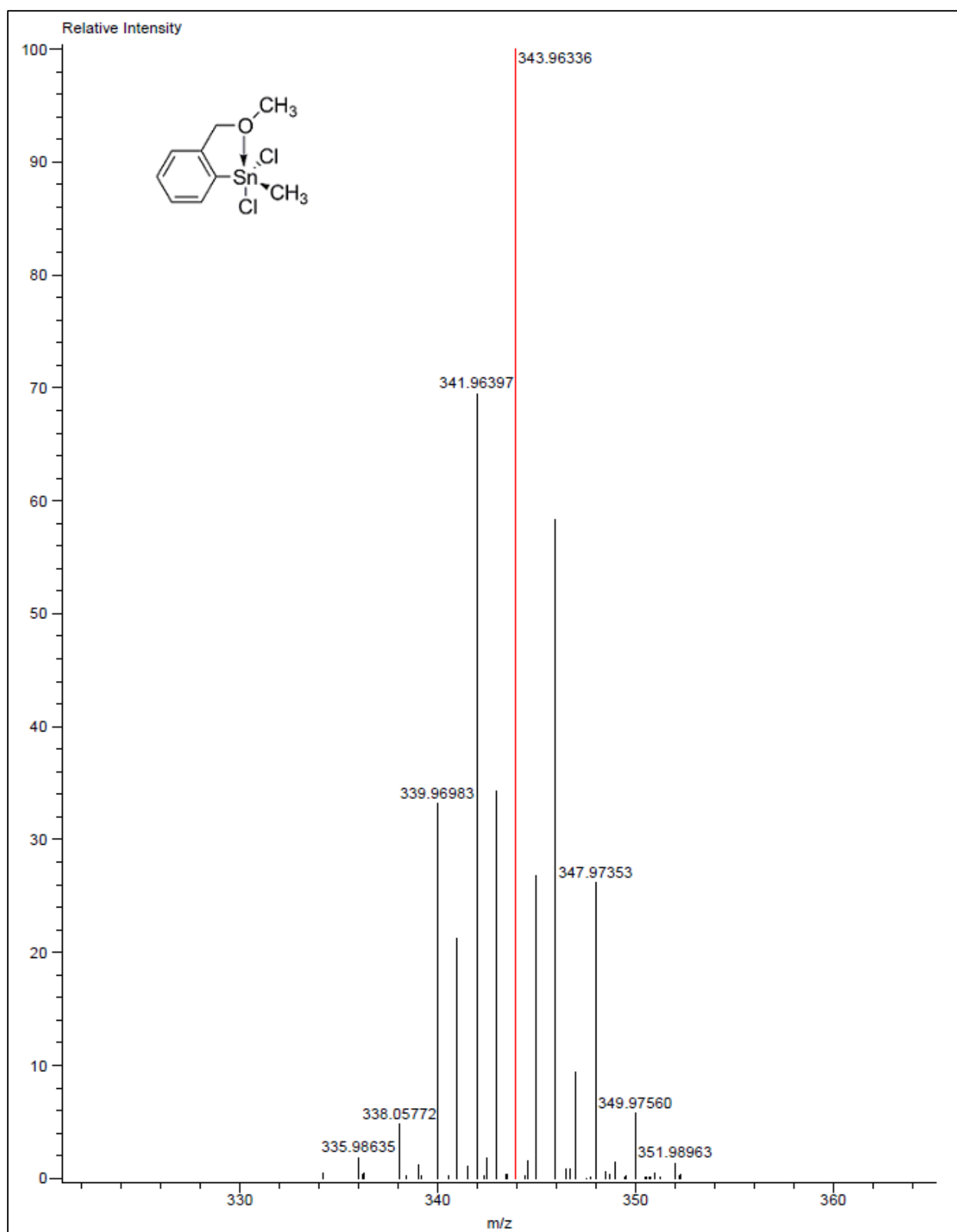
Figure A 139: HRMS-DART spectrum of compound 218
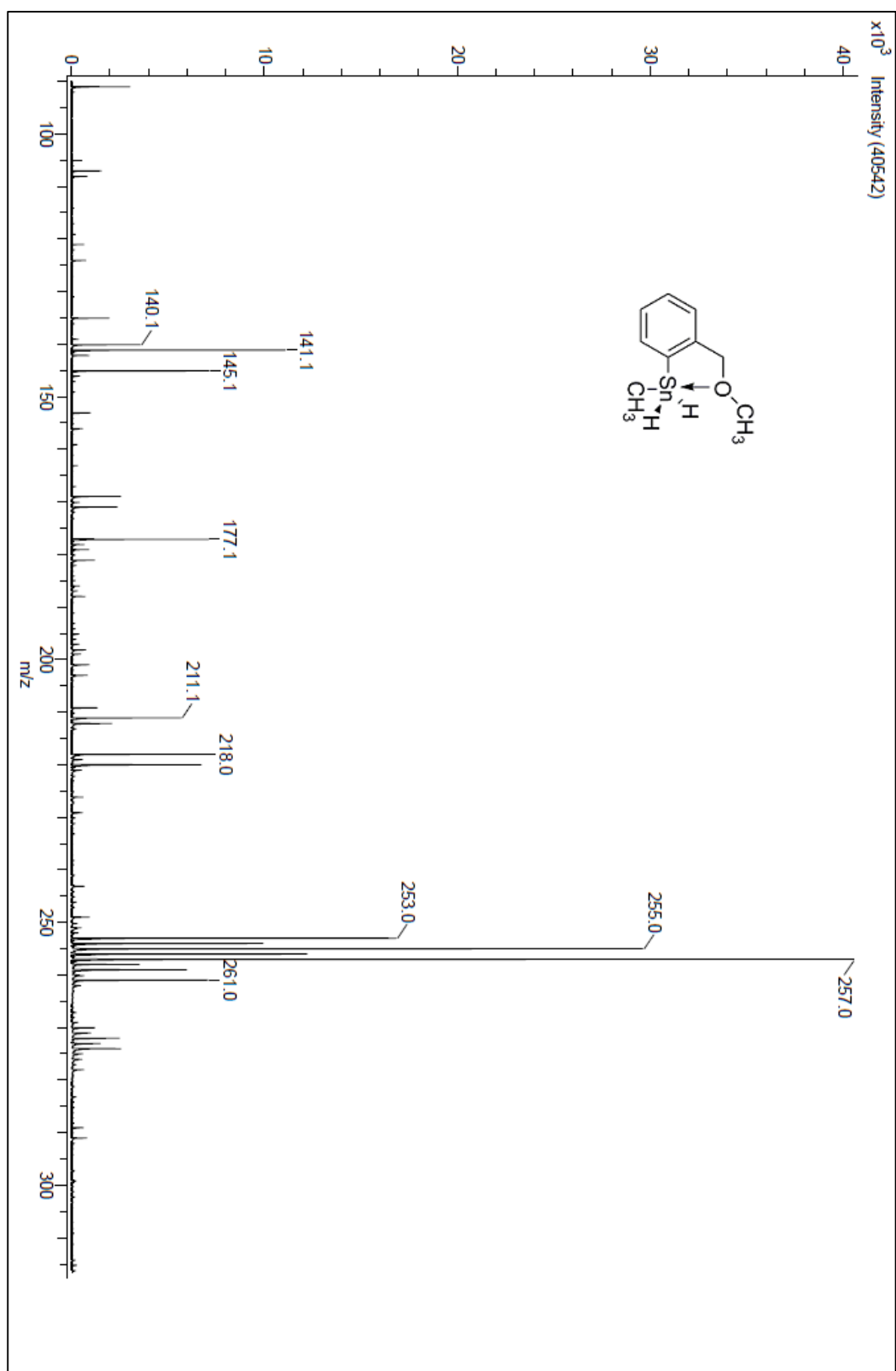
Figure A 140: DART spectrum of compound 226
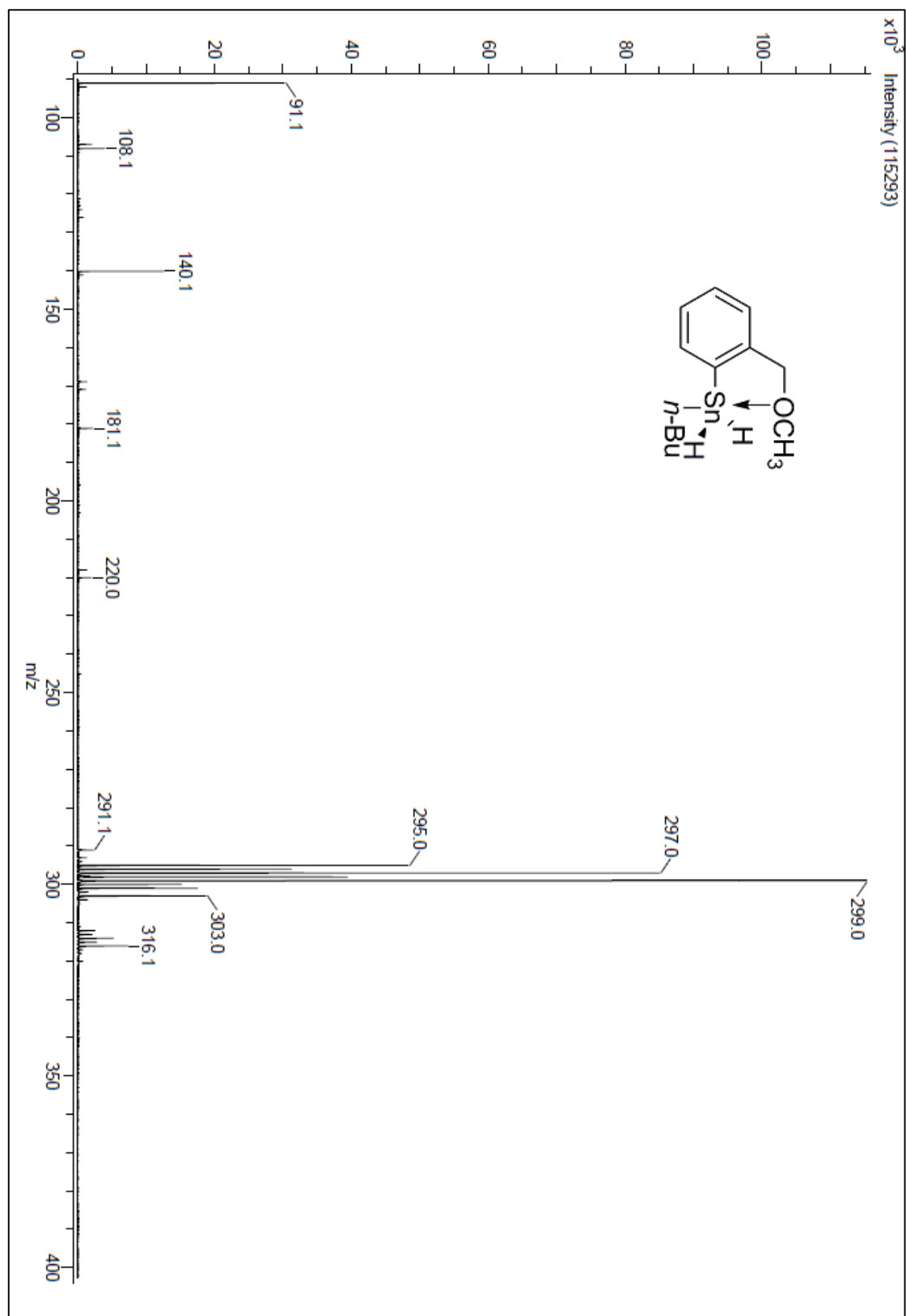
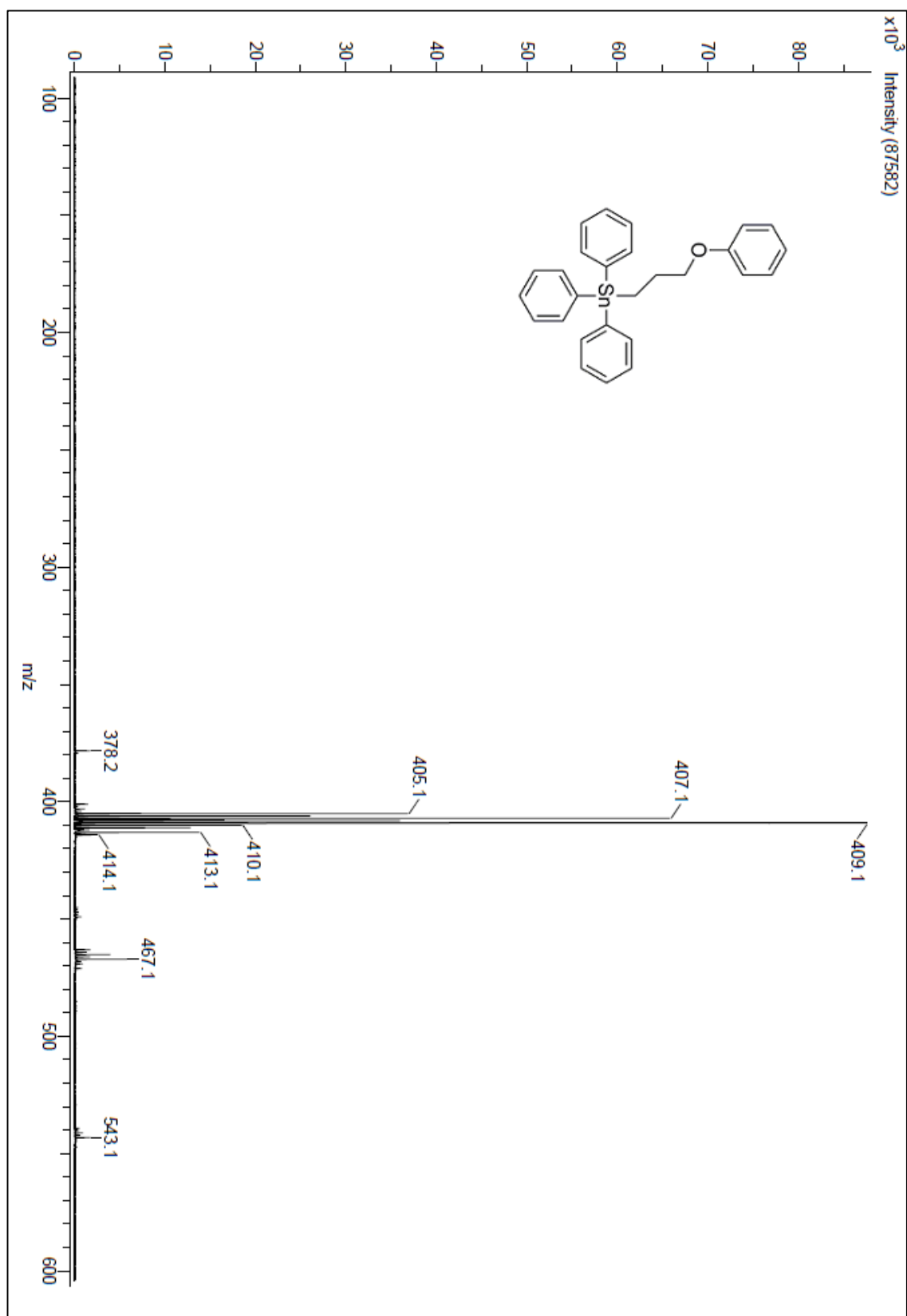**Figure A 141: DART spectrum of compound 227**
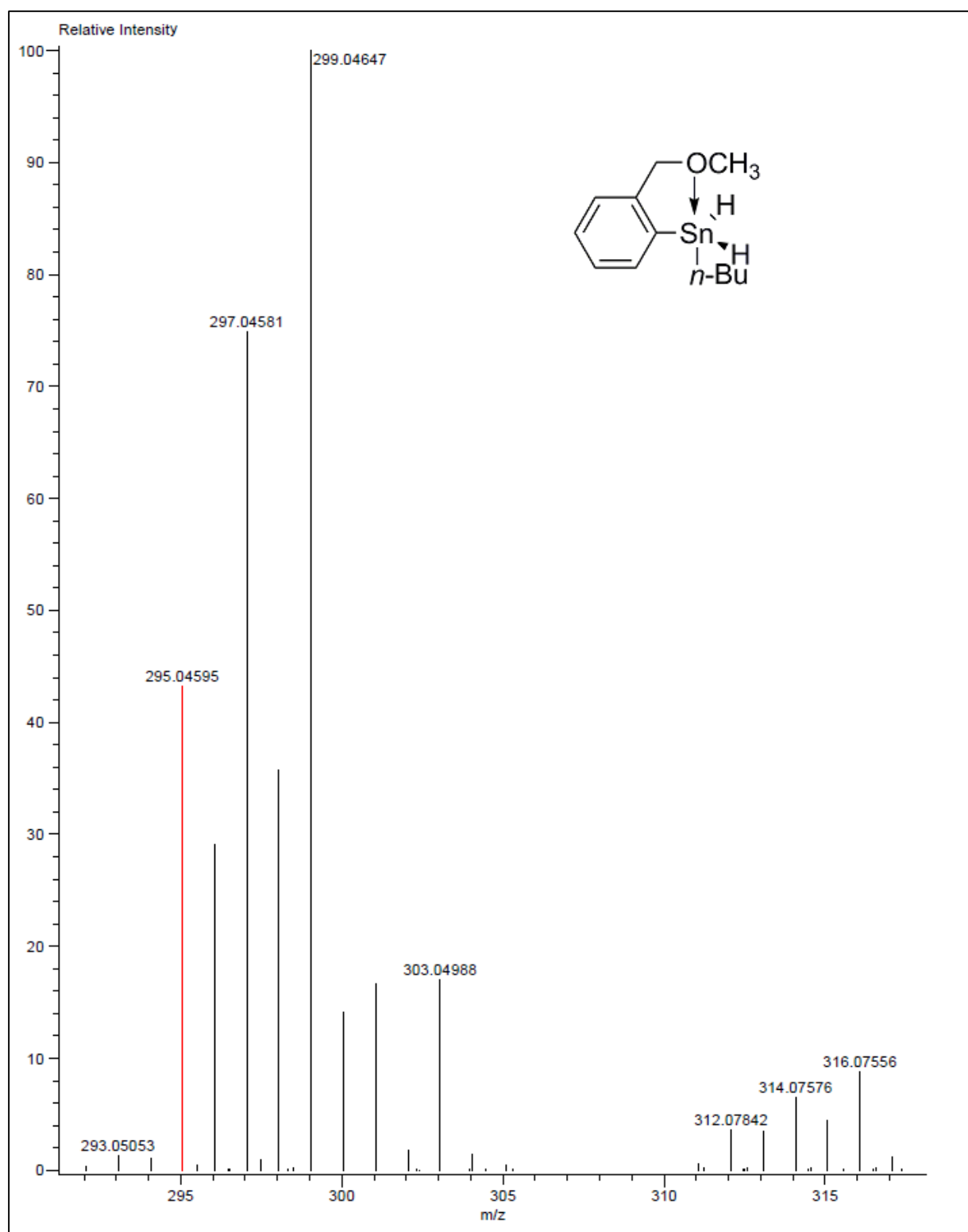
Figure A 142: HRMS-DART spectrum of compound 227
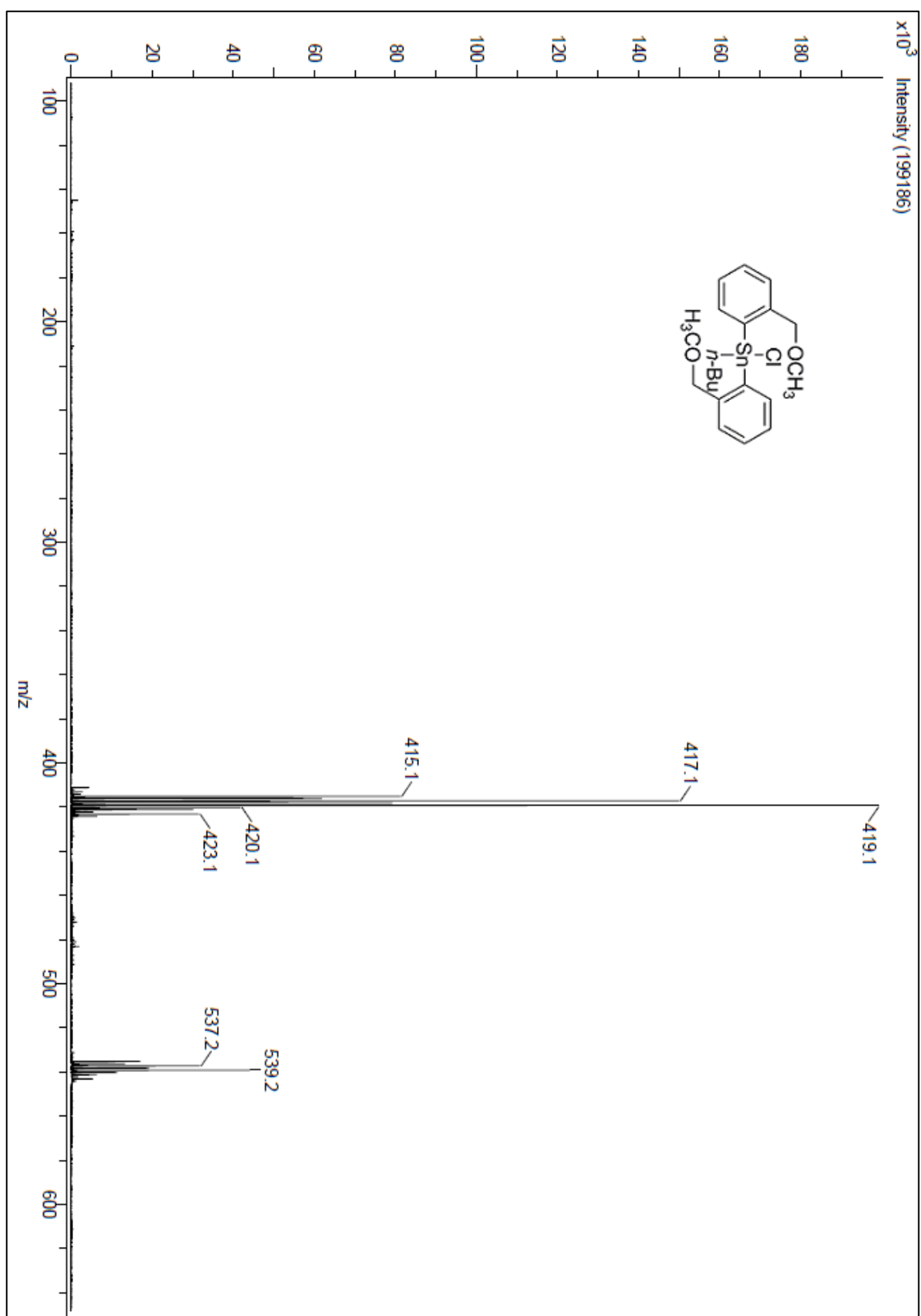
Figure A 143: DART spectrum of compound 224
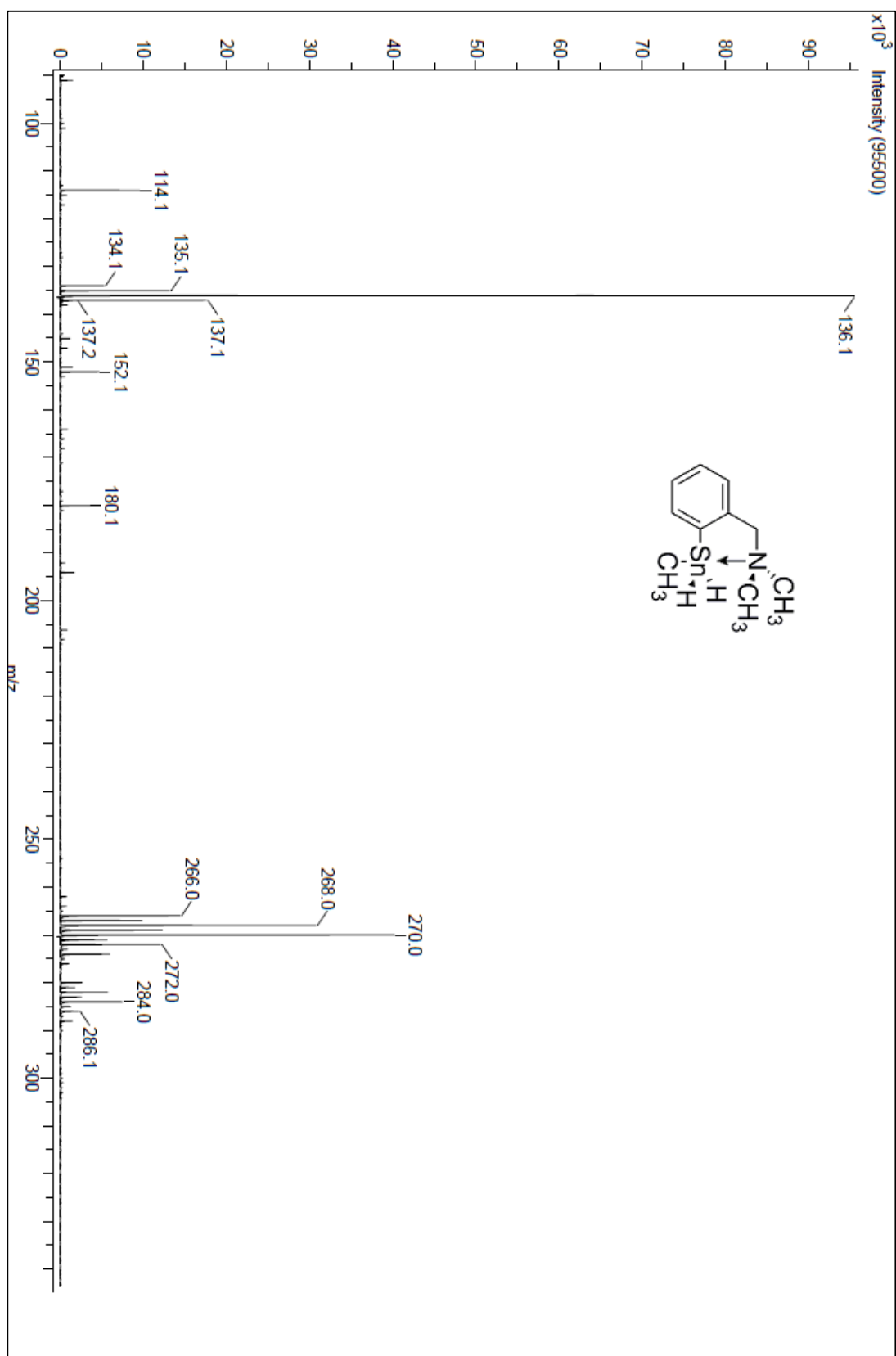
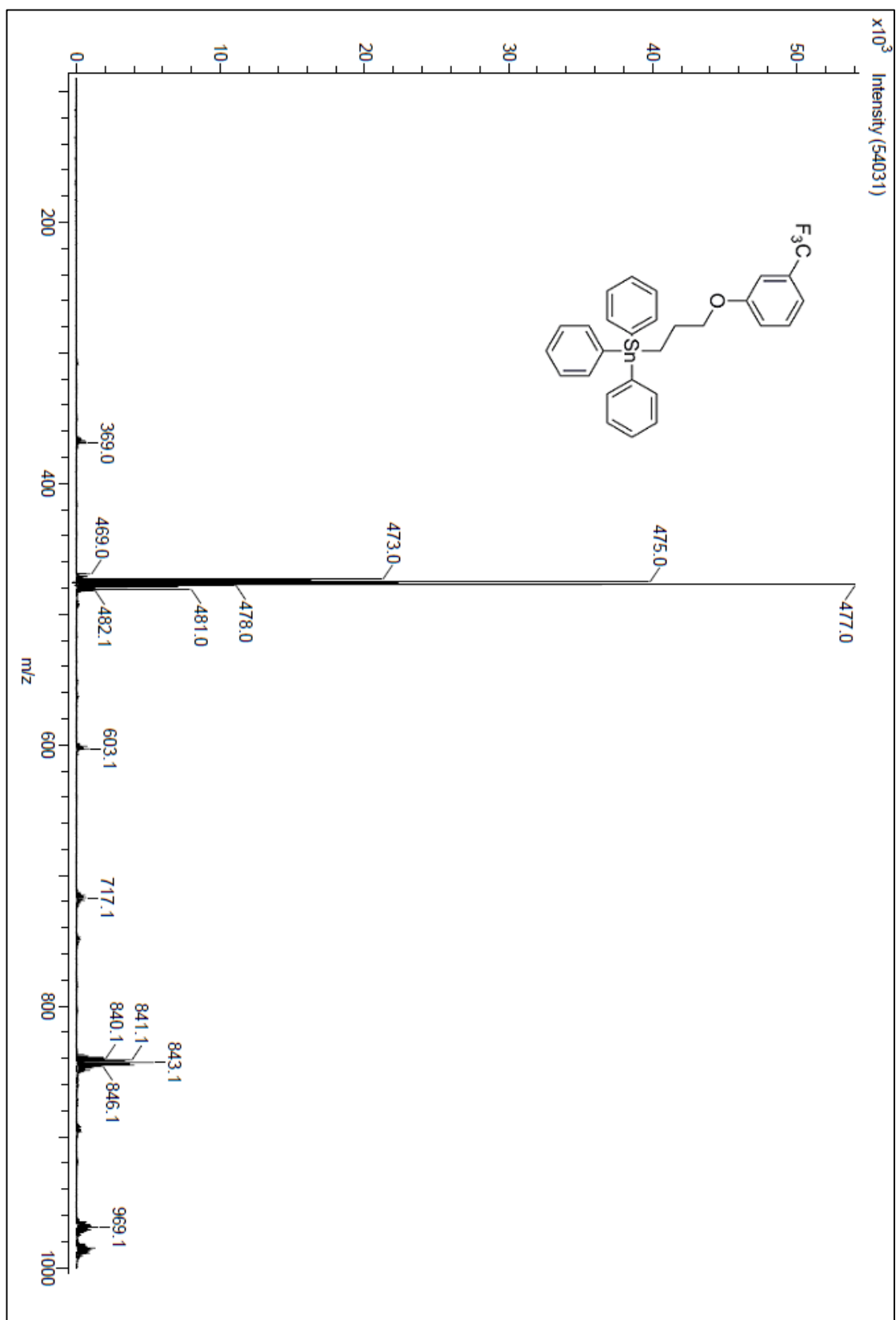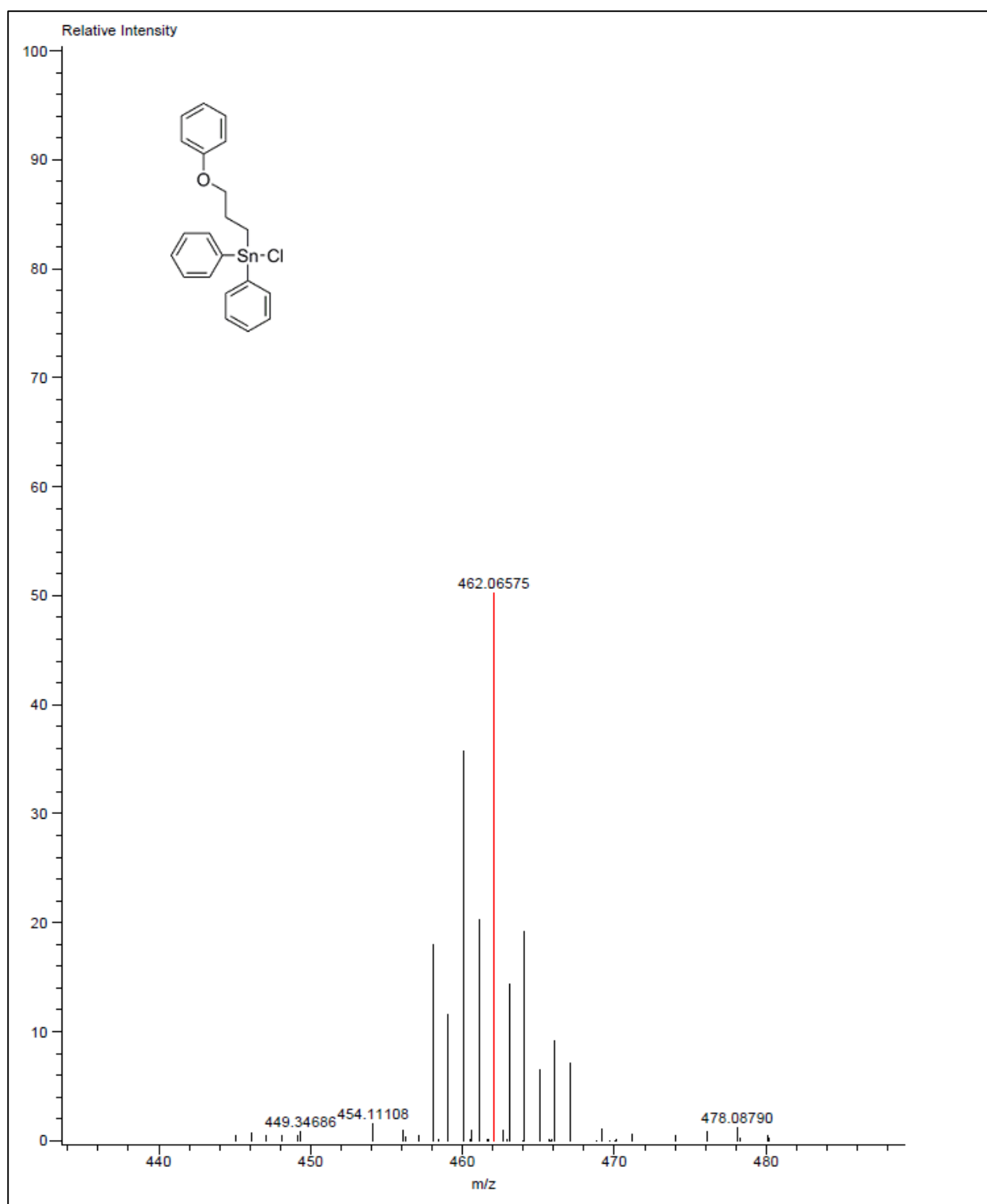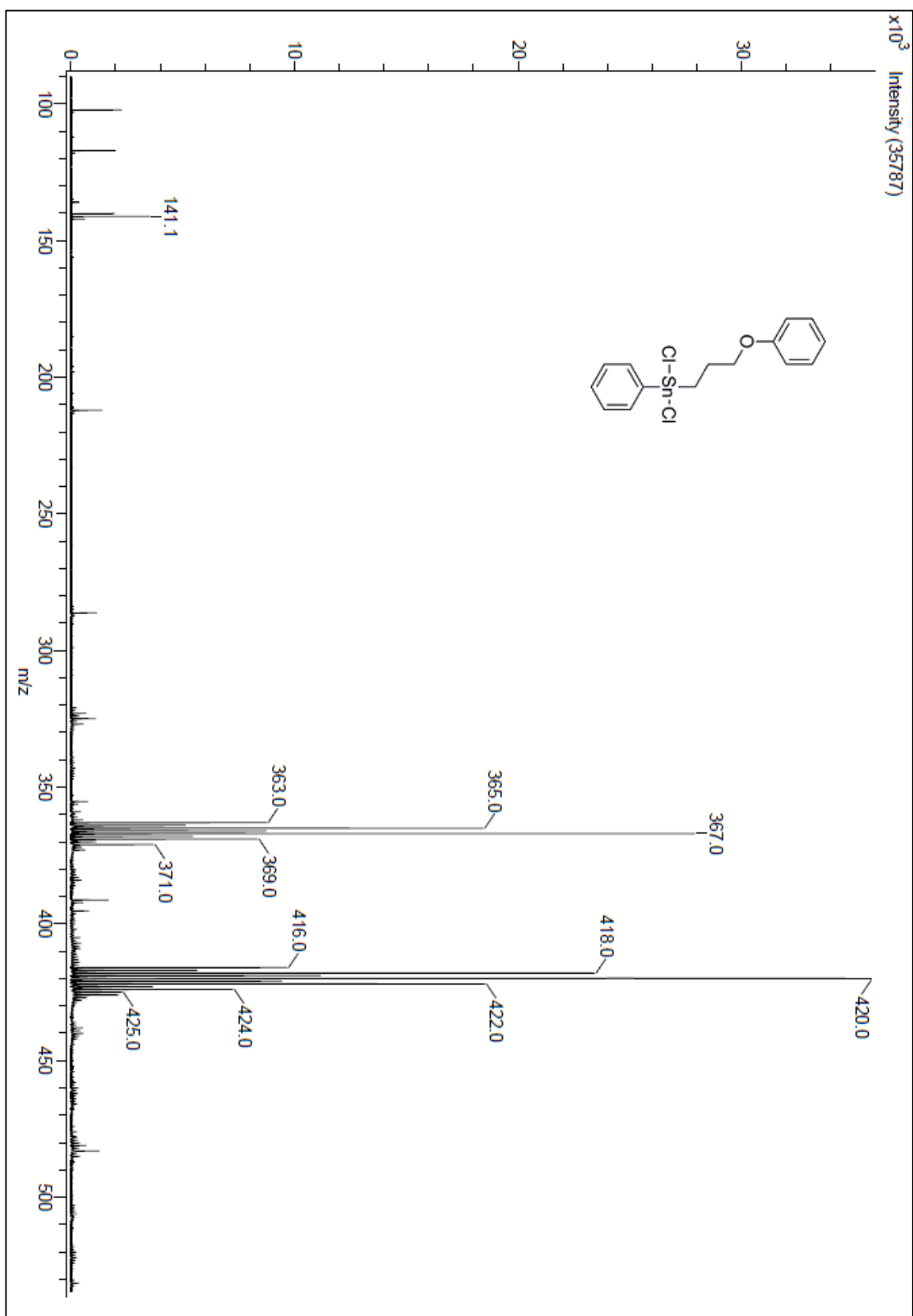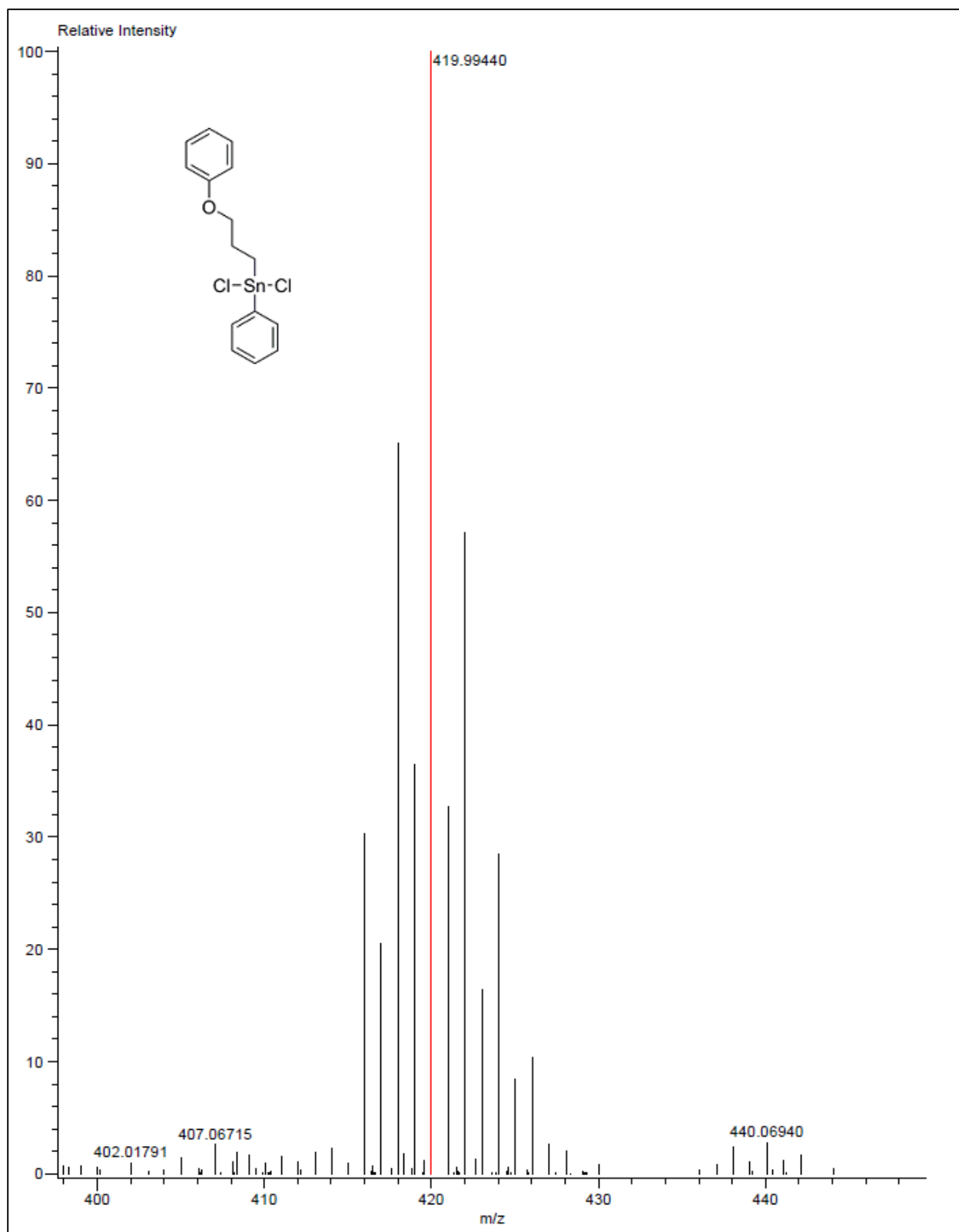**Figure A 144: DART spectrum of compound 230**
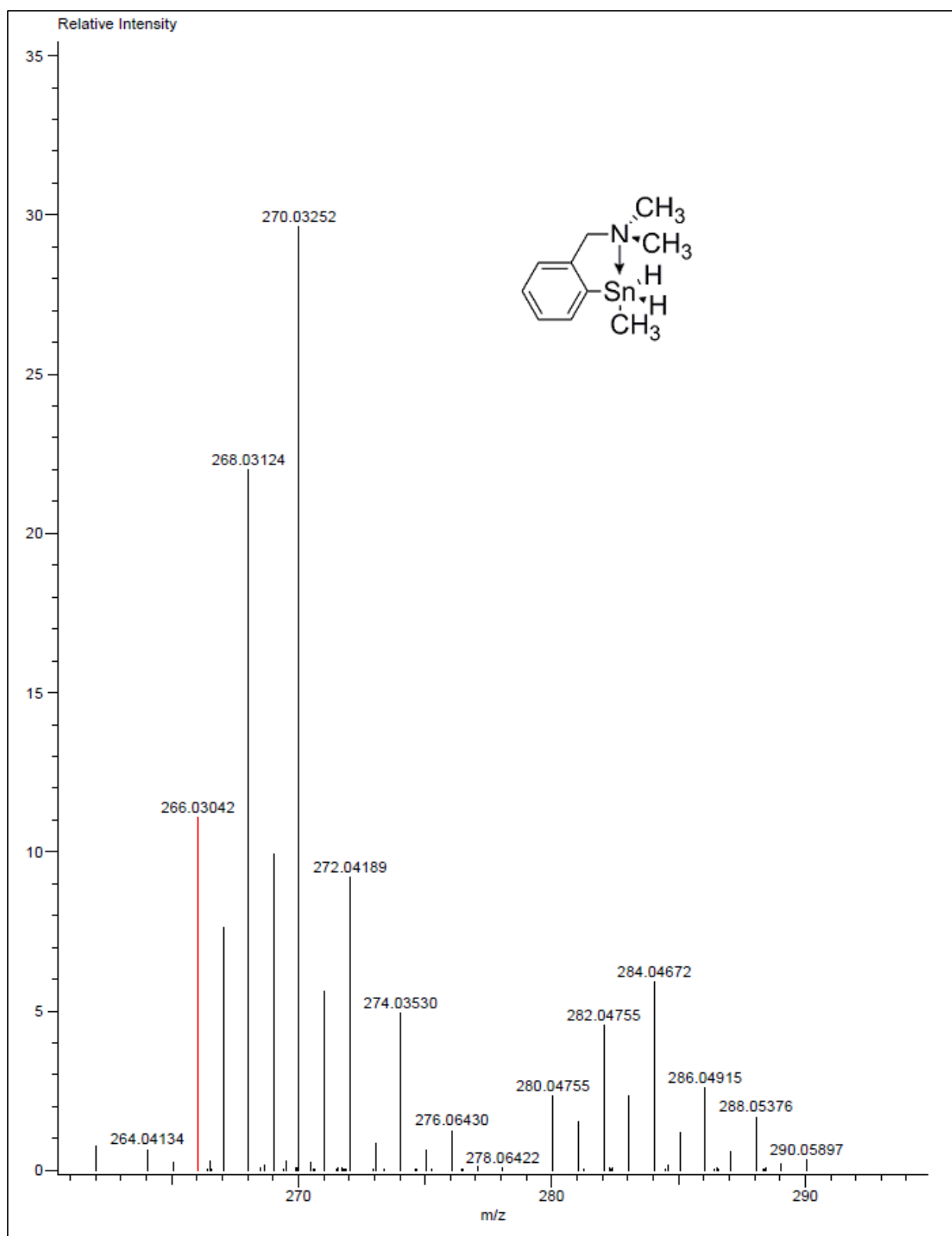
Figure A 145: HRMS-DART spectrum of compound 230
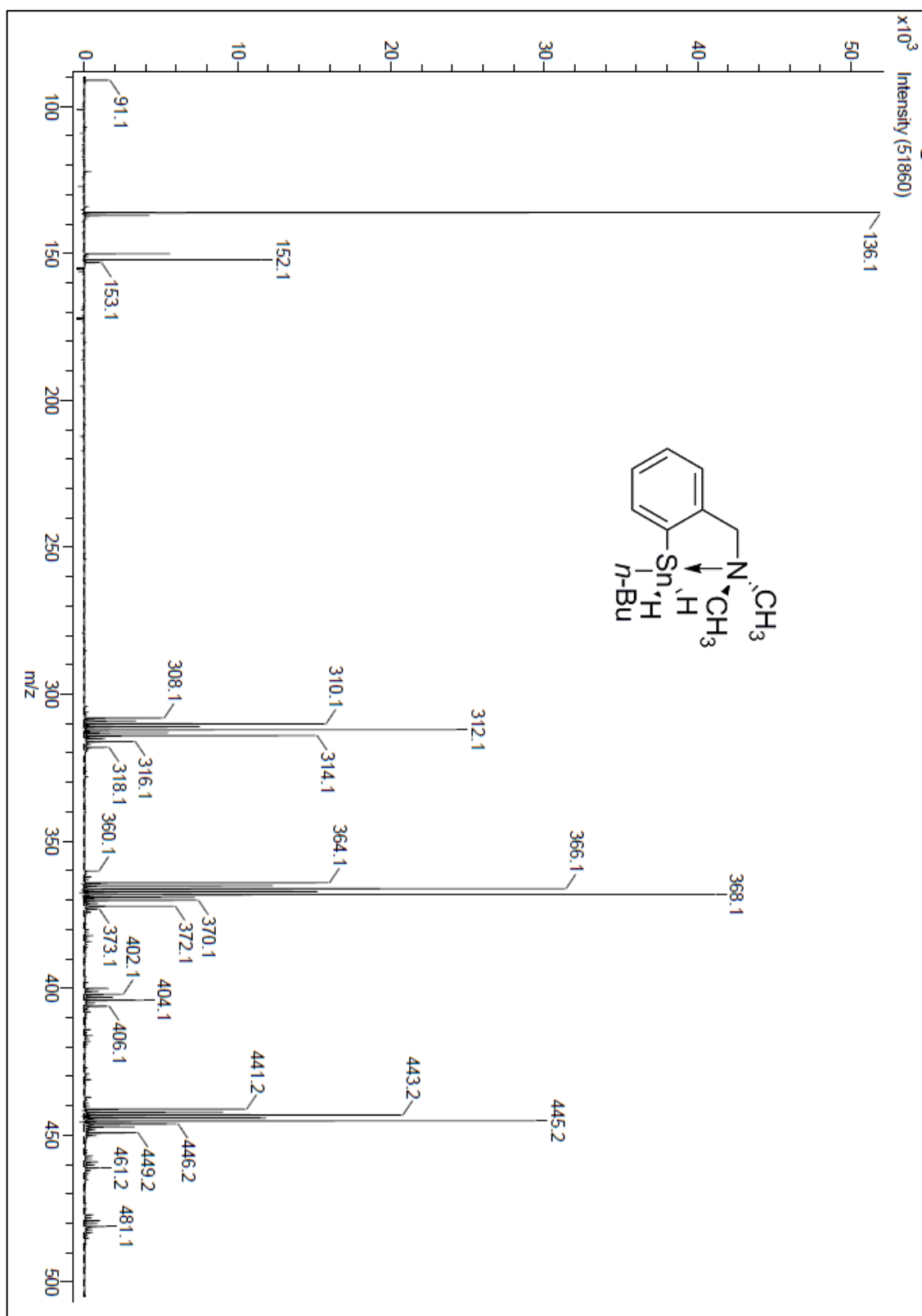
Figure A 146: DART spectrum of compound 231

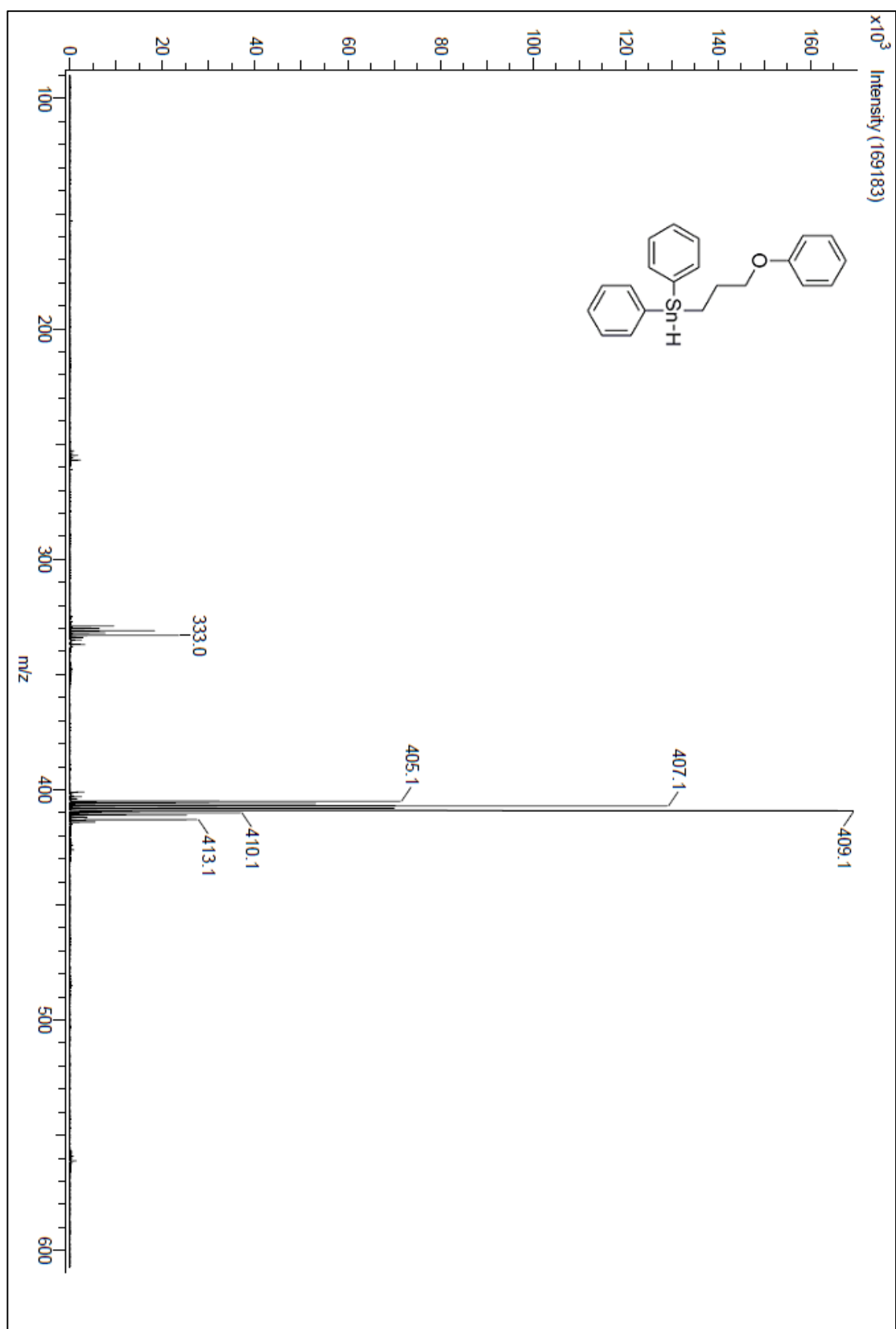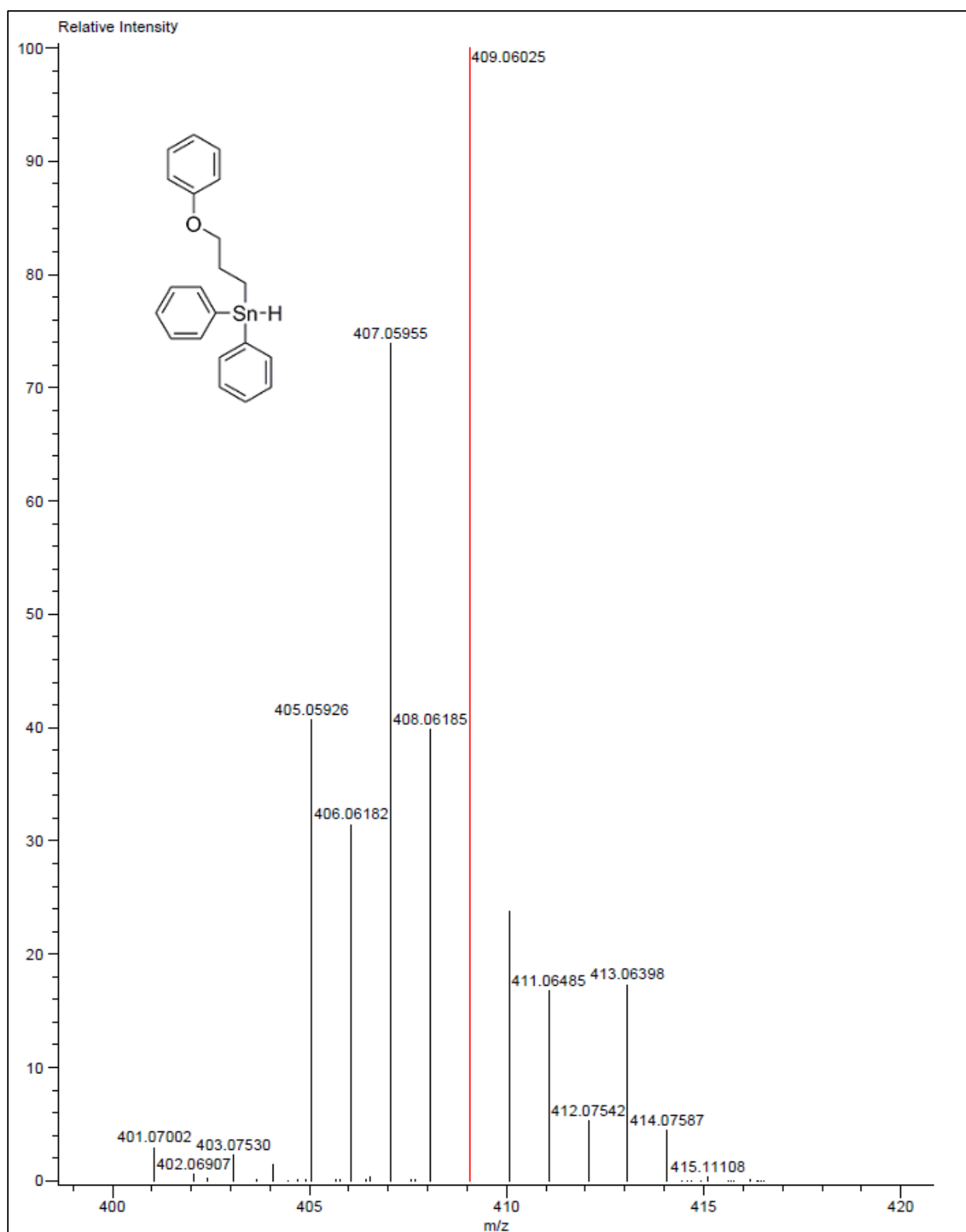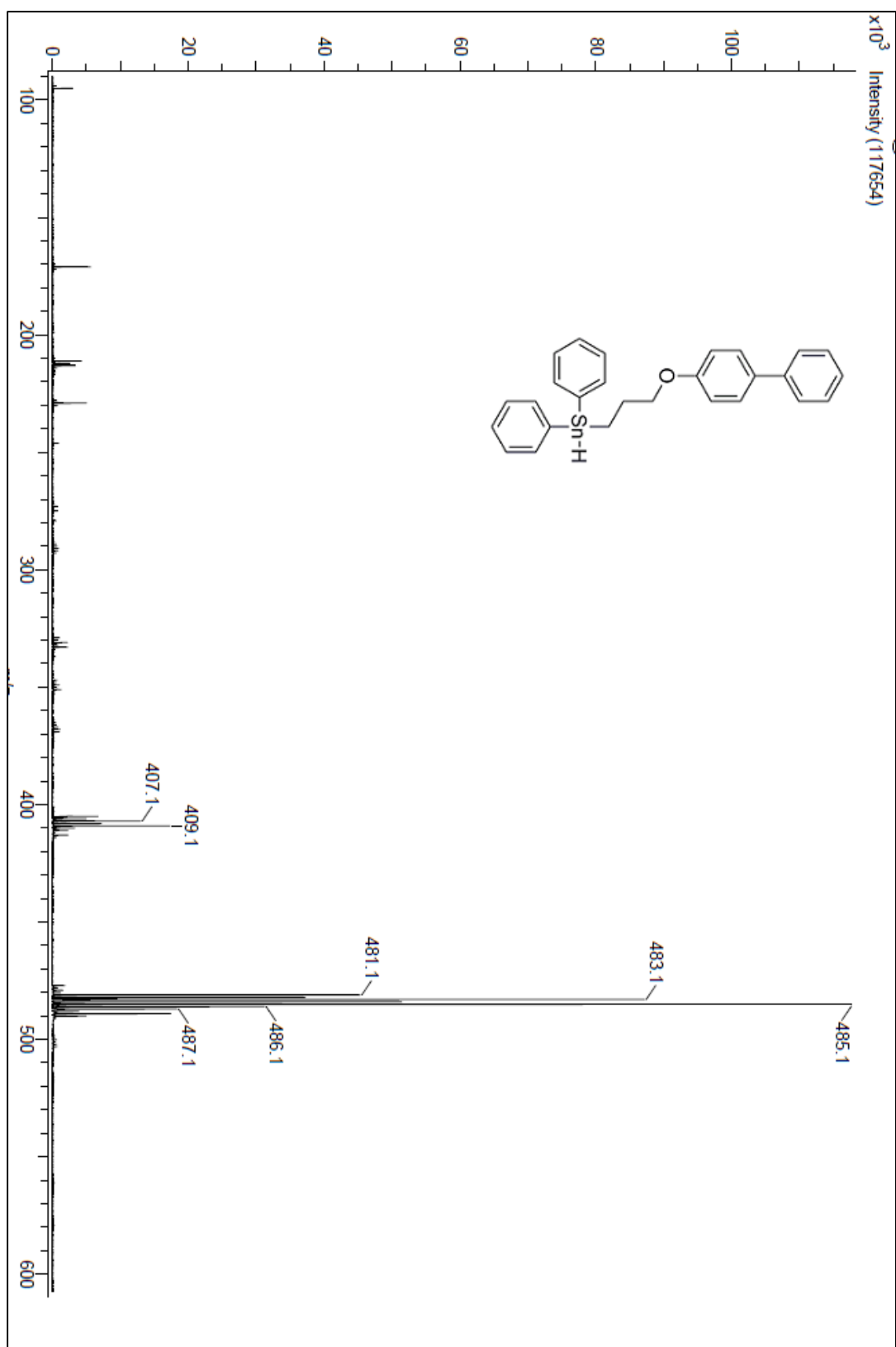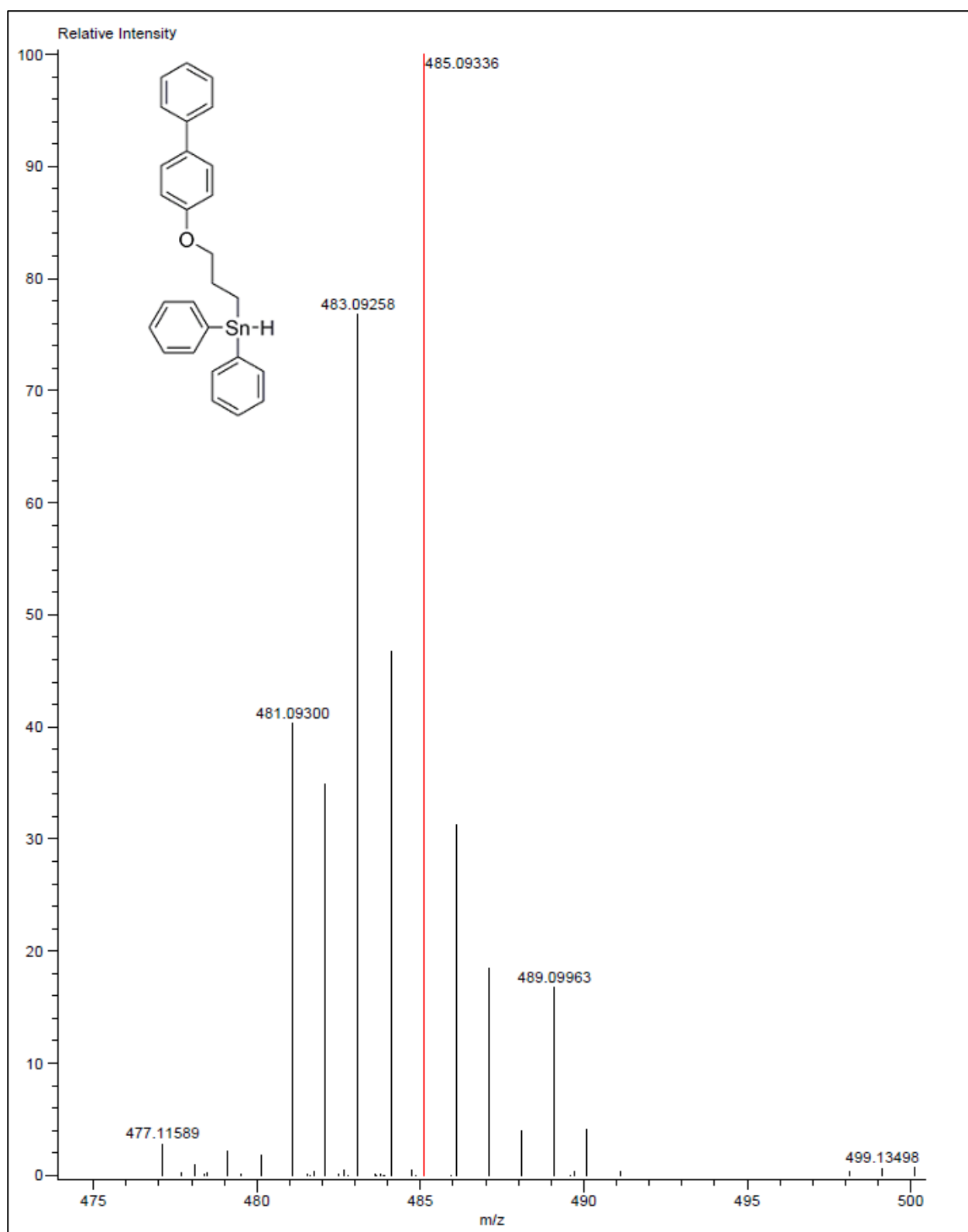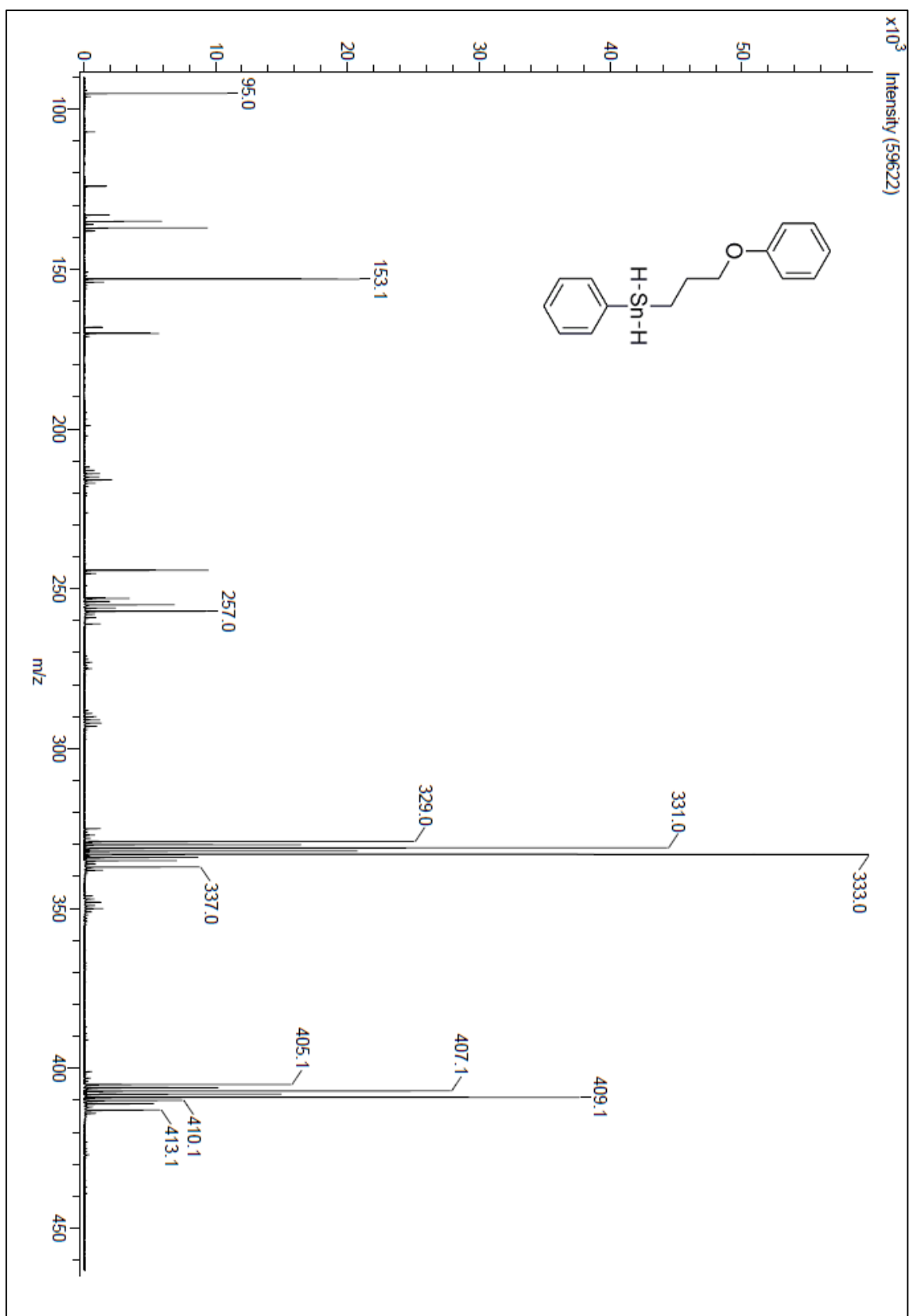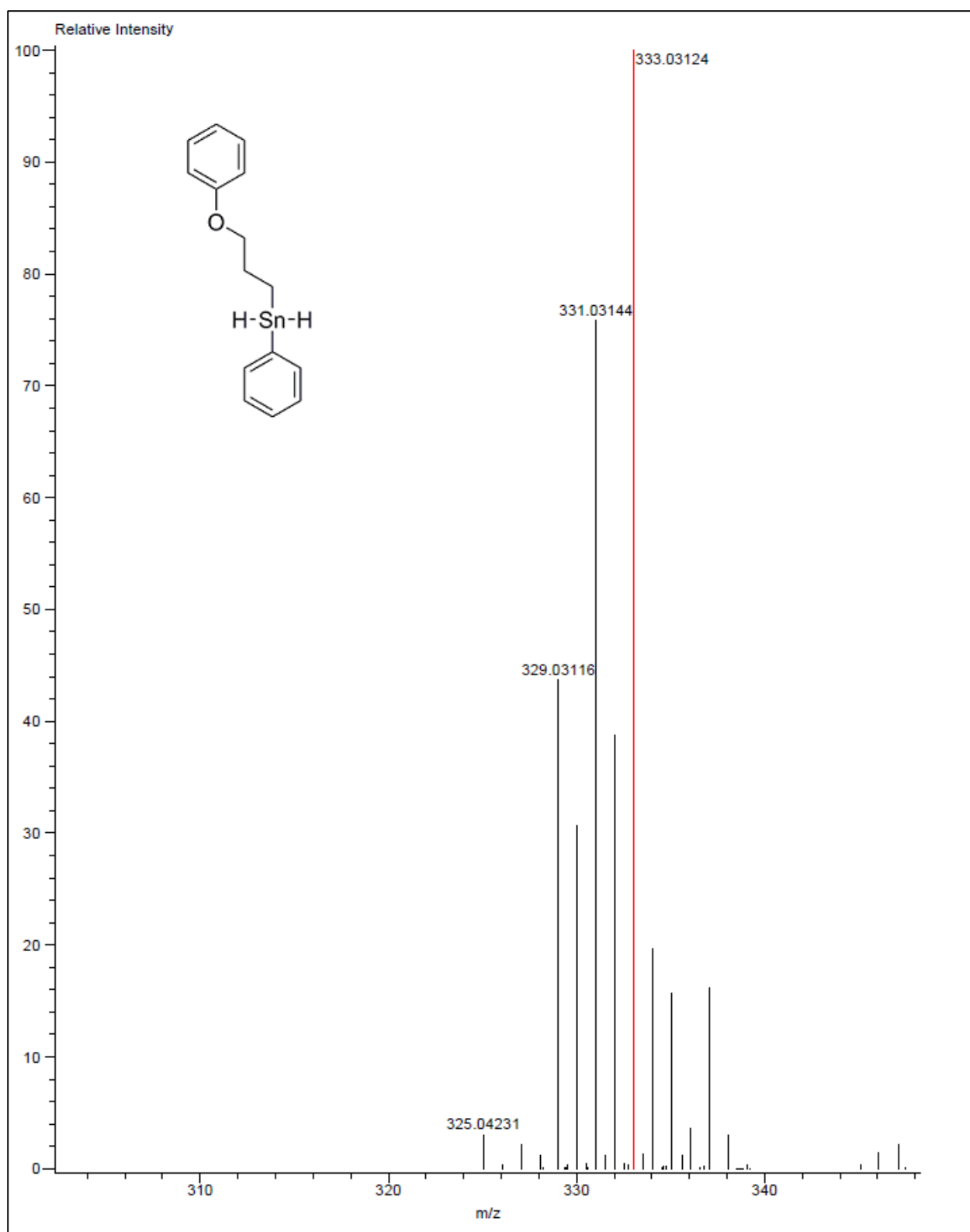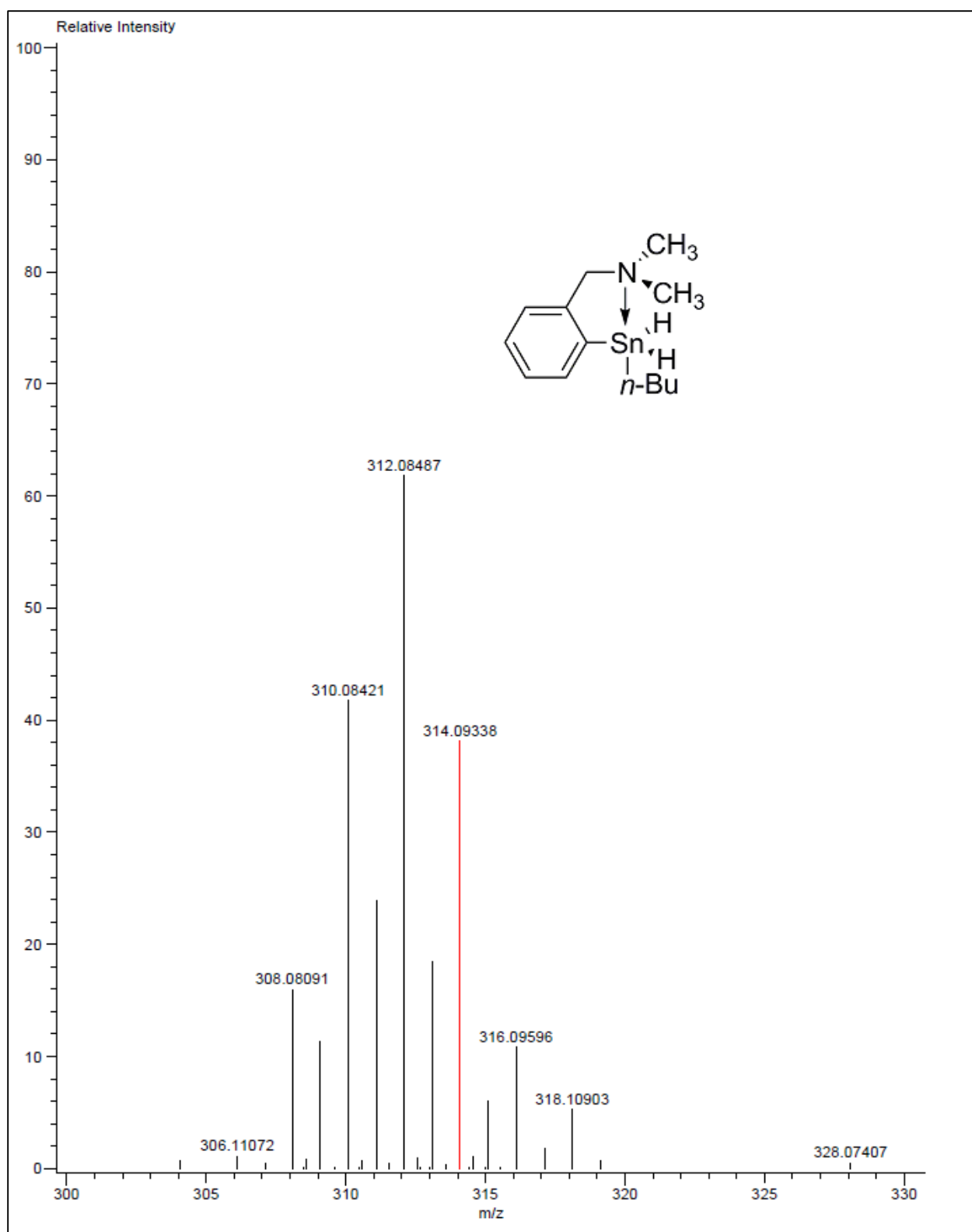**Figure A 147: HRMS-DART spectrum of compound 231**

7.0 References:

1.   Chaudhary, A.; Singh, R. V. *Main Group Met. Chem.* **2008**, *31*, 107.

2.   Tin Chemistry: Fundamental, Frontiers, and Applications, Edited by Gielen, M.; Davies, A.; Pannell, K.; Tiekink, E. John Willey & Sons, Ltd., New York, 2000.

3.   Frankland, E. *Q. J. Chem. Soc*. **1850**, *2*, 263.

4.   Löwig, C. *Liebigs, Ann. Chem*. **1852**, *84*, 308.

5.   Pope, W. J.; Peachy, S. J. *Proc. Chem. Soc*. **1903**, *19*, 290.

6.   Kocheshkov, K. A. *Ber*., **1929**, *62*, 996.

7.   Krause, E.; Von Grosse, A. *Die Chemie der Metal-organization verbindungen, Verlag Borntraeger*, Berlin, **1937**.

8.   Akiba, K.-Y. Chemistry of hypervalent compounds, John Willey & Sons, Ltd. New York, 1999.

9.   Tandura, S. N.; Voronkov, M. G.; Alekseev, N. A. *Top. Curr. Chem*. **1986**, *131*, 101

10.   Chuit, C.; Corriu, R. J. P.; Reye, C.; Young. J. C. *Chem. Rev*. **1993**, *93*, 1371.

11.   Holmes, R. R. *Chem. Rev*. **1996**, *96*, 927.

12.   Voronkov, M. G.; Trofimova, O. M.; Bolgova, Y. I.; Chernov, N. F. *Russ. Chem. Rev*. **2007**, *76*, 825.

13.   Baukov, Y, I.; Tandura, S. N. The Chemistry of Organic Germanium, Tin and Lead Compounds, Rappoport, Z., Eds.; John Willey & Sons, Ltd., New York, 2002; Vol. 2.

14.   Jastrzebski, J. T. B. H.; van Koten, G. *Adv. Organometal. Chem.* **1993**, *35*, 241.

15.   Janseen, M. J.; Lujiten, J. G. A.; van der Kerk, G. J. M.; *J. Organometal. Chem.* **1964**, *1*, 286.

16.   Beattie, I. R.; Gilson, T.; *J. Chem. Soc*. **1961**, 2582.

17.   Musher, J. I. *Angew. Chem. Int. Ed. Engl*. **1969**, *8*, 54.

18.   Hulme, R. *J. Chem. Soc.* **1963**, 1524.

19.   Perkins, C. W.; Martin, J. C.; Arduengo, A. J.; Lau, W.; Alegria, A.; Koci, J. K. *J. Am. Chem. Soc.* **1985**, *107*, 6359.

20.   (a) Pimentel, G. C. J. *Chem. Phys*. **1951**, *19*, 446. (b) Hackand, R. J.; Rundle, R. E. *J. Am. Chem. Soc.* **1951**, *73*, 4321.

21.   Kutzelning, W. *Angew. Chem. Int. Ed. Engl*. **1984**, *23*, 272.

22.   Reed, A. E.; Schleyer, P. V. R. *J. Am. Chem. Soc.* **1990**, *112*, 134.

23.   Janseen, M. J.; Lujiten, J. A.; van der Kerk, G. J. M. *J. Organomet. Chem*. **1964**, *1*, 286.

24.   Colton, R.; Dakternieks, D. *Inorg. Chim. Acta*. **1988**, *31*, 148.

25.   Li, Q.; Yang, P.; Hau, E.; Tian, C. *J. Coord. Chem*. **1996**, *40*, 227.

26.   Jastrzebski, J. T. B. H.; Grove, D. M.; Boersma, J.; van Koten, G. *J. Magn. Reson*. **1991**, *29*, S25.

27.   Jastrzebski, J. T. B. H.; Knapp, C. T.; van Koten, G. *J. Organomet. Chem*. **1983**, *255*, 287.

28.   Jastrzebski, J. T. B. H.; Boersma, J.; Esch, P. M.; van Koten, G. *Organometallics* **1991**, *10*, 930.

29.   a) Novák, P.; Padělková, Z.; Kolářová, L.; Císařová, I; Růžička, A.; Holeček, J. *Appl. Organometal. Chem*. **2005**, *19*, 1101. b) Růžička, A.; Pejchal, V.; Holeček, J.; Lyčka, A.; Jacob, K. *Collect. Czech. Chem. Commun*. **1998**, *63*, 977.

30.   Mitchell, T. N. *J. Organomet. Chem*. **1973**, *59*, 189.

31.   Gielen, M. *Pure Appl. Chem*. **1980***, 52, 657.*

32.   Jastrzebski, J. T. B. H.; van Koten, G.; Knaap, C. T.; Schreurs, A. M. M.; Kroon, J.; Spek, A. L. *Organometallics* **1986**, *5*, 1551.

33. van Koten, G.; Jastnebki, J. T. B. H.; Noltes, J. G.; Pontenagel, W. M. G. F.; Kroon, J.; Spek, A. L. *J. Am. Chem. Soc*. **1978**, *100*, 5021.

34. Jastrzebski, J. T. B. H. Ph.D. Thesis, University of Utrecht, The Netherland, 1991.

35. Rippstein, R.; Kickelbick, G.; Schubert, U. *Inorg. Chim. Acta* **1999**, *290*, 100.

36. Kitching, W.; Drew, D.; Adcock, W.; Abeywickrema, A. N. *J. Org. Chem*. **1981**, *46*, 2252.

37. Gielen, M. *Bull. Soc. Chim. Belg*. **1983**, *92*, 409.

38. Kroth, H. J.; Schumann, H.; Kuivila, H. G.; Schaeffer, C. D.; Zuckerman, J. J. *J. Am. Chem. Soc.* **1975**, *97*,1754.

39. Hunter, B. K.; Reeves, L. W. *Can. J. Chem*. **1968**, *46*, 1399.

40. Choffat, F.; Kaser, S.; Wolfer, P.; Schmid, D.; Mezzenga, R.; Smith, P.; Caseri, W. *Macromolecules* **2007,** *40*, 7878.

41. Choffat, F.; Buchmuller, Y.; Mensing, C.; Smith, P.; Caseri, W. *J. Inorg. Organomet. Polym*. **2009**, *19*, 715.

42. Zeppek, C.; Pichler, J.; Torvisco, A.; Flock, M.; Uhlig, F. *J. Organomet. Chem*. **2013**, *740*, 41.

43. Deacon, P. R.; Devylder, N.; Hill, M.; Mahon, M. F.; Molloy, K. C.; Price, G. J. *J. Organomet. Chem*. **2003**, *687*, 46.

44. Jastrzebski J. T. B. H, van Koten, G. *Adv. Organomet. Chem.* **1993**, *35*, 241.

45. Růžička, A.; Jambor. R.; Brus, J.; Císařová, I.; Holeček, J. *Inorg. Chim. Acta* **2001**, *323*, 163.

46. Růžička, A.; Jambor, R.; Císařová, I.; Holeček, J. *Chem. Eur. J*. **2003**, *9*, 2411.

47. van Koten, G.; Schaap, C. A.; Noltes, J. G. *J. Organomet. Chem*. **1975**, *99*, 157.

48. Rippstein, R.; Kickelbick, G.; Schubert, U. *Monatsh. Chem.* **1999**, *130*, 385.

49.   Varga, R. A.; Rotar, A.; Schürmann, M.; Jurkschat, K.; Silvestru, C. *Eur. J. Inorg. Chem.* **2006**, 1475.

50.   van Koten, G.; Jastrzebski, J. T. B. H.; Noltes, J. G.; Godefridus J. V.; Anthony L. S.; and Jan K. *J.Chem. Soc. Dalton Trans.* **1980**, 1352.

51.   Varga, R. A.; Jurkschat, K.; Silvestru, C. *Eur. J. Inorg. Chem.* **2008**, 708.

52.   Novák, P.; Císařová, I; Jambor, R.; Růžička, A.; Holeček, J. *Appl. Organomet. Chem.* **2004**, *18*, 241.

53.   Oki, M.; Ohira, M. *Chem. Lett.* **1982**, *11*, 1267.

54.   van Koten, G.; Noltes, J. G.; Spek, A. L.; *J. Organomet. Chem.* **1976**, *118*, 183.

55.   van Koten, G.; Noltes, J. G. *J. Am. Chem. Soc.* **1976**, *98*, 5393.

56.   a)Jastrzebski, J. T. B. H.; Boersma, J.; Esch, P. M.; van Koten, G. *J. Organomet. Chem.* **1991**, *413*, 43. b) Wrackmeyer, B. *Annu. Reports NMR Spectrosc*. **1985**, 16, 73.

57.   van Koten, G.; Noltes, J. G. *J. Am. Chem. Soc.* **1976**, *98*, 5393.

58.   Švec, P.; Padělková, Z.; Císařová, I; Růžička, A.; Holeček, J. *Main group met. Chem.* **2008**, *31*, 305.

59.   van Koten, G.; Jastrzebski, J. T. B. H.; Noltes, J. G. *J. Organometal. Chem.* **1979**, *177*, 283.

60.   Padělková, Z.; Brus, J.; Císařová, I; Růžička, A.; Holeček, J. *J. Fluorine Chem.* **2005**, *126*, 1531.

61.   Novák, P.; Padělková, Z.; Císařová, I; Kolářová, L.; Růžička, A.; Holeček, J. *Appl. Organomet. Chem.* **2006**, *20*, 226.

62.   Pejchal, V.; Holeček, J.; Lyčka, A. *Sci. Pap. Univ. Pardubice Ser. A* **1996**, *2*, 35. [*Chem. Abstr.* **1997**, *126*]

63. Kraus, C. A.; Greer, N. W. *J. Am. Chem. Soc*. **1922**, *44*, 2629.

64. Finholt, A. E.; Bond, A. C.; Wilzbach Jr., K. E.; Schlesinger, H. I. *J. Am. Chem. Soc.* **1947**, *69*, 2692.

65. Komsta, Z.; Cmoch, P.; Staliński, K. *Polish J. Chem*. **2006**, *80*, 1259.

66. Turek, J.; Padělková, Z.; Černošek, Z.; Milan, E.; Lyčka, A.; Nechaev, M. S.; Císařová, I; Růžička, A.; *J. Organomet. Chem.* **2009**, *694*, 3000.

67. Vedejs, E.; Duncan, S. M.; Haight. A. R. *J. Org. Chem.* **1993**, *58*, 3046.

68. Dakternieks, D.; Dunn, K.; Carl H. Schiesser, C. H.; Tiekink, E. R. T. *J. Organomet. Chem.* **2000**, *605*, 209.

69. Cmoch, P.; Urbańczyk-Lipkowski, Z.; Petrosyan, A.; Stępień, A.; Staliński, K. *J. Mol. Struct*. **2005**, *733*, 29.

70. Rupnicki, L.; Urbańczyk-Lipkowski, Z.; Stępień, A.; Cmoch, P.; Pianowski, Z.; Staliński, K. *J. Organomet. Chem.* **2005**, *690*, 3690.

71. Staliński, K.; Urbańczyk-Lipkowski, Z.; Cmoch, P.; Rupnicki, L.; Grachev, A. *J. Organomet. Chem.* **2006**, *691*, 2394.

72. Matkowska, D.; Gola, M.; Śnieżek, M.; Cmoch, P.; Staliński, K. *J. Organomet. Chem.* **2007**, *692*, 2036.

73. Birchall, T.; Pereira, A. R. *J. Chem. Soc*., *Dalton Trans*. **1975**, 1087.

74. Blunden, S. J.; Cusack, P. A.; Hill, R. The Industrial Uses of Tin Chemicals, Royal Society of Chemistry, London, 1985.

75. Gielen, M.; Willem, R.; Holeček, J.; Lyčka, A. *Main Group Met. Chem.* **1993**, *16*, 29.

76. Schumann, H.; Wassermann, B. C.; Ekkehardt H. F. *Organometallics* **1992**, *11*, 2803.

77. a) Gay-Lussac, J. L.; Thenard, L. J. *Mémoires de Physique et de Chimie de la Société d' Arceuil*, **1809**, *2*, 317. b) Davy, J. *Philos. Trans.* **1812**, *2*, 352; *Liebigs Ann. Chem.* **1813**, *86,* 178.

78. Boyer, J.; Breliére, C.; Carré, F.; Corriu, R. J. P.; Kpoton, A.; Poirier, M.; Royo, G.; Young, J. C. *J. Chem. Soc. Dalton Trans*. **1989**, 43.

79. Klebe, G.; Nix, M.; Hensen, K. *J. Chem. Soc. Dalton Trans.* **1985**, 5.

80. Klebe, G. *J. Organomet. Chem.* **1987**, *332*, 35.

81. Breliere, C.; Carre, F.; Corriu, R. J. P.; De Saxce, A.; Poirier, M.; Royo, G. *J. Organomet. Chem*. **1981**, *205*, C1.

82. Klebe, G.; Nix, M.; Hensen, K. *Chem. Ber*. **1984**, *117*, 797.

83. Klanberg, F.; Muetterties, E. L. *Inorg. Chem.* **1968**, *7*, 155.

84. De Wit, P. P.; Van Der Kooi, H. O.; Wolters, J. *J. Organomet. Chem.* **1981**, *216*, C9.

85. Christea, A.; Silvestru, A.; Silvestru, C. Studia Universitatis Babeş-Bolyai, Chemia, **2009**, *LIV*, 4.

86. Krause, E.; Reissaus, G. G. *Ber*. **1922**, *55*, 888.

87. GiIman, H.; Summers, L.; Leeper. R. W. *J. Org. Chem*. **1922**, *17*, 630.

88. GlockIing, F.; Hooton, K.; Kingston, D. *J. Chem. Soc*. **1961**, 4405.

89. Appeerson. L. D. *Coll. J. Sci*. **1941**, 16, 7; *Che. Abstr*. **1942**, *36*, 4476.

90. Willemsens, L. C.; van der Kerk. G. J. M. *J. Organomet. Chem*. **1964**, *2*, 271.

91. Lenka Kolářová, L.; Holčapek, M.; Jambor, R.; Dostál, L.; Nádvorník, M.; Růžička, A. *J. Mass Spectrom.* **2004**, *39*, 621.

92. Jambor, R.; Dostál, L.; Růžička, A.; Císařová, I; Brus, J.; Holčapek, M.; Holeček, J. *Organometallics* **2002**, *21*, 3996.

93. Mehring, M.; Schurmann, M.; Jurkschat, K. *Organometallics* **1998**, *17*, 1227.

94. GiIman, H.; Artzen, C. E. *J. Am. Chem. Soc.* **1950**, 3823.

95. Reich, H. J.; Goldenberg, W. S.; Sanders, A. W.; Jantzi, K. L.; Tzschucke, *C. C. J. Am. Chem. Soc.* **2003**, *125*, 3509.

96. Munguia, T.; Lopez-Cardoso, M.; Cervantes-Lee, F.; Pannell, K. H. *Inorg. Chem.* **2007,** *46*, 1305.

97. Jousseaume, B.; Duboudin, J. G. *J. Organomet. Chem.* **1982**, *238*, 171.

98. Dostál, L.; Jambor, R.; Růžička, A.; Císařová, I; Holeček, J.; Biesemans, M.; Willem, R.; De Proft. F.; Geerlings, P. *Organometallics* **2007**, *26*, 6312.

99. Kemmer, M.; Biesemans, M.; Gielen, M.; Tiekink, E. R. T.; Willem, R. *J. Organomet. Chem.* **2001**, *634*, 55.

100. Susperregui, J.; Bayle, M.; Leger, J. M.; Deleris, G.; Biesemans, M.; Willem, R.; Kemmer, M.; Gielen, M. *J. Organomet. Chem.* **1997**, *545*, 559.

101. Jurkschat, K.; Schilling, J.; Mugge, C.; Tzschach, A.; Meunier- Piret, J.; van Meerscsche, M. Gielen, M.; Willem, R. *Organometallics* **1988**, *7*, 38.

102. Takeuchi, Y.; Yamamoto, H.; Tanaka, K.; Ogawa, K.; Harada, J.; Iwamoto, T.; Yuge, H. *Tetrahedron* **1998**, *54*, 5822.

103. Traynelis, V. J.; Borgnaes. D. M. *J. Org. Chem.* **1972**, *37*, 3824.

104. Yan, Y. Y.; Rajan Babu, T. V. *J. Org. Chem.* **2000**, *65*, 900.

105. Takeda, N.; Nakamura, T.; Imamura, A.; Unno, M. *Heteroatom Chem.* **2011**, *22*, 438.

106. Munguia, T.; Pavel. L. S.; Kapoor, A. N.; Cervantes-Lee, F.; Párkányi, L.; Pannell, K. H. *Inorg. Chem.* **2003,** *81*, 1388.

107. Berlekamp, U. H.; Mix, A.; Neumann, B.; Stammler, H.-G.; Jutzi. P. *J. Organomet. Chem.* **2003**, *667*, 167.

108. Williams, E. A. In The Chemistry of Organic Silicon Compounds, Part 1; Patai, S.; Rappoport, Z. (Eds.); 1989, Wiley: Chichester, UK,.

109. Schoeller, W. W.; Rozhenko, A. *Eur. J. Inorg. Chem.* **2000**, 375.

110. Lin, T. -P.; Gualco, P.; Ladeira, S.; Amgoune, A.; Bourissou, D.; Gabbaï, F. P. *C. R. Chimie* **2010**, *13*, 1168.

111. Weichmann, H.; Meunier-Piret, J.; Van Meerssche, M. *J. Organomet. Chem.* **1986**, *309*, 267.

112. von Abicht, H.-P.; Mügge, C.; Weichmann, H. *Z. Anorg. Allg. Chem.* **1980**, *467*, 203.

113. Gualco, P.; Lin, T. -P.; Sircoglou, M.; Mercy. M.; Ladeira, S.; Bouhadir, G.; Perez, L. M.; Amgoune, A. Maron, L.; Gabbaï, F. P.; Bourissou, D. *Angew. Chem. Int. Ed.* **2009**, *48*, 9892.

114. Hoppe, S.; Weichmann, H.; Jurkschat, K.; Schneider-Koglin. C.; Dräger, M. *J. Organomet. Chem.* **1995**, *505*, 63.

115. Gossage, R. A.; McLennan, G. D.; Stobart, S. R. *Inorg. Chem.* **1996**, *35*, 1729.

116. Lu, V.; Tilley, T. D., *Marcromolecules* **2000**, *33*, 2403.

117. Adams, S.; Dräger, M. *Angew, Chem. Int. Ed. Engl.* **1987**, *26*, 1255.

118. Imori, T.; Lu, V.; Cai, H.; Tilley, T. D. *J. Am. Chem. Soc.* **1995**, *117*, 9931.

119. Choffat, F.; Smith, P.; Caseri, W. *J. Mater. Chem.* **2005**, *15*, 1789.

120. Choffat, F.; Käser, S.; Wolfer, P.; Schmid, D.; Mezzenga, R.; Smith, P.; Caseri, W. *Macromolecules* **2007**, *40*, 7878.

121. Babcock, J. R.; Sita, L. R. *J. Am. Chem. Soc.* **1996**, *118*, 12481.

122. Choffat, F.; Wolfer, P.; Smith, P.; Caseri, W. *Macromol. Mater. Eng.* **2010**, *295*, 210.

123. Pfeiffer, P.; Prade, R.; Rekate, H. *Chem. Ber.* **1911**, *44*, 1269.

124. Trummer, M.; Nauser, T.; Lechner, M-L.; Uhlig, F.; Caseri, W. *Polym. Degrad. Stab.* **2011**, *96*, 1841.

125. Kipping, F. S. *J. Chem. Soc.* **1924**, *125*, 2291.

126. Zou, W. K.; Yang, N.-L. *Polym. Prepr. (Am. Chem. Soc. Div. Polym.Chem.)* **1992***, 33,* 188.

127. Devylder, N.; Hill, M.; Molloy, K. C.; Price, G. J. *Chem. Commun.* **1996**, 711.

128. Miles, D., Burrow. T.; Lough, A.; Foucher, D. *J. Inorg. Organomet. Polym.* **2010**, *20*, 544.

129. Trummer, M.; Zemp, J.; Sax, C.; Smith, P.; Caseri, W. *J. Organomet. Chem.* **2011**, *696*, 3041.

130. Lechner, M-L.; Trummer, M.; Bräunlich, I.; Smith, P.; Caseri, W. *J. Appl. Organometal. Chem.* **2011**, *25*, 769.

131. (a) Trefonas, P., III; Damewood, J. R., Jr; West, R.; Miller, R. D.; *Organometallics* **1985**, *4*, 1318. (b) Harrah, L. A.; Zeigler, J. M.; *Macromolecules* **1987**, *20*, 601. (c) Fujino, M.; Hishaki, T.; Fujiki, M.; Matsumoto, N. *Macromolecules* **1992**, *25*, 1079.

132. Okano, M.; Matsumoto, N.; Arakawa, M.; Tsuruta, T.; Hamano, H. *Chem. Commun.* **1998**, 1799.

133. Elangovan, M.; Muthukumaran, A.; Kulandainathan, M. A. *Mat. Lett.* **2006**, *60*, 1099.

134. Okano, M.; Watanabe, K.; Totsuka, S. *Chem. Commun.* **2003**, *4*, 257.

135. Harrod, J. F.; MU, Y. *Polyhedron* **1991**, *10*, 123.

136. Imori, T.; Tilley, T**.** D. *J. Chem. Soc., Chem. Commun.* **1993**, 1607.

137. Woo, H-G.; Park, J-M.; Song, S-J.; Yang, S-Y.; Kim, I-S, Kim, W-G. *Bull. Korean Chem. Soc.* **1997**, *18*, 1291.

138. Neale, N. R.; Tilley, T. D. *Tetrahedron*, **2004**, *60*, 7247.

139. Thompson, S. M.; Schubert, U. *Inorg. chim. Acta* **2004**, *357*, 1959.

140. Choffat, F.; Buchmuller, Y.; Mensing, C.; Smith, P.; Caseri, W. *J. Inorg. Organomet. Poylm.* **2009**, *19*, 715.

141. Choffat, F.; Smith, P.; Caseri, W. *Adv. Mater.* **2008**, *20*, 2225.

142. Beckmann, J.; Duthie, A.; Grassmann, M.; Semisch, A. *Organometallics* **2008**, *27*, 1495.

143. Mochida, K.; Azemi, T.; Hayakawa, M.; Yokoyama, Y. *J. Chem. Soc., Chem. Commun.* **1995**, 2275.

144. Hayashi, H.; Wasaka, M.; Yokoyama, Y.; Tsuchikawa, T.; Hayakawa, M.; Mochida, K. *Chem. Lett*. **1998**, 91.

145. Drenth, W.; Noltes, J. G.; Bulten, E. J.; Creemers, H. M. J. C. *J. Organomet. Chem.* **1969**, *17*, 173.

146. Sita, L.R. *Organometallics* **1992**, *11*, 1442.

147. Brunclich, I.; Trummer, M.; Lechner, M-L.; Smith, P.; Caseri, W.; Uhlig, F. *Appl. Organomet. Chem.* **2011**, *25*, 769.

148. Sanford, E. M.; Lis, C. C.; McPherson, N. R. *J. Chem. Edu.* **2009,** *86* (12), 1422.

149. Brimble, M. A.; Flowers, C. L.; Trzoss, M.; Tsang, K. Y. *Tetrahedron* **2006,** *62* (25), 5883.

150. Porosa, L. Detection and antimirobial avtivity of immobilized quaternary ammonium anitmicrobial monolayers on porous and non-porous surfaces. Ph.D. thesis, Ryerson University , 2014.

151. Mitchell, T. N.; Walter, G. *J. Chem. Soc., Perkin Trans. 2*, **1977**, 1842.

152.   a) Tzeng, D.; Weber, W. P. *J. Org. Chem.* **1981***, 46,* 265. b) Tsai, C.-Y.; Robert Sung, R.; Zhuang, B.-R.; Sung, K. *Tetrahedron* **2010**, *66*, 6869.

153.   Dutta, D. K.; Deb, B.; Hua, G.; Woollins, J. D. *J. Mol. Catal. A* **2012**, *7*, 353.

154.   Lloyd, N. C.; Brian K. Nicholson, B. K.; Wilkins, A. L. *J. Organomet. Chem.* **2006**, *691*, 2757.

155.   Wrackmeyer, B. *Annu. Reports NMR Spectrosc.* **1999**, *38*, 203.

156.   Wrackmeyer, B.; Vosteen, M.: Storch, W. *J. Mol. Struct.* **2002**, *177*, 602.

157.   Sonika.; Narula, A. K. *Int. J. Chem. Sci.* **2003**, *1*, 141.

158.   Mahmud, T.; Iqbal, J.; Imran, M.; Mckee, V. *J. Appl. Sci.* **2007**, *7*, 1347.

159.   Šindelář, K.; Holubek, J.; Svátek, E.; Matoušová, O.; Metyšová, J.; Protiva, M. *J. Heterocyclic Chem.* **1989**, *26*, 1325.

160.   Biesemans, M.; Martin, J. C.; Willem, R.; Lyčka, A.; Růžička, A.; Holeček, J. *Magn. Reson.* **2002**, *40*, 65.

161.   Zhou, D.; Reiche, C.; Nag, M.; Soderquist, J. A.; Gaspar, P. P. *Organometallics*, **2009**, *28*, 2595.

162.   Müller, G.; Waldkirch, M.; Winkler, M. *Z. Naturforsch. Teil.* **1994**, *B 49*, 106.

163.   Morales-Morales, D.; Redón, R.; Zheng, Y.; Dilworth, J. R. *Inorg. Chim. Acta* **2002**, *328*, 39.

164.   Tolleson, G. S.; Puckette, T. A. U.S. Patent 20090299099, 03 Dec 2009.

165.   O'Keefe, M.; Brese, N. E. *J. Am. Chem. Soc.* **1991**, *113*, 3226.

166.   (a) Dräger, M.; Guttmann, H. J. *J. Organomet. Chem.* **1981**, *212*, 171. (b) Kolb, U.; Beuter, M.; Dräger, M. *Organometallics* **1994**, *13*, 4413.

167.   Kolb, U.; Beuter, M.; Drager, M. *Inorg. Chem.* **1994**, *33*, 4522.

168.   Kolb, U.; Dräger, M.; Jousseaume, B. *Organometallics* **1991**, *10*, 2737.

169.   Cox, P. J.; Doidge-Harrison, S. M. S. V.; Nowell, I. W.; Howie, R. A.; Wardell, J. L.; Wigzell, J. M. *Acta Crystallogr.* **1990**, *C46*, 1015.

170.   Dräger, M. *Z. Anorg. Allg. Chem.* **1976**, *423*, 53.

171.   Turek, J.; Padělková, Z.; Nechaev, M. S.; Růžička, A.; *J. Organometal. Chem.* **2010**, *695*, 1843.

172.   (a) Farrar, W. V.; Skinner, H. A. *J. Organomet. Chem.* **1964**, *1*, 434. (b) Neumann, W. P.; Pedain, J.; Sommer, R. *Ann. Chem.* **1966**, *694*, 9.

173.   Davies, A. G.; Osei-Kissi, D. K. *J. Organomet. Chem.* **1994**, *474*, C8.

174.   Woo, B. Y. PCT Int. Appl., 2010002209, 07 Jan 2010.

175.   El-Qisairi, A. K.; Qaseer, H. A.; Henry, P. M. *J Organomet. Chem.* **2002**, *656*, 168.

176.   Manzer, L. E. *J. Am. Chem. Soc.* **1978**, *100*, 8068.